

YS
34
66YY

ABSTRACT

ON THE KINETICS OF PHASE TRANSITIONS IN BINARY ALLOYS

by
Joaquin Marro

We report the computer simulation of the time evolution of a model binary alloy following quenching. The model is a simple-cubic lattice whose sites are occupied either by A or B particles. Particles on nearest neighbor sites can exchange positions with a probability per unit time proportional to $\exp(-\beta \Delta U) / [1 + \exp(-\beta \Delta U)]$ where $\beta = (k_B T)^{-1}$ and ΔU is the change in the energy of the system resulting from the exchange. Two different types of interactions are considered; a 'ferromagnetic' interaction which produces, at low temperatures, a segregation into two phases (one A-rich and one B-rich), and an 'antiferromagnetic' interaction which produces, at low temperatures and certain system compositions, some "alternate" ordering. The model is isomorphic to a ferromagnetic/antiferromagnetic Ising spin-one-half system with stochastic spin exchange dynamics and also to a lattice gas with attractive/repulsive interactions.

The model is started with an initial random configuration ($T = \infty$) and its evolution and equilibrium properties are studied at different temperatures and compositions in the one- and two-phase regions of the corresponding phase diagram.

Comparison is made with various theories of the processes.

involved and with experiments. We analyse in particular the validity of theories concerning the phase segregation which occurs when a binary alloy is quenched from a very high temperature molten state to a temperature T . Results are presented for the evolution of the structure function, Fourier transform of the spatial correlation function, and of the energy; also for the evolution and equilibrium properties of the distribution of clusters of different sizes. Our results, which are very similar to experimental ones on real alloys, are in disagreement with the "classical" theory of the process.

ON THE KINETICS OF PHASE TRANSITIONS IN BINARY ALLOYS

by

Joaquin Marro

Submitted in partial fulfillment of the requirements for the degree of
Doctor of Philosophy
in the Belfer Graduate School of Science
Yeshiva University
New York
September 1975

Copyright © 1975
by
Joaquin Marro

The committee for this doctoral dissertation consisted of:

Joel L. Lebowitz, Ph.D., Chairman

Graham Frye, Ph.D.

M. H. Kalos, Ph.D.

To Julia.

To my mother.

ACKNOWLEDGEMENTS

It is with pleasure that I express here my deep appreciation to Joel Lebowitz, his advice, collaboration, friendship and very kind hospitality at the Belfer Graduate School of Science, Yeshiva University, will be long remembered.

I am greatly indebted to Mal Kalos for his warm hospitality at the Courant Institute of Mathematical Sciences, New York University, and for very valuable assistance during the completion of this work. Interactions with Michael Aizenman, Alfred Bortz and Mikkilin Rao have been very fruitful. I am also indebted to Kurt Binder, James Langer and Oliver Penrose for several discussions and critical comments. To Mrs. Anne Cooper my gratitude for the patient typing of the manuscript, and to my wife, Julia, for helpful collaboration in the preparation of tables, graphs and bibliography.

Finally, I wish to acknowledge with gratitude the interest and help of Prof. L.M. Garrido which made this work possible, and the financial support from the Program for Cultural Interchange between Spain and the U.S.A., Fulbright-Hays Program, Madrid, Spain, and from the United States Air Force Office of Scientific Research (Grant No. 73-2430B). Computer time was granted by the E.R.D.A. Computing and Mathematics Laboratory at New York University under contract AT(11-1)-3077.

TABLE OF CONTENTS

I.	INTRODUCTION	
1.1.	- Motivation	1
1.2.	- Kinetics	6
II.	THE MODEL SYSTEM	
2.1.	- "Ising-like" models	19
2.2.	- Binary alloy model	22
2.3.	- Kinetics of the model	29
2.4.	- Computation of time-dependent properties	34
III.	THEORY	
3.1.	- Classical theory	38
3.2.	- "Ostwald ripening" theory	48
3.3.	- Modern formulations	50
3.4.	- Cluster dynamics	57
3.5.	- Order-Disorder transition	61
IV.	RESULTS	
4.1.	- Structure function	71
4.2.	- Energy	103
4.3.	- Scaling analysis	114
4.4.	- Clusters analysis	126
4.5.	- Antiferromagnetic interaction	166
4.6.	- Equilibrium behavior	178
4.7.	- Comparison with experiments	189
4.8.	- Discussion	192
V.	REFERENCES	196
VI.	APPENDICES	205
A.	- Numerical data	208
B.	- Lattice configurations	237
C.	- Cluster distributions	275

I. INTRODUCTION

1.1. - Motivation

The analysis of cooperative phenomena in real matter is beset by many problems of a mathematical nature and attention is still concentrated on the simplest ("Ising-like") model systems. Peierls, Kramers, Wannier and, particularly, Onsager showed that phase transitions can emerge from a rigorous treatment of simple lattice systems without the need for any additional assumption or information. The similarity between the results obtained from lattice models and those observed experimentally led to the now common belief that these models, in the beginning regarded as mathematical curiosities, actually capture many of the essential physical features of cooperative phenomena. In fact, the Ising model is now recognised to have certain relevance for all phase transitions, the only exceptions being the transitions to superfluid or superconducting states for which quantum effects are dominant on a macroscopic level.

The physical relevance of Ising-like models in the study of the kinetics of phase transitions is less clear-cut at the present time. The necessary assumptions about the transition probabilities make them more artificial when considering the dynamical problem. Also the general situation here is definitely worse: the difference in the present understanding of equilibrium and nonequilibrium problems holds also for the theory of phase transitions. As a

consequence, the consideration of more realistic systems is at the moment a difficult task and the kinetic studies are by necessity centered on simple lattice models which provide a first but significant insight into the time evolution of systems undergoing a phase transition.

The work we are reporting here represents a small contribution to this exciting area of physics and we expect it to be useful for the understanding of certain processes in real systems. We present results obtained from a computer simulation of the time evolution of an Ising model system and its comparison with various theories of the processes involved, and with some experiments. In particular we are concerned with the following situation (Fig. 1.1): a binary system in a molten state of thermal equilibrium at high temperature is suddenly quenched to a lower temperature. Immediately after the quench the system remains with a spatially uniform composition (one thermodynamic phase) but thermal equilibrium requires the coexistence of two phases. Certain atomic mixtures, e.g. Al-Zn, Cu-Ti, Ni-Si,..., quenched to temperatures below some critical value undergo coarsening which in some circumstances is referred to as "spinodal decomposition" and in others as "nucleation and growth". "Ostwald ripening" and "Smoluchowski coagulation", which refer to specific mechanisms, are also familiar denominations. The phenomenon is in some ways very similar (and in others different, see section 1.2)

to the development of liquid droplets in a supersaturated vapor. It also resembles the appearance of magnetic domains in a ferromagnetic material (if one ignores the quantum nature of the magnets). Other mixtures, e.g. Au-Cd, Mg-Cd, Cu-Zn, Au-Cu, ..., on the contrary, favor at low temperatures some "alternate" ordering so that the tendency is to the formation of "superlattices". The process then bears a similarity to the liquid-solid transition and also to anti-ferromagnetism. These are usually known as "order-disorder phenomena". Our main interest here is in the occurrence of coarsening and ordering phenomena in binary alloy systems where they are of great practical interest.

The nature of the kinetic evolution of the system towards its equilibrium state in the above conditions presents a difficult challenge to the theorist, as will be analysed in chapter III. The phenomenological approaches are hampered by several serious problems (Sato 1970, Langer 1973, Yamauchi and de Fontaine 1974, Binder et al. 1975), and any microscopic theory will have to deal with two of the less understood areas of modern physics: phase transitions and irreversibility. Furthermore, although some number of x-ray and neutron scattering studies have been performed on binary alloys, experimental results are not yet very clear-cut. Thus, the computer simulation of those processes seems to be a good way of attacking the problem. We believe that despite the many crude over-simplifications of reality necessarily

made in the model of our simulations it contains the essential features of the phenomena of interest as they occur in real systems; indeed we obtain results very similar to experimental observations (section 4.7). If this is granted, then it follows that any theory claiming to describe these processes in real physical systems should also be able to describe what happens in our model system. The model is thus useful as a test of theory. Even more important, the model, because of its flexibility, can be used in some cases to identify the important physical steps in the phase separation processes which need to be built into a good theory.

Next in this chapter we present a qualitative description of the phenomena of interest that incorporates our knowledge from theory and experiments as well as from the computer simulations. Also in this chapter the occurrence of these phenomena in real materials and their relation with other familiar processes are considered. In chapter II we make a detailed description of the model system and give details of the computational techniques employed in this work. The binary (AB) alloy is modeled as a simple-cubic, Ising-spin system with nearest-neighbor spin exchanges and periodic boundary conditions. The two possible spin states will then correspond to the two different kind of particles, A or B, at every lattice site. Starting from a random configuration, corresponding to the alloy system at infinite temperature,

the system is quenched to and evolves at a temperature $(k_B \beta)^{-1}$ where the probability of an exchange between an A and a B atom on nearest neighbor sites is assumed proportional to $e^{-\beta \Delta U} [1 + e^{-\beta \Delta U}]^{-1}$. ΔU is the change in energy resulting from the exchange. The evolution simulates a stochastic process according to the Monte-Carlo technique. We are then mainly interested in the time evolution of the energy of the system and the structure function, Fourier transform of the spatial-correlation function, as it would be observed by means of x-ray or neutron scattering.

In chapter III we analyze the theories for the processes involved. The main general conclusion from chapters I and III is that insufficient knowledge of the microscopic properties of the samples and complicated additional effects which may influence the kinetic evolution make a meaningful comparison of experiments with theory very difficult. Chapter IV is devoted to the analysis of the results from our computer experiments. These results are then compared with the theory and with some experiments. While we obtain an excellent qualitative agreement with experimental results, some of the predictions of the classical theory are in disagreement with the computer simulation of the phenomena in our idealized system. Some equilibrium numerical computations for our model system are also reported in section 4.6.

1.2. - Kinetics

We are concerned here with the separation of a single, thermodynamically unstable phase into two stable phases which occurs in its simplest form when an AB-alloy is quenched (i.e. cooled very rapidly) from some high temperature, where the system is in a molten state, to a temperature T below T_c , the critical temperature for phase separation in the solid alloy.

The system, initially with a uniform spatial composition, will develop local inhomogeneities that one expects to describe by means of some order parameter. For instance one can think in terms of the variables $n_A(\underline{r})$ and $n_B(\underline{r})$ giving respectively the concentration of atomic species A and B in a region of some size around the position \underline{r} . Denoting by \bar{n}_A and \bar{n}_B the average of these variables in the system, we can have $\bar{n}_A + \bar{n}_B = 1$ and define a single local parameter $\eta(\underline{r}) = n_A(\underline{r}) - n_B(\underline{r})$ that describes the composition in those regions throughout the system. Then $1 \geq \eta(\underline{r}) \geq -1$ with the extremum values corresponding to an A-pure or a B-pure region respectively. The average composition will be $\bar{\eta} = \bar{n}_A - \bar{n}_B$. We define the spatial correlation function

$$G(\underline{r}, t) = \langle (\eta(\underline{r}') + \bar{\eta})(\eta(\underline{r}', t) - \bar{\eta}) \rangle \quad (1.1)$$

where the angular brackets refer to an average over \underline{r}' in the macroscopic system. The structure function $S(\underline{k}, t)$ is the Fourier transform of (1.1):

$$S(\underline{k}, t) = \int d\underline{r} e^{i\underline{k} \cdot \underline{r}} G(\underline{r}, t); \quad (1.2)$$

it can be measured experimentally by means of x-ray or neutron scattering and is thus a quantity of interest in the analysis.

The features of the equilibrium state of the system are recognized to be fundamentally different according to the position of its representative point in the temperature-composition plane of the phase diagram (Fig. 1 of this chapter). At very high temperatures, say T_0 , where the components of the system are miscible in all proportions, one expects essentially no correlation between the composition in different microscopic regions (Appendix B, Fig. 1). Then $\bar{\eta}(\underline{r})$ will be independent of \underline{r} and equal to $\bar{\eta}$, and the microscopic $S(\underline{k})$ effectively zero everywhere. If the temperature is not so high, however, microscopic correlations can develop. The structure function is then expected to have approximately an Ornstein-Zernicke form, $S(\underline{k}) \sim 1/(1+k^2 \xi^2)$, with a very short correlation length ξ . If one considers somewhat bigger regions in the system, whose size has to increase with decreasing temperature, the correlations will disappear. This would also be essentially the situation outside the coexistence

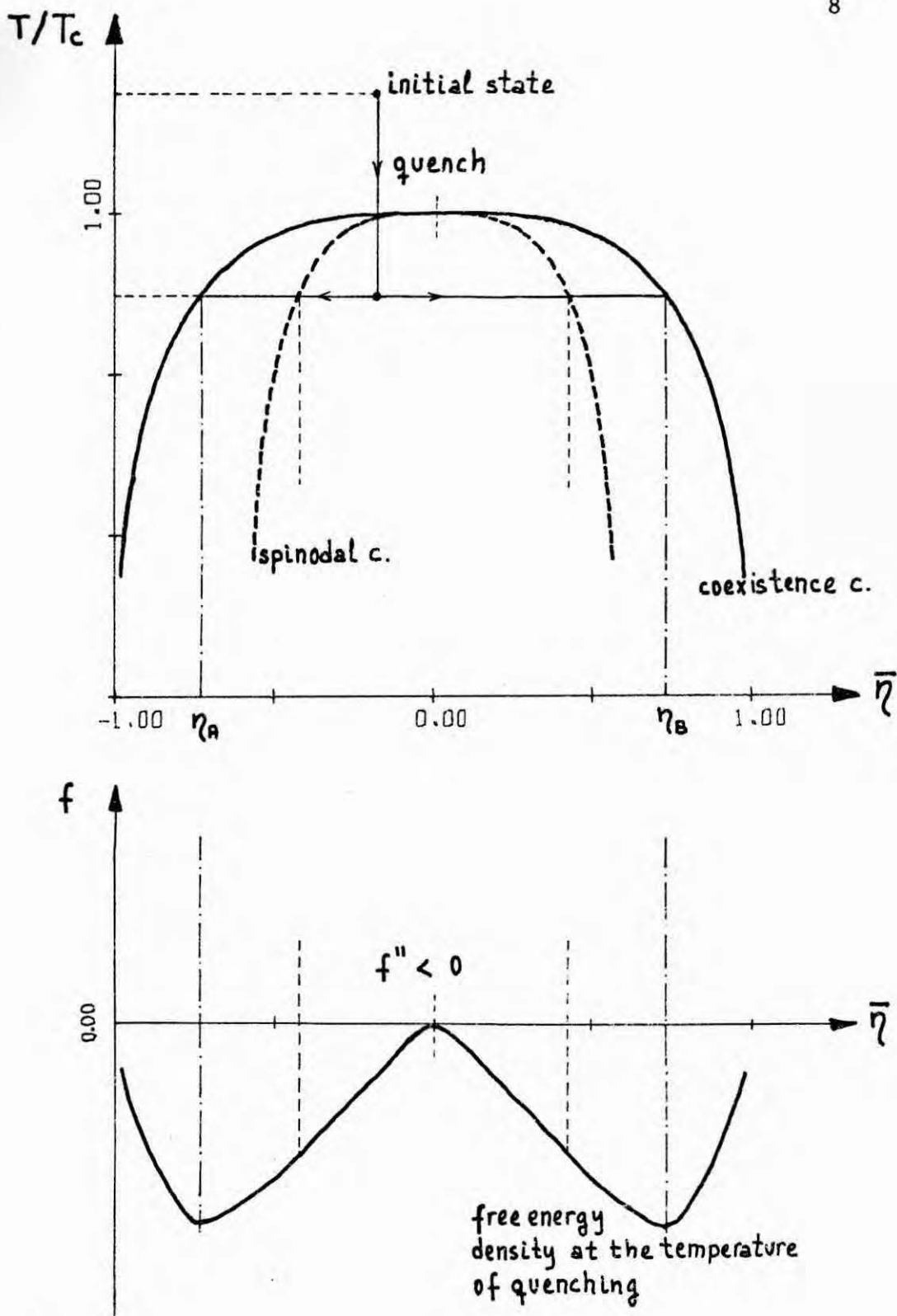


Fig. 1.1 Schematic representation of the general process considered in this work in order to study the kinetics of phase transitions in binary systems. See the text for details.

curve at $T < T_c$. On the other hand, at temperatures below T_c and for certain ranges of composition the equilibrium state is one of coexistence of two phases, one A-rich of composition η_A and one B-rich of composition η_B if there is a predominance of attraction between atoms of the same species. These values are determined by the end of the miscibility region at the temperature T as shown in Fig. 1. This means that $\eta(r)$ will have spatial dependence (with, however, $n_A(r) + n_B(r) = 1$), and $S(k)$ will also reveal the two-phase structure. In particular it will have a peak at a value of k whose inverse is a measure of the size of the differentiated single-phase regions. The height of the peak will indicate in some way how well defined these regions are.

Suppose now that a system, in equilibrium at the high temperature T_0 , is cooled very rapidly so that its homogeneity is not altered during the process. After the quench it will be left in a thermodynamically unstable state, still without correlations. It will then undergo a process of phase separation as it approaches its equilibrium state at the temperature of quenching. This kinetic evolution will lead to different final states depending on the nature of the atomic interaction in the system. Let us consider first the case of a net attraction between like atoms. According to the classical theory of the process (section 3.1) one has to distinguish two regimes of different kinetic behavior. If the quench is to a state within the so-called "spinodal curve", the

system is supposed to be unstable with respect to weak delocalized (i.e. long wave-length) fluctuations and the phase separation proceeds then by the "spinodal decomposition" mechanism. If the alloy is quenched to some phase point in the region between the coexistence and spinodal lines (Fig. 1) the corresponding state is supposed to be metastable. Some activation energy is then required for the system to undergo a phase separation; that is, nuclei of a certain size (strong localized fluctuations), built up by some mechanism, have to be present. It seems however that the distinction between spinodal decomposition and nucleation is not as dramatic as stated by the classical theory.

The process will begin with the formation throughout the system of small regions in which there is an excess of one of the phases, $n_A > \bar{n}_A$. The scattering intensity will then have a maximum at some comparatively large value of k . The coarsening of these initial "grains" may then proceed essentially by two different mechanisms*. One may consider single atom processes which cause the growth of larger grains at the expenses of smaller ones. This is the basis of the "Ostwald ripening" theory as considered in section 3.2. The "Smoluchowski coagulation", on the contrary, assumes the preponderance of an effective diffusion of the clusters and their coalescence with other clusters

*This point is being expressly analyzed nowadays in a two-dimensional system (Rao et al., to appear).

of a comparable size. This is considered in section 3.4. During the coarsening it is observed that the maximum of the scattering intensity shifts toward smaller values of k while it becomes sharper. These facts are respectively associated with the growth of the linear dimensions of the differentiated regions and with the increasing compactness in the clusters.

Spinodal decomposition in alloys is formally similar to the spin diffusion in ferromagnets. We shall frequently use the spin language keeping in mind that the concentration, composition and chemical potential in an alloy correspond to the spin density, magnetization and magnetic field in a magnet. The corresponding critical point is the Curie point. One outstanding difference consists in that the total magnetization need not be conserved in a magnetic system while the average composition is constant during the time evolution of the alloy.

The condensation of liquid droplets in a supersaturated vapor is also a similar phenomenon. The conceptual difference comes from the fact that in the vapor the thermal atomic motion is closely associated with temporal changes in the spatial composition, an effect that can be disregarded in the alloy problem. This might also be true, to a lesser extent, when considering fluid mixtures in which the coarsening process should be qualitatively very similar to the one in alloys. In this case, however, there is a finite viscosity and hydrodynamic effects may be expected to be dominant over atomic diffusion.

Spinodal decomposition is supposed to be characteristic of all alloy systems as far as they present a miscibility gap, the experimental difficulties in obtaining a rapid enough quenching, however, lead to its being mixed up with other competing processes. Also, imperfections of the alloy, grain boundaries, elastic strain fields, etc. can modify its development, by limiting the phase separation in a later stage. These difficulties are not present in the computer simulations, where the phenomenon can be isolated.

The typical experimental evidence of spinodal decomposition corresponds to the situation in which a metallic alloy, such as Zn - Al, rich in aluminum, is rapidly quenched from about 400° C and then annealed at 100° C (Rundman and Hilliard 1967, Rundman 1970, Butler and Thomas 1970, and others to be quoted later). The phenomenon has also been reported in some glassy mixtures (Zarzycki and Naudin 1967, Nielsen 1969, Andreev et al. 1970, and Tomozawa et al. 1970). When the scattering length of the two kinds of atoms in the alloy is sufficiently different, it is possible to determine experimentally the structure function, $S(k)$, which is proportional to the intensity of the radiation scattered with momentum transfer k . In sections 4.3 and 4.7 some such experiments are compared with our results. In some cases magnetic measurements techniques (Butler and Thomas 1970), as well as measurements of the electrical resistivity (Richter et al. 1974),

have been used to determine the structure of the alloy. More directly comparable with this work are the analysis of thin foils of the sample by means of electron microscopy and direct estimation of the particles size (Ardell 1969). Some of these experiments are considered in section 3.2 where it is pointed out that while they are consistent with power-laws with small exponents, these exponents cannot be determined unambiguously in that way (Speich and Oriani 1965, Smith 1967), even apart from other difficulties (section 4.7).

In the case of an antiferromagnetic coupling the process involved is in some sense the opposite to the clustering described above. It occurs in the development of antiferromagnetism in magnetic systems, the absorption of a gas upon a crystalline surface, the formation of "superlattices" in alloy systems and the solid-liquid transitions. In the latter case, the liquid state possesses only short-range order while the crystalline structure of a solid is a long-ranged ordered structure (there is a certain degree of correlation between the positions of different atoms which is almost independent of their distance apart); the transition from liquid to solid thus requires the building of some order in the system. We shall use here the widely-accepted (Green and Hurst 1964) term "order-disorder" (although "disorder-order" might be more appropriate to our case) to refer to this kind of transition, in spite of the fact that the clustering processes

are sometimes also called by that name.

A quenched binary alloy undergoes such an ordering process when unlike atoms attract each other more strongly than like atoms. This interaction favors having different kinds of atoms as nearest-neighbors. For a simple-cubic lattice at zero temperatures and 50% concentration of A-atoms the equilibrium state is one in which each atom is surrounded by atoms of the other species. This type ordering will persist for higher temperatures (below T_c) for certain range of compositions. When there is an appreciable difference between the concentrations of the two atomic species ($\bar{n} \neq 0$), most of the A-atoms will be separated from each other by distances larger than the interaction range. The A-atoms are then allowed to keep "travelling" in a sea of B-atoms without changing the total energy of the system and there will be no long range order in the system. This peculiarity of ordering phenomena^(*), which is observed in our simulation, is associated with a degeneracy in the ordered state (Sato and Kikuchi 1973).

(*) A difficulty of a similar nature (Kikuchi and Sato 1974), not present in clustering phenomena, may induce essential differences between the ordering process in a simple-cubic lattice and body- or face-centered cubic lattices, which is of more practical interest.

An accurate description of the processes involved is more complex than in the case of the spinodal decomposition; every proposed order parameter fails to describe some aspect of the phenomenon, and this usually hampers the theoretical approaches (Guttman 1966). A convenient way of dealing with binary systems is the consideration of two equivalent sublattices (or superlattices): at zero temperature and equal concentrations all of the A-atoms will occupy a sublattice, α , and all of the B-atoms the other sublattice, β . This suggests (Bragg and Williams 1934) the consideration of a "long-range order parameter",

$$\sigma = (N_r - N_w)/(N_r + N_w) \quad (1.3)$$

where N_r refers to the total number of atoms occupying the proper sublattice and N_w to the total number of "misplaced" atoms in the system. Thus σ varies from 0 (the completely random distribution of atoms favored by the thermal agitation at "infinite" temperature) to one (the completely ordered state at $T = 0$ and $\sigma = 1$). This long-range order (LRO) parameter, however, provides on some occasions a poor description of the state of order in the system; one can construct atomic arrangements (such as the one shown in Fig. 1.2) with a high degree of order, for which $\sigma = 0$. Other order parameters have been proposed (Bethe 1935, Cowley 1950, Klein 1951, Fowler and Guggenheim 1949) for specific or general purposes.

A	B	A	B	A	B	A	B		B	A	B
B	A	A	B	A	A	B	A		A	B	A
A	B	B	A	B	B	A	B		B	A	B
A	B	A	B	A	A	B	A		B	A	B
B	A	B	A	B	B	B	A		B	B	A
B	A	B	A	B	A	A	B		A	A	B
A	B	A	B	A	B	B	A		B	B	A
B	A	A	B	A	B	B	A		B	A	B
A	B	B	A	B	A	A	B		A	B	A
B	A	A	B	A	B	B	A		B	A	B
A	B	B	A	B	A	A	B		A	B	A

Fig. 1.2 Highly ordered atomic arrangement in a
 11 x 11 lattice in which the "out-of-step"
 domains cause the LRO parameter to be zero.

The description via the structure function (1.2) is still very useful in this case. In fact, the scattering intensity from a partially ordered system is essentially the sum of two differentiated parts. A disordered system will cause diffuse scattering with a small number of peaks ("fundamental reflections") which correspond to the presence of some short-range order (SRO) in the system. When the system undergoes an ordering process, some of the diffuse intensity will concentrate into sharp lines ("superlattice reflections"). This corresponds to the development of LRO and is intimately associated with the lowering of the lattice symmetry. These superlattice lines have been detected in a number of different systems; the classic experiments by Jones and Sykes (1938) and Wilson (1949) refer to the temporal evolution of binary alloys. The typical example of a substitutional alloy in which ordering takes place, and where the above effect are observed (Dietrich and Nielsen 1966), is the so-called β -brass (Cu-Zn at 50%). This crystalline alloy presents a BCC structure that, in the ordered state, can be considered as made up of two interpenetrating simple cubic lattices, each occupied by one of the atomic species. Some more experimental evidence, as well as some related theoretical concepts are analysed in section 3.5.

The mathematical problem (Green and Hurst 1964) associated with ordering phenomena in the Ising model is very similar to that of clustering phenomena, and they are equivalent in the case of

zero external field for loose-packed lattices. In fact (section 2.1), the spins are dummy variables in the expression for the partition function so that one may change the sign of all the spin variables on one sublattice without altering that function and, in consequence, without altering the thermodynamic properties of the system. Our model system can simulate the kinetics of the transition as it occurs in the simple-cubic binary alloys, and in section 4.5 we report some results in this system.

II. THE MODEL SYSTEM

2.1. - "Ising-like" models

"Ising-like" models (Brush 1967) have often been used for the modelling of alloy systems for the study of cooperative phenomena. We describe them in this section since they form the basis of the kinetic alloy model studied in this work.

Consider a regular lattice with N sites and dimensionality d , and assume well-localized spins (angular momenta) so that we can associate a spin variable $\underline{\sigma}_i$, $\sigma \geq 1/2$, to each lattice site i . The system is placed in a magnetic field \underline{h} , and there is an isotropic, pairwise spin interaction. Under these conditions the energy of the system is given by the Heisenberg Hamiltonian (Heisenberg 1928),

$$H_H = \sum_{i < j} J_{ij} \underline{\sigma}_i \cdot \underline{\sigma}_j - g\mu_B \sum_i \underline{\sigma}_i \cdot \underline{h} \quad (2.1)$$

where J_{ij} is the "exchange energy" between spins i and j and $g\mu_B$ is the magnetic moment per spin (g is a pure number and μ_B the Bohr magneton). The spin operators $\underline{\sigma}$ satisfy the usual commutation rules $([\sigma_{xj}, \sigma_{yj}] = i \sigma_{zj})$, while $\underline{\sigma}_j$ and $\underline{\sigma}_k$ commute for $j \neq k$) and $\underline{\sigma}^2 = \sigma(\sigma + 1)$.

Equation (2.1) can be seen as a particular case of the more general Ising-Heisenberg Hamiltonian,

$$H_{IH} = \sum_{i < j} J_{ij} [\sigma_{zi} \sigma_{zj} + \alpha(\sigma_{xi} \sigma_{xj} + \sigma_{yi} \sigma_{yj})] - g\mu_B \sum_i \sigma_i \cdot \underline{h}. \quad (2.2)$$

H_{IH} reflects the fact that actual magnetic materials exhibit neither pure isotropic nor pure anisotropic interactions. The Ising case (Lenz 1920, Ising 1925) follows from (2.2) when $\alpha = 0$. If the field \underline{h} is parallel to the z-axis the Hamiltonian has a trivial diagonalization and, upon identifying the operators σ_{zi} with semiclassical variables with $2\sigma + 1$ values, one can write

$$H_I = \sum_{i < j} J_{ij} \sigma_i \sigma_j - h \sum_i \sigma_i, \quad (2.3)$$

where we included $g\mu_B$ in h , the constant intensity of the field.

The most familiar realizations of the Ising model keep a short-ranged interaction specified by setting $J_{ij} = J$ when i and j are nearest neighbor spins and zero otherwise. The Hamiltonian is then written

$$H = -J \sum_{i,j} \sigma_i \sigma_j - h \sum_i \sigma_i \quad (2.4)$$

The value $\sigma = 1/2$, with $\sigma_{zi} = \pm 1/2$ corresponding to "up and down" spins, is appropriate when simulating the two atomic species in a

binary alloy, and $\sigma = 1$ when vacancies (or a third species) are allowed in the lattice. The case $J > 0$, in general $J_{ij} \geq 0$, is associated with ferromagnetic coupling since the energy is minimized for $\underline{\sigma}_i$ parallel to $\underline{\sigma}_j$. Likewise $J < 0$ generally corresponds to an antiferromagnetic interaction.

One can think of the above formulae as referring to a system confined to a certain domain of finite volume V . The free-energy per lattice site is then given by

$$f = \frac{1}{V} k_B T \ln Z \quad (2.5)$$

where k_B is Boltzmann constant, T the temperature and Z the partition function of the system. Z is a function of the configurations,

$$Z = \sum_{\sigma_1} \sum_{\sigma_2} \dots \sum_{\sigma_N} \exp (-H/k_B T) \quad (2.6)$$

in the classical case, whose determination thus implies the "solution" of the model. One is generally concerned with bulk properties so that it is important to know if the above quantities have a well defined limit when the linear dimensions of the system are allowed to become infinite. The existence of the thermodynamic limit has been proved (Lebowitz 1968, Griffiths 1972) for the cases considered here.

2.2. - Binary alloy model

Let us consider a system made up of two different atomic species, A and B, in which we can distinguish N disjoint regions of the same volume, each containing ν atoms. The region i , $i = 1, \dots, N$, whose center is determined by the position vector \underline{r}_i , presents the concentrations $n_A(\underline{r}_i)$ and $n_B(\underline{r}_i)$ for A- and B-atoms respectively, with $n_A(\underline{r}_i) + n_B(\underline{r}_i) = 1$. In order to simulate a metallic alloy we have to provide for some structure; then we suppose each region attached to one of the N sites of a regular lattice. This picture helps when considering the extension of the model to the continuum case, but only one atom per site, $\nu = 1$, will be considered in the following. This precisely determines the size of the regions considered in section 1.2 and in consequence the results of the computer simulation will always refer to the lowest "microscopic" level. In these conditions the Hamiltonian of the system can be written:

$$H = \sum_{i < j} \sum_{\alpha, \beta} n_\alpha(\underline{r}_i) n_\beta(\underline{r}_j) \Psi_{\alpha\beta} (\underline{r}_i - \underline{r}_j) + \sum_i \sum_{\alpha} n_\alpha(\underline{r}_i) g_\alpha \quad (2.7)$$

where $\alpha, \beta = A$ or B , and g_α is the chemical potential corresponding to species α . The interaction energy of the system is supposed to be the sum of pair potentials $\Psi_{\alpha\beta}$ that should have a hard-core part and reflect the fundamental property in coarsening (ordering) phenomena of a predominant attraction (repulsion) between like atoms.

The common repulsive part automatically enters in the model when one requires that each lattice site can be occupied at most once; this hard-core potential has a range $a_o/2$, with a_o the lattice spacing which is set equal to the unity in the following. The simplest realization for the attractive (repulsive) part consists of an interaction between atoms when they are nearest neighbors in the lattice and zero otherwise, $\Psi_{AA} < 0$, $\Psi_{BB} < 0$, $\Psi_{AB} > 0$ ($\Psi_{AA} > 0$, $\Psi_{BB} > 0$, $\Psi_{AB} < 0$). More general interactions might also be considered, but they would increase unsuitably the computer time necessary for the simulation; only the allowance for vacancies (or the simulation of defects in the lattice) seems to be at the present time inside of reasonable limits, but they were also neglected in this work. We can arrange then the Hamiltonian (2.7) to get

$$H = -J \sum'_{i,j} \eta(\underline{r}_i) \eta(\underline{r}_j) - h \sum_i \eta(\underline{r}_i), \quad (2.8)$$

where the prime indicates that the sum is over nearest neighbor sites, $-J = \Psi_{AA} + \Psi_{BB} - 2\Psi_{AB}$, $h = g_B = -g_A$, independent of \underline{r} , and we have introduced the composition at site i , $\eta(\underline{r}_i) = n_A(\underline{r}_i) - n_B(\underline{r}_i)$, as in section 1.2.

The system is then isomorphic to a spin one-half Ising system of Hamiltonian (2.4) in which there is at each lattice site i a spin variable, $\eta(\underline{r}_i) = \pm 1$, which can either "point up or

down". Spin up will correspond to an A-atom and spin down to a B-atom. The system is also isomorphic to a lattice gas where each site can be either occupied or empty.

The Hamiltonian (2.8) reflects predominance of attraction between alike atoms (ferromagnetic interaction) when $J > 0$; this is the situation considered here. Eventually an antiferromagnetic interaction, $J < 0$, is also considered. The results we present here refer to a simple cubic lattice which allows the direct comparison with experiments and with the current three-dimensional theories. In this case the position \underline{r}_i ranges over an L by L by L cubical region containing $L^3 = N$ sites. In every case we use periodic (toroidal) boundary conditions so that corresponding atoms on opposite faces are considered nearest neighbors.

In a zero magnetic field, $h = 0$, the interaction energy between atoms on nearest neighbor sites is given by

$$U = -J \sum' \eta(\underline{r}_i) \eta(\underline{r}_j) . \quad (2.9)$$

The composition $\eta(\underline{r}_i)$ corresponds to the local magnetization in the spin representation and the microscopic state of the system is specified by giving the value of $\eta(\underline{r}_i)$ at each lattice site,

$$x = \{\eta(\underline{r}_i), i = 1, \dots, N\} \quad (2.10)$$

(Sometimes in the following we shall use $\eta_i \equiv \eta(\underline{r}_i)$ in order to simplify the notation.) The variable x can thus take on 2^N values. The total magnetization, $\bar{\eta} = \bar{n}_A - \bar{n}_B$ (average values in the system), is conserved. This is a consequence of considering a spin exchange mechanism as the elementary dynamical process in our system. We have

$$\bar{\eta} = \frac{1}{N} \sum_i \eta(\underline{r}_i) = 2\bar{n}_A - 1 \quad (2.11)$$

that corresponds to the difference between the total number of A- and B-atoms divided by N. Sometimes we use $c \equiv \bar{\eta}$ in the figures.

The equilibrium properties of the model can be directly obtained from the free-energy density, (2.5), which is simply related to the partition function of the system. The computation of the partition function (2.6), however, involves a complicated combinatorial analysis and, as is well-known, has only been exactly determined in a few particular cases, mainly in one and two dimensions with zero external field (Ising 1925, and Onsager 1944, respectively; Newell and Montroll 1953, Mattis 1965). In other cases, in particular for the simple-cubic lattice of relevance here, most of the equilibrium properties have been accurately determined by approximate methods (Fisher 1967, Kadanoff et al. 1967). The most accurate procedure consists essentially in the

expansion of certain physical quantities in power series about $T = 0$ and $T = \infty$ and the application of standard techniques (for instance Padé approximants) in the determination (or guessing) of the radius of convergence of these series. In this way it has even been possible to obtain knowledge about the behavior of those quantities near singularities. (Domb 1974).

The critical point for the binary alloy model in the thermodynamic limit $L \rightarrow \infty$ is located by this method at $T_c \approx 4.5103 \text{ J}/k_B$ (Fisher 1967). The phase diagram of the infinite system is shown in Fig. 2.1 where it is drawn using low temperature Padé's and a $5/16$ power law near T_c (Essam and Fisher 1963).

Here appears an interesting question: how large has a model system to be in order to simulate cooperative macroscopic behavior. The problem has been studied both by means of exact analytic computations (Ferdinand and Fisher 1969, Fisher 1970) and computer simulations (Yang 1963, Binder et al. 1970) in small systems. The finite size causes a "rounding phenomena" which smoothes the singularities (for instance the peak of the specific heat as a function of the temperature) as the number of particles in the system decreases, and the critical point is replaced by a "transition region" in which one can localize a "transition temperature", T'_c . For a finite three-(or two-) dimensional system with periodic boundary conditions this transition temperature is always above T_c , the critical temperature for

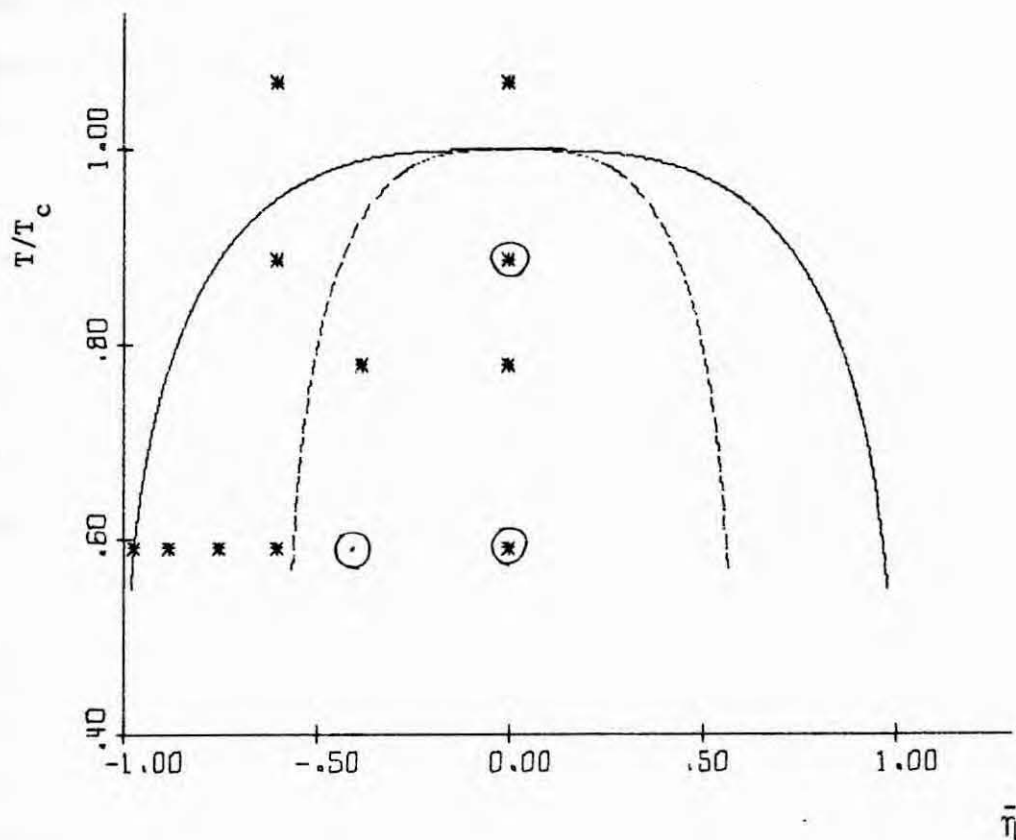


Fig. 2.1 Phase diagram for the AB-alloy or for the infinite 3-dimensional Ising model. The coexistence curve (solid line) is drawn according to a low-temperature series expansion (Essam and Fisher 1963). The "spinodal curve" (dashed line), supposed boundary between metastable and unstable states, is characterized by $\partial^2 f(\bar{\eta}) / \partial \bar{\eta}^2 = 0$ and is drawn assuming a free-energy density of the form $f(\bar{\eta}) = -\alpha \bar{\eta}^2 + \beta \bar{\eta}^4$ below T_c . The asterisks denote points discussed here in connection with a ferromagnetic interaction, and the circles in connection with an antiferromagnetic interaction. The case $T/T_c = 1.5$, $\bar{\eta} = 0$ is not included in the figure.

the infinite system, and rapidly approaches T_c with increasing size. For free boundary conditions the transition temperature is always below T_c . Ferdinand and Fisher (1969) conjecture

$$T'_c = T_c (1 \pm a/\tilde{L}^b), \quad (2.12)$$

with a of order unity, \tilde{L} some characteristic linear dimension of the system in units of the lattice spacing, and the sign + (-) standing for periodic (free) boundary conditions. The exponent b in (2.12) is $b \approx 1$ for very small systems and the relation seems to be confirmed by Monte Carlo analysis (Binder 1972) for free boundaries. For larger systems it is $b \approx 3/2$. In the case of periodic boundaries the coefficient a in (3.12) is somewhat bigger than that for free boundaries. As a consequence it seems reasonable to admit that the critical behavior of our system of 27000 spins should be practically indistinguishable from the one of the corresponding infinite system. We also computed some of the equilibrium properties in our model system, and the comparison with the ones approximately known for the infinite system seems to confirm this point. Some results for a system of 125000 spins are also reported.

The free energy density for our model has a rigorous symmetry about $\tilde{\eta} = 0$ and for the scaling analysis performed in section 4.3 is assumed the conventional Ginzburg-Landau polynomial (3.2)

(Fig. 2.1). The form suggested by Wilson and Kogut (1975) for the critical region, with a sixth-order term in \tilde{N} , should do a better work in the neighborhood of T_c (see also section 3.1). This is in any case a delicate point. The spinodal curve (as drawn in Fig. 2.1) is only an artifact of the phenomenological approach which does not follow from equilibrium statistical mechanics; non-equilibrium considerations, however, can lead to a distinction between unstable and metastable states (Penrose and Lebowitz 1971, Binder 1973).

The time evolution of the models so far described has been studied in the consideration of a number of different phenomena. Flinn (1974), Binder (1974) and Bortz et al. (1974, Bortz 1974) carried out machine computations on this model using essentially the kinetics described in the next section. Our kinetic model is also similar in some ways to models discussed by Kawasaki (1966, 1972). This model differs from the spin-flip models considered by Glauber (1963) and Gotlib (1970), where the total magnetization is not conserved and thus cannot be used to simulate the binary-alloy problems of interest here. A simulation of ordering kinetics has been performed by Flinn and McManus (1961) using second-neighbor interactions and exchanges via vacancies on a rather small ($N = 2000$) BCC lattice.

2.3. - Kinetics of the model

An alloy system after the quench is usually in a solid phase

which makes atomic migration difficult. The lattice vibrations or phonons, nevertheless, can supply the energy necessary for an evolution of the system. This picture provides the basis for the kinetics of the model. The microscopic time evolution thus depends on the interaction with a heat or phonon reservoir which helps atoms overcome the potential barriers necessary to change their positions. The reservoir is in equilibrium at the temperature T during the evolution and provides the driving force for the configurational part of the system to approach its equilibrium state at that temperature.

We consider a Gibbs ensemble of the systems so far described and denote by $P(x)$ the probability of the microscopic state x in the ensemble. The reservoir is always in equilibrium and $P(x)$ is the fraction of systems in the ensemble with the configuration x , (2.10). Then, when the ensemble is in equilibrium at temperature T one has

$$P_{eq}(x) = \frac{1}{Z} \exp [-\beta U(x)] , \quad Z = \sum_x \exp [-\beta U(x)] , \quad (2.13)$$

where $\beta = 1/k_B T$ and $U(x)$ is the configurational part of the Hamiltonian, (2.9).

Immediately after the quench, which we shall take as the time origin for the evolution, the ensemble finds itself with a non-equilibrium probability distribution $P(x,0)$. $P(x,t)$ will in general evolve according to an equation of the form

$$\frac{\partial P}{\partial t} = \left(\frac{\partial P}{\partial t} \right)_L + \left(\frac{\partial P}{\partial t} \right)_R \quad (2.14)$$

where the first term in the right hand side contains the own internal dynamical evolution of the lattice system and the second term refers to the interaction with the reservoir. But our model has no dynamics of its own (the Hamiltonian (2.9) commutes with the spin variable at each lattice site) so that only the fluctuation part has to be considered in (2.14). It is assumed that this part evolves according to a "master equation":

$$\frac{\partial P(x,t)}{\partial t} = \sum_{x'} [K(x' \rightarrow x) P(x',t) - K(x \rightarrow x') P(x,t)] \quad (2.15)$$

where $K(x \rightarrow x')$ represents the probability per unit time of a transition induced by the reservoir from the state x to the state x' .

The determination of the transition probabilities $K(x \rightarrow x')$ is in general a difficult matter. It is well known that the condition of detailed balance,

$$K(x \rightarrow x') \exp [-\beta U(x)] = K(x' \rightarrow x) \exp [-\beta U(x')] \quad (2.16)$$

is sufficient, although not necessary, to ensure that the equilibrium distribution (2.13) is a stationary solution of the master equation. When, as in the model considered here, all the configurations x are accessible from any initial state then the equilibrium distribution will actually be approached as $t \rightarrow \infty$, even for an infinite system (Holley 1974). The elementary process in the model consists of a spin interchange between nearest neighbors so that $K(x \rightarrow x')$ must have the form

$$K(x \rightarrow x') = \sum_{i,j} W(\eta_i, \eta_j; \eta'_i, \eta'_j) \delta(x - \eta_i - \eta_j, x' - \eta'_i - \eta'_j) \delta(\eta_i + \eta_j, \eta'_i + \eta'_j). \quad (2.17)$$

(2.17) is a sum over all nearest neighbor pairs, and W gives the probability for the spin variables η_i and η_j to become η'_i and η'_j . The first δ -function ensures that all spin variables other than η_i and η_j are not altered in the interchange. The second δ -function in (2.17) ensures that the total magnetization is conserved so that only spin exchanges (and not spin flips) are performed. The violation of any of these two conditions will annul the corresponding term in the sum (2.17). W has to reflect the relative probability of the configuration x and x' that, according to (2.13), is

$$p_{ij} = \exp [-2\beta J \Delta_{ij}] \quad (2.18)$$

with $2J \Delta_{ij} = U(x) - U(x')$, and thus Δ_{ij} is simply the change in the number of unlike nearest neighbor pairs that would result from the interchange. This change depends on the configuration of spins on the ten sites surrounding the pair i, j . W in (2.17) was chosen as

$$W(\eta_i, \eta_j; \eta'_i, \eta'_j) = \alpha p_{ij} / (1 + p_{ij}) . \quad (2.19)$$

This satisfies the detailed balance condition. α^{-1} , which is assumed to be independent of x and x' , is taken to determine the unit of time and treated as a temperature-independent quantity. Nevertheless, in comparisons with experiments on real systems α will certainly need to be taken temperature dependent since the strength of the phonon reservoirs decrease with temperature. In this case our time scale will have to be rescaled for each temperature, apart from the necessary rescaling necessary to model different materials (section 4.7).

To carry out the computer simulation we start the system with a magnetization $\bar{\eta}$ in a "random configuration" x_0 , i.e. we choose the sites at which to place the A particles 'at random' from among all sites. Then we select at random a pair of nearest neighbor spins and the Markov transition probability (2.19) is

calculated for this case. The value of W is then compared to a random fraction R that is chosen each time with uniform probability over the interval $(0,1)$. If $W \geq R$ the interchange is performed, otherwise the process ("try") is repeated by selecting a new pair of nearest neighbor spins. In this way a stochastic evolution is simulated in which the number of tries per lattice site is the natural unit of time.

As the system approaches the equilibrium state, it becomes more unlikely that a pair of nearest neighbors selected at random will be different, that is, more tries are necessary in order to perform an interchange. Thus, after a relatively rapid early evolution it is necessary to use a large amount of computer time, especially at low temperatures, to proceed further in the simulation. This problem can be largely avoided when studying long time effects by means of an a priori classification of the spins according to their probability of interchange; the time variable is then computed in a stochastic way (Bortz et al. 1975).

The "programs" were written in Fortran Extended (FTN) Language for a CDC-6600 computer; the (Central Processor) time the machine employed in the simulations is indicated in some of the tables.

2.4. - Computation of time-dependent system properties.

The expected value of any function of the configuration at time t is obtained by taking the average over the ensemble with the initial state x_0 distributed according to the probability $P(x_0; 0)$. This means that we can obtain it by averaging over

"many" independent evolutions of our model system. We expect, however, that for functions which are "extensive" (like the energy and a "smoothed" structure function) the number of runs needed should decrease with increasing system size (for a macroscopic size system almost every run should produce typical results). The results presented here correspond to averages over eight statistically independent evolutions, unless otherwise indicated.

We define the pair correlation function $G(\underline{r}, t)$ as

$$G(\underline{r}, t) = \frac{1}{N} \sum_{\underline{r}_i} [\eta(\underline{r}_i, t) \eta(\underline{r}_i + \underline{r}, t) - \bar{\eta}^2] \quad (2.20)$$

where \underline{r} and \underline{r}_i run over the N sites and we have indicated explicitly the time dependence of $\eta(\underline{r}_i)$. Thus, the structure function is given by

$$S(\underline{k}, t) = \sum_{\underline{r}} e^{i\underline{k} \cdot \underline{r}} G(\underline{r}, t), \quad \underline{k} = (2\pi/L) \underline{\mu} \quad (2.21)$$

where

$$\underline{\mu} = (\mu_x, \mu_y, \mu_z), \quad \mu_\alpha = 0, 1, \dots, L-1, \quad \alpha = x, y, z \quad (2.22)$$

Note that from our definition,

$$\frac{1}{N} \sum_{\underline{k}} S(\underline{k}, t) = (1 - \bar{\eta}^2), \quad (2.23)$$

$$S(\underline{k} = 0, t) = 0, \quad (2.24)$$

and that corresponding to the random initial configuration present at $t = 0$,

$$S(\underline{k}, 0) = (1 - \bar{\eta}^2) \quad \text{for } \underline{k} \neq 0. \quad (2.25)$$

We also define the spherically averaged structure function

$$S(k, t) = \sum_{\underline{k}}'' S(\underline{k}, t) / \sum_{\underline{k}}'' 1 \quad (2.26)$$

where $k = (2\pi/L)\mu$, $\mu = 1, 2, \dots$, and the sum $\sum_{\underline{k}}''$ goes over all values of \underline{k} such that $(2\pi/L)\mu \leq |\underline{k}| < (2\pi/L)(\mu + 1)$. In the actual simulation in three dimensions we computed $S(\underline{k}, t)$ for \underline{k} in one octant of the reciprocal lattice up to $|\underline{k}| = 2\pi/3$, i.e. in ten shells in which there were 6, 13, 19, 39, 55, 72, 91, 114, 169 and 178 different \underline{k} values respectively (for $L = 30$).

The energy U , given by (2.9), is related simply to the value of $G(\underline{r}, t)$ for \underline{r} a nearest neighbor vector. If we denote this value of $G(\underline{r}, t)$ (averaged over the three orientations) by $\frac{1}{3} g$, we have

$$U/N = -3J(g + \bar{n}^2) = J[2N_{AB}/N - 3] = J(2u-3) \quad (2.27)$$

where N_{AB} is the number of bonds between spins of opposed orientation (A-B bonds).

A "cluster" is defined as a group of spins with "up orientation" (A-atoms) linked together by nearest-neighbor bonds on the lattice.

In the case of antiferromagnetic interactions ($J < 0$) we also computed, in addition to the quantities above, the "sublattice magnetization"

$$\sigma = (1/N) \sum_{\alpha, \beta, \gamma=1}^L (-1)^{\alpha+\beta+\gamma} n_{\alpha\beta\gamma}(t) \quad (2.28)$$

where each set of integer numbers $\alpha, \beta, \gamma (= 1, 2, \dots, L)$ specifies a given lattice site ($n_{\alpha\beta\gamma} \equiv n(r_i)$). The quantity (2.28) corresponds to the so-called "long-range-order parameter", (1.3). The usual "short-range order parameter" corresponds to the pair-correlation function over nearest-neighbors, g , and is related simply to the energy of the system by eq. (2.27).

III. THEORY

3.1. - Classical Theory.

The production of alloys with desirable properties by rapid cooling of a molten mixture has a very long history but systematic attempts to understand the nature of the processes involved are relatively recent. The concept of spinodal (but not the term which is probably due to Cahn) as the limit of metastability in a fluid solution goes back to Gibbs and van der Waals. On the temperature-composition section of the phase diagram (Fig. 2.1) it is generally believed to correspond to a line that can be characterized by the condition $(\partial^2 f / \partial \eta^2)_{T,P} = 0$, where f is some "Gibbs free-energy density" and η , as before, the composition of the system. The regions in which that derivative is negative correspond to unstable states (Fig. 3.1.). The division of the phase diagram in this case is more subtle and very far from being as rigorously justified as the one implied by the coexistence curve. A spatially uniform solution with a concentration and temperature corresponding to a point in the region between the coexistence and spinodal curves is metastable with respect to small fluctuations. Some thermal activation energy is then required for the appearance of two stable phases; only a nucleation and growth mechanism can account for the separation in this case. On the contrary, if the solution is held at a temperature inside the spinodal curve, it is unstable and spontaneously separates into

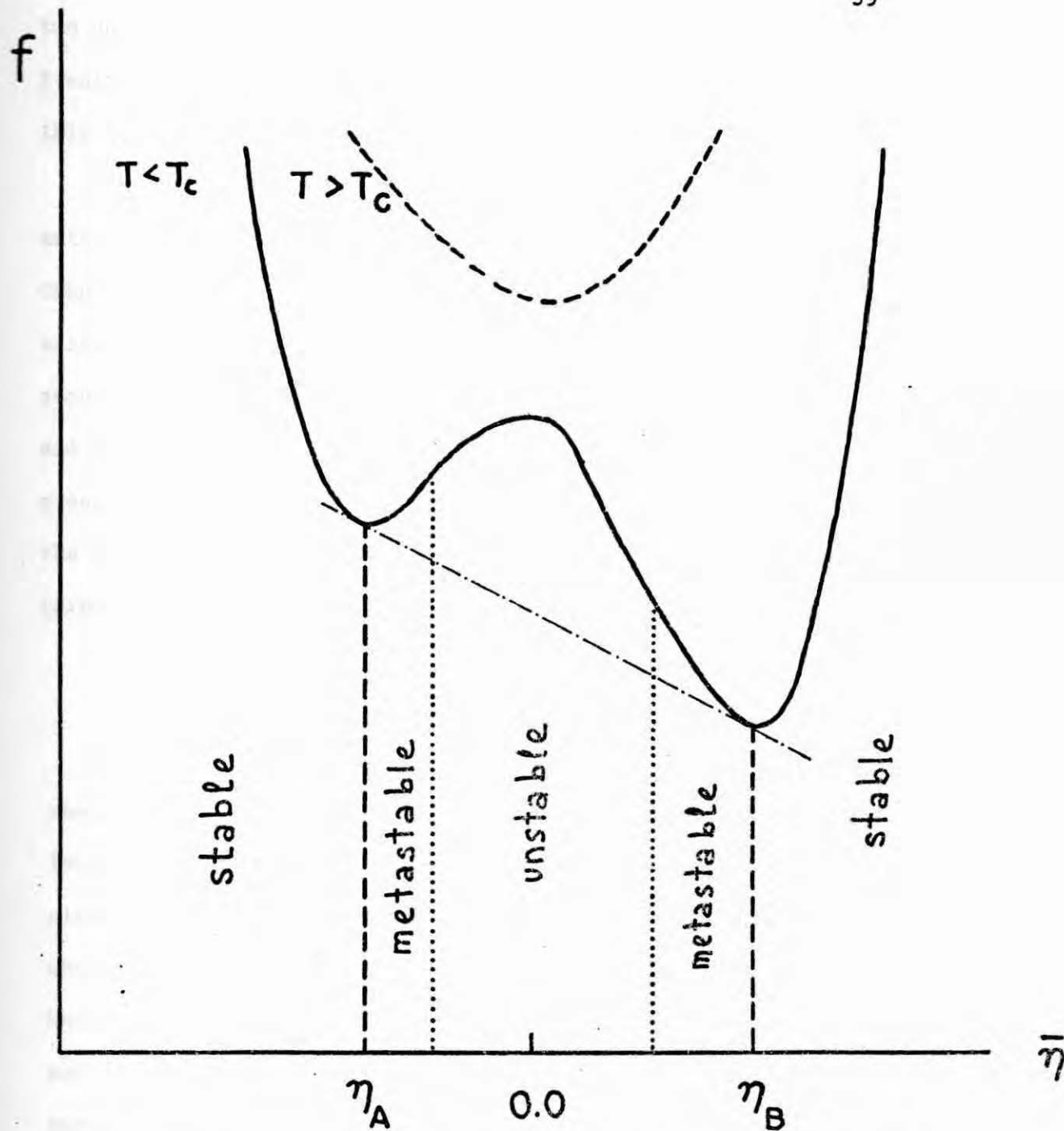


Fig. 3.1 Schematic expected form for the free-energy of an AB-alloy below and above the critical temperature in clustering processes.

two phases by what is called the spinodal decomposition mechanism. Eventually, also nucleation and growth is expected to occur in this region as a competing mechanism (Cahn 1962).

The great metallurgical interest of the problem led to the extension of the spinodal concept to solid systems (Hillert 1956, Cahn 1961) and to the development during the last decade of an essentially phenomenological theory which is apparently quite successful (Hilliard 1970). Hillert (1961), Cahn (1961, 1962) and others (see Cahn 1968 for further references) supposed the process entirely governed by diffusion. First they assumed that the system can be described by a free-energy (functional) of the form

$$F\{\eta\} = \int d\mathbf{r} [f(\eta) + \frac{1}{2} K (\nabla \eta)^2] \quad (3.1)$$

where $K = \epsilon \xi^2$, with ϵ an energy density and ξ a characteristic length for the variations of η . An elastic energy term can be included in (3.1), in order to account for strains in the system when atoms of different nature are interchanged (Cahn 1962, Christian 1969), but it is not essential and will be omitted in our discussion. What is essential in (3.1) is the gradient energy term that gives rise to the necessary surface tension; as expressed in (3.1) it can be interpreted as the first term of an expansion for the additional free-energy due to gradients in composition (Cahn and Hilliard 1959). The free-energy density f is expected to have two distinct minima at temperatures below T_c ,

corresponding to the two stable phases (Fig. 3.1.). Assuming a symmetry about $\bar{\eta} = 0$, Cahn and Hilliard(1958) suggested the form

$$f = -\alpha\eta^2 + \beta\eta^4, \quad (3.2)$$

with $\alpha \sim (1 - T/T_c)^a$ and β a positive constant. This form has been generally accepted as a reasonable approximation. In Fig. 1.1 f is plotted as a function of η . Also plotted is the spinodal line corresponding to (3.2); (which implies $\eta_s = \eta_c/\sqrt{3}$, with η_s and η_c the respective abscissas of the spinodal and co-existence curves at a given temperature). The parameters in (3.2) can also be adjusted to more realistic situations (de Fontaine 1967); the form sketched in Fig. 3.1 is believed to be more appropriate for alloys (Cahn 1966). It is important here (Langer 1971) to make the distinction between f in (3.1), where it has the meaning of a "coarse-grained" free energy density, and the true, statistical mechanical, free-energy density, (2.5), obtained from Z the partition function of the real system, which would be observed in the true equilibrium state. In fact they only are approximately equivalent at very low temperatures where atomic thermal fluctuations are negligible.

The classical kinetic analysis essentially proceeds as follows. The driving force that causes the interdiffusion of the atomic species is taken to be $-\delta F/\delta\eta(x)$, which is interpreted as the local chemical potential, so that there is a current density

$$\underline{j}(\underline{r}, t) = -M \nabla [\delta F / \delta \eta(\underline{r}, t)], \quad (3.3)$$

where M is a phenomenological mobility (temperature-dependent in actual systems). Equation (3.3) only differs from Fick's first law in the interpretation of the force. It follows then from the continuity equation that,

$$\frac{\partial \eta}{\partial t} = -\nabla \cdot \underline{j} = M \nabla^2 \left[\frac{\partial f}{\partial \eta} - K \nabla^2 \bar{\eta} \right]. \quad (3.4)$$

Eq. (3.4) is due to Cahn and Hilliard.

The introduction in this equation of the fluctuation variable

$$\zeta(\underline{r}, t) = \eta(\underline{r}, t) - \bar{\eta} \quad (3.5)$$

to describe what were supposed small deviations from the average composition of the system, $\bar{\eta}$, and the expansion of f around $\bar{\eta}$, leads to a linear equation,

$$\frac{\partial \zeta}{\partial t} = M \nabla^2 \left[\left(\frac{\partial^2 f}{\partial \eta^2} \right)_{\eta=\bar{\eta}} - K \nabla^2 \right] \zeta, \quad (3.6)$$

when only the first term in that expansion is kept. This is the Cahn's equation (Cahn 1961), which is the basis of the classical theory. In Fourier space one has

$$\frac{\partial \zeta(\underline{k}, t)}{\partial t} = R(\underline{k}) \zeta(\underline{k}, t) \quad (3.7)$$

where $R(\underline{k})$ is the amplification factor of the fluctuation given by

$$R(\underline{k}) = -Mk^2 \left[\left(\frac{\partial^2 f}{\partial \eta^2} \right)_{\eta=\bar{\eta}} + K k^2 \right] , \quad (3.8)$$

with K and M positive constants. The quantity $M(\partial^2 f / \partial \eta^2)_{\eta=\bar{\eta}}$ is identified with the chemical or diffusion constant, so that there is "negative diffusion" below the spinodal line, where that derivative is negative. In this case (3.8) will be positive for small values of k , $k < K^{-\frac{1}{2}} |(\partial^2 f / \partial \eta^2)_{\eta=\bar{\eta}}|^{\frac{1}{2}}$, and the solutions of equation (3.7), proportional to $\exp[tR(\underline{k})]$, will increase exponentially with time. The structure function $S(\underline{k}, t)$ is proportional to $\zeta(\underline{k}, t) \zeta^*(\underline{k}, t)$ so that if one multiplies the solution of (3.7) by $\zeta^*(\underline{k}, t)$ it follows that

$$\frac{\partial S(\underline{k}, t)}{\partial t} = 2 R(\underline{k}) S(\underline{k}, t) , \quad (3.9)$$

with solutions proportional to $\exp[2tR(\underline{k})]$: the structure function also increases exponentially with time for small values of k . At the value $k = k_m$,

$$k_m^2 = \frac{1}{2K} \left| \left(\frac{\partial^2 f}{\partial \eta^2} \right)_{\eta=\bar{\eta}} \right| , \quad (3.10)$$

the amplification factor (3.8) has a maximum; it vanishes at $k = k_o \equiv \sqrt{2} k_m$ and becomes negative for greater values of k . Fig. 3.2 is a schematic representation according to this picture of the variation of $R(k)$ with k for a mixture inside and outside the spinodal region. (Note that the inclusion of a strain energy term in the expression for the free-energy, (3.1), would be reflected in the expression (3.8) for $R(k)$ so that the values k_o and k_m would be slightly decreased).

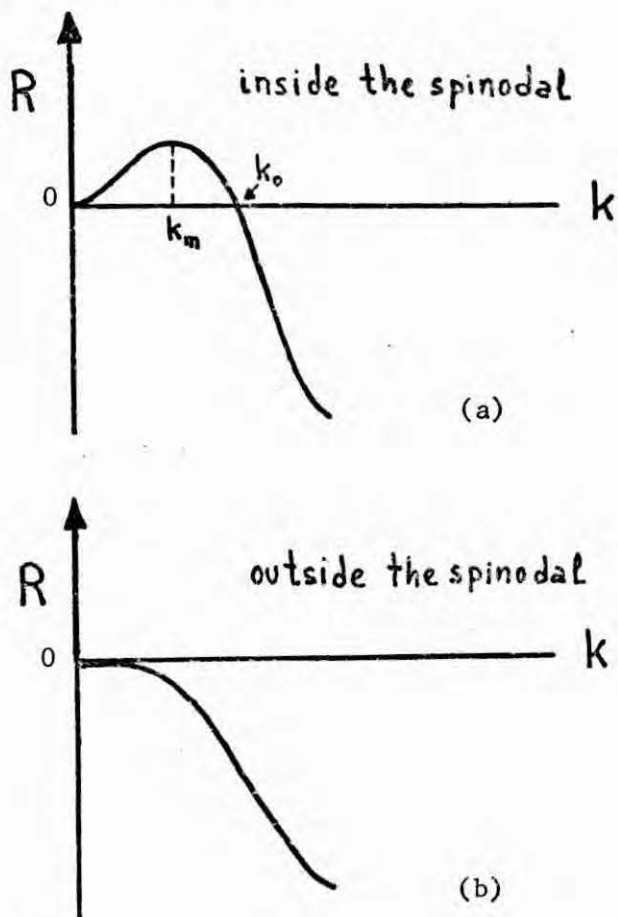


Fig. 3.2 Amplification factor $R(k)$, (3.8), inside the spinodal region (a) and in the stable or metastable regions (b).

The resulting picture implies that one should observe, after quenching from a single phase, composition modulations symmetric around the average composition of the system, that eventually would lead to a two phase structure. Looking through the microscope one should early observe a precipitate of grains with typical linear dimensions proportion to $\lambda_m = 2\pi/k_m$ in which there is an excess of one of the phases. These grains would essentially maintain their initial size during the "early" process while becoming purer in the predominant phase. Grains with characteristic linear dimensions smaller than $\lambda_o = 2\pi/k_o$ should rapidly dissolve. The scattering intensity should develop a clear maximum at k_m which would grow exponentially with time while remaining at that location. For $k > k_o$ the x-ray scattering intensity should rapidly decay to zero with time.

This basic theory has led to the experimental identification of spinodal decomposition in a number of alloys and in other different mixtures (section 1.2) and to the recognition of the importance of this process in the temporal evolution of a mixture after a rapid cooling. The available x-ray and neutron scattering studies (although the reported results are not yet very clear-cut) indicate, however, some systematic discrepancies with the theory. For instance, the theory allows via eq. (3.9) the determination of the amplification factor $R(k)$ from measurements of the scattering intensity, and eq. (3.8) predicts a linear variation of

$R(k)/k^2$ with k^2 with coefficients corresponding to some quantities of interest. In general the theoretical fit of the data grows worse with increasing values of k (Rundman 1967, Neilsen 1969, Cook and Hilliard 1969, Philofsky and Hilliard 1969). Some authors reported a definite bending for any k when plotting $R(k)/k^2$ vs. k^2 (Zarzycki and Nandin 1967, Andreev et al. 1970). This curvature was also observed by Erb and Hilliard (1970; Hilliard 1970) who attributed it to the neglect by the theory of thermal effects in the process. Other authors reported a temporal dependence of $R(k)$ (Tomozawa et al. 1970). Recent experiments in fluids have observed the collapsing of the ring of scattered light which corresponds to the maximum intensity of $S(k)$ (Huang et al. 1974).

Since the theory described above neglects nonlinear terms in the free-energy (passage from eq. (3.4) to (3.6)) its applicability, if any, is certainly restricted to the "early stages" of the process. Some aspects of this limitation have been analysed by Hillert (1961) by means of machine calculations on a one-dimensional equation derived from (3.4). In a slightly different direction, Cahn (1966) proposed starting with the equation,

$$\frac{\partial \eta}{\partial t} = D \nabla^2 \eta - 2M K \nabla^4 \eta + \frac{\partial D}{\partial \eta} (\nabla \eta)^2, \quad (3.11)$$

that contains some nonlinear terms. Expanding the three coefficients in this equation around $\bar{\eta}$ Cahn obtained a linear equation, with

more information than (3.6), that we shall not write here. The computer treatment of one-dimensional versions of that equation (de Fontaine 1967, Swanger et al. 1970) showed that the nonlinear effects were not essential during the early decomposition. In the current formulation of the theory they had the effect of limiting the exponential growth in the later stage, but they did not include the necessary corrections to account for most of the experimental discrepancies. More recent work by Langer and co-workers has shown, however, that any realistic formulation should avoid such a linearization around $\bar{\eta}$ given that we are expecting the appearance of regions with composition near η_A and η_B , which are in general very different from $\bar{\eta}$ (Fig. 1.1).

The suggestion by Erb and Hilliard was examined, on a linear approximation, by Cook (1970) who pointed out that the effect of thermal fluctuations in the system might fundamentally affect the process from the earliest stages. The formal modification in Cook's equation, which will be further considered in section 3.3, comes from the introduction in the expression for the current density, (3.3), of a random current derived from a fluctuating scalar field. It represents the counterpart to the Langevin force in Brownian motion and thus it corresponds to the interaction with the thermal reservoir in the model system described in section 2.4. While in a fluid mixture this could be of less importance, in an

alloy it decisively helps the atoms to overcome the potential barriers that prevent their migration. A one-dimensional study (Bortz 1974) that compares the predictions of a conventional diffusion equation with the evolution of a model system in which these fluctuations are included indicates their possible importance in a more accurate description of the phenomenon.

3.2. - "Ostwald ripening" Theory.

At the beginning of the last decade there was developed, on a different basis from that so far discussed, a theory for the clustering process which a mixture undergoes after a rapid cooling. Following Ostwald's earlier ideas (Lifshitz and Slyozov 1961, Wagner 1961) these studies are directly concerned with the growth of the clusters and with their size distribution. Originally the approach referred to particles dispersed in a fluid but it has been widely accepted (Ardell 1969) for alloy systems following the work of Oriani (Oriani 1964, Li and Oriani 1967).

Lifshitz and Slyozov, and also Wagner, assumed the process governed by diffusion and concluded that the distribution of cluster sizes will evolve towards a "quasi-steady-state" distribution whose dependence on A , the cluster radius, and on the time, t , has the separable form:

$$\tilde{\rho}(A, t) \simeq \rho'(t) (A/\bar{A})^2 \rho''(A/\bar{A}), \quad (3.12)$$

with \bar{A} the average cluster radius at time t , independent of the initial distribution $\tilde{\rho}(A, 0)$. These authors presented an explicit form for $\rho''(A/\bar{A})$ which is identically equal to zero for $A \geq A_c = 1.5\bar{A}$ so that no clusters greater than $1.5\bar{A}$ should exist. This theory also predicts that

$$\bar{A}^3 - \bar{A}_o^3 = \kappa t, \quad (3.13)$$

where \bar{A}_o is \bar{A} at the onset of coarsening and the coefficient κ is proportional to the diffusion constant and inversely proportional to the temperature. Wagner showed on the other hand that if one assumes a predominance of interface control in the process, the appropriate size distribution has the form

$$\tilde{\rho}(A, t) \simeq \rho'_w(t) (A/\bar{A}) \rho''_w(A/\bar{A}) \quad (3.14)$$

where $A_c = 2\bar{A}$ in this case. From this distribution one has

$$\bar{A}^2 - \bar{A}_o^2 = \kappa_w t \quad (3.15)$$

with κ_w proportional to κ in (3.13).

Since these theories permit a direct determination of the diffusion constants via the easily measured \bar{A} they have

attracted much attention.

The Lifshitz-Slyozov prediction (3.13) has been reported (Dalal and Grant 1973, Cornie et al. 1973, Flewitt 1974, Richter et al. 1974) to be essentially confirmed in a number of different alloys, typically the ones made up of nickel with other elements (Al, Ti, Si). The predicted cut-off in the cluster radius at any time turns out to be not so dramatic in experiments (Smith 1967, Ardell 1969). Wagner's law (3.15) has also been reported to hold in similar alloys (Higgins et al. 1974) and, interesting enough, Smith (1967) showed how the data from an experiment with manganese in magnesium can reasonably well fit both relations (3.13) and (3.15) (Fig.3.3). In any case we are in the presence of definitely slower time-power laws for the coarsening process than the ones predicted by Cahn and Hilliard. Langer (1971) has shown that the relation (3.13) can be consistent with a theory including thermal fluctuations, and Binder and Stauffer (1974) suggest that this 1/3 law might be quantitatively characteristic of spinodal decomposition in binary liquid mixtures rather than in alloys, what seems to be confirmed by some recent experiment (Huang et al. 1975).

3.3. - Modern Formulations.

The identification of the physical steps in the phenomenon is at the present time a difficult matter by means of experiments in real materials and some effort has therefore been directed toward computer simulations in model systems. In this direction are the works by Bortz (1971) on a one-dimensional

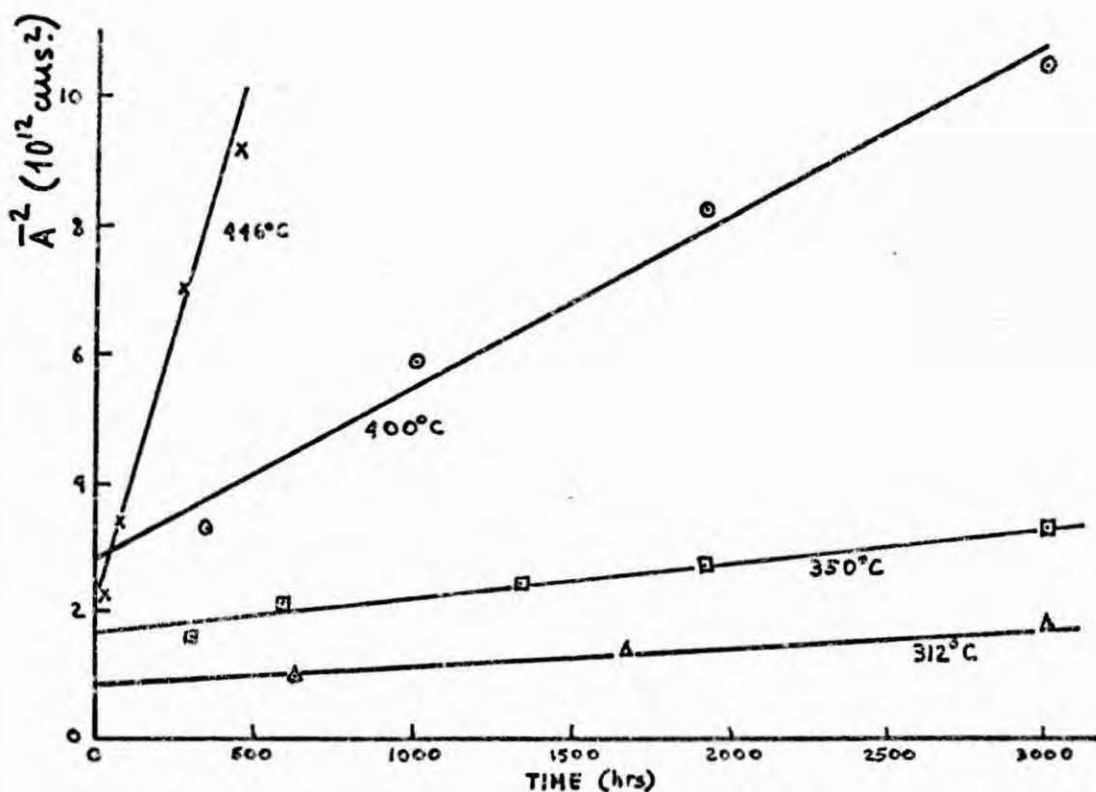
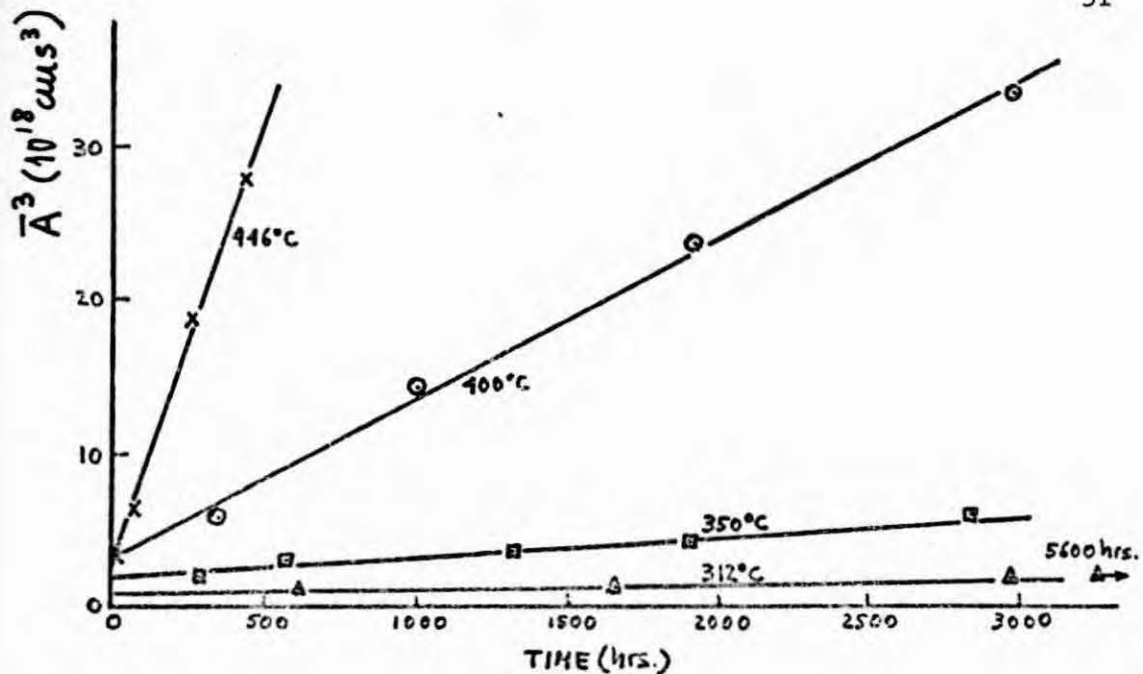


Fig. 3.3 The same data, from the observation through the electronic microscope of a quenched magnesium-manganese alloy (Smith 1967), can be used to verify both a $t^{1/3}$ and a $t^{1/2}$ law. A similar ambiguity in this kind of experiments follows from a paper by Speich and Oriani (1965).

model, by Shendelman and O'Toole (1968), Flinn (1974), Binder (1974), Bortz, et al. (1974), and Rao et al. (1975) in two dimensions, and by Marro et al. (1975) in three dimensions that have led to recent modifications of the theory, particularly those due to Langer and Binder and Stauffer. In particular the last analytic computations by Langer et al. (1975) produce an excellent agreement with the results we report here.

Langer and coworkers (Langer 1971, Langer and Bar-on 1973, Langer 1973) still assume a Ginzburg-Landau free-energy, F , (3.1), for the system, but they present a much more elaborate formulation for the phenomenon based on the importance of both the thermal fluctuations and the non-linear effects. The fluctuations are accounted for by assuming that the atomic migration is driven by interaction with a phonon reservoir, just in the same sense as in the model of our simulations. The system then evolves according to a master equation of the form (2.14). Defining the distribution-functional $\rho(\{\eta\})$ (the counterpart of our ensemble distribution) on the space of functions $\eta(\underline{r})$ where \underline{r} specifies a small region in the system, the theory transforms that master equation in the continuum limit to the form

$$\frac{\partial \rho(\{\eta\})}{\partial t} = - \int d\underline{r} \frac{\delta \varphi(\underline{r})}{\delta \eta(\underline{r})} , \quad (3.16)$$

where the probability current $\varphi(\underline{r})$ is given by

$$\varphi(\underline{r}) = M^2 \left[\frac{\delta F}{\delta \bar{\eta}} \rho + k_B T \frac{\delta \rho}{\delta \bar{\eta}} \right]. \quad (3.17)$$

Now, taking the first moment in (3.16) with (3.17) one formally recovers almost exactly the non-linear equation (3.4) of Cahn and Hilliard. The difference is obvious; here the equation will refer to the average of $\bar{\eta}(\underline{r}, t)$ in some region, that only will coincide with the point function of the classical theory if ρ is a sharply peaked function of the $\bar{\eta}$'s, which usually is not the case.

Alternatively, multiplying eq. (3.16) by $[\bar{\eta}(\underline{r}, t) - \bar{\eta}] [\bar{\eta}(\underline{r}', t) - \bar{\eta}]$ and integrating over the space of functions $\bar{\eta}$ one gets in the Fourier space, with the same notation as before,

$$\frac{\partial S(k, t)}{\partial t} = -2Mk^2 [Kk^2 S(k, t) + \Omega(k, t) - k_B T]. \quad (3.18)$$

Here $\Omega(k, t)$ has the explicit form

$$\Omega(k, t) = \sum_{n=2}^{\infty} \frac{1}{(n-1)!} \left(\frac{\partial^n f}{\partial \eta^n} \right)_{\eta=\bar{\eta}} S_n(k, t), \quad (3.19)$$

where f was introduced in (3.1) and

$$S_n(k, t) = \int d\underline{r} e^{i\underline{k} \cdot \underline{r}} \langle [\bar{\eta}(\underline{r} + \underline{r}', t) - \bar{\eta}]^n [\bar{\eta}(\underline{r}', t) - \bar{\eta}] \rangle \quad (3.20)$$

with $S_2(\underline{k}, t) \equiv S(\underline{k}, t)$ a semi-microscopic structure function.

The non-closed form of equation (3.18) makes it necessary to introduce some approximation in order to proceed to its analysis. As a matter of fact, it can be seen in that equation what are the differences between the proposed theories for all practical purposes. The linearized theories formally follow from eq. (3.18) when one only considers the first term in (3.19). In this case we have

$$\frac{\partial S(\underline{k}, t)}{\partial t} = 2R(k) S(\underline{k}, t) + 2M k_B T k^2, \quad (3.21)$$

with $R(k)$ given in (3.8). Cahn's linear equation, (3.9), is a particular case of this equation in the sense that we can recover it by neglecting the last term in (3.21), which appears as a consequence of the thermal fluctuations. Eq. (3.21) was first derived by Cook (1970) and one sees that it also, like Cahn's equation, predicts an unbounded growth of $S(\underline{k}, t)$. Besides, although the last term introduces some limitation when $k \gtrsim k_0$ (Fig. 3.4) in the decay of $S(\underline{k}, t)$ to zero predicted by the classical theory, Langer and Bar-on (1973) noted that the limit solution of (3.21) is not consistent with the expected form of the equilibrium structure function.

The application of standard many-body techniques leads to the approximation

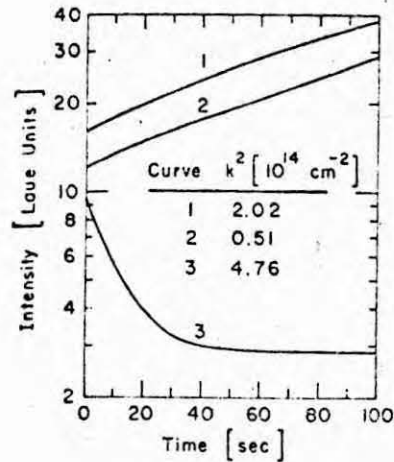


Fig. 3.4 Semi-logarithmic plot of the solution
 $S(k, t)$ of Cook's (1970) equation, (3.21),
 for parameters corresponding approximately
 to the Zn-Al alloy quenched to $\sim 0.7T_c$.

$$\Omega(k, t) = \left(\frac{\partial^2 f}{\partial \eta^2} \right)_{\eta=\bar{\eta}} + \frac{1}{2} \bar{u}(t) \left(\frac{\partial^4 f}{\partial \eta^4} \right)_{\eta=\bar{\eta}}, \quad (3.22)$$

with the "mean-field" $\bar{u}(t) = (1/8\pi^3) \int dk S(k, t)$. The resulting equation has the form (3.21) with a modified amplification factor that only differs from $R(k)$, (3.8), by the inclusion in R of the last term in (3.22). This gives a smaller and time-dependent value of k_m , more in accord with the observation, but the description is soon invalidated by non-linear effects (Langer 1973). Also, as in the case of a linearization of the generalized diffusion equation around its stationary solutions (Langer 1971), there is some trouble here in the predicted form for the equilibrium structure function. This can be avoided by introducing in the analysis of the master equation a certain cell-phase space (Wilson 1971) intermediate between the Fourier space and the position space, but the resulting picture only refers to a few values of k (Langer and Bar-on 1973). The results of this analysis, however, have provided important information regarding the phenomenon.

First it made evident the implicit high non-linearity and asymmetry, not clear at all from the classical theory, that appears when dealing with eqs. (3.18) and (3.19) (or similar equations); second, two new features arise for the expected behavior of $S(k, t)$ and both are evidenced by the existing experimental data. The structure function in this picture soon develops a peak at a value k_m sensibly smaller than the classical one, which will

slightly shift toward $k = 0$ with time; in the mean time, $S(k, t)$ decreases for values $k > k_m$. As we shall see this behavior is also present in our model.

A recent approximation (Langer et al. 1975) for the expression (3.19) provides the best current (excellent indeed) quantitative description of the phenomenon, at least as it occurs in our oversimplified model. The basis of the approximation consists in supposing that $S_n(k, t)$, (3.20), is linear in $S(k, t)$, $S_n(k, t) \approx \langle \tau^n \rangle / \langle \tau^2 \rangle S(k, t)$, so that

$$\Omega(k, t) \approx \gamma(t) S(k, t) \quad (3.23)$$

where $\gamma(t)$, see (3.19), depends both on $f(\tau)$ and on $S(k, t)$ in a highly non-linear way, but is independent of k . We shall make, later on, some detailed comparisons of these calculations with our results.

3.4. - Cluster Dynamics.

Binder and Stauffer (1974; Binder 1975) have suggested a semi-phenomenological approach that provides some definite predictions concerning some of the most characteristic parameters in the phenomenon. The theory assumes the process governed by diffusion of large clusters.

Consider a cluster in the system with a given volume V_ℓ (which, at low temperatures, is proportional to ℓ , the number of A-particles linked together). According to our model kinetics, there will be random interchanges between the A-particles in the cluster surface and the surrounding B-particles. The frequency of these interchanges can be taken, at least when the cluster is compact enough, proportional to the cluster surface area, $V_\ell^{(d-1)/d}$, and two interchanges of opposite sign (an A-particle is changed to a B-particle in some place of the surface and an A-particle is added to the cluster) will shift the center of masses of the cluster in an amount proportional to $1/V_\ell$. This suggests a random diffusion of the cluster with diffusivity of the form $D_\ell \sim (1/V_\ell)^2 \cdot V_\ell^{(d-1)/d} = V_\ell^{-(d+1)/d}$. During this diffusion the cluster may grow by coalescing with other clusters. Binder and Stauffer (1974) argued that a cluster moving the mean distance between clusters ($\sim V_\ell^{1/d}$) in the time Δt will increase its volume in an amount $\Delta V_\ell \sim V_\ell$, so that $V_\ell^{2/d} \sim D_\ell \Delta t$ and $(dV_\ell/dt) \sim V_\ell D_\ell V_\ell^{-2/d} \sim V_\ell^{-3/d}$. Thus, the volume will grow as

$$V_\ell \sim t^{d/(3+d)}, \quad T < T_c. \quad (3.24)$$

This yields a definite prediction for the behavior of the energy u as defined in (2.27). The quantity $u - u_p(T)$ (sections 2.5 & 4.2) at any time is proportional to the total surface of the clusters at that time. Assuming that the cluster distribution is strongly

peaked at some value ℓ and denoting by $n_\ell(t)$ the number of clusters with ℓ particles at time t , we have $n_\ell(t) \cdot \ell = \text{constant}$ by conservation of the number of particles. Then

$$u - u_p(T) \sim n_\ell v_\ell^{(d-1)/d} \sim v_\ell^{-1/d}. \quad (3.25)$$

Inserting (3.24),

$$u - u_p(T) \sim t^{-b''}, \quad b'' = 1/(3+d), \quad T < T_c. \quad (3.26)$$

It is interesting to note that the introduction in (3.25) of the Lifshitz-Slyozov Law, (3.13), and the Wagner Law, (3.15), give respectively the exponents $-1/3$ and $-1/2$, independent of d .

Now one can introduce some form for the structure function; for instance Binder (1975) assumes that

$$S(k, t) \simeq \frac{c_1(t)}{k^2 + k_m^2(t)} \{1 - \exp[-D_m(t) k^2 t]\}, \quad (3.27)$$

for small values of k and "low temperatures", where D_m is the diffusivity associated with clusters having the characteristic length $k_m^{-1}(t)$. The combination of this equation with previous results (Binder and Stauffer 1974) leads to the relation

$$S(k_m(t), t) \sim k_m(t)^{-d}, \quad T < T_c, \quad (3.28)$$

and

$$k_m(t) \sim t^{-a'}, \quad a' = b'' = 1/(3+d), \quad T < T_c. \quad (3.29)$$

In the neighborhood of T_c (one- or two-phase regions) the composition fluctuations are not so dramatic and the situation is quite different (Fisher 1967b, Müller-Krumbhaar and Binder 1972). In these cases the corresponding cluster diffusion constant is $D_\ell \sim \ell^{(1-\delta)/\delta}$, $T \gtrsim T_c$, where the exponent δ is introduced so that the average cluster volume is $\xi^d \sim (1 - T/T_c)^{-\beta\delta(1+1/\delta)}$, with ξ the correlation length. Then (Binder and Stauffer 1974):

$$k_m(t) \sim t^{-a'_c}, \quad a'_c = 1/(2+\gamma'), \quad T \gtrsim T_c, \quad (3.30)$$

where $\gamma' = d(\delta-1)/(\delta+1)$, and

$$u - u_p(T) \sim t^{-b''_c}, \quad b''_c = a'_c d(\alpha' - 1)/\alpha', \quad T \gtrsim T_c, \quad (3.31)$$

where $\alpha' = \beta(1+\delta)$, with β the critical exponent for the total magnetization in the Ising model, and δ previously introduced ($a'_c \simeq 0.25$, $b''_c \simeq 0.36$ for a three dimensional system; $a'_c = 4/15$, $b''_c \simeq 4/15$ in two dimensions). Also the exponent $b''_c = 2a'_c d \beta/\alpha'$ ($\simeq 0.97 a'_c$ for three dimensions)

has been suggested (Binder 1975). On the other hand it is expected that outside the critical region:

$$k_m(t) \sim t^{-a'}, \quad a' = 1/2, \quad T > T_c \quad (3.32)$$

and

$$u - u_p(T) \sim t^{-b''}, \quad b'' = da', \quad T > T_c. \quad (3.33)$$

These expected behaviors are analysed in sections 4.1 and 4.2.

3.5. - Order-Disorder Transition.

The "antiferromagnetic" coupling favors some alternate spin ordering rather than the clustering of spins with the same orientation (section 1.2), and the processes involved are of an essentially different nature. Even the kind of the transition is, in principle, different; while spinodal decomposition is associated with a first-order transition in the Ehrenfest (1933) classification, order-disorder phenomena generally correspond to a second-order transition (although the distinction is not so great in real systems; Guttman 1966, Kikuchi and van Baal 1974). The analysis of these processes in multicomponent systems, where clustering and ordering can occur simultaneously, seems to indicate (Morral and Cahn 1971, de Fontaine 1973), however, that both are essentially governed by diffusion in a very similar way. The same was concluded by Borelius (1947)

and Nyström (1950) from measurement of the activation energy. This suggests, a formulation of ordering kinetics parallel to that in the ferromagnetic case. Cook et al. (1969, de Fontaine and Cook 1971) have developed a phenomenological approach within the framework of the linear classical theory for spinodal decomposition (section 3.1). The basic equation in this case is again equivalent to eqs. (3.7) or (3.9), which predict exponential behavior for $S(k,t)$ with the amplification factor in this case given by

$$R(k) = -M w(k) \left[\left(\frac{\partial^2 f}{\partial \eta^2} \right)_{\eta=\bar{\eta}} + K w(k) \right]. \quad (3.34)$$

Here M is a phenomenological mobility (always positive),

$$w(k) = (z/a_0^2) (1 - \kappa), \quad \kappa = (1/z) \sum_i \cos(\underline{k} \cdot \underline{r}_i), \quad (3.35)$$

with z the coordination number of the lattice, and a_0 the lattice spacing. K , the coefficient of the gradient energy term in the free energy (see eq. (3.1)), is negative for ordering systems.

Now Cook et al. expand $w(k)$ in (3.34) about $k = 0$ up to the fourth order. In this way these authors retain the first gradient energy term in f that was neglected to find eq. (3.8), and which seems to play an important role in the diffusion of ordering (Cook and Hilliard 1969, Yamauchi and Hilliard 1972). Finally,

$$R(k) = -Mk^2 \left[\left(\frac{\partial^2 f}{\partial \eta^2} \right)_{\eta=\bar{\eta}} + Kk^2 - \frac{(\partial^2 f / \partial \eta^2)_{\eta=\bar{\eta}} \Sigma(r \cdot k)^4}{24 a_0^2 k^2} \right] \quad (3.36)$$

The last term in the bracket of (3.38), and the sign of K , differentiates this equation from (3.8); the dependence of $R(k)$ on k is sketched in Fig. 3.5 (Yamauchi and de Fontaine 1974). Accordingly, the structure function for a system quenched to $T < T_c$ should decay exponentially with

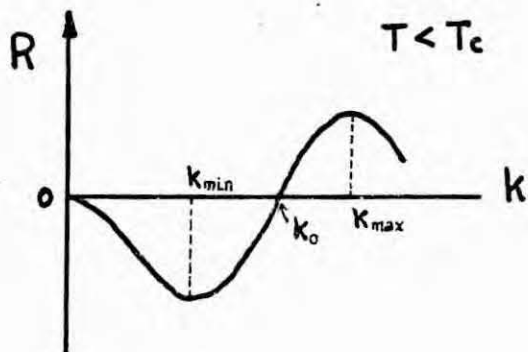
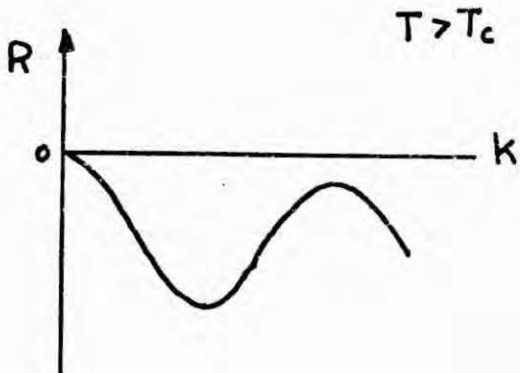


Fig. 3.5 Amplification factor, (3.36), below and above T_c for an ordering system.



time for small values of k and increase, also exponentially, for certain values of $k > k_o$ developing a sharp peak at k_m . The values of k_o and k_m can easily be obtained from eq. (3.36). For $T > T_c$ an exponential decay is expected for any value of k .

Yamauchi (1973; also Yamauchi and de Fontaine 1974) have investigated the validity of this approach starting from the master equation (2.15). Multiplying both sides of this equation by $\eta(\underline{r}, t)$ or by $[\eta(\underline{r}', t) - \bar{\eta}] [\eta(\underline{r} + \underline{r}', t) - \bar{\eta}]$ and integrating over the possible configurations (see sections 2.4 and 3.3) one can again recover the simple equations (3.7) or (3.9) in Fourier space. To this end one has to introduce several drastic simplifications. First, the intermediate formal kinetic equation is expanded about $J/k_B T = 0$, which corresponds for all practical purposes to the zeroth order approximation introduced by Bragg and Williams (1934). Further, it is assumed that there are only very small deviations of $\eta(\underline{r}, t)$ from $\bar{\eta}$ for all \underline{r} . Thus, the range of applicability of these approaches is limited to systems at very high temperatures ($T \approx \infty$) during the early stage of the evolution. Yet, it seems that there is some qualitative experimental evidence when one creates unstable composition modulations and then up-quenches the alloy into the stable region. Thus x-ray scattering on Au-Cu, 16% Cu, at 225°C (just above T_c) shows (Paulson 1972) a variation of $R(k)$ versus k that resembles the graph at the bottom of Fig. 3.5. Similarly Murakami et al.

(1975) report, from the scattering analysis of an up-quenched (to 250°C) sample of Ag-Au, that $\log [S(k,t)/S(k,0)]$ varies approximately linearly with time during the whole duration of the experiment. In other cases, however, the agreement is not so good. In Fig. 3.6 we collect some results from scattering

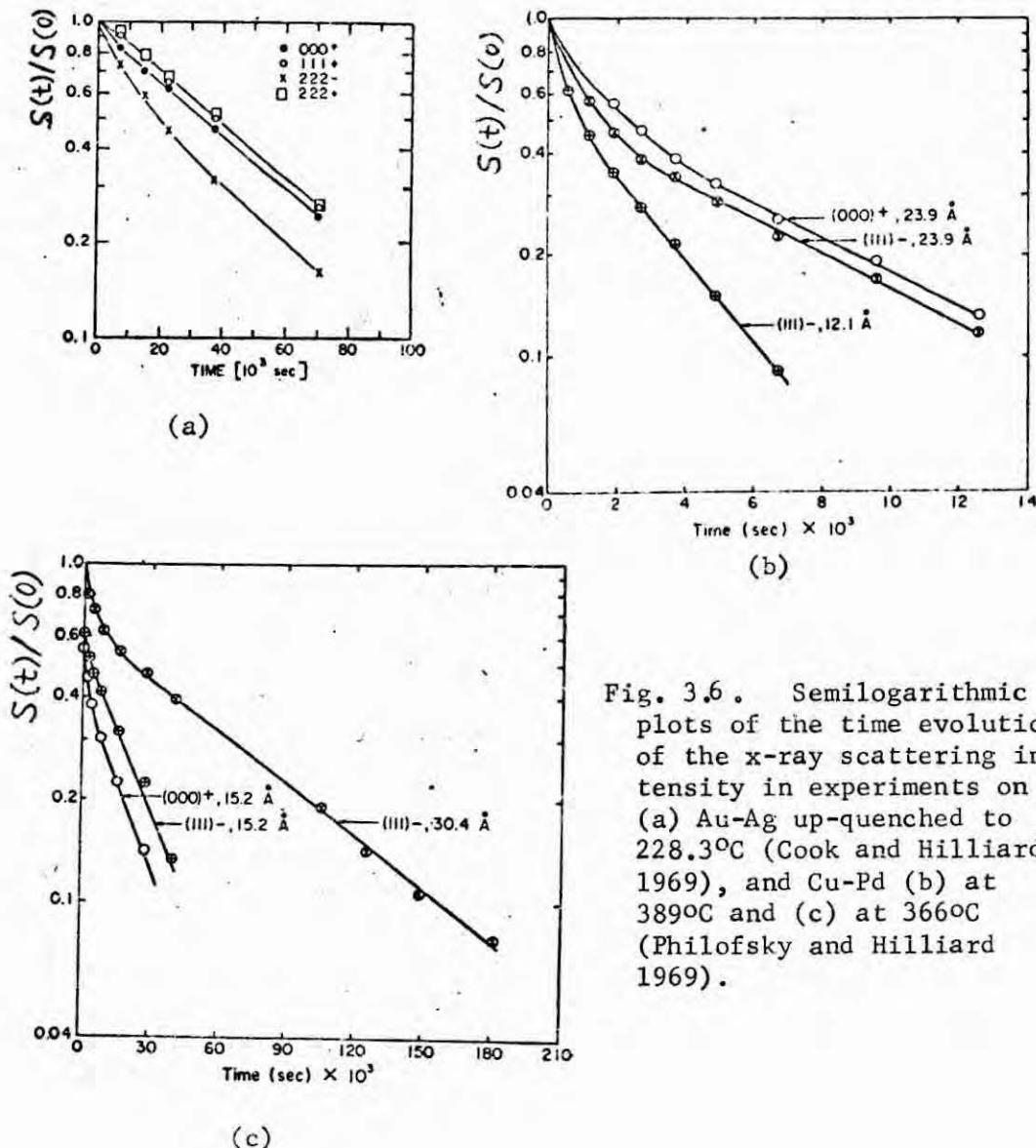


Fig. 3.6. Semilogarithmic plots of the time evolution of the x-ray scattering intensity in experiments on (a) Au-Ag up-quenched to 228.3°C (Cook and Hilliard 1969), and Cu-Pd (b) at 389°C and (c) at 366°C (Philofsky and Hilliard 1969).

experiments on the alloys Au-Ag, 32% Au, and Cu-Pd, ~ 20% Pd, which show deviations from the straight line behavior predicted by the above theories.

A kinetic equation for the LRO parameter σ , as defined in eqs. (1.3) or (2.28), can also be derived by phenomenological treatments (Dienes 1955, Vineyard 1956) or from the master equation (2.15) (Yamauchi 1973) using the Bragg-Williams' zeroth order approximation. The basic equation has the form

$$\frac{d\sigma}{dt} = K_o (1 - \bar{\eta}^2) (1 - \sigma)^2 - K_D [(1 + \sigma)^2 - \bar{\eta}^2 (1 - \sigma)^2] \quad (3.37)$$

The solution of this equation corresponding to a BCC lattice, $\bar{\eta} = 0$, is shown in Fig. 3.7 for the case (Dienes 1955):

$K_o = v' \exp(-V'/k_B T)$, $K_D = v' \exp[(V' + U'\sigma)/k_B T]$, where v' , V' and U' are thermodynamic parameters of the system (Yamauchi and

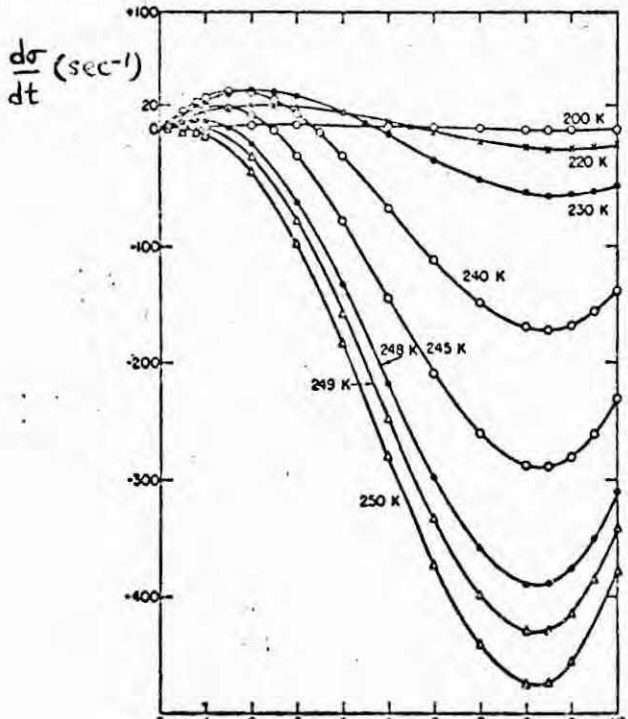


Fig. 3.7 Solution of eq. (3.37) for an AB-alloy with a BCC structure quenched to various temperatures ($T_c = 250^\circ\text{K}$) (Dienes 1955).

de Fontaine 1974).

A striking peculiarity of ordering kinetics, whose actual relevance has not yet been clearly established (Sato 1970), concerns the existence of two differentiated stages in the approach of the system to equilibrium. Lord (1953) presented some evidence, Figs. 3.8-3.9, based on the analysis of Young's modulus on the alloy Cu₃ Au quenched from 414.2°C to various temperatures T < T_c. A qualitatively similar effect has been reported in a number of

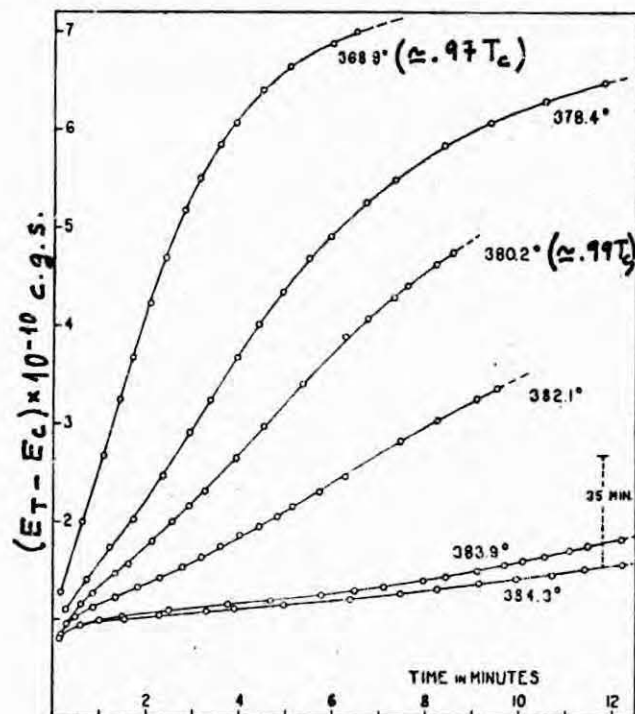


Fig. 3.8 Variation of Young's modulus, E_T, with time after quenching a sample of Cu₃^T Au to various temperatures (Lord 1953). E_c is the value of E_T immediately before the quench.

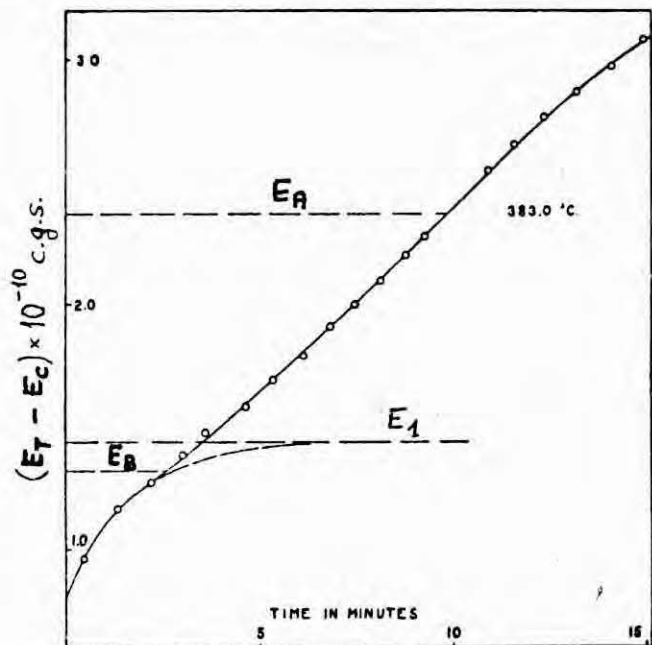


Fig. 3.9 The variation of Young's modulus, as in Fig. 3.8, showing the separation of the stages (Lord 1953). E_A and E_B correspond to the inflection points, and the initial stage (including the extrapolated dashed line) is fitted by the formula $(E_1 - E_T) = (E_1 - E_C)(1 - e^{-t/\tau})$, with τ the associated relaxation time.

different alloys (Kaya et al. 1943, Weisberg and Quimby 1963).

Although there is no adequate theory, (Jones and Sykes 1938, Sato 1970) the first "fast" stage might be associated with the development of short-range order throughout the system by means of normal atomic interdiffusion. After a relatively short time "out-of-step" ordered domains ("antiphase domains") would appear in the system. These domains are supposed to be highly ordered,

but in the opposite way as are their neighbors (as was shown in Fig. 1.3). Once the system presents such a structure, which is sometimes evidenced by electron micrography (Marcinkowski 1963, Stoloff and Davies 1966), there is a much slower approach to equilibrium. This stage is then associated with the coalescence of the antiphase domains: certain domains are absorbed by others and the excess atoms diffuse along the domain boundaries.

The theories above do not account for this peculiar effect, although eq. (3.37) can be shown to be consistent (Yamauchi and de Fontaine 1974) with the critical slowing down (divergence of the relaxation time when the critical temperature is approached from below) observed by Lord (1953). Finally we shall mention that a modification of the linear theory by Bragg and Williams (1935) and Dienes (1955) to include non-linear terms in $(\sigma - \sigma_e)$, where σ_e is the equilibrium value of the LRO parameter at the considered temperature, leads to (Nowick and Weisenberg 1958):

$$\sigma = 1 + (1-\sigma_e) [\gamma - (1-\gamma)\mu(t)]. \quad (3.38)$$

Here γ stands for a thermodynamic parameter which vanishes as the temperature approaches the absolute zero, and

$$\mu(t) = \coth(\gamma't + c), \quad (3.39)$$

with γ' also a thermodynamic parameter and c an integration constant, when eq. (3.38) refers to a sample quenched below T_c . This equation was shown to fit well some data from the evolution of up-quenched states when $\mu(t) = \tanh(\alpha' t + c)$ is used instead of eq. (3.39).

IV. RESULTS

4.1. - Structure function

We report first the results of our observations of the time evolution of $S(k, t)$ after quenching the system at two different concentrations to various temperatures. For $\bar{\eta} = 0$ ($\bar{n}_A = \bar{n}_B = 1/2$) the system was quenched to temperatures $T/T_c = 0.591, 0.780, 0.887, 1.068$ and 1.501 . The three lower temperatures are in the two phase region of the phase diagram, the spinodal region, while $T/T_c = 1.1$ and 1.5 are in the one phase region; see Fig. 2.1. For $\bar{\eta} = -0.6$ ($\bar{n}_A = 0.2, \bar{n}_B = 0.8$) the system was quenched to temperatures $T/T_c = 0.591, 0.887$ and 1.068 . The two lower temperatures are in the two phase region of the phase diagram but, according to the spinodal line drawn in Fig. 2.1, they are outside of the spinodal region. As we shall see, however, the evolution of the system at $T = 0.6 T_c$ in this case is very similar to the evolution at the same temperature for $\bar{\eta} = 0$. At $T = 0.9 T_c$ and $\bar{\eta} = -0.6$, on the contrary, the evolution is qualitatively quite different from the one at the same temperature for $\bar{\eta} = 0$, and resembles more the cases $T = 1.1 T_c, \bar{\eta} = -0.6$ and $T = 1.1 T_c, \bar{\eta} = 0$. The last two points of the phase diagram are sufficiently close to the coexistence curve so that significant "local ordering", which for short times looks similar in some sense to coarsening, may be expected.

All our results for the different reported quantities are averages over eight independent runs which appeared sufficient to wash out most fluctuations. In the case of the energy, the typical r.m.s. fluctuations between the eight runs, $[\sum_{i=1}^8 (\bar{u}(t) - u_i(t))^2 / 8]^{1/2}$, with $\bar{u}(t)$ the value reported here for each time and $u_i(t)$ the corresponding value for each run, are approximately 0.5% - 2%. The corresponding typical r.m.s. fluctuations for $S(k, t)$ (whose average values for each time and for each value of $\mu = Lk/2\pi$ are given in Tables A.1 - A.8) are approximately 5% - 15% but, for the latest time and for values of k in the neighborhood of the maximum of $S(k, t)$ (where the largest uncertainty is), the r.m.s. fluctuations are sometimes as large as 50%. The data reported were collected at initially assigned intervals of a certain number of (actual) exchanges. The intervals were increased as time progressed and the evolution slowed down.

The spherically averaged structure function is plotted in Figs. 1 - 8 of this chapter as a function of k for different values of t after quenching to the temperatures mentioned earlier. An interesting result (also reported in the two dimensional study; Bortz et al. 1974, Rao et al. 1975) is the shift of the peak of $S(k, t)$ to smaller values of k as time passes. The shift is very rapid at early times continuing more slowly at late times. As the peak shifts from large k to small k , it grows considerably. The growth and the

shift of the peak (in disagreement with the classical theory) is similar to what is reported by experimentalists on some occasions (section 4.7) and agrees fairly well with the solution of eq. (3.18) with the approximation (3.23). One outstanding difference in qualitative behavior at different temperatures and compositions can be seen in Figs. 1 - 8. In the one-phase region, and for $T = 0.9 T_c$ and $\bar{\eta} = -0.6$, $S(k,t)$ initially grows rapidly for large k , then quickly decays to its apparent equilibrium value. This shows up as the common tail of all the curves in Figs. 4, 5, 7 and 8. In Figs. 1 - 3 and 6, however, the tail as well as the peak is changing, thus in what seems to be the spinodal region, $S(k,t)$ continues to change at large k , even at late times. These "crossovers" in the spinodal region are consistent with the approximations (3.22) and (3.23) at $\bar{\eta} = 0$. Cook's equation, (3.21), however, predicts a common tail in that region, and is not supported by these results.

The point $T = 0.6 T_c$, $\bar{\eta} = -0.6$ is sufficiently close to the spinodal line drawn in Fig. 2.1 so that the behavior in that case should be very similar to the one predicted for points lying on that line. According to the linearized classical theory we would have $k_m = 0$ and no decomposition at all. Langer et al. (1975) predict a broad but well-defined peak for $S(k,t)$, with considerably less intensity than in the case of the spinodal region, and a common tail for $S(k,t)$ (Fig. 9). The computer solution of the one-

dimensional diffusion equation with parameters corresponding to the Al-Zn alloy, 20% Zn, (de Fontaine 1967) also presents a similar behavior. The observed $S(k, t)$ in Fig. 6 is similar to that shown in Fig. 4 (note our normalization (2.23)) and there is a cross-over in the tail as in the case $\tilde{\eta} = 0$, very similar to what is observed in the x-ray scattering spectra from Al-Zn, 22% Zn (Fig. 96). Langer's calculation, Fig. 9, more resembles our Fig. 7. Fig. 8. bis and Fig. 31 bis corresponds to a $50 \times 50 \times 50$ lattice at $T = 0.6T_c$ and $\tilde{\eta} = -0.75$. Although the cross-over effect is less pronounced here than in Figs. 1 and 6, the maximum intensity at, say $t = 1000$ is comparable to the one at the same time in Fig. 6. This fact may indicate, as also suggests a dynamical definition of spinodal (Binder and Müller-Krumbhaar 1974), that the spinodal curve is much closer to the coexistence curve than is shown in Fig. 2.1.

We have also investigated the shape of $S(k, t)$ for $k > k_m$, the location of the peak, by fitting it to the formula

$$S(k, t) = c_1(t)/[k^2 + c_2(t)] \quad (4.1)$$

This is plotted in Figs. 10-11 for the latest times. For $\tilde{\eta} = 0$ at $T = 1.1T_c$ and $T = 1.5T_c$, and for $\tilde{\eta} = -0.6$ at $T = 1.1T_c$ and, perhaps, $T = 0.9T_c$, c_1 and c_2 become time independent very early while for the other cases the c 's definitely change with time.

(see Figs. 12-15 where $1/c_1(t)$ and $c_2(t)$ are plotted vs. time).

Note that $c_2 < 0$ for $\tilde{\eta} = 0$, $T/T_c = 0.6$ and 0.8 , and for $\tilde{\eta} = -0.6$, $T/T_c = 0.6$, as one would expect in that region (Langer 1971).

The behavior (4.1) was also found in the two dimensional study for $T/T_c = 1.1$, where $c_2 \approx 0$, in agreement with the calculations of Fisher and Burford (1967) of the equilibrium $S(k)$ for the two-dimensional Ising model above T_c (see section 4.6).

In Figs. 16-31 $S(k,t)$ is plotted as a function of time for different values of k , Figs. 16-23 corresponding to the very early time behavior. It is clear from these figures that there is no time regime in which $S(k,t)$ can be said to grow exponentially with time as is predicted by the classical theory. In fact $S(k,t)$ for each value of k , has an initial growth in time, reaches a peak and decays. The time required to reach the peak increases as k decreases and the peak is never reached, during the course of the experiment, for the smallest values of k . The slope of $S(k,t)$ vs. t appears to decrease monotonically with t (for almost all values of k) until $S(k,t)$ is past its peak. As the temperature is increased, the decay after the peak is reached becomes less pronounced, and for $T = 1.1 T_c$ and $T = 1.5 T_c$, $S(k,t)$ appears to reach its maximum value for each k , beginning with the largest values of k , and remain there. This agrees with some predictions of Langer (1973). (Note that at $T = 0.9 T_c$, $\tilde{\eta} = -0.6$,

$S(k, t)$ almost follows a similar pattern). At $T = 1.5T_c$ for $\tilde{\eta} = 0$ and at $T = 1.1T_c$ for $\tilde{\eta} = -0.6$ we ran our computer simulation to values of t for which the system seems to have reached equilibrium.

Two important parameters characterizing the time evolution of $S(k, t)$ are the location of the peak $k_m(t)$ and the height of the peak $S(k_m(t), t)$. Due to the finite (small) size of our system, which leads to a wide spacing between the values of k we can measure, it is difficult to determine these parameters precisely. Using a parabolic fit for three values of k around k_m we find a reasonable fit, Figs. 32 -35, with the following formulae:

$$k_m(t) \simeq \alpha'(t + 10)^{-a'} \pm \Delta' \quad (4.2)$$

$$S(k_m(t), t) \simeq \alpha''(t + 10)^{a''} \pm \Delta'' \quad (4.3)$$

We also computed the first moment of $S(k, t)$, $\bar{k}(t) = \sum_k k \cdot S(k, t) / \sum_k S(k, t)$. This quantity is plotted in Figs. 36-37 and has the "asymptotic" behavior

$$\bar{k}(t) \simeq \alpha(t + 10)^{-a} \pm \Delta \quad (4.4)$$

The values of a , a' and a'' are listed in Table 4.1. Table 4.2 lists the values of α , α' and α'' , which, of course, only have a qualitative significance, and the values of Δ , Δ' and Δ'' , the standard errors of the estimates (4.4), (4.2) and (4.3) respectively, in percent.

	$\bar{\eta} = 0$					$\bar{\eta} = -0.6$		
$T/T_c =$	0.6	0.8	0.9	1.1	1.5	0.6	0.9	1.1
a	0.17	0.21	0.23	0.12	0.06	0.19	0.12	0.07
a'	0.21	0.25	0.25	0.22	0.25	0.20	-	-
a''	0.69	0.74	0.65	0.38	0.19	0.70	0.41	0.24

Table 4.1. Values of a , a' and a'' for different points in the phase diagram.

Figs. 4.1-4.8

Development with time of the spherical averaged structure function $S(k, t)$ vs. k at different temperatures. In each figure the increasing values of the time (in units of α^{-1} , eq. (2.19)) correspond to the different graphs from the bottom of the picture to the top ($C \equiv \bar{N}$ in all the figures.)

In every case the peak grows and shifts toward small k . Inside the two-phase region (Figs. 1-3 and 6) the intensity at a given time decreases with increasing temperature and seems independent of composition; the tail shifts toward small k producing a characteristic cross-over. In the one-phase region (Figs. 4-5 and 7-8) the intensity is much smaller and clearly depends on composition (Figs. 4 and 8); the tail is common for all the times. In these cases, the shift of the peak for the latest times, if any, is very slow. Note the similar behavior shown in Fig. 8 bis and in Figs. 6 and 1.

Figs. 8.bis and 8.ter correspond to the $50 \times 50 \times 50$ lattice.

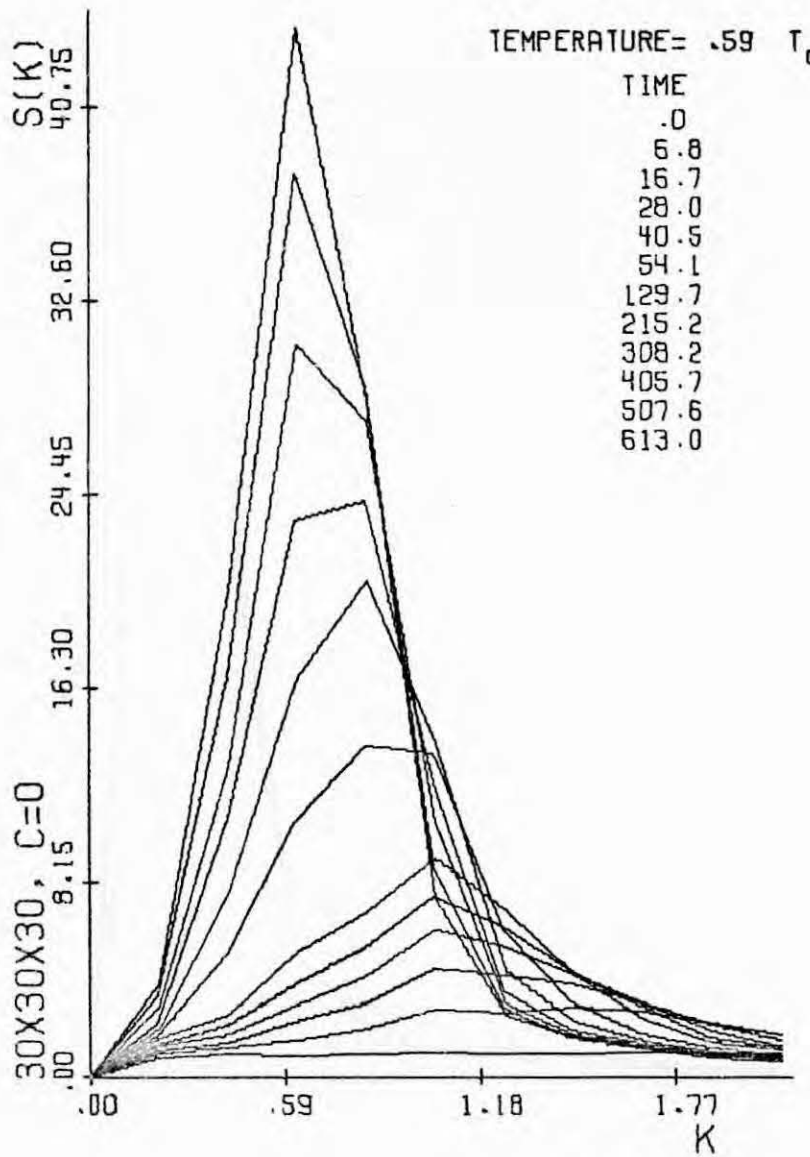


Fig. 4.1

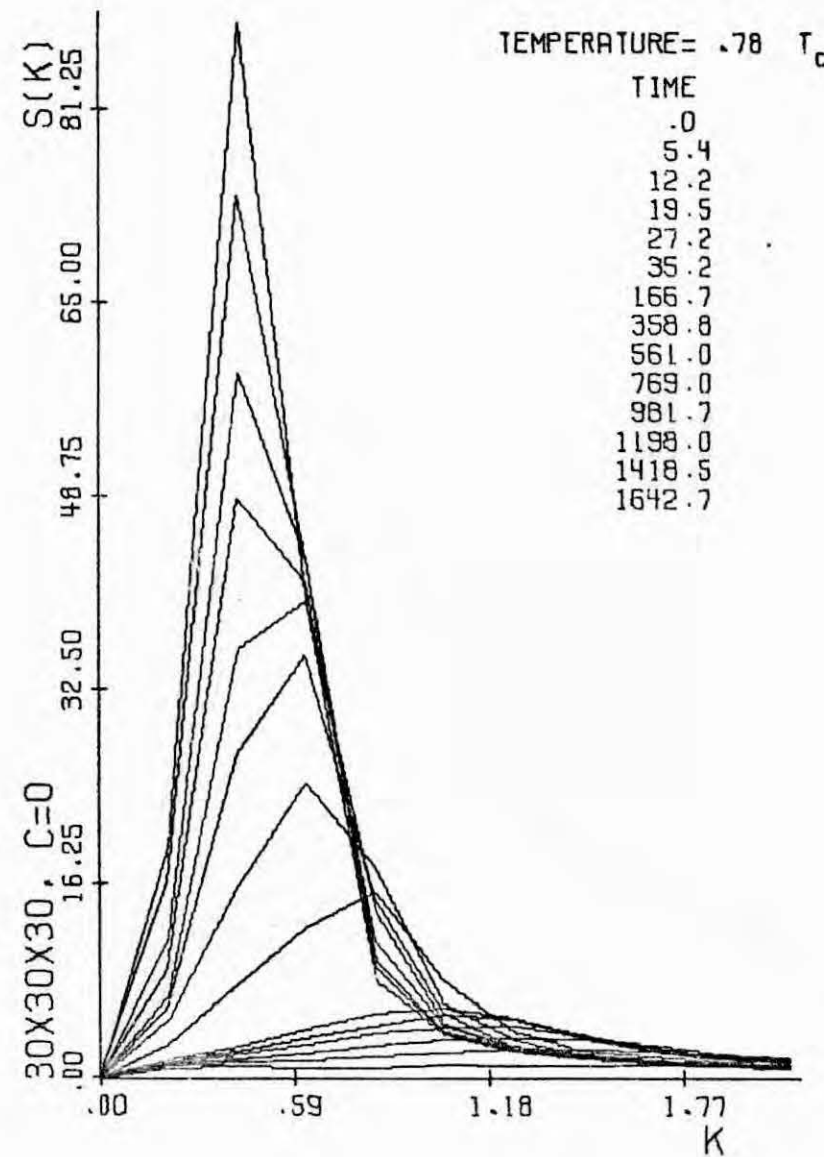


Fig. 4.2

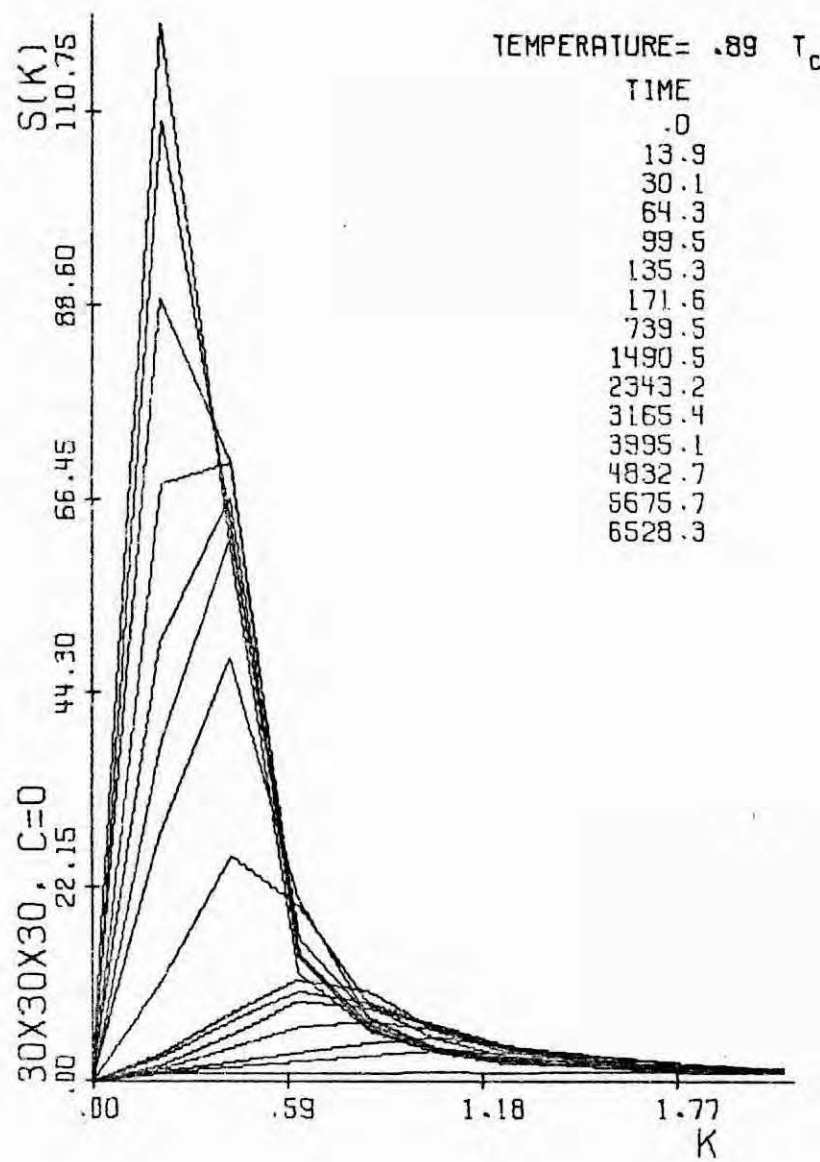


Fig. 4.3

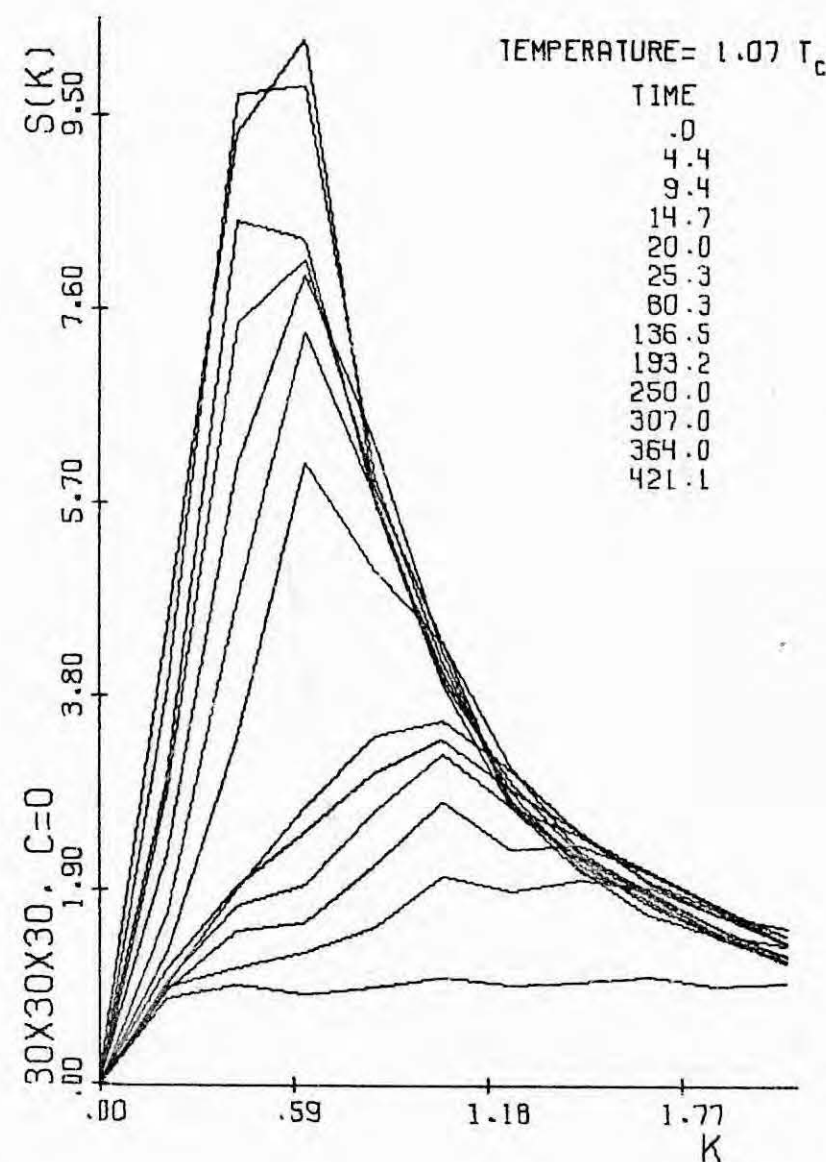


Fig. 4.4

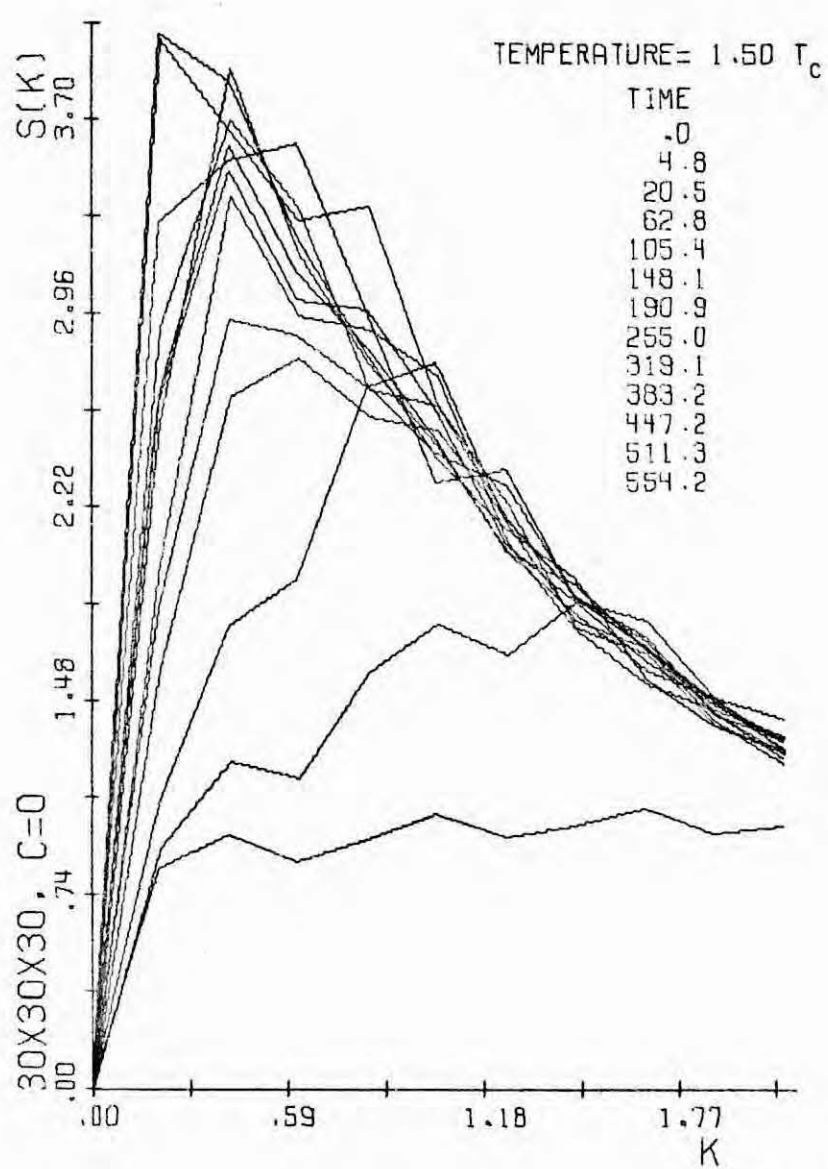


Fig. 4.5

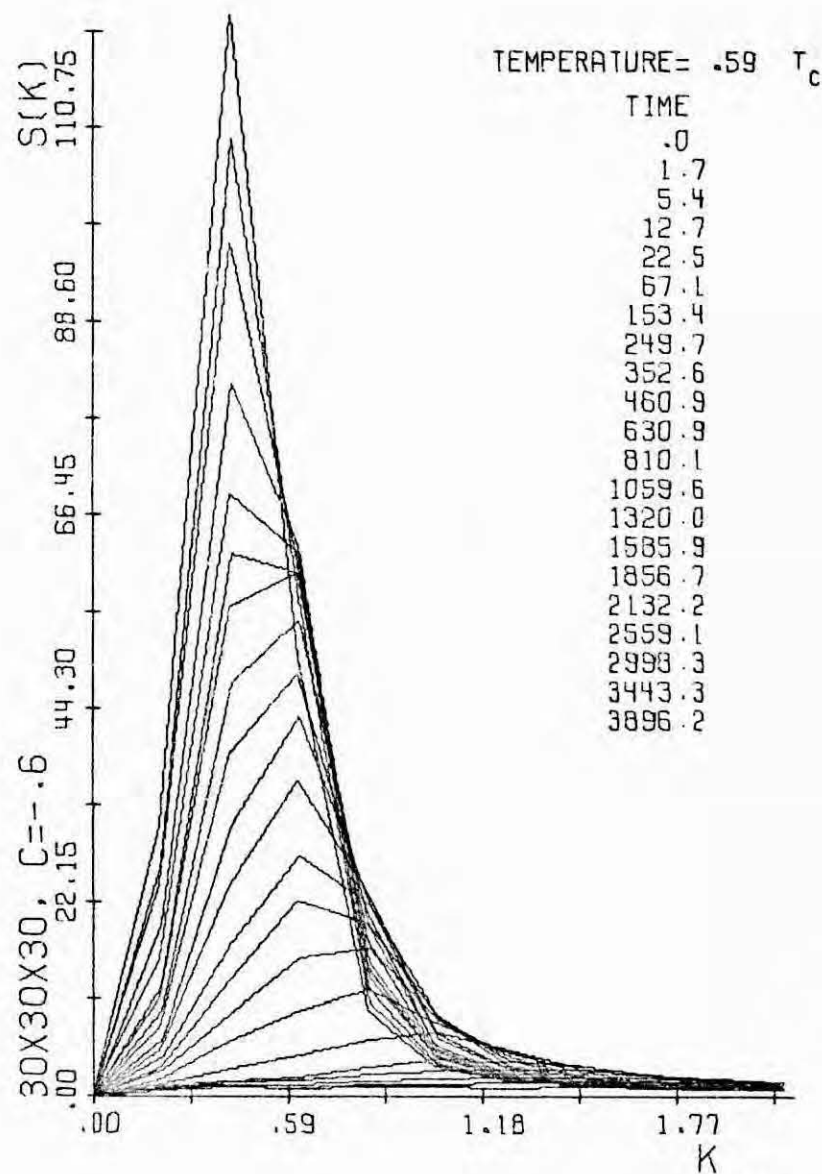


Fig. 4.6

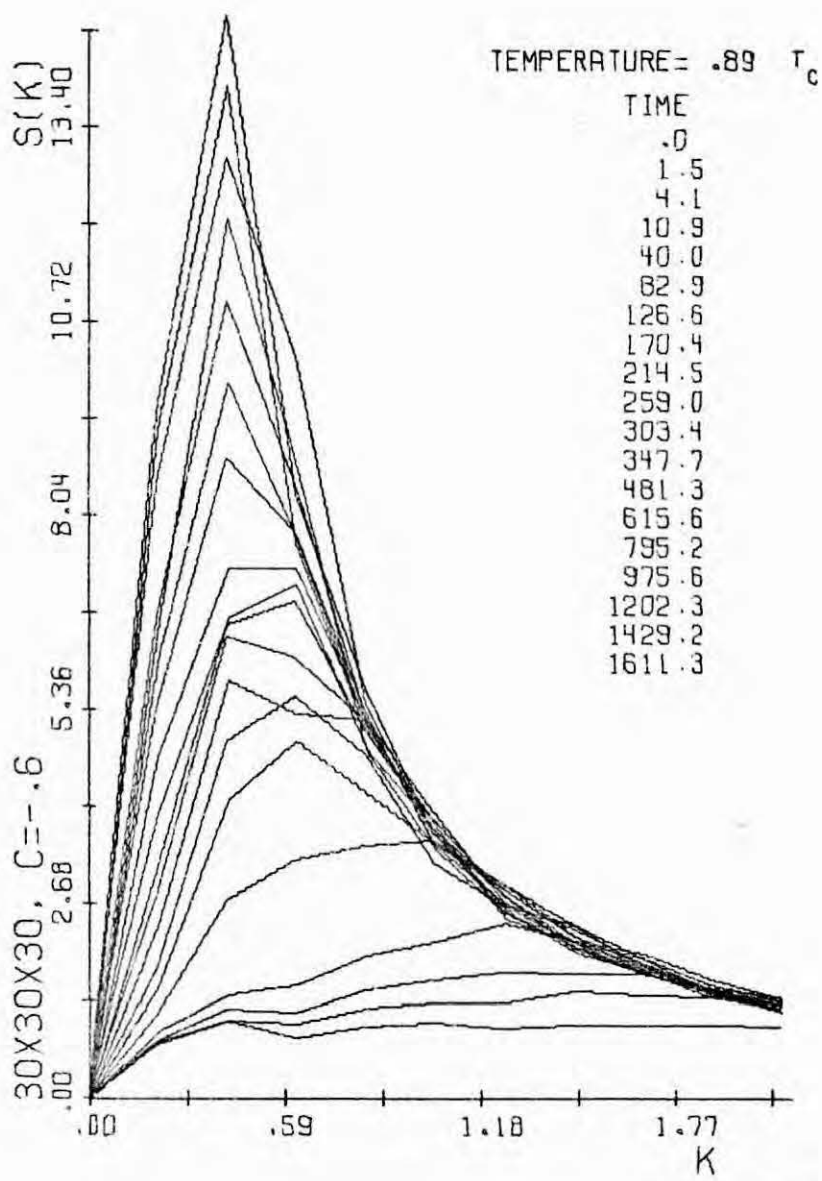


Fig. 4.7

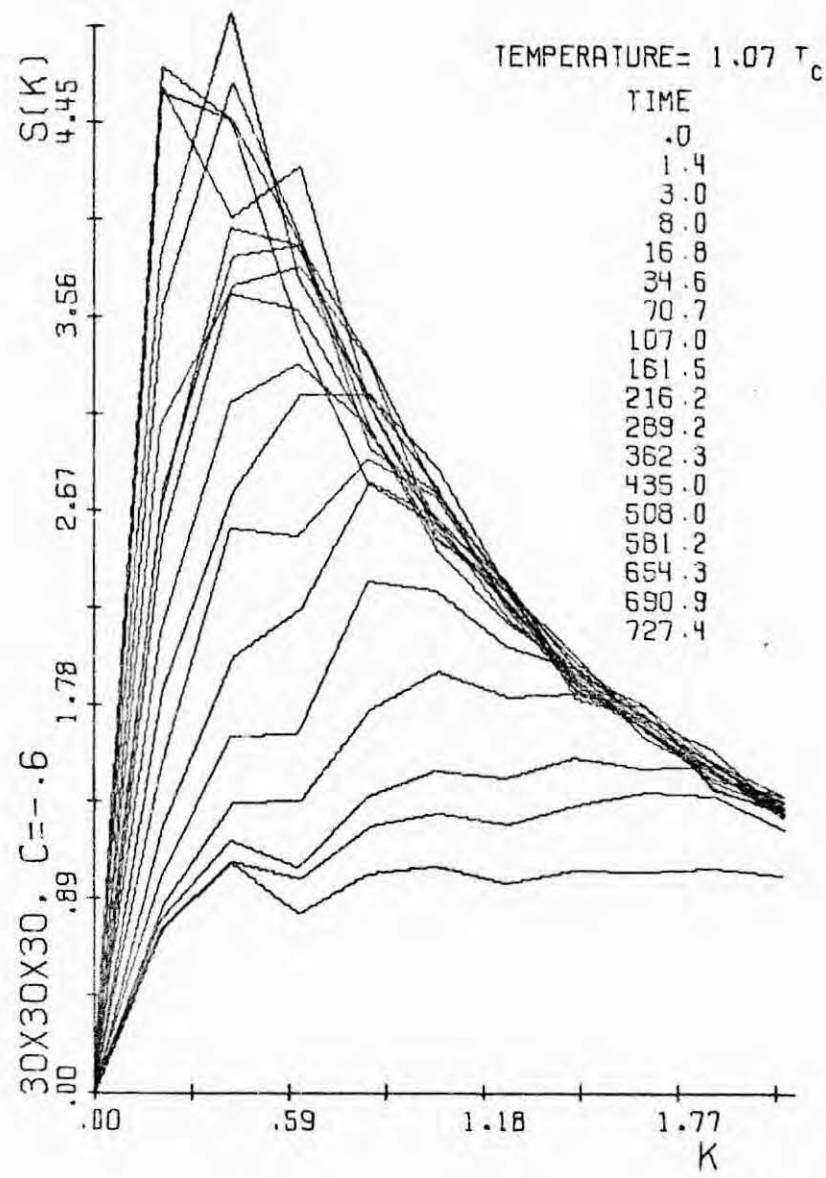
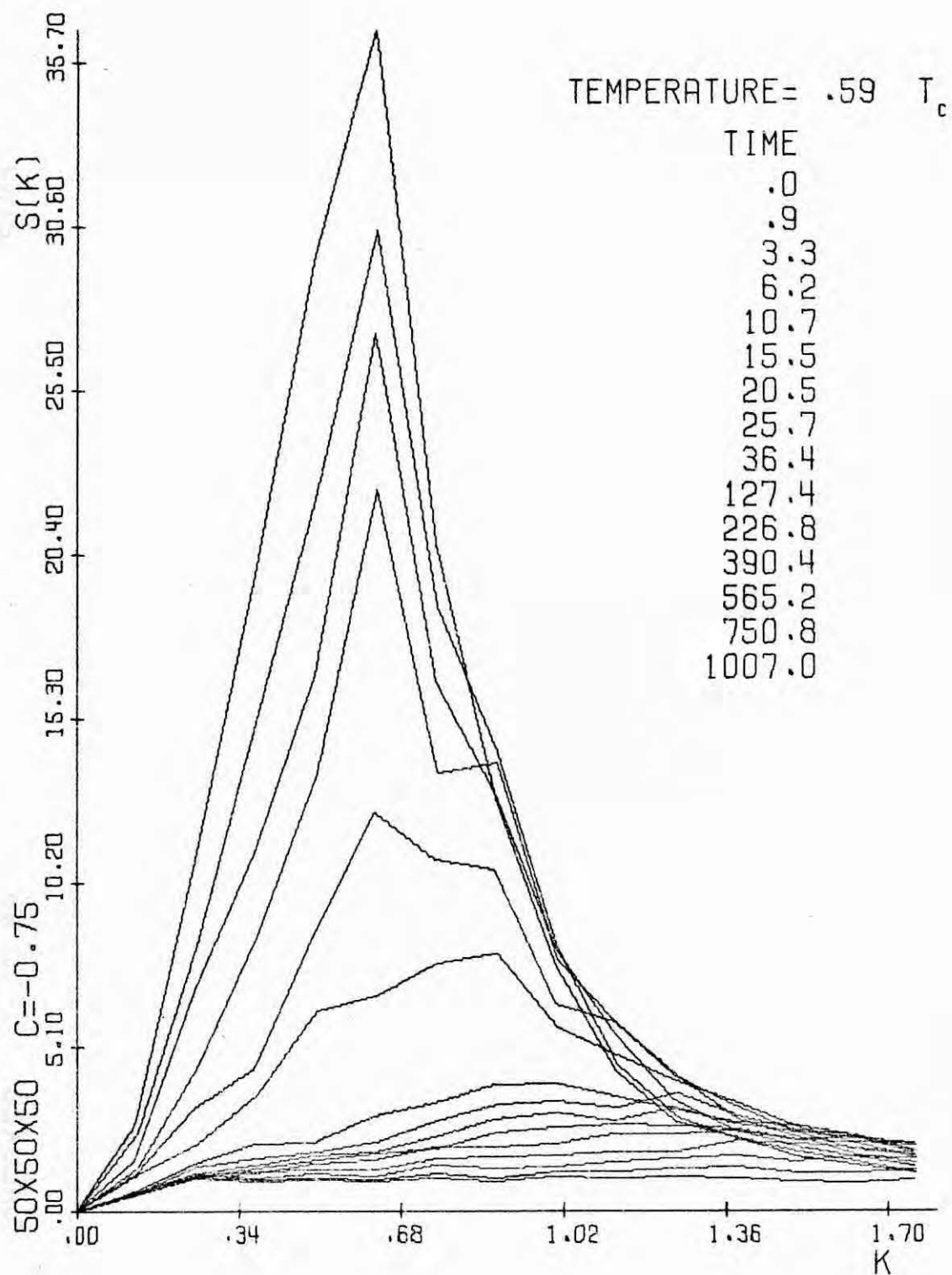


Fig. 4.8



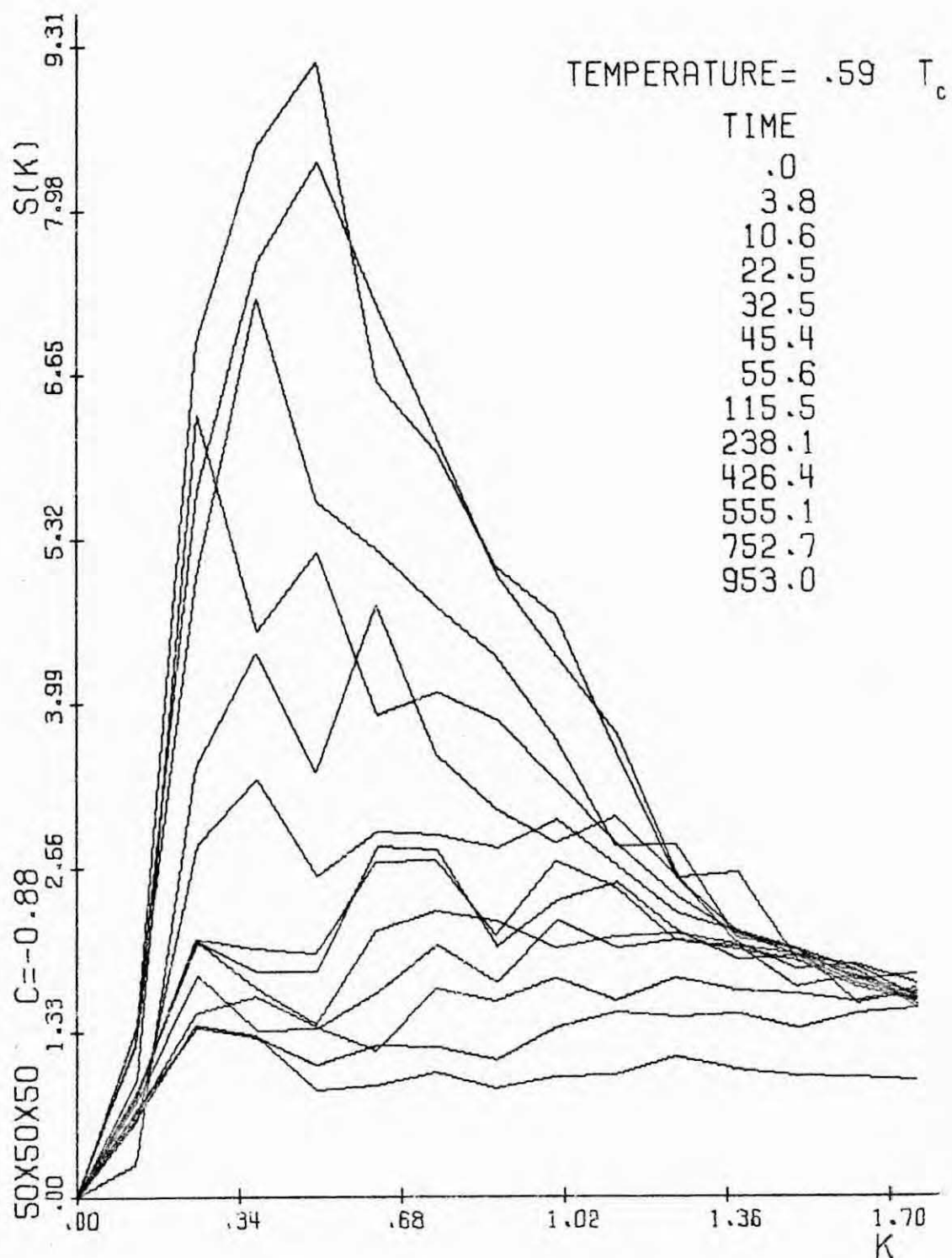


Fig. 4.8.ter

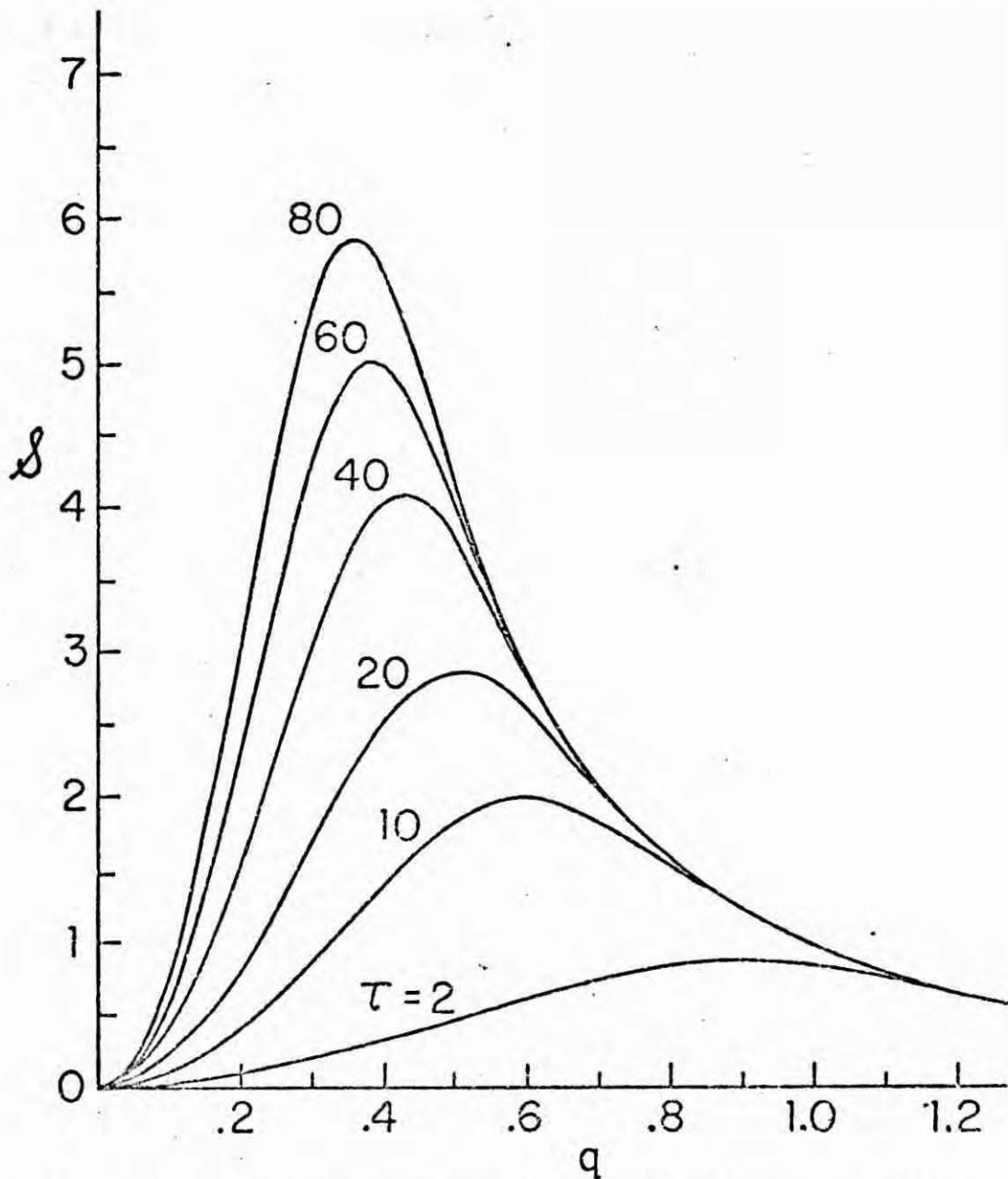


Fig. 4.9 Development with time of the structure function versus k (reduced units; section 4.3), for a system quenched to a point on the spinodal curve drawn on Fig. 2.1, according to the computations by Langer et al. (1975). This is to be compared with Figs. 6 and 8 bis, and Fig. 7.

Figs. 4.10-4.11. Plot and least-squares fit of $S(k,t)^{-1}$,
 $k > k_m(t)$, vs. k^2 . The slopes shown correspond
 to $1/c_1(t)$ in eq. (4.1) at $t = 613, 1643, 6528,$
 $421, 554, 3896, 1611$ and 727 for increasing
 temperatures and decreasing concentration, re-
 spectively.

Figs. 4.12-4.15. Time evolution of $1/c_1(t)$ and $c_2(t)$ assuming
 the form of eq. (4.1). In the one-phase region
 (with perhaps the exception $T/T_c = 1.5, \bar{\eta} = 0$) and
 for $T/T_c = 0.9, \bar{\eta} = -0.6$ they soon become time-
 independent. See also section 4.6.

Figs. 4.16-4.23. Early time evolution of $S(k,t)$ as a function
 of time for different values of k . At the end
 of each line is shown the corresponding value of
 $\mu = 30k/2\pi$.

Figs. 4.24-4.31. Complete evolution with time of the spherical
 averaged structure function for different values
 of k . No exponential growth is seen in any case.

Figs. 4.31.bis and 4.31.ter correspond to the
 $50 \times 50 \times 50$ lattice.

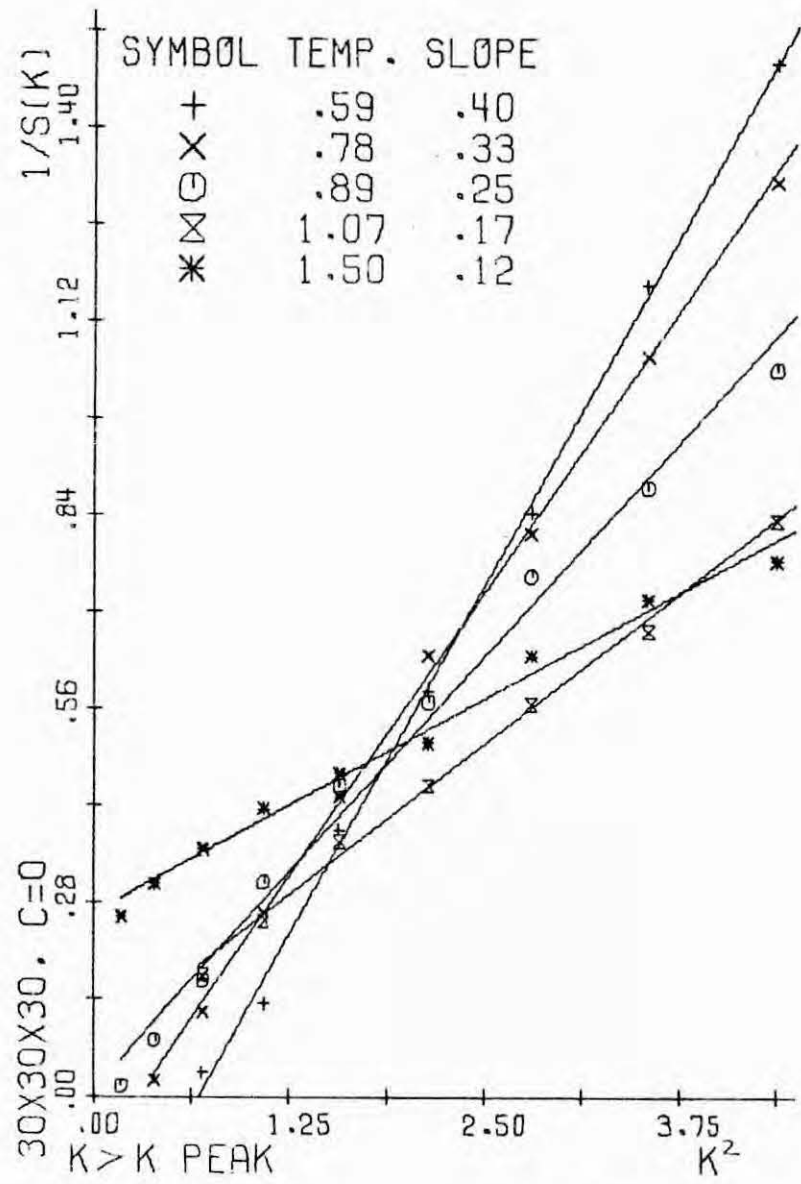


Fig. 4.10

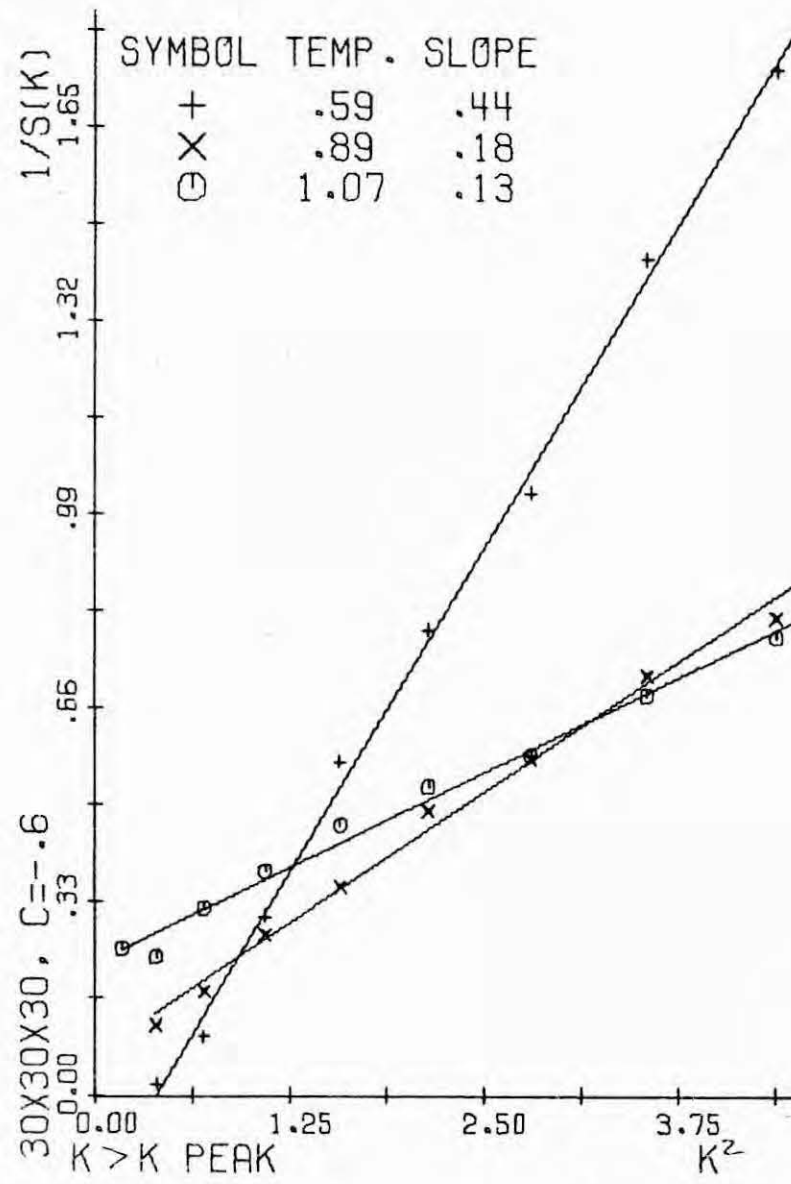


Fig. 4.11

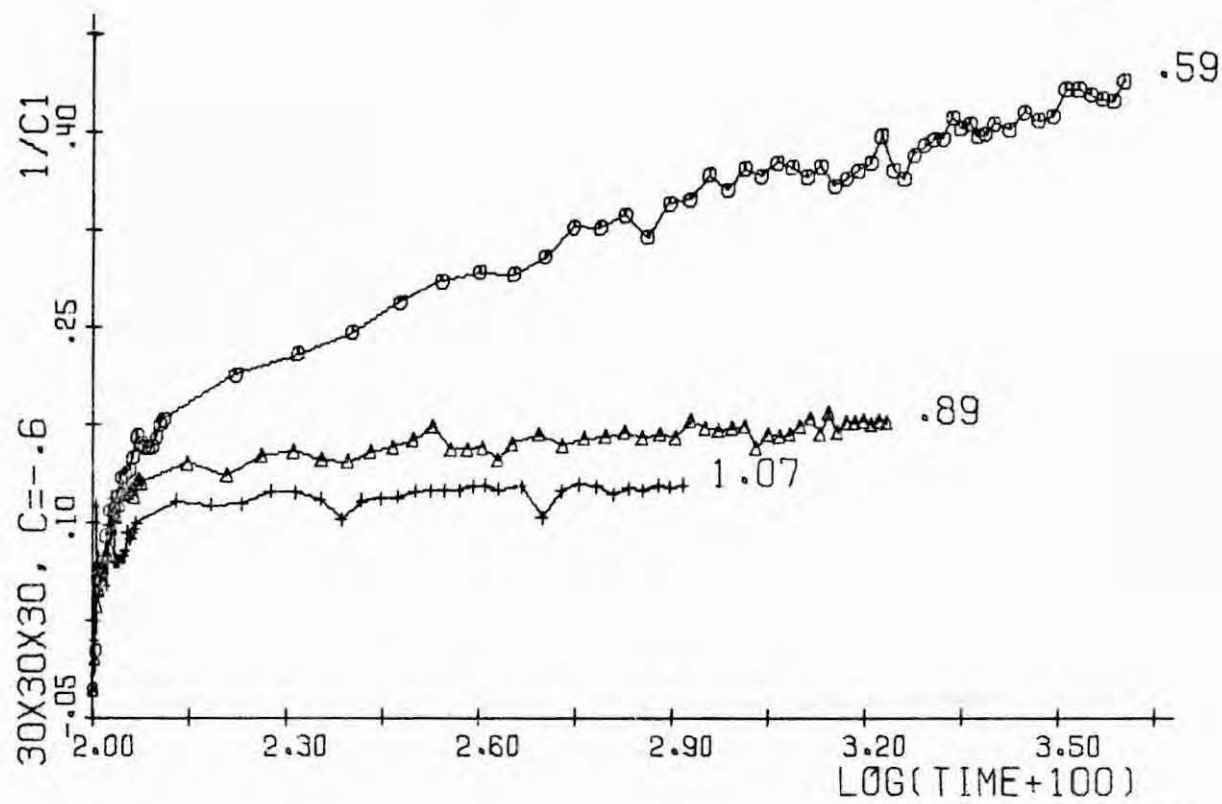


Fig. 4.13

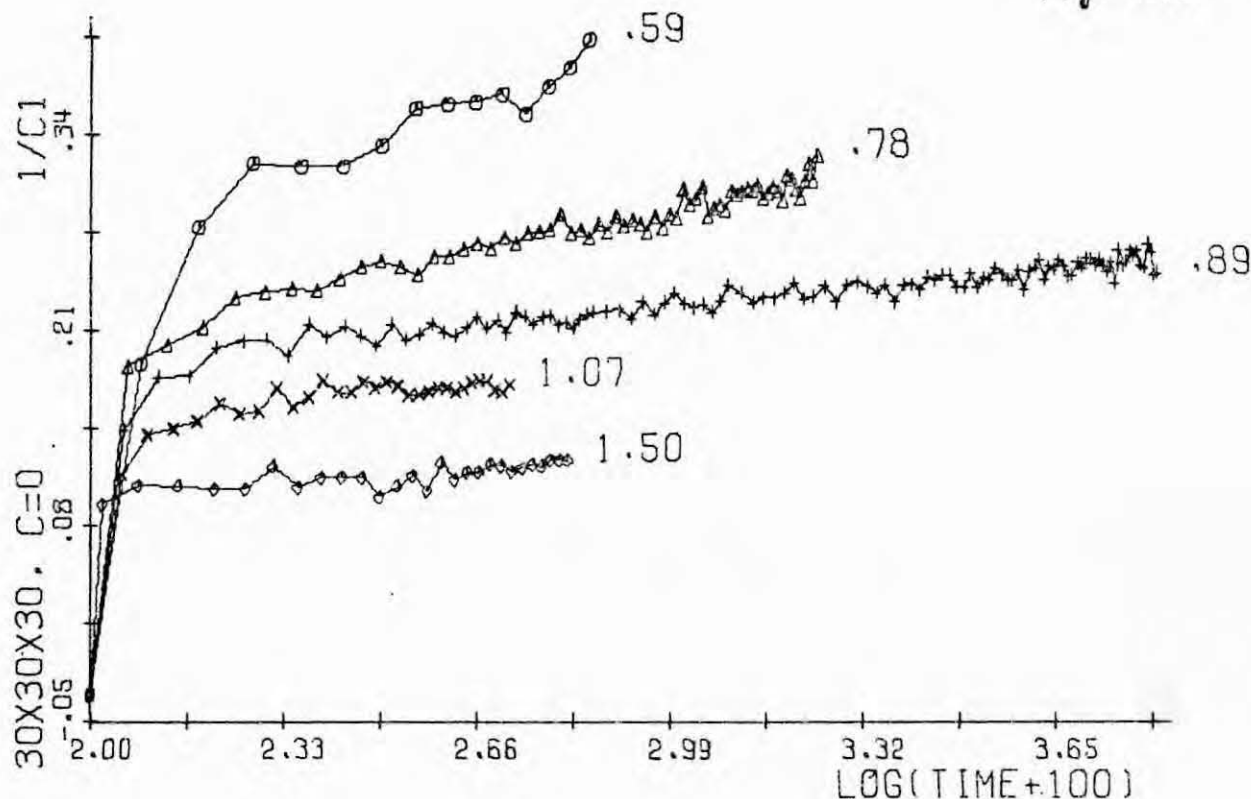


Fig. 4.12

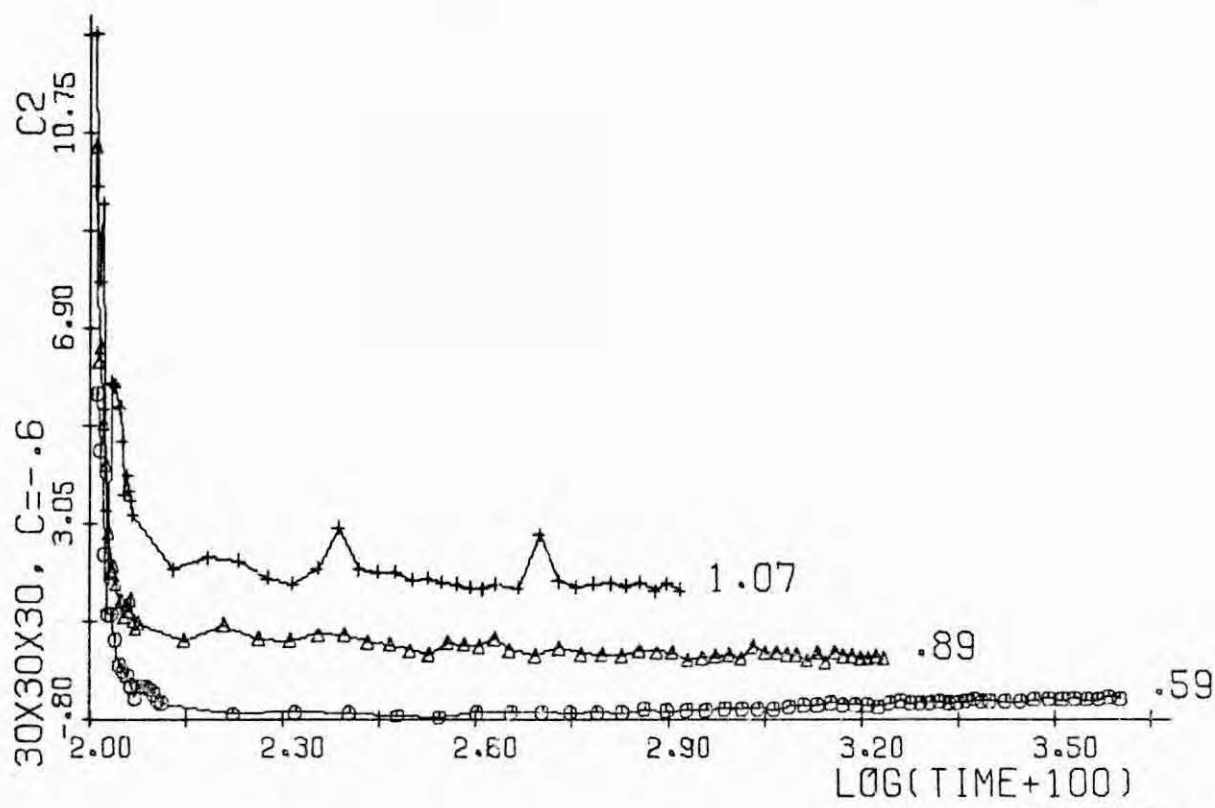


Fig. 4.15

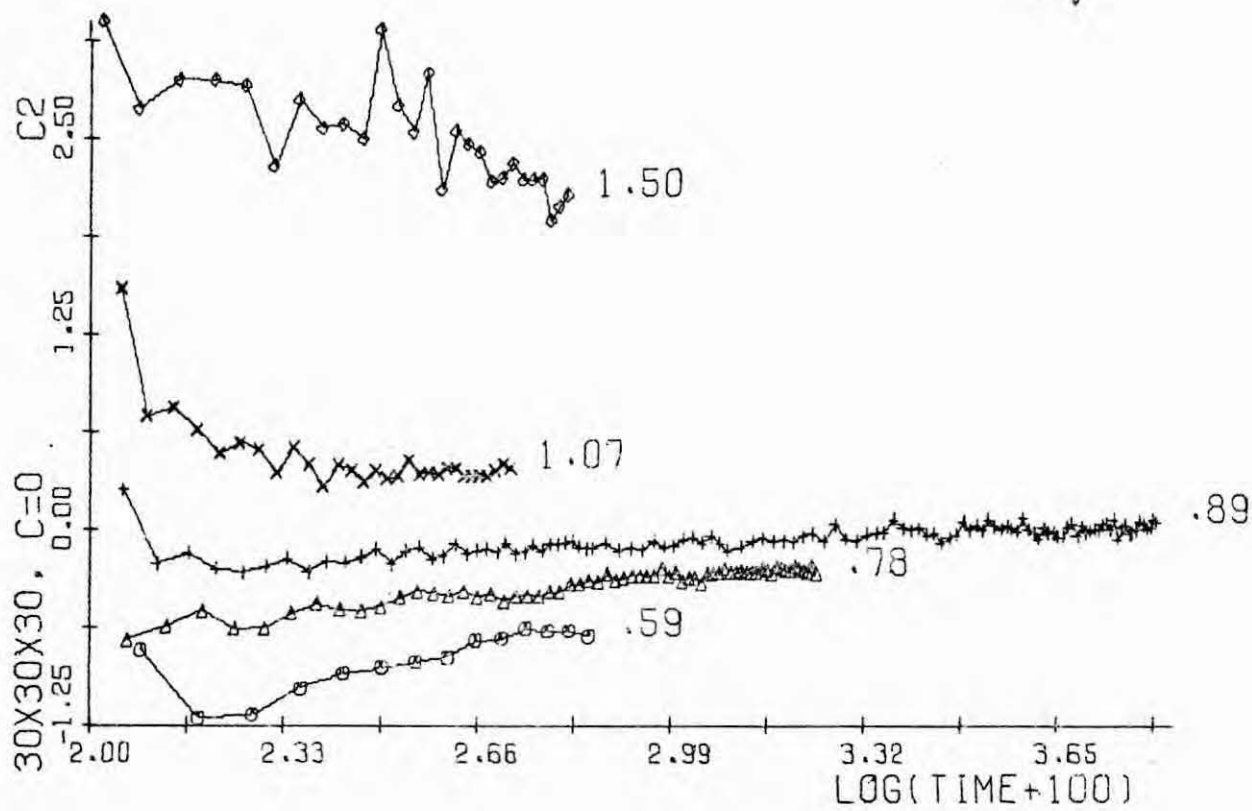


Fig. 4.14

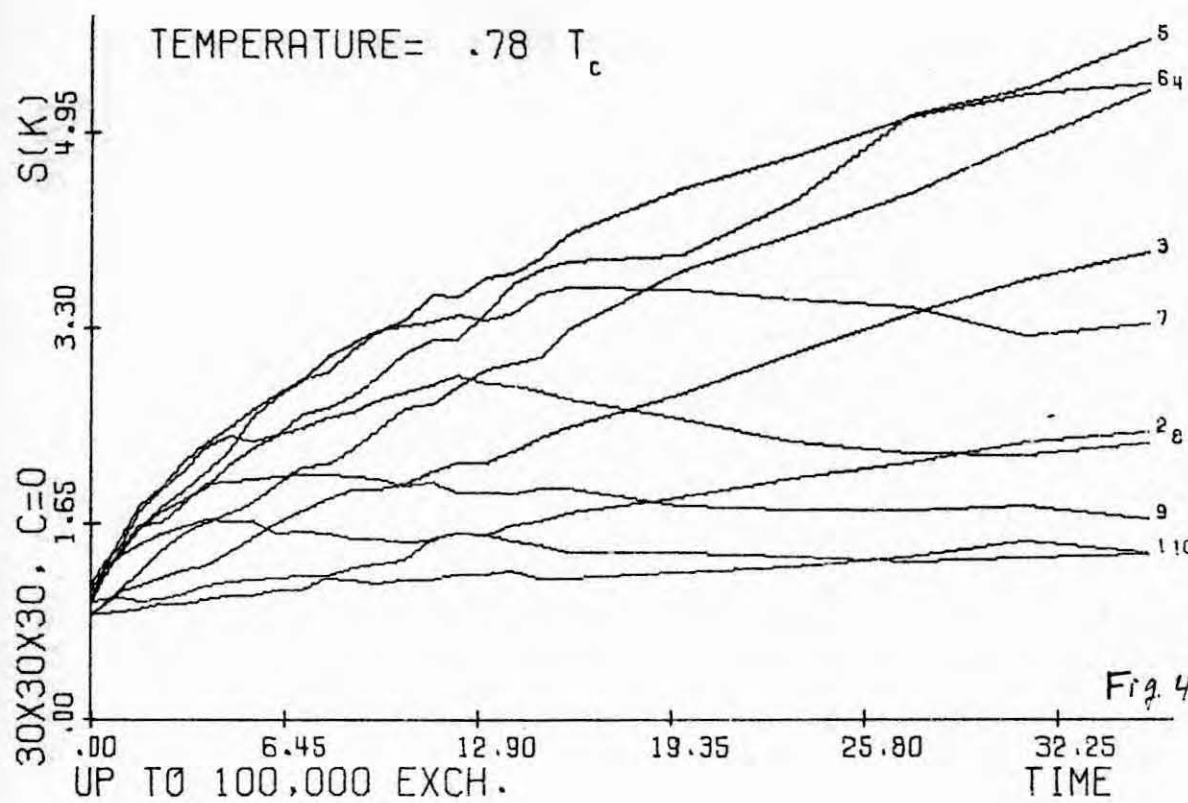


Fig. 4.17

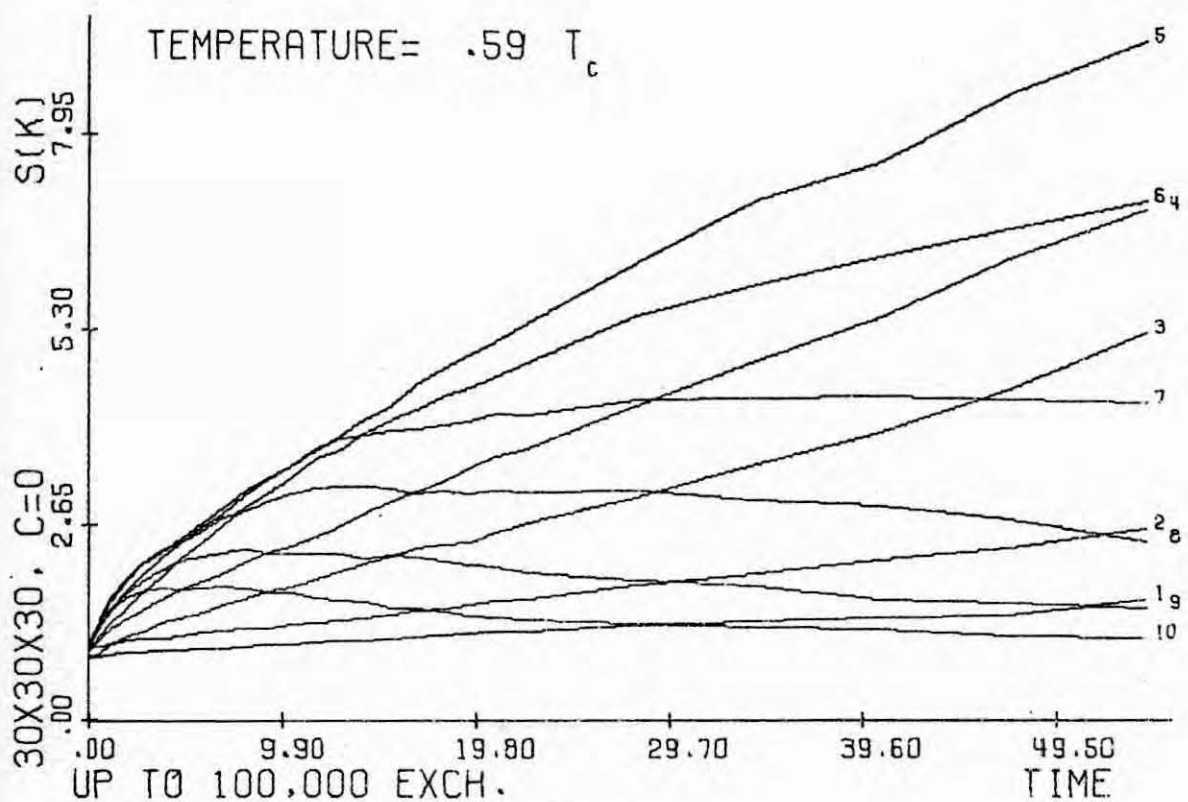
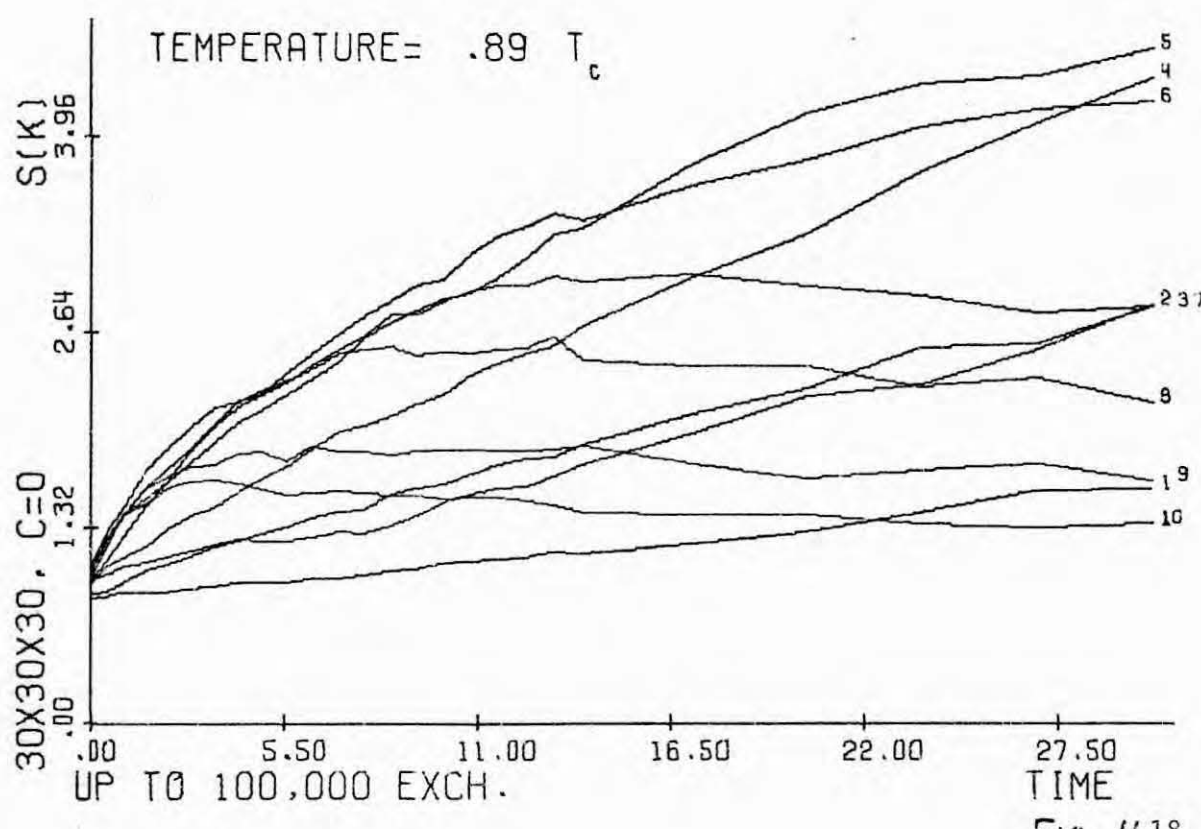
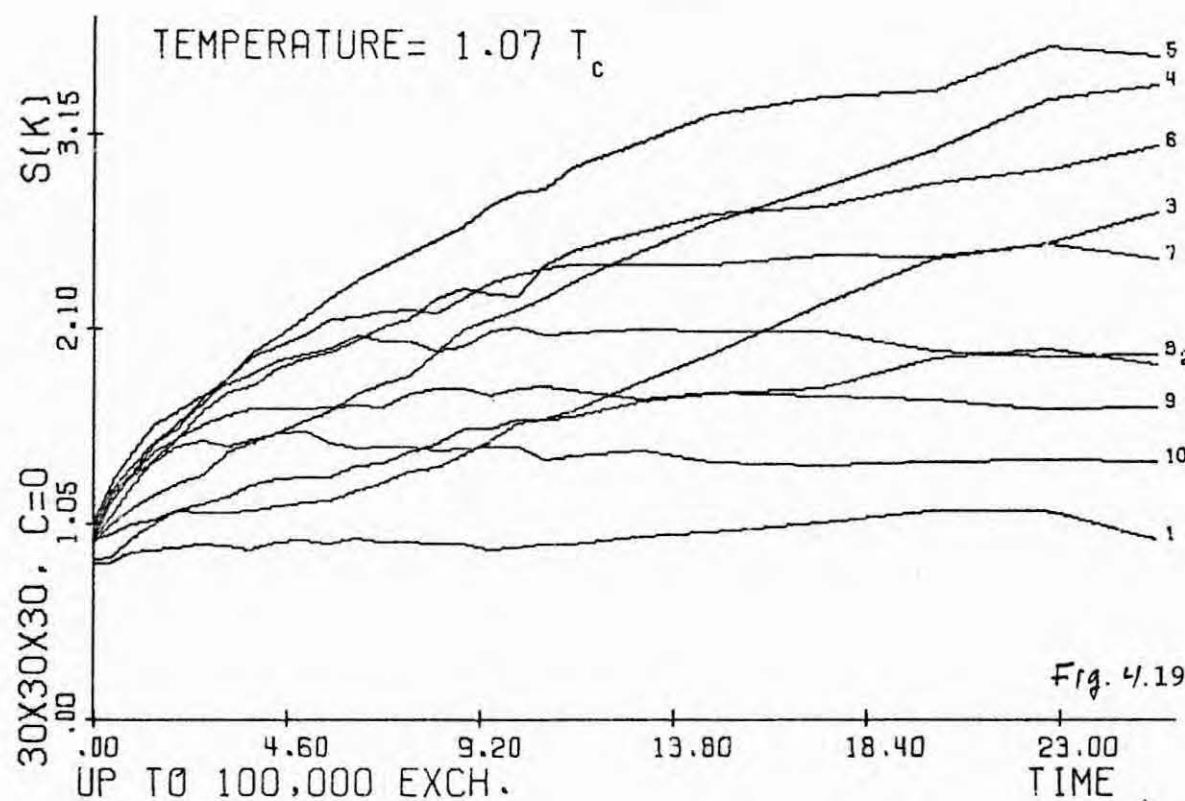


Fig. 4.16



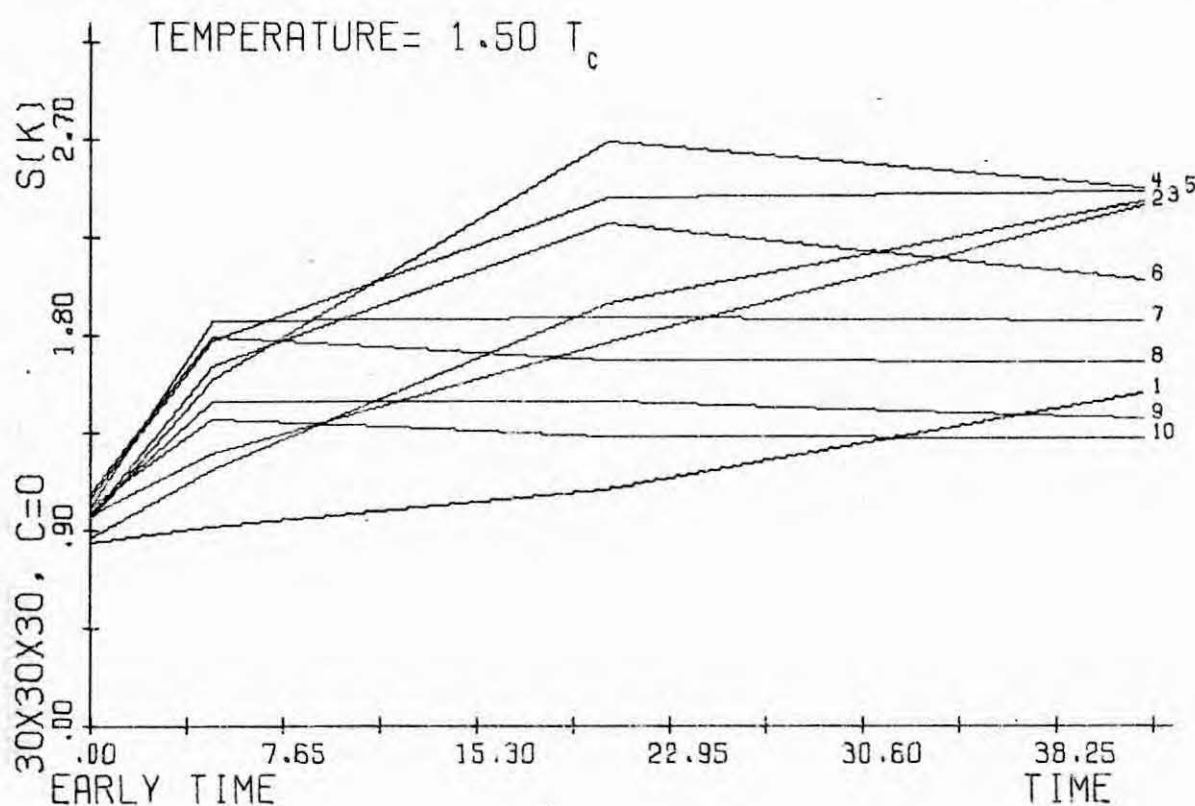
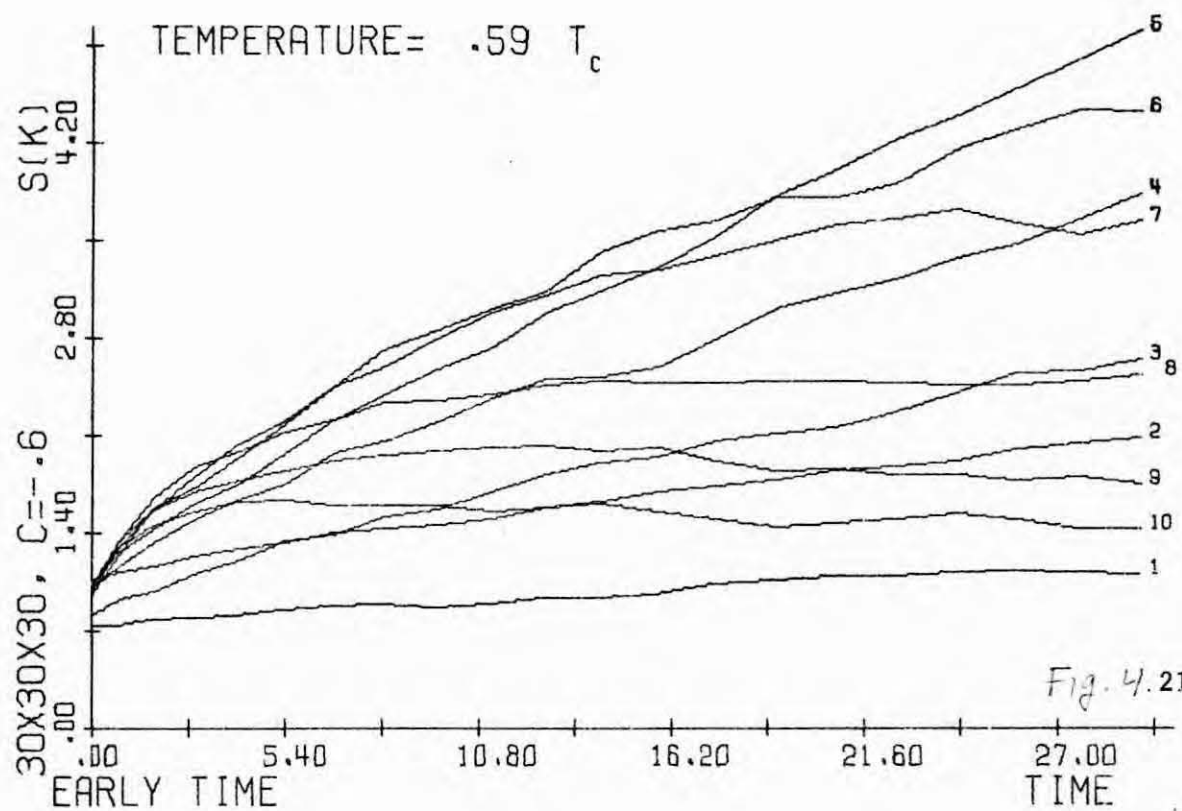


Fig. 4.20

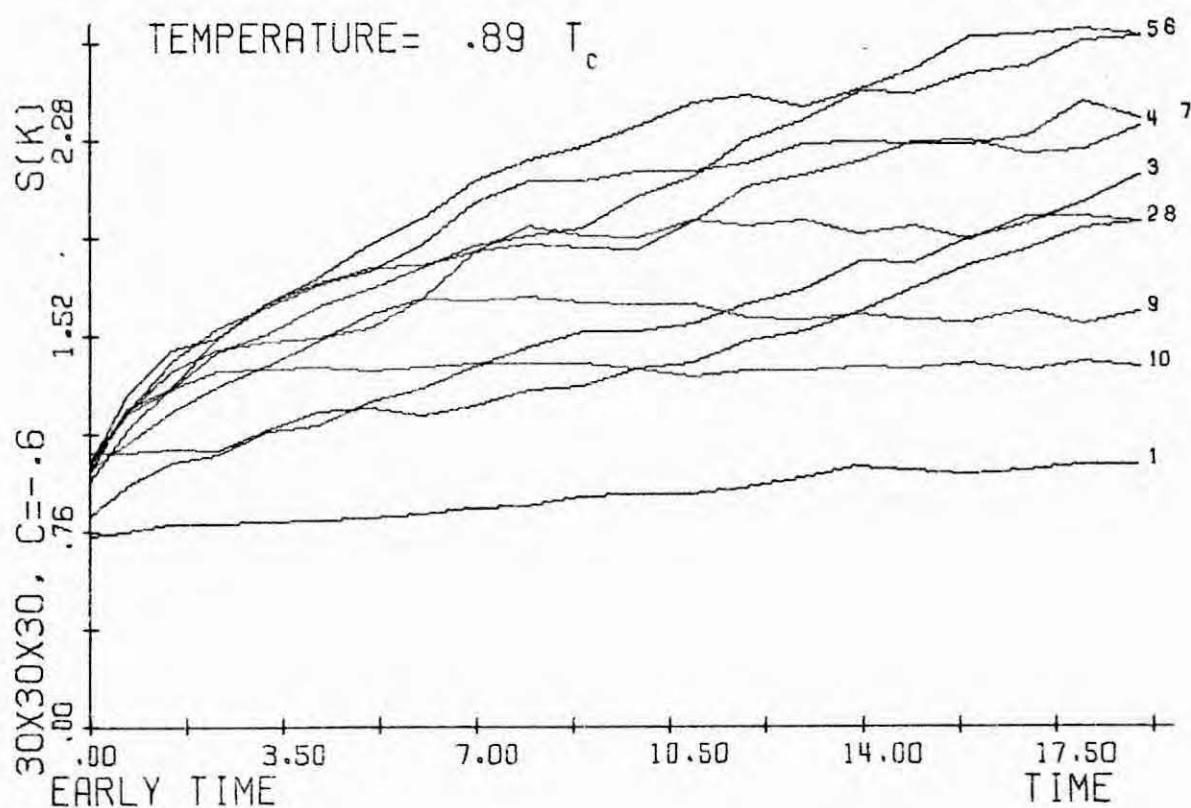
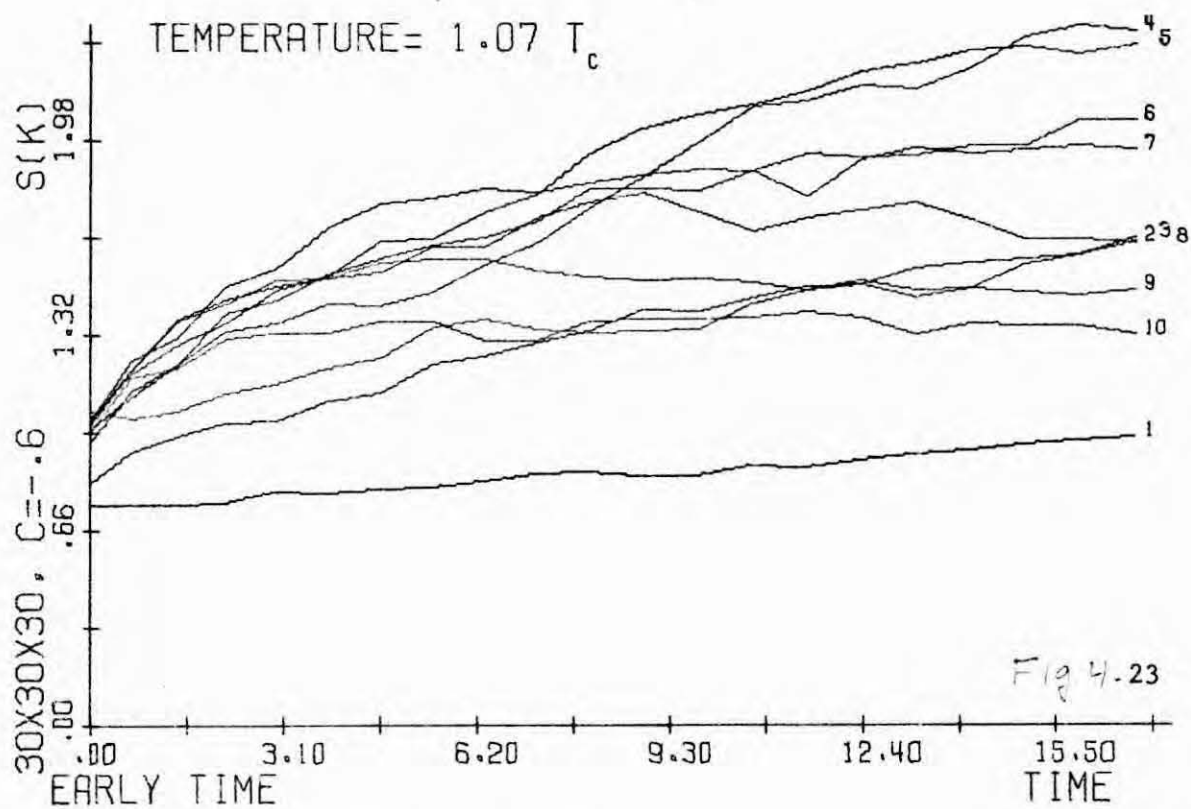


Fig. 4.22

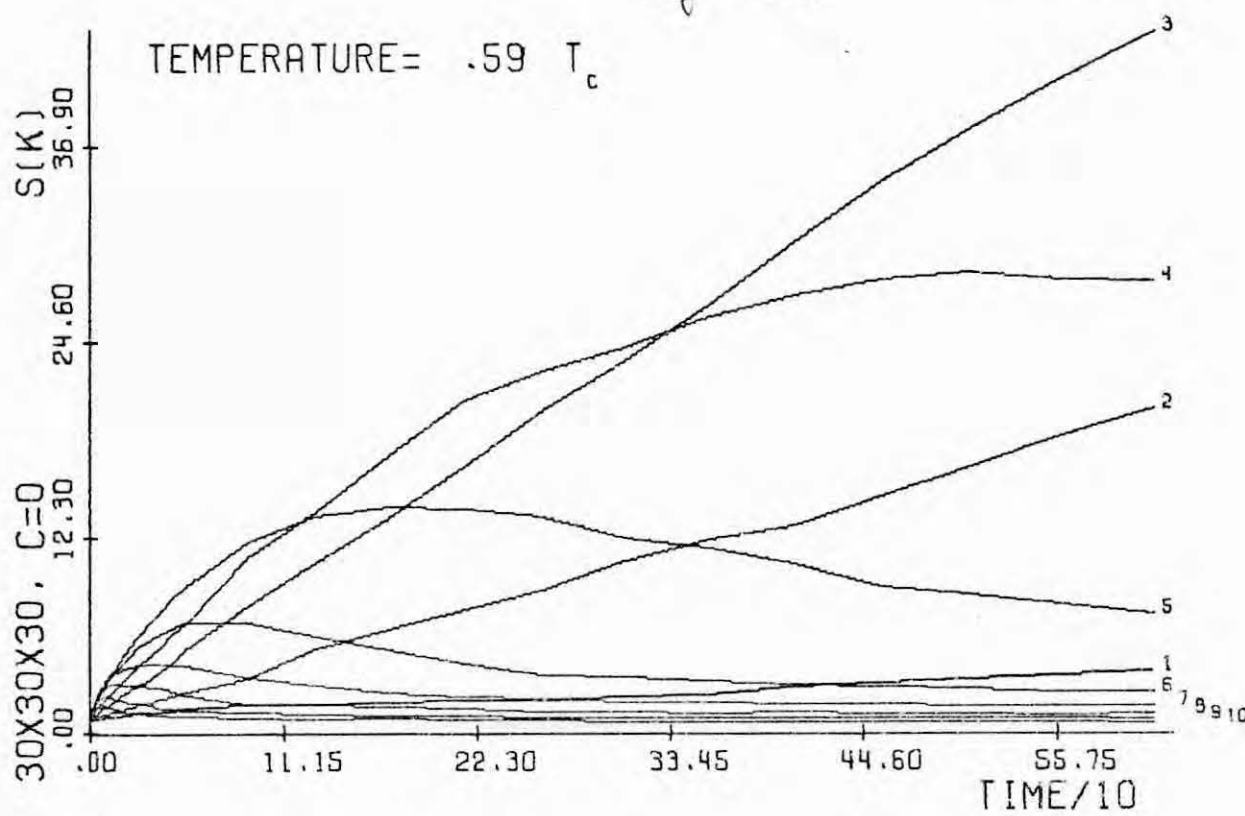
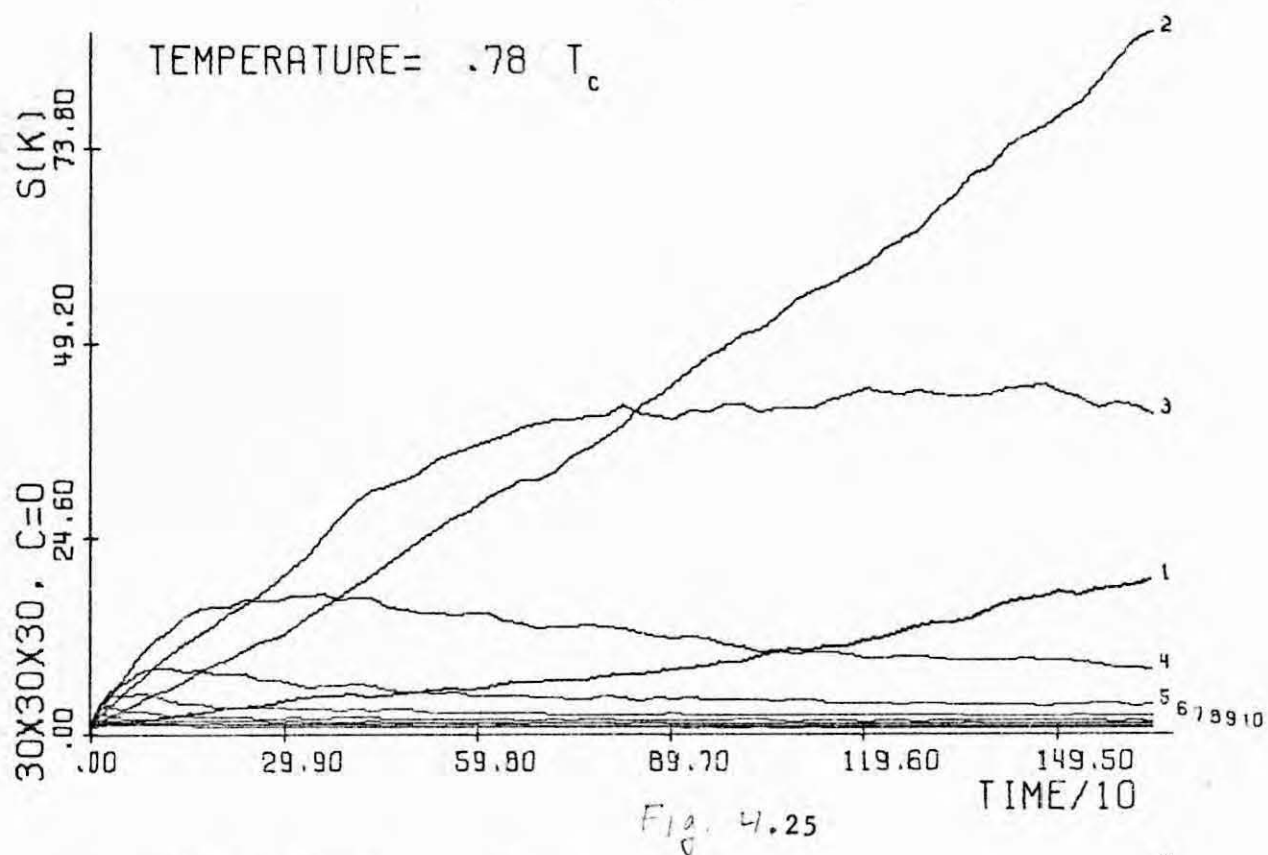


Fig. 4. 24

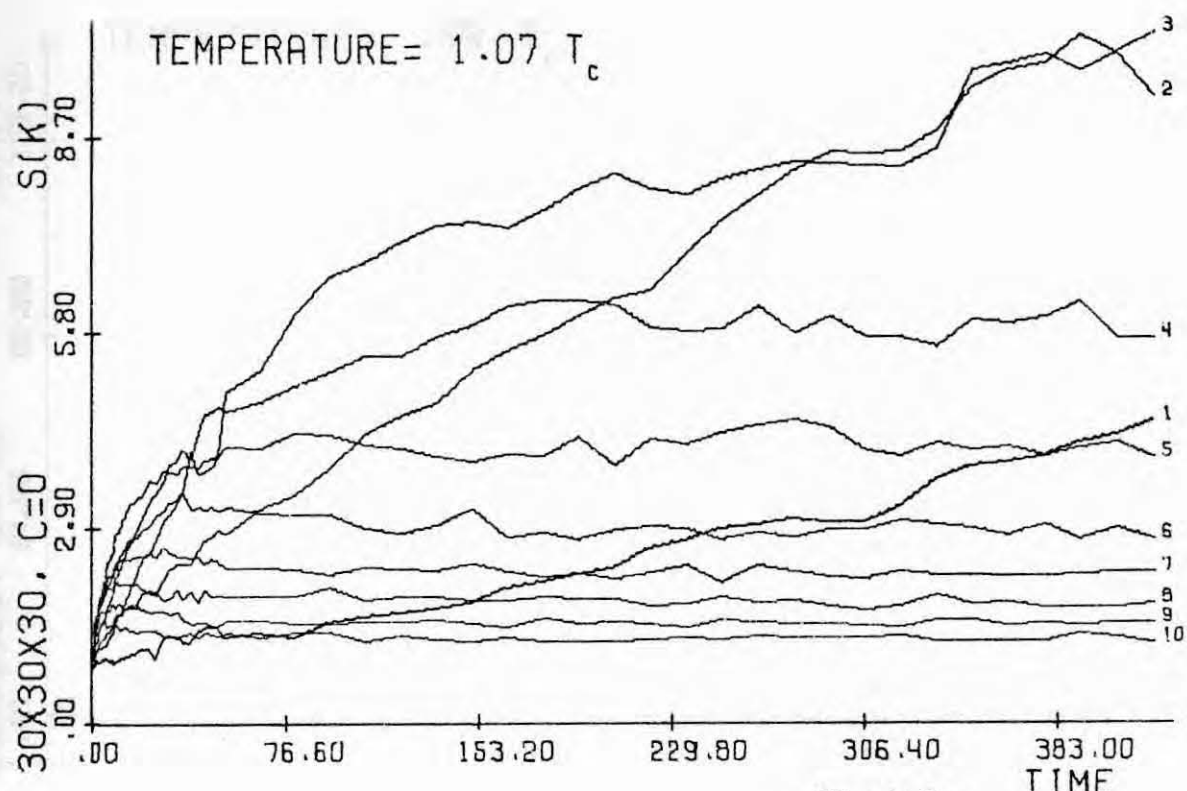


Fig. 4.27

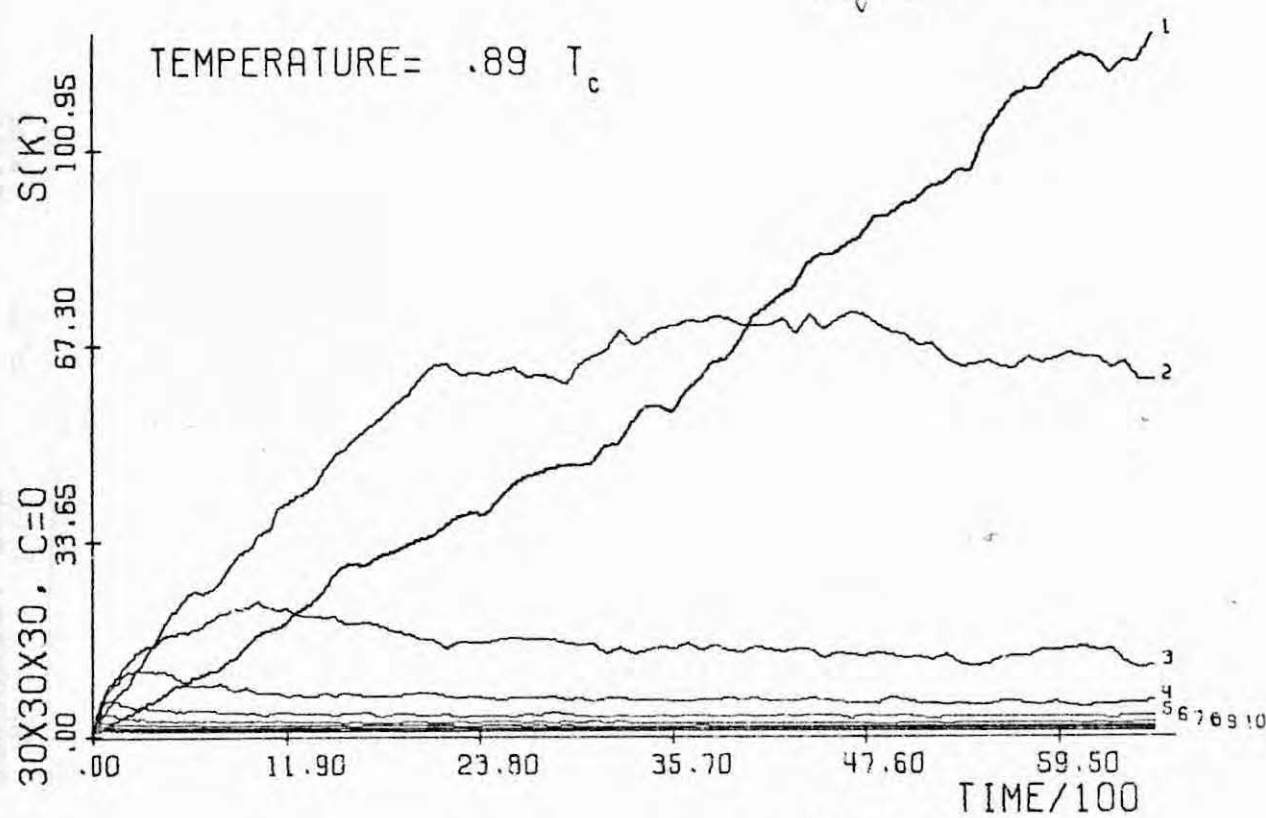
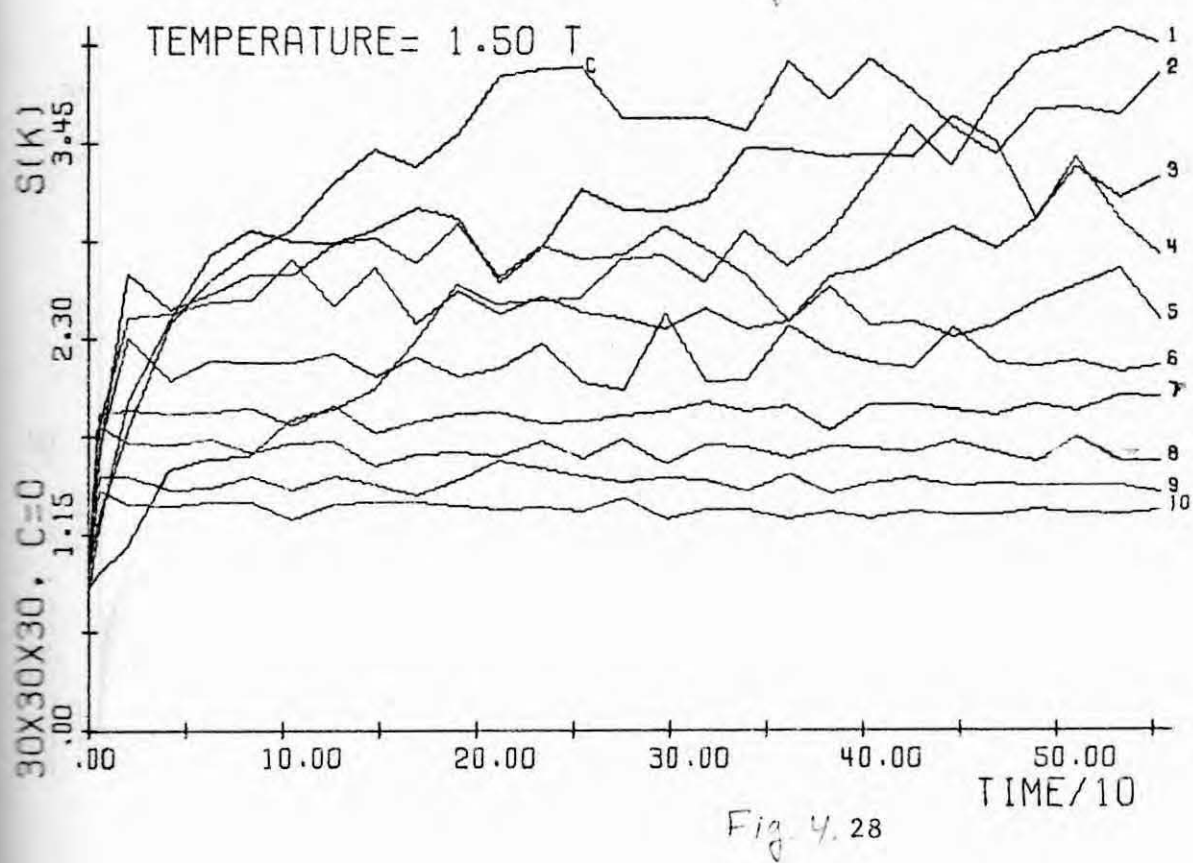
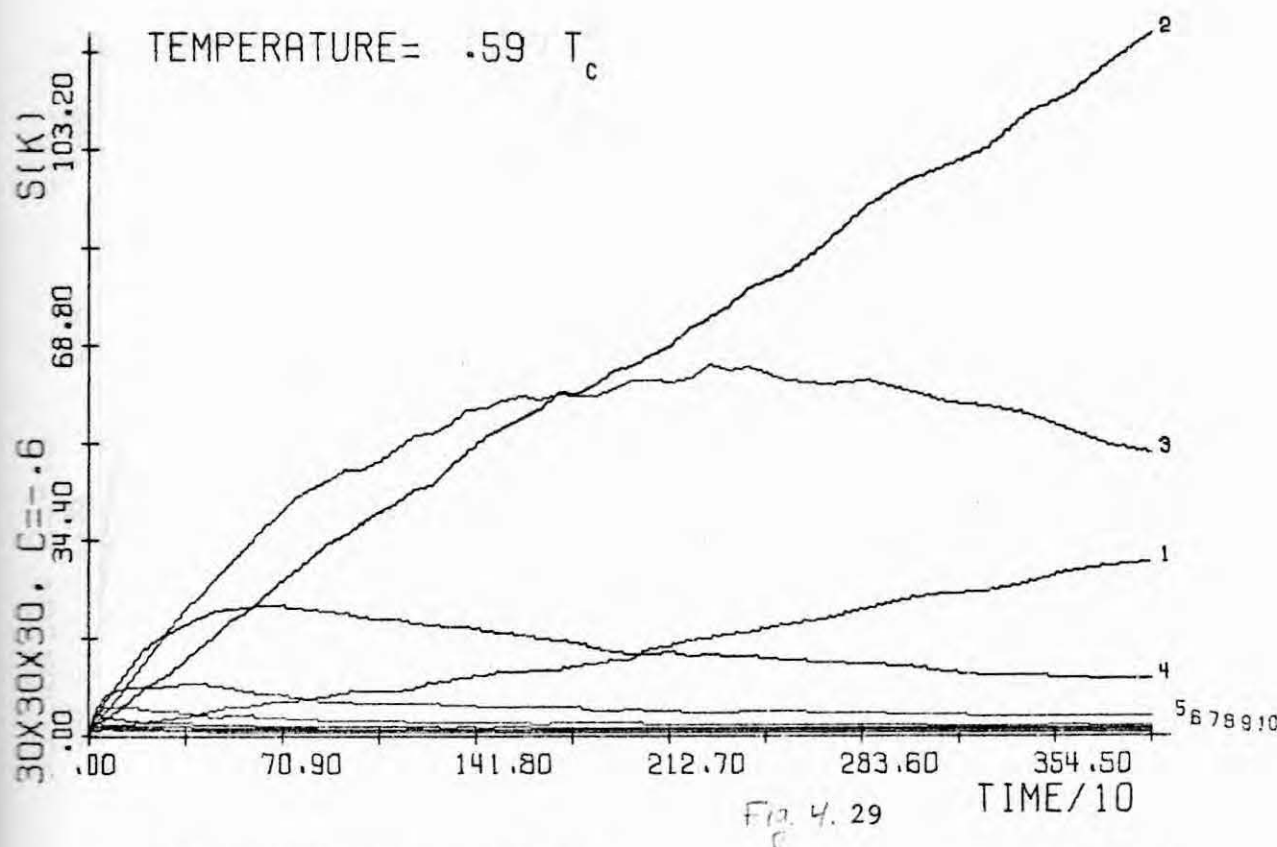


Fig. 4.26



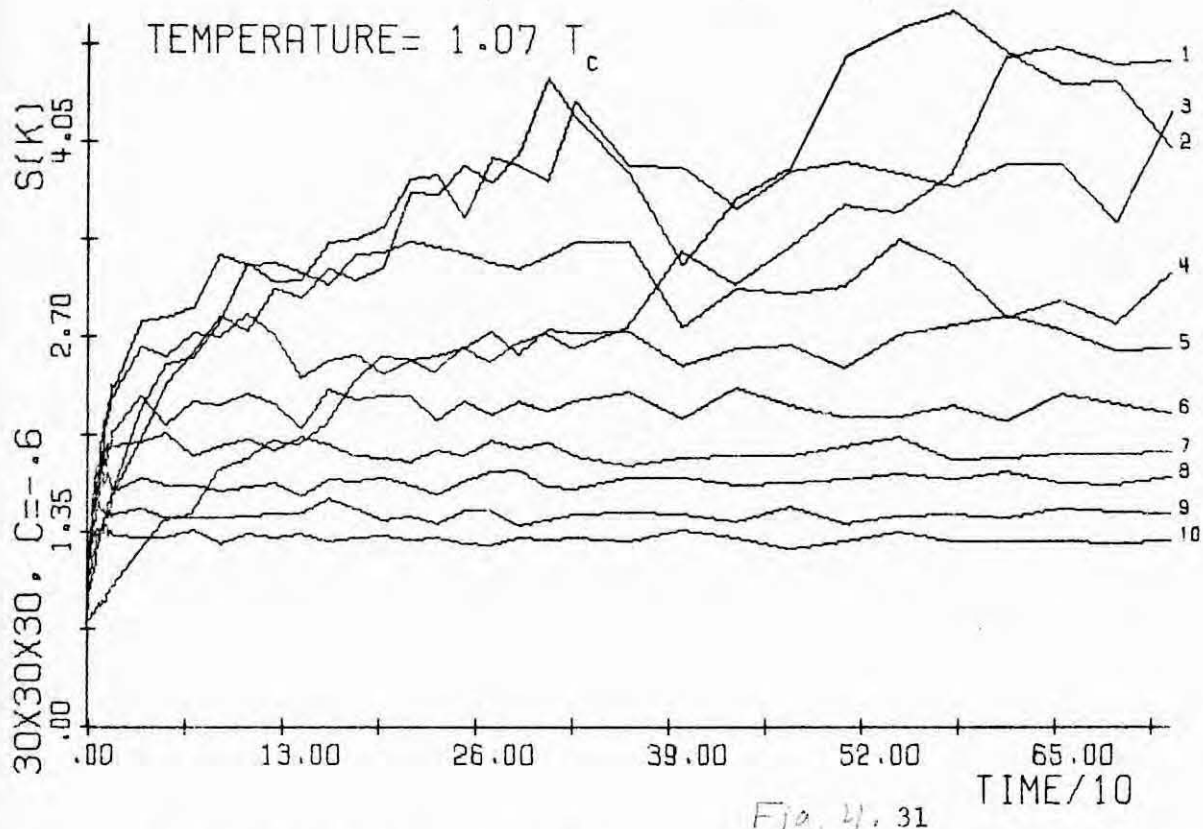


Fig. 4.31

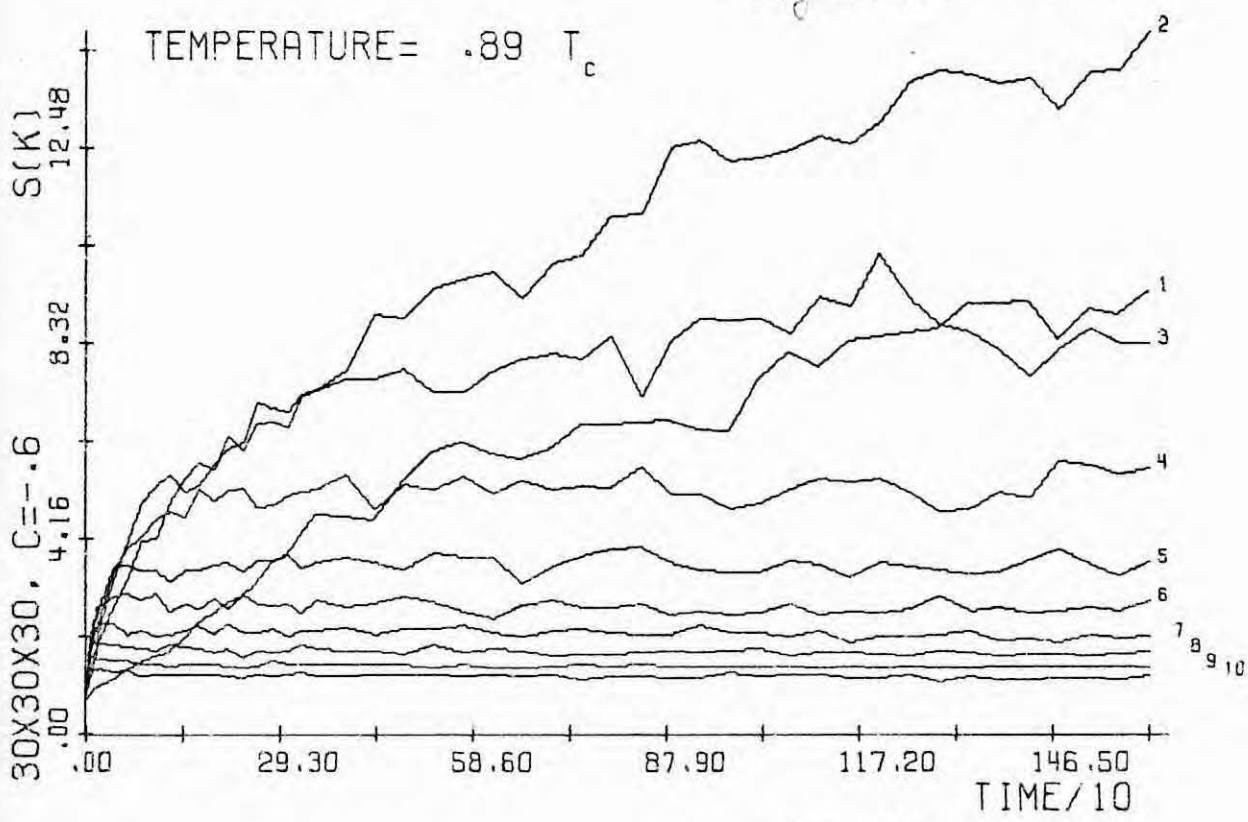
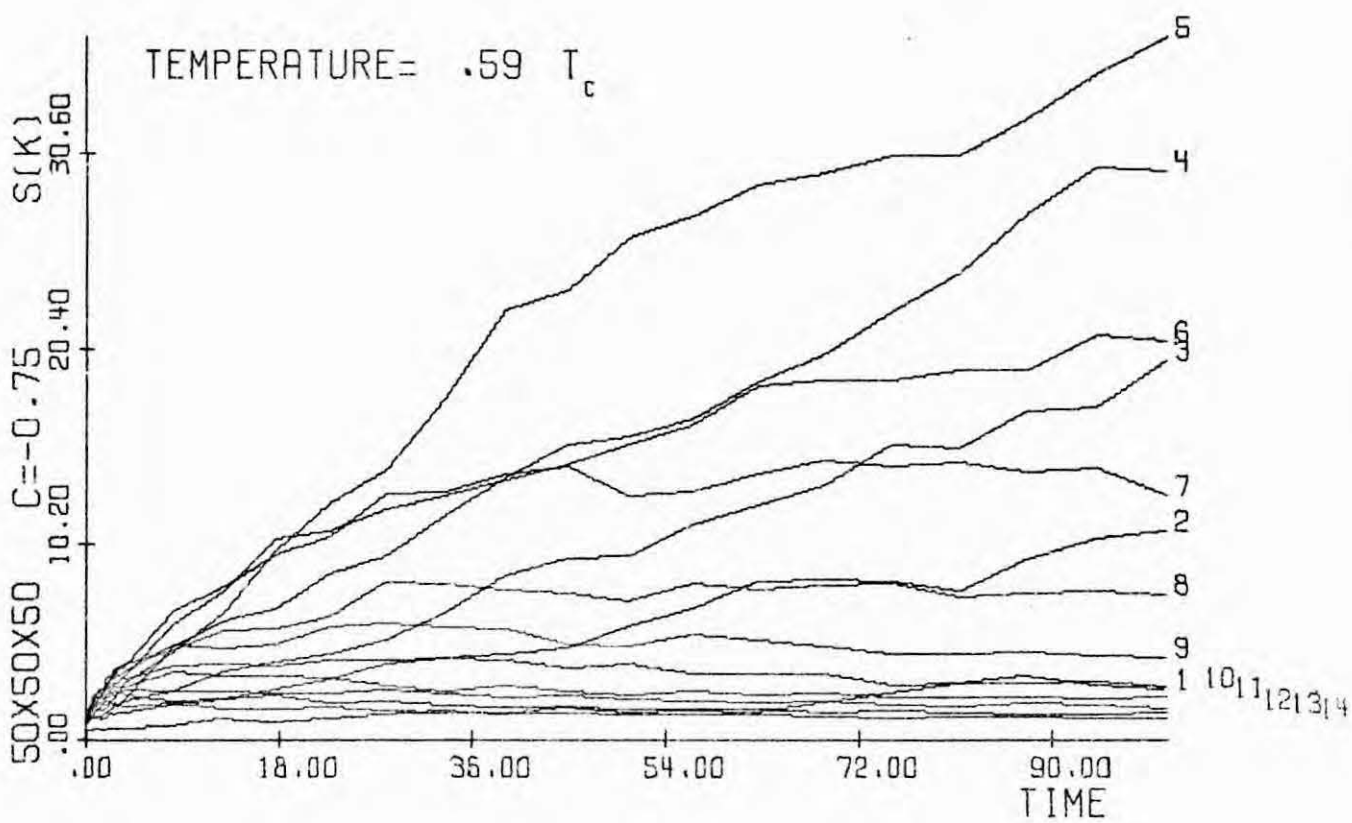
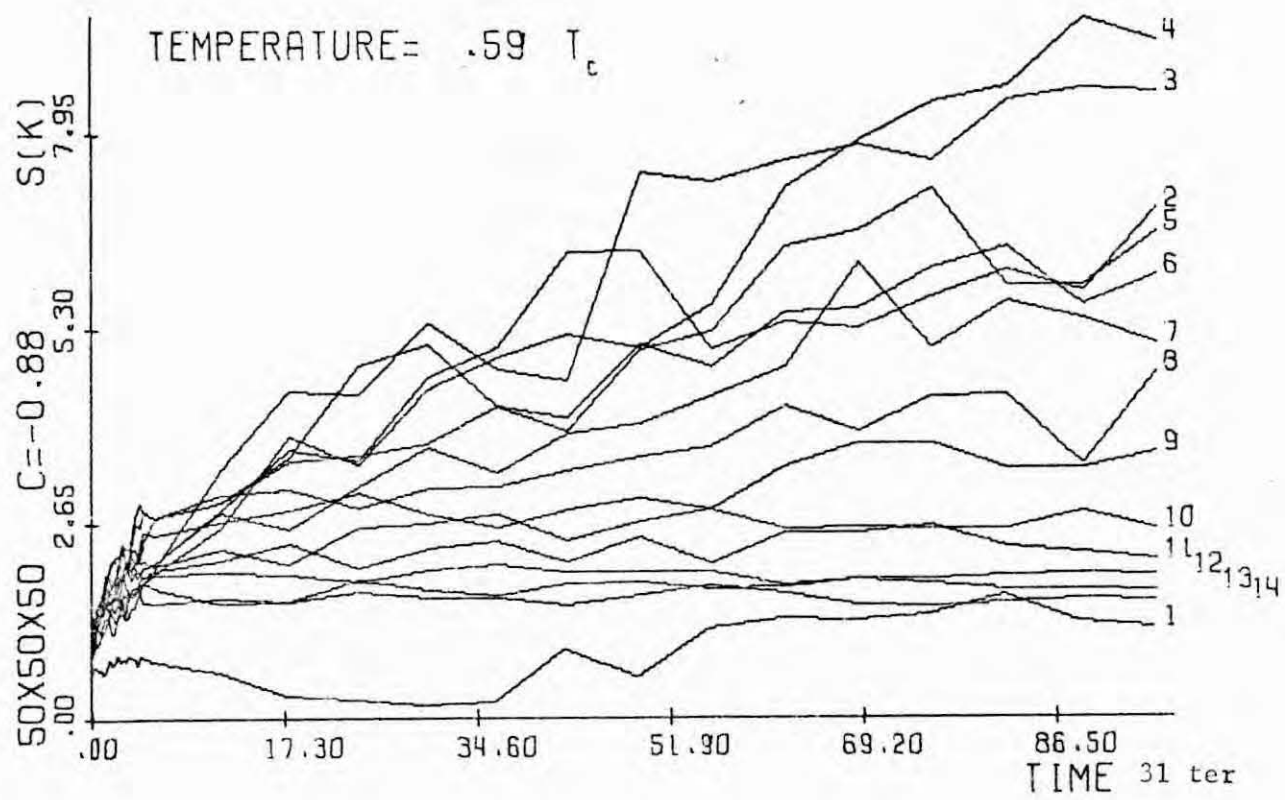
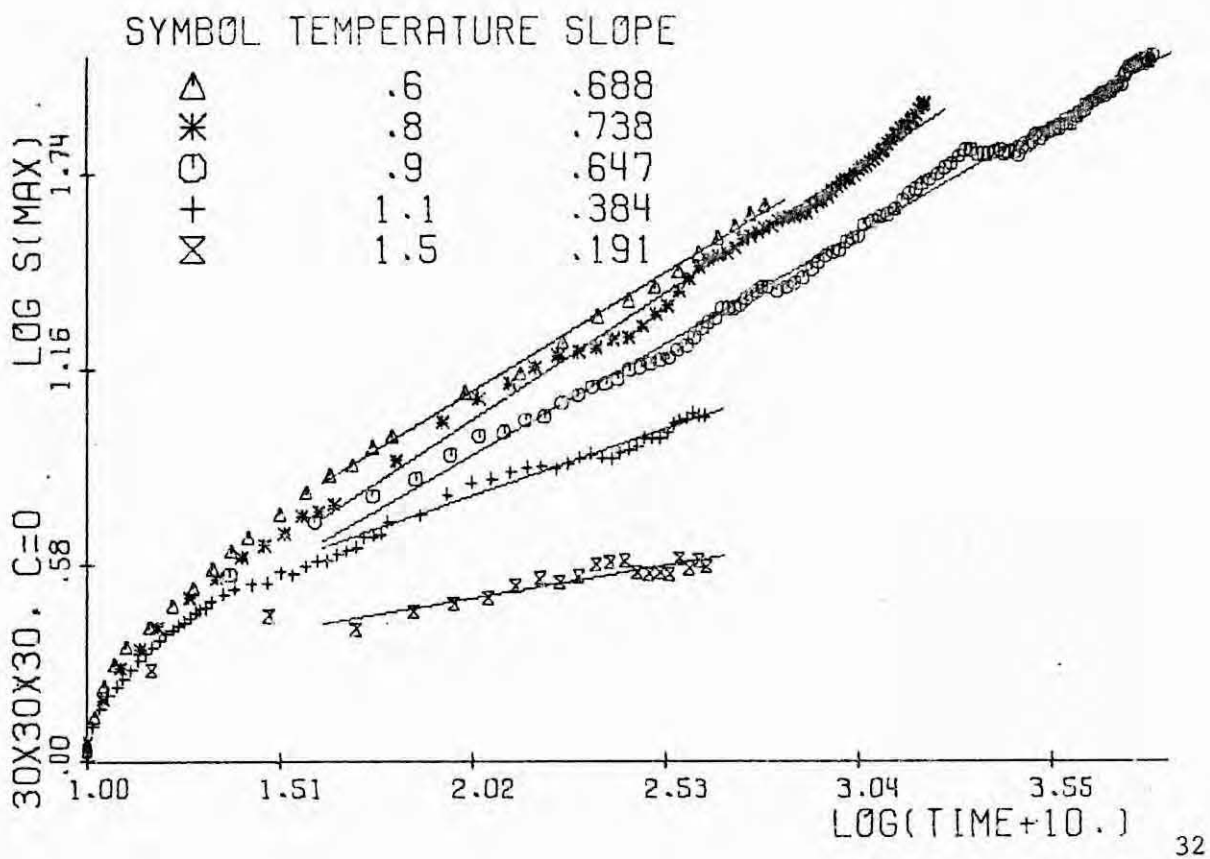
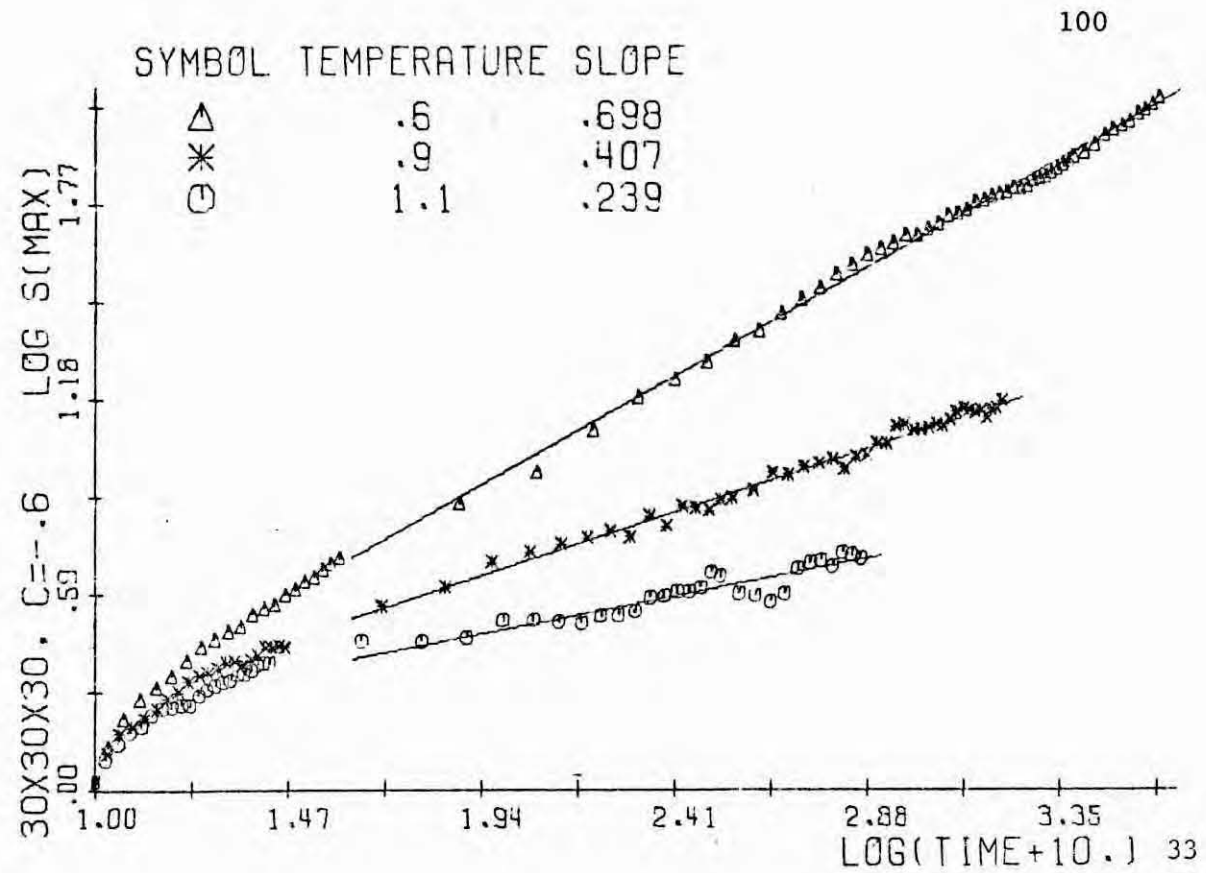


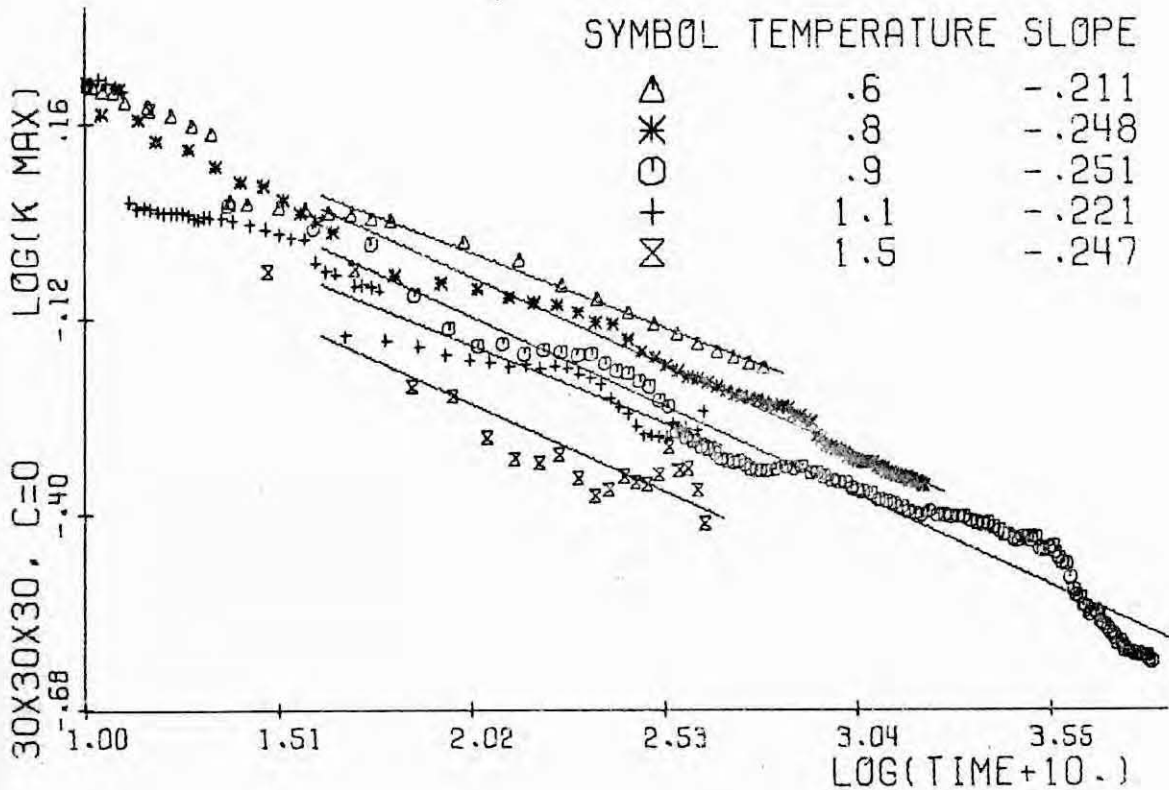
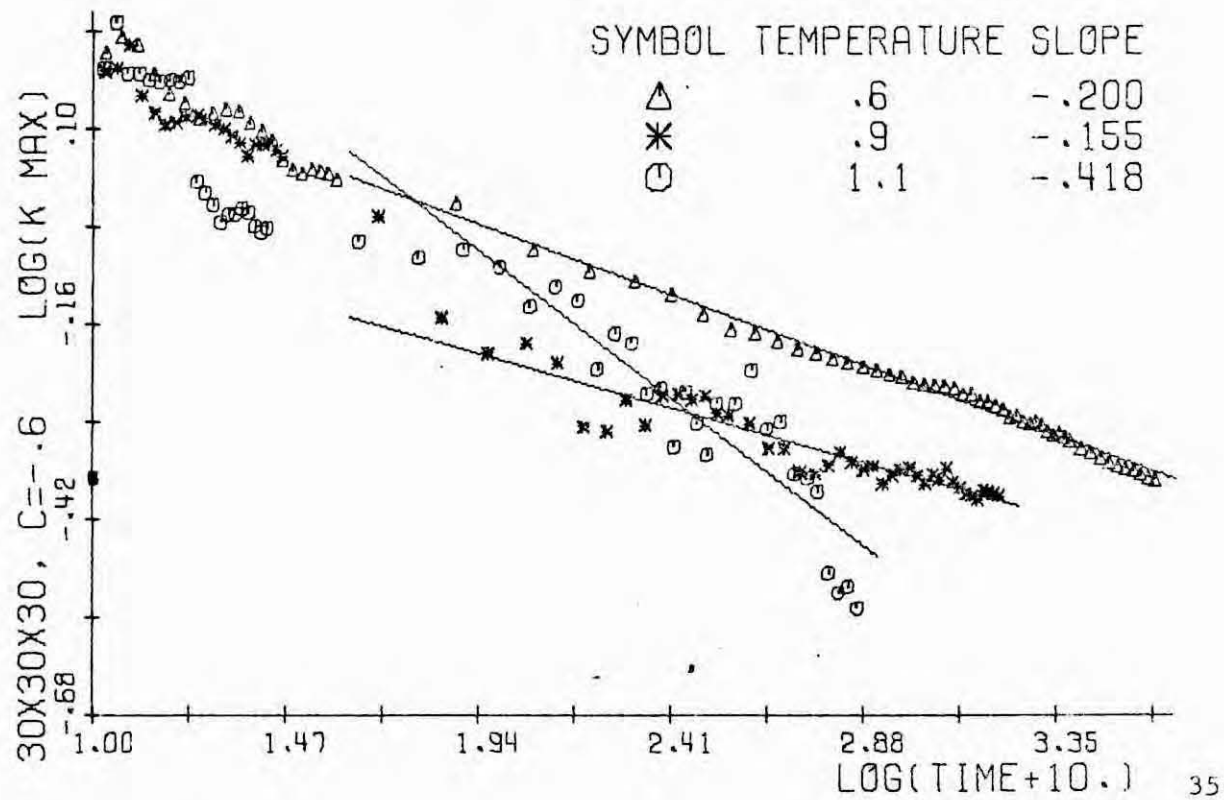
Fig. 4.30

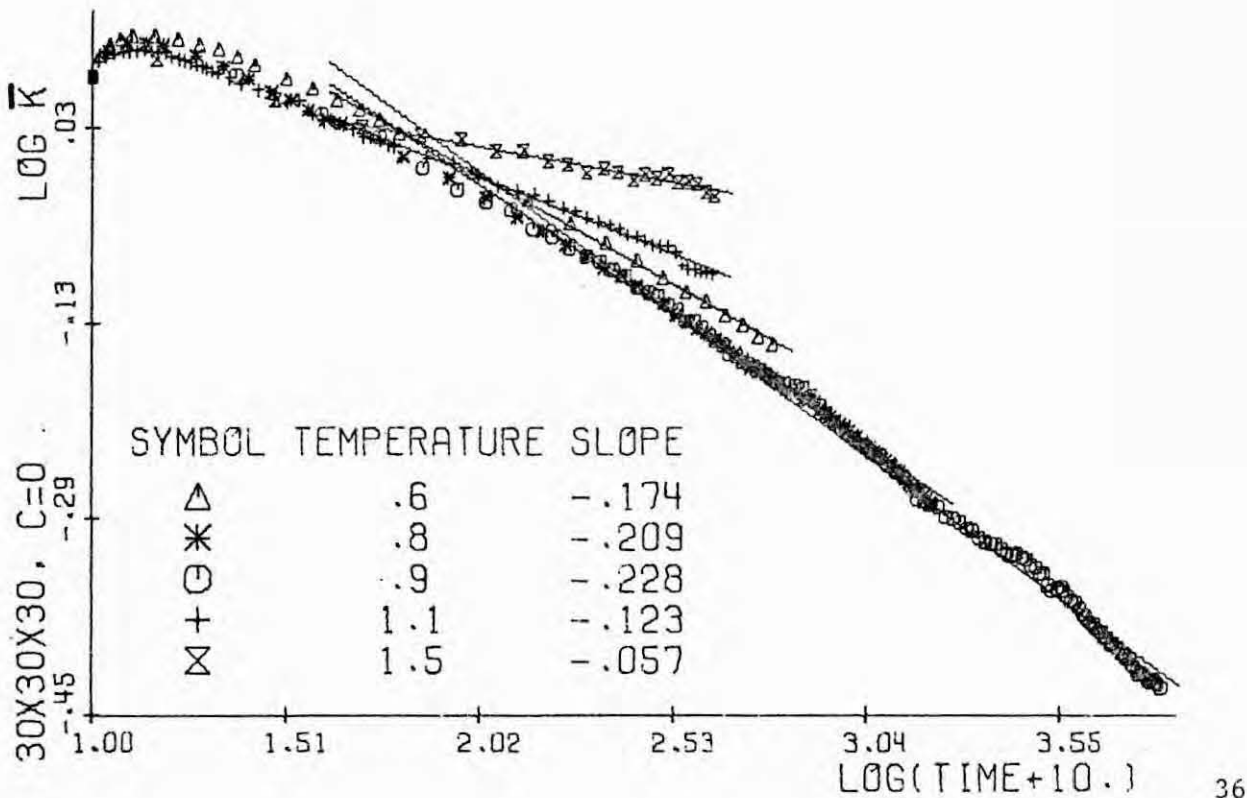
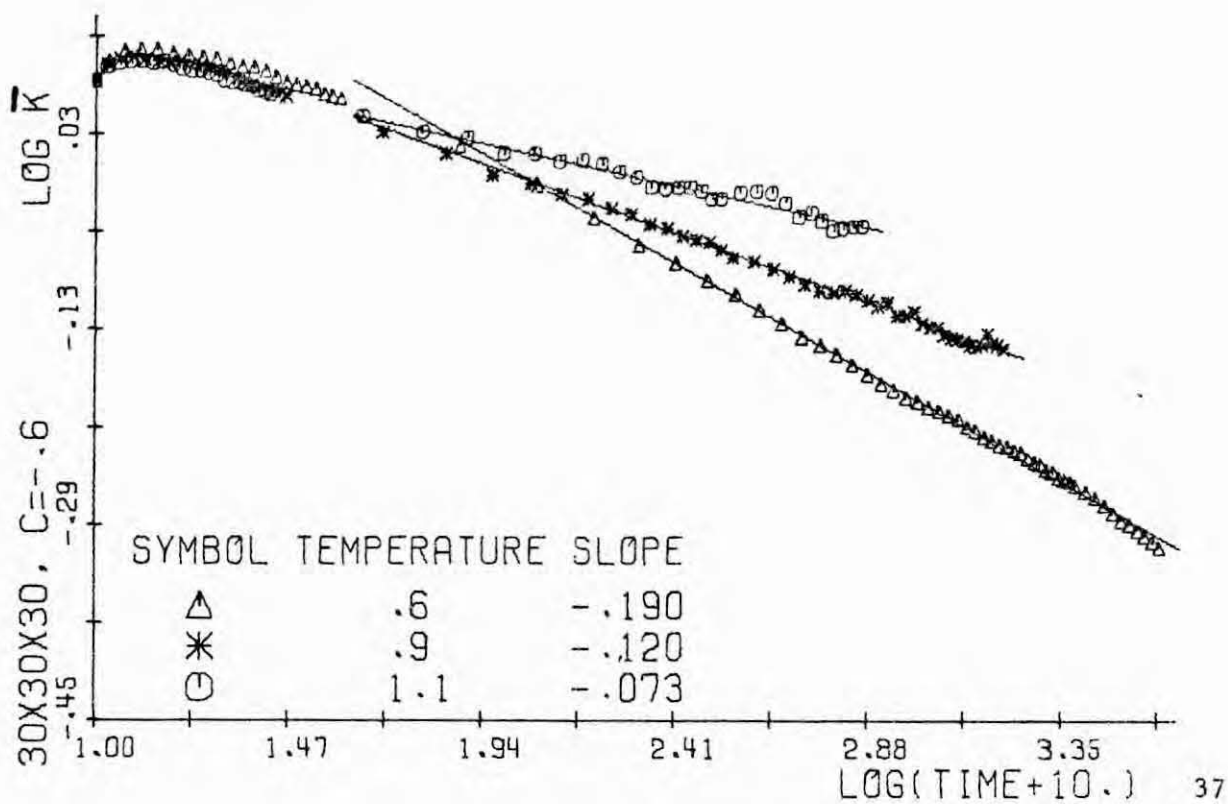


Tables 4.32-4.37 Least-square determination of the parameters
in eqs. (4.2)-(4.4) for $t \geq 50$. In Figs. 32-35 is
assumed that the highest points of $S(k,t)$ around k_m
follow a parabola; the inadequacy of this fit
probably accounts for most of the fluctuations in
those figures. Note that for $T/T_c = 1.5$ in Fig. 32
and for $T/T_c = 1.1$ in Fig. 33 the slope correspond-
ing to the latest times is practically zero, indicat-
ing the end of the growth of the peak of $S(k,t)$.
This effect is less transparent for the location
of the peak in Figs. 36-37 for the same cases.

It seems again evident from the figures that
the evolution is independent of the composition when
the system is quenched to some "spinodal region"
(this would include $T/T_c = 0.6$, $\bar{\eta} = -0.6$, but not
 $T/T_c = 0.9$, $\bar{\eta} = -0.6$ nor $T/T_c = 0.6$, $\bar{\eta} = -0.94$).







$T/T_c =$	$\bar{\eta} = 0$					$\bar{\eta} = -0.6$		
	0.6	0.8	0.9	1.1	1.5	0.6	0.9	1.1
α	2.21	2.54	2.84	1.73	1.35	2.42	1.73	1.46
Δ	0.4	1.3	2.2	0.8	0.6	0.7	0.8	1.1
α'	2.53	2.77	2.46	1.95	1.81	2.30	-	-
Δ'	1.5	2.8	7.2	4.8	9.9	1.9	-	-
α''	0.51	0.33	0.40	1.03	1.25	0.37	0.73	1.02
Δ''	3.5	6.5	5.9	4.5	5.0	4.6	4.2	6.4

Table 4.2. Values of α , α' and α'' , and values of Δ , Δ' and Δ'' in percent corresponding to the relations (4.4), (4.2) and (4.3).

A basic cluster dynamics theory (section 3.4) predicts $a'' = 3a'$ and $a' = 1/6$ at "low temperatures". The first of these predictions seems to be satisfied well for $T = 0.6 T_c$ and $T = 0.8 T_c$, the second apparently not. For $T \approx T_c$ the prediction is $a' \approx 1/4$ and for $T > T_c$, $a' = 1/2$. Only the first of these predictions seems in agreement with some of our results. On the other hand, the solution of eq. (3.18) with the approximation (3.23) is consistent with $a' \approx 0.21$ (Langer 1975).

4.2. - Energy

The behavior of u defined in (2.27) is plotted in Figs. 38-41 and a part of the numerical data (the energy was collected more frequently than the rest of the quantities) is listed in Tables A.9 - A.16. At $t = 0$, the number of A-B bonds is

approximately $N_{AB} = (zn_B)(n_A N)$, with $z = 6$ the coordination number of the lattice; then $u = 3/2$ for $\bar{\eta} = 0$ and $u = 24/25$ for $\bar{\eta} = -0.6$. This quantity, excluding the very early times, appears to behave (Figs. 38 and 40) as

$$u \approx \alpha(t + 10)^{-b} \pm \Delta . \quad (4.5)$$

This behavior must clearly be modified for still longer times when u should approach a finite value $u_\infty(T)$ which will be very small at low temperatures. The parameters for eq. (4.5) are given in Table 4.3 for $t \geq 100$. Figs. 39 and 41 correspond to the early behavior of the form $u \sim t^{-b}$.

Unfortunately we have no reliable way of estimating $u_\infty(T)$, the equilibrium value of u for our system, at $T < T_c$. What exists in the literature (Baker 1963, Binder 1972) are estimates based on Padé approximants for the equilibrium energy in the pure phase, $u_p(T)$, i.e. along the coexistence line, and in the one phase region $\bar{\eta} = 0$, for $T \geq T_c$. As discussed in section 2.2, the size effect corrections to this energy can be expected to be very small for our system. What is not negligible for our system are the interfacial energies, which since we have a finite system (with a fixed value of $\bar{\eta}$) give a non vanishing $u_\infty(T)$ even for $T = 0$. Fisher (1975) suggested that we estimate this interfacial energy, $u_I(T)$, for $T < T_c$, by multiplying $u_I(0)$ by the surface tension $\sigma(T)$. This would give

$$u_{\infty}(T) \simeq u_I(0) \sigma(T) + u_p(T), \quad (4.6)$$

where $\sigma(T) = 0$ and $u_p(T)$ is the one-phase equilibrium u for $T \geq T_c$, and $\sigma(0) = 1$, $u_p(0) = 0$. The values of $u_{\infty}(T)$ obtained in this way, using for $\sigma(T)$ the results of Monte-Carlo computations (Leamy et al. 1973), are listed in Table 4.6 ; its accuracy is uncertain (see section 4.6). Above T_c it was possible to obtain the value of $u_{\infty}(T)$ in our system from the Padé approximation and/or by means of the simulation technique, as described in section 4.6. This gives, excluding the very early times, an asymptotic behavior, Figs. 42 - 45,

$$u - u_{\infty}(T) \simeq \alpha'(t + 10)^{-b'} \pm \Delta' \quad (4.7)$$

We have also looked at the behavior of $\log[u - u_p(T)]$ and find that

$$u - u_p(T) \simeq \alpha''(t + 10)^{-b''} \pm \Delta'' \quad (4.8)$$

The parameters in relations (4.5), (4.7) and (4.8) at different temperatures and compositions are listed in Table 4.3. In the two dimensional case Bortz et al. (1974) found for

$T/T_c =$	$\bar{\eta} = 0$				$\bar{\eta} = -0.6$			
	0.6	0.8	0.9	1.1	1.5	0.6	0.9	1.1
b	0.17	0.10	0.06	0.01	0.002	0.16	0.02	0.003
b'	0.22	0.23	0.24	0.79	1.26	0.28	0.14	1.06
b''	0.18	0.16	0.13	0.79	-	-	-	-
Δ	0.3	0.5	0.5	0.2	0.2	0.5	0.3	0.2
Δ'	0.7	1.5	2.1	12.8	61.2	2.1	2.7	18.5
α	1.78	1.55	1.35	1.20	1.27	1.31	0.80	0.81
α'	1.78	1.59	1.32	1.33	1.71	1.71	0.19	0.83

Table 4.3. Values of b , b' , b'' , α , α' and α'' and values of Δ , Δ' and Δ'' in percent corresponding to the relations (4.5), (4.7) and (4.8).

$\bar{\eta} = 0$, $b \approx b'' \approx 1/5$ at $T = 0.6 T_c$ and $b' \approx 7/12$ for $T = 1.1 T_c$ (the only two points analysed there). The extension of the computations at $T = 0.6 T_c$ in that case to much longer times gives $b \approx 1/4$ (Rao et al. 1975).

The behavior of b at the lowest temperatures is in good accord with the prediction of the cluster dynamics theory in section 3.4 which gives, at "low temperatures", $b'' = (d + 3)^{-1}$ with d the dimensionality of the space considered. For $T > T_c$

this theory predicts $b' \simeq d/2$ and a change-over effect at $T \simeq T_c$ with $b'' \simeq 0.36$ or $b'' \simeq 0.24$, that might still affect the behavior at $T = 1.1 T_c$ (Binder 1975); there is also in this case some support from our data.

It is not clear to us at the present time how much weight one should put on the fits or misfits between our results and the predictions. Our data is limited and the theory may or may not be adequate. In fact, as also has been pointed out by Binder (1975), the inspection of the figures 43 and 45 seems to indicate a certain time dependence in b' (and also in a) and perhaps a change-over effect in the behavior of $u - u_\infty(T)$ vs. time at a definite, temperature-dependent value of the time. The data from very early times is reasonably fitted by a power law with the exponents given in Figs. 43 and 45 (or in Figs. 39 and 41 for the behavior of u with time). After a temperature dependent interval of time there is a short interval during which the exponents change rapidly to a new value. After this, and during most of the evolution we have studied, the exponents in Figs. 42 and 44 describe fairly well the temporal dependence of the excess energy. We have at the present time no adequate explanation of this effect, nor do we know if it has any actual significance, but it is interesting to note that Langer et al. (1975) have found a similar temporal break on certain occasions in the solution of eq. (3.18) with (3.23). One cannot

Figs. 4.38-4.41

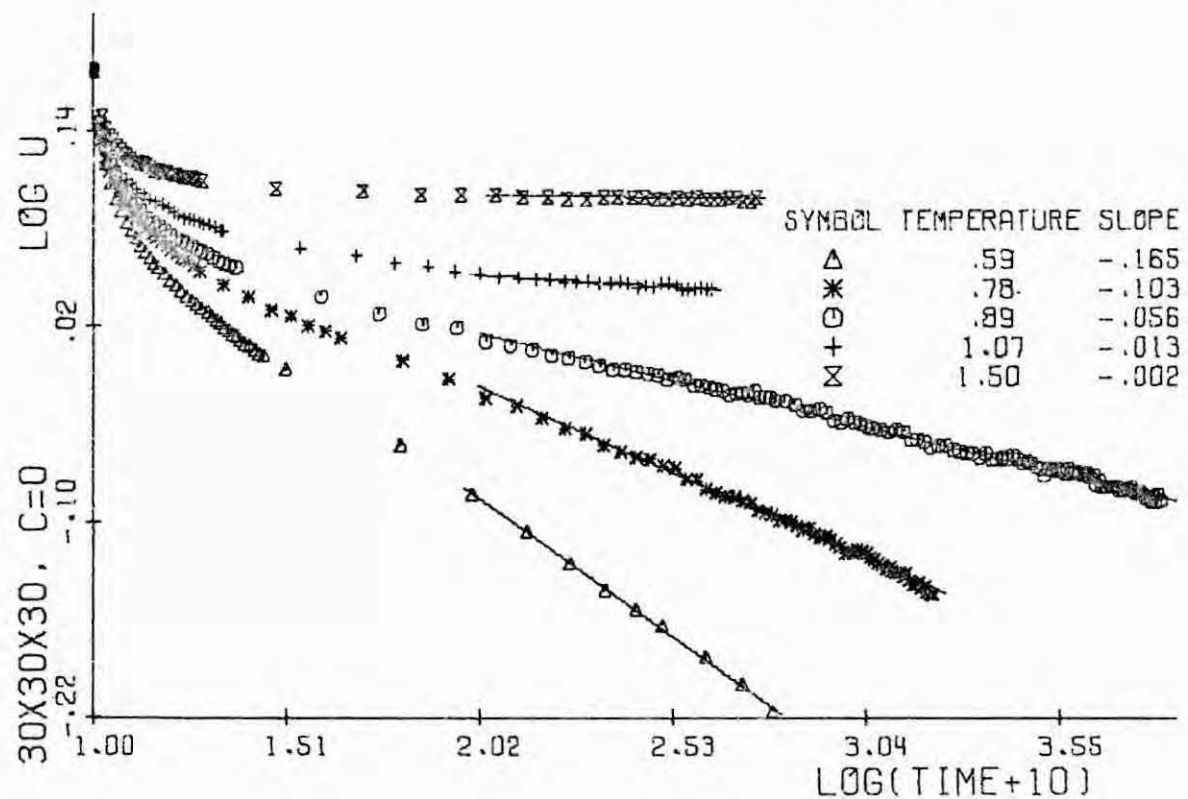
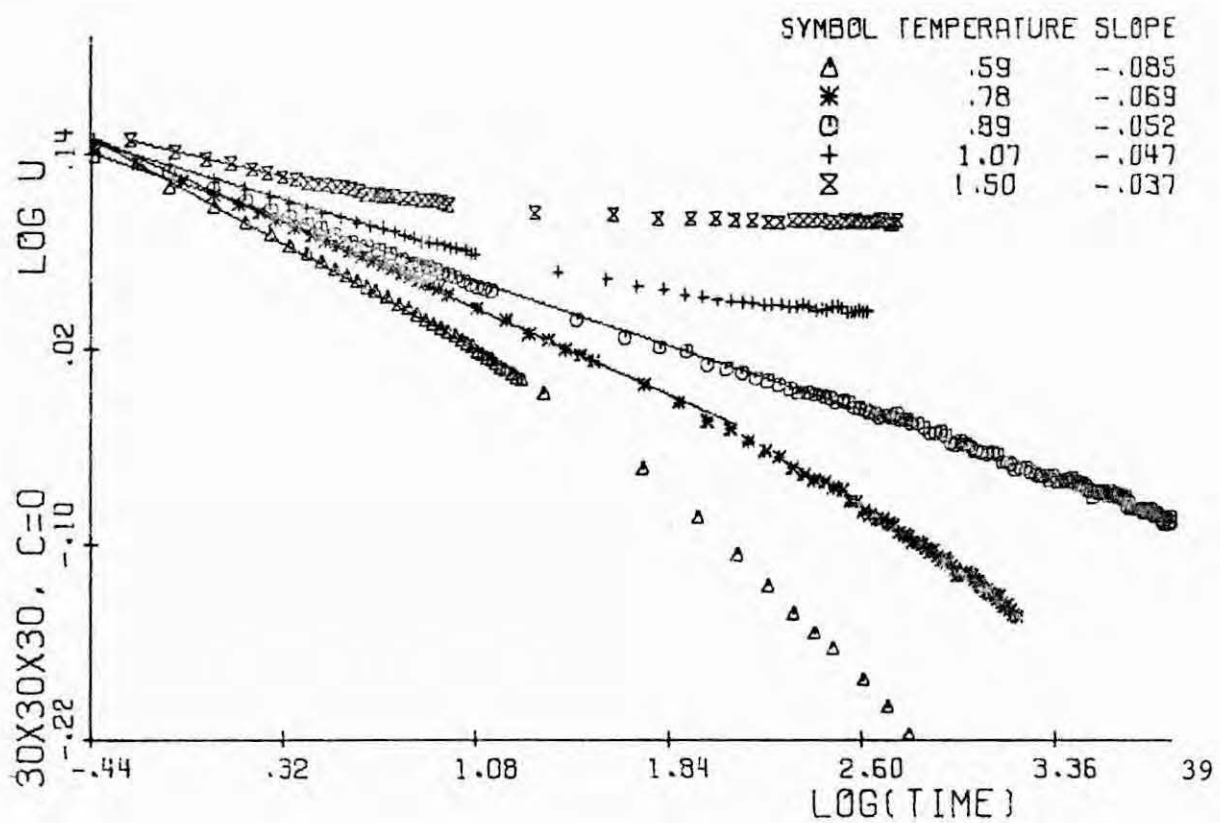
Logarithmic plot of u , a measure of the energy of the system, vs. t for different temperatures. In Figs. 39 and 41 the early data is fitted. Note in these figures a temporal variation (of different sign below T_c than above T_c) of the slope.

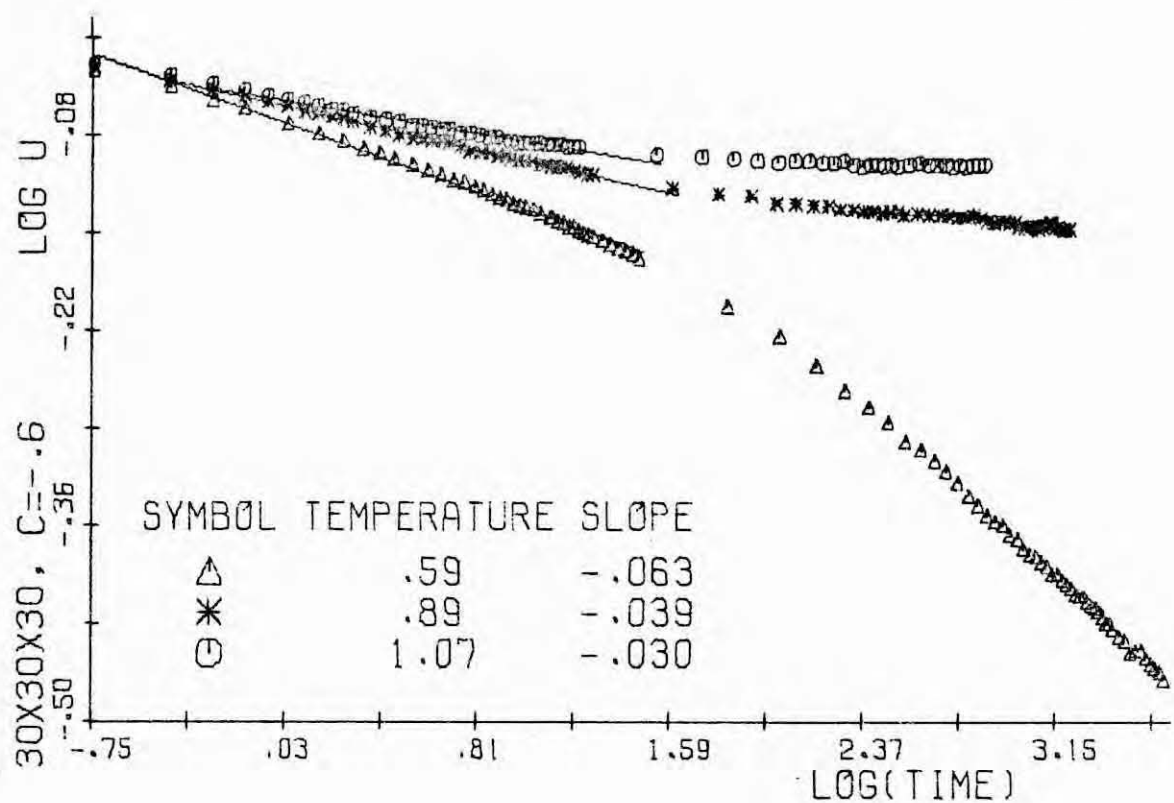
Figs. 4.42-4.45

Logarithmic plot of $u - u_\infty(T)$, $u_\infty(T)$ is the equilibrium energy of the system, vs. time. In Figs. 43 and 45 the early evolution is emphasized. The change-over effect described in the text, is clear. Note the peculiar graph for $T/T_c = 0.9$, $\bar{\eta} = -0.6$ in Fig. 45.

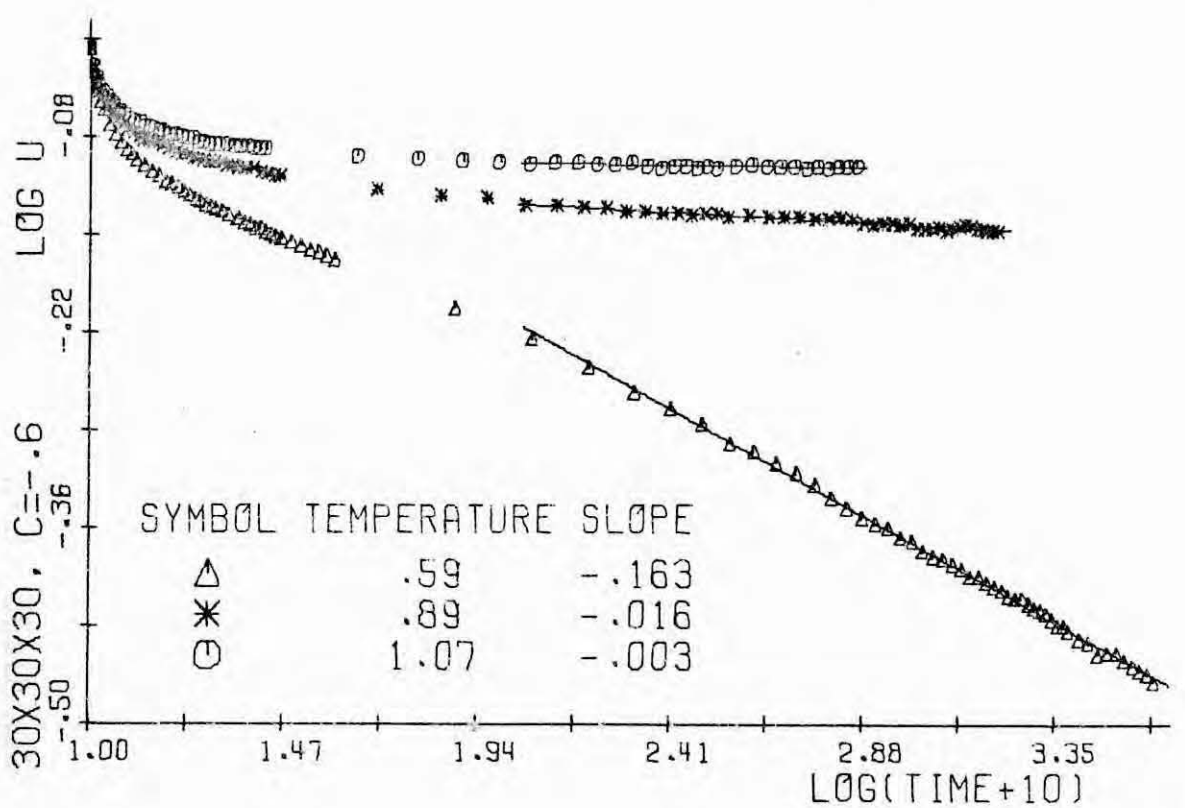
Figs. 4.46-4.47

Logarithmic plot of the number of (actual) exchanges vs. time for different temperatures. The straight lines, whose slope is shown, correspond to a least-square fit to the data for $t \geq 50$.

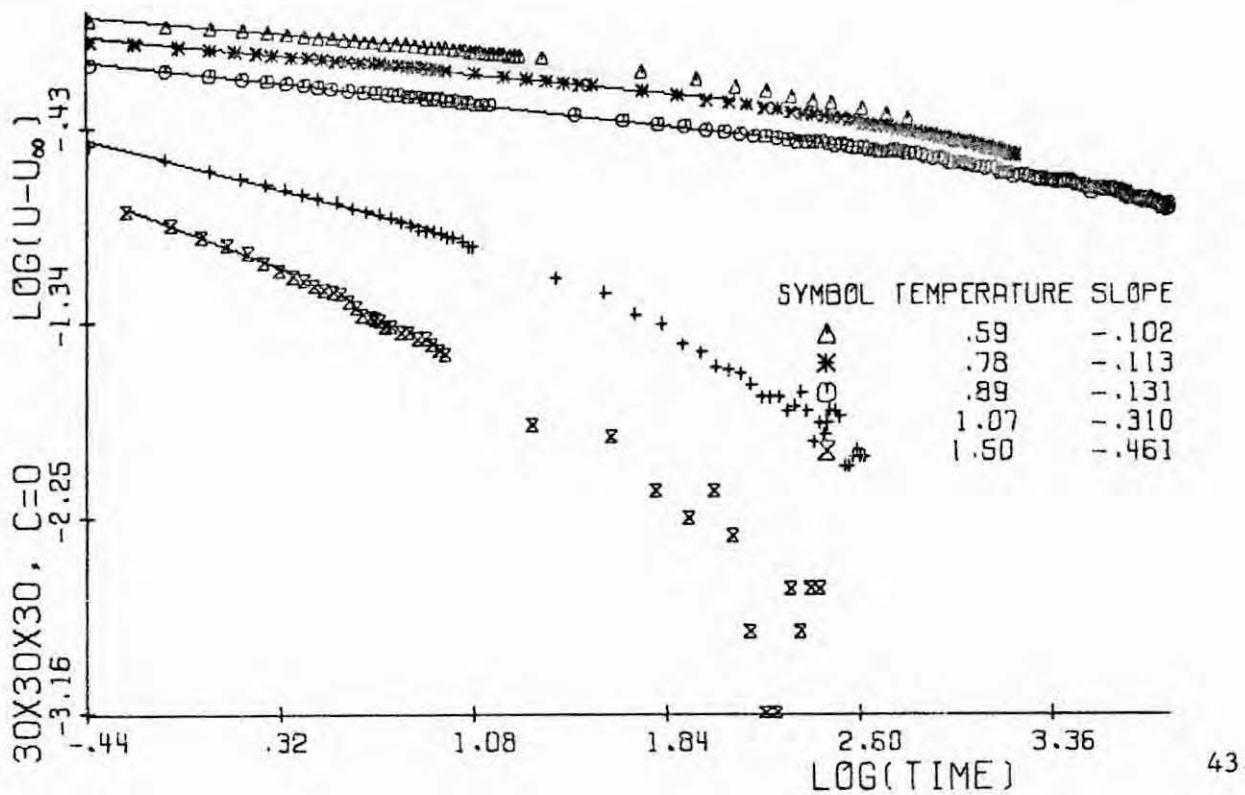




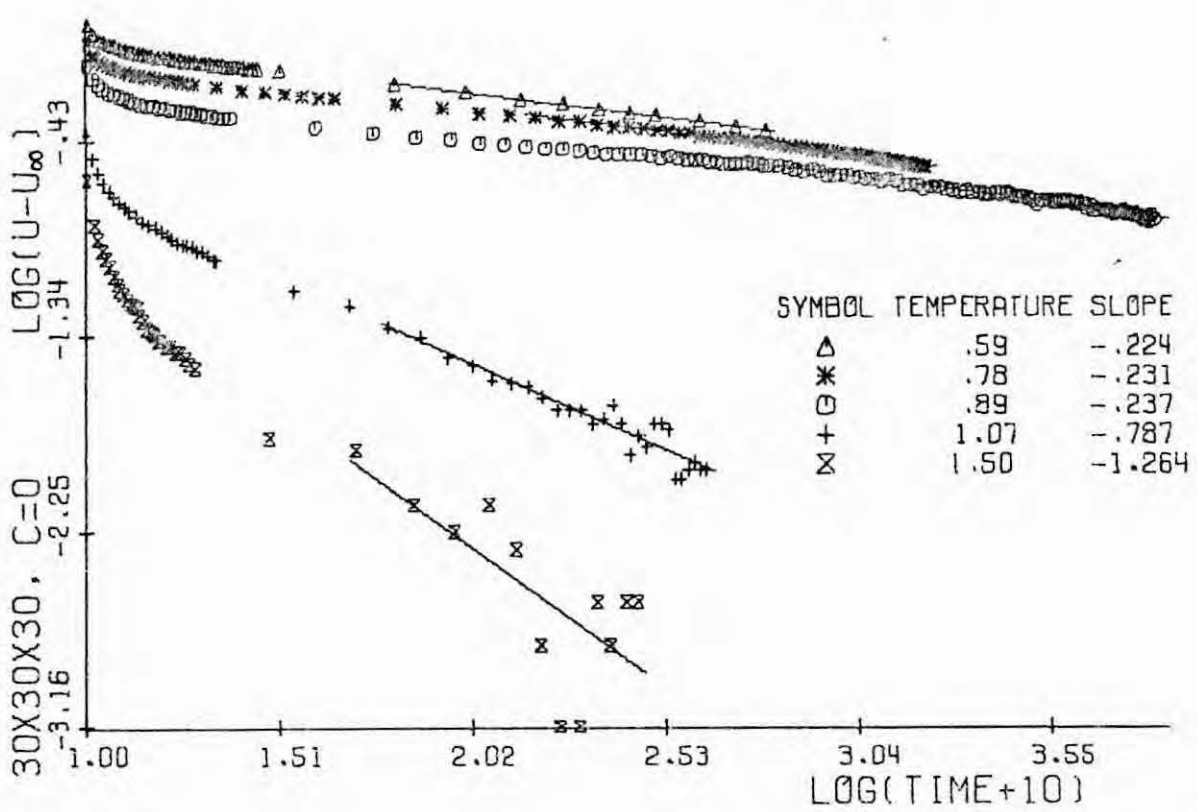
41



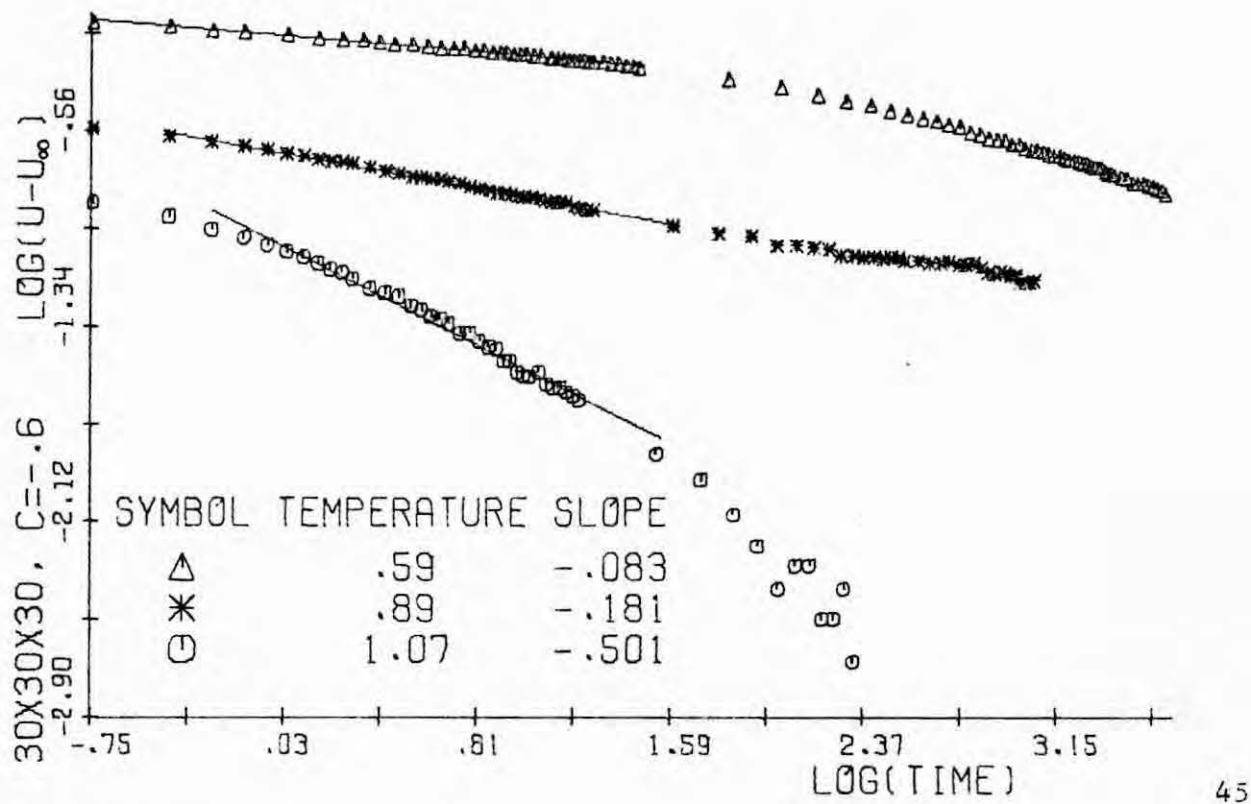
40



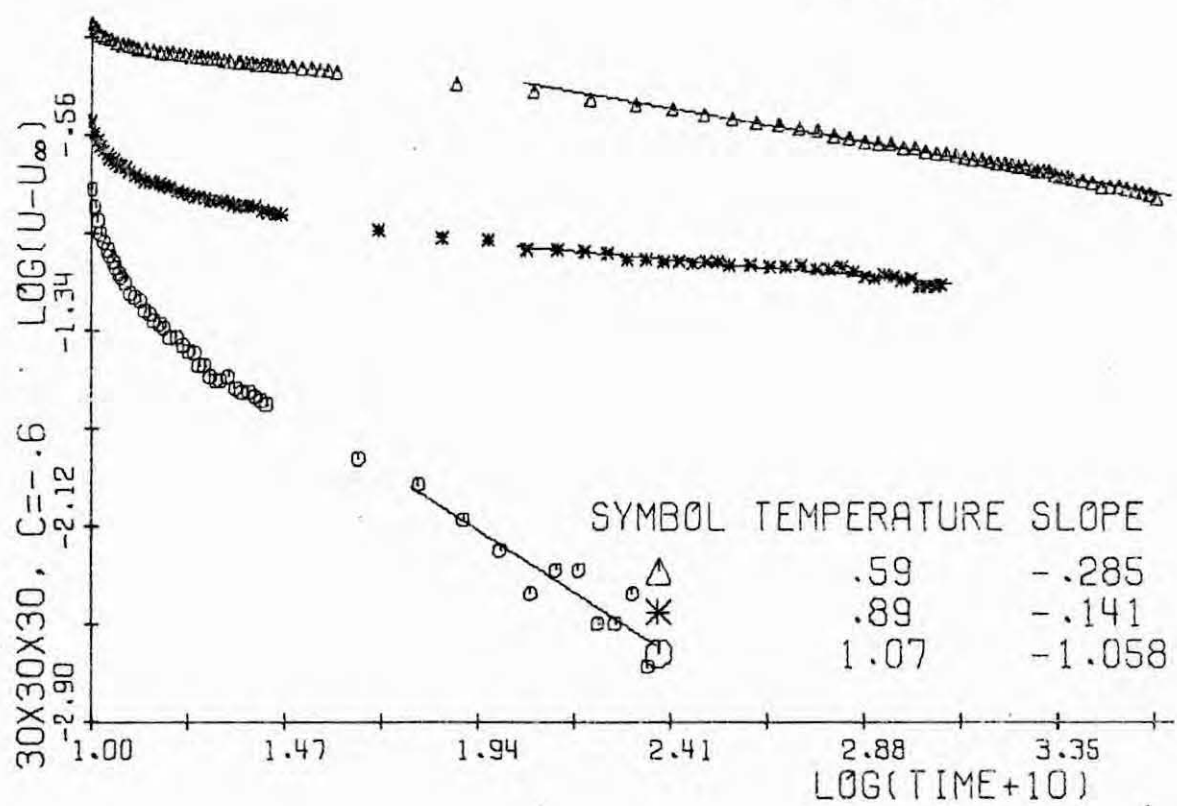
43



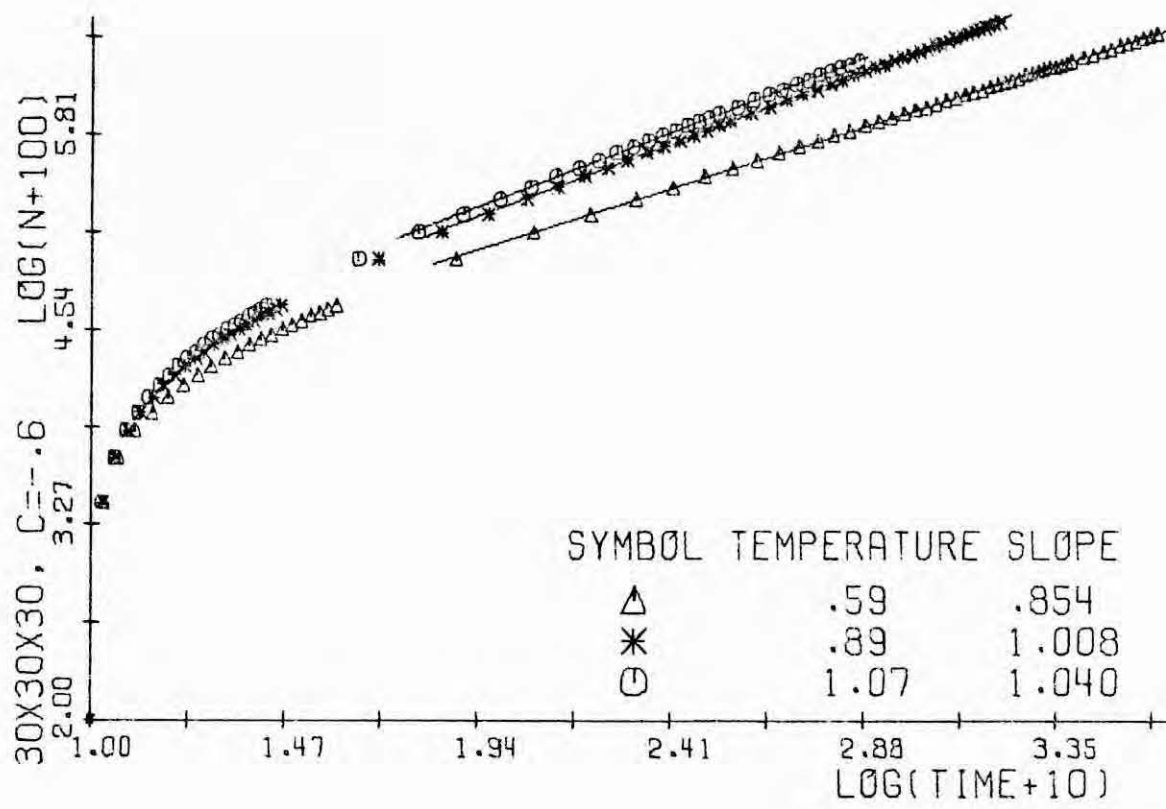
42



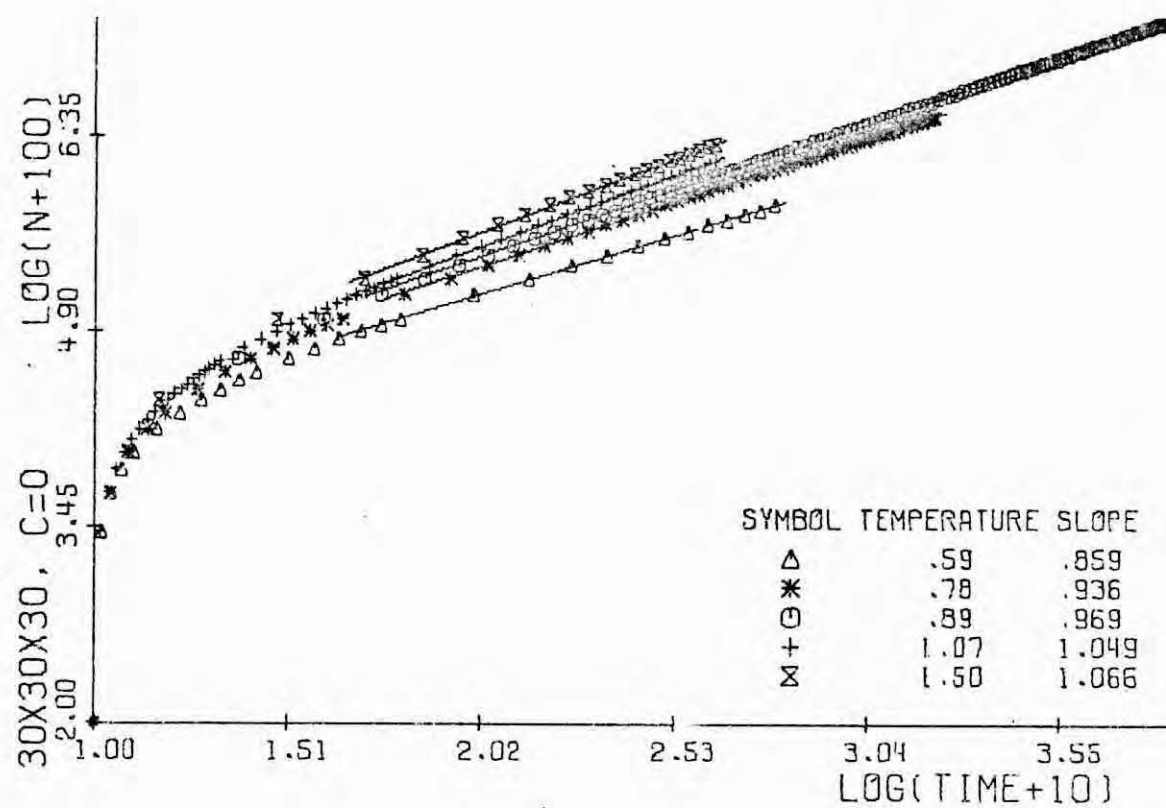
45



44



47



46

expect, on the other hand, the basic cluster dynamics sketched in section 3.4 to account for this effect. This may indicate a slight change in the clustering mechanism below T_c (see Fig. 43) when a certain cluster size is predominant in the system. Note that the time at which the change-over is observed below T_c increases with temperature, while above T_c the effect appears much earlier, the time of its appearance becoming smaller for higher temperatures.

The number of exchanges vs. time is plotted in Figs. 46-47. We expect that the slope of this graph, the number of exchanges per unit time, should behave, at the lower temperatures, approximately like the number of A-B bonds, and this is confirmed by the results. It is not exactly the same since the probability of an exchange depends on the configuration on the sites surrounding the A-B pair. When the A and B regions are well segregated however this should affect the rate only through a constant factor.

4.3. - Scaling Analysis.

The introduction of dynamical scaling can, in principle, remove the temperature and composition dependence from our data allowing a detailed comparison with Langer's theory. Assuming the validity of dynamical scaling (Kawasaki 1966, Kadanoff et al.

1967, Tarko and Fisher 1975) the function $S(k, t)$ may be expressed in the vicinity of the critical temperature $T \lesssim T_c$ in a "universal form" $\mathcal{J}(q, \tau)$ in terms of the dimensionless variables

$$\tau = \alpha_1(1 - \tilde{\eta}^2) (1 - T/T_c)^{\gamma+2\nu} t, \quad q = \alpha_2(1 - T/T_c)^{-\nu} k \quad (4.9)$$

$$\mathcal{J}(q, \tau) = \alpha_3(1 - T/T_c)^\gamma S(k, t). \quad (4.10)$$

The values of the parameters in these equations for the kinetic three dimensional model simulated here are given by Langer et al. (1975) as

$$\gamma = 5/4, \nu = 9/14, \alpha_1 = 3.51, \alpha_2 = 0.35 \text{ and } \alpha_3 = 2.59. \quad (4.11)$$

The power-law temperature dependence in (4.9) and (4.10) with the above exponents is known to be valid only very near T_c . In order to extend the validity of the scaling to other temperatures, low (or high) temperature expansions (Essam and Fisher 1963) should be used instead. On the other hand, the calculation of α_1 , α_2 , and α_3 , (4.11), involves the assumption of a Ginzburg-Landau polynomial for the free energy density of the system and this may seriously affect the results, especially at $\tilde{\eta} \neq 0$. These

assumptions may cause (at least in part) the reported disagreement between the calculation by Langer et al. at the spinodal line and our results at $\bar{\eta} = -0.6 T_c^*$, and therefore we shall only perform here the scaling analysis of our data at $\bar{\eta} = 0$.

In Fig. 48 we plot $\mathcal{J}(q, \tau)$ for $\bar{\eta} = 0$ as a function of τ for selected values of q . If scaling is valid and we were in the region of scaling (which we definitely are not for $T = 0.6 T_c$ and only marginally for $T = 0.8 T_c$) then, for a given q , $\mathcal{J}(q, \tau)$ should be the same function of τ for different temperatures. Surprisingly enough for $q \approx 1$ this is the case even for $T = 0.6 T_c$. For smaller values of q the deviations increase as τ increases. The dotted lines in Fig. 48 correspond to Langer's calculations for values of q close to the ones reported by us. It is because of the scaling of t that we ran our computer simulations to larger values of t for $T = 0.9 T_c$.

*We note that the position of this phase point relative to the spinodal line is critically affected by the definition of that line. If one defines the spinodal by $\bar{\eta}_s = (1.57/\sqrt{3})|T-T_c|^{5/16}$, implied by (4.9) and (4.10) with (4.11), the point ($\bar{\eta} = -0.6, T/T_c = 0.6$) lies, at difference from the case in Fig. 2.1, well inside of the spinodal region. According to a molecular-field-free-energy density (Suzuki and Kubo (1968)), this point is also inside this region, but very close to the spinodal line.

In terms of the reduced variables q and τ , eq. (3.18) with Langer's approximation (3.23) leads to

$$\frac{\partial \mathcal{J}(q, \tau)}{\partial \tau} = -q^2[q^2 + \tilde{\gamma}(\tau)] \mathcal{J}(q, \tau) + q^2 \quad (4.12)$$

with $\tilde{\gamma}(\tau)$ the scaled $\gamma(t)$ in (3.23). It was this equation which was solved by Langer et al. (1975) and the results compared in part with preliminary data from our computer simulation. We make such a comparison in Figs. 49 - 52 where we compare the function $\mathcal{J}(q, \tau)$ obtained from (4.12) (and an equation for $\tilde{\gamma}(\tau)$ obtained from (3.19) after simplifying assumptions; Langer et al. 1975) with the results of our simulation. The agreement for $T = 0.8 T_c$ and $0.9 T_c$ in this case is quite impressive. As a more direct, and more stringent, test of the approximation (4.12) we have also plotted in Fig. 53 the function

$$\Gamma(q, \tau) \equiv \left[\frac{1}{q^2} \frac{\partial \mathcal{J}(q, \tau)}{\partial \tau} - 1 \right] \mathcal{J}^{-1}(q, \tau) + q^2 \quad (4.13)$$

which is taken directly from our computer simulation. Function (4.13) corresponds to the negative of $\tilde{\gamma}(\tau)$ in eq. (4.12); thus, according to the approximation (3.23), $\Gamma(q, \tau)$ should be independent of q and of the temperature T if $T \lesssim T_c$. Fig. 53

shows again a surprising temperature independence, even outside the scaling region, and a definite dependence in q that is not included in Langer's approximation (which gives the dashed line in Fig. 53).

We also note that Cook's equation, (3.21), follows from eq. (4.21), using the scaling relations (4.9) and (4.10), when $\tilde{\gamma}(\tau)$ is given by

$$\tilde{\gamma}(\tau) = \frac{2M(\partial^2 f / \partial \eta^2)_{\eta=\bar{\eta}}}{\alpha_2^2 \alpha_3} (1 - T/T_c)^{2\nu-\gamma}, \quad (4.14)$$

where, according to (4.11), $2\nu-\gamma$ is close to zero and $M(\partial^2 f / \partial \eta^2)_{\eta=\bar{\eta}}$ is the classical diffusion constant. Thus, the linear fluctuation theory implies a constant value for our function (4.13).

In Figs. 54 - 55 we plot the function $R(q, \tau)/q^2$ where R is the logarithmic derivative of \mathcal{L} ,

$$R(q, \tau) \equiv \frac{\partial}{\partial \tau} \ln \mathcal{L}(q, \tau). \quad (4.15)$$

The linear classical theory predicts a straight line in this case (see eq. (3.8)) whose intersection at $k = 0$ would give the negative of the diffusion constant. For this reason this is a quantity usually plotted by experimentalists, and they also

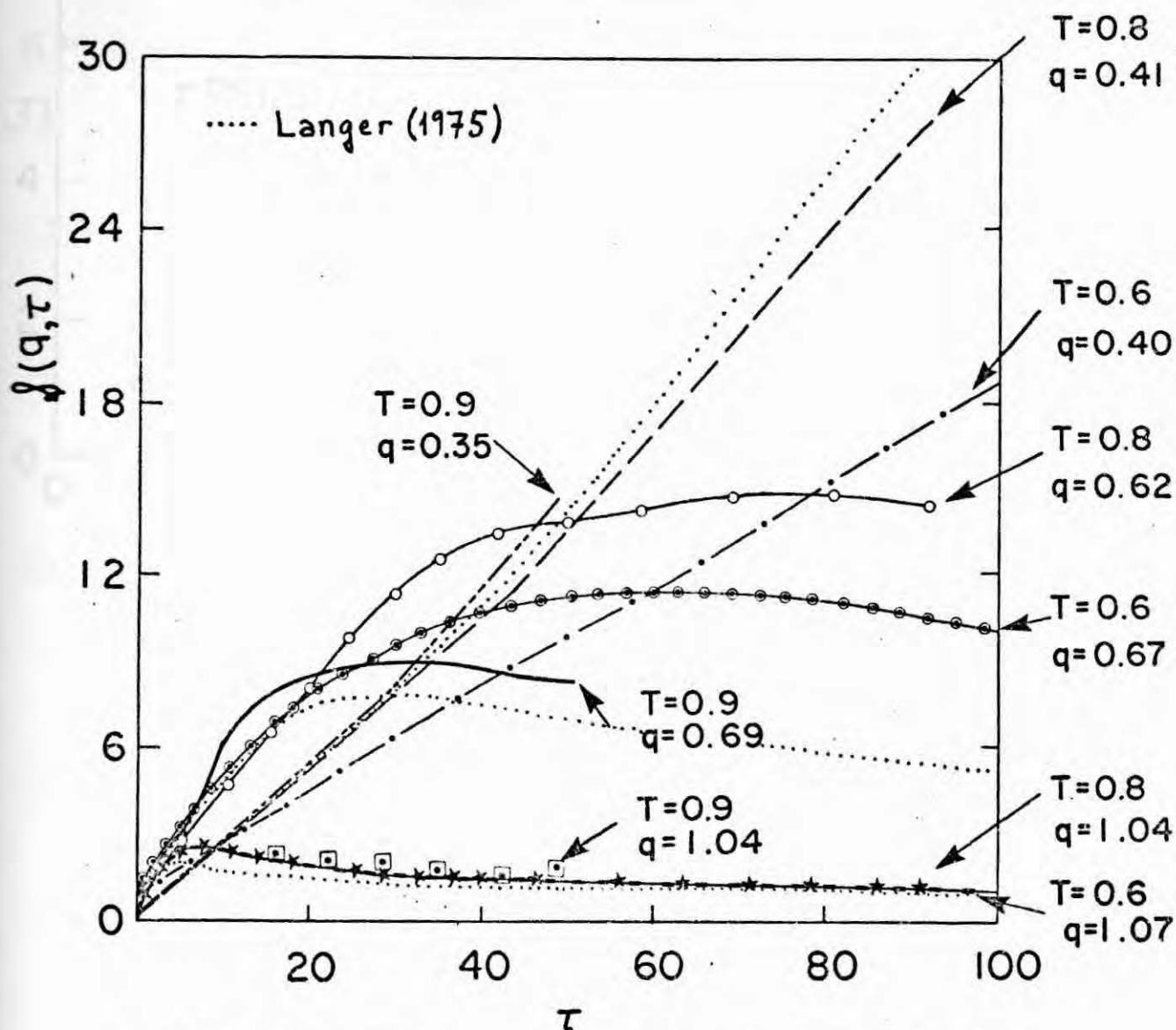


Fig. 4.48 Structure function vs. time in reduced units for three different values of q (scaled k) and different temperatures. Note that for $q \approx 0.65$ (which is in the neighborhood of $\mathcal{S}(q, \tau)$ for intermediate times; see Figs. 49-52) the results for $T/T_c = 0.9$ can be affected by the slight differences between the chosen values of q . The dotted lines correspond to the predictions by Langer et al. (1975) for similar values of q .

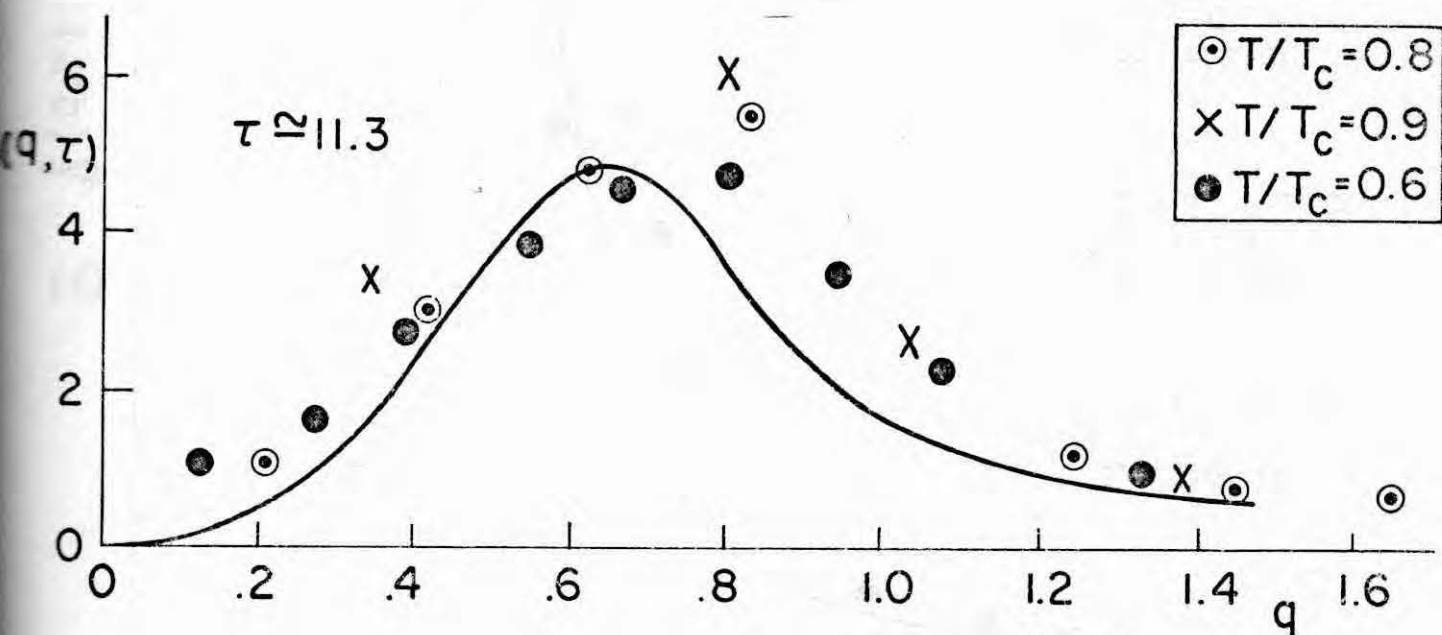
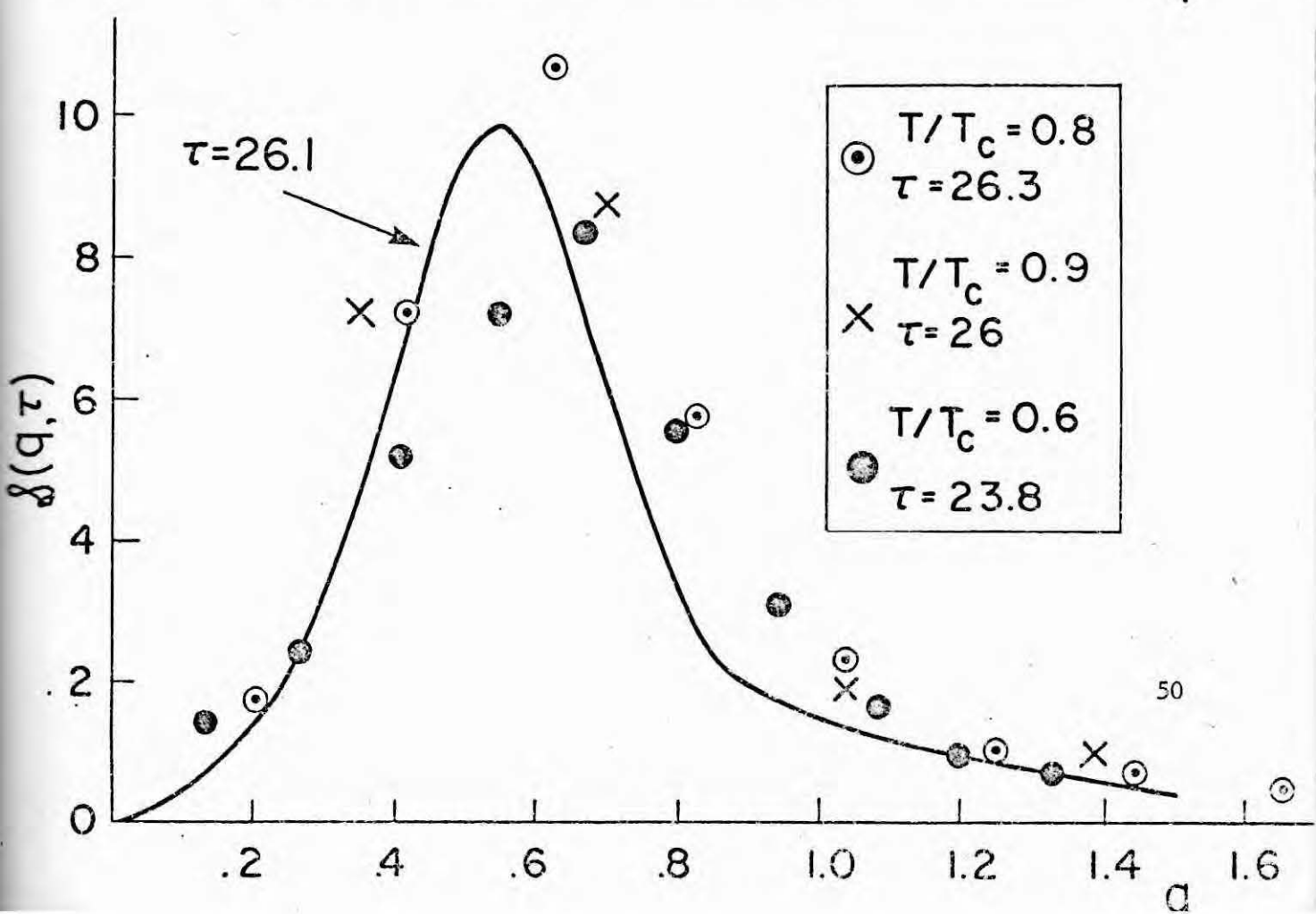
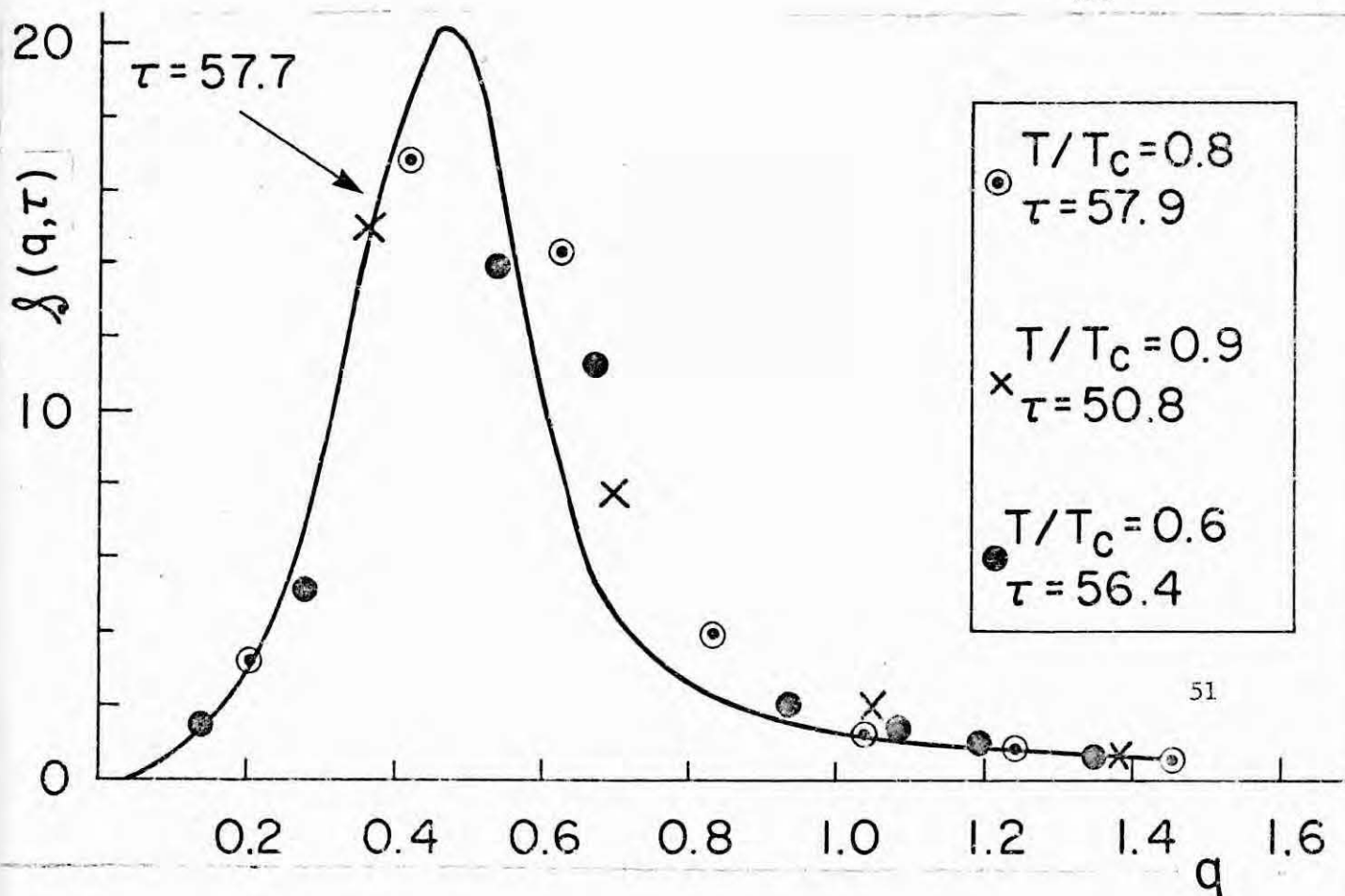


Fig. 4.49

Figs. 4.49-4.52 Comparison of the computer simulation results at different temperatures (scaled data) with the solution (solid lines; Langer et al. 1975) of equation (3.18) with the approximation (3.23) for different values of the time.

Fig. 4.53 Time evolution of the function $\Gamma(q, \tau)$ as defined in equation (4.13). The dashed line is obtained using the approximation by Langer et al. (1975).



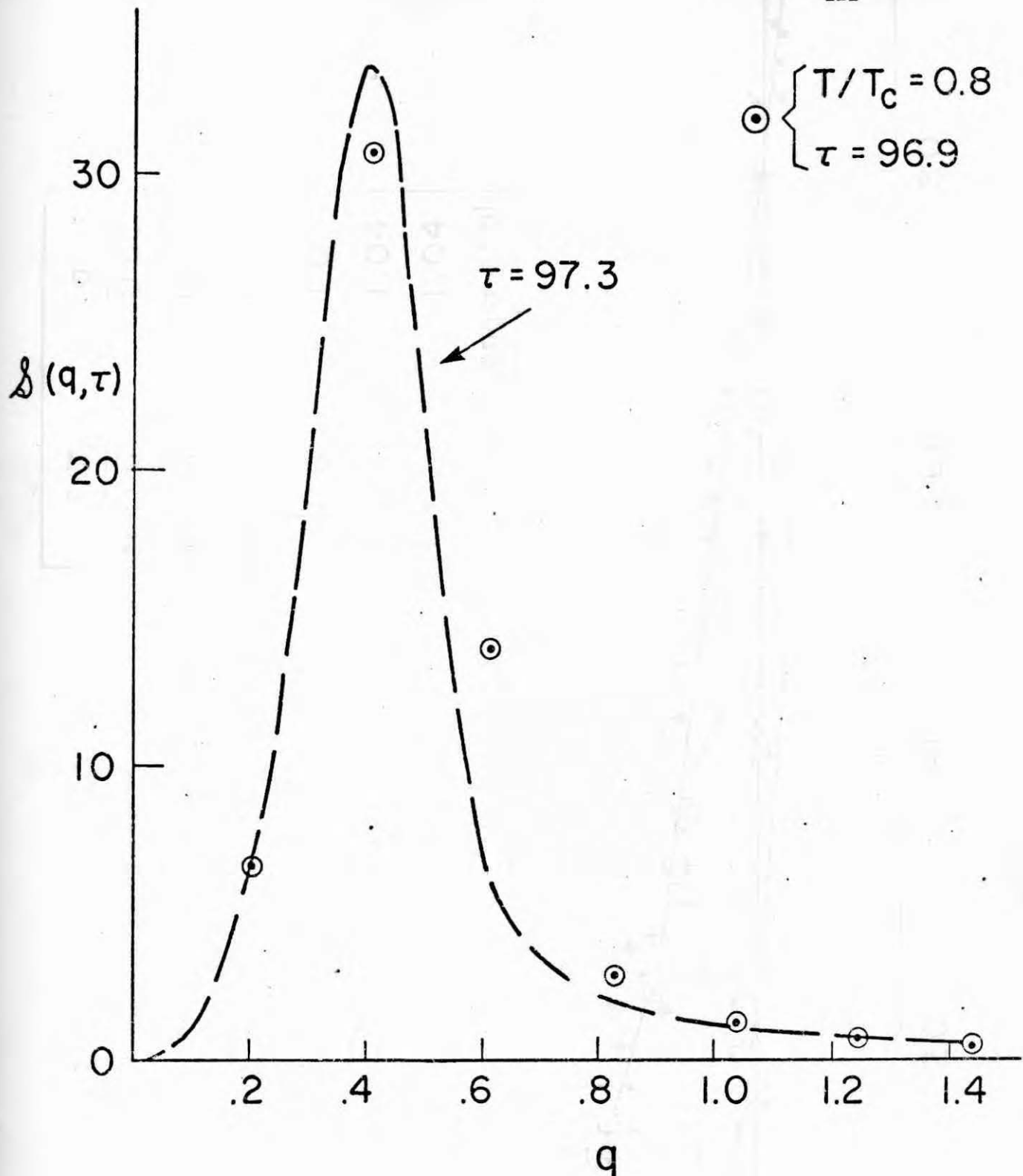


Fig. 52

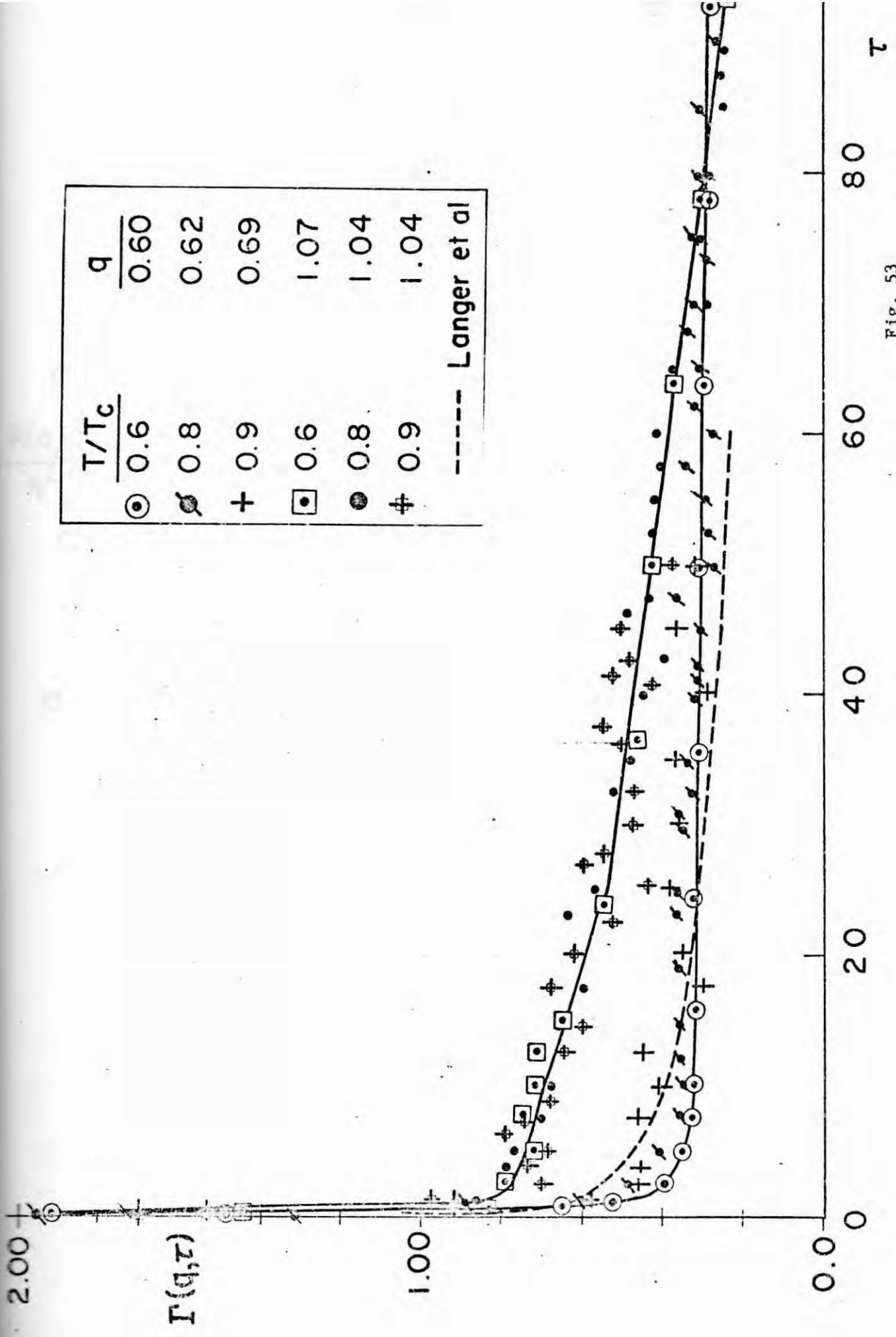
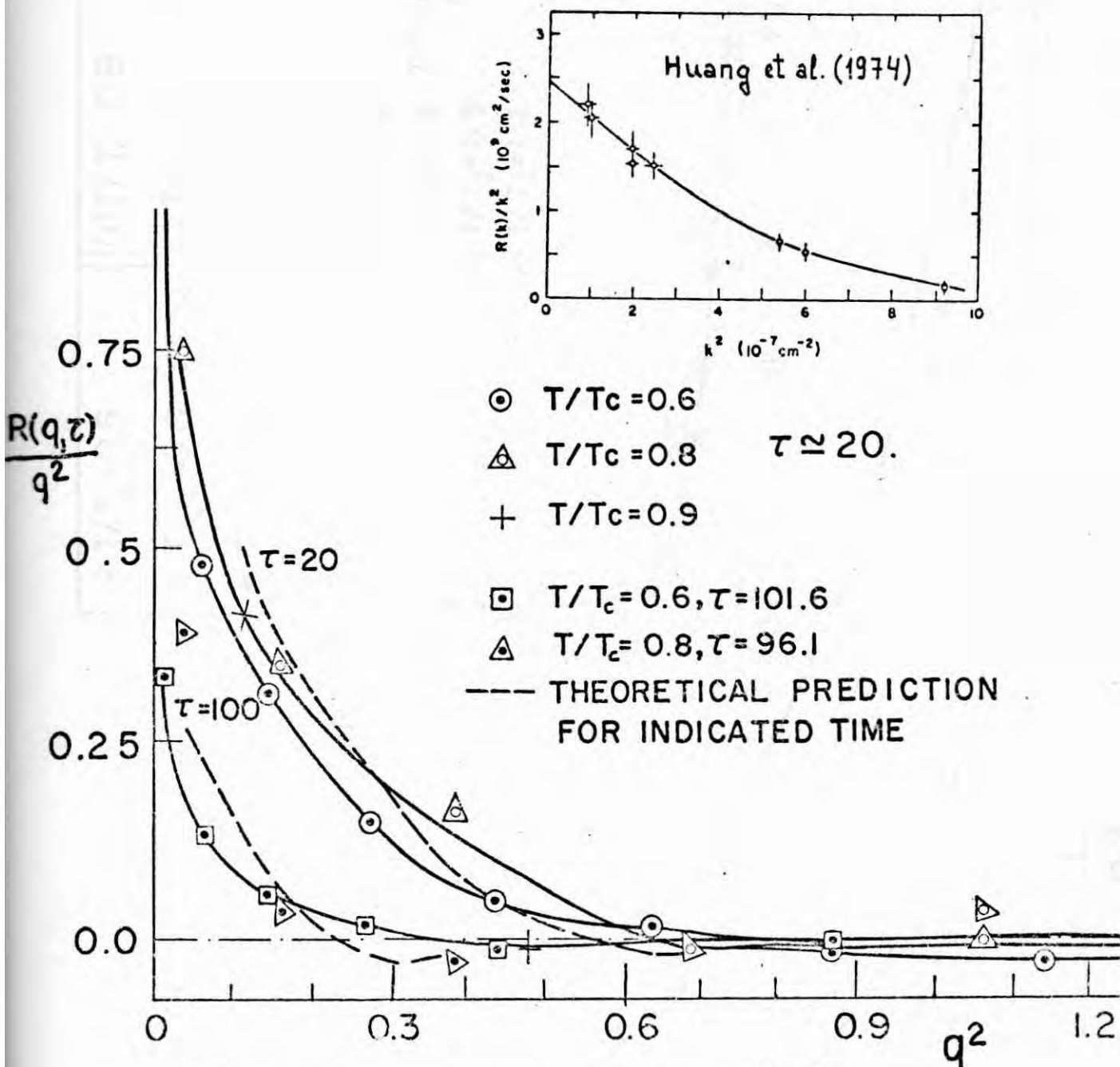
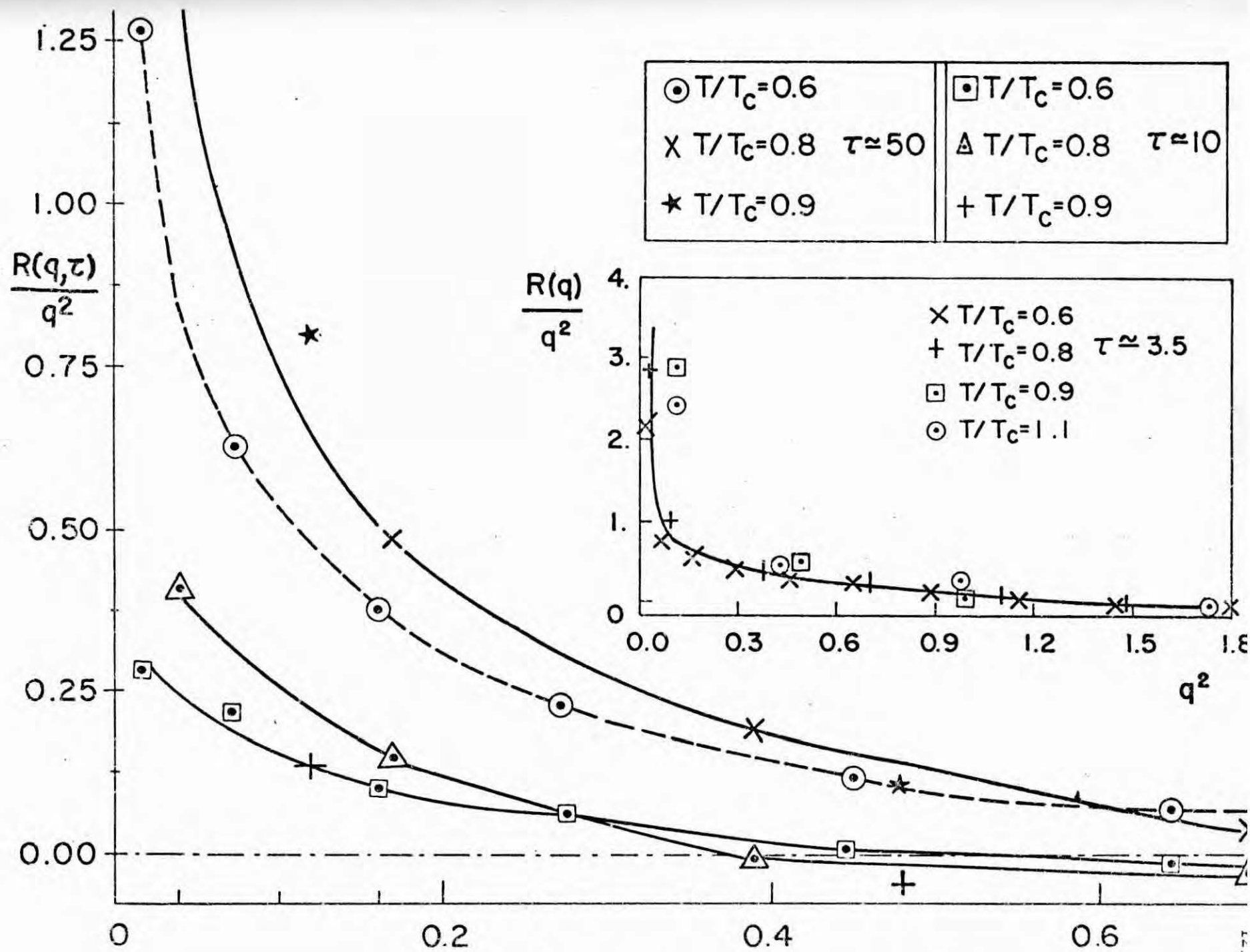


Fig. 53



Figs. 4.54-4.55 The function $R(q, \tau) / q^2$ (see eq. (4.15)) vs. q^2 for different times. The inset in Fig. 55 corresponds to very early times. There is only little temperature dependence but a definite time dependence, that has also been reported in experiments. In Fig. 54 we include the comparison for $\tau \approx 20$ and $\tau \approx 100$ with the calculations by Langer et al. The inset in that figure corresponds to a scattering experiment on the methanol-cyclohexane mixture.

Fig. 54



report a bending (and sometimes a time-dependence) qualitatively similar to the situation in Figs. 54 - 55 . Fig. 54 also contains the predictions by Langer, and the inset there corresponds to the observations (Huang et al. 1974) of the same quantity in a binary mixture of methanol and cyclohexane quenched to about 2mK below its critical temperature ($T_c = 45.14^{\circ}\text{C}$). Surprisingly enough for a liquid mixture (where hydrodynamic effects are expected to be of importance in the coarsening process) these detailed observations of phase separation (also Huang et al. 1975) bears, during most of the evolution, a great qualitative similarity with our observations near T_c .

4.4. - Clusters analysis.

We report here our observations concerning the formation of "clusters" as the system evolves in time. A "cluster" is defined as a group of A-atoms linked together by nearest-neighbor bonds. It turns out that there is an essential difference between two- and three-dimensional systems with the same composition so that, in addition to the $30 \times 30 \times 30$ lattice so far considered, we have also studied cluster formation in the 80×80 , 200×200 and $50 \times 50 \times 50$ lattices*.

* Other results on these systems will be reported elsewhere
(Rao et al. 1975).

In two dimensions we are reporting the cluster analysis corresponding to six statistically independent evolutions for the 80×80 system and one evolution for the 200×200 system, all of them (which were run to comparatively very large values of t) at $T/T_c = 0.588$ and $\tilde{\eta} = -0.6$. In three dimensions we report an average over eight independent evolutions for the $30 \times 30 \times 30$ system at $\tilde{\eta} = -0.6$ and each of the following temperatures: $0.6T_c$, $0.9T_c$, and $1.1T_c$; and one evolution for the $50 \times 50 \times 50$ lattice at each of the phase-points: $(\tilde{\eta} = -0.6, T/T_c = 0.59)$, $(\tilde{\eta} = -0.75, T/T_c = 0.59)$ and $(\tilde{\eta} = -0.88, T/T_c = 0.59)$.

For two-dimensions we present in Appendix C, Figs. C.1-C.16, histograms at different values of the time showing the per cent of A-particles in the system which constitute clusters of a given size. In this case, given the similarity of the results from the two different studied lattices, we combined the results from the seven evolutions, each weighted according to the number of particles in the corresponding system. In addition, each graph there includes the information from a certain time interval (see figures captions). The qualitative behavior shown by these figures is much as expected, and they look similar to experimental histograms. In Fig. 56 are sketched, from left to right, the theoretical cluster distributions at some given "late" time according to Lifshitz and Slyozov, eq. (3.12), to Wagner, eq. (3.14), and a characteristic experimental one (Smith 1967). On occasions

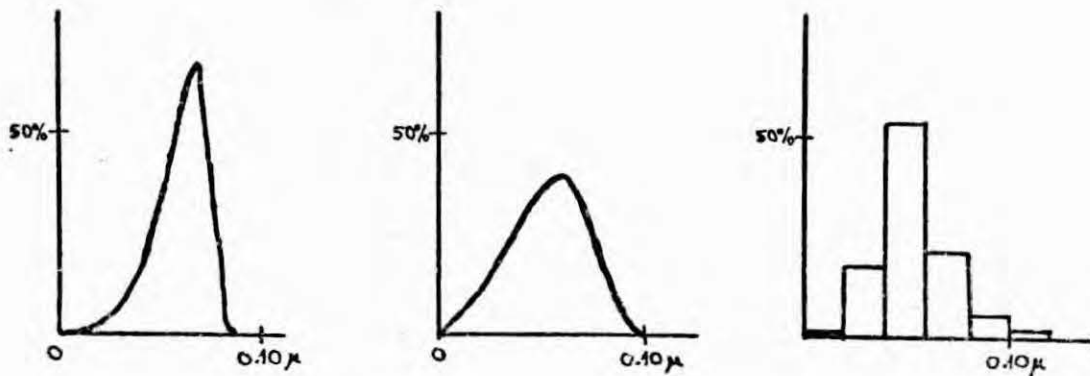


Fig. 4.56 Clusters distributions (per cent of particles vs. clusters size in microns) at some late time after the quench according to, from left to right, Lifshitz and Slyozov, Wagner, and experimental observation on Mn-Mg (Smith 1967).

(Ardell 1969), the experimental histograms agree better with the Lifshitz-Slyozov distribution (and, in consequence, worse with our Figs. C.1-C.16 corresponding to a two-dimensional system) than the one transcribed in Fig. 56.

We have also looked at the behavior of the following quantities in the system: the average cluster size,

$$\bar{\ell} = \frac{\sum_{\ell_i < \ell < \ell_f} \ell n_\ell}{\sum_{\ell_i < \ell < \ell_f} n_\ell}, \quad (4.16)$$

with n_ℓ the number of clusters made up of ℓ particles, the standard deviation for the distribution of sizes,

$$\Delta \ell = \sqrt{\ell^2 - \bar{\ell}^2}, \quad (4.17)$$

the average cluster "radius",

$$\bar{A} = c \bar{\ell}^{1/d}, \quad (4.18)$$

with d the dimensionality of the system and $c = (3/4\pi)^{1/3}$ for $d = 3$ and $c = 1/\sqrt{\pi}$ for $d = 2$, the average cluster energy,

$$\bar{\epsilon} = \frac{\sum_{\ell_i < \ell < \ell_f} \epsilon_\ell n_\ell}{\sum_{\ell_i < \ell < \ell_f} n_\ell}, \quad (4.19)$$

and the average ratio ("surface/volume"):

$$\overline{\epsilon/\ell} = \frac{\sum_{\ell_i < \ell < \ell_f} (\epsilon_\ell n_\ell / \ell)}{\sum_{\ell_i < \ell < \ell_f} n_\ell}. \quad (4.20)$$

ϵ_ℓ is the number of A-B bonds of a given cluster of size ℓ . For the two-dimensional system, $\ell_i = 10$ and ℓ_f is large enough to include all clusters. The numerical data is tabulated in Tables A.17-A.18, and its analysis, according to predictions in chapter III, is summarized in Figs. 57-63. Fig. 57, including the data from the 80×80 and 200×200 lattices and the mentioned temporal average, indicates

$$\bar{\ell} \approx \alpha t^\alpha \quad (4.21)$$

with $a \simeq 0.36$ for $t \geq 1000$; the earlier evolution does not seem to follow (4.21), as seen in Fig. 58. This later figure also shows that the medium cluster size for any time is slightly larger in the 80×80 lattice. Binder and Stauffer (1974) predicted (4.21) with $a = 0.4$ at "low temperatures". We also find for the average radius:

$$\bar{A} \sim t^{a'} \quad (4.22)$$

with $a' \simeq 0.18$ ($\simeq \frac{1}{2} a$) for $t \geq 1000$. In Figs. 59-60, which refer to the same data as above, we emphasize the fact of the ambiguity of that kind of plots, which are used by experimentalists to confirm Lifshitz-Slyozov, (3.13), or Wagner, (3.15), laws. Figs. 59-60, however, show more transparently than Figs. 57-58 a change-over effect similar to the one discussed in section 4.2.

According to Fig. 61,

$$\overline{\epsilon/\ell} \sim \beta t^{-b} \quad (4.23)$$

with $b \simeq 0.44$ for $t \geq 1000$ (and $b \simeq 0.47$ for $t \geq 4000$); the data in tables A.17-A.18, however, shows a size-dependence (the only one which affects the temporal behavior) in the decay with time of $\overline{\epsilon/\ell}$ (actually we obtain for $t \geq 4000$, $b \simeq 0.60$ for the system of 6400 spins and $b \simeq 0.43$ for the one with 40,000 spins.)

Fig. 62 also refers to the evolution with time of the clusters compactness; we obtain (size-independently)

$$\epsilon \simeq \beta' \bar{\lambda}^{b'} \quad (4.24)$$

with $b' \simeq 0.488$ for $t \geq 1000$ and $b' \simeq 0.492$ for $t \geq 4000$, very close to the value $1/2$ of the contour/area ratio. Fig. 63 shows the evolution with time of the standard deviation (4.17).

The evolution with time of the cluster distribution in the $30 \times 30 \times 30$ lattice at $\tilde{\eta} = -0.6$ and different temperatures is shown in Figs. C.17-C.50. There becomes evident an essential difference with clustering in a two-dimensional system with the same composition. Instead of the peaked distribution of the later, the histograms for three dimensions present (or have the tendency to), after a relatively very short time which increases with temperature, two different maxima. In fact, each of the eight evolutions at $T/T_c = 0.6$ showed very early one or two clusters totalizing between 2000 and 5000 particles (see for instance the cluster distribution accompanying Figs. B.1-B.19 which correspond to a single run). At $T/T_c = 0.9$ (Figs. C.31-C.40 and B.20-B.24) the big clusters appear much later and, at a given time, their size is smaller than at $0.6T_c$. Above T_c (Figs. C.41-C.50 and B.25-B.30) only one out of the eight runs developed a big cluster of about 1500 particles and the

distributions present no second maximum as it occurs below T_c .

This interesting behavior, very different from the one reported by experimentalists for real alloys (see Fig. 56 and section 4.7), seems to be a consequence of the natural extension of the "percolation" effect (Shante and Kirkpatrick 1971, Essam 1972) to interacting systems, a phenomenon rarely considered (Müller-Krumbhaar 1974) in the literature. In this case, of course, the system, when quenched to a low temperature, is crossed by thick layers of the minority phase instead of presenting the diluted network of connected particles which is characteristic of the familiar "random percolation".

We have also studied a $50 \times 50 \times 50$ lattice; Figs. C.51-C.56 contain the corresponding histograms for the cluster distribution at different values of the time for $T/T_c = 0.6$ and $\bar{\eta} = -0.6$. A big cluster (~ 9000 particles) develops very early; then its size increases very rapidly up to about 17000 particles and its size fluctuates around that value for the rest of the considered evolution. Thus, we note that the size of the big cluster has roughly increased, as compared with the eight evolutions of the $30 \times 30 \times 30$ system, in an amount proportional to the ratio between the total number of particles in the systems ($50^3/30^3 \approx 4.63$), and this strongly suggests that we are in the presence of an "infinite cluster" in the sense of percolation theory (connected by periodic boundary conditions).

In Figs. C.57-C.64 we present similar histograms for the evolution of the $50 \times 50 \times 50$ lattice at $\bar{\eta} = -0.75$ and $T/T_c = 0.6$. Regarding our latest distributions in this case we note that, although the biggest clusters are only of a few hundred particles, the situation is qualitatively similar to the case of composition $\bar{\eta} = -0.6$. In fact, it is also present here the peculiar gap between a "typical" distribution for small clusters and a few big clusters, and we think that, letting the system evolve long enough in time, one would finally observe the appearance of an infinite cluster.

We also mention that the "typical" distribution for the small clusters, as clearly observed for instance in Fig. C.64, is also characteristic of the temperatures below T_c and concentrations previously reported; Figs. C.17-C.50 do not show this typical distribution due to our choice there of wide bands to smooth the fluctuations between the eight evolutions. Figs. C.65-C.66 contain the same information as before (approximately as C.23 and C.37, respectively), but this time the bands are more sensible and the mentioned "typical distribution" is clearly seen. This suggests the separate analysis in the system of properties (4.16)-(4.20) corresponding to "small" clusters and "big" clusters. We shall take $10 \leq \ell \leq 300$ as "small" clusters, and $\ell > 300$ as "big" clusters. We prepared in this way Figs. 64-66 corresponding to the $30 \times 30 \times 30$ system, $\bar{\eta} = -0.6$, at different temperatures.

An interesting difference between the qualitative behavior at $T = 0.6T_c$ and $T = 0.9T_c, 1.1T_c$ is shown by Fig. 64. After a relatively short interval of time, the mean size of the small clusters decreases slightly for the later temperatures, while at $0.6T_c$ the mean size increases very fast (as $t^{0.42}$). Note that the rapid decrease which is observed at $0.6T_c$ after $t \approx 1500$ only means that clusters with more than 300 particles are predominant in the system after that time. This fact also affects the interpretation of the behavior at $T = 0.6T_c$ shown by Fig. 65, which corresponds to "big" clusters. Again, the decrease of the mean size for this temperature corresponds to the formation and growth of clusters of size between 300 and 1500 particles (at the expense of the smaller clusters) while the total number of particles in the (few) very big clusters is approximately stationary (although important fluctuations are seen due to the breaking, and subsequent recombination, of these big clusters). Fig. 66 corresponds to the evolution with time of the quantity $\overline{\epsilon/\ell}$ for small clusters.

In fig. 67 we analyse the temporal behavior of the mean cluster size including all the clusters with $\ell \geq 10$ (Tables A.19-A.21). Given the "untypical" form of the cluster distribution in three dimensions, one has to be cautious when interpreting this figure; this is obvious when one compares Fig. 67 with Fig. 68 for the temporal evolution of the clusters radius ($\sim \ell^{1/3}$). We emphasize in Fig. 67 two different temporal behaviors; for

$t \geq 500$ a least-square fit according to eq. (4.21) gives $a = 0.385$, as compared with the prediction $a = 1/3$ of the Ostwald ripening theory and with $a = 1/2$ which is given by the cluster dynamics in section 3.4. Figs. 69-70 refer to the quantities defined in eqs. (4.20) and (4.19) respectively.

When the fraction of A-particles in the system, \bar{n}_A , is below the critical value for percolation (this value is 0.307 ± 0.01 for site percolation, as computed by the series method; Essam 1972), one expects the initial, random, cluster distribution to decrease monotonically with cluster size. Fig. 71 corresponds to the average of eight infinite-temperature configurations for the $30 \times 30 \times 30$ lattice at $\bar{n}_A = 0.2$. At higher concentrations, "infinite size" clusters appear in the system. This is shown in Figs. C.67-C.84 which correspond to the average over twelve random configurations of the $30 \times 30 \times 30$ lattice for \bar{n}_A ranging from 0.282 to 0.350 at intervals of 0.004.

Also of interest is the analysis of the behavior of the very small clusters (monomers, dimers, etc.) in the system. The variation of the percentage of A-particles constituting clusters of small sizes as a function of \bar{n}_A is given in Fig. 72, while Figs. 73-80 bis are concerned with the evolution in time of the same quantity for different situations. A common fact to all these situations is that, apart from fluctuations, the number of monomer, dimers, trimers, etc. reaches very early the corresponding

equilibrium values. We denote these values by n_i^S , $i = 1, 2, 3, \dots$, and they are tabulated in Table 4.5 for different situations as computed by a temporal average over the part of the corresponding evolution after stabilization. Note the qualitatively different behavior shown by Fig. 80 bis (the only one at $\bar{\eta} = 0$) for early times as compared with the one in Figs. 71-80.

In the lattice-gas-model language, one may think of the "very small" clusters in the system as constituting the vapor phase; then, large clusters would correspond to the solid phase. The mean density of the system is then given by

$$\rho = x \rho_v + (1 - x) \rho_s \quad (4.25)$$

with ρ_v and ρ_s , respectively, the density of the vapor and solid phases, and $x, (1 - x)$ the corresponding fractions. When ρ_v is small, $n_1^S \approx \rho N$ with N the number of sites in the lattice. One may write

$$n_1^S \approx \lambda N, \quad \lambda = \begin{cases} zN & \text{in the one-phase region} \\ xz'N & \text{in the two-phase region,} \end{cases} \quad (4.26)$$

and

$$n_2^S \approx 3 \lambda^2 \exp(4J/kT), \quad (4.27)$$

$$n_3^S \simeq 15 \lambda^3 [\exp(4J/kT)]^2, \dots \quad (4.28)$$

From these equations,

$$r \equiv n_1^S n_3^S / (n_2^S)^2 = 15/9. \quad (4.29)$$

This value reasonably agrees with the one computed from the evolution of our model system (rightmost column in Table 4.5), especially if one has in mind that ρ_v is not so small in the cases considered in Table 4.5. From the values for the $30 \times 30 \times 30$ lattice one observes, however, that r slightly depends on the temperature. The value of r for the 80×80 lattice is 8.6% higher than (4.29) (while the one for the 200×200 lattice is 2.2% smaller) perhaps corresponding to size effects in the smallest system. A similar (less pronounced) difference affects the values for the $30 \times 30 \times 30$ and $50 \times 50 \times 50$ lattices, and is remarkable the fact that the largest lattices at $T = 0.6T_c$ and $\bar{\eta} = -0.6$ give almost the same value for r , very close to the prediction (4.29). We do not expect (4.27)-(4.29) to hold at $\bar{\eta} = 0$.

Other cluster properties will be considered in section 4.6.

lattice	T/T_c	$\bar{\eta}$	n_1^S	n_2^S	n_3^S	n_4^S	n_5^S	n_6^S	n_7^S	n_8^S	n_9^S	n_{10}^S	r
80 x 80	0.6	-0.6	15.62	1.99	0.46	0.27	0.16	0.14	0.09	0.05	0.03	0.06	1.81
200 x 200	0.6	-0.6	90.38	12.11	2.64	1.38	0.93	0.70	0.78	0.67	0.56	0.56	1.63
30 x 30 x 30	0.6	-0.6	226.92	38.48	11.42	4.15	1.85	1.08	0.33	0.29	0.11	0.09	1.75
30 x 30 x 30	0.9	-0.6	474.13	113.60	50.59	27.74	17.60	11.67	9.10	6.32	5.38	4.39	1.86
30 x 30 x 30	1.1	-0.6	573.9	140.25	65.13	37.15	24.48	17.76	12.59	10.27	8.25	6.86	1.90
30 x 30 x 30	1.1	0	112.13	7.81	1.78	0.395	0.194	0.157	0.046	0.020	0.018	0.010	3.27
30 x 30 x 30	1.5	0	114.31	6.18	1.32	0.315	0.174	0.047	0.033	0.013	0.003	0.005	3.95
50 x 50 x 50	0.6	-0.6	1066.0	193.6	56.9	-	-	-	-	-	-	-	1.62
50 x 50 x 50	0.6	-0.75	1425.3	296.8	108.3	43.7	24.0	18.0	9.5	5.3	3.0	3.3	1.75
50 x 50 x 50	0.9	-0.38	1157.1	213.8	-	-	-	-	-	-	-	-	-

Table 4.5 Equilibrium value of the number of monomers, n_1^S , dimers, n_2^S , etc. computed as an average over the stationary evolution shown in Figs. 73-80, in the cases for which it was clear the stabilization of these values. The right most column corresponds to

$$r = \frac{n_1^S n_3^S}{(n_2^S)^2}$$

Figs. 4.57-4.58 Logarithmic plot of the average cluster size (number of particles) vs. time as obtained from six evolutions of the 80×80 lattice and one evolution of the 200×200 lattice at $T/T_c = 0.6$ and $\tilde{\eta} = -0.6$ (Fig. 58) and the combination of the seven evolutions (Fig. 57). The straight lines shown are a least-square fit to the data; the figures show the slope and intersection of these lines with the vertical axis for zero value of the horizontal axis, and the standard error of the estimate (RMSF) in percent.

Figs. 4.59-4.60 Same data as before, this time referring to the average cluster radius, plotted in the way experimentalists use to do. The RMSF are in absolute value. This kind of plots do not determine unambiguously a law for the temporal evolution.

Figs. 4.61-4.62 Logarithmic plots of the decay with time of $\bar{\epsilon}/\ell$, eq. (4.20), and of $\bar{\epsilon}$ vs. ℓ , eqs. (4.19) and (4.16), for a combination of the results from the two-dimensional systems.

Fig. 4.63 Evolution with time of the standard deviation of the distribution of clusters sizes corresponding to the two different two-dimensional lattices.

Figs. 4.64-4.70 Same as Figs. 4.57, 4.58, 4.61 and 4.62, this time referring to the $30 \times 30 \times 30$ lattice, $\tilde{\eta} = -0.6$, at different temperatures. Figs. 4.64 and 4.66 refer to "small" clusters and Fig. 4.65 to "big"

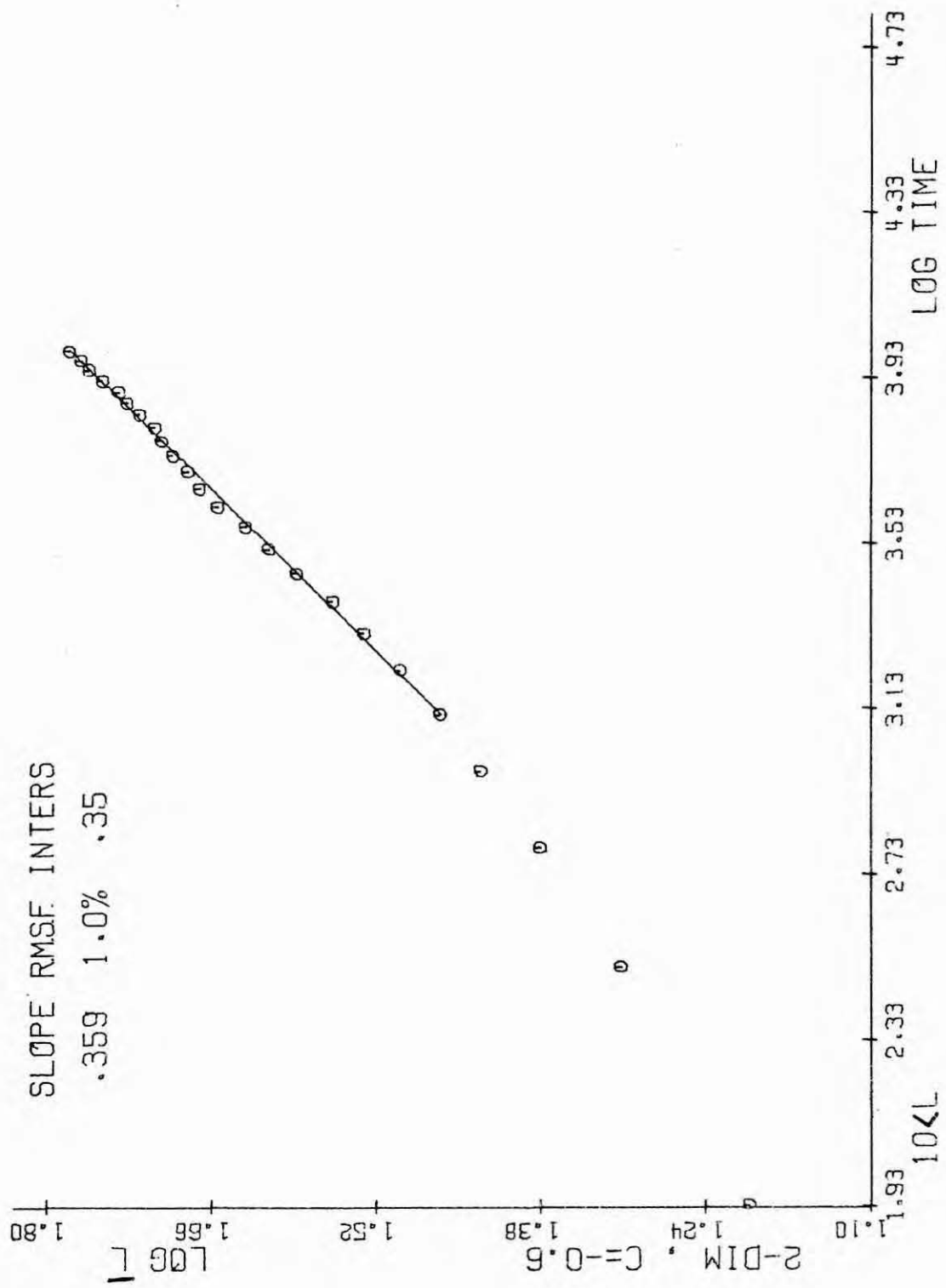
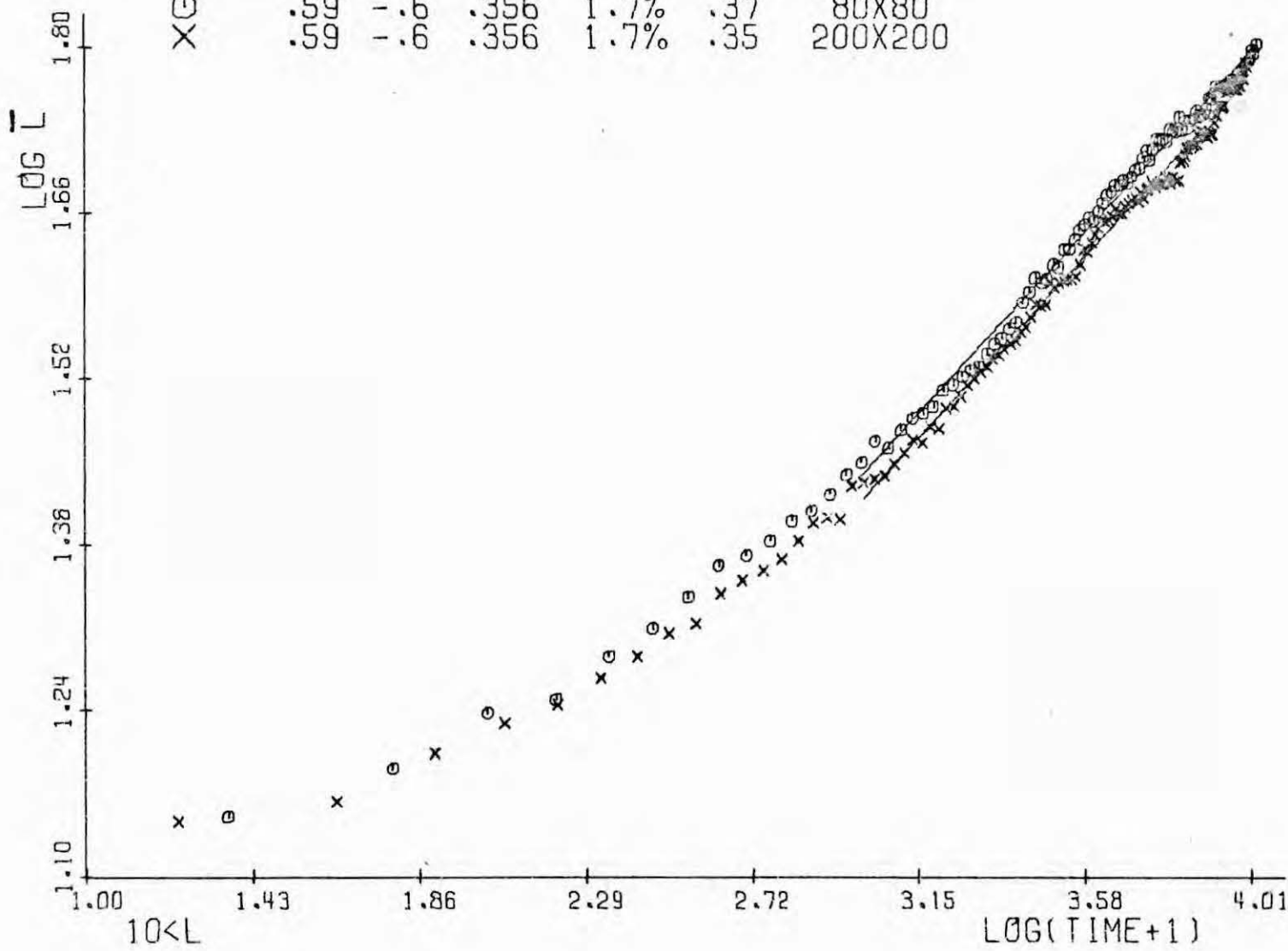


Fig. 57

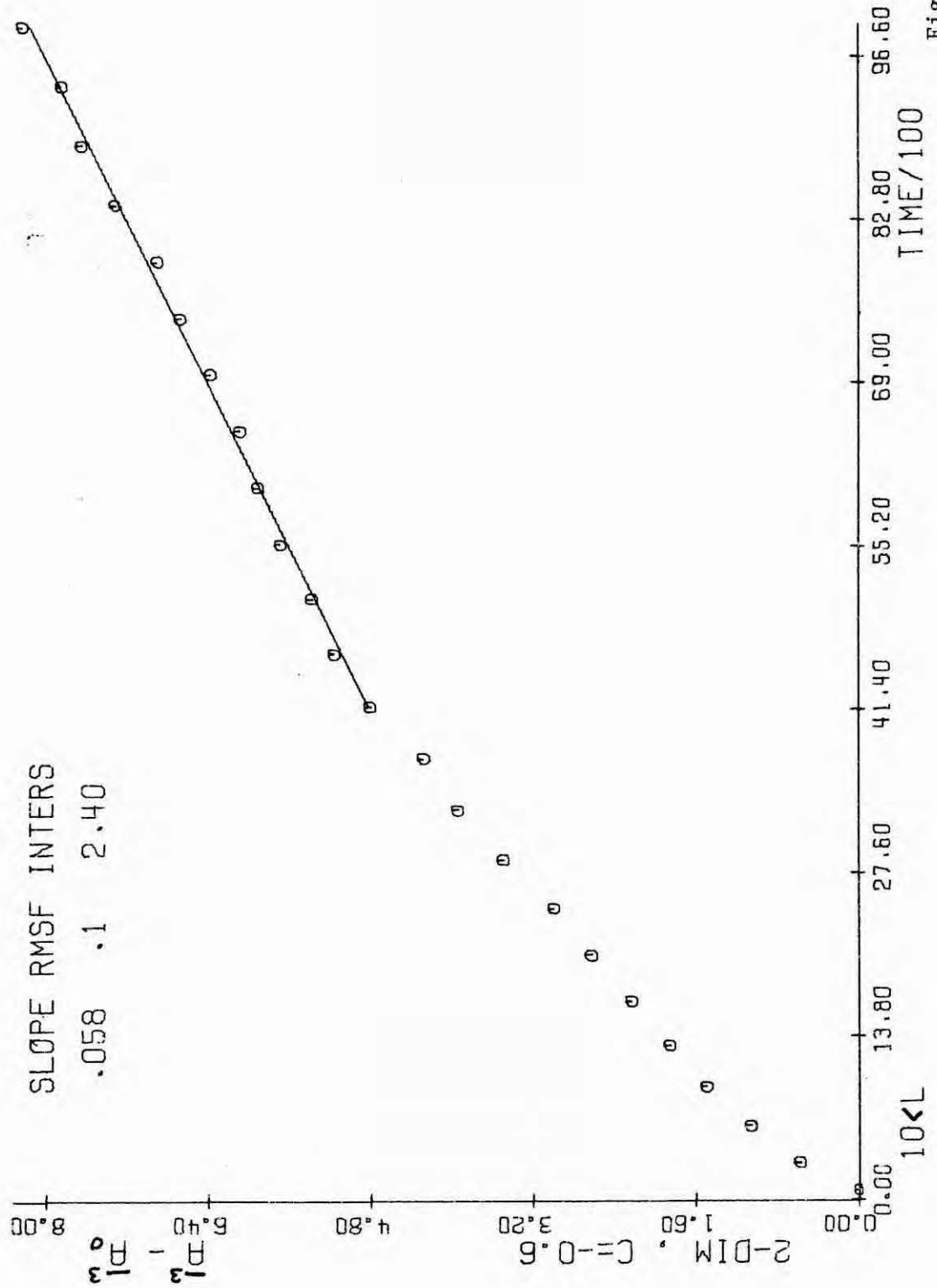
SYMBOL T/T_c C SLOPE RMSF INTERS LATTICE

○	.59	-.6	.356	1.7%	.37	80X80
×	.59	-.6	.356	1.7%	.35	200X200



141

Fig. 58



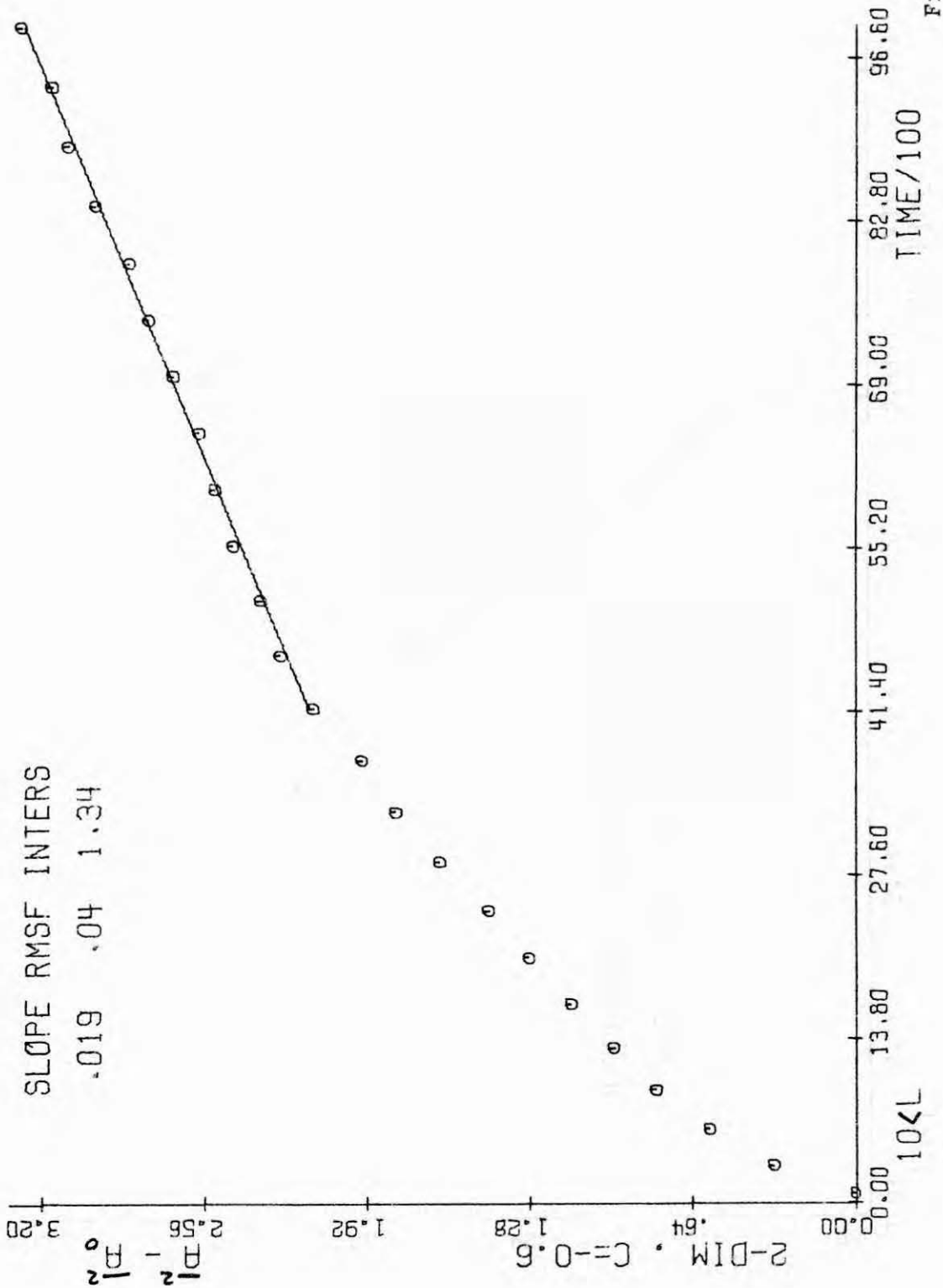
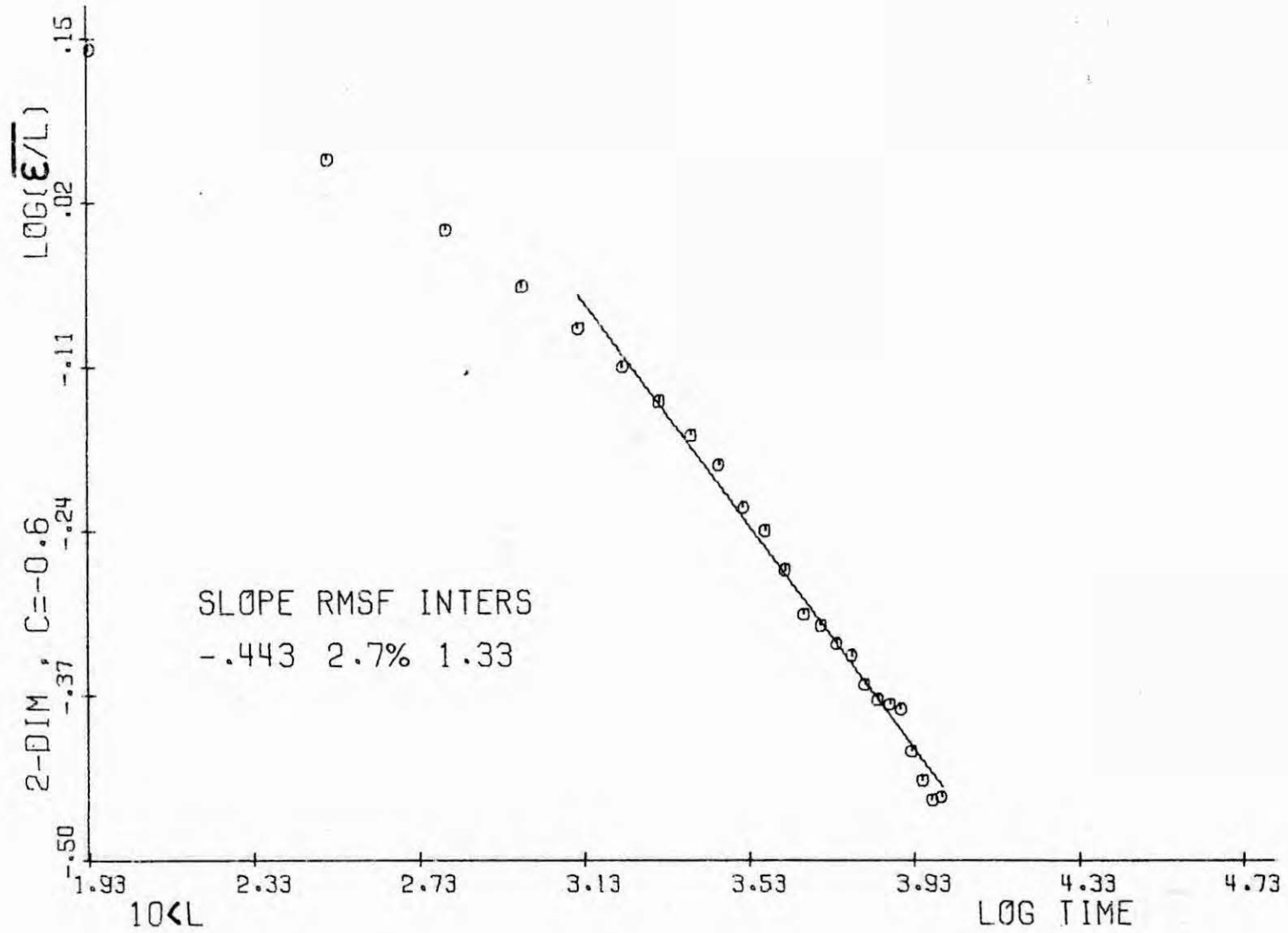


Fig. 60



144

Fig. 61

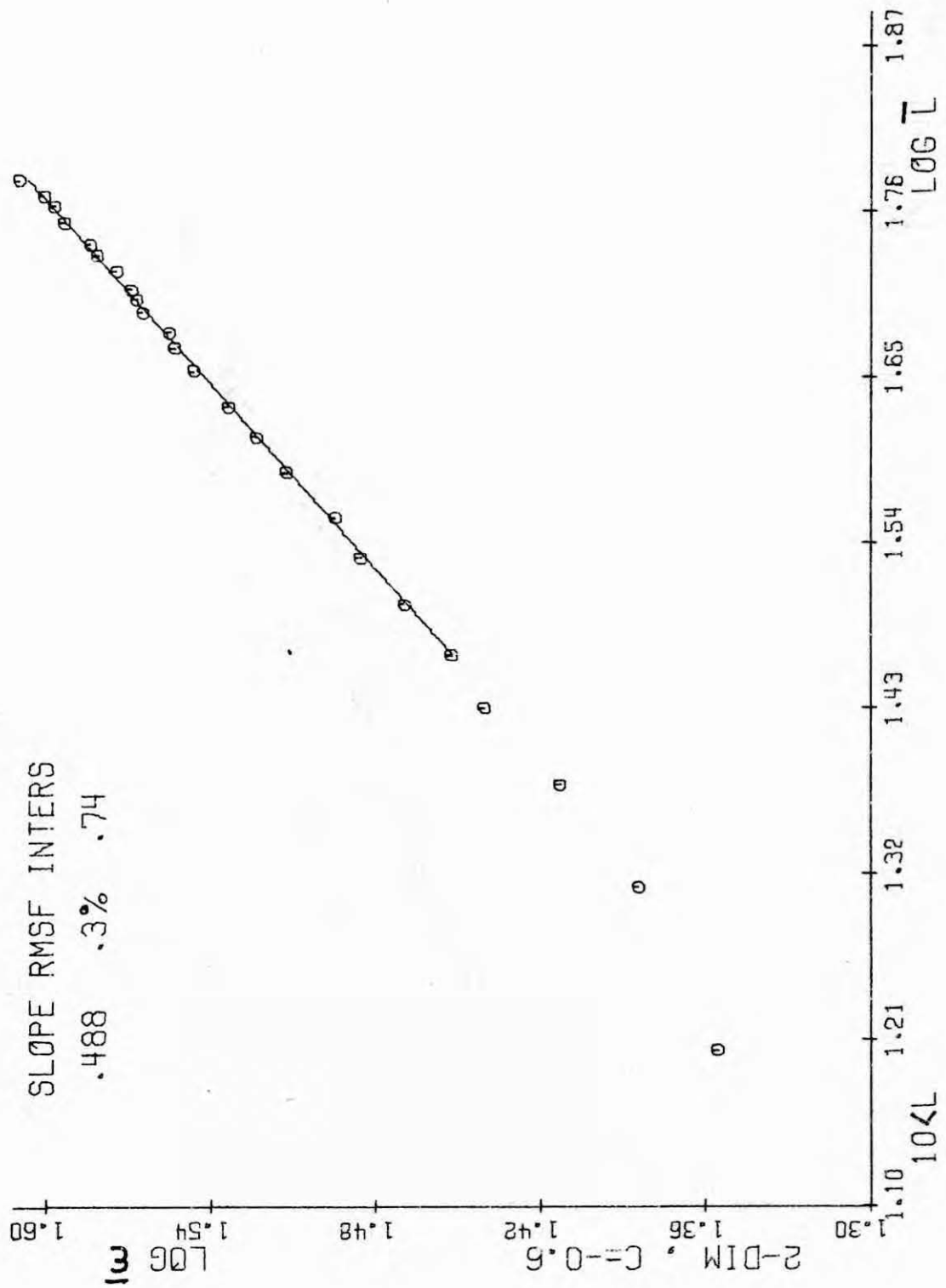
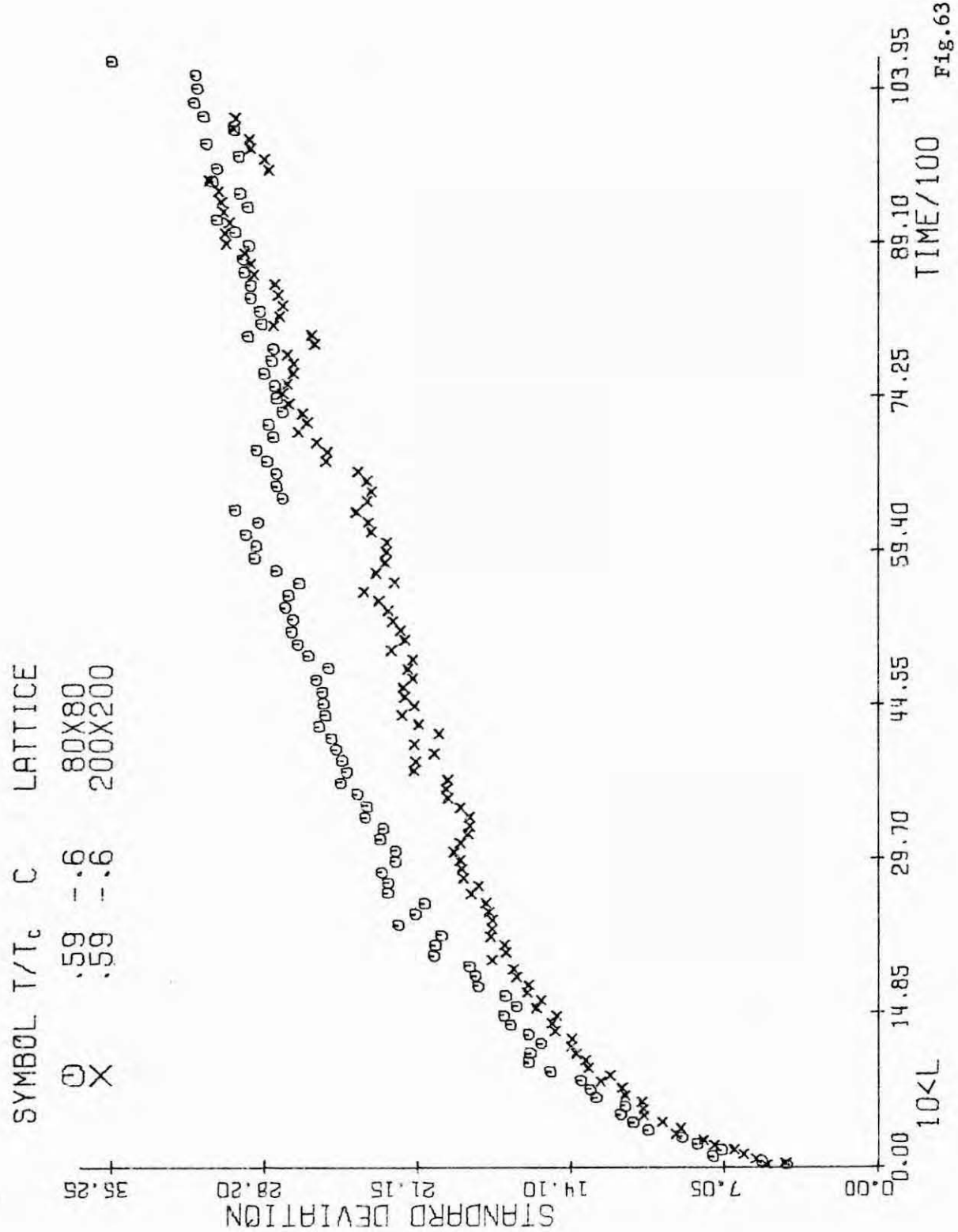
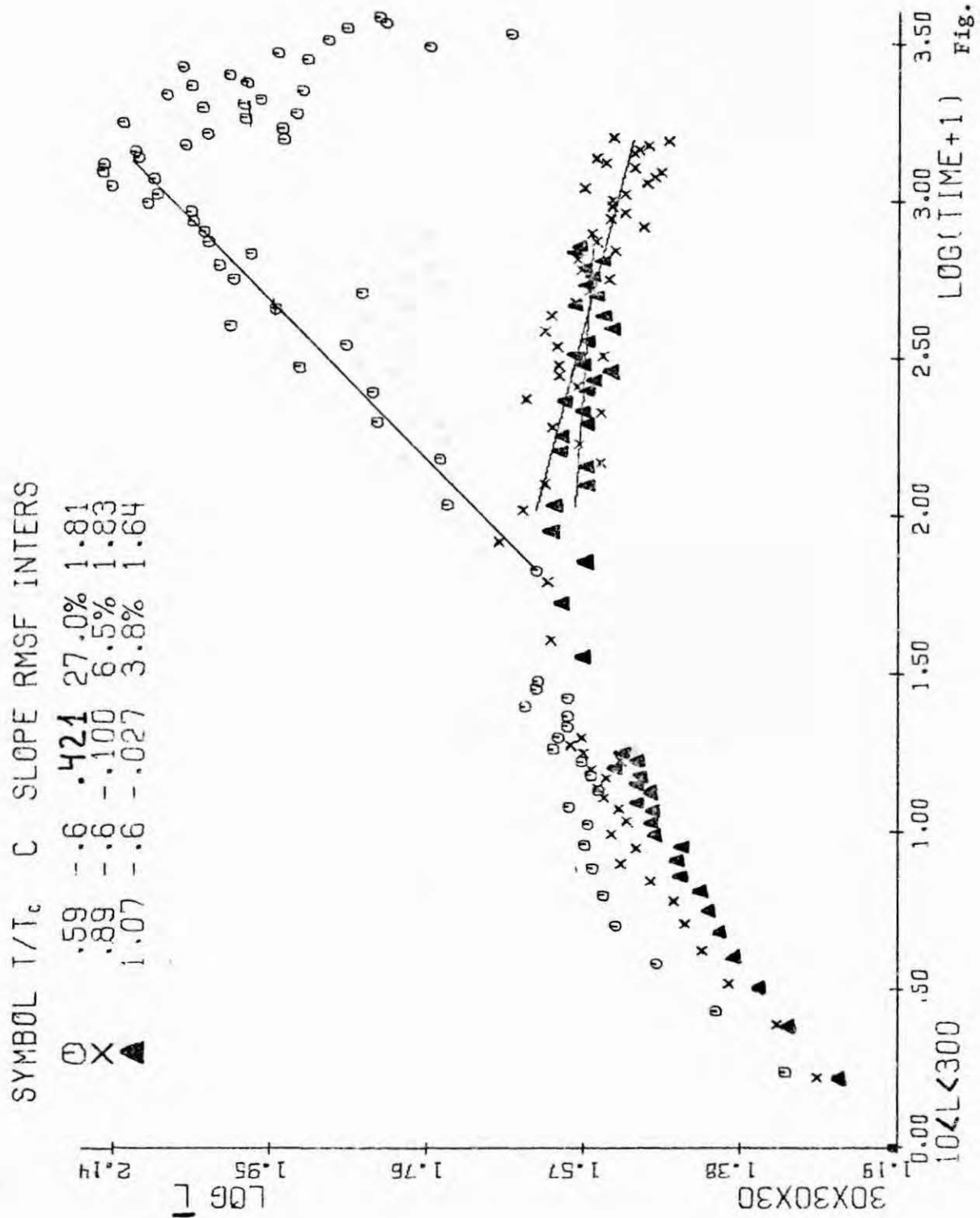
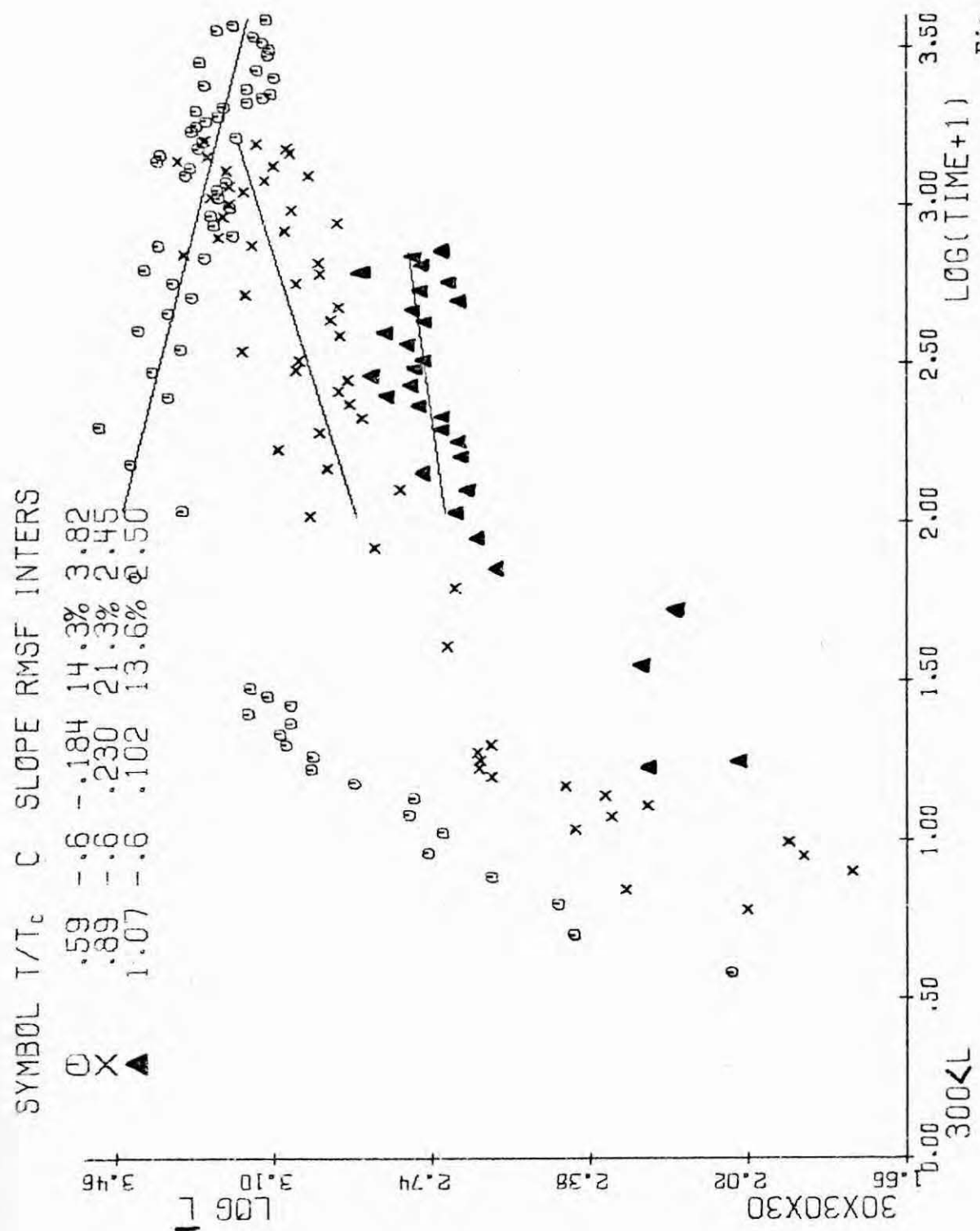
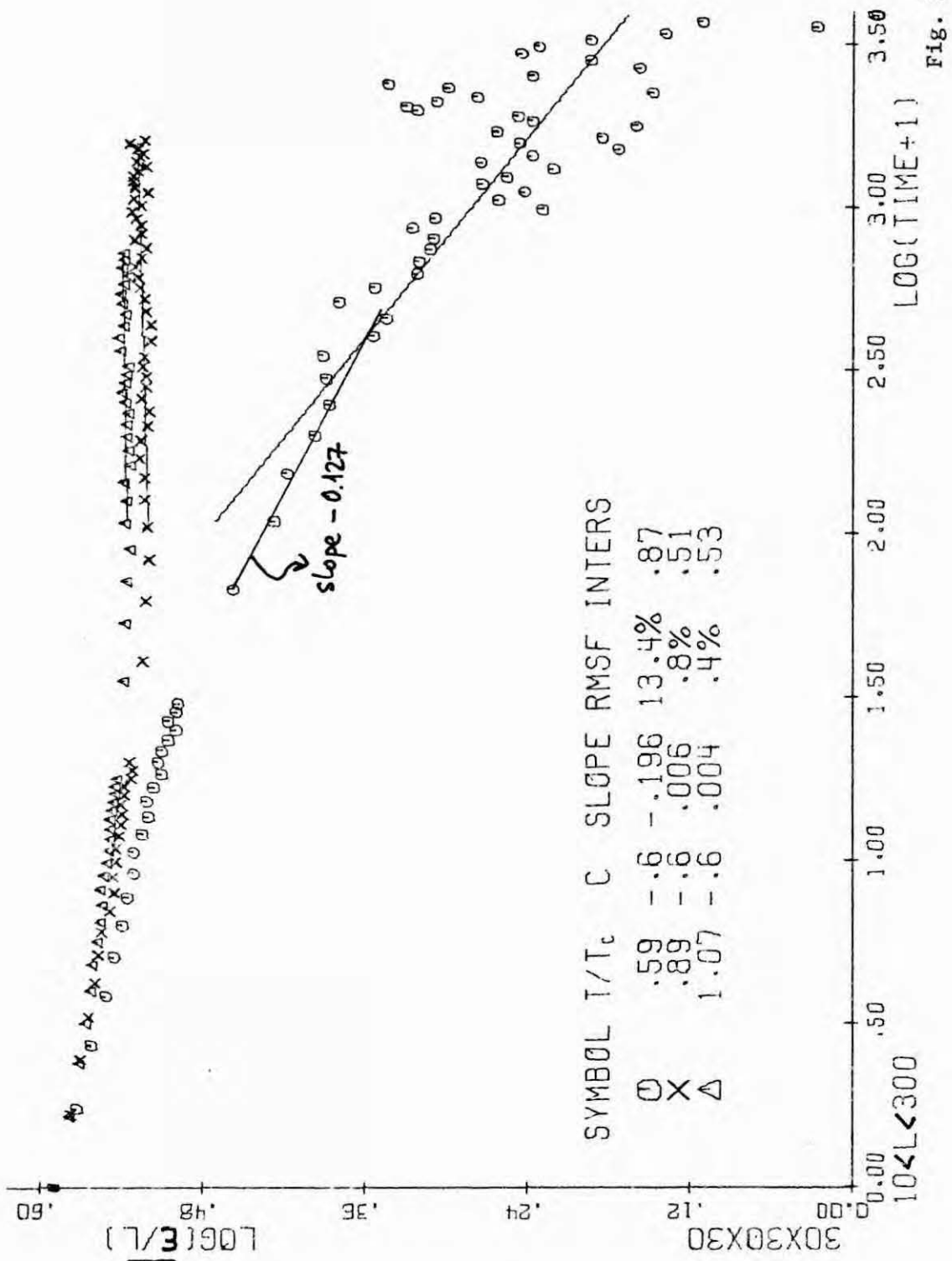


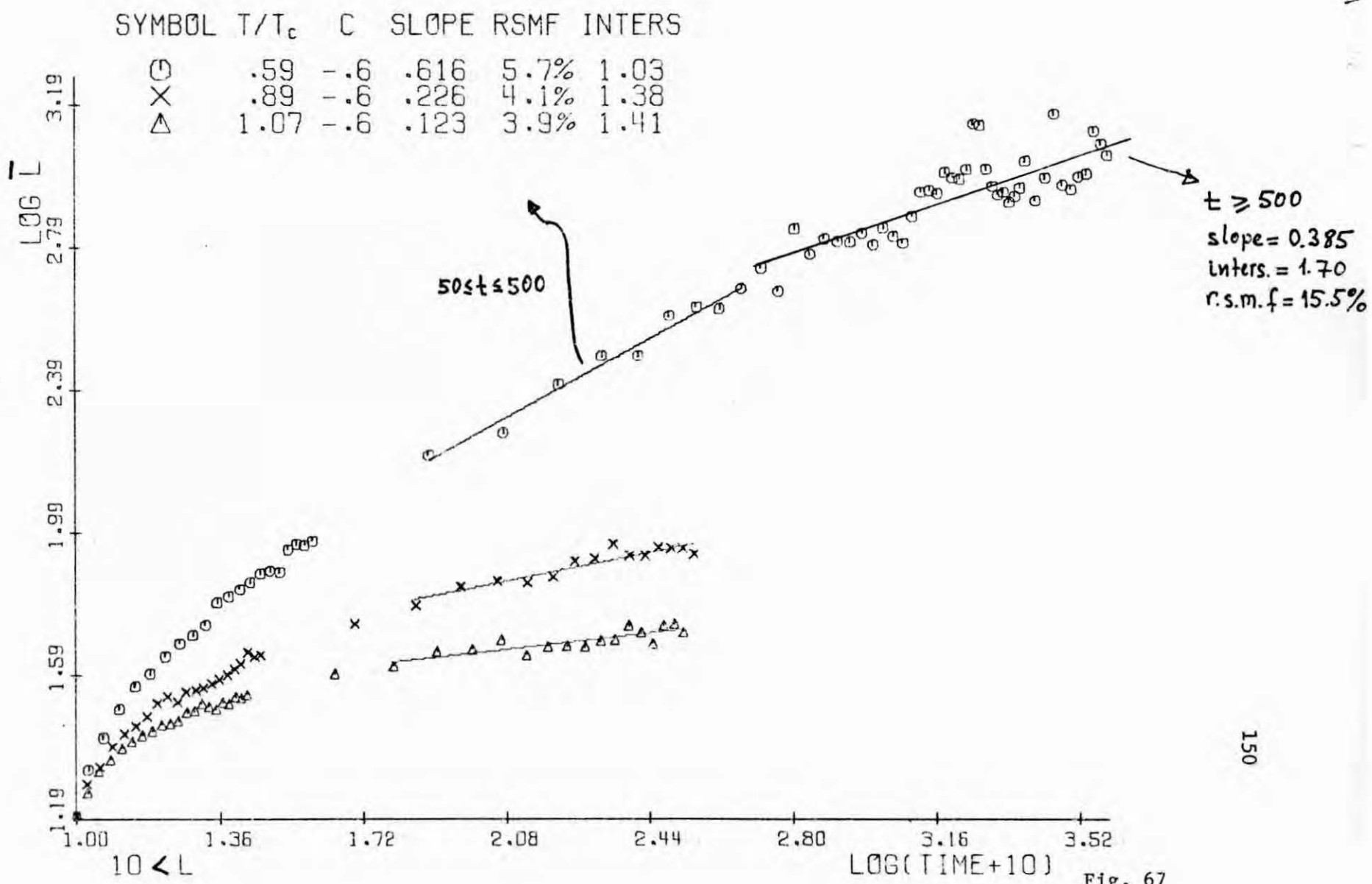
Fig. 62











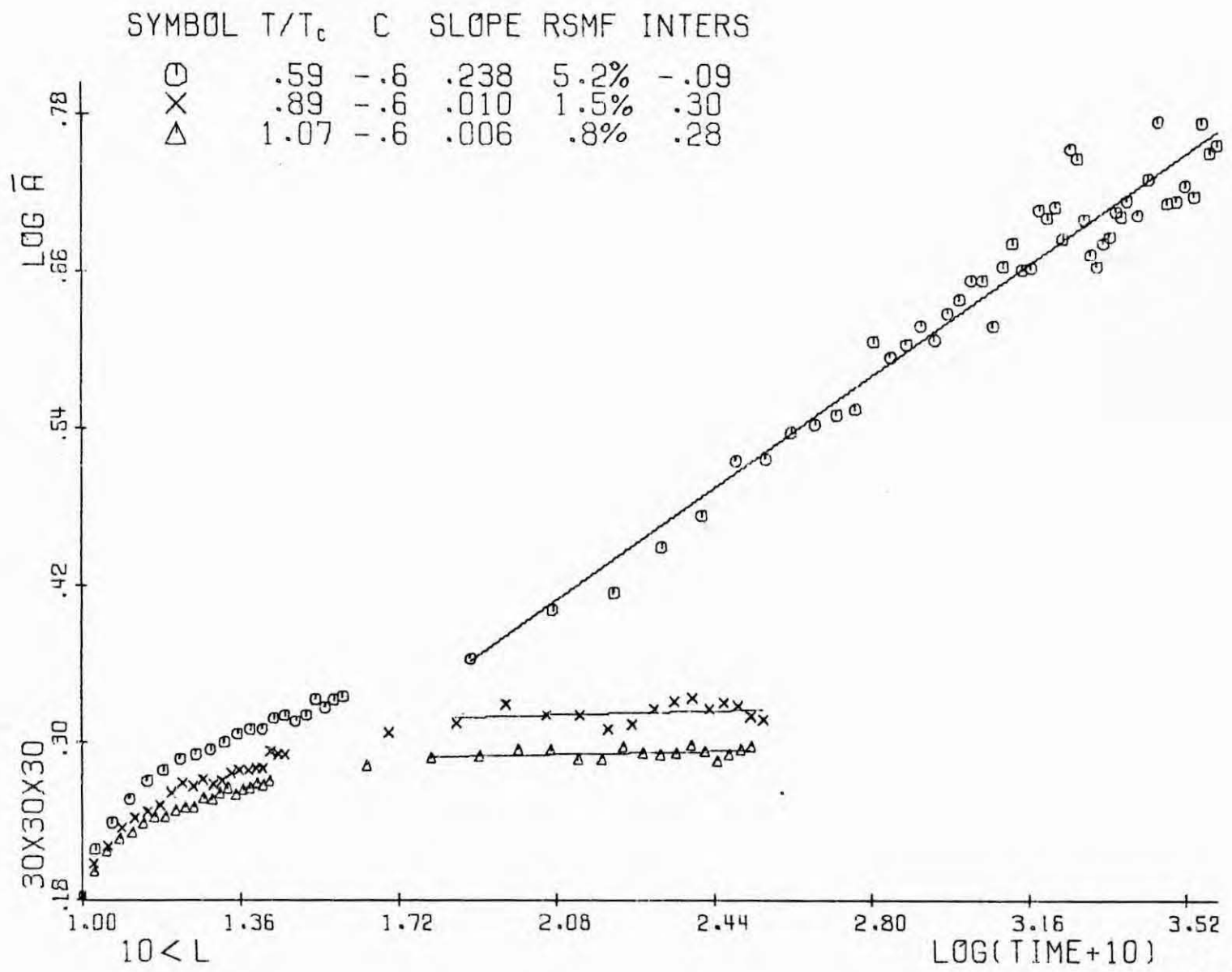
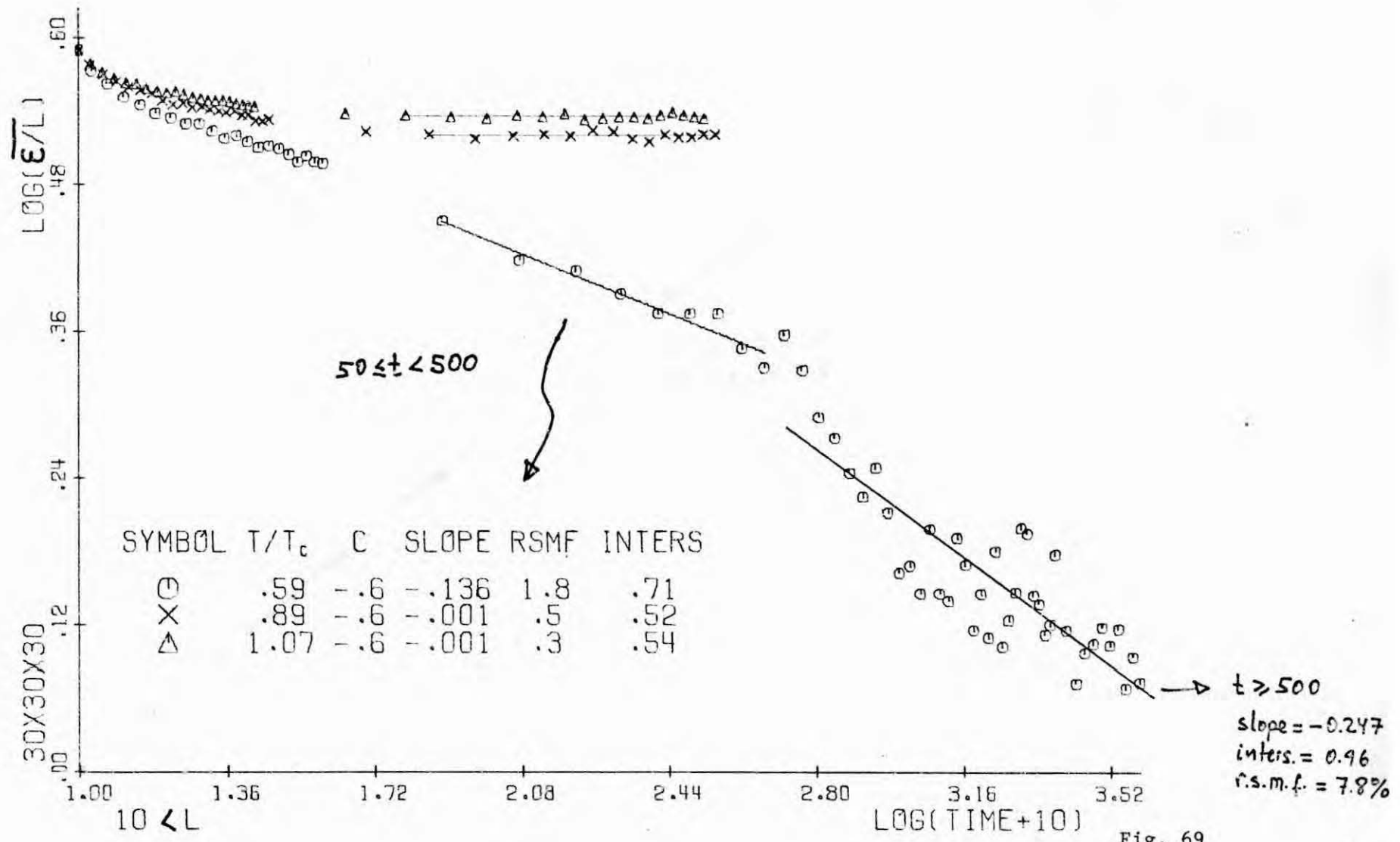


Fig. 68



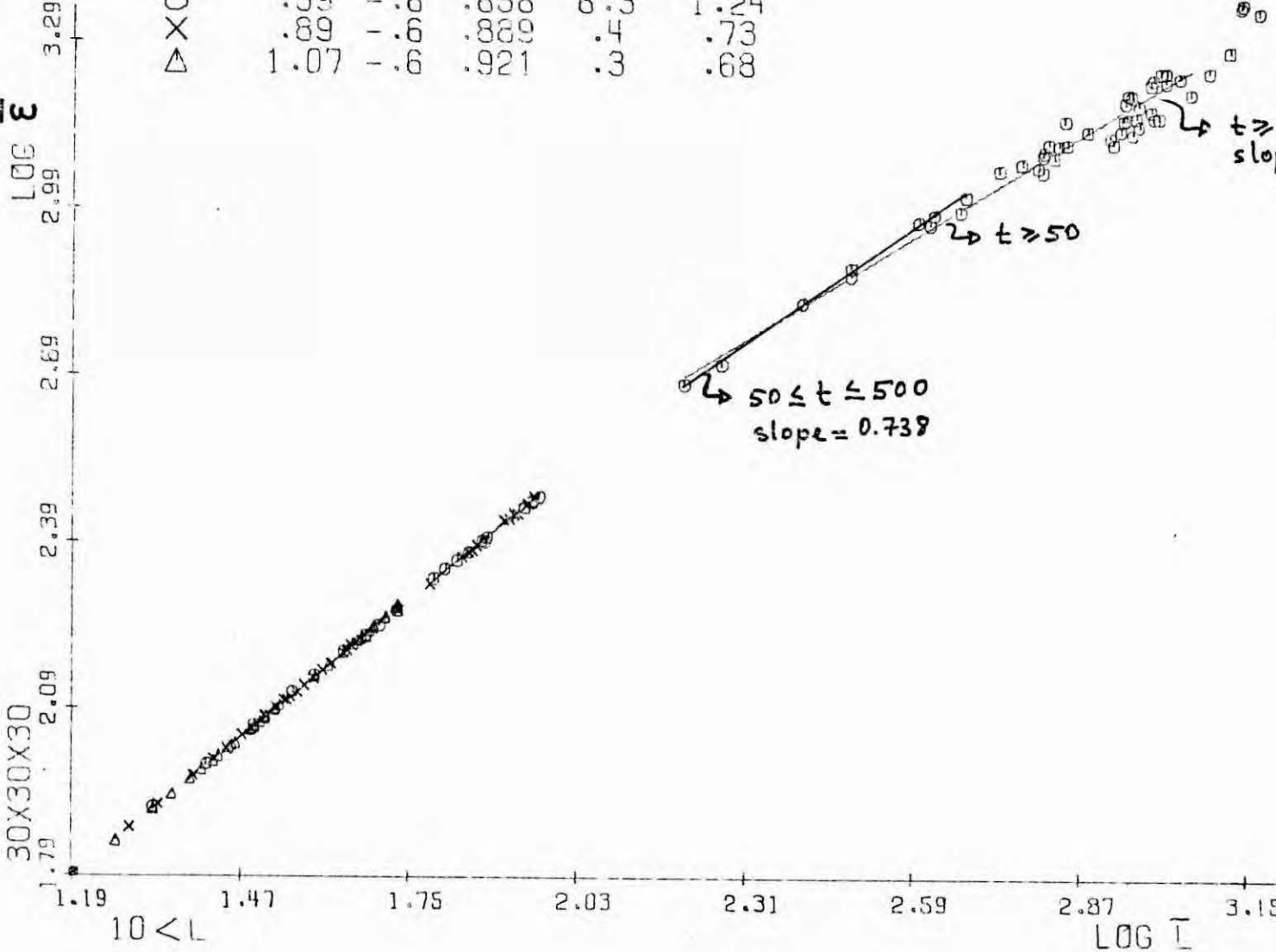


Fig. 70

Fig. 4.71 Initial cluster distribution, average of eight random configurations for the $30 \times 30 \times 30$ lattice at $\bar{\eta} = -0.6$. The horizontal axis was divided in bands of 5 particles up to size 51 and in bands of 10 particles for the rest.

Fig. 4.72 Percentage of A-atoms constituting very small clusters as a function of the fraction \bar{n}_A of A-atoms in the system. The corresponding cluster size is indicated at the end of each line.

Figs. 4.73-4.80bis Evolution with time of the percentage of A-atoms constituting very small clusters for different systems, compositions and temperatures. The number at the end of each line corresponds to the cluster size to which it refers. Note that the very early times are not considered in any of the graphs.

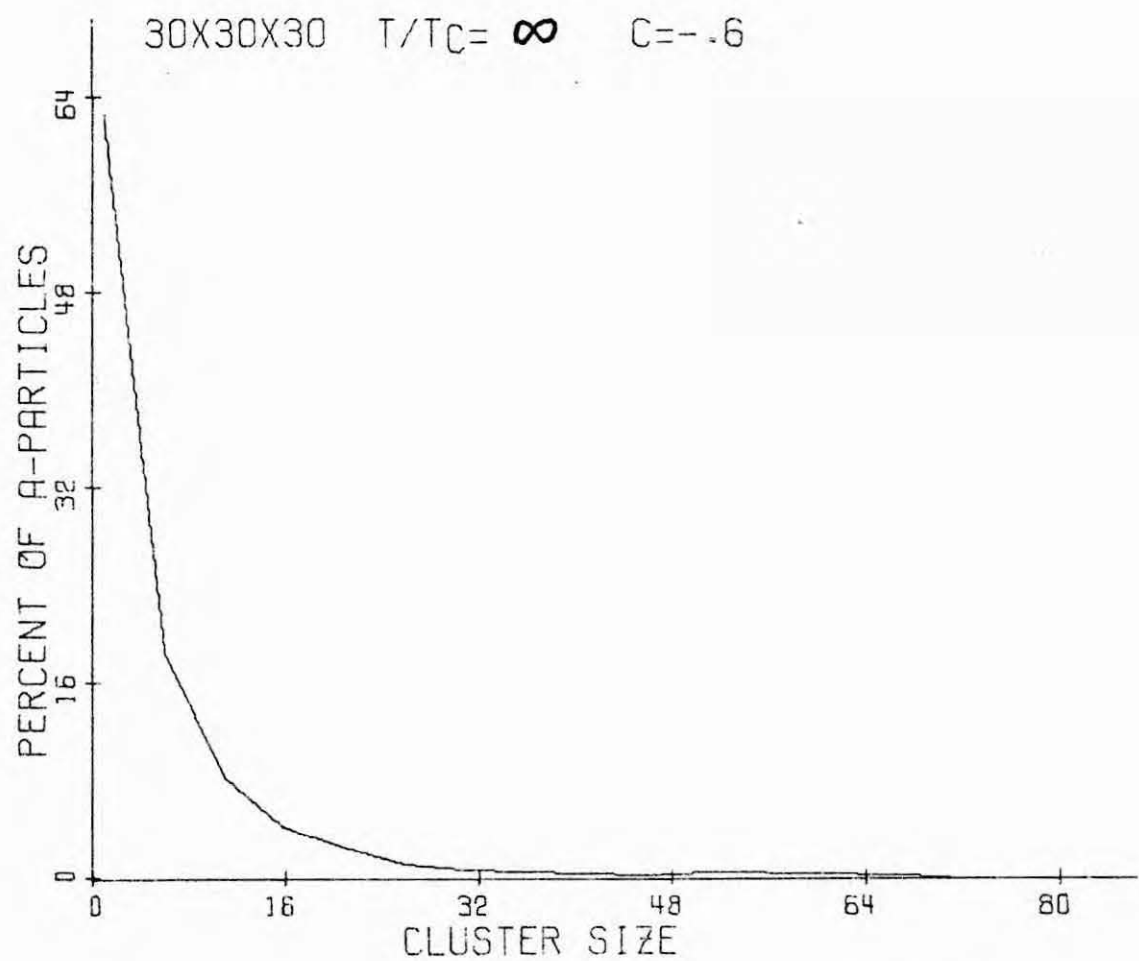
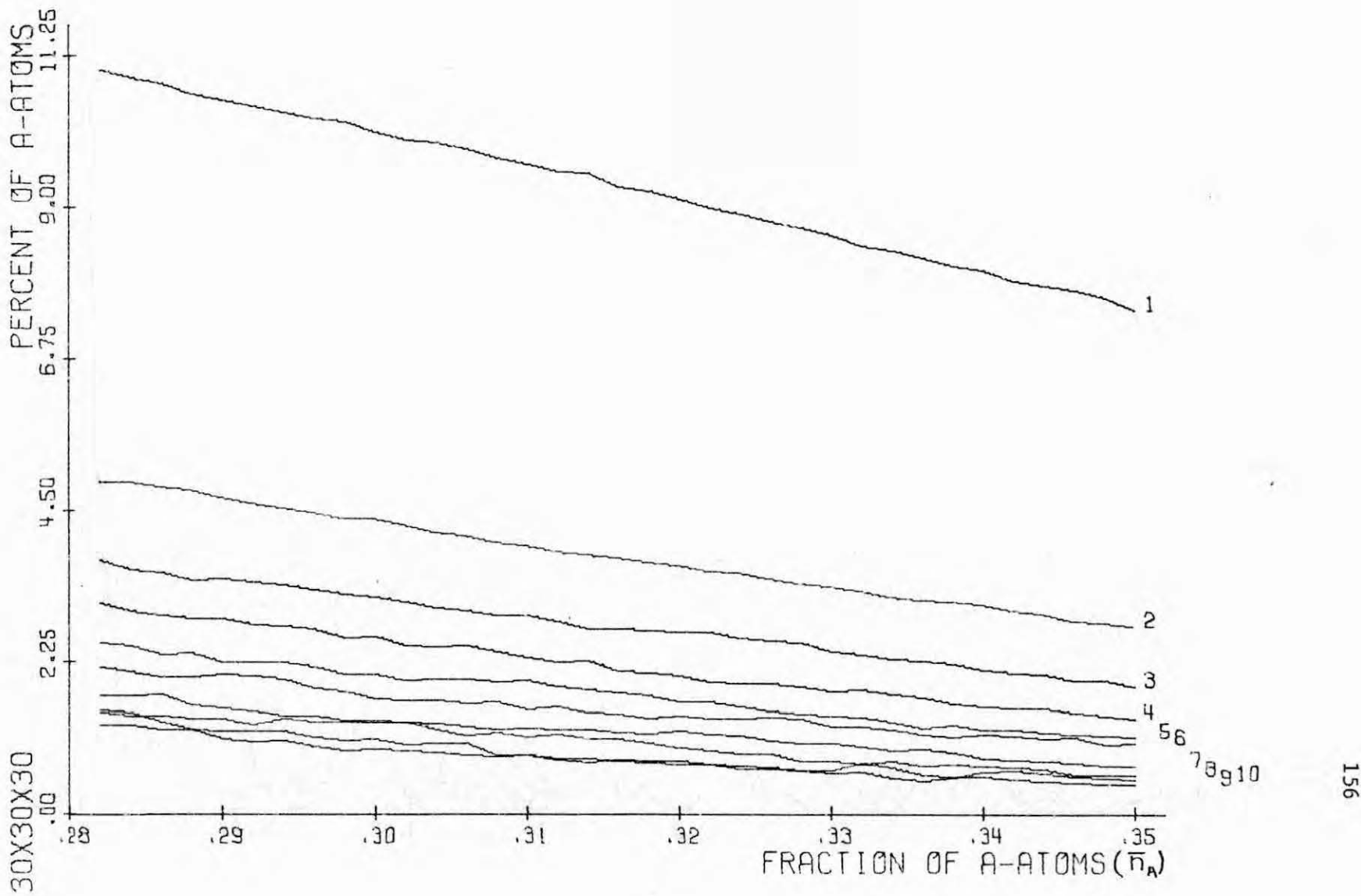
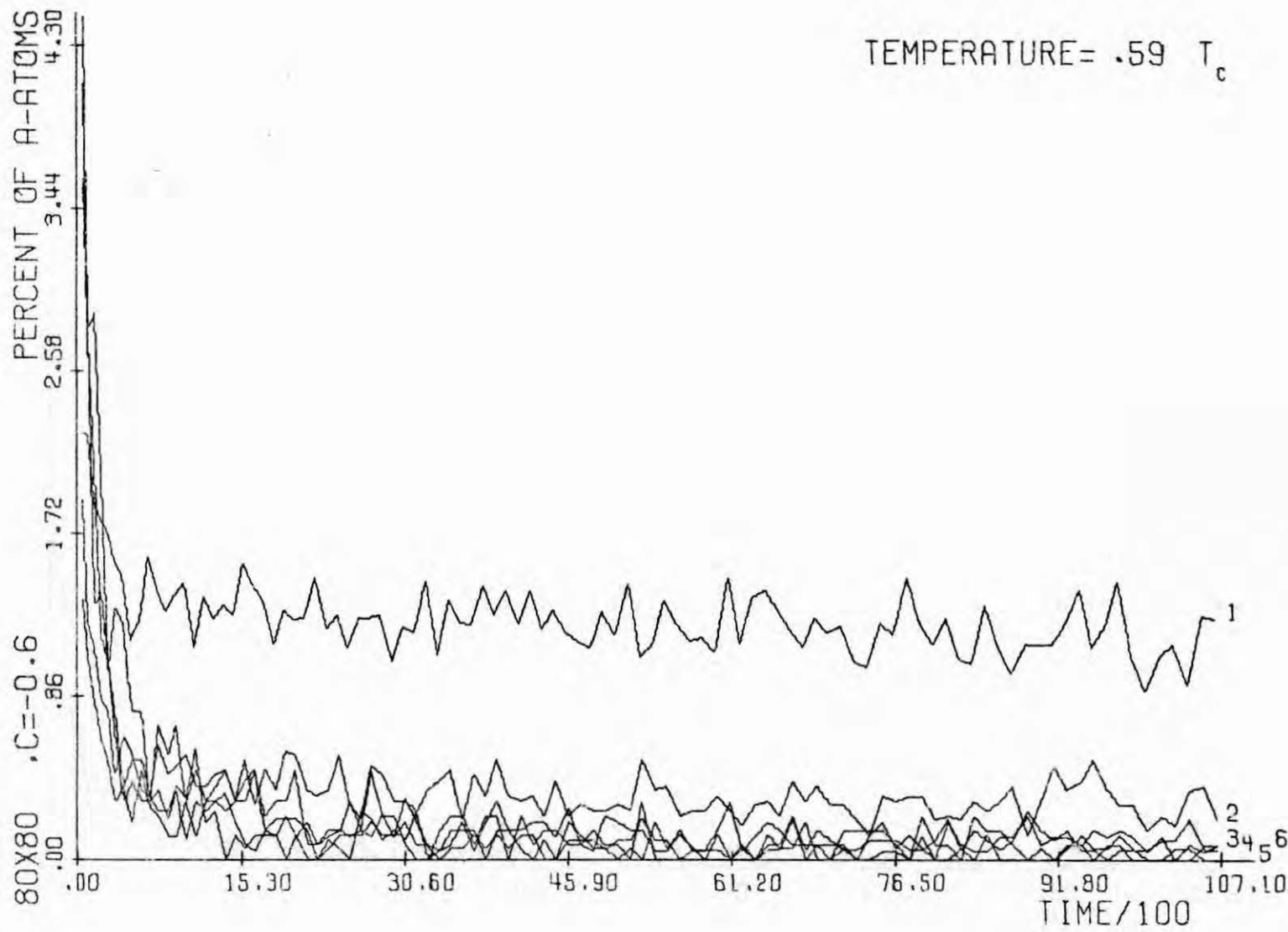


Fig. 71





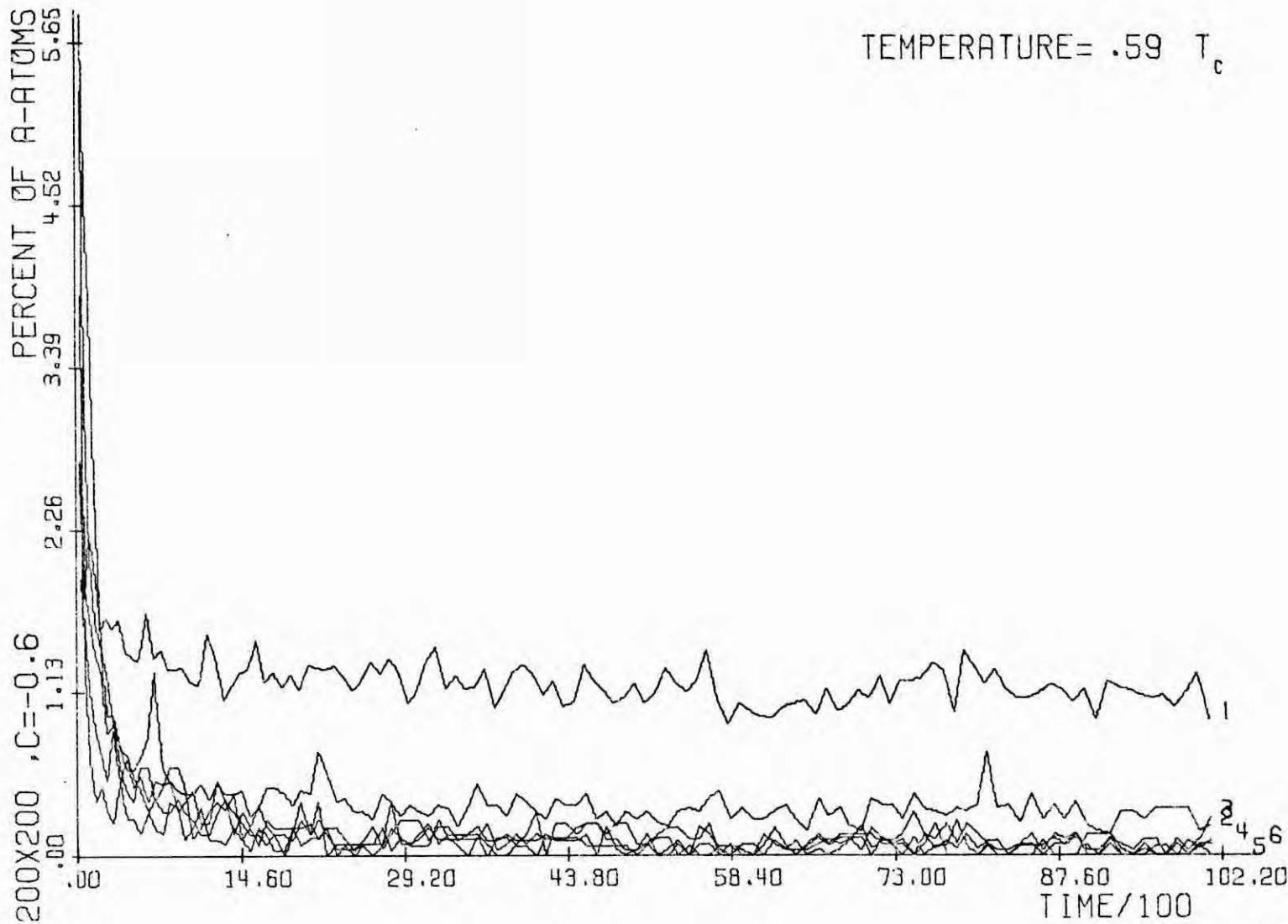


Fig. 74

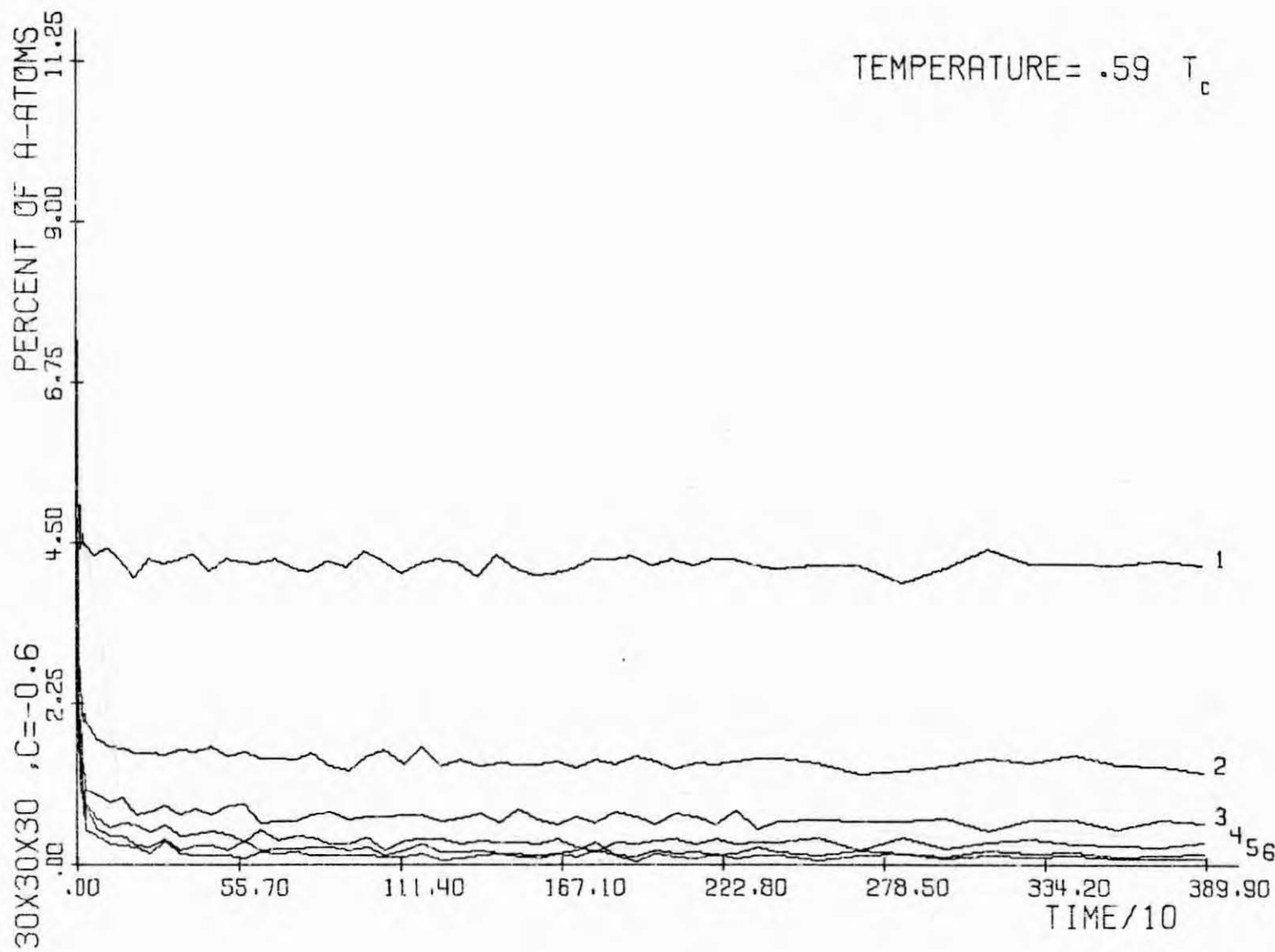


Fig. 75

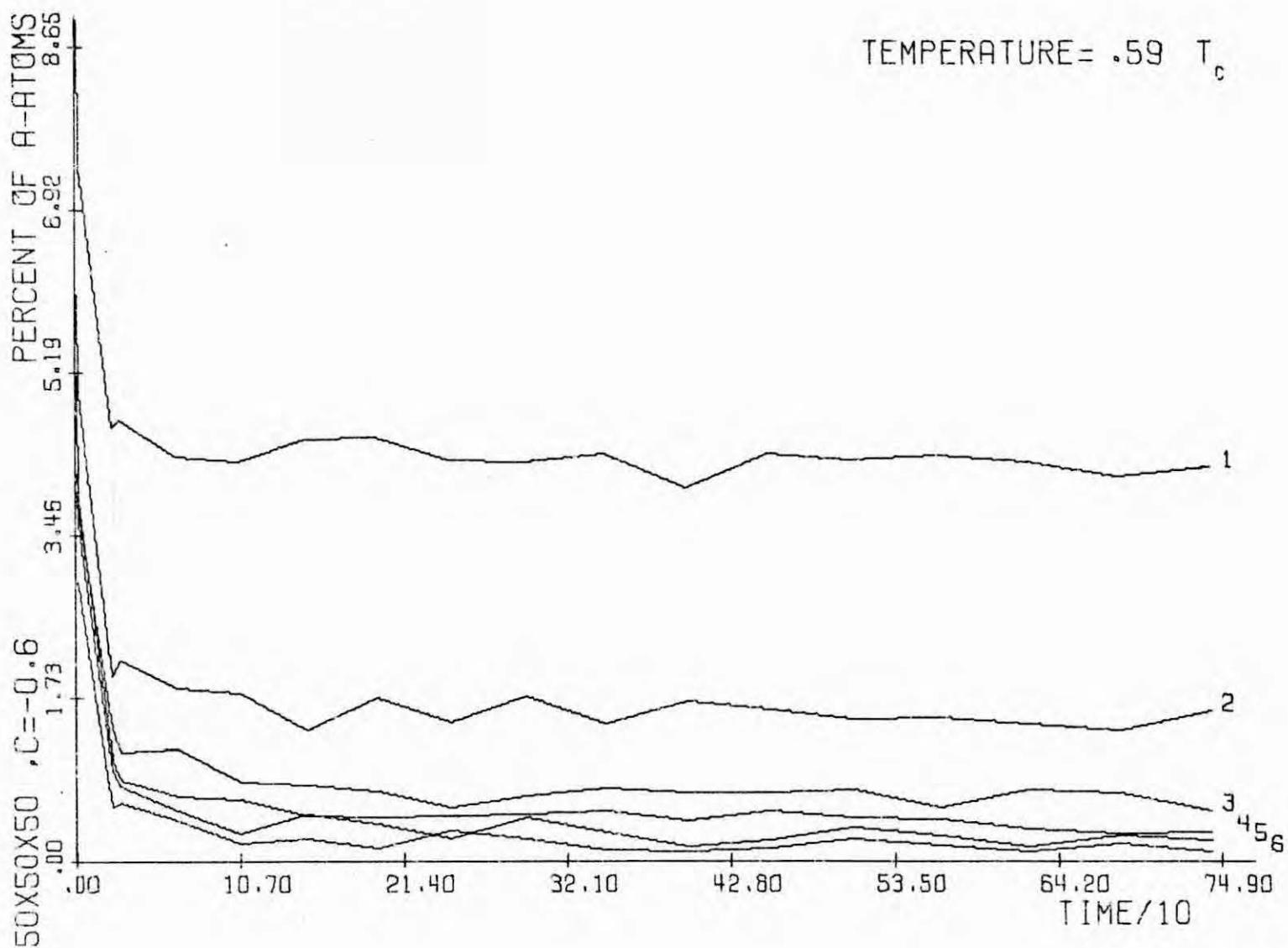


Fig. 76

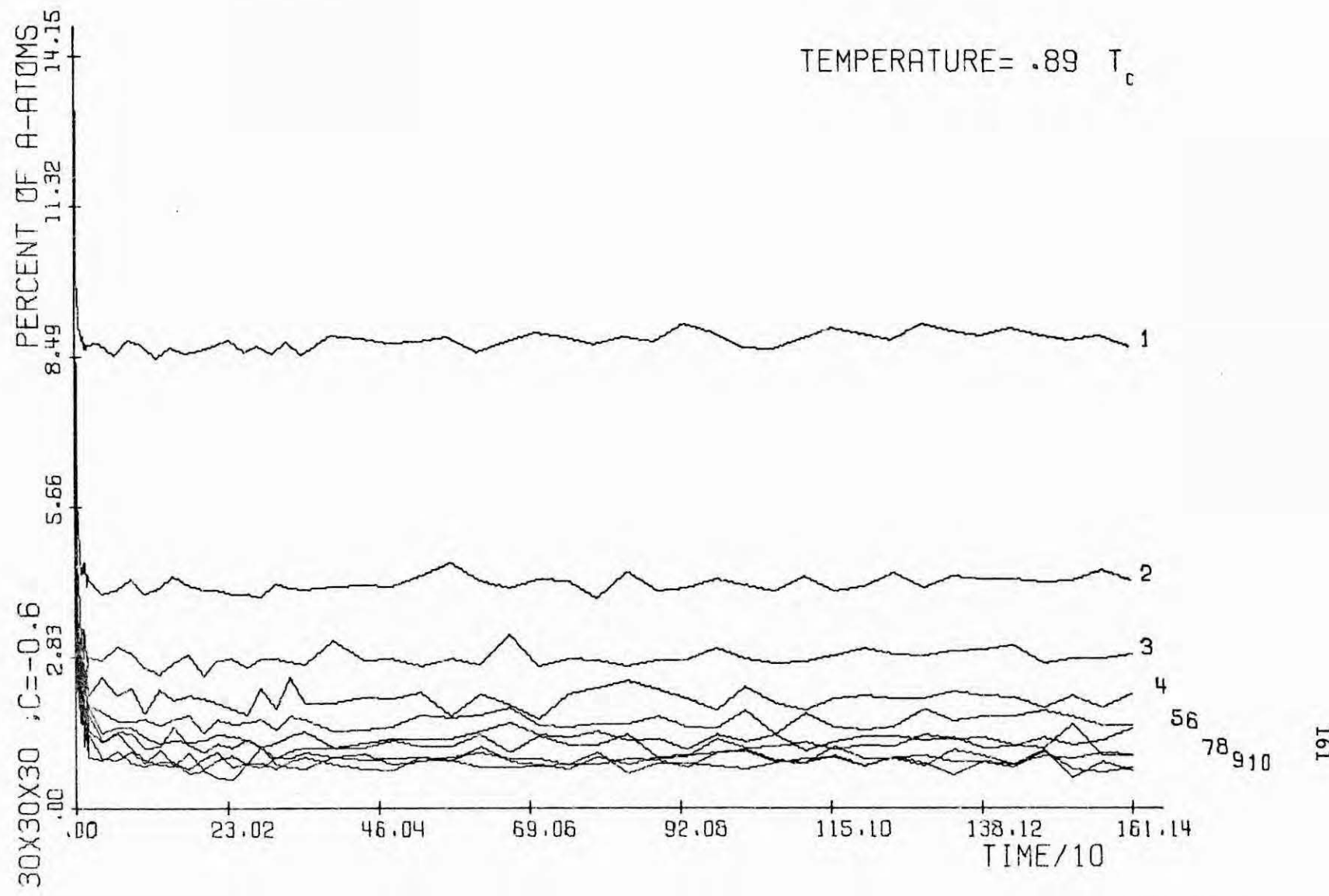


Fig. 77

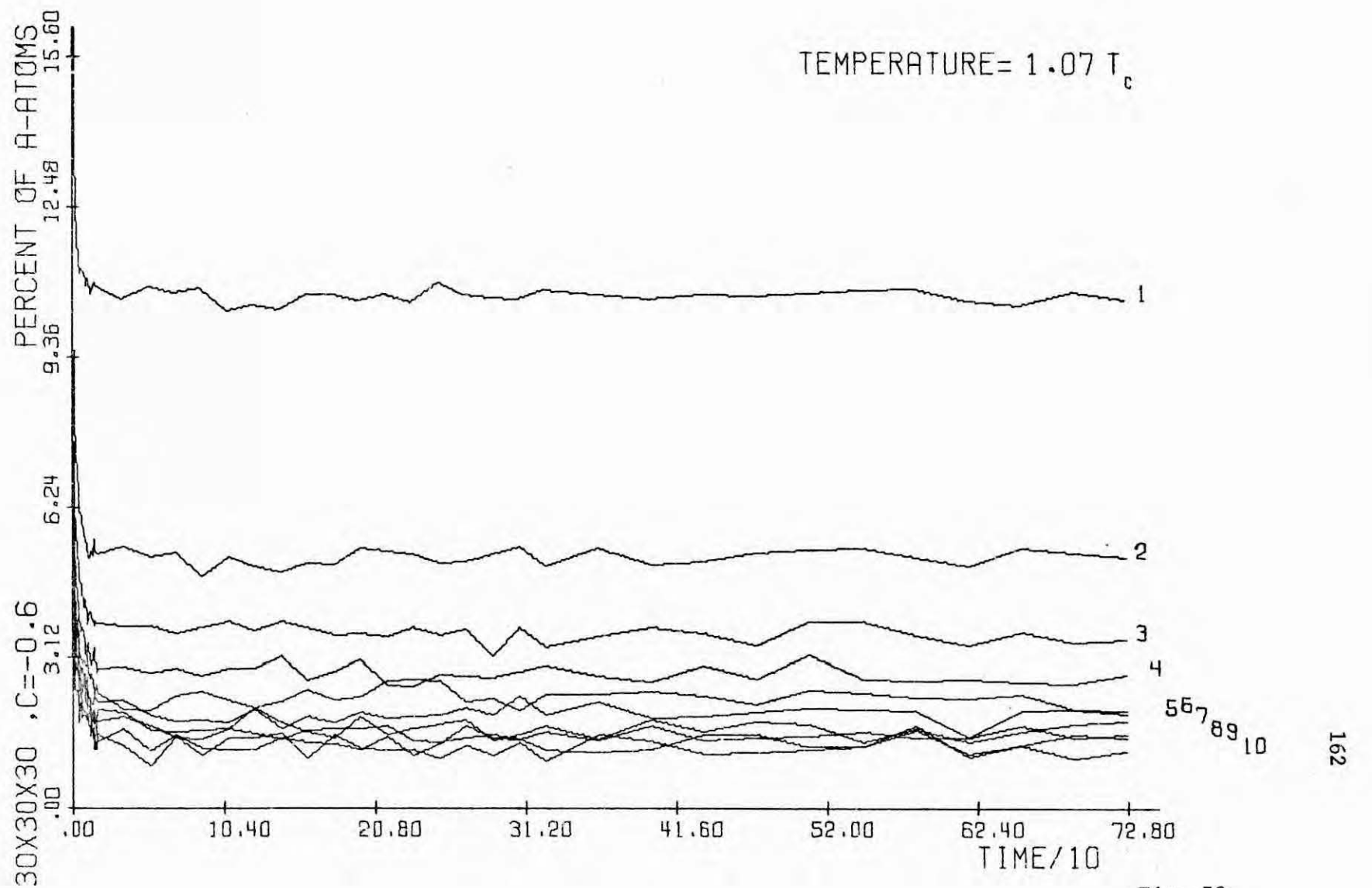


Fig. 78

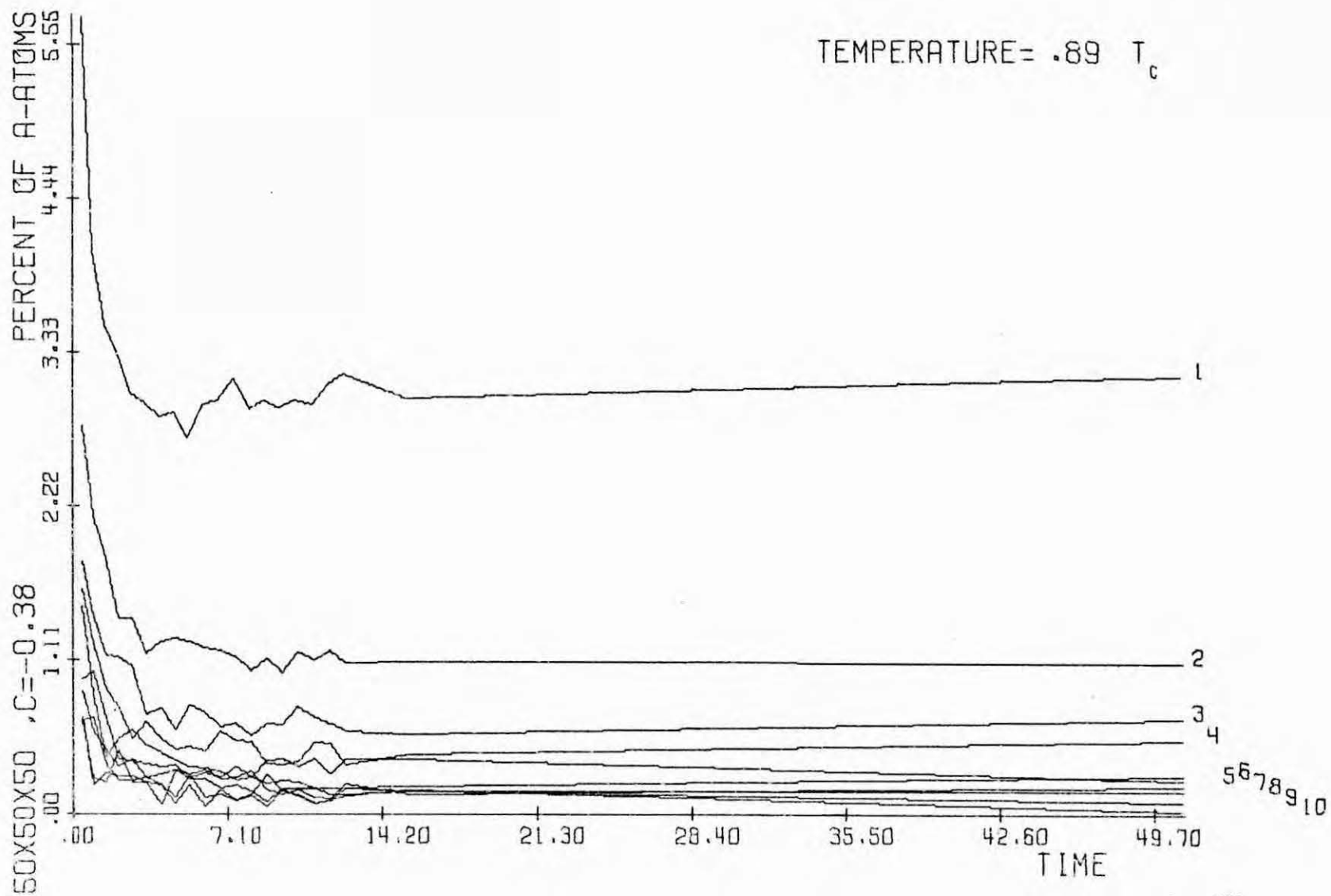


Fig. 79

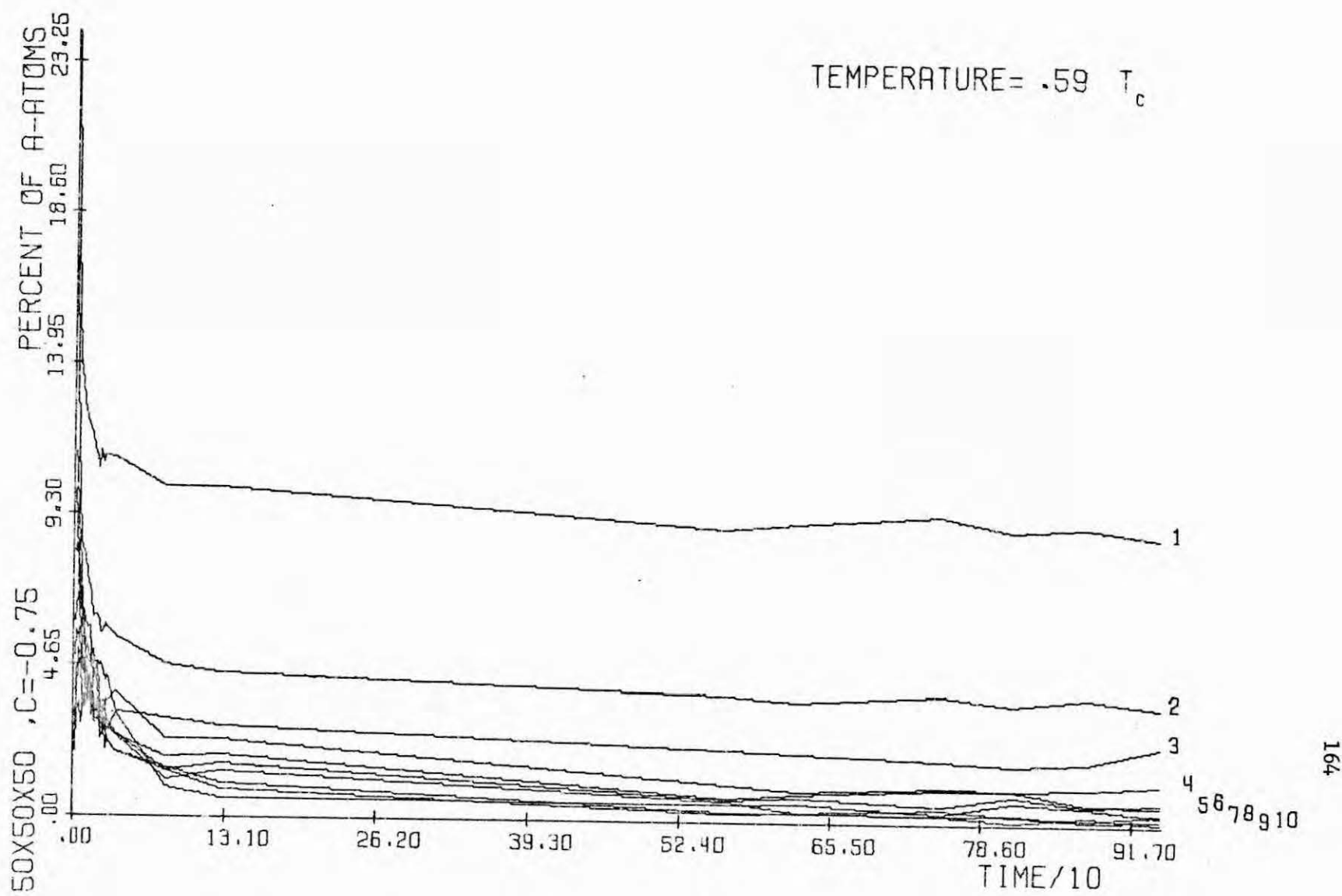


Fig. 80

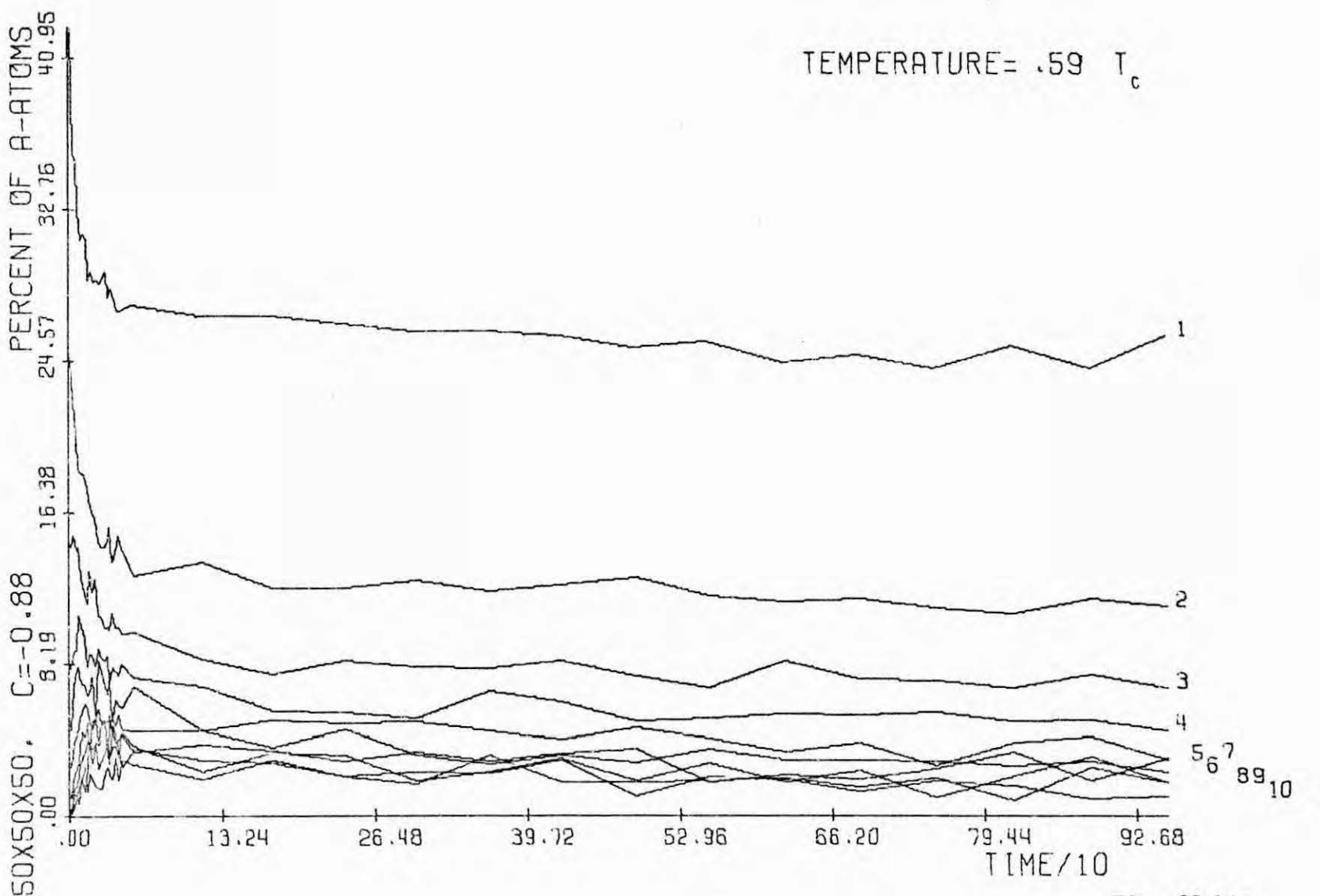


Fig. 80 bis

4.5. - Anti-ferromagnetic interaction.

We present in this section some results on the temporal evolution after quench of the Ising anti-ferromagnet as discussed in Chapter II. They refer to an average over eight independent evolutions (Tables A.22-A.27) of the $30 \times 30 \times 30$ lattice at the phase-points (Fig. 2.1): ($\tilde{\eta} = 0$, $T = 0.591T_c$), ($\tilde{\eta} = -0.4$, $T = 0.591T_c$) and ($\tilde{\eta} = 0$, $T = 0.887T_c$).

The spherically averaged structure function, (2.26), is plotted in Figs. 81-82 as a function of k for different values of t after quenching the system with different compositions to $T = 0.6T_c$. Figs. 83-84 refer to the evolution with time of $S(k,t)$ for different values of k . All these figures show a rapid decay of $S(k,t)$ with time which corresponds to the decay of the short (microscopic) ranged correlations. According to Fig. 83, this decay is quantitatively similar to all the studied k values with the exception of the very small ones. This is also seen, although less transparently, in Fig. 84 and might indicate the appearance of a peak for $S(k,t)$ at $k < 2\pi/30$ (the smallest value of k we can measure in our finite system). The visual inspection of Figs. 81-82 also helps to guess the presence of this peak. On the other hand, these figures show no "superlattice reflection" corresponding to the development of correlations of order $\sim 2 a_0$; this may be due to the spherical average performed in $S(k,t)$. If one avoids this average, however, the fluctuations in $S(k,t)$ will probably hamper the usefulness of the resulting picture.

These figures evidence that the system reaches its equilibrium state much earlier than the corresponding ferromagnet; this is also true for quenched real alloys favoring ordering for which the relaxation time (though may vary from several seconds to several days) is, generally speaking, one order of magnitude smaller than in the case of alloys with a tendency to clustering. In our model system the relaxation time at $0.6T_c$ is larger for $\bar{\eta} = 0$ than for $\bar{\eta} = -0.4$. On the other hand, a remarkable fact shown by the preceding graphs is that one can clearly distinguish two different stages in the approach to equilibrium. This evolution, however, presents no exponential regime for any case. $S(k, t)$ seems to vary almost linearly with time during most part of the evolution.

The energy u varies with time as shown in Figs. 85 (very early times) and 86 for the cases studied here. The last figure also evidences the two different stages in the relaxation of the system. The first stage is a very fast one and, according to Figs. B.31 - B.33 for the lattice configurations at early times, it is associated with single atoms processes which built up small ordered regions in the system. These regions ("antiphase domains") clearly show up in Figs. B.35 - B.37; in Fig. B.37 we limited the boundary of two of these domains by a dashed line. The "diffusion" and reaction of the antiphase domains is a much slower process and will then correspond to the flat part of the

evolution of u in Fig. 86. Note, however, that one can still distinguish two different slopes in the upper succession of points in Fig. 86; the latest, slightly slower, part of the evolution seems to correspond to the diffusion of "defects" (very small clusters which break the general order) throughout the lattice.

Fig. 87 corresponds to the variation with time of $u_\infty - u(t)$, where the equilibrium energy u_∞ is given in section 4.6 as computed from the evolution of our model system to long times; that figure shows a similar behavior of $u_\infty - u(t)$ for $\tilde{\eta} = 0$ at different temperatures. In Fig. 88 we present the temporal dependence of $\partial u / \partial t$ for all the cases considered here; this is to be compared with Fig. 89 corresponding to Iida's classical experiment in which a sample of the $Ni_3 Fe$ alloy ($T_c \approx 550^\circ C$) is quenched from $600^\circ C$ to the indicated temperatures (Iida 1955). Finally, Fig. 90 shows the evolution with time of $\sigma_\infty - \sigma$ at $\tilde{\eta} = 0$, $T = 0.9T_c$, where σ is the long range order parameter defined in (2.28) and its equilibrium value is given in the next section.

We mention that we find not much support from the present data for some of the predictions in section 3.5. In particular, when our data for $S(k, t)$ is plotted in the same fashion as in Fig. 3.6 we find a much more serious deviation from exponential behavior; we expect to report soon on higher temperatures which will be more comparable to those studied. Neither the evolution with time of the long range order parameter seems to agree with the theoretical

expectations (3.37) or (3.38) which are supposed to hold below T_c .

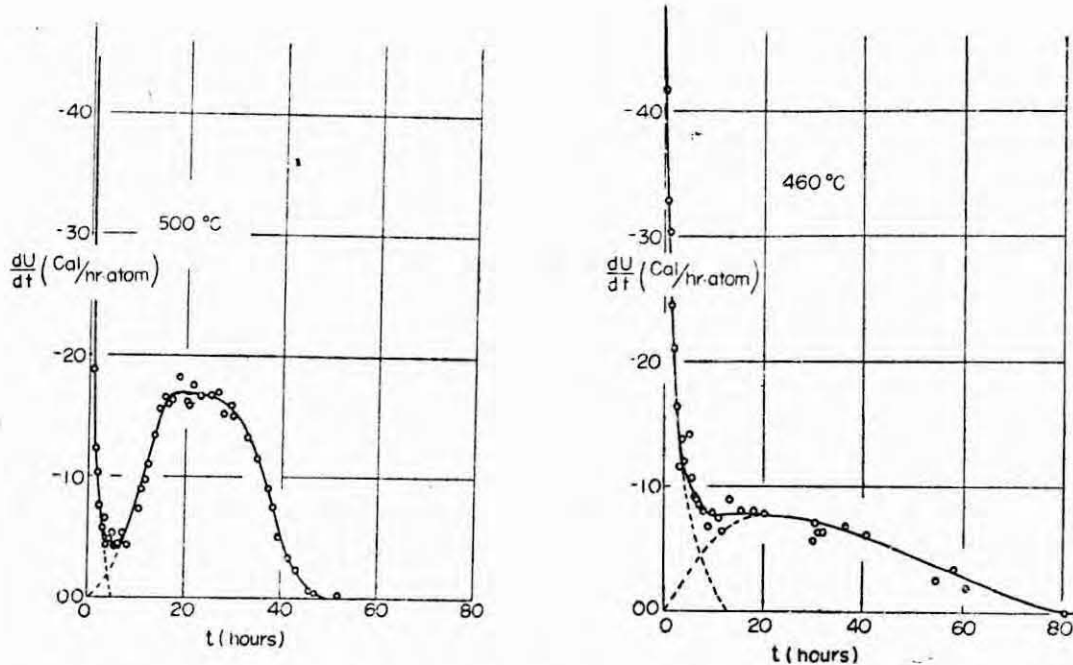


Fig. 4.89 The rate of the internal energy decrease plotted against time for Ni_3Fe quenched to the indicated temperatures ($T \approx 0.94T_c$, $0.89T_c$, respectively) (Iida 1955).

Figs. 4.81-4.82 Decay with time of the spherical averaged structure function $S(k, t)$ vs. k at $T = 0.6T_c$ for total magnetizations $\bar{\eta} = 0$ and -0.4 , respectively, in the antiferromagnetic model system.

Figs. 4.83-4.84 Evolution with time of $S(k, t)$ for different values of k . The corresponding value of $\mu = 30k/2\pi$ is shown at the end of each line.

Figs. 4.85-4.88 Temporal behavior of the energy u (number of AB-bond per site), as indicated in the figures, for the given compositions and temperatures.

Fig. 4.90 Evolution with time of $\sigma_\infty - \sigma$ at $T = 0.9T_c$ and $\bar{\eta} = 0$. σ is the long range order parameter defined in eq. (2.28) and σ_∞ the corresponding equilibrium value (sec. 4.6).

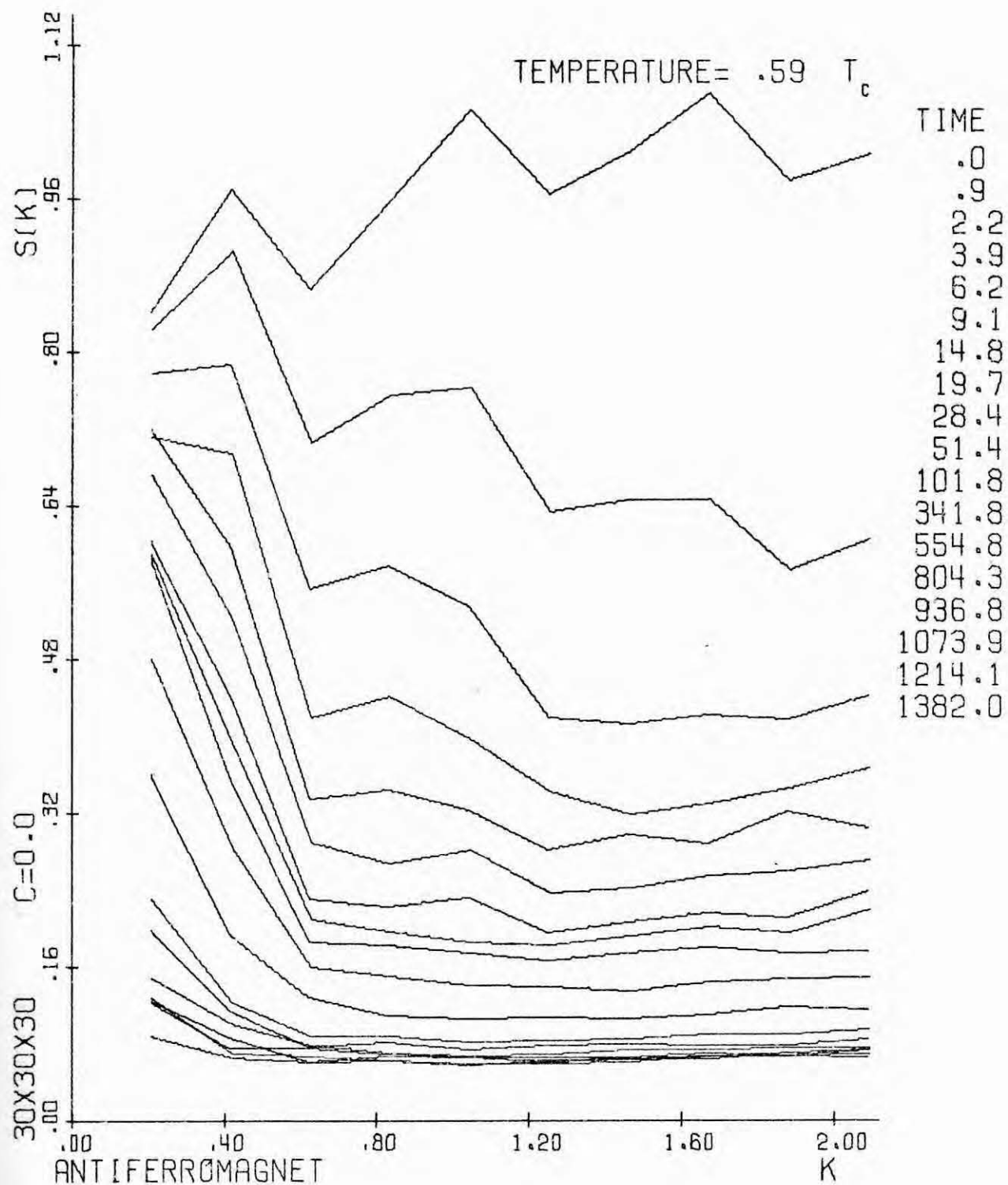


Fig. 81

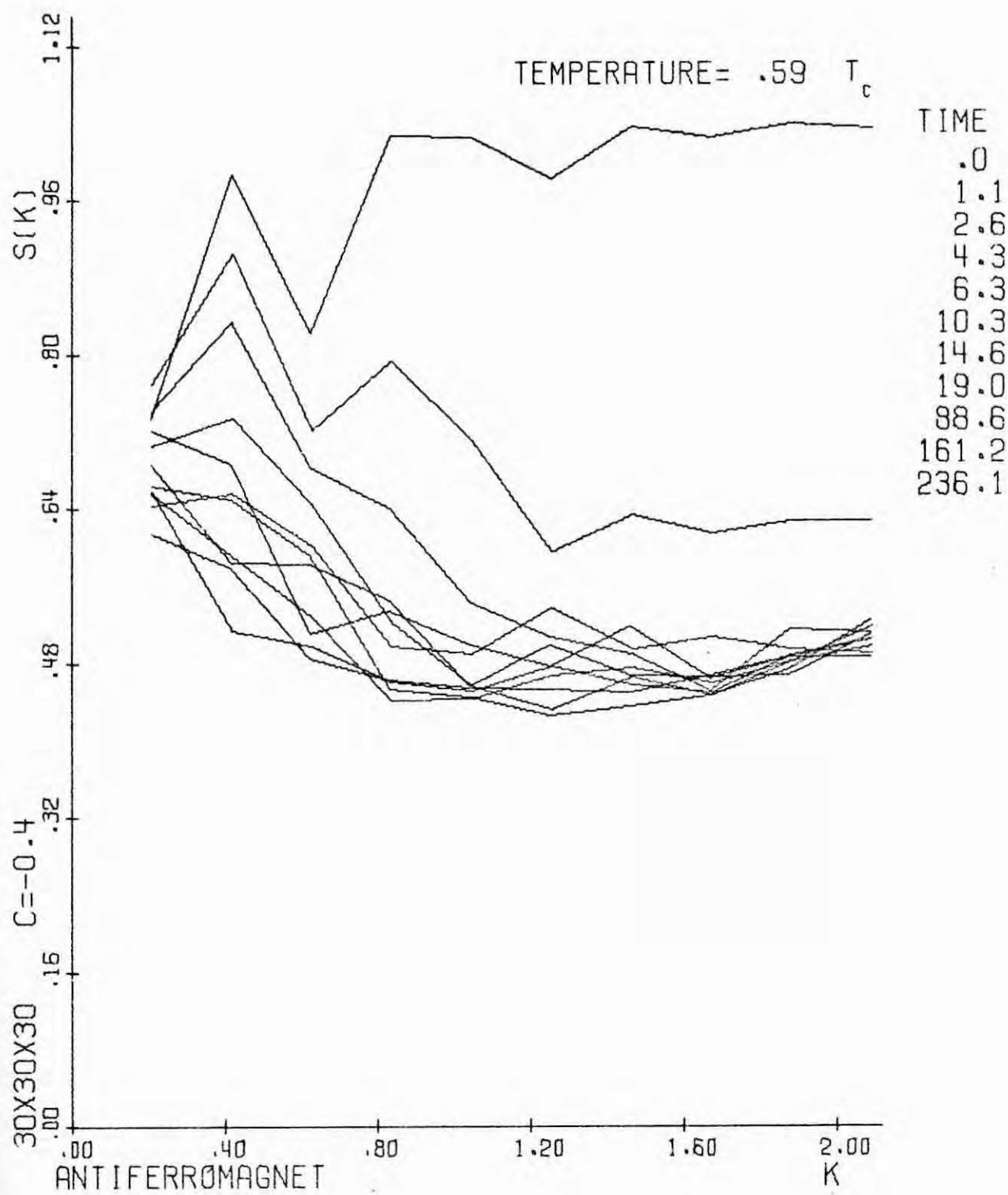


Fig. 82

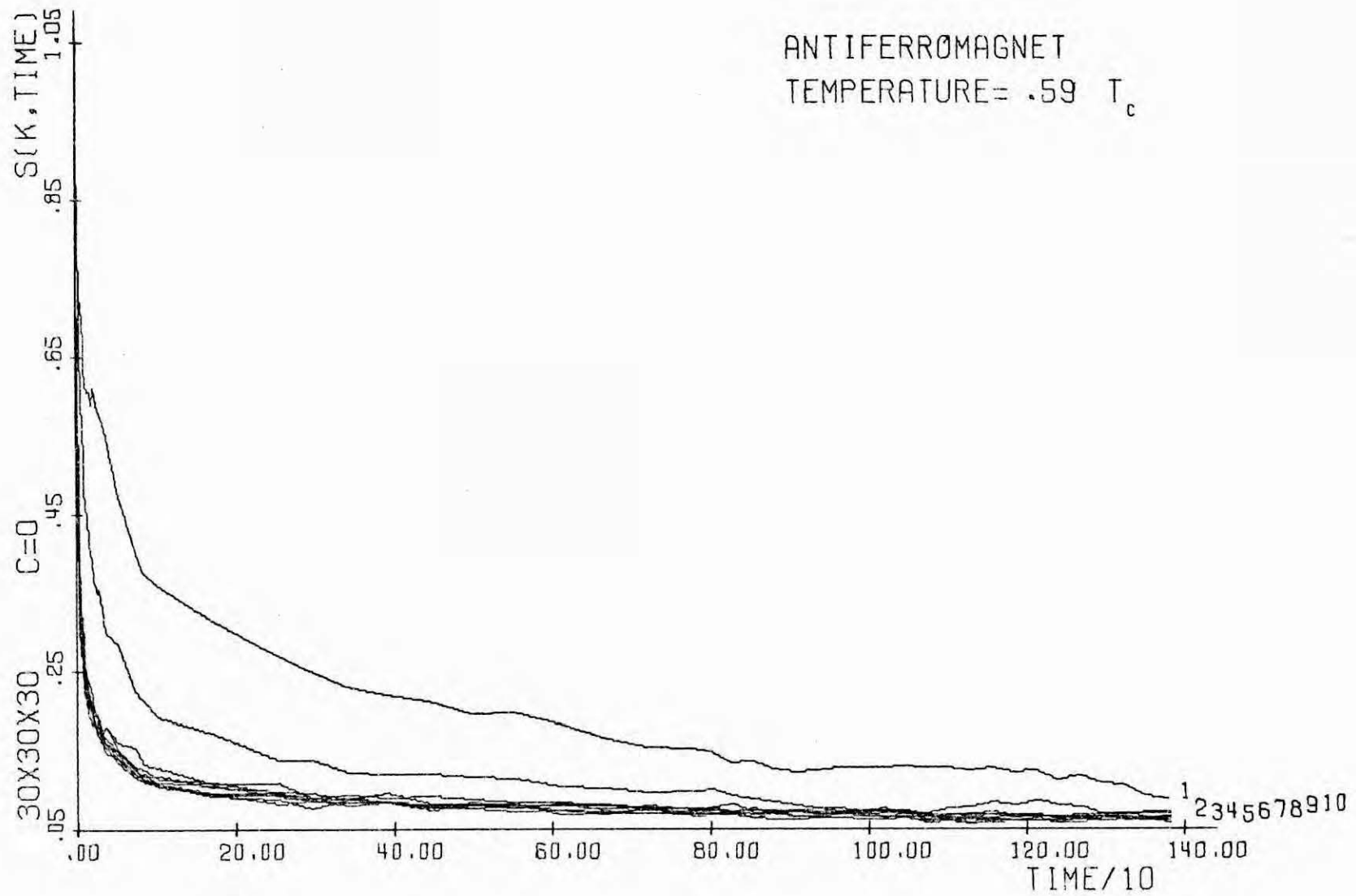


Fig. 83

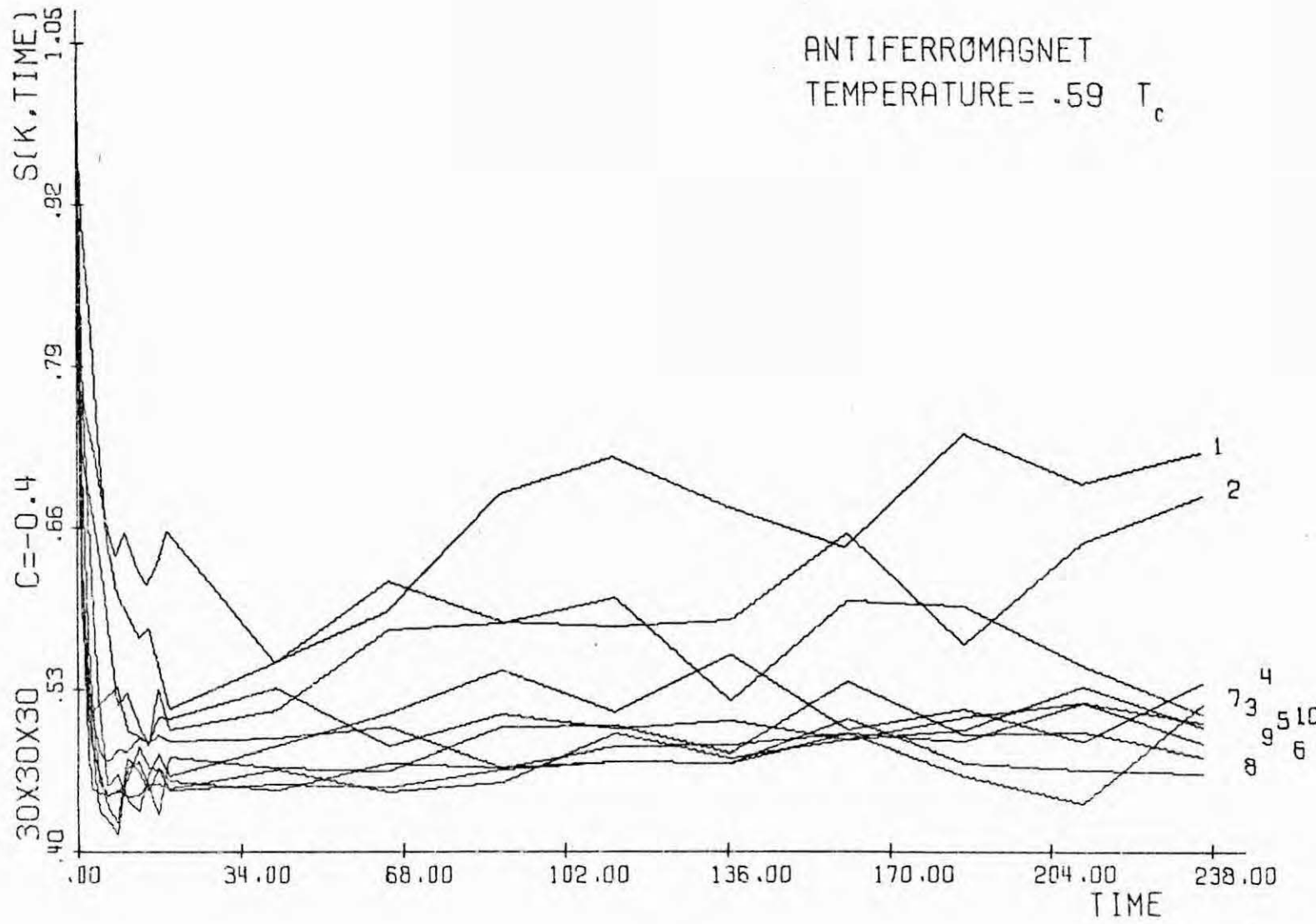
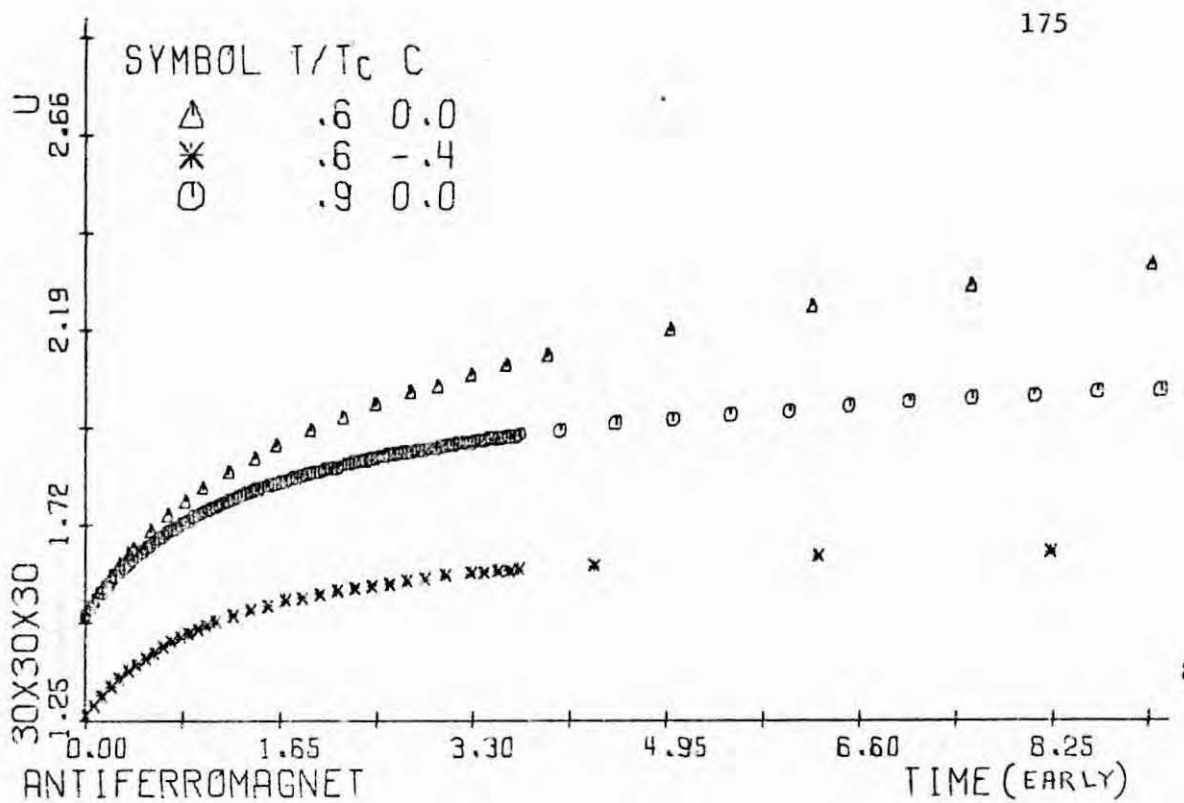
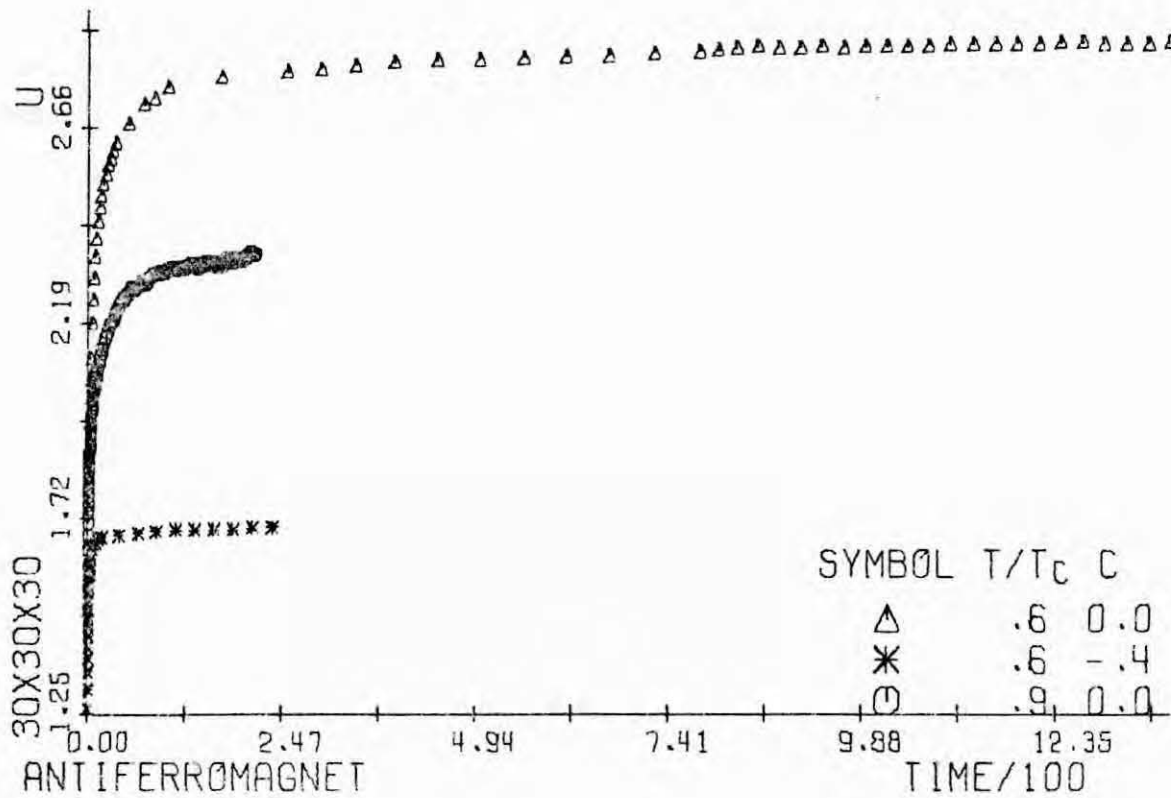


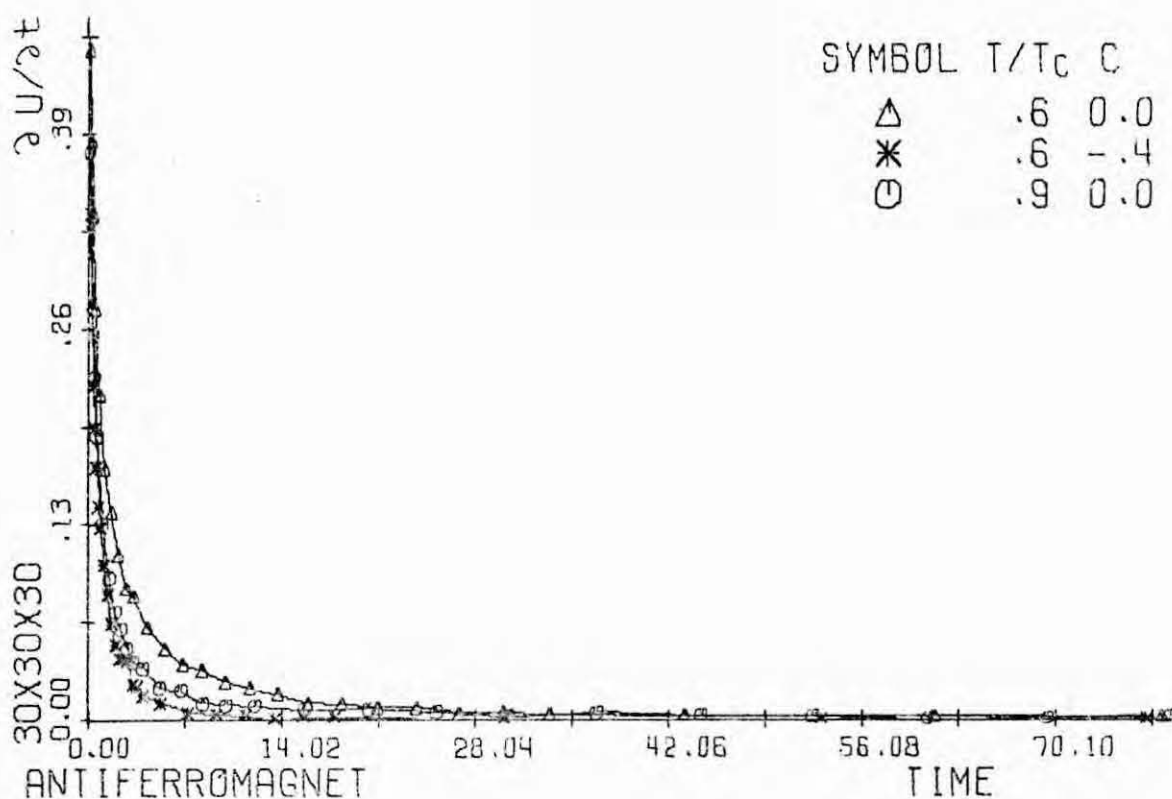
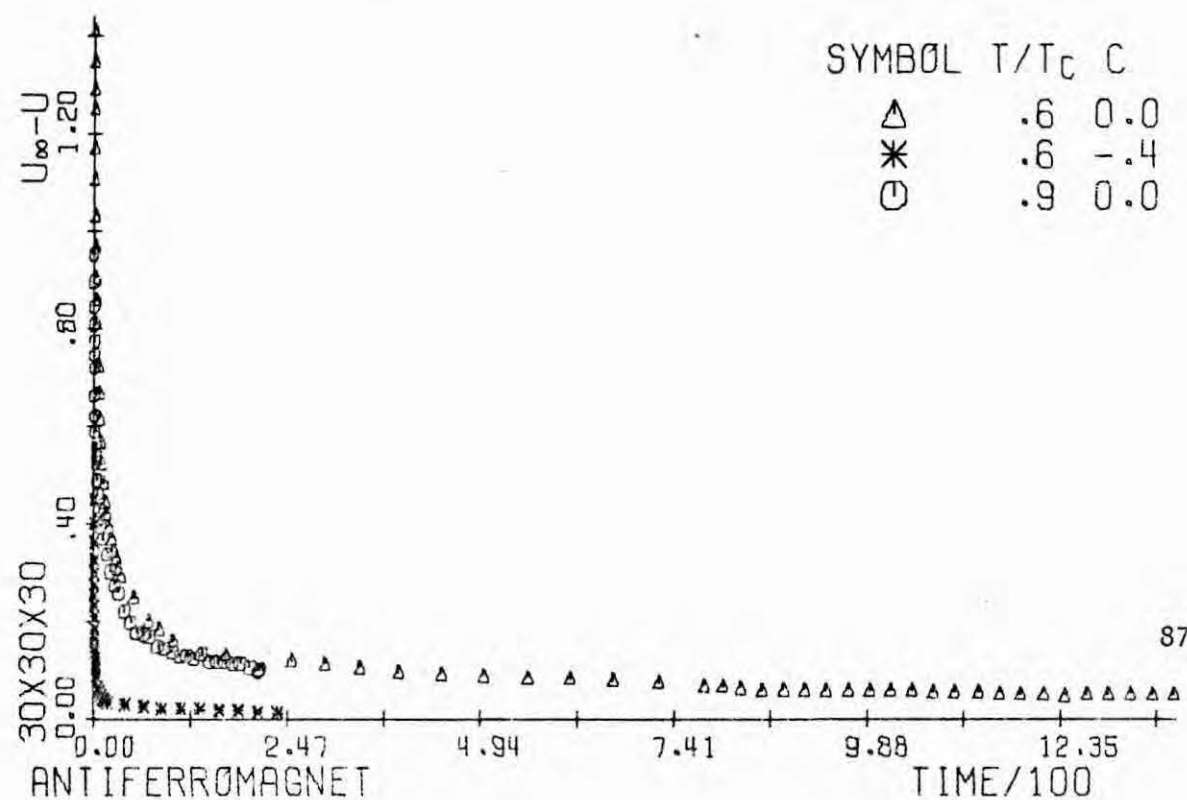
Fig. 84

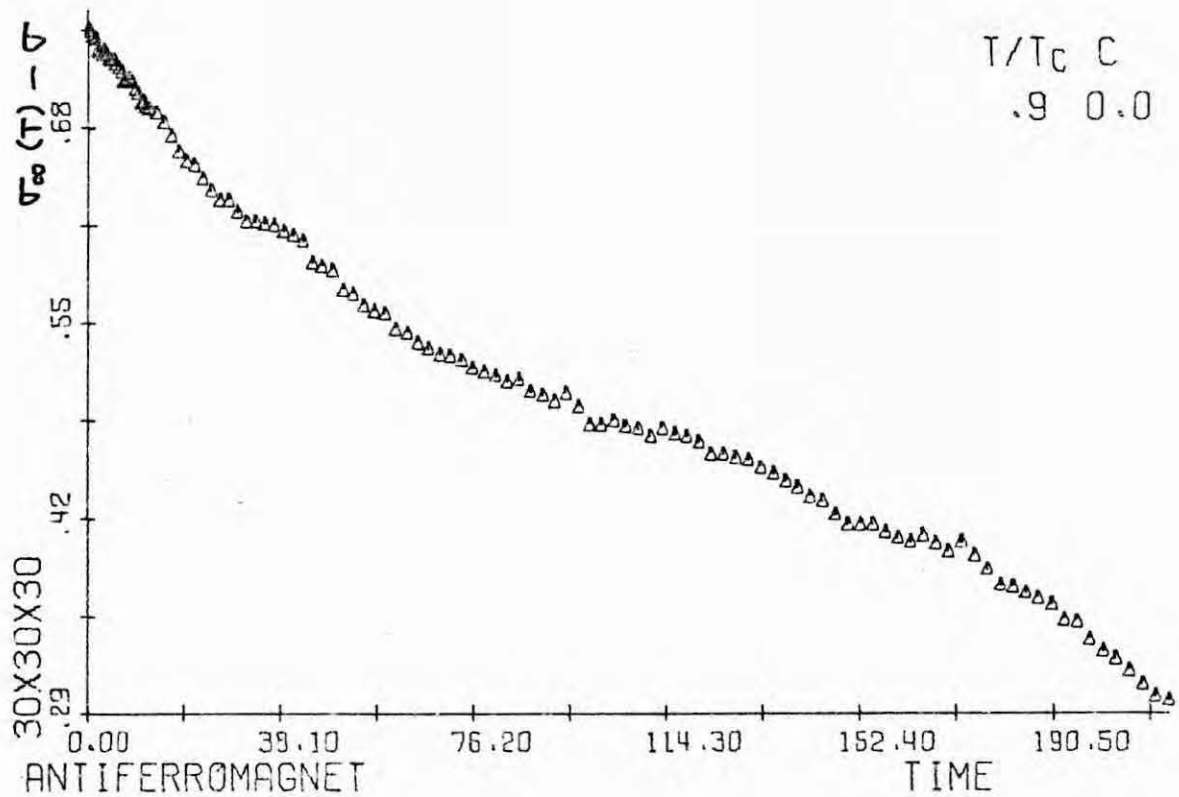


85



86





4.6. - Equilibrium behavior.

The minimum interfacial energy $u_I^{(1)}$ at zero temperature in our three-dimensional system is given, depending on the composition, by three possible different configurations: (1) a rectangular parallelepiped ($\bar{n}_A L \times L \times L$, with L the number of sites on a lattice side and \bar{n}_A the fraction of A-particles in the system) with four faces connected by periodic boundary conditions; (2) a rectangular parallelepiped ($\bar{n}_A^{1/2} L \times \bar{n}_A^{1/2} L \times L$) with two connected faces; and (3) a cube ($\bar{n}_A^{1/3} L \times \bar{n}_A^{1/3} L \times \bar{n}_A^{1/3} L$). When the system is large enough, the corresponding zero-temperature interfacial energies are

$$u_I^{(1)}(0) = 2/L, \quad u_I^{(2)}(0) = 4\bar{n}_A^{1/2}/L, \quad u_I^{(3)}(0) = 6\bar{n}_A^{2/3}/L. \quad (4.30)$$

(Note that for small systems for which $\bar{n}_A L$, $\bar{n}_A^{1/2} L$ or $\bar{n}_A^{1/3} L$ are not integer numbers, the expressions (4.30) should be corrected; this correction, however, may be neglected here.) Then we have

$$u_I^{(2)}(0) \leq u_I^{(1)}(0), \text{ for } \bar{n}_A \leq \frac{1}{4}, \quad \text{and} \quad (4.31)$$

$$u_I^{(3)}(0) \leq u_I^{(2)}(0), \text{ for } \bar{n}_A \leq 64/729 (\approx 0.088).$$

Thus, $\bar{n}_A \approx 0.088$ corresponds approximately to the, so to speak, critical value for "percolation" in our interacting system at zero temperature. The determination of the temperature dependence of this critical value is an open problem. Our simulation for the $50 \times 50 \times 50$ lattice seems to indicate that this value is between $\bar{n}_A = 0.03$ and $\bar{n}_A = 0.125$ at $T = 0.6T_c$ (and less than $\bar{n}_A = 0.2$ at $0.9T_c$ and $1.1T_c$ for the $30 \times 30 \times 30$ lattice.) The "random percolation" theory gives the value 0.307 for the infinite system at infinite temperature.

In two dimensions the situation is similar (case (1) would then correspond to a cross with bars connected by p.b.c.), but in this case

$$u_I^{(3)}(0) \leq u_I^{(2)}(0), \text{ for } \bar{n}_A \leq \frac{1}{4}, \quad (4.32)$$

with $u_I^{(2)}(0) = 2/L$ and $u_I^{(3)}(0) = 4\bar{n}_A^{\frac{1}{2}} L$. Thus, in two dimensions we expected no percolation effects at $\bar{n}_A = 0.2$ for any temperature, and this is the case in our simulation at $0.6T_c$.

The surface tension $\sigma(T)$ for the Ising model has been computed using the Monte-Carlo method (Leamy et al. 1973); Fig. 91. The relation $U(T)/U(0)$ between the equilibrium energies in the pure phase can be determined by integration of the low and high temperatures expansions (Baker 1963) for the specific heat. This value is then simply related to our energy $u_p(T)$ (section 4.2) by

eq. (2.27) $(U(0)/N = (\frac{1}{2}) zJ)$.

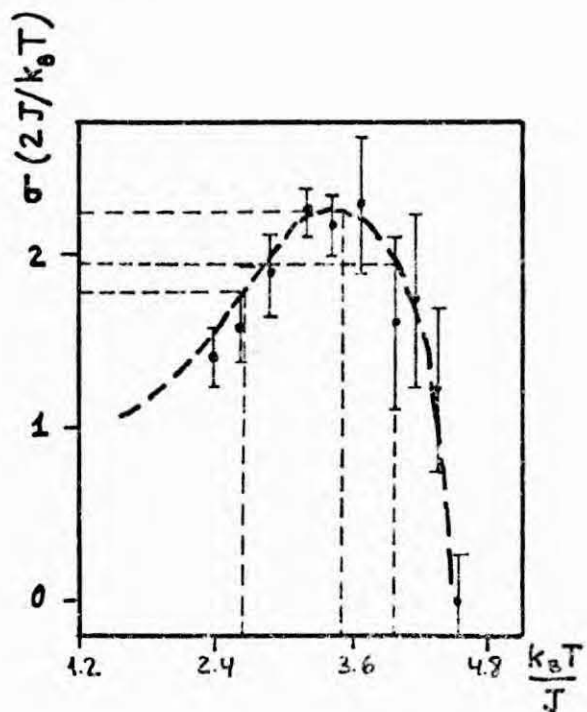


Fig. 4.91 Temperature dependence of the interfacial energy $\sigma(T)$ for an Ising system from Monte-Carlo simulations (Leamy et al. 1973). The values of relevance here are indicated.

The combination of all of this quantities according to relation (4.6) finally gives the values in Table 4.6 for the equilibrium energy, $u_\infty(T)$. In the cases for which the simulation was run to large enough values of t , we were able to compute directly $u_\infty(T)$ for our model system. The inspection of the temporal variation of the quantities in the system was the criterion we use to

T/T_c	$u_p(T)$	$u_\infty(T)$				
		30 x 30 x 30 lattice		50 x 50 50 lattice		
		$\bar{\eta} = 0$	$\bar{\eta} = -0.6$	$\bar{\eta} = -0.38$	$\bar{\eta} = -0.6$	$\bar{\eta} = -0.75$
0.6	0.08	0.20	0.18	0.15	0.14	0.13
0.8	0.29	0.44	0.43	0.38	0.37	0.35
0.9	0.53	0.66	0.65	0.61	0.60	0.59
1.1	1.10	1.10	-	-	-	-
1.5	1.26	1.26	-	-	-	-

Table 4.6 Equilibrium energy $u_\infty(T)$, (4.6), in the cases of interest here, as computed from relation (4.6).

T/T_c	ferromagnetic interaction			antiferromagnet		
	1.068	1.068	1.501	0.591	0.591	0.887
$\bar{\eta}$	0	-0.6	0	0	-0.4	0
n	57	67	117	52	72	81
$u_\infty(T)$	1.097 ± 0.0064	0.792 ± 0.0050	1.255 ± 0.0065	2.917 ± 0.0042	1.709 ± 0.0044	2.457 ± 0.0152
$C(T)/k$	0.19	0.22	0.10	0.27	0.30	1.56
σ : long range order parameter				0.970 ± 0.0018	0.407 ± 0.0149	0.752 ± 0.010

Table 4.7 Equilibrium energy $u_\infty(T)$ for our system as given by the computer simulation. n is the number of the different time points considered in the corresponding average. Our computed values for the specific heat and LRO parameter are also shown.

determine whether or note the system had reached its equilibrium state. Then the system was allowed to evolve during a certain time, and the latest values of the quantities of interest were averaged (these late parts of the evolutions are generally not included in the previous analysis.) In this way we obtain for

$u_{\infty}(T) \pm \Delta u$, $\Delta u = [\sum_{i=1}^n (\bar{u} - u_i)^2 / n]^{1/2}$, the values in Table 4.7; there is good agreement for the cases contemplated in both tables.

As seen in eq. (2.27), in equilibrium we have

$U_{AB}^{\text{ferr}} = -JN_{AB}^{\text{ferr}} + J(N_{AA} + N_{BB}) = -2JN_{AB}^{\text{ferr}} + 3JN$, in the case of a ferromagnetic coupling. For an antiferromagnetic interaction and $T > T_c$, $U_{AB}^{\text{ant}} = 2JN_{AB}^{\text{ant}} - 3JN = U_{AB}^{\text{ferr}}$, which implies $u_{\infty}^{\text{ferr}}(T) = 3 - u_{\infty}^{\text{ant}}(T)$. We note that our data in Table 4.7 for $T/T_c = 0.6, 0.9, \tilde{\eta} = 0$, gives $u_{\infty}^{\text{ferr}}(T) = 0.08, 0.54$, in agreement with the values of $u_p(T)$, the equilibrium energy for the infinite system. The same procedure gives $u_p(T) = 1.29$ for $\tilde{\eta} = -0.4$ and $T = 0.6T_c$.

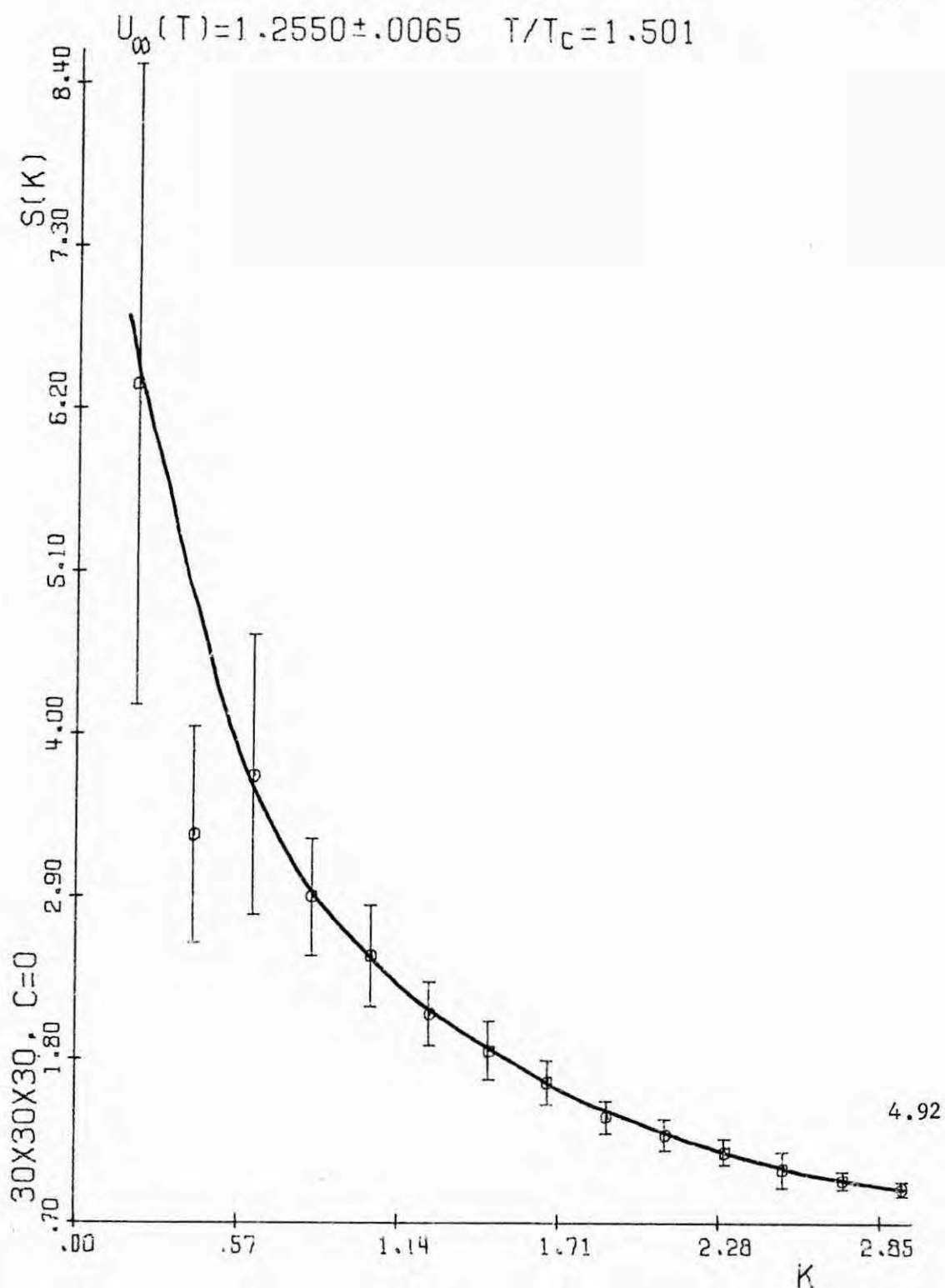
From Einstein's formula for the energy fluctuations in the system, ΔU (simply related to Δu by eq. (2.27)),

$$\overline{(\Delta U)^2} = k_B T^2 N C(T), \quad (4.33)$$

one can also determine the corresponding values for the specific heat $C(T)$; these values are also given in Table 4.7, as well as the equilibrium values we computed for the long range order parameter in the case of antiferromagnetic interactions.

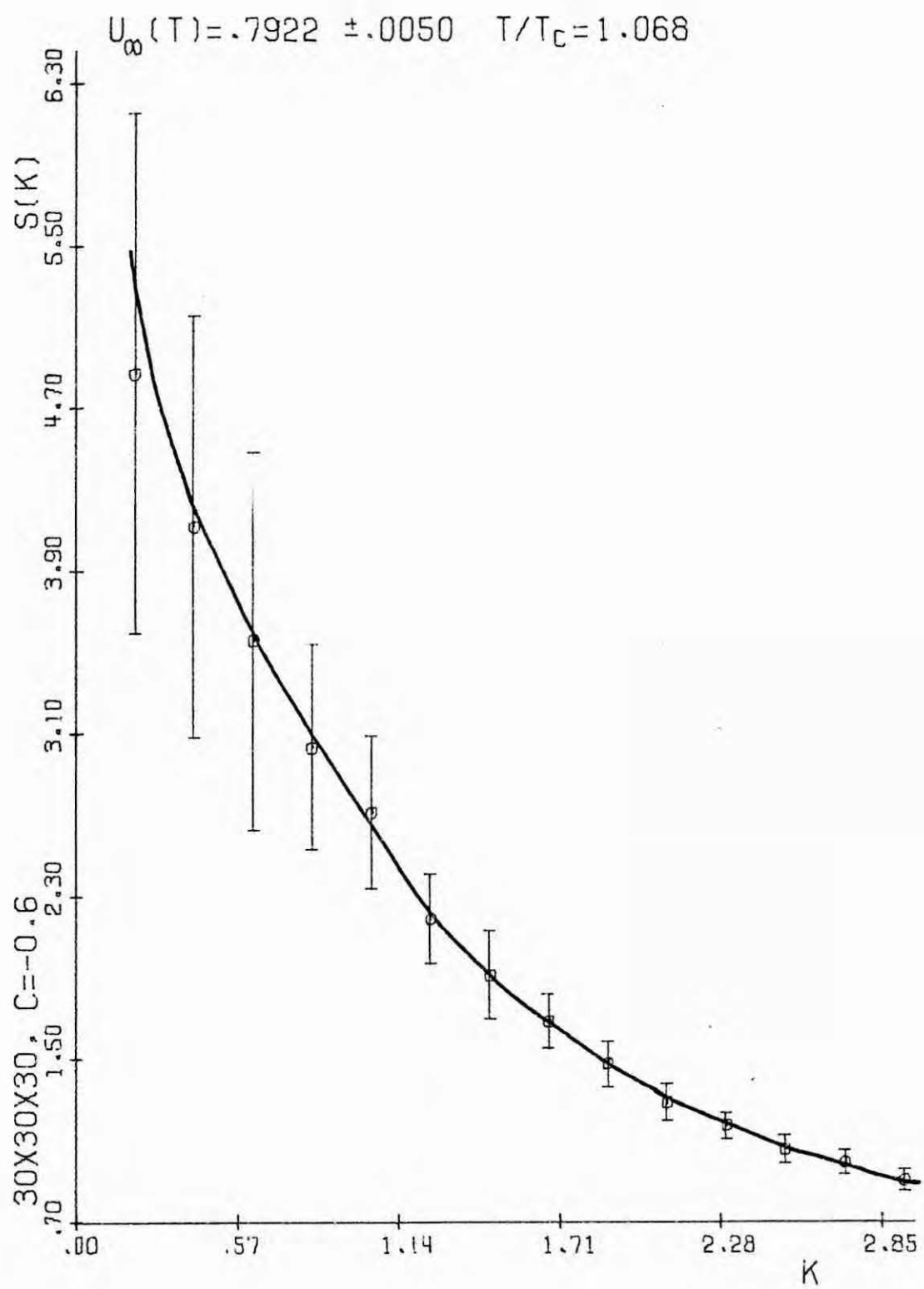
We have also looked at the equilibrium shape of the structure function $S(k)$ in some of the studied cases; this is shown in Figs. 92-95 where also are indicated the equilibrium fluctuations. The data in Figs. 92-93 for $k \lesssim 2/a_0$ fits fairly well an Ornstein-Zernicke expression for $S(k)$ but, as expected, there is a strong deviation for larger values of k ; this will be reported elsewhere.

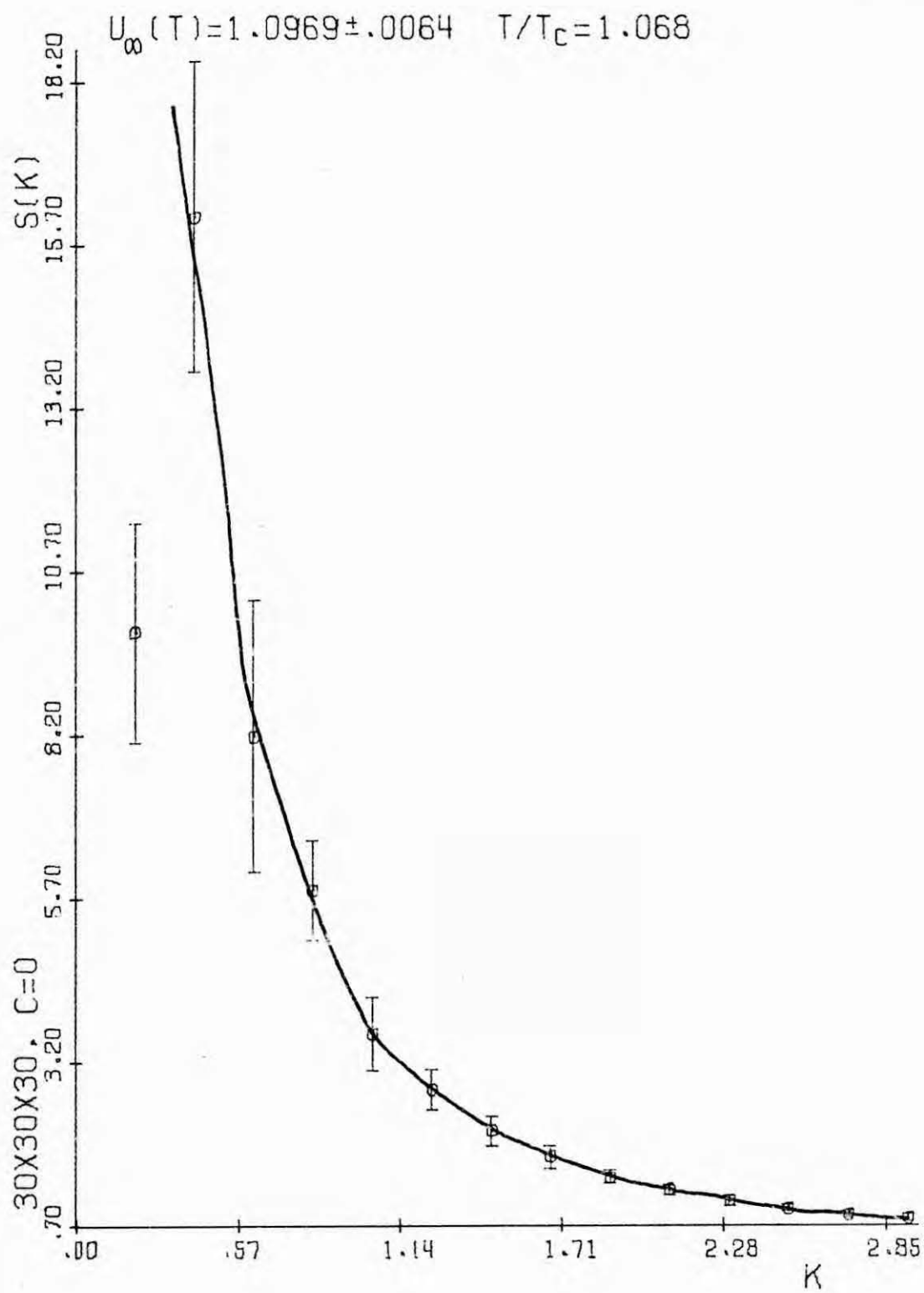
In Fig. C.86 we present the equilibrium cluster distribution at $T = 1.1T_c$ and $\bar{\eta} = -0.6$. This is calculated by means of an average over an interval of time (whose mean time is shown in the figure) in which were performed 1,350,000 exchanges in each of the eight independent evolutions (corresponding to the last 17 time points in Table A.21). The same procedure (average over 1,900,000 exchanges) gives Fig. C.85 at $T = 0.9T_c$, $\bar{\eta} = -0.6$; although in this case the system had not reached the equilibrium state, Table A.20 shows that there is no appreciable change in the cluster distribution during the averaged temporal interval. In other cases we computed the equilibrium cluster distributions corresponding to small clusters; this is given in Table 4.5.

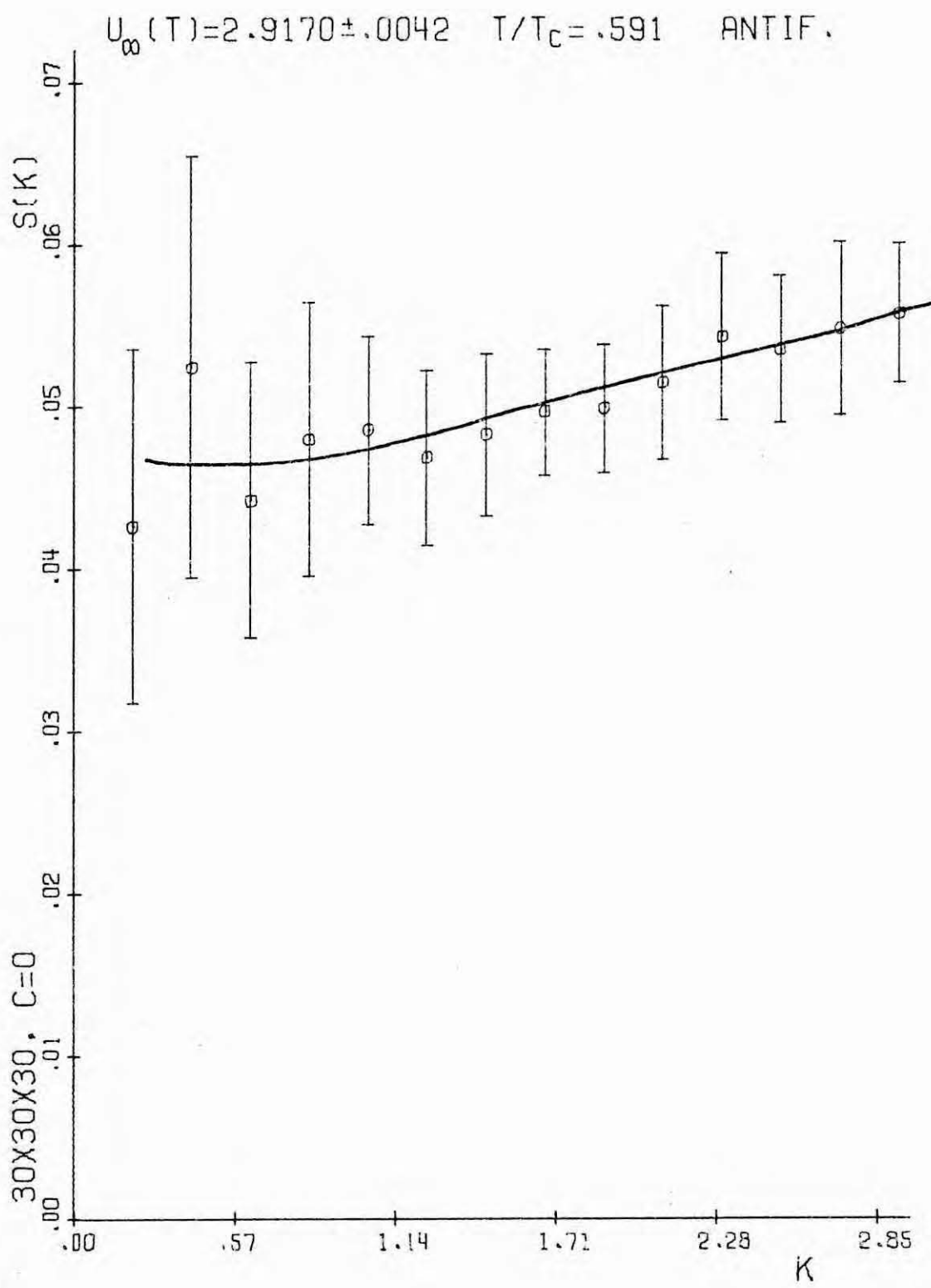


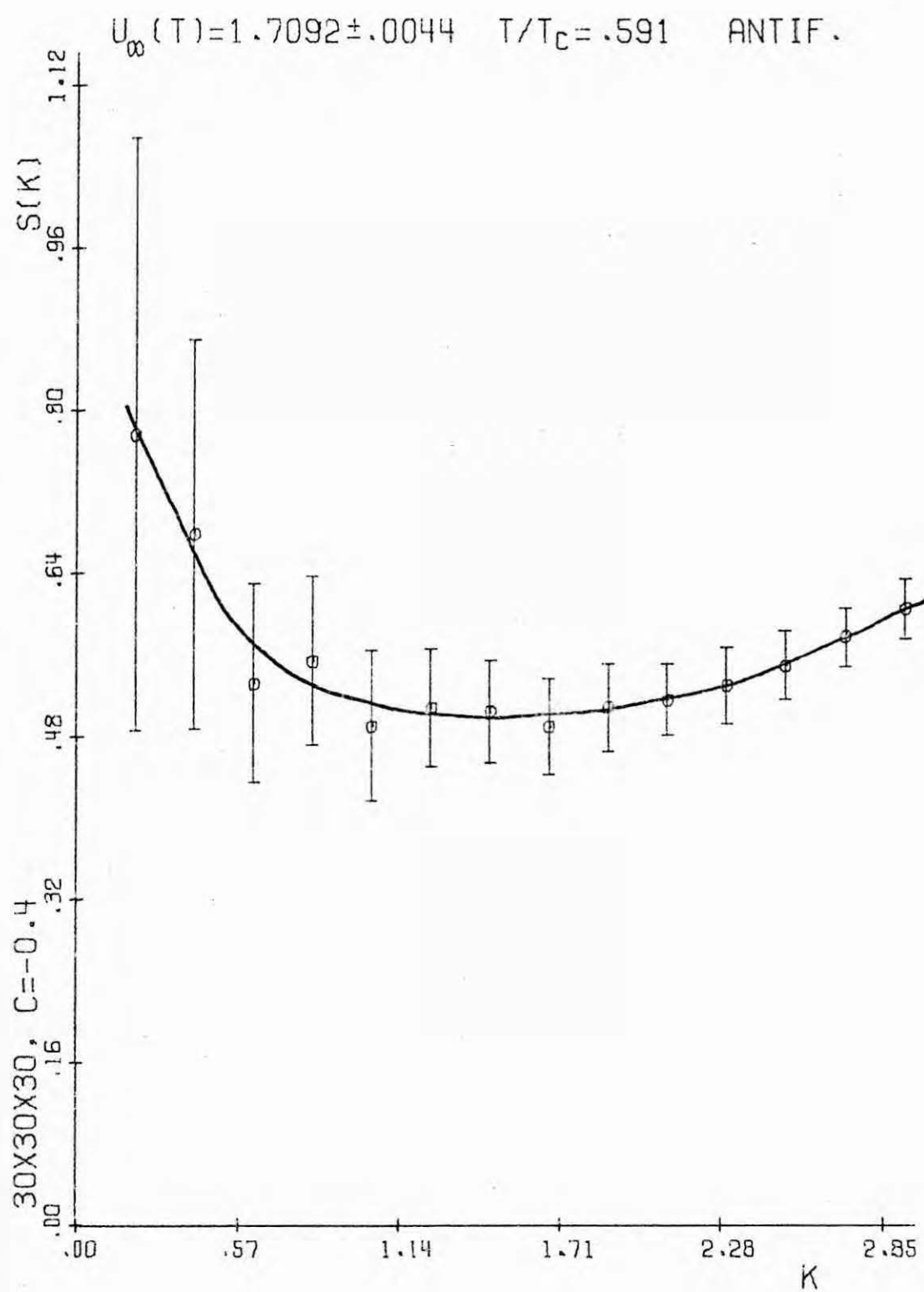
Figs. 4.92-4.95

Equilibrium spherically averaged structure function $S(k)$ as a function of k for the indicated temperatures and compositions. The equilibrium fluctuations are also indicated.









For $\bar{\eta} = 0$ at every temperature we considered, the system in equilibrium showed, in addition to the very small clusters, most of the particles connected in a single cluster. At $T = 1.1T_c$, the corresponding values in Table 4.5 are to be completed with $n_{11}^S = 0$, $n_{12}^S = 0.005$, $n_{13}^S = 0$, $n_{14}^S = 0.002$ and $n_\lambda^S = 0$ for $L > 14$ with the only exception of a big cluster whose mean size we computed as 13316.61 (98.64% of the particles.) The corresponding average values of the energy per particle are:

$$\lambda = 1, 2, 3, 4, 5, 6, 7, 8, 9, 10, 12, 14, 13316.61$$

$$\epsilon_\lambda/\lambda = 6, 5, 4.67, 4.46, 4.35, 4.18, 4.04, 4.20, 4.04, 3.80, 3.75, 4, 2.43.$$

At $T = 1.5T_c$, $\bar{\eta} = 0$:

$$\lambda = 1, 2, 3, 4, 5, 6, 7, 8, 9, 10, 11, 13336.49$$

$$\epsilon_\lambda/\lambda = 6, 5, 4.67, 4.44, 4.34, 4.30, 4.22, 3.94, 4, 3.90, 4.09, 2.75,$$

with $n_{11}^S = 0.005$ and $n_\lambda^S = 0$ for the values of λ not shown above.

Note that for $8 \leq \lambda \leq 13000$ our statistics are poor and the corresponding values above are not accurate.

4.7. - Comparison with experiments.

In order to compare the results of the computer simulation with possible real experiment (i.e being able to neglect vacancies, defects, etc.) we have to establish some (order of magnitude) relation between our units of length and time and those of real systems. Our unit of length is the lattice spacing, a_0 , which is of the order of several Angstroms. In the experiments of Rundman and Hilliard (1967, Rundman 1970) on the Zn-Al (22% Zn alloy)

at 423°K ($\approx 0.7T_c$) is $a_0 \approx 2.5 \text{ \AA}$. Thus we have $k = 2\pi\mu/a_0 \approx 0.84\mu 10^7 \text{ cm}^{-1}$.

The location of the peak in the Rundman-Hilliard experiment, Fig.

96, is around $k \approx 10^7 \text{ cm}^{-1}$, as is also, according to the above

value of a_0 , in Fig. 3 from our "experiment". Interestingly

enough, the location and height of the peak in the real experiment described in Fig. 96 appears to behave in accordance with eqs.

(4.2) and (4.3) with $a' \approx 0.2$ and $a'' \approx 0.7$, which are close to the values found by us.

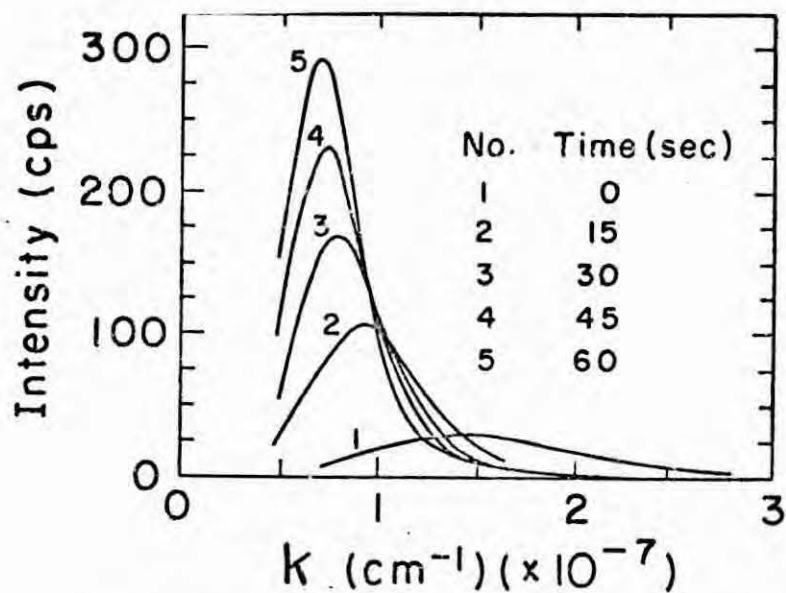


Fig. 4.96 Development with time of the scattering intensity as a function of k in the Rundman-Hilliard experiment on the Zn-Al alloy at $0.7T_c$. Note the resemblance with our Figs. 1-3 and 6.

Our unit of time is α^{-1} which according to (2.19) is just one half of the average time between exchanges which do not change the energy of a configuration, e.g. $2/\alpha$ is the mean time between jumps to a neighboring site for an A-atom in a sea of B-atoms. Hence, according to (2.19), α^{-1} is related simply to $\tilde{D}(T)$, the diffusion coefficient of an A-atom in a crystal of B-atoms (and vice versa),

$$\alpha^{-1}(T) = a_0^2 [12 \tilde{D}(T)], \quad (4.34)$$

where $\tilde{D}(T)$ is the diffusion constant at temperature T in the limit of zero concentration of A(or B)-atoms (when the system would of course be in a one-phase). If we set (deFontaine 1967, Cook 1970; see, for instance, Ardell 1969 for other alloys) $\tilde{D}(T) \simeq 8.8 \cdot 10^{-16} \text{ cm}^2/\text{sec}$ for the Rundman-Hilliard experiment, then $\alpha^{-1} \simeq 3/50 \text{ sec}$. Accordingly, the time limit in our simulations below T_c runs from 37 sec to 392 sec and we are reporting evolution intervals which can be observed experimentally.

On the other hand, we mention that there is an outstanding difference between the cluster distribution reported in a certain kind of experiments on real alloys (Fig. 56) and the corresponding graphs we report in Figs. C.1 - C.51. Those experiments (Ardell 1969) report a direct counting of clusters size and number which is performed on a thin foil of the alloy separated from a "frozen"

extraction replica. This procedure is justified if the clusters are spherical, but cannot detect the presence of "infinite size" clusters in the sample. To obtain comparable results we would have to determine the cluster size from Figs. B.1 - B.30 which correspond to sections of the system (and doing so we approximately obtain at $T = 0.6T_c$ $a' \approx 1/3$ for eq. (4.22)), but this is not justified here. An experimental analysis of this point on real alloys, as well as detailed scattering studies (similar to the Rundman-Hilliard experiment) at different phase-points on different alloys would be very interesting.

4.8. - Discussion.

We want to summarize here some qualitative conclusions which emerged during the preceding analysis.

The coarsening process in our model binary alloy is accompanied by a growth of the structure function $S(k,t)$ for certain values of k which is no faster than linear with time (sec. 4.1). This result is in serious disagreement with the linearized Cahn-Hilliard theory (sec. 3.1), including Cook's modification (sec. 3.3), and we conclude that these theories, which have been usually considered as a reasonable approximation for the early stages of phase segregation in quenched binary alloys, do not provide a valid description.

The computer treatment of one-dimensional diffusion equations (sec. 3.1) and statistical-mechanics formulations of

the above theories (secs. 3.3 and 3.5) have shown that the introduction of non-linear corrections is not enough by itself to obtain a proper description. A partial, very satisfactory picture of the coarsening process is provided by a recent analytic model by Langer, Bar-on and Miller (sec. 3.3), and we have shown (sec. 4.3) in relation with this model that usual dynamical scaling laws seem to be valid at temperatures surprisingly lower than expected in the case of zero total magnetization. Several approximations contained by this model might be improved (sec. 4.3), in particular the assumption about a Ginzburg-Landau free-energy which prevents it of a more general applicability.

The "Ostwald ripening" theory, as formulated by Lifshitz and Slyozov and Wagner (sec. 3.2), quantitatively disagrees with our results. Nevertheless, there is some evidence about the relevance of simple power laws in the temporal evolution of the system. If this is so, some of the preceding analysis (secs. 4.1, 4.2 and 4.4) indicates an important role of the "Smoluchowski coagulation" mechanism and the predictions by Binder and Stauffer (sec. 3.4) are approximately correct, at least for some early stages of the evolution. Later, if one accepts the existence of a rapid change in the mechanism of cluster growth, our empirical exponents for the corresponding power laws are closer to the ones predicted by the Lifshitz-Slyozov theory.

The main conclusion, however, should be stated at this stage in terms of the lack of a satisfactory theory for "spinodal decomposition". In fact, the last conjecture is not quite consistent with the reported good agreement between the computations by Langer, Bar-on and Miller at $\tilde{\eta} = 0$ and the evolution of our model, although it is interesting to note that those authors report a crossover effect when trying to fit the temporal evolution of the peak of $S(k,t)$ by a simple power law. Also, as a consequence of the possible inadequacy of theory, some of our empirical fits in sections 4.1, 4.2 and 4.3 are to be quarantined.

The results we report here for the ordering binary alloy (sec. 4.5) are of very little support for the corresponding approaches considered in section 3.5. There is also little hope from those preliminary results for an exponential decrease of $S(k,t)$ which is predicted by an extension of the Cahn-Hilliard theory to the case of an antiferromagnetic model quenched to $T > T_c$.

Another interesting conclusion concerns the concept of limit of metastability as introduced by Gibbs. We have seen that our results at $\tilde{\eta} = 0$ and $\tilde{\eta} = -0.6$ are practically independent of composition for $T < 0.9T_c$; this is not consistent with a Ginzburg-Landau polynomial for the free-energy of the system, so far always assumed by theory. More than that, the gradual change observed in the behavior of the system when quenched to different

points inside the coexistence line (and its comparison with the behavior outside that line) indicates that there is no well-defined limit of metastability for our system, but some transition region very close to the coexistence line

Finally, we want to comment that some of our results bear a close similarity with observations from scattering experiments on real alloys, and this supports our belief that the model analysed in this work contains the essential physical features of the phenomena of interest. This, of course, does not mean that experimentalists will always report a behavior similar to the one of the model. They deal with systems in which there are vacancies, strain fields, grain boundaries, long ranged interactions, lower symmetries, etc., etc. and, on the other hand, the reliable scattering experiments on real quenched alloys seem to present a very difficult realization. There is no apparent reason, however, to assume that a theory failing to describe what happens in our oversimplified model will work better in more realistic systems. A deeper understanding of these systems may partly follow from the incorporation of complications in the flexible computer simulations.

V. References.

- Andreev, N.S., Boiko, G.G. and Bokov, N.A. (1970), J. Non-Cryst. Solids 5, 41.
- Ardell, A.J. (1969), in The Mechanics of Phase Transitions in Crystalline Solids, Institute of Metals Monograph Series, London 1969, 33, 111.
- Baker, J.A. (1963), Phys. Rev. 129, 99.
- Bethe, H.A. (1935), Proc. Roy. Soc. (London) A150, 552.
- Binder, K. (1972), Physica 62, 508.
- (1973), Phys. Rev. B8, 3423.
 - (1974a), Z. Phys. 267, 213.
 - (1974b), in Nucleation, Vol. II, A.C. Zettlemoyer ed. M. Dekker, N.Y.
 - (1975), private communication.
 - and Müller-Krumbhaar, H. (1974), Phys. Rev. B9, 2328.
 - Rauch, H. and Wildpaner, V. (1970), J. Phys. Chem. Solids, 31, 391.
 - and Stauffer, D. (1974), Phys. Rev. Lett. 33, 1006.
 - et al. (1975), in Nucleation, Vol. III, A.C. Zettlemoyer, Dekker, N.Y., to be published.
- Borelius, G. (1947), J. Inst. Metals 74, 17.
- Bortz, A.B. (1971), Ph.D. Thesis, Carnegie-Mellon Univ. Penn.
- (1974), J. Stat. Phys. 11, 181.
 - Kalos, M.H., Lebowitz, J.L. and Zendejas, M.A. (1974), Phys. Rev. B10, 535.

References, con't.

- Bortz, A.B., Kalos, M.H. and Lebowitz, J.L. (1975), J. Comp. Phys. 17, 10.
- Bragg, W.L. and Williams, E.J. (1934), Proc. Roy. Soc. (London) A145, 340; 151, 540; 152, 231 (1935).
- Brush, S.G. (1967), Rev. Mod. Phys. 39, 883.
- Butler, E.P. and Thomas, G. (1970), Acta Met. 18, 347.
- Cahn, J.W. (1961), Acta Met. 9, 795.
- (1962), Acta Met. 10, 179.
- (1966), Acta Met. 14, 1685.
- (1968), Trans. Metl. Soc. AIME 242, 166.
- and Hilliard, J.E. (1958), J. Chem. Phys. 28, 258.
- and Hilliard, J.E. (1959), J. Chem. Phys. 31, 688.
- Christian, J.W. (1969), Comm. Sol. State Phys. 1, 145; 2, 143.
- Cook, H.E. (1970), Acta Met. 18, 297.
- deFontaine, D. and Hilliard, J.E. (1969), Acta Met. 17, 765.
- and Hilliard, J.E. (1969), J. Appl. Phys. 40, 2191.
- Cornie, J.A. et al. (1973), Met. Trans. 4, 727.
- Cowley, J.M. (1950), J. Appl. Phys. 21, 24; Phys. Rev. 77, 669.
- Dalal, H. and Grant, N.J. (1973), Met. Trans. 4, 381.
- deFontaine, D. (1967), Ph.D. Thesis, Northwestern University,
Evanston, Ill.
- (1973), J. Phys. Chem. Solids 34, 1285.

References, con't.

- deFontaine, D. and Cook, H.E. (1971), in Critical Phenomena in Alloys, Magnets and Superconductors, R. Mills et al. ed., McGraw-Hill, N.Y.
- and Kikuchi, R. (1974), *Acta Met.* 22, 1139.
- Dienes, G.J. (1955), *Acta Met.* 3, 549.
- Dietrich, O.W. and Nielsen, J.A. (1966), Proc. Conf. Critical Phenomena, Washington, D.C. 1966, NBS Publ. 273, 144.
- Domb, C. (1974), in Phase Transitions and Critical Phenomena, Vol. 3, C. Domb and M.S. Green, eds., Academic Press, London.
- Ehrenfest, P. (1933), *Proc. K. Akad. Amst.* 36, 153.
- Erb, D. and Hilliard, J.E. (1970), preprint.
- Essam, J.W. (1972), in Phase Transitions and Critical Phenomena, Vol. 2, Domb, C and Green, M.S. eds., Academic Press, London.
- and Fisher, M.E. (1963), *J. Chem. Phys.* 38, 802.
- Ferdinand, A.E. and Fisher, M.E. (1969), *Phys. Rev.* 185, 832.
- Fisher, M.E. (1967a), *Repts. Progr. Phys.* 30, 615.
- (1967b), *Physica* 3, 255.
- (1970), in *Lecture Notes of the International School of Physics "Enrico Fermi"*, L.I. Course, Critical Phenomena, Varenna.
- (1975), private communication.

References, con't.

- Flewitt, P.E. (1974), *Acta Met.* 22, 47.
- Flinn, P.A. (1974), *J. Stat. Phys.* 10, 89.
- and McManus, G.M. (1961), *Phys. Rev.* 124, 54.
- Fowler, R.H. and Guggenheim, E.A. (1949), Statistical Thermodynamics, Cambridge Univ. Press, London.
- Glauber, R.J. (1963), *J. Math. Phys.* 4, 294.
- Gotlib, Y.Y. (1970), *Soviet Phys. Solid State* 3, 1574.
- Green, H.S. and Hurst, C.A. (1964), Order-Disorder Phenomena, Interscience, London.
- Griffiths, R.B. (1972), in Phase Transitions and Critical Phenomena, Vol. 1, C. Domb and M.S. Green eds., Academic Press, London.
- Guttmann, L. (1956), *Solid State Phys.* 3, 145.
- Hammersley, J.M. and Handscomb, D.C. (1964), Monte Carlo Methods, Methuen, London.
- Heisenberg, W. (1928), *Physik. Z.* 49, 619.
- Higgins, J. et al. (1974), *Acta Met.* 22, 201.
- Hillert, M. (1956), Ph.D. Thesis, M.I.T., Cambridge, Mass.
- (1961), *Acta Met.* 9, 525.
- Hilliard, J.E. (1970), in Phase Transformations, H.I. Aaronson ed., Am. Soc. Met., Metals Park, Ohio.
- Holley, R. (1974), *Rocky Mountain J. Math.*, to appear.

References, con't.

- Huang, J.S., Goldburg, W.I. and Bjerkaas, A.W. (1974), Phys. Rev. Lett. 32, 921.
- et al. (1975), communication to the 33rd U.S. East Statistical Mech. Meeting, Yeshiva, Univ. N.Y., May 1975.
- Iida, S. (1955), J. Phys. Soc. Japan 10, 9; and references therein.
- Ising, E. (1925), Physik. Z. 31, 253.
- Jones, F.W. and Sykes, C. (1938), Proc. Roy. Soc. (London) A166, 376; A157, 213 (1936).
- Kadanoff, L.P., et al. (1967), Rev. Mod. Phys. 39, 395.
- Kawasaki, K. (1966), Phys. Rev. 145, 224; 148, 375; 150, 285.
- (1972), in Phase Transitions and Critical Phenomena, Vol. 2, cited above.
- Kaya, S. Nakayama, M. and Sato, H. (1943), Proc. Phys. Math. Soc. Japan 25, 179.
- Kikuchi, R. and Sato, H. (1974), Acta Met. 22, 1099.
- and van Baal, C.M. (1974), Scrip. Met. 8, 425.
- Klein, M.J. (1951), Am. J. Phys. 19, 153.
- Langer, J.S. (1971), Ann. Phys. (N.Y.) 65, 53.
- (1973), Acta Met. 21, 1649.
- (1975), private communication.
- and Bar-on, M. (1973), Ann. Phys. (N.Y.) 78, 421.
- Bar-on, M. and Miller, H.D. (1975), Phys. Rev., to appear.

References, con't.

- Leamy, H.J., Gilmer, G.H. and Jackson, K.A. (1973), Phys. Rev. Lett. 30, 601.
- Lebowitz, J.L. (1968), Ann. Rev. Phys. Chem. 19, 389.
- Lenz, W. (1920), Physik. Z. 21, 613.
- Li, C.Y. and Oriani, R.A. (1967), in "Proceedings of Bottom Landing Conference on Oxide-Dispersion Strengthening", pre-print.
- Lifshitz, I.M. and Slyozov, V.V. (1961), J. Phys. Chem. Solids 19, 35.
- Lord, N.W. (1953), J. Chem. Phys. 21, 692.
- Marcinkowski, M.J. (1963), Electron Microscopy and Strength of Crystals, Wiley, N.Y.
- Marro, J., Bortz, A.B., Kalos, M.H. and Lebowitz, J.L. (1975), Phys. Rev., to appear.
- Mattis, D.C. (1965), The Theory of Magnetism; and Introduction to the Study of Cooperative Phenomena, Harper & Row, N.Y.
- Morral, J.E. and Cahn, J.W. (1971), Acta Met. 19, 1037.
- Müller-Krumbhaar, H. (1974), Phys. Lett. 50A, 27.
- and Binder, K. (1972), Z. Phys. 254, 269.
- Murakami, M., deFontaine, D., Sánchez, J.M. and Fodor, J. (1975), to be published.
- Nagarajan, A. and Flinn, P.A. (1967), Appl. Phys. Lett. 11, 120.
- Nagy, E. and Nagy, I. (1962), J. Phys. Chem. Sol. 23, 1605.

References, con't.

- Neilsen, G.F. (1969), Phys. Chem. Glasses 10, 54.
- Newell, G.F. and Montroll, E.W., (1953), Rev. Mod. Phys. 25, 353.
- Nowick, A.S. and Weisenberg, L.R. (1958), Acta Met. 6, 260.
- Nyström, J. (1950), Arkiv Fysik 2, 151.
- Oriani, R.A. (1964), Acta Met. 12, 1399.
- Paulson, W.M. (1972), Ph.D. Thesis, Northwestern Univ., Evanston,
Ill.
- Peierls, R. (1936), Proc. Cambridge, Phil. Soc. 32, 477.
- Penrose, O. and Lebowitz, J.L. (1971), J. Stat. Phys. 3, 211.
- Philofsky, E.M. and Hilliard, J.E. (1969), J. Appl. Phys. 40,
2198.
- Raeside, D.E. (1974), AJP 42, 21.
- Rao, M., Marro, J., Kalos, M.H., and Lebowitz, J.L. (1975), to
appear.
- Richter, F., Bendick, W. and Pepperhoff, W. (1974), Z. Metallkde.
65, 42.
- Rundman, K.B. (1967), Ph.D. Thesis, Northeastern Univ., Evanston,
Ill.
- .. and Hilliard, J.E. (1967), Acta Met. 15, 1025.
- Sato, H. (1970), in Physical Chemistry, Vol. X: Solid State,
Jost, W. ed., Academic Press, N.Y.
- and Kikuchi, R. (1973), in Magnetism and Magnetic
Materials, 1972 AIP Conference Proceedings 10, 505.

References, con't.

- Shante, V.K. and Kirkpatrick, S. (1971), *Advan. Phys.* 20, 325.
- Shendalman, L.H. and O'Toole, J.H. (1968), *J. Colloid. Interface Sci.* 27, 145.
- Smith, A.F. (1967), *Acta Met.* 15, 1867.
- Speich and Oriani, R.A. (1965), *AIME* 233, 623.
- Stoloff, N.S. and Davies, R.G. (1966), *Progr. Mat. Sci.* 13, 1.
- Suzuki, M. and Kubo, R. (1968), *J. Phys. Soc. (Japan)* 24, 51.
- Swanger, L.A., Gupta, P.K. and Cooper, A.R. (1970), *Acta Met.* 18, 9.
- Syozi, I. (1972), in Phase Transitions and Critical Phenomena, Vol. 1, cited above.
- Tarko, H.B. and Fisher, M.E. (1975), *Phys. Rev. B* 11, 1217.
- Temperley, H.N.V. (1972), in Phase Transitions and Critical Phenomena, Vol. 1, cited above.
- Takagi, Y. and Oguchi, T. (1950), *Bull. Tokyo Inst. Tech. Ser. V* 3, 211.
- Tomozawa, M., MacCrone, R.K. and Herman, H. (1970), *J. Amer. Ceramic Soc.* 53, 62.
- Vineyard, G.H. (1956), *Phys. Rev.* 102, 981.
- Wagner, C. (1961), *Z. Electrochem.* 65, 581.
- Weisberg, L.R. and Quimby, S.M. (1963), *J. Phys. Chem. Solids* 24, 1251.
- Wilson, A.J.C. (1949), X-Ray Optics, Methuen, London; *Proc. Roy. Soc. (London)* A181, 360 (1943).
- Wilson, K.G. (1971), *Phys. Rev. B* 4, 3184.
- and Kogut, J. (1975), *Phys. Reports*, to appear.

References, con't.

- Yamauchi, H. (1973), Ph.D. Thesis, Northwestern Univ., Evanston,
Ill.; Scripta Met. 7, 109.
- and deFontaine, D. (1974), in Order-Disorder Transitions in Alloys, H. Warlimont ed., Springer-Verlag, Berlin, 1974.
- and Hilliard, J.E. (1972), Scripta Met. 6, 909.
- Yang, C.P. (1963), in Proceedings of the 15th Symposium in Applied Math. of the American Mathematical Soc., Chicago 1962, Metropolis, N.C. et al. eds., American Mathematical Society.
- Zarzycki, J. and Naudin, F. (1967), C.R. Acad. Sci., Ser. B 265, 1456.

VI. APPENDICES.

In part A of this section we collect selected numerical data from the computer simulation to which we refer in the preceding analysis. In the tables for the structure function we indicate the value of $\mu = kL/2\pi$, with L the number of sites on a lattice side. See section 4.7 for the appropriate units of k and t ("time" in the tables). The term "energy" in the tables refers to the number of A-B bonds in the system. In tables A.17-A.21 we denote by $\langle \text{SIZE} \rangle$, $\langle E/L \rangle$, $\langle EN \rangle$ and $\langle \text{RADIO} \rangle$ the quantities defined in eqs. (4.16), (4.20), (4.19) and (4.18), respectively; the cluster size interval to which the corresponding average refers is also indicated in the mentioned tables.

Part B groups some lattice configurations at different temperatures and for different interactions. Each figure contains, in this order, the values of the temperature and composition ($\tilde{\eta}$) of the system which corresponds to the instant of time at which the "picture was taken", the number of interchanges performed up to that time, the value of the energy of the system (u) and the corresponding cluster distribution. The occupation state of four equidistant sections in the system is represented in each figure. Three different symbols are used: \odot denotes an "interior" A-particle (surrounded by B-particles at the nearest neighbor sites), * denotes a non-interior A-particle, and / denotes an interior B-particle; the absence of any symbol denotes

a non-interior B-particle. Figures B.1 - B.30 correspond to a ferromagnetic interaction (clustering), and Figs. B.31 - B.38 to an antiferromagnetic interaction.

Part C is devoted to the temporal evolution of the cluster distribution, Figs. C.1-C.16, in our two-dimensional and, Figs. C.17-C.66, for the three-dimensional systems. The graphs for two dimensions correspond to the weighted combination of six runs for an 80×80 lattice and one run for a 200×200 lattice; in addition, each graph includes information from a certain time interval (four time-points from the 80×80 lattice and corresponding five time-points from the 200×200 lattice). The different cluster sizes in the system are grouped in bands of ten particles-wide. In three dimensions, Figs. C.18 - C.50 refer to a temporal average of four different time-points, Fig. C.51 to three time-points, and Figs. C.60 - C.64 to two time-points. The bands are 500 particles wide most of the times in Figs. C.17 - C.56, 5 particles wide in Figs. C.57 - C.59, and 10 particles wide in Figs. C.60 - C.64. Figs. C.85 - C.86, which correspond to the steady, or quasi-steady, part of the evolution whose mean time is shown in the figures, refer respectively to 20 and 17 time points and bands are of 200 and 100 particles.

Figs. C.65 - C.66 refer to an average over the eight evolutions of the $30 \times 30 \times 30$ lattice (no temporal average), but this time the intervals for the horizontal axis are of 5 particles up

to size 51, of 10 particles up to 201, of 20 up to 501, of 50 up to 2001, and of 100 particles in the rest.

Figs. C.67 - C.84 correspond to an average over twelve independent initial (random) configurations, and show the evolution of the cluster distribution with the fraction of A-particles in the system in the interval $\bar{n}_A = 0.282, 0.350$.

Appendix A.

TABLE A.1

30X30X30 LATTICE

50.00 PERCENT OF A MOLECULES

TEMPERATURE = .591 TIMES THE CRITIC TEMPERATRE

AVERAGE OF 8 RUNS WITH INFORMATION AT 29 POINTS

COMPUTER TIME = 217.6 MINUTES

STRUCTURE FUNCTION, S(μ)

EXCHANGES	TIME	S(1)	S(2)	S(3)	S(4)	S(5)	S(6)	S(7)	S(8)	S(9)	S(10)
0	0.0	.84	.97	.87	.96	1.05	.96	1.01	1.07	.98	1.01
2500	.5	.87	1.01	.91	1.08	1.27	1.13	1.31	1.35	1.26	1.30
5000	1.1	.90	1.04	1.05	1.24	1.51	1.32	1.61	1.66	1.50	1.52
7500	1.8	.92	1.09	1.14	1.37	1.74	1.52	1.87	1.92	1.73	1.66
10000	2.7	.92	1.11	1.20	1.50	1.97	1.73	2.13	2.11	1.89	1.74
15000	4.6	.95	1.13	1.39	1.77	2.41	2.19	2.47	2.41	2.18	1.78
20000	6.8	.99	1.23	1.56	2.00	2.82	2.66	2.90	2.74	2.28	1.82
25000	9.1	1.03	1.26	1.76	2.28	3.26	3.08	3.23	2.96	2.29	1.76
30000	11.5	1.06	1.31	1.90	2.50	3.66	3.54	3.69	3.16	2.29	1.67
35000	14.1	1.09	1.39	2.12	2.81	4.09	3.89	3.87	3.17	2.21	1.62
40000	16.7	1.15	1.46	2.34	3.11	4.55	4.22	3.94	3.08	2.22	1.53
50000	22.4	1.23	1.65	2.68	3.69	5.38	4.85	4.15	3.10	2.00	1.38
60000	28.1	1.31	1.83	3.03	4.27	6.20	5.48	4.35	3.12	1.92	1.34
70000	34.2	1.36	1.98	3.48	4.88	7.05	5.90	4.38	3.01	1.82	1.27
80000	40.5	1.40	2.16	3.88	5.46	7.57	6.28	4.39	2.92	1.65	1.25
90000	47.1	1.44	2.34	4.48	6.25	8.49	6.66	4.36	2.72	1.59	1.15
100000	54.1	1.65	2.60	5.24	6.93	9.19	7.03	4.28	2.41	1.50	1.12
150000	90.3	1.85	3.49	8.04	11.03	12.05	7.04	3.57	1.87	1.32	.97
200000	129.7	1.83	5.23	10.73	13.95	13.64	6.11	3.09	1.79	1.22	.92
250000	171.3	1.95	6.49	13.49	17.47	14.27	5.30	2.58	1.70	1.13	.93
300000	215.2	2.07	7.71	16.71	20.90	14.13	4.44	2.39	1.57	1.09	.88
350000	261.1	2.04	9.04	20.26	22.76	13.63	3.71	2.24	1.38	.99	.82
400000	308.2	2.28	10.85	23.36	24.18	12.33	3.62	1.93	1.37	1.01	.79
450000	356.3	2.45	12.23	26.93	26.14	11.66	3.31	1.91	1.26	.96	.75
500000	405.7	2.90	13.05	30.82	27.55	10.64	3.09	1.80	1.29	.95	.74
550000	456.3	3.20	14.91	34.65	28.54	9.19	2.94	1.79	1.22	.97	.77
600000	507.6	3.41	16.77	38.01	28.98	8.73	2.87	1.67	1.23	.92	.73
650000	559.8	3.74	18.73	41.19	28.50	8.12	2.63	1.68	1.17	.93	.69
700000	613.0	3.95	20.39	44.21	28.47	7.51	2.60	1.71	1.19	.85	.67

TABLE A.2

30X30X30 LATTICE

50.00 PERCENT OF A MOLECULES

TEMPERATURE = .780 TIMES THE CRITIC TEMPERATJRE

AVERAGE OF 8 RUNS WITH INFORMATION AT 75 POINTS

COMPUTER TIME = 809.1 MINUTES

STRUCTURE FUNCTION, S(μ)											
EXCHANGES	TIME	S(1)	S(2)	S(3)	S(4)	S(5)	S(6)	S(7)	S(8)	S(9)	S(10)
0	0.0	.89	.99	.87	.88	1.09	.99	1.03	1.14	.98	1.00
5000	1.0	.90	1.02	1.07	1.09	1.39	1.42	1.52	1.46	1.43	1.37
10000	2.3	.90	1.07	1.18	1.46	1.66	1.78	1.81	1.88	1.68	1.58
15000	3.8	.93	1.12	1.35	1.65	1.95	2.07	2.15	2.08	1.83	1.69
20000	5.4	.96	1.23	1.51	1.84	2.16	2.48	2.48	2.28	1.98	1.70
30000	8.7	1.02	1.33	1.86	2.34	2.61	3.04	2.97	2.55	1.98	1.62
40000	12.2	1.10	1.56	2.10	2.80	3.23	3.48	3.22	2.83	1.91	1.55
50000	15.8	1.12	1.79	2.44	3.23	3.85	3.98	3.43	2.75	1.91	1.43
60000	19.5	1.19	1.94	2.79	3.76	4.19	4.34	3.50	2.60	1.78	1.41
70000	23.3	1.25	2.09	3.18	4.08	4.67	4.58	3.63	2.41	1.73	1.40
80000	27.2	1.33	2.22	3.48	4.41	5.31	4.80	3.64	2.27	1.69	1.35
90000	31.2	1.41	2.48	3.76	4.91	5.52	4.96	3.39	2.25	1.72	1.33
100000	35.2	1.39	2.53	4.05	5.41	5.77	5.04	3.41	2.27	1.64	1.34
150000	55.6	1.54	3.32	5.65	7.74	6.73	4.96	3.03	2.00	1.56	1.22
200000	76.8	1.79	4.11	6.84	10.11	7.82	5.22	2.92	1.90	1.50	1.15
250000	98.8	2.00	5.10	8.51	11.89	8.45	4.86	2.83	1.87	1.46	1.14
300000	121.1	2.23	5.73	9.97	13.12	8.28	4.22	2.50	1.80	1.37	1.12
350000	143.7	2.43	6.76	11.29	14.65	8.00	3.87	2.43	1.75	1.32	1.12
400000	166.7	2.81	7.86	12.55	15.67	8.10	3.90	2.29	1.80	1.31	1.08
450000	190.0	2.95	8.85	13.83	15.99	7.67	3.41	2.28	1.83	1.37	.99
500000	213.6	3.47	9.45	15.19	16.06	7.52	3.44	2.22	1.74	1.26	1.01
550000	237.3	3.49	10.54	16.17	16.91	7.67	3.35	2.13	1.69	1.24	1.03
600000	261.3	3.69	11.60	17.51	16.81	6.92	3.36	2.07	1.62	1.27	1.05
650000	285.6	3.96	12.02	19.13	16.78	6.77	3.35	1.94	1.58	1.16	1.03
700000	309.8	4.35	13.28	20.83	17.47	6.44	3.09	2.16	1.63	1.20	1.00
750000	334.2	4.71	14.78	22.29	17.51	5.98	3.17	2.02	1.47	1.21	.98
800000	358.8	4.81	16.01	24.74	17.60	6.17	3.32	1.98	1.54	1.17	.98
850000	383.7	5.00	17.18	27.06	16.86	6.23	3.00	2.10	1.53	1.20	.97
900000	408.5	5.06	18.63	29.23	17.30	6.50	3.17	2.17	1.44	1.20	.95
950000	433.7	4.77	20.01	30.74	17.26	6.13	2.85	2.16	1.61	1.14	.97
1000000	458.9	4.90	21.48	31.36	16.01	5.63	3.09	1.96	1.56	1.11	.95
1050000	484.4	5.07	22.99	31.88	15.76	5.46	3.14	1.97	1.53	1.17	.92
1100000	509.8	5.35	24.46	32.94	15.18	5.32	3.00	2.02	1.49	1.08	.95
1150000	535.4	5.67	25.93	34.81	15.22	5.18	2.77	1.86	1.49	1.09	.88
1200000	561.0	5.91	27.21	35.48	15.01	5.35	2.65	1.91	1.50	1.11	.93
1250000	586.8	5.78	28.00	36.11	15.15	5.02	2.78	1.97	1.37	1.14	.92
1300000	612.7	5.82	29.67	36.92	15.13	4.93	2.69	1.94	1.49	1.09	.94
1350000	638.5	6.29	30.70	37.56	14.29	4.83	2.66	1.88	1.42	1.11	.90
1400000	664.5	6.67	31.93	38.65	14.06	4.82	2.63	1.83	1.32	1.11	.92
1450000	690.7	6.74	31.92	39.21	13.33	4.71	2.61	1.85	1.43	1.00	.91
1500000	716.6	6.77	32.90	39.57	13.59	4.57	2.56	1.93	1.41	1.10	.90
1550000	742.8	6.99	34.84	39.61	13.60	4.37	2.43	1.84	1.44	1.05	.88
1600000	769.0	6.79	35.91	39.98	13.81	4.47	2.44	1.85	1.44	1.09	.88
1650000	795.4	7.36	37.32	40.17	13.46	4.89	2.45	1.86	1.48	1.10	.91
1700000	821.8	7.66	38.94	41.55	13.20	4.69	2.46	1.83	1.34	1.07	.88

CONT.

TABLE A.2, CONT'D

STRUCTURE FUNCTION, S(μ)

EXCHANGES	TIME	S(1)	S(2)	S(3)	S(4)	S(5)	S(6)	S(7)	S(8)	S(9)	S(10)
1750000	848.2	7.69	41.24	40.29	12.79	4.21	2.49	1.66	1.36	1.09	.90
1800000	874.8	7.88	42.61	40.03	12.37	4.56	2.55	1.76	1.36	1.09	.87
1850000	901.3	8.20	44.05	39.56	12.14	4.52	2.59	1.74	1.27	1.08	.89
1900000	928.0	8.44	45.84	40.76	12.31	4.62	2.52	1.72	1.28	1.06	.81
1950000	954.9	8.60	47.39	40.70	12.10	4.50	2.57	1.79	1.32	.98	.89
2000000	981.7	9.12	48.65	41.65	11.30	4.44	2.53	1.79	1.28	1.04	.85
2050000	1008.8	9.18	50.35	41.48	11.05	4.35	2.46	1.86	1.30	1.04	.81
2100000	1035.8	9.95	50.91	40.57	10.24	4.41	2.56	1.89	1.31	1.04	.89
2150000	1062.7	10.43	52.65	41.09	10.62	4.29	2.48	1.70	1.33	1.07	.85
2200000	1089.5	10.82	54.51	41.15	10.21	4.32	2.46	1.60	1.38	1.05	.84
2250000	1116.6	10.61	55.89	41.18	10.39	4.40	2.35	1.62	1.28	1.04	.87
2300000	1143.6	11.02	56.46	42.03	10.32	3.90	2.47	1.62	1.28	.99	.83
2350000	1170.7	11.18	58.03	42.87	10.07	3.99	2.48	1.61	1.29	1.05	.82
2400000	1198.0	11.78	59.08	43.51	9.69	3.83	2.49	1.57	1.25	1.06	.80
2450000	1225.4	12.17	61.00	43.14	9.54	3.84	2.45	1.73	1.22	.98	.83
2500000	1252.9	12.86	62.22	42.75	9.83	3.75	2.37	1.68	1.32	1.00	.81
2550000	1280.5	13.49	63.53	43.35	9.77	3.86	2.38	1.60	1.27	1.02	.80
2600000	1308.2	14.02	66.26	42.76	9.65	3.85	2.36	1.69	1.30	1.00	.84
2650000	1335.8	13.94	67.83	42.58	9.32	3.71	2.46	1.68	1.25	.99	.83
2700000	1363.4	14.55	70.64	42.49	9.30	3.78	2.27	1.73	1.36	1.01	.79
2750000	1390.9	15.48	71.31	42.85	9.46	3.66	2.11	1.68	1.27	.99	.81
2800000	1418.5	16.45	74.16	43.60	9.23	3.74	2.28	1.83	1.26	1.02	.84
2850000	1446.4	17.04	75.53	43.79	9.49	3.62	2.20	1.70	1.22	.96	.79
2900000	1474.2	17.31	76.42	44.13	9.25	3.50	2.33	1.60	1.33	.94	.80
2950000	1502.1	17.87	78.25	43.08	9.31	3.59	2.30	1.61	1.31	.96	.82
3000000	1530.0	17.51	79.74	42.33	9.01	3.66	2.40	1.71	1.32	.99	.83
3050000	1558.1	18.12	82.12	41.13	8.95	3.88	2.29	1.61	1.23	.98	.80
3100000	1586.2	18.44	84.83	41.94	8.46	3.98	2.23	1.58	1.25	.91	.79
3150000	1614.4	18.79	87.62	41.26	8.28	3.55	2.23	1.62	1.23	.94	.81
3200000	1642.7	19.32	88.53	40.43	8.13	3.78	2.31	1.57	1.23	.93	.75

TABLE A.9

30X30X30 LATTICE

50.00 PERCENT OF A MOLECULES ($\bar{q} = 0.0$)

TEMPERATURE = .591 TIMES THE CRITIC TEMPERATURE

AVERAGE OF 8 RUNS WITH INFORMATION AT 47 POINTS

TIME	ENERGY	TIME	ENERGY	TIME	ENERGY	TIME	ENERGY
0.00	1.503	.37	1.380	.74	1.320	1.11	1.282
1.43	1.256	1.89	1.234	2.22	1.215	2.59	1.200
2.96	1.167	3.33	1.174	3.70	1.164	4.07	1.156
4.44	1.147	4.81	1.139	5.37	1.129	5.92	1.118
6.48	1.112	7.03	1.103	7.59	1.094	8.14	1.087
8.70	1.080	9.25	1.074	10.30	1.068	10.55	1.062
11.11	1.056	11.66	1.053	12.22	1.046	12.77	1.042
13.33	1.037	13.88	1.033	14.44	1.028	15.00	1.024
15.74	1.020	16.66	1.013	17.40	1.009	18.14	1.006
22.26	.986	54.91	.885	90.34	.827	129.68	.785
171.33	.751	215.16	.722	261.11	.702	308.16	.688
405.69	.657	507.64	.632	613.03	.609		

TABLE A.3

30X30X30 LATTICE

50.00 PERCENT OF A MOLECULES

TEMPERATURE = .887 TIMES THE CRITICAL TEMPERATURE

AVERAGE OF 8 RUNS WITH INFORMATION AT 115 POINTS

COMPUTER TIME = 2608.2 MINUTES

STRUCTURE FUNCTION, S(μ)

EXCHANGES	TIME	S(1)	S(2)	S(3)	S(4)	S(5)	S(6)	S(7)	S(8)	S(9)	S(10)
0	0.0	.84	.97	.87	.96	1.05	.96	1.01	1.07	.98	1.01
50000	13.9	.93	1.64	2.30	2.83	3.53	3.32	3.01	2.45	1.87	1.43
100000	30.1	1.13	2.28	3.35	4.35	5.14	3.91	3.03	2.16	1.64	1.34
150000	47.0	1.12	2.98	4.47	5.69	5.99	4.10	2.70	2.05	1.55	1.32
200000	64.3	1.35	3.77	6.28	6.85	6.06	3.87	2.62	1.96	1.49	1.24
250000	81.8	1.56	4.65	7.93	7.95	6.47	3.97	2.58	1.87	1.41	1.25
300000	99.5	1.77	5.30	8.97	8.22	6.51	3.94	2.57	1.84	1.48	1.19
350000	117.3	2.20	6.06	9.23	8.65	6.40	4.04	2.50	1.91	1.53	1.25
400000	135.3	2.61	6.76	10.16	8.94	6.29	3.90	2.37	1.77	1.43	1.14
450000	153.4	3.07	7.27	10.37	9.47	6.47	3.50	2.32	1.92	1.37	1.21
500000	171.6	3.17	7.86	11.47	10.28	5.86	3.26	2.33	1.79	1.40	1.14
550000	190.0	3.43	8.54	12.09	10.72	5.69	3.25	2.37	1.78	1.43	1.19
600000	208.4	3.84	8.83	12.83	11.34	5.87	3.31	2.24	1.80	1.40	1.25
650000	227.0	4.07	9.67	13.14	11.11	5.31	3.32	2.33	1.85	1.37	1.14
700000	245.5	4.09	10.65	13.67	11.21	5.02	3.38	2.24	1.82	1.45	1.17
750000	264.1	4.36	11.51	14.53	11.80	5.12	2.98	2.24	1.72	1.41	1.16
800000	282.6	4.76	12.13	14.74	11.57	5.30	3.25	2.32	1.69	1.34	1.16
850000	301.3	5.12	12.53	15.17	11.30	5.24	3.26	2.23	1.80	1.42	1.15
900000	320.0	5.22	13.81	15.32	11.31	5.27	3.04	2.26	1.60	1.41	1.19
950000	338.7	5.68	14.36	15.54	11.28	5.21	3.18	2.17	1.78	1.36	1.15
1000000	357.3	6.09	15.47	15.42	11.33	4.96	2.92	2.22	1.64	1.34	1.10
1050000	376.1	6.07	16.06	15.52	11.21	4.97	3.04	2.24	1.71	1.39	1.12
1100000	395.1	6.43	17.08	16.21	11.55	5.03	3.18	2.00	1.75	1.39	1.10
1150000	414.0	6.84	18.25	16.66	11.38	4.99	3.04	2.10	1.67	1.40	1.16
1200000	433.0	7.04	19.14	17.15	11.43	4.85	3.00	2.12	1.69	1.31	1.09
1250000	452.0	7.41	19.89	17.37	11.15	4.93	3.07	2.16	1.65	1.30	1.12
1300000	471.0	7.94	21.43	17.82	11.13	4.70	2.92	2.01	1.75	1.33	1.12
1350000	490.1	8.36	21.39	17.56	10.91	4.69	2.86	2.17	1.76	1.35	1.08
1400000	509.1	8.82	21.43	17.40	10.24	4.50	2.85	2.05	1.66	1.30	1.10
1450000	528.2	9.15	22.04	18.10	10.01	4.57	2.98	2.15	1.67	1.34	1.13
1500000	547.3	8.70	23.13	18.03	9.61	4.53	3.02	2.12	1.59	1.34	1.12
1550000	566.4	9.12	23.85	17.97	9.58	4.64	2.97	2.23	1.64	1.29	1.17
1600000	585.5	9.43	24.47	17.98	9.16	4.82	2.85	2.16	1.76	1.29	1.10
1650000	604.7	9.63	25.02	18.44	8.76	4.59	2.80	2.30	1.68	1.28	1.09
1700000	623.8	10.28	25.16	18.49	8.59	4.84	2.87	2.20	1.60	1.30	1.09
1800000	662.2	10.57	24.48	18.81	9.04	4.73	2.71	2.00	1.61	1.30	1.08
1900000	700.8	11.11	24.94	19.72	8.77	4.84	2.92	2.08	1.68	1.32	1.05
2000000	739.5	11.32	25.66	20.03	8.74	4.82	2.99	2.17	1.66	1.30	1.11
2100000	778.4	11.54	26.73	21.16	9.40	4.26	2.72	2.15	1.65	1.26	1.04
2200000	817.3	12.74	28.44	21.28	8.87	4.48	2.65	2.04	1.66	1.27	1.09
2300000	856.1	13.44	29.89	22.30	8.17	4.36	2.84	2.03	1.56	1.32	1.03
2400000	895.2	13.96	31.28	21.93	8.18	4.37	2.56	2.08	1.44	1.30	1.01
2500000	934.5	15.64	32.35	22.17	8.66	4.03	2.71	1.97	1.53	1.23	1.07
2600000	973.8	16.58	32.80	22.65	7.91	4.24	2.72	1.90	1.51	1.30	1.06
2700000	1013.3	17.46	34.52	23.50	7.64	4.17	2.90	2.04	1.59	1.24	1.07

CONT.

TABLE A.3, CONT'D

STRUCTURE FUNCTION, S(μ)

EXCHANGES	TIME	S(1)	S(2)	S(3)	S(4)	S(5)	S(6)	S(7)	S(8)	S(9)	S(10)
2800000	1052.7	18.07	35.45	22.46	7.62	3.71	2.73	2.08	1.65	1.27	1.05
2900000	1092.1	18.50	36.06	22.06	7.72	4.15	2.59	2.06	1.66	1.22	1.04
3000000	1131.9	18.89	39.22	22.00	7.58	4.27	2.95	1.94	1.50	1.22	1.00
3150000	1191.5	19.50	39.91	22.22	7.21	4.23	2.79	2.07	1.54	1.23	1.02
3300000	1251.2	21.67	41.35	21.07	7.42	4.17	2.65	2.07	1.55	1.28	1.03
3450000	1310.9	22.30	41.95	21.02	7.18	4.00	2.78	1.93	1.53	1.22	1.04
3600000	1370.5	23.71	43.25	20.72	7.18	4.13	2.86	1.96	1.49	1.23	1.04
3750000	1430.4	25.31	45.95	20.51	7.65	4.03	2.61	1.89	1.59	1.18	1.02
3900000	1490.5	28.07	48.30	20.73	6.99	3.84	2.55	1.99	1.50	1.20	.97
4050000	1550.8	29.48	49.51	19.60	7.58	4.07	2.48	2.01	1.53	1.18	1.05
4200000	1611.3	30.05	51.25	19.52	7.50	4.04	2.67	1.85	1.44	1.21	1.05
4400000	1692.2	29.61	53.28	19.84	7.04	4.44	2.49	1.86	1.49	1.25	.98
4600000	1773.0	31.35	54.77	19.17	7.16	3.50	2.44	1.92	1.48	1.19	1.04
4800000	1853.6	32.04	57.05	18.17	6.97	4.01	2.51	1.98	1.47	1.20	.98
5000000	1934.8	32.97	58.74	17.84	7.28	3.90	2.72	1.90	1.44	1.16	1.00
5200000	2016.2	33.94	61.67	16.99	7.64	3.58	2.54	1.93	1.45	1.16	1.00
5400000	2097.6	34.79	64.00	16.86	7.61	3.73	2.38	1.94	1.53	1.24	.98
5600000	2179.4	36.41	64.23	15.21	7.21	4.09	2.28	1.88	1.51	1.13	1.00
5800000	2261.1	37.92	62.30	16.39	6.79	3.34	2.55	1.77	1.56	1.18	1.02
6000000	2343.2	38.89	62.49	16.09	7.20	3.61	2.42	1.75	1.41	1.21	.97
6200000	2425.0	38.26	62.18	16.13	6.65	3.66	2.53	1.93	1.41	1.10	1.02
6400000	2507.2	41.20	62.98	16.85	6.46	3.69	2.59	1.86	1.41	1.20	1.00
6600000	2589.2	43.38	63.60	17.22	6.74	3.48	2.59	1.94	1.39	1.14	.97
6800000	2671.0	44.78	62.07	16.91	6.72	3.87	2.41	1.79	1.41	1.23	.95
7000000	2752.9	45.28	62.10	16.87	6.76	3.83	2.79	1.92	1.44	1.15	.97
7200000	2835.0	46.40	61.93	15.69	6.93	4.29	2.29	1.85	1.40	1.22	.94
7400000	2917.3	46.69	60.60	16.04	6.29	3.99	2.66	1.86	1.50	1.17	.99
7600000	2999.8	46.61	64.33	15.70	6.59	3.67	2.38	1.67	1.41	1.18	.98
7800000	3082.4	47.21	65.29	16.04	6.13	3.45	2.65	1.74	1.40	1.14	.95
8000000	3165.4	50.17	66.57	14.27	6.64	3.53	2.45	1.76	1.49	1.19	.95
8200000	3248.5	50.58	69.88	15.43	6.66	3.71	2.53	1.72	1.43	1.14	.98
8400000	3331.7	54.08	67.21	14.22	6.39	3.34	2.39	1.70	1.33	1.14	.97
8600000	3414.7	56.71	69.12	14.76	6.25	3.42	2.31	1.67	1.43	1.09	.93
8800000	3497.6	56.93	70.34	15.37	6.45	3.62	2.32	1.76	1.43	1.15	.94
9000000	3580.5	55.77	70.83	15.31	6.17	3.43	2.42	1.78	1.41	1.20	.94
9200000	3663.6	59.44	71.74	16.18	6.22	3.72	2.44	1.83	1.35	1.16	.97
9400000	3746.1	61.59	71.34	14.85	6.38	3.55	2.36	1.90	1.33	1.17	.93
9600000	3829.1	64.72	72.38	15.95	6.36	3.47	2.31	1.74	1.43	1.15	.99
9800000	3912.2	65.09	72.02	14.96	6.65	3.47	2.45	1.70	1.40	1.15	.94
10000000	3995.1	68.19	70.67	14.35	6.38	3.71	2.45	1.75	1.40	1.11	.94
12000000	4078.3	72.28	70.70	15.42	6.57	3.48	2.38	1.79	1.41	1.11	.92
14000000	4161.6	73.91	70.51	15.29	5.95	3.52	2.29	1.81	1.42	1.12	.99
16000000	4244.8	76.00	71.90	14.48	5.90	3.74	2.38	1.66	1.39	1.15	.93
18000000	4328.0	77.28	69.47	15.14	5.97	3.53	2.35	1.80	1.34	1.15	.94
20000000	4411.7	81.38	72.55	15.05	6.64	3.57	2.31	1.71	1.37	1.17	.91
22000000	4495.8	83.14	70.10	13.38	6.24	3.68	2.52	1.76	1.41	1.11	.95
24000000	4579.8	83.28	71.79	14.45	6.13	3.68	2.28	1.63	1.46	1.11	.98
26000000	4664.1	84.70	73.13	14.29	5.58	3.17	2.30	1.74	1.40	1.10	.97
28000000	4748.4	86.02	72.73	13.96	5.87	3.54	2.39	1.79	1.42	1.10	.92
30000000	4832.7	89.49	70.97	14.38	5.75	3.33	2.10	1.77	1.39	1.11	.93
32000000	4916.8	89.35	69.77	13.98	6.59	3.52	2.15	1.66	1.36	1.13	.91
34000000	5000.9	91.38	69.19	13.52	6.38	3.56	2.24	1.67	1.32	1.07	.95
36000000	5085.4	92.26	67.42	13.83	5.85	3.24	2.30	1.74	1.37	1.10	.93

CONT.

TABLE A.3, CONT'D

STRUCTURE FUNCTION, $S(\mu)$

EXCHANGES	TIME	$S(1)$	$S(2)$	$S(3)$	$S(4)$	$S(5)$	$S(6)$	$S(7)$	$S(8)$	$S(9)$	$S(10)$
12800000	5169.9	94.71	67.79	13.26	5.73	3.18	2.38	1.76	1.29	1.15	.90
13000000	5254.2	95.17	65.03	14.01	5.55	3.35	2.19	1.63	1.33	1.15	.92
13200000	5338.4	97.73	63.73	12.46	5.76	3.25	2.44	1.59	1.35	1.14	.95
13400000	5422.5	97.35	64.02	11.97	5.35	3.47	2.42	1.68	1.46	1.08	.92
13600000	5506.7	103.51	64.66	12.57	5.53	3.51	2.26	1.69	1.41	1.10	1.01
13800000	5591.1	1106.80	63.43	13.57	6.01	3.37	2.46	1.78	1.41	1.07	.89
14000000	5675.7	109.94	63.42	13.88	5.96	3.26	2.37	1.71	1.33	1.09	.95
14200000	5760.5	111.55	65.34	13.69	5.81	3.24	2.23	1.63	1.34	1.07	.94
14400000	5845.2	111.37	64.11	14.89	5.50	3.52	2.22	1.69	1.36	1.11	.83
14600000	5930.1	1114.44	64.78	14.71	6.01	3.39	2.27	1.62	1.38	1.12	.90
14800000	6015.3	1115.97	65.80	15.22	5.44	3.46	2.21	1.64	1.31	1.06	.91
15000000	6100.7	1117.31	65.39	15.37	4.97	3.28	2.08	1.66	1.41	1.07	.93
15200000	6186.6	1116.69	65.24	14.84	5.27	3.25	2.19	1.68	1.39	1.11	.93
15400000	6272.0	1113.97	63.14	15.28	5.46	3.17	2.05	1.72	1.30	1.01	.90
15600000	6357.7	1116.42	64.59	12.84	5.81	3.52	2.07	1.62	1.26	1.11	.90
15800000	6443.2	1115.96	61.15	11.65	5.80	3.22	2.24	1.66	1.38	1.10	.97
16000000	6528.3	1120.96	61.08	12.20	5.98	3.24	2.23	1.75	1.33	1.14	.95

TABLE A.10

30X30X30 LATTICE

50.00 PERCENT OF A MOLECULES ($\bar{\eta} = 0.0$)

TEMPERATURE = .780 TIMES THE CRITIC TEMPERATURE

AVERAGE OF 8 RUNS WITH INFORMATION AT 93 POINTS

TIME	ENERGY	TIME	ENERGY	TIME	ENERGY	TIME	ENERGY
0.00	1.500	.37	1.392	.56	1.363	.83	1.330
1.11	1.306	1.39	1.287	1.67	1.273	1.94	1.260
2.32	1.245	2.69	1.232	3.06	1.222	3.43	1.213
3.80	1.203	4.29	1.195	4.72	1.188	5.19	1.182
5.65	1.173	6.11	1.168	6.57	1.161	7.04	1.156
7.50	1.152	7.96	1.148	8.51	1.141	9.26	1.134
12.17	1.112	15.80	1.092	19.52	1.073	23.35	1.062
27.20	1.050	31.15	1.040	35.15	1.030	55.61	.998
76.78	.973	98.80	.947	121.12	.937	143.75	.920
166.67	.907	190.00	.900	213.50	.887	237.33	.878
261.34	.872	285.57	.869	309.33	.861	334.21	.859
358.80	.845	363.71	.845	408.52	.833	433.72	.830
453.94	.825	464.35	.824	509.78	.820	535.40	.817
561.04	.809	586.75	.807	612.53	.804	638.52	.798
664.52	.797	690.67	.796	716.52	.792	742.79	.787
769.01	.789	795.43	.782	821.78	.779	848.24	.781
874.78	.776	901.27	.771	927.99	.768	954.90	.762
981.70	.764	1008.83	.761	1035.79	.765	1062.70	.764
1089.46	.760	1116.62	.756	1143.50	.755	1170.69	.750
1197.97	.748	1225.41	.744	1252.93	.746	1280.46	.742
1308.16	.740	1335.78	.741	1363.41	.737	1390.91	.740
1418.51	.733	1446.40	.728	1474.20	.729	1502.10	.731
1530.02	.725	1558.11	.726	1586.17	.721	1614.37	.719
1642.66	.719						

TABLE A,4

30X30X30 LATTICE

50.00 PERCENT OF A MOLECULES

TEMPERATURE = 1.068 TIMES THE CRITICAL TEMPERATURE

AVERAGE OF 8 RUNS WITH INFORMATION AT 62 POINTS

COMPUTER TIME = 222.3 MINUTES

STRUCTURE FUNCTION, S(μ)

EXCHANGES	TIME	S(1)	S(2)	S(3)	S(4)	S(5)	S(6)	S(7)	S(8)	S(9)	S(10)
0	0.0	.84	.97	.87	.96	1.05	.96	1.01	1.07	.98	1.01
2500	.4	.84	1.00	.88	1.05	1.23	1.10	1.20	1.27	1.17	1.19
5000	.9	.90	1.05	.98	1.13	1.36	1.26	1.32	1.44	1.33	1.31
7500	1.4	.91	1.08	1.05	1.20	1.49	1.40	1.48	1.58	1.44	1.38
10000	2.0	.93	1.12	1.12	1.27	1.57	1.52	1.59	1.66	1.52	1.47
12500	2.6	.94	1.12	1.15	1.32	1.73	1.66	1.71	1.75	1.58	1.50
15000	3.2	.93	1.12	1.20	1.43	1.84	1.76	1.84	1.80	1.64	1.47
17500	3.8	.92	1.12	1.26	1.50	1.98	1.79	1.95	1.86	1.67	1.50
20000	4.4	.96	1.15	1.29	1.54	2.06	1.89	2.01	1.93	1.67	1.54
22500	5.0	.97	1.16	1.30	1.61	2.16	1.94	2.06	1.96	1.67	1.55
25000	5.6	.94	1.17	1.30	1.66	2.26	1.98	2.16	2.00	1.68	1.50
27500	6.2	.97	1.23	1.36	1.75	2.37	2.04	2.16	2.07	1.69	1.46
30000	6.9	.95	1.28	1.37	1.81	2.44	2.11	2.19	2.04	1.68	1.48
32500	7.5	.96	1.34	1.44	1.85	2.51	2.15	2.21	2.04	1.76	1.47
35000	8.1	.94	1.36	1.48	1.98	2.58	2.27	2.18	1.99	1.79	1.45
37500	8.8	.94	1.42	1.57	2.10	2.66	2.32	2.27	2.00	1.79	1.45
40000	9.4	.91	1.50	1.57	2.15	2.77	2.29	2.36	2.09	1.74	1.47
42500	10.1	.92	1.59	1.62	2.20	2.83	2.28	2.40	2.11	1.78	1.47
45000	10.7	.95	1.62	1.62	2.27	2.85	2.45	2.43	2.07	1.80	1.40
47500	11.4	.95	1.63	1.66	2.35	2.97	2.52	2.45	2.08	1.78	1.42
50000	13.0	.98	1.71	1.81	2.52	3.11	2.62	2.45	2.10	1.72	1.45
60000	14.7	1.01	1.75	1.97	2.68	3.25	2.72	2.45	2.09	1.76	1.39
70000	17.3	1.06	1.78	2.24	2.86	3.35	2.77	2.50	2.09	1.75	1.36
80000	20.0	1.12	1.94	2.47	3.07	3.38	2.88	2.49	1.99	1.72	1.39
90000	22.7	1.13	2.00	2.57	3.34	3.62	2.96	2.56	1.96	1.67	1.40
100000	25.3	.97	1.91	2.73	3.41	3.57	3.08	2.48	1.97	1.68	1.38
110000	28.1	1.23	2.14	3.02	3.59	3.77	3.17	2.64	1.81	1.68	1.32
120000	30.8	1.33	2.30	3.09	3.86	3.75	3.28	2.54	1.85	1.63	1.31
130000	33.5	1.29	2.37	3.26	3.93	3.70	3.33	2.50	1.99	1.67	1.29
140000	36.3	1.26	2.38	3.45	4.08	3.82	3.45	2.51	1.87	1.57	1.32
150000	38.8	1.20	2.37	4.06	3.94	3.83	3.18	2.47	1.98	1.49	1.35
160000	41.8	1.37	2.59	3.71	4.31	3.80	3.22	2.49	1.79	1.50	1.28
170000	44.5	1.41	2.72	3.74	4.62	3.92	3.19	2.38	1.99	1.50	1.36
180000	47.3	1.45	2.77	3.82	4.65	3.94	3.23	2.45	1.90	1.45	1.35
190000	50.0	1.44	2.88	3.99	4.73	3.96	3.15	2.41	1.91	1.45	1.31
200000	52.6	1.28	2.80	4.94	4.65	4.12	3.22	2.31	1.87	1.54	1.37
250000	66.4	1.37	3.18	5.24	4.78	4.08	3.12	2.32	1.87	1.54	1.27
300000	80.3	1.28	3.39	6.09	5.03	4.33	3.10	2.20	1.89	1.49	1.38
350000	94.3	1.49	3.80	6.64	5.22	4.29	3.12	2.21	2.03	1.49	1.35
400000	108.3	1.58	4.28	5.83	5.44	4.16	2.90	2.32	1.83	1.51	1.22
450000	122.4	1.66	4.60	7.18	5.46	4.10	2.80	2.28	1.88	1.52	1.30
500000	136.5	1.70	4.77	7.39	5.76	3.97	2.94	2.26	1.90	1.54	1.25
550000	150.6	1.80	5.26	7.46	5.92	3.88	3.19	2.39	1.82	1.48	1.22
600000	164.8	2.04	5.53	7.36	6.20	3.99	2.75	2.27	1.82	1.43	1.20
650000	179.0	2.11	5.77	7.62	6.30	3.98	2.84	2.18	1.88	1.56	1.23

CONT.

TABLE A.4, CONT'D

STRUCTURE FUNCTION, S(μ)											
EXCHANGES	TIME	S(1)	S(2)	S(3)	S(4)	S(5)	S(6)	S(7)	S(8)	S(9)	S(10)
700000	193.2	2.24	6.06	7.94	6.28	4.26	2.72	2.24	1.86	1.48	1.22
750000	207.4	2.31	6.33	8.18	6.22	3.84	2.87	2.15	1.85	1.51	1.22
800000	221.6	2.61	6.44	7.95	5.87	4.24	2.92	2.23	1.73	1.47	1.24
850000	235.8	2.74	7.00	7.85	5.84	4.15	2.90	2.34	1.78	1.43	1.25
900000	250.0	2.69	7.47	8.09	5.85	4.32	2.71	2.09	1.89	1.54	1.25
950000	264.2	2.97	7.87	8.23	6.22	4.43	2.86	2.35	1.81	1.52	1.29
1000000	278.5	3.04	8.22	8.35	5.79	4.52	2.76	2.28	1.83	1.48	1.27
1050000	292.8	2.99	8.49	8.31	6.06	4.41	2.86	2.18	1.74	1.47	1.29
1100000	307.0	2.99	8.48	8.29	5.74	4.05	2.88	2.13	1.68	1.46	1.28
1150000	321.3	3.21	8.51	8.27	5.74	3.97	3.03	2.25	1.75	1.43	1.32
1200000	335.4	3.64	8.83	8.55	5.61	4.18	2.95	2.20	1.91	1.54	1.23
1250000	349.7	3.83	9.44	9.71	6.02	4.07	2.90	2.20	1.76	1.52	1.21
1300000	364.0	3.89	9.72	9.81	5.95	4.13	2.78	2.17	1.80	1.44	1.22
1350000	378.2	3.96	9.80	9.93	6.03	3.98	2.96	2.19	1.71	1.48	1.22
1400000	392.5	4.18	10.22	9.70	6.26	4.10	2.74	2.20	1.70	1.46	1.32
1450000	406.9	4.28	9.94	9.98	5.70	4.19	2.90	2.24	1.72	1.49	1.28
1500000	421.1	4.49	9.32	10.27	5.72	3.94	2.72	2.23	1.77	1.49	1.20

TABLE A.5

50X50X30 LATTICE

51.00 PERCENT OF A MOLECULES

TEMPERATURE = 1,501 TIMES THE CRITICAL TEMPERATURE

AVERAGE OF 8 RUNS WITH INFORMATION AT 28 POINTS

COMPUTER TIME = 331.5 MINUTES

STRUCTURE FUNCTION, S(μ)											
EXCHANGES	TIME	S(1)	S(2)	S(3)	S(4)	S(5)	S(6)	S(7)	S(8)	S(9)	S(10)
0	0.0	.84	.97	.87	.96	1.05	.97	1.01	1.07	.98	1.01
25000	4.8	.92	1.25	1.18	1.59	1.78	1.66	1.86	1.79	1.50	1.41
100000	20.5	1.09	1.77	1.95	2.69	2.43	2.31	1.88	1.69	1.49	1.33
200000	41.7	1.23	2.39	2.41	2.47	2.46	2.06	1.87	1.68	1.42	1.32
300000	52.8	1.60	2.65	2.79	2.57	2.52	2.17	1.88	1.71	1.43	1.34
400000	34.1	1.61	2.82	2.94	2.68	2.53	2.16	1.90	1.63	1.49	1.35
500000	105.4	1.63	2.94	2.88	2.68	2.77	2.16	1.79	1.69	1.41	1.24
600000	126.7	1.83	3.22	2.86	2.86	2.49	2.22	1.91	1.70	1.50	1.33
700000	148.1	2.01	3.42	2.95	2.90	2.72	2.08	1.75	1.55	1.45	1.35
800000	169.5	2.26	3.31	3.07	2.75	2.39	2.19	1.82	1.62	1.38	1.34
900000	190.9	2.62	3.51	3.01	2.98	2.59	2.08	1.86	1.64	1.47	1.32
1000000	212.2	2.50	3.84	2.63	2.67	2.45	2.13	1.83	1.61	1.59	1.30
1100000	233.6	2.53	3.89	2.84	2.85	2.56	2.27	1.81	1.70	1.54	1.31
1200000	255.0	2.54	3.90	3.19	2.77	2.46	2.05	1.81	1.60	1.50	1.29
1300000	276.3	2.77	3.60	3.06	2.80	2.43	2.00	1.85	1.71	1.46	1.37
1400000	297.7	2.80	3.60	3.05	2.97	2.36	2.45	1.87	1.56	1.49	1.24
1500000	319.1	2.64	3.61	3.11	2.83	2.48	2.05	1.93	1.68	1.48	1.30
1600000	340.5	2.94	3.52	3.43	2.68	2.35	2.05	1.87	1.67	1.40	1.30
1700000	361.8	2.73	3.93	3.42	2.41	2.40	2.38	1.91	1.60	1.51	1.25
1800000	383.2	2.91	3.70	3.37	2.67	2.61	2.24	1.76	1.67	1.39	1.22
1900000	404.5	3.22	3.94	3.38	2.72	2.39	2.17	1.92	1.66	1.45	1.25
2000000	425.8	3.56	3.76	3.37	2.85	2.40	2.12	1.92	1.63	1.49	1.23
2100000	447.2	3.31	3.55	3.61	2.95	2.31	2.37	1.88	1.70	1.44	1.27
2200000	468.6	3.71	3.38	3.45	2.83	2.38	2.17	1.85	1.63	1.45	1.25
2300000	489.9	3.97	3.64	3.02	3.00	2.52	2.14	1.92	1.58	1.44	1.30
2400000	511.3	4.01	3.66	3.31	3.38	2.61	2.18	1.88	1.72	1.43	1.23
2500000	532.8	4.13	3.62	3.13	3.01	2.72	2.10	1.97	1.57	1.43	1.27
2600000	554.2	4.03	3.85	3.25	2.80	2.41	2.14	1.95	1.57	1.39	1.29

TABLE A.6

30X30X30 LATTICE

20.00 PERCENT OF A MOLECULES

TEMPERATURE = .591 TIMES THE CRITICAL TEMPERATURE

AVERAGE OF 8 RUNS WITH INFORMATION AT 70 POINTS

COMPUTER TIME = 1636.9 MINUTES

EXCHANGES	TIME	STRUCTURE FUNCTION, S(μ)									
		S(1)	S(2)	S(3)	S(4)	S(5)	S(6)	S(7)	S(8)	S(9)	S(10)
0	0.0	.75	1.06	.82	1.00	1.05	.96	1.03	1.02	1.03	1.00
2500	.7	.75	1.12	.92	1.17	1.26	1.25	1.34	1.35	1.30	1.30
5000	1.7	.79	1.17	.98	1.33	1.43	1.58	1.57	1.65	1.57	1.45
7500	2.9	.80	1.23	1.11	1.50	1.62	1.73	1.81	1.88	1.69	1.55
10000	4.1	.82	1.29	1.20	1.63	1.75	1.95	2.04	1.99	1.78	1.63
12500	5.4	.85	1.34	1.34	1.75	1.98	2.19	2.21	2.12	1.85	1.63
15000	6.7	.88	1.41	1.39	1.97	2.22	2.45	2.45	2.22	1.92	1.60
17500	8.2	.89	1.43	1.51	2.06	2.40	2.72	2.60	2.34	1.96	1.60
20000	9.7	.87	1.45	1.57	2.21	2.58	2.86	2.80	2.36	1.99	1.59
22500	11.2	.90	1.50	1.70	2.36	2.73	3.00	2.98	2.40	2.02	1.55
25000	12.7	.93	1.59	1.83	2.50	2.98	3.14	3.11	2.46	2.03	1.53
27500	14.2	.94	1.62	1.90	2.52	3.14	3.42	3.25	2.49	1.98	1.61
30000	15.8	.97	1.69	1.94	2.59	3.30	3.57	3.29	2.48	2.02	1.55
32500	17.4	1.04	1.73	2.05	2.78	3.52	3.64	3.39	2.47	1.92	1.53
35000	19.1	1.06	1.78	2.11	3.01	3.83	3.81	3.50	2.49	1.85	1.44
37500	20.8	1.09	1.85	2.16	3.13	4.01	3.81	3.61	2.49	1.87	1.46
40000	22.5	1.10	1.88	2.27	3.22	4.23	3.91	3.65	2.47	1.83	1.50
42500	24.2	1.12	1.92	2.40	3.37	4.39	4.16	3.73	2.47	1.82	1.54
45000	25.9	1.13	2.00	2.55	3.47	4.59	4.30	3.63	2.46	1.78	1.50
47500	27.6	1.12	2.05	2.57	3.66	4.81	4.44	3.54	2.50	1.81	1.43
50000	29.3	1.11	2.09	2.65	3.84	5.01	4.42	3.64	2.53	1.76	1.42
100000	67.1	1.38	3.19	4.62	6.41	7.35	5.25	3.34	2.22	1.57	1.29
150000	108.9	1.78	4.61	7.00	9.21	8.10	5.18	3.06	2.10	1.46	1.18
200000	153.4	2.05	6.40	9.83	12.27	8.45	5.00	2.79	1.88	1.41	1.10
250000	200.5	2.39	8.41	12.71	15.12	8.76	4.83	2.57	1.78	1.32	1.01
300000	249.7	2.80	9.58	15.79	16.90	8.75	4.64	2.48	1.83	1.23	.95
350000	300.3	2.98	11.10	18.87	18.14	8.80	4.36	2.37	1.57	1.19	.91
400000	352.6	3.30	13.38	22.47	19.65	9.33	4.22	2.26	1.61	1.14	.93
450000	405.9	3.84	15.38	24.27	20.81	9.36	3.75	2.15	1.54	1.13	.86
500000	460.9	4.32	17.49	27.57	21.96	9.03	3.48	2.12	1.43	1.01	.84
550000	516.6	5.14	20.16	30.34	22.44	8.54	3.67	2.07	1.38	1.02	.84
600000	573.1	5.12	21.63	32.99	22.74	8.06	3.68	1.98	1.39	.99	.82
650000	630.9	5.39	24.03	36.13	23.17	7.41	3.43	1.89	1.38	1.01	.85
700000	689.4	6.04	26.66	38.64	23.01	7.49	3.42	1.88	1.30	.97	.79
750000	749.2	6.28	28.81	41.58	22.74	6.86	3.15	1.81	1.28	.94	.73
800000	810.1	6.49	30.96	43.32	22.21	6.61	3.00	1.69	1.21	.92	.73
850000	871.6	6.92	33.59	44.62	22.05	6.17	2.86	1.82	1.18	.91	.77
900000	933.6	7.72	35.16	46.80	21.70	6.12	2.85	1.60	1.17	.91	.72
950000	996.0	7.82	37.17	46.73	20.92	5.94	2.72	1.73	1.20	.92	.72
1000000	1059.6	8.03	39.26	48.27	20.76	5.81	2.73	1.67	1.20	.87	.71
1050000	1124.3	7.80	41.07	50.73	20.64	5.75	2.69	1.58	1.10	.86	.73
1100000	1189.0	8.24	43.36	53.14	19.98	5.84	2.44	1.55	1.21	.89	.73
1150000	1254.3	9.18	43.92	53.49	19.67	5.84	2.37	1.63	1.11	.88	.71
1200000	1320.0	9.67	47.22	54.56	19.22	5.33	2.39	1.53	1.11	.91	.73
1250000	1386.1	10.39	49.86	57.44	19.29	5.37	2.45	1.63	1.13	.89	.73

CONT.

TABLE A.6, CONT'D

EXCHANGES	TIME	STRUCTURE FUNCTION, S(μ)									
		S(1)	S(2)	S(3)	S(4)	S(5)	S(6)	S(7)	S(8)	S(9)	S(10)
1300000	1452.0	10.78	52.74	57.78	18.63	5.33	2.42	1.53	1.12	.89	.71
1350000	1518.3	11.51	54.39	59.32	18.11	5.17	2.33	1.70	1.12	.84	.71
1400000	1585.9	11.21	56.09	59.85	17.72	5.04	2.25	1.59	1.12	.84	.66
1450000	1653.1	11.76	57.49	59.31	17.28	5.10	2.19	1.47	1.20	.68	.69
1500000	1721.3	11.73	60.51	60.08	16.69	5.01	2.25	1.53	1.12	.86	.71
1550000	1789.1	12.34	60.28	60.00	16.36	5.01	2.40	1.50	1.13	.85	.66
1600000	1856.7	12.69	62.06	59.86	15.32	4.57	2.31	1.48	1.13	.85	.64
1650000	1925.5	13.57	64.43	61.24	14.95	4.55	2.33	1.42	1.16	.81	.64
1700000	1994.3	13.54	65.05	62.53	14.55	4.66	2.26	1.40	1.08	.81	.65
1750000	2063.0	15.33	67.12	62.62	14.46	4.57	2.09	1.49	1.06	.77	.62
1800000	2132.2	15.82	68.88	62.14	14.66	4.45	2.19	1.42	1.08	.81	.63
1850000	2202.0	16.85	71.97	63.02	14.16	4.14	2.07	1.42	1.00	.84	.51
1900000	2272.8	17.21	73.47	65.41	14.38	4.19	2.09	1.34	.99	.81	.65
1950000	2343.8	17.93	75.52	64.20	14.17	4.26	2.09	1.44	1.00	.81	.64
2000000	2415.4	18.36	78.87	64.96	14.11	4.38	2.07	1.38	.99	.79	.63
2100000	2559.1	19.65	81.60	62.60	13.57	4.43	2.02	1.40	1.11	.76	.64
2200000	2704.0	20.57	86.80	62.02	13.23	4.16	2.16	1.36	1.01	.74	.65
2300000	2850.5	22.43	93.16	62.63	12.61	4.17	1.92	1.35	1.04	.78	.62
2400000	2998.3	24.25	97.70	60.81	12.32	3.84	1.93	1.29	1.03	.74	.53
2500000	3145.7	25.24	100.35	58.96	11.37	3.70	1.89	1.22	.99	.76	.57
2600000	3293.6	25.61	103.58	58.24	10.80	3.49	1.86	1.25	.98	.69	.60
2700000	3443.3	26.90	109.60	56.71	10.57	3.48	1.81	1.36	1.01	.73	.58
2800000	3593.0	28.80	112.85	53.86	10.24	3.59	1.92	1.38	.94	.74	.60
2900000	3743.6	29.86	118.79	51.24	9.93	3.55	1.65	1.27	.99	.74	.59
3000000	3896.2	30.77	123.76	50.01	9.81	3.29	1.76	1.26	.97	.70	.57

30X30X30 LATTICE

20.00 PERCENT OF A MOLECULES

TEMPERATURE = .887 TIMES THE CRITICAL TEMPERATURE

AVERAGE OF 8 RUNS WITH INFORMATION AT 64 POINTS

COMPUTER TIME = 782.9 MINUTES

STRUCTURE FUNCTION, S(μ)

EXCHANGES	TIME	S(1)	S(2)	S(3)	S(4)	S(5)	S(6)	S(7)	S(8)	S(9)	S(10)
0	0.0	.75	1.06	.82	1.00	1.05	.96	1.03	1.02	1.03	1.00
2500	.7	.76	1.06	.93	1.11	1.22	1.15	1.29	1.23	1.23	1.24
5000	1.5	.79	1.08	1.03	1.22	1.32	1.32	1.47	1.42	1.39	1.31
7500	2.3	.79	1.08	1.06	1.32	1.46	1.52	1.52	1.55	1.46	1.38
10000	3.2	.80	1.16	1.15	1.41	1.53	1.65	1.65	1.63	1.50	1.39
12500	4.1	.81	1.22	1.17	1.50	1.63	1.75	1.72	1.72	1.51	1.40
15000	5.1	.81	1.24	1.26	1.60	1.70	1.88	1.77	1.79	1.55	1.39
17500	6.0	.83	1.21	1.32	1.66	1.79	1.98	1.88	1.80	1.67	1.40
20000	7.0	.85	1.25	1.40	1.65	1.87	2.12	2.04	1.84	1.66	1.41
22500	8.0	.86	1.31	1.48	1.88	1.91	2.20	2.12	1.95	1.67	1.42
25000	8.9	.90	1.33	1.54	1.87	1.94	2.26	2.12	1.91	1.65	1.42
27500	9.9	.91	1.39	1.54	1.86	2.06	2.34	2.16	1.90	1.65	1.39
30000	10.9	.90	1.42	1.56	1.96	2.14	2.42	2.16	1.97	1.64	1.36
32500	11.9	.93	1.50	1.64	2.09	2.28	2.45	2.19	1.95	1.59	1.39
35000	12.9	.96	1.54	1.70	2.14	2.35	2.41	2.26	1.97	1.58	1.38
37500	13.9	1.01	1.61	1.81	2.19	2.47	2.48	2.27	1.91	1.60	1.40
40000	14.9	1.00	1.71	1.80	2.28	2.47	2.55	2.27	1.94	1.58	1.39
42500	15.9	.98	1.79	1.90	2.28	2.54	2.69	2.27	1.90	1.58	1.41
45000	17.0	.99	1.85	1.95	2.23	2.57	2.69	2.30	1.98	1.62	1.38
47500	18.0	1.02	1.94	2.04	2.24	2.67	2.71	2.43	1.98	1.57	1.43
50000	19.0	1.02	1.96	2.14	2.33	2.68	2.69	2.36	1.96	1.61	1.40
100000	40.0	1.16	2.73	3.29	3.49	3.56	2.94	2.38	1.93	1.57	1.34
150000	61.4	1.37	3.30	4.06	3.94	3.62	2.99	2.13	1.86	1.60	1.36
200000	82.9	1.52	4.11	4.92	4.21	3.52	2.88	2.22	1.85	1.51	1.27
250000	104.7	1.66	4.17	5.26	4.58	3.48	2.98	2.10	1.79	1.48	1.29
300000	126.6	1.77	4.93	5.54	4.74	3.24	2.64	2.14	1.93	1.46	1.30
350000	148.4	2.05	5.45	5.15	4.63	3.47	2.77	2.19	1.88	1.51	1.31
400000	170.4	2.38	5.77	5.30	5.22	3.49	2.68	2.33	1.83	1.48	1.28
450000	192.4	2.57	5.63	5.75	4.93	3.62	2.89	2.13	1.74	1.48	1.29
500000	214.5	2.78	6.38	6.08	5.20	3.65	2.65	2.39	1.81	1.46	1.24
550000	236.9	2.95	6.02	6.20	5.22	3.45	3.00	2.16	1.64	1.42	1.21
600000	259.0	3.22	5.63	7.09	4.83	3.69	2.80	2.14	1.79	1.44	1.31
650000	281.2	3.65	6.65	6.95	4.85	3.70	2.75	2.23	1.76	1.56	1.25
700000	303.4	3.84	6.55	6.87	5.07	3.82	2.78	2.10	1.78	1.51	1.29
750000	325.6	4.24	7.19	7.23	5.14	3.56	2.60	2.22	1.92	1.51	1.33
800000	347.7	4.70	7.31	7.31	5.19	3.67	2.86	2.22	1.83	1.50	1.26
900000	392.2	4.67	7.75	7.56	5.55	3.80	2.72	2.28	1.78	1.52	1.24
1000000	436.8	4.58	8.95	7.56	4.80	3.68	2.80	2.11	1.78	1.50	1.30
1100000	481.3	5.40	8.85	7.79	5.32	3.51	2.94	2.25	1.71	1.50	1.28
1200000	525.9	6.04	9.50	7.27	5.21	3.86	2.81	2.25	1.90	1.42	1.27
1300000	570.7	6.26	9.68	7.29	5.51	3.79	2.61	2.32	1.73	1.49	1.23
1400000	615.6	5.99	9.88	7.74	5.12	3.77	2.47	2.15	1.82	1.41	1.23
1500000	660.3	5.88	9.26	8.01	5.42	3.21	2.76	2.08	1.80	1.42	1.25
1600000	705.1	6.11	10.04	8.09	5.19	3.60	2.86	2.20	1.68	1.47	1.29
1700000	750.1	6.61	10.20	7.99	5.28	3.80	2.70	2.24	1.71	1.48	1.17

CONT.

TABLE A.7, CONT'D

EXCHANGES	TIME	STRUCTURE FUNCTION, S(μ)									
		S(1)	S(2)	S(3)	S(4)	S(5)	S(6)	S(7)	S(8)	S(9)	S(10)
1800000	795.2	6.62	11.01	8.48	5.24	3.95	2.72	2.15	1.71	1.47	1.23
1900000	840.3	6.64	11.07	7.20	5.69	3.99	2.78	2.13	1.76	1.49	1.24
2000000	885.2	6.70	12.49	8.34	5.13	3.67	2.55	2.13	1.78	1.46	1.21
2100000	930.3	6.49	12.67	8.87	5.12	3.51	2.63	2.34	1.77	1.44	1.20
2200000	975.6	6.43	12.18	8.80	4.80	3.44	2.56	2.17	1.78	1.46	1.33
2300000	1020.7	7.57	12.26	8.88	4.91	3.44	2.60	2.16	1.83	1.45	1.23
2400000	1065.9	8.17	12.44	8.54	5.18	3.69	2.81	2.09	1.65	1.48	1.30
2500000	1111.4	7.82	12.72	9.30	5.46	3.63	2.52	2.19	1.75	1.43	1.29
2600000	1156.7	8.38	12.57	9.10	5.37	3.33	2.61	1.96	1.76	1.45	1.20
2700000	1202.3	8.47	13.00	10.25	5.44	3.64	2.58	2.09	1.71	1.43	1.19
2800000	1247.9	8.59	13.88	9.28	5.16	3.56	2.68	2.08	1.68	1.45	1.28
2900000	1293.3	8.64	14.16	8.73	4.75	3.48	2.97	2.12	1.80	1.40	1.13
3000000	1338.5	9.18	14.06	8.56	4.76	3.41	2.63	2.20	1.73	1.40	1.25
3100000	1383.8	9.18	13.86	8.18	5.17	3.45	2.70	1.99	1.65	1.46	1.19
3200000	1429.2	9.23	13.99	7.63	5.05	3.69	2.60	2.02	1.71	1.47	1.17
3300000	1474.6	8.39	13.30	8.20	5.84	3.97	2.63	1.97	1.69	1.44	1.22
3400000	1520.2	9.09	14.12	8.66	5.74	3.62	2.71	2.13	1.68	1.46	1.23
3500000	1565.8	8.94	14.16	8.34	5.53	3.36	2.64	2.03	1.72	1.45	1.17
3600000	1611.3	9.46	14.97	8.33	5.66	3.66	2.82	2.07	1.74	1.40	1.23

TABLE A.14

30X30X30 LATTICE

20.00 PERCENT OF A MOLECULES ($\bar{\eta} = .6$)

TEMPERATURE = .591 TIMES THE CRITICAL TEMPERATURE

AVERAGE OF 8 RUNS WITH INFORMATION AT 91 POINTS

TIME	ENERGY	TIME	ENERGY	TIME	ENERGY	TIME	ENERGY
0.00	.9e2	.18	.926	.37	.902	.55	.884
.74	.871	1.11	.850	1.48	.836	1.85	.824
2.22	.815	2.59	.808	2.96	.802	3.51	.794
4.07	.727	4.62	.780	5.18	.774	5.74	.770
6.29	.765	6.85	.760	7.40	.756	7.96	.752
8.51	.749	9.07	.745	9.52	.743	10.18	.740
10.92	.736	11.66	.733	12.58	.728	12.96	.727
13.70	.724	14.44	.721	15.18	.717	15.92	.715
16.56	.712	17.44	.710	18.14	.707	19.12	.704
20.79	.701	22.47	.696	24.17	.692	25.87	.688
27.60	.684	29.32	.680	67.15	.628	103.88	.597
153.40	.569	200.49	.547	249.71	.532	300.31	.518
352.59	.503	405.90	.495	460.93	.487	516.61	.478
573.05	.470	630.92	.459	689.37	.452	749.19	.444
810.14	.440	871.64	.437	933.50	.430	995.99	.428
1059.60	.420	1124.33	.416	1188.96	.415	1254.29	.411
1319.99	.409	1386.09	.403	1452.02	.404	1518.26	.399
1585.95	.397	1653.13	.395	1721.27	.391	1789.05	.389
1856.67	.389	1925.49	.385	1994.34	.383	2062.97	.382
2132.19	.380	2201.97	.376	2272.34	.372	2343.78	.372
2415.43	.369	2559.11	.364	2704.00	.361	2850.53	.355
2998.29	.356	3145.74	.356	3293.58	.351	3443.30	.348
3593.02	.345	3743.64	.343	3896.20	.339		

30X30X30 LATTICE

20.00 PERCENT OF A MOLECULES

TEMPERATURE = 1,068 TIMES THE CRITIC TEMPERATJRE

AVERAGE OF 8 RUNS WITH INFORMATION AT 49 POINTS

COMPUTER TIME = 403.1 MINUTES

STRUCTURE FUNCTION, S(μ)

EXCHANGES	TIME	S(1)	S(2)	S(3)	S(4)	S(5)	S(6)	S(7)	S(8)	S(9)	S(10)
0	0.0	.75	1.06	.82	1.00	1.05	.96	1.03	1.02	1.03	1.00
2500	.6	.75	1.04	.92	1.11	1.19	1.13	1.24	1.20	1.20	1.18
5000	1.4	.75	1.06	.98	1.22	1.29	1.22	1.31	1.38	1.37	1.21
7500	2.2	.75	1.12	1.02	1.33	1.36	1.39	1.49	1.44	1.43	1.31
10000	3.0	.79	1.16	1.03	1.36	1.48	1.44	1.54	1.49	1.50	1.33
12500	3.8	.79	1.21	1.09	1.43	1.52	1.53	1.69	1.51	1.51	1.33
15000	4.6	.80	1.24	1.12	1.42	1.64	1.58	1.77	1.53	1.56	1.36
17500	5.5	.80	1.35	1.22	1.46	1.64	1.62	1.78	1.62	1.58	1.36
20000	6.3	.82	1.38	1.25	1.56	1.74	1.65	1.81	1.62	1.58	1.30
22500	7.2	.85	1.34	1.30	1.63	1.79	1.71	1.80	1.72	1.54	1.30
25000	8.0	.86	1.33	1.33	1.75	1.93	1.82	1.83	1.77	1.52	1.36
27500	8.9	.84	1.33	1.41	1.85	2.02	1.82	1.86	1.80	1.51	1.33
30000	9.8	.85	1.34	1.40	1.97	2.07	1.81	1.88	1.74	1.51	1.37
32500	10.6	.88	1.43	1.44	2.09	2.10	1.88	1.87	1.67	1.50	1.36
35000	11.5	.87	1.47	1.48	2.11	2.14	1.94	1.79	1.72	1.47	1.40
37500	12.4	.90	1.49	1.49	2.16	2.21	1.92	1.91	1.75	1.51	1.35
40000	13.2	.92	1.54	1.45	2.15	2.24	1.93	1.95	1.77	1.47	1.32
42500	14.1	.93	1.57	1.48	2.23	2.28	1.96	1.93	1.71	1.48	1.36
45000	15.0	.95	1.58	1.56	2.33	2.29	1.96	1.94	1.65	1.47	1.35
47500	15.9	.96	1.59	1.59	2.37	2.27	2.05	1.96	1.65	1.45	1.36
50000	16.8	.98	1.64	1.65	2.35	2.30	2.05	1.95	1.63	1.47	1.32
100000	34.6	1.22	2.00	2.22	2.81	2.63	2.30	1.97	1.72	1.51	1.31
150000	52.6	1.43	2.37	2.51	2.83	2.57	2.09	2.03	1.68	1.45	1.31
200000	70.7	1.47	2.59	2.56	2.91	2.73	2.25	1.88	1.67	1.44	1.35
250000	88.8	1.78	2.86	2.81	3.26	2.70	2.22	1.94	1.64	1.45	1.28
300000	107.0	1.84	2.75	3.21	3.20	2.87	2.30	2.00	1.66	1.46	1.34
350000	125.2	1.98	3.04	3.08	3.21	2.71	2.24	1.92	1.68	1.47	1.31
400000	143.3	1.96	2.97	3.10	3.14	2.42	2.07	2.01	1.60	1.47	1.34
450000	161.5	2.11	3.17	3.35	3.06	2.54	2.33	1.95	1.72	1.58	1.28
500000	179.7	2.39	3.10	3.37	3.26	2.57	2.27	1.87	1.70	1.51	1.31
550000	197.9	2.57	3.17	3.46	3.29	2.44	2.30	1.87	1.73	1.43	1.32
600000	216.2	2.56	3.70	3.79	3.36	2.54	2.30	1.84	1.67	1.46	1.30
650000	234.5	2.46	3.68	3.83	3.32	2.57	2.13	1.92	1.60	1.41	1.31
700000	252.7	2.63	3.89	3.52	3.28	2.63	2.26	1.88	1.70	1.50	1.28
750000	270.9	2.52	3.77	3.94	3.21	2.74	2.16	1.98	1.77	1.50	1.28
800000	289.2	2.66	3.97	3.89	3.17	2.58	2.26	1.93	1.78	1.39	1.30
850000	307.5	2.73	4.49	3.78	3.26	2.76	2.19	1.97	1.65	1.44	1.30
900000	325.7	2.62	4.22	4.33	3.37	2.72	2.26	1.87	1.64	1.47	1.31
1000000	362.3	2.76	3.84	3.89	3.37	2.74	2.33	1.81	1.73	1.48	1.28
1100000	398.7	3.29	3.20	3.87	2.77	2.50	2.13	1.86	1.73	1.47	1.36
1200000	435.0	3.06	3.66	3.59	3.04	2.62	2.35	1.88	1.68	1.42	1.31
1300000	471.5	3.32	3.88	3.85	3.00	2.64	2.23	1.87	1.69	1.52	1.23
1400000	508.0	3.62	4.64	3.92	3.05	2.48	2.15	1.95	1.71	1.40	1.23
1500000	544.6	3.57	4.84	3.84	3.38	2.72	2.15	2.01	1.76	1.46	1.35
1600000	581.2	3.84	4.96	3.74	3.20	2.78	2.22	1.85	1.71	1.48	1.29
1700000	617.8	4.64	4.67	3.90	2.83	2.84	2.12	1.86	1.76	1.45	1.28
1800000	654.3	4.71	4.46	3.90	2.96	2.75	2.31	1.89	1.69	1.51	1.28
1900000	690.9	4.59	4.47	3.49	2.79	2.60	2.25	1.89	1.67	1.48	1.26
2000000	727.4	4.61	4.01	4.26	3.15	2.62	2.18	1.90	1.73	1.47	1.28

TABLE A.11

30X30X30 LATTICE

50.00 PERCENT OF A MOLECULES ($\bar{\eta} = 0.0$)TEMPERATURE = .887 TIMES THE CRITIC TEMPERATURE
AVERAGE OF 8 RUNS WITH INFORMATION AT 140 POINTS

TIME	ENERGY	TIME	ENERGY	TIME	ENERGY	TIME	ENERGY
0.00	1.503	.37	1.397	.74	1.347	1.11	1.316
1.48	1.294	1.85	1.276	2.22	1.264	2.59	1.253
2.96	1.243	3.33	1.233	3.88	1.220	4.44	1.213
5.00	1.206	5.55	1.200	6.11	1.191	6.66	1.185
7.22	1.182	7.77	1.178	8.33	1.173	8.88	1.169
9.44	1.164	10.00	1.160	10.74	1.156	11.48	1.149
12.22	1.146	12.96	1.142	13.90	1.138	30.15	1.093
47.01	1.067	64.30	1.051	81.78	1.046	99.45	1.027
117.29	1.021	135.26	1.014	153.38	1.007	171.63	1.002
189.95	.997	208.39	.991	226.97	.986	245.47	.986
264.06	.983	262.64	.981	301.29	.979	320.01	.972
338.65	.976	357.30	.972	376.14	.966	395.07	.964
413.99	.963	432.97	.959	451.96	.957	470.98	.952
490.11	.954	509.14	.955	528.21	.952	547.29	.956
566.40	.950	585.48	.950	604.59	.948	623.79	.944
662.24	.944	700.80	.939	739.49	.932	778.38	.931
817.27	.933	856.06	.928	895.16	.918	934.53	.916
973.84	.920	1013.29	.917	1052.71	.914	1092.14	.911
1131.90	.907	1191.48	.906	1251.18	.904	1310.91	.905
1370.53	.904	1430.38	.894	1490.53	.894	1550.84	.891
1611.34	.884	1692.15	.886	1772.99	.886	1853.59	.881
1934.83	.879	2016.21	.875	2097.52	.876	2179.35	.872
2261.08	.875	2343.20	.869	2424.99	.870	2507.16	.872
2589.22	.868	2670.98	.873	2752.87	.869	2835.04	.864
2917.28	.866	2999.76	.863	3082.38	.859	3165.41	.857
3248.52	.849	3331.75	.858	3414.56	.855	3497.59	.856
3580.54	.854	3663.57	.853	3746.11	.857	3829.09	.853
3912.22	.855	3995.10	.853	4078.34	.850	4161.65	.852
4244.79	.847	4327.99	.849	4411.72	.839	4495.84	.843
4579.77	.835	4664.09	.836	4748.39	.835	4832.66	.837
4916.78	.837	5000.90	.835	5085.43	.832	5169.91	.831
5254.23	.832	5338.45	.834	5422.49	.836	5506.74	.831
5591.07	.830	5675.72	.831	5760.53	.826	5845.16	.828
5930.07	.825	6015.35	.823	6100.73	.820	6186.63	.818
6272.01	.824	6357.72	.817	6443.16	.826	6528.35	.819

TABLE A.12

30X30X30 LATTICE

50.00 PERCENT OF A MOLECULES ($\bar{\eta} = 0.0$)TEMPERATURE = 1.068 TIMES THE CRITIC TEMPERATURE
AVERAGE OF 8 RUNS WITH INFORMATION AT 54 POINTS

TIME	ENERGY	TIME	ENERGY	TIME	ENERGY	TIME	ENERGY
0.00	1.503	.37	1.408	.74	1.363	1.11	1.334
1.48	1.315	1.85	1.300	2.22	1.290	2.59	1.280
2.96	1.272	3.51	1.263	4.07	1.254	4.62	1.249
5.18	1.243	5.74	1.238	6.29	1.231	6.85	1.226
7.40	1.221	7.96	1.219	8.51	1.218	9.07	1.215
9.62	1.212	10.18	1.210	10.92	1.206	11.66	1.200
11.99	1.200	25.29	1.170	39.54	1.159	52.60	1.146
66.40	1.141	80.33	1.132	95.06	1.129	108.34	1.124
122.45	1.123	136.50	1.122	150.54	1.119	164.80	1.116
179.01	1.116	193.19	1.116	207.36	1.113	221.58	1.114
235.78	1.117	250.00	1.113	264.22	1.108	278.52	1.111
292.79	1.109	307.01	1.113	321.27	1.113	335.41	1.112
349.66	1.105	363.96	1.105	378.23	1.106	392.55	1.107
406.87	1.106	421.14	1.106				

TABLE A.13

30X30X30 LATTICE

50.00 PERCENT OF A MOLECULES ($\bar{\eta} = 0.0$)TEMPERATURE = 1.501 TIMES THE CRITIC TEMPERATURE
AVERAGE OF 8 RUNS WITH INFORMATION AT 55 POINTS

TIME	ENERGY	TIME	ENERGY	TIME	ENERGY	TIME	ENERGY
0.00	1.504	.52	1.409	.78	1.386	1.04	1.372
1.30	1.362	1.56	1.353	1.82	1.344	2.07	1.337
2.33	1.332	2.59	1.328	2.85	1.324	3.11	1.321
3.37	1.320	3.63	1.318	3.89	1.314	4.15	1.310
4.41	1.306	4.79	1.304	4.93	1.303	5.19	1.302
5.44	1.300	5.70	1.300	6.22	1.297	6.74	1.297
7.26	1.294	7.78	1.294	8.30	1.292	8.82	1.290
9.33	1.288	20.49	1.271	41.69	1.269	62.83	1.263
84.10	1.261	105.38	1.263	126.73	1.260	148.11	1.257
169.48	1.256	190.87	1.256	212.22	1.258	233.58	1.257
254.96	1.258	276.32	1.258	297.72	1.255	319.08	1.256
340.48	1.260	361.83	1.256	383.16	1.260	404.47	1.255
425.77	1.256	447.19	1.255	468.56	1.257	489.94	1.257
511.32	1.251	532.78	1.253	554.20	1.258		

TABLE A.15

30X30X30 LATTICE

20.00 PERCENT OF A MOLECULES ($\bar{\eta} = .6$)

TEMPERATURE = .887 TIMES THE CRITIC TEMPERATURE

AVERAGE OF 8 RUNS WITH INFORMATION AT 72 POINTS

TIME	ENERGY	TIME	ENERGY	TIME	ENERGY	TIME	ENERGY
0.00	.962	.18	.932	.37	.912	.55	.898
.74	.888	.92	.879	1.11	.873	1.29	.867
1.48	.862	1.66	.857	1.35	.855	2.03	.851
2.40	.844	2.77	.839	3.14	.834	3.51	.829
3.88	.828	4.25	.825	4.52	.824	5.00	.822
5.55	.818	6.11	.812	6.56	.810	7.22	.808
7.77	.805	8.33	.804	8.38	.802	9.44	.800
10.00	.798	10.74	.798	11.48	.795	12.22	.793
12.96	.792	13.93	.791	14.93	.790	15.94	.785
16.97	.783	17.99	.781	19.02	.780	39.99	.763
61.42	.756	82.93	.753	104.56	.745	126.55	.742
148.39	.743	170.36	.741	192.37	.736	214.55	.736
236.89	.734	259.04	.735	281.23	.733	303.39	.734
325.57	.734	347.75	.731	392.23	.732	436.81	.730
481.28	.730	525.91	.731	570.70	.728	615.58	.728
660.28	.730	705.10	.727	750.14	.723	795.23	.721
840.26	.724	885.22	.723	930.27	.720	975.56	.722
1020.68	.716	1065.93	.717	1111.43	.717	1156.73	.718

TABLE A.16

30X30X30 LATTICE

20.00 PERCENT OF A MOLECULES ($\bar{\eta} = .6$)

TEMPERATURE = 1.068 TIMES THE CRITIC TEMPERATURE

AVERAGE OF 8 RUNS WITH INFORMATION AT 48 POINTS

TIME	ENERGY	TIME	ENERGY	TIME	ENERGY	TIME	ENERGY
0.00	.962	.18	.935	.37	.918	.55	.905
.74	.896	.92	.890	1.11	.884	1.29	.879
1.48	.875	1.66	.870	1.35	.868	2.03	.864
2.40	.858	2.77	.855	3.14	.853	3.51	.848
3.88	.846	4.25	.843	4.52	.842	5.00	.840
5.55	.836	6.11	.836	6.56	.833	7.22	.831
7.77	.830	8.33	.826	8.38	.826	9.44	.823
10.00	.822	10.63	.822	11.50	.823	12.37	.820
13.24	.819	14.13	.819	15.00	.818	15.88	.817
16.76	.816	34.60	.807	52.50	.804	70.70	.801
88.79	.799	107.00	.797	125.19	.798	143.32	.796
161.53	.796	179.70	.796	197.92	.797	216.16	.795

TABLE A.17

80X80 LATTICE

CLUSTER DISTRIBUTION PROPERTIES(10⁵⁶)

20.00 PERCENT OF A MOLECULES

TEMPERATURE = .586 TIMES THE CRITIC TEMPERATURE

AVERAGE OF 6 RUNS WITH INFORMATION AT 100 POINTS

ENERGY	TIME	EXCHAN.	<SIZE>	<SIZE >	<E/L>	<EN>	<RADIO>
.367	22.35	100000	14.15	213	1.497	22.77	1.051
.334	61.13	200000	15.54	270	1.341	22.40	1.098
.309	106.17	300000	17.29	356	1.235	23.26	1.151
.287	163.40	400000	17.76	367	1.132	22.63	1.168
.274	223.53	500000	19.32	442	1.146	23.07	1.214
.261	290.36	600000	20.37	496	1.059	24.01	1.245
.255	359.40	700000	21.65	580	1.018	25.13	1.279
.243	432.22	800000	23.03	656	.970	25.67	1.319
.236	510.34	900000	23.56	692	.950	25.73	1.329
.231	589.90	1000000	24.19	720	.872	25.91	1.351
.229	670.75	1100000	25.18	801	.859	26.74	1.374
.225	752.20	1200000	25.62	830	.852	26.78	1.385
.222	837.67	1300000	26.48	887	.794	27.26	1.406
.220	924.66	1400000	27.43	981	.805	27.88	1.430
.219	1010.33	1500000	28.14	1050	.763	28.47	1.445
.212	1098.96	1600000	29.33	1115	.696	28.91	1.477
.212	1191.67	1700000	28.94	1077	.706	28.27	1.468
.208	1282.54	1800000	29.99	1157	.704	28.94	1.494
.206	1374.46	1900000	30.74	1229	.667	29.24	1.510
.202	1465.71	2000000	30.99	1256	.639	29.19	1.510
.204	1555.14	2100000	31.35	1253	.649	29.52	1.527
.200	1651.08	2200000	32.38	1342	.597	30.14	1.553
.197	1747.64	2300000	32.72	1409	.608	29.81	1.555
.195	1845.61	2400000	33.30	1451	.617	30.37	1.568
.195	1943.30	2500000	33.74	1490	.578	30.46	1.579
.193	2039.63	2600000	33.97	1571	.593	30.58	1.577
.191	2140.26	2700000	34.78	1624	.576	31.08	1.600
.189	2238.19	2800000	35.44	1659	.551	31.20	1.617
.186	2337.52	2900000	35.89	1774	.535	31.26	1.621
.187	2440.41	3000000	36.59	1792	.548	31.27	1.641
.182	2541.94	3100000	36.96	1801	.504	31.61	1.651
.183	2645.54	3200000	36.44	1985	.509	32.67	1.680
.185	2743.09	3300000	39.26	2048	.499	33.29	1.700
.181	2840.53	3400000	40.32	2146	.500	33.69	1.724
.179	2952.12	3500000	39.98	2091	.458	33.37	1.718
.179	3053.06	3600000	40.23	2169	.489	33.46	1.725
.176	3166.02	3700000	41.39	2236	.445	33.98	1.749
.175	3270.22	3800000	41.17	2211	.463	33.46	1.744
.174	3376.36	3900000	42.61	2371	.437	34.69	1.774
.174	3481.60	4000000	42.70	2375	.404	34.08	1.777
.171	3597.53	4100000	43.51	2467	.442	34.62	1.792
.171	3706.26	4200000	44.31	2574	.389	35.01	1.807
.172	3814.24	4300000	44.82	2606	.369	35.45	1.820
.170	3921.22	4400000	45.31	2660	.397	35.23	1.831

CONT.

TABLE A.17, CONT'D

ENERGY	TIME	EXCHAN.	<SIZE>	<SIZE >	<E/L>	<EV>	<RADIUS>
,169	4028.71	450000	45.07	2652	.335	35.01	1.824
,166	4139.50	460000	45.91	2739	.391	35.30	1.842
,163	4248.72	470000	46.65	2837	.372	35.81	1.855
,163	4361.00	480000	47.38	2989	.409	35.85	1.875
,164	4472.10	490000	47.77	2932	.353	36.23	1.882
,164	4585.70	500000	48.35	2991	.311	36.86	1.894
,160	4701.30	510000	48.36	3006	.298	35.86	1.892
,160	4819.54	520000	48.84	3022	.314	36.47	1.906
,161	4932.73	530000	48.45	3033	.331	36.23	1.893
,159	5040.18	540000	49.09	3121	.296	36.33	1.905
,161	5164.64	550000	49.79	3203	.279	36.90	1.917
,160	5280.74	560000	49.90	3213	.277	36.89	1.921
,160	5396.56	570000	51.04	3343	.268	37.93	1.944
,159	5511.83	580000	51.73	3410	.276	37.87	1.961
,158	5630.63	590000	50.71	3278	.300	37.34	1.940
,158	5747.77	600000	51.87	3456	.308	36.24	1.960
,155	5866.95	610000	52.96	3623	.266	36.32	1.977
,156	5984.67	620000	52.71	3597	.287	36.30	1.973
,158	6102.33	630000	52.86	3640	.303	36.36	1.973
,154	6216.21	640000	52.65	3584	.275	38.07	1.972
,154	6339.87	650000	53.90	3779	.228	38.28	1.995
,157	6451.75	660000	53.76	3639	.253	38.72	2.002
,156	6568.79	670000	53.58	3635	.261	36.45	1.997
,156	6680.31	680000	55.20	3813	.223	39.30	2.031
,153	6802.50	690000	53.82	3687	.314	36.23	1.998
,152	6918.67	700000	54.86	3623	.250	36.33	2.017
,152	7040.48	710000	53.93	3680	.234	38.04	2.000
,151	7161.25	720000	54.83	3793	.251	38.45	2.018
,148	7285.17	730000	54.98	3774	.253	38.24	2.025
,148	7410.70	740000	55.93	3893	.252	38.79	2.042
,153	7532.39	750000	55.18	3815	.250	39.00	2.028
,152	7650.21	760000	55.31	3656	.277	38.96	2.030
,152	7775.67	770000	55.53	3662	.286	38.46	2.038
,150	7890.76	780000	56.09	3920	.231	38.30	2.050
,149	8012.48	790000	57.46	4141	.209	39.96	2.073
,149	8134.25	800000	57.18	4073	.262	39.13	2.068
,148	8255.31	810000	57.94	4166	.237	40.02	2.083
,147	8382.21	820000	58.76	4287	.223	40.33	2.097
,148	8505.73	830000	58.46	4252	.247	39.77	2.092
,146	8631.61	840000	58.61	4287	.185	39.60	2.093
,145	8757.64	850000	58.66	4296	.212	39.73	2.094
,146	8887.21	860000	58.89	4303	.213	40.01	2.099
,146	9014.09	870000	58.60	4309	.193	39.61	2.091
,144	9135.87	880000	59.50	4466	.223	39.66	2.105
,145	9260.75	890000	58.94	4314	.178	39.53	2.098
,147	9385.60	900000	59.31	4361	.203	39.65	2.103
,146	9505.23	910000	60.21	4561	.209	40.56	2.116
,146	9632.53	920000	60.39	4572	.249	40.57	2.120
,147	9752.93	930000	60.14	4681	.245	40.46	2.119
,144	9874.27	940000	60.96	4673	.231	40.89	2.130
,142	10006.68	950000	61.25	4629	.218	41.06	2.141
,143	10138.79	960000	61.51	4747	.224	41.17	2.141
,141	10271.62	970000	61.90	4621	.206	40.67	2.146
,143	10403.27	980000	63.07	4952	.202	42.14	2.171
,145	10535.14	990000	62.53	4893	.176	41.70	2.160
,143	10665.55	1000000	63.56	5283	.169	42.10	2.174

TABLE A.18

200X200 LATTICE

CLUSTER DISTRIBUTION PROPERTIES(10SL.)

20.00 PERCENT OF A MOLECULES

TEMPERATURE = .588 TIMES THE CRITIC TEMPERATURE

AVERAGE OF 1 RUNS WITH INFORMATION AT 120 POINTS

ENERGY	TIME	EXCHAN.	<SIZE>	<SIZE >	<E/L>	<EN>	<RADIO>
.403	16.40	500000	14.00	222	1.645	23.32	1.043
.351	43.35	1000000	14.56	230	1.506	21.90	1.066
.319	70.37	1200000	16.03	263	1.395	22.48	1.114
.304	119.25	2000000	16.95	325	1.338	22.64	1.144
.283	164.20	2500000	17.56	352	1.303	22.67	1.163
.276	212.27	3000000	18.51	399	1.253	23.12	1.192
.266	264.63	3500000	19.31	437	1.229	23.52	1.216
.262	319.92	4000000	20.18	493	1.197	23.90	1.239
.255	377.13	4500000	20.55	504	1.173	23.99	1.252
.248	436.59	5000000	21.78	572	1.152	24.91	1.285
.243	497.26	5500000	22.40	617	1.131	25.25	1.302
.236	561.62	6000000	22.81	635	1.109	24.88	1.314
.235	627.13	6500000	23.31	661	1.085	25.20	1.328
.232	692.60	7000000	24.19	720	1.071	26.04	1.351
.229	759.41	7500000	25.04	765	1.047	26.54	1.375
.226	824.74	8000000	25.33	803	1.130	26.57	1.380
.225	889.42	8500000	25.18	785	1.043	26.31	1.377
.221	956.29	9000000	26.91	901	1.072	27.64	1.422
.213	1026.83	9500000	27.11	915	1.089	27.70	1.427
.216	1096.21	10000000	27.28	937	1.071	27.54	1.429
.216	1165.55	10500000	27.46	952	1.066	27.59	1.434
.214	1233.99	11000000	28.05	984	1.067	27.82	1.451
.203	1307.42	11500000	28.68	1042	1.048	27.99	1.464
.206	1382.51	12000000	29.44	1090	1.035	28.38	1.485
.203	1457.17	12500000	29.27	1075	1.028	27.81	1.481
.204	1532.13	13000000	30.20	1159	1.029	28.86	1.503
.204	1607.41	13500000	30.07	1143	1.002	28.53	1.499
.199	1680.05	14000000	31.39	1239	1.091	29.20	1.529
.198	1757.90	14500000	31.41	1245	1.099	29.27	1.531
.197	1836.48	15000000	32.02	1300	1.077	29.73	1.545
.197	1914.39	15500000	32.73	1351	1.069	30.14	1.563
.194	1992.18	16000000	33.13	1411	1.050	30.22	1.569
.194	2068.95	16500000	33.64	1423	1.059	30.43	1.585
.195	2144.84	17000000	33.90	1444	1.055	30.56	1.591
.191	2220.53	17500000	34.50	1507	1.026	30.63	1.603
.183	2299.63	18000000	34.65	1515	1.030	30.50	1.606
.186	2379.81	18500000	35.15	1549	1.005	30.62	1.621
.184	2463.75	19000000	35.53	1582	1.004	30.89	1.629
.185	2545.65	19500000	35.71	1600	1.026	31.06	1.632
.184	2629.05	20000000	36.31	1663	1.099	31.18	1.644
.184	2711.59	20500000	36.68	1692	1.001	31.31	1.655
.183	2791.36	21000000	37.31	1755	1.069	31.83	1.666
.180	2874.03	21500000	36.33	1636	1.054	32.15	1.692
.177	2959.93	22000000	38.18	1827	1.090	31.94	1.680

CONT.

TABLE A.18, CONT'D

ENERGY	TIDE	EXCHAN.	<SIZE>	<SIZE >	<E/L>	<EN>	<RADIO>
.178	3046.37	2250000	38.31	1848	.765	32.02	1.688
.177	3129.29	2300000	40.03	1971	.737	32.92	1.732
.180	3211.77	2350000	39.66	1930	.723	32.82	1.726
.176	3296.05	2400000	39.94	1943	.738	32.96	1.733
.173	3384.75	2450000	40.10	1961	.697	32.60	1.735
.175	3472.70	2500000	40.28	1991	.742	33.10	1.737
.175	3561.40	2550000	40.19	2007	.737	32.80	1.732
.175	3648.76	2600000	40.45	2030	.731	33.06	1.737
.171	3733.49	2650000	41.42	2103	.720	33.50	1.761
.170	3822.42	2700000	42.72	2280	.683	34.16	1.784
.172	3911.54	2750000	42.49	2256	.699	33.98	1.780
.171	3994.11	2800000	43.16	2279	.689	34.16	1.798
.170	4082.54	2850000	43.56	2385	.673	34.77	1.814
.168	4175.42	2900000	44.46	2353	.634	34.93	1.831
.171	4262.52	2950000	45.18	2483	.634	35.74	1.843
.167	4352.01	3000000	45.06	2509	.559	35.19	1.836
.166	4446.31	3050000	45.15	2492	.636	35.02	1.840
.168	4534.44	3100000	45.43	2537	.626	35.22	1.845
.167	4623.34	3150000	46.17	2603	.615	35.81	1.862
.165	4714.25	3200000	45.77	2552	.632	35.23	1.856
.162	4802.23	3250000	45.72	2558	.645	35.11	1.853
.163	4895.51	3300000	46.34	2604	.645	35.54	1.869
.162	4988.07	3350000	46.67	2673	.649	35.48	1.872
.160	5083.06	3400000	46.95	2678	.623	35.32	1.886
.160	5179.45	3450000	47.27	2715	.614	35.58	1.887
.161	5271.44	3500000	46.83	2620	.623	35.05	1.874
.162	5364.11	3550000	47.73	2787	.634	36.16	1.894
.159	5456.11	3600000	47.08	2744	.617	35.23	1.876
.160	5547.24	3650000	47.85	2642	.616	35.70	1.892
.163	5639.52	3700000	48.04	2802	.599	36.03	1.903
.159	5729.76	3750000	48.66	2901	.573	36.21	1.912
.157	5820.81	3800000	48.26	2844	.520	35.82	1.905
.157	5926.69	3850000	46.51	2865	.593	35.89	1.910
.155	6028.21	3900000	46.59	2870	.574	35.73	1.912
.157	6123.43	3950000	46.59	2904	.593	36.05	1.908
.156	6220.39	4000000	49.09	2960	.575	36.04	1.919
.157	6316.50	4050000	49.19	2997	.594	36.33	1.918
.155	6412.48	4100000	48.53	2903	.580	35.42	1.907
.156	6516.17	4150000	49.19	2964	.581	36.35	1.922
.156	6612.54	4200000	48.76	2932	.547	35.67	1.912
.156	6705.10	4250000	48.21	2954	.621	35.60	1.910
.154	6803.10	4300000	50.62	3207	.563	36.50	1.944
.156	6897.53	4350000	50.68	3209	.555	37.12	1.946
.153	6991.10	4400000	51.28	3296	.523	36.76	1.957
.156	7086.11	4450000	51.88	3402	.556	37.58	1.965
.153	7176.07	4500000	52.16	3411	.527	37.03	1.973
.155	7266.68	4550000	52.29	3435	.567	37.99	1.974
.155	7358.85	4600000	52.22	3463	.560	37.67	1.970
.153	7455.97	4650000	52.42	3429	.517	37.15	1.973
.153	7552.37	4700000	53.21	3571	.531	37.70	1.992
.153	7647.83	4750000	53.79	3618	.545	38.00	2.005
.153	7745.75	4800000	53.58	3594	.562	38.04	2.000
.153	7839.22	4850000	53.40	3538	.558	38.31	1.995

CONT.

TABLE A.18, CONT'D

ENERGY	TIME	EXCHAN.	<SIZE>	<SIZE>	<E/L>	<EN>	<RADIUS>
.154	7931.59	4900000	53.14	3495	.544	37.52	1.994
.152	8025.69	4950000	53.60	3553	.548	37.66	2.003
.154	8116.38	5000000	53.46	3630	.521	37.74	1.992
.151	8210.16	5050000	53.42	3612	.544	37.57	1.990
.150	8308.35	5100000	54.58	3728	.521	38.40	2.016
.149	8410.56	5150000	55.42	3833	.500	38.80	2.034
.150	8509.21	5200000	56.45	3957	.482	39.37	2.054
.149	8609.00	5250000	56.53	4021	.511	39.30	2.053
.149	8709.57	5300000	56.35	4010	.525	38.85	2.047
.148	8807.42	5350000	56.48	4038	.496	39.05	2.049
.146	8905.30	5400000	57.96	4257	.482	39.36	2.079
.147	9004.23	5450000	58.13	4282	.459	39.94	2.081
.144	9105.83	5500000	58.69	4335	.463	39.83	2.094
.145	9207.70	5550000	58.61	4343	.433	39.63	2.091
.146	9310.42	5600000	58.32	4315	.489	39.73	2.084
.144	9412.36	5650000	58.39	4329	.496	39.45	2.085
.147	9515.63	5700000	58.31	4349	.437	40.00	2.081
.147	9615.47	5750000	58.63	4225	.463	40.12	2.093
.146	9715.43	5800000	58.69	4242	.493	40.05	2.098
.145	9817.19	5850000	59.56	4381	.477	40.35	2.112
.146	9918.95	5900000	59.48	4376	.447	40.49	2.110
.146	10017.08	5950000	61.41	4652	.422	41.53	2.145
.142	10119.77	6000000	61.04	4599	.419	40.76	2.136

TABLE A.19

30X30X30 LATTICE

CLUSTER DISTRIBUTION PROPERTIES(10SL)

20.00 PERCENT OF A MOLECULES

TEMPERATURE = .591 TIMES THE CRITIC TEMPERATURE

AVERAGE OF 8 RUNS WITH INFORMATION AT 70 POINTS

ENERGY	TIME	EXCHAN.	<SIZE>	<SIZE>	<E/L>	<EN>	<RADIUS>
.962	0.00	0	15.65	303	3.889	62.38	1.524
.871	.74	2500	21.22	683	3.743	81.99	1.654
.829	1.73	5000	26.00	1362	3.652	98.00	1.735
.804	2.56	7500	31.24	2397	3.561	115.50	1.810
.788	4.09	10000	36.19	3608	3.511	131.95	1.866
.774	5.38	12500	39.38	4710	3.457	141.50	1.901
.762	6.75	15000	44.08	7346	3.425	156.54	1.940
.751	8.18	17500	47.92	10435	3.390	167.84	1.956
.743	9.65	20000	50.42	11632	3.385	174.87	1.970
.736	11.16	22500	54.01	17285	3.337	185.71	1.996
.728	12.68	25000	62.32	23701	3.298	212.12	2.027
.723	14.23	27500	65.09	29729	3.311	219.80	2.042
.716	15.61	30000	68.03	49787	3.273	227.86	2.044
.710	17.44	32500	71.11	44333	3.235	236.21	2.062
.704	19.12	35000	75.16	54239	3.250	248.11	2.092
.701	20.79	37500	76.43	65584	3.230	250.70	2.073
.696	22.47	40000	75.76	56789	3.194	246.89	2.094

CONT.

TABLE A.19, CONT'D

ENERGY	TIME	EXCHAN.	<SIZE>	<SIZE >	<E/L>	<EN>	<RADIUS>
,692	24.17	42500	88.18	87526	3.152	285.33	2.153
,688	25.87	45000	91.03	89171	3.182	293.28	2.125
,684	27.60	47500	90.62	96412	3.151	290.28	2.151
,680	29.32	50000	93.16	99232	3.144	296.42	2.163
,628	67.15	100000	162.12	376431	2.820	474.47	2.314
,597	108.88	150000	196.66	371309	2.623	515.18	2.517
,569	155.40	210000	255.07	722700	2.562	666.56	2.595
,547	200.42	250000	306.67	914766	2.458	771.91	2.612
,532	249.71	300000	307.24	711831	2.370	745.88	2.974
,518	300.31	350000	397.95	1032323	2.369	932.42	3.278
,503	352.59	400000	422.29	1066350	2.369	940.95	3.287
,495	402.93	450000	415.33	1018933	2.219	923.76	3.441
,487	460.93	500000	475.26	1325233	2.141	1039.53	3.493
,478	510.61	550000	541.07	1665567	2.078	1156.23	3.553
,470	573.05	600000	460.09	1196053	2.131	973.84	3.585
,459	630.92	650000	695.09	2308421	1.949	1423.65	4.042
,452	689.37	700000	590.23	1522414	1.875	1187.01	3.932
,444	749.12	750000	655.46	1932809	1.757	1294.53	4.023
,440	819.14	800000	643.30	1653693	1.677	1249.64	4.156
,437	871.64	850000	640.95	1796606	1.772	1234.93	4.052
,430	933.60	900000	679.76	1810543	1.630	1286.07	4.249
,428	995.99	950000	629.54	1354947	1.455	1171.20	4.359
,420	1059.60	1000000	701.84	1557506	1.474	1288.77	4.501
,415	1124.83	1050000	668.17	1353093	1.399	1220.02	4.501
,415	1188.96	1100000	639.45	1595192	1.579	1152.95	4.153
,411	1254.29	1150000	759.91	1889984	1.399	1361.70	4.613
,409	1319.99	1200000	687.92	2355060	1.380	1583.92	4.805
,403	1386.09	1250000	698.93	2635915	1.553	1579.41	4.588
,404	1452.02	1300000	677.31	2742996	1.477	1535.87	4.602
,399	1510.28	1350000	1004.84	2506873	1.305	1734.49	5.105
,397	1585.95	1400000	975.25	2681925	1.398	1626.40	5.028
,395	1653.13	1450000	966.76	2511194	1.287	1654.95	5.127
,391	1721.27	1500000	1027.63	3452790	1.517	1734.65	4.847
,389	1789.05	1550000	1377.51	405607	1.265	2375.49	5.681
,389	1856.57	1600000	1370.24	506213	1.330	2279.56	5.584
,385	1925.49	1650000	1020.01	3212692	1.401	1673.41	5.019
,383	1994.34	1700000	924.59	2690099	1.582	1515.83	4.714
,382	2062.97	1750000	872.34	2643673	1.567	1420.85	4.619
,380	2132.19	1800000	684.87	2779079	1.395	1429.56	4.815
,379	2201.97	1850000	629.85	1841534	1.373	1330.62	4.668
,372	2272.84	1900000	663.26	1649133	1.295	1364.54	5.087
,372	2343.78	1950000	914.15	2277049	1.320	1445.47	5.044
,369	2415.43	2000000	1081.94	3135523	1.506	1709.28	5.187
,364	2559.11	2100000	640.37	1520592	1.306	1295.54	5.057
,361	2704.00	2200000	971.23	1940600	1.183	1484.23	5.384
,355	2850.53	2300000	1469.62	4906633	1.251	2239.16	5.964
,356	2998.29	2400000	926.87	2142279	1.272	1393.10	5.164
,356	3145.74	2500000	904.12	1759982	1.314	1349.61	5.186
,351	3295.58	2600000	981.05	2141297	1.269	1442.80	5.325
,348	3445.36	2700000	997.44	2520709	1.310	1441.72	5.230
,345	3595.02	2800000	1315.48	3351635	1.171	1899.10	5.950
,343	3745.64	2900000	1212.95	3421424	1.243	1744.41	5.642
,339	3895.20	3000000	1126.22	2693829	1.185	1587.70	5.720

30X30X30 LATTICE

CLUSTER DISTRIBUTION PROPERTIES(10SL)

20.00 PERCENT OF A MOLECULES

TEMPERATURE = .887 TIMES THE CRITICAL TEMPERATURE

AVERAGE OF 8 RUNS WITH INFORMATION AT 64 POINTS

ENERGY	TIME	EXCHAN.	<SIZE>	<SIZE >	<E/L>	<EN>	<RADIO>
.962	0.00	0	15.65	303	3.889	62.38	1.524
.891	.67	2500	19.37	539	3.782	75.37	1.614
.863	1.47	5000	21.65	708	3.724	83.09	1.664
.848	2.32	7500	24.74	1035	3.667	93.65	1.721
.834	3.22	10000	26.74	1327	3.627	100.21	1.750
.827	4.14	12500	28.07	1536	3.607	104.34	1.771
.822	5.07	15000	29.81	2078	3.588	110.22	1.791
.814	6.01	17500	32.52	2686	3.536	119.39	1.820
.809	6.98	20000	35.94	2658	3.511	123.92	1.853
.805	7.95	22500	32.70	2204	3.523	116.99	1.849
.802	8.92	25000	35.08	2806	3.496	127.47	1.871
.799	9.92	27500	35.36	3865	3.498	127.70	1.855
.798	10.91	30000	35.96	3781	3.481	129.49	1.866
.795	11.90	32500	36.83	3514	3.469	132.11	1.888
.793	12.91	35000	37.95	3797	3.460	135.61	1.903
.791	13.93	37500	39.23	4780	3.470	140.11	1.900
.790	14.93	40000	40.63	7223	3.448	144.50	1.907
.789	15.94	42500	42.00	7910	3.446	148.79	1.907
.783	16.97	45000	45.37	6887	3.409	164.29	1.967
.781	17.99	47500	44.05	6635	3.401	155.13	1.955
.780	19.02	50000	44.65	6941	3.417	156.72	1.952
.763	39.99	100000	54.41	11591	3.338	186.06	2.034
.756	61.42	150000	61.26	21113	3.322	206.64	2.063
.753	62.93	200000	69.37	25726	3.299	231.65	2.136
.745	104.66	250000	71.90	47764	3.315	238.38	2.096
.745	126.55	300000	71.11	31002	3.323	236.24	2.093
.743	146.39	350000	73.55	51724	3.316	242.32	2.045
.741	170.36	400000	81.73	73628	3.349	268.73	2.362
.736	192.37	450000	83.68	55513	3.337	271.56	2.115
.736	214.55	500000	91.40	64142	3.291	297.13	2.145
.734	236.89	550000	94.94	52022	3.280	275.64	2.157
.735	259.04	600000	84.80	56197	3.322	276.68	2.116
.733	281.23	650000	89.15	61749	3.307	287.76	2.139
.734	303.39	700000	88.97	68452	3.305	289.49	2.127
.734	325.57	750000	86.84	83815	3.323	286.77	2.091
.731	347.75	800000	85.86	93137	3.321	276.83	2.077
.732	392.23	900000	90.51	73941	3.280	221.33	2.137
.730	436.61	1000000	92.08	70150	3.275	224.95	2.139
.730	431.29	1100000	86.76	72761	3.304	223.45	2.112
.731	525.91	1200000	94.64	316268	3.323	303.31	2.032
.728	570.70	1300000	92.29	88057	3.333	295.54	2.095
.728	615.53	1400000	87.75	66113	3.337	279.55	2.092
.730	660.29	1500000	89.81	77989	3.366	226.76	2.081
.727	705.10	1600000	100.00	184202	3.334	337.83	2.066

CONT.

TABLE A.20, CONT'D

ENERGY	TIME	EXCHAN.	<SIZE>	<SIZE >	<E/L>	<EN>	<RADIUS>
.723	750.14	1700000	103.02	124159	3.304	325.06	2.097
.721	795.23	1800000	100.83	149421	3.362	317.33	2.059
.724	840.26	1900000	94.18	89318	3.307	297.09	2.072
.723	885.22	2000000	92.34	71730	3.316	291.99	2.100
.720	930.27	2100000	109.80	170142	3.342	344.29	2.072
.722	975.56	2200000	92.84	98777	3.368	291.80	2.052
.716	1020.68	2300000	100.57	157271	3.305	330.32	2.079
.717	1060.93	2400000	105.24	151115	3.355	329.44	2.054
.717	1111.43	2500000	104.19	130304	3.287	322.23	2.103
.718	1150.73	2600000	90.64	114169	3.354	232.82	2.005
.714	1202.32	2700000	103.14	137273	3.335	318.74	2.048
.717	1247.86	2800000	94.32	87473	3.339	293.00	2.061
.719	1293.27	2900000	91.63	107495	3.334	222.37	2.015
.721	1338.45	3000000	94.69	95591	3.282	295.67	2.078
.720	1383.79	3100100	104.77	157095	3.346	326.25	2.057
.717	1429.12	3200000	107.89	176051	3.322	332.54	2.051
.716	1474.59	3300000	98.44	105664	3.258	315.46	2.077
.713	1520.17	3400000	105.07	126259	3.307	324.32	2.090
.714	1565.79	3500000	97.68	112461	3.352	302.60	2.041
.713	1611.30	3600000	100.55	134742	3.294	311.45	2.066

TABLE A.21

30X30X30 LATTICE

CLUSTER DISTRIBUTION PROPERTIES(10SL.)

20.00 PERCENT OF A MOLECULES

TEMPERATURE = 1.063 TIMES THE CRITICAL TEMPERATURE

AVERAGE OF 9 RUNS WITH INFORMATION AT 49 POINTS

ENERGY	TIME	EXCHAN.	<SIZE>	<SIZE >	<E/L>	<EN>	<RADIUS>
.962	0.00	0	15.65	303	3.839	52.38	1.524
.901	.65	2500	18.35	457	3.792	71.64	1.592
.877	1.40	5000	21.13	719	3.735	91.37	1.651
.863	2.13	7500	22.79	839	3.691	86.92	1.686
.855	2.93	10000	24.44	1074	3.560	92.65	1.709
.847	3.81	12500	25.47	1111	3.650	95.98	1.737
.842	4.64	15000	26.65	1318	3.615	99.80	1.754
.837	5.47	17500	27.20	1495	3.599	101.40	1.757
.835	6.32	20000	28.36	1629	3.530	105.51	1.776
.833	7.16	22500	28.62	1573	3.597	106.03	1.782
.829	8.01	25000	29.00	1816	3.576	107.00	1.782
.826	8.88	27500	30.74	1943	3.555	113.24	1.812
.823	9.75	30000	31.03	2200	3.552	115.64	1.808
.822	10.63	32500	32.59	2621	3.541	119.13	1.828
.823	11.50	35000	31.94	1972	3.541	117.04	1.842

CONT.

TABLE A.21, CONT'D

ENERGY	TIME	EXCHAN.	<SIZE>	<SIZE >	<E/L>	<EN>	<RADIOS>
.820	12.37	37500	31.20	1950	3.539	114.51	1.826
.819	13.24	40000	32.68	2404	3.529	119.27	1.838
.819	14.13	42500	32.60	2342	3.518	118.69	1.843
.818	15.00	45000	33.91	2489	3.508	123.37	1.857
.817	15.88	47500	33.59	2592	3.508	122.37	1.856
.816	16.76	50000	34.43	2608	3.497	125.23	1.865
.807	34.80	100000	39.38	4340	3.456	141.00	1.919
.804	52.68	150000	41.41	4349	3.448	147.55	1.941
.803	70.70	200000	45.52	7515	3.438	151.38	1.949
.799	88.79	250000	46.30	7612	3.421	153.73	1.972
.797	107.00	300000	49.30	9696	3.415	173.80	1.970
.795	125.19	350000	44.62	7197	3.434	157.49	1.937
.795	143.32	400000	47.17	11663	3.450	165.46	1.940
.795	161.53	450000	47.24	7396	3.415	165.76	1.953
.795	179.70	500000	46.93	8492	3.429	165.11	1.959
.795	197.92	550000	46.72	10997	3.434	171.31	1.957
.795	216.16	600000	49.36	10572	3.435	172.80	1.959
.792	234.47	650000	53.75	14255	3.420	187.55	1.989
.795	252.71	700000	51.68	16949	3.444	190.43	1.967
.795	270.91	750000	47.94	11079	3.460	167.82	1.932
.792	289.17	800000	53.93	22313	3.440	188.47	1.955
.794	307.50	850000	54.20	17713	3.435	189.00	1.971
.792	325.72	900000	51.71	14010	3.426	189.06	1.982
.794	362.29	1000000	50.25	14635	3.470	175.50	1.947
.796	390.69	1100000	47.19	13602	3.483	165.91	1.920
.795	435.00	1200000	48.89	13126	3.455	171.38	1.944
.793	471.56	1300000	51.55	13926	3.444	180.11	1.956
.795	508.02	1400000	50.66	13541	3.461	175.63	1.937
.792	544.62	1500000	50.69	13015	3.465	175.94	1.955
.793	581.19	1600000	49.97	12289	3.424	173.01	1.942
.791	617.89	1700000	56.08	19904	3.422	196.20	1.995
.793	654.29	1800000	47.86	11677	3.457	165.97	1.930
.793	691.87	1900000	54.27	16282	3.447	189.30	1.980
.794	727.30	2000000	49.83	11883	3.450	174.47	1.959

30X30 LATTICE

ANTIFERROMAGNETIC INTERACTION
50.00 PERCENT OF A MOLECULESTEMPERATURE = .591 TIMES THE CRITICAL TEMPERATURE
AVERAGE OF 8 RUNS WITH INFORMATION AT 59 POINTS

Table A.22

EXCHANGES	TIME	STRUCTURE FUNCTION, S(μ)									
		S(1)	S(2)	S(3)	S(4)	S(5)	S(6)	S(7)	S(8)	S(9)	S(10)
0	0.0	.842	.970	.865	.957	1.053	.965	1.010	1.071	.979	1.006
2500	.4	.829	.944	.793	.853	.925	.771	.819	.814	.712	.759
5000	.9	.824	.906	.706	.756	.764	.634	.646	.646	.573	.605
7500	1.5	.813	.635	.608	.647	.614	.522	.511	.503	.492	.515
10000	2.2	.778	.787	.553	.577	.535	.419	.413	.422	.417	.442
12500	3.0	.747	.738	.484	.504	.472	.385	.367	.364	.392	.399
15000	3.9	.712	.694	.420	.441	.397	.343	.319	.329	.345	.366
17500	5.0	.716	.667	.367	.398	.362	.302	.296	.307	.337	.348
20000	6.2	.720	.597	.334	.344	.323	.281	.297	.288	.321	.304
22500	7.6	.690	.559	.309	.297	.320	.258	.245	.278	.289	.292
25000	9.1	.672	.523	.290	.267	.282	.237	.241	.255	.260	.270
27500	10.8	.637	.479	.253	.268	.262	.221	.225	.223	.249	.254
30000	12.7	.618	.467	.241	.240	.246	.214	.230	.222	.228	.245
32500	14.6	.603	.442	.230	.222	.232	.196	.207	.216	.212	.238
35000	17.1	.606	.397	.198	.215	.207	.186	.200	.203	.201	.229
37500	19.7	.589	.394	.210	.197	.185	.182	.192	.201	.195	.220
40000	22.4	.612	.367	.197	.184	.183	.182	.195	.185	.187	.200
42500	25.3	.588	.351	.194	.171	.174	.169	.193	.181	.181	.194
45000	28.4	.585	.355	.186	.183	.174	.166	.174	.181	.175	.175
47500	31.7	.573	.330	.173	.179	.164	.157	.158	.169	.164	.171
50000	35.3	.559	.301	.180	.181	.159	.149	.154	.160	.160	.167
52500	51.4	.486	.285	.160	.150	.141	.139	.134	.144	.148	.149
55000	71.5	.413	.226	.155	.128	.117	.122	.116	.121	.127	.131
57500	84.1	.376	.212	.132	.113	.123	.113	.111	.114	.119	.127
60000	101.8	.360	.193	.128	.109	.105	.108	.106	.110	.118	.115
62500	120.1	.317	.172	.108	.093	.096	.097	.094	.107	.104	.110
65000	253.6	.271	.139	.109	.089	.096	.083	.094	.092	.099	.096
67500	296.7	.250	.139	.090	.077	.089	.086	.086	.087	.096	.091
70000	341.8	.230	.123	.088	.088	.081	.084	.085	.090	.089	.094
72500	391.1	.221	.121	.096	.084	.084	.084	.084	.085	.087	.090
75000	445.5	.212	.120	.083	.078	.081	.083	.073	.074	.077	.093
77500	499.9	.195	.117	.081	.082	.077	.083	.077	.081	.084	.088
80000	554.8	.198	.114	.077	.082	.073	.078	.081	.079	.079	.083
82500	609.7	.165	.104	.082	.069	.075	.075	.081	.075	.083	.085
85000	665.5	.166	.103	.083	.071	.073	.069	.081	.076	.075	.081
87500	722.8	.155	.096	.074	.071	.071	.076	.077	.075	.080	.078
90000	781.0	.152	.099	.072	.070	.068	.067	.076	.070	.075	.077
92500	804.3	.149	.100	.079	.071	.068	.069	.074	.074	.076	.076
95000	828.6	.134	.093	.083	.072	.072	.068	.071	.072	.073	.073
97500	855.3	.137	.089	.076	.068	.076	.064	.064	.069	.068	.074
100000	882.5	.125	.085	.071	.070	.069	.063	.070	.070	.072	.075
102500	909.9	.123	.081	.072	.072	.067	.063	.065	.072	.074	.075
105000	936.8	.124	.076	.076	.069	.066	.065	.070	.068	.073	.073
107500	964.7	.128	.077	.073	.069	.072	.064	.071	.073	.072	.071
110000	991.9	.129	.072	.073	.066	.067	.062	.063	.070	.073	.074

CONT.

TABLE A.22, CONT'D

STRUCTURE FUNCTION, S(μ)												
EXCHANGES	TIME	S(1)	S(2)	S(3)	S(4)	S(5)	S(6)	S(7)	S(8)	S(9)	S(10)	
160000	1019.4	.129	.077	.065	.070	.067	.063	.065	.166	.074	.072	
170000	1046.3	.131	.069	.070	.072	.067	.064	.070	.166	.073	.075	
172000	1073.9	.128	.070	.066	.063	.059	.059	.061	.067	.067	.069	
174000	1101.6	.126	.077	.064	.068	.062	.061	.064	.063	.069	.067	
176000	1130.0	.125	.078	.064	.067	.059	.057	.064	.063	.069	.070	
178000	1158.0	.129	.084	.062	.069	.064	.061	.058	.165	.069	.072	
180000	1185.6	.122	.061	.060	.066	.061	.061	.060	.168	.064	.066	
182000	1214.1	.125	.086	.060	.067	.065	.061	.064	.168	.068	.066	
184000	1242.3	.113	.080	.060	.066	.059	.058	.059	.063	.064	.064	
186000	1270.1	.118	.078	.062	.069	.067	.058	.064	.162	.065	.067	
188000	1297.9	.109	.069	.064	.067	.067	.065	.067	.167	.070	.067	
190000	1325.7	.107	.079	.062	.061	.066	.065	.063	.163	.070	.069	
192000	1353.7	.092	.065	.061	.064	.063	.065	.063	.064	.070	.073	
194000	1382.0	.088	.066	.061	.062	.058	.063	.064	.164	.070	.073	

TABLE A.23

50X30X30 LATTICE

ANTIFERROMAGNETIC INTERACTION

50.00 PERCENT OF A MOLECULES

TEMPERATURE = .591 TIMES THE CRITICAL TEMPERATURE

AVERAGE OF 8 RUNS WITH INFORMATION AT 20 POINTS

STRUCTURE FUNCTION, S(μ)												
EXCHANGES	TIME	S(1)	S(2)	S(3)	S(4)	S(5)	S(6)	S(7)	S(8)	S(9)	S(10)	
0	0.0	.733	.986	.522	1.027	1.025	.982	1.037	1.026	1.040	1.036	
5000	1.1	.720	.986	.721	.793	.711	.595	.633	.515	.528	.527	
10000	2.6	.741	.933	.684	.640	.542	.507	.489	.452	.516	.512	
15000	4.4	.766	.734	.645	.524	.456	.432	.465	.447	.481	.513	
20000	6.3	.664	.649	.590	.453	.445	.426	.436	.446	.473	.525	
25000	8.3	.637	.607	.517	.463	.450	.414	.423	.448	.482	.532	
30000	10.3	.656	.591	.528	.441	.444	.467	.476	.459	.481	.497	
35000	12.4	.627	.572	.501	.433	.446	.473	.465	.484	.491	.492	
40000	14.6	.615	.580	.485	.463	.455	.453	.449	.467	.487	.487	
45000	16.8	.627	.551	.530	.479	.455	.430	.463	.466	.494	.508	
50000	19.0	.658	.514	.497	.461	.451	.477	.457	.449	.488	.504	
100000	41.6	.552	.552	.513	.484	.466	.467	.450	.455	.491	.531	
150000	64.9	.593	.617	.578	.511	.448	.465	.472	.452	.500	.485	
200000	88.6	.687	.584	.583	.546	.456	.500	.467	.466	.467	.510	
250000	112.6	.717	.581	.604	.512	.495	.502	.473	.473	.485	.493	
300000	136.8	.677	.586	.521	.558	.475	.479	.472	.471	.486	.505	
350000	161.2	.644	.656	.602	.498	.490	.537	.495	.507	.495	.491	
400000	185.9	.736	.566	.598	.514	.498	.494	.461	.472	.488	.508	
450000	210.9	.695	.646	.550	.489	.532	.496	.439	.466	.519	.519	
500000	236.1	.721	.686	.510	.535	.500	.477	.518	.464	.487	.504	

TABLE A.24

30X30X30 LATTICE

ANTIFERROMAGNETIC INTERACTION

50.00 PERCENT OF A MOLECULES ($\bar{\eta} = 0.0$)

TEMPERATURE = .591 TIMES THE CRITIC TEMPERATURE

AVERAGE OF 8 RUNS WITH INFORMATION AT 63 POINTS

TIME	ENERGY	TIME	ENERGY	TIME	ENERGY	TIME	ENERGY
0.00	1.504	.15	1.570	.30	1.627	.41	1.666
.70	1.746	1.00	1.810	1.44	1.884	1.93	1.951
2.48	2.012	3.01	2.058	3.59	2.106	5.00	2.192
6.21	2.250	7.56	2.300	9.10	2.351	10.83	2.395
12.71	2.435	14.83	2.472	17.13	2.498	19.66	2.525
22.36	2.549	25.30	2.574	28.44	2.589	31.71	2.608
35.25	2.624	51.38	2.671	71.53	2.717	84.14	2.735
101.78	2.759	170.08	2.785	253.59	2.798	296.71	2.805
341.83	2.813	391.10	2.822	445.46	2.825	499.92	2.828
554.85	2.832	609.71	2.834	665.50	2.838	722.76	2.843
780.99	2.848	804.34	2.850	828.65	2.853	855.35	2.858
882.45	2.856	909.91	2.856	936.80	2.859	964.66	2.857
991.93	2.858	1019.41	2.859	1046.32	2.859	1073.87	2.862
1101.58	2.863	1130.04	2.863	1158.00	2.865	1185.57	2.866
1214.09	2.865	1242.34	2.868	1270.06	2.867	1297.92	2.866
1325.69	2.864	1353.67	2.866	1381.95	2.867		

TABLE A.25

30X30X30 LATTICE

ANTIFERROMAGNETIC INTERACTION

30.00 PERCENT OF A MOLECULES ($\bar{\eta} = -.4$)

TEMPERATURE = .591 TIMES THE CRITIC TEMPERATURE

AVERAGE OF 8 RUNS WITH INFORMATION AT 34 POINTS

TIME	ENERGY	TIME	ENERGY	TIME	ENERGY	TIME	ENERGY
0.00	1.261	.15	1.311	.30	1.352	.44	1.385
.59	1.414	.74	1.439	.89	1.460	1.04	1.479
1.26	1.502	1.56	1.527	1.85	1.546	2.15	1.561
2.44	1.573	2.74	1.585	3.07	1.598	3.41	1.606
3.63	1.611	4.35	1.623	6.26	1.648	8.25	1.655
10.32	1.663	12.42	1.669	14.56	1.670	16.77	1.673
18.96	1.677	41.58	1.682	64.86	1.686	88.63	1.691
112.59	1.692	136.80	1.692	161.19	1.694	185.94	1.694
210.87	1.697	236.12	1.700				

TABLE A.26

30X30X30 LATTICE

ANTIFERROMAGNETIC INTERACTION

50.00 PERCENT OF A MOLECULES ($\bar{\eta} = 0.0$)

TEMPERATURE = .887 TIMES THE CRITIC TEMPERATURE

AVERAGE OF 7 RUNS WITH INFORMATION AT 116 POINTS

TIME	LRO P.						
0.00	.005	.31	.006	.56	.010	1.02	.011
1.41	.011	1.82	.019	2.23	.021	2.67	.022
3.12	.019	3.58	.022	4.05	.024	4.54	.025
5.02	.026	5.51	.028	6.02	.030	6.53	.033
7.04	.039	7.57	.039	8.11	.038	8.65	.040
9.19	.044	9.75	.048	10.30	.054	10.86	.053
11.43	.057	12.00	.058	13.46	.061	14.93	.068
16.44	.076	17.97	.087	19.53	.093	21.12	.096
22.75	.104	24.41	.113	26.11	.119	27.86	.119
29.61	.128	31.38	.133	33.16	.134	34.97	.135
36.82	.136	38.70	.140	40.59	.143	42.52	.147
44.49	.161	46.45	.163	48.46	.166	50.50	.179
52.53	.181	54.61	.189	56.72	.193	58.85	.195
60.95	.205	63.10	.207	65.24	.214	67.40	.218
69.59	.222	71.78	.223	73.96	.226	76.17	.231
78.43	.233	80.67	.236	82.97	.241	85.29	.239
87.63	.247	89.97	.250	92.33	.253	94.65	.247
97.00	.256	99.36	.269	101.72	.269	104.11	.265
106.48	.270	108.88	.272	111.30	.277	113.70	.271
116.07	.275	118.45	.277	120.34	.281	123.25	.288
125.69	.288	128.15	.291	130.58	.292	133.03	.297
135.48	.301	137.93	.307	140.36	.311	142.79	.316
145.21	.320	147.65	.329	150.13	.335	152.63	.335
155.10	.336	157.59	.340	160.06	.344	162.56	.347
165.04	.342	167.51	.348	169.97	.353	172.49	.347
175.01	.355	177.53	.365	180.07	.376	182.61	.376
185.11	.381	187.63	.384	190.14	.389	192.67	.398
195.20	.400	197.73	.411	200.27	.420	202.84	.425
205.40	.432	208.03	.442	210.63	.450	213.25	.452

TABLE A.27

30X30X30 LATTICE

ANTIFERROMAGNETIC INTERACTION

50.00 PERCENT OF A MOLECULES ($\bar{\eta} = 0.0$)

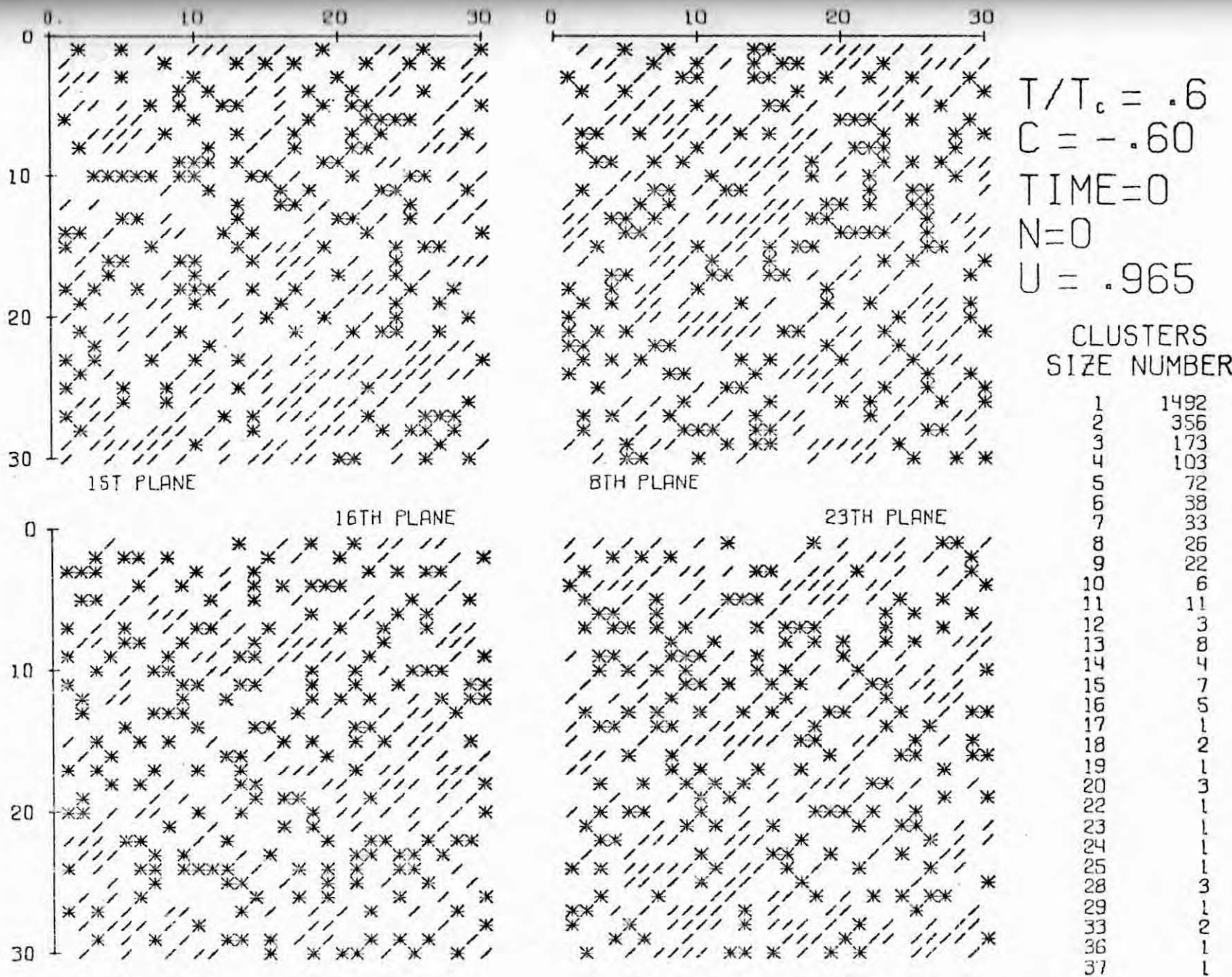
TEMPERATURE = .887 TIMES THE CRITIC TEMPERATURE

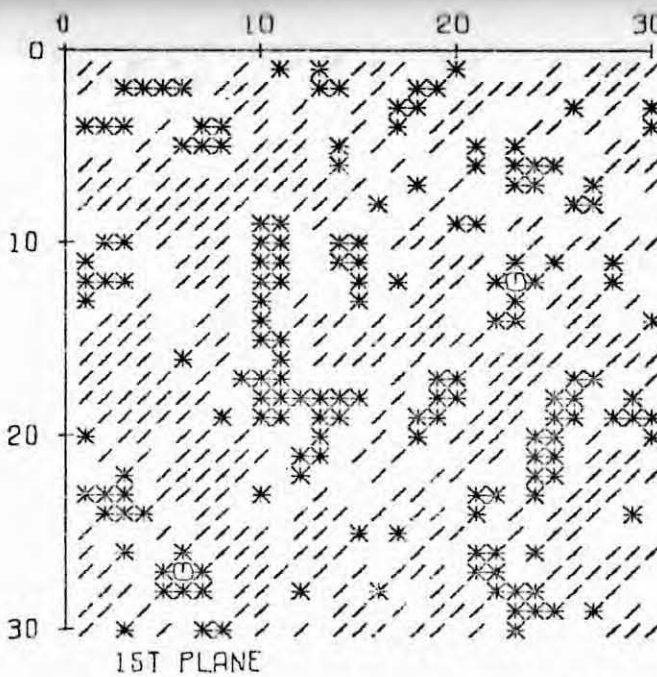
AVERAGE OF 7 RUNS WITH INFORMATION AT 43 POINTS

TIME	ENERGY	TIME	ENERGY	TIME	ENERGY	TIME	ENERGY
0.00	1.504	.15	1.560	.30	1.609	.44	1.647
.59	1.681	.74	1.709	.89	1.734	1.33	1.792
1.78	1.834	2.22	1.866	2.67	1.893	3.11	1.914
3.56	1.931	4.54	1.965	6.02	1.996	7.57	2.027
9.19	2.045	10.86	2.062	13.46	2.087	17.97	2.118
22.75	2.154	27.86	2.182	33.16	2.198	40.59	2.236
48.46	2.258	56.72	2.277	65.24	2.281	73.96	2.288
82.97	2.308	92.33	2.312	101.72	2.318	111.30	2.325
120.84	2.326	130.58	2.332	140.36	2.324	150.13	2.337
160.06	2.339	169.97	2.339	180.07	2.342	190.14	2.342
200.27	2.349	210.63	2.358	213.25	2.356		

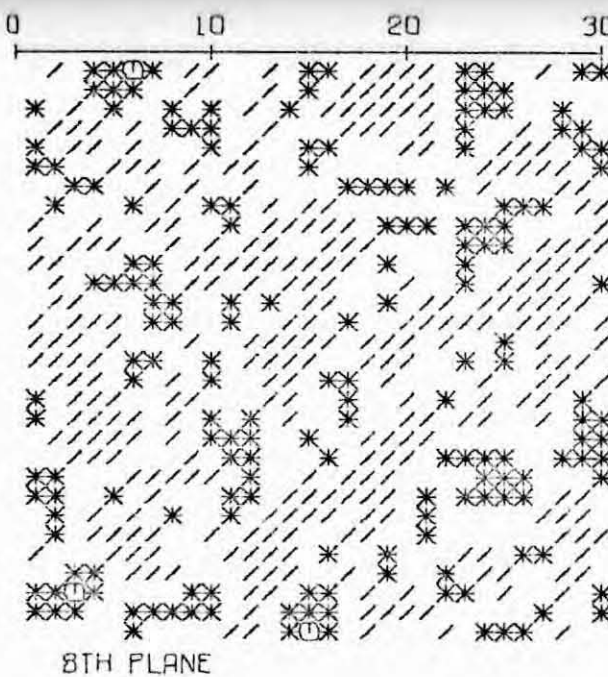
Appendix B

FIG. B.1

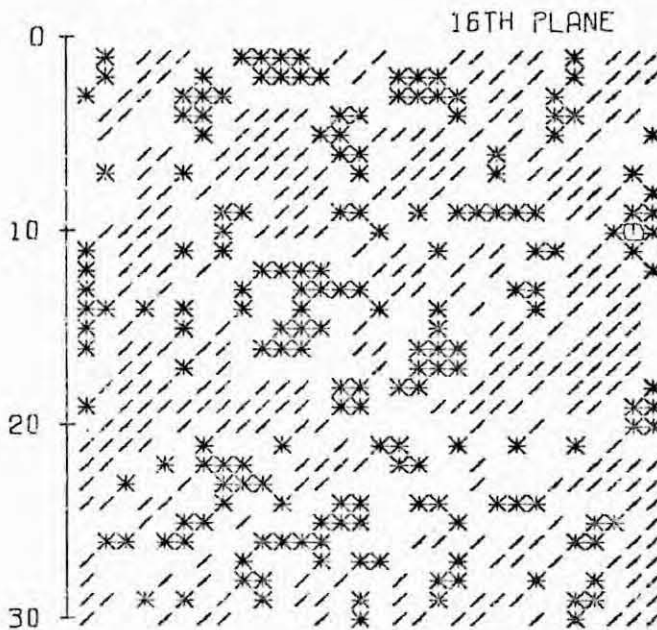




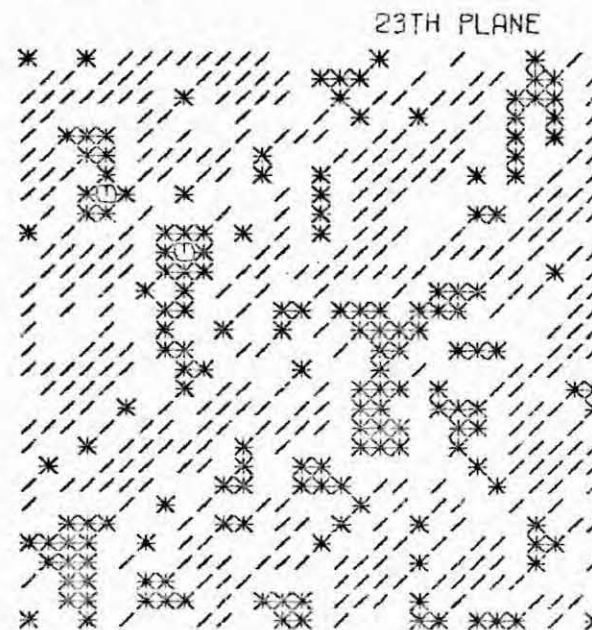
1ST PLANE



8TH PLANE



16TH PLANE



23TH PLANE

$T/T_c = .6$
 $C = -.60$
 TIME=29
 $N=50000$
 $U = .683$
 CLUSTERS
 SIZE NUMBER

257
 50
 17
 12
 8
 6
 2
 4
 13
 14
 15
 16
 17
 19
 20
 21
 22
 23
 25
 28
 30
 32
 34
 36
 37
 39
 42
 48
 62
 67
 73
 81
 82
 84
 95
 108
 139
 229
 376
 461
 556
 1353

Fig. B2

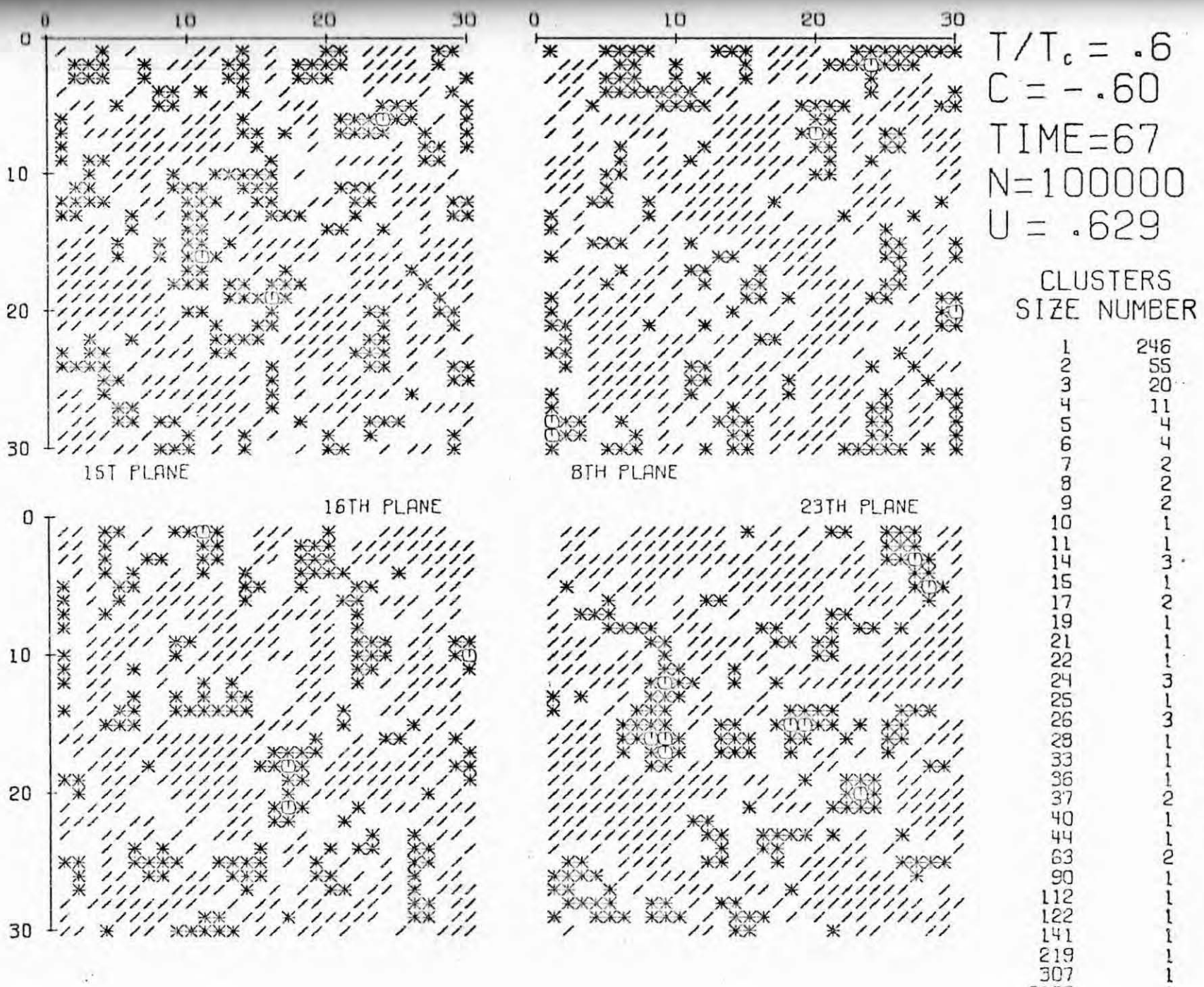
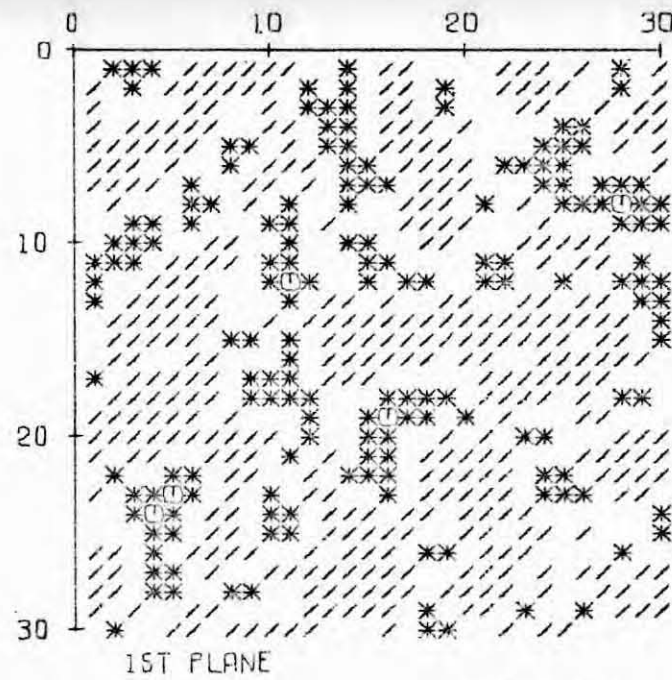
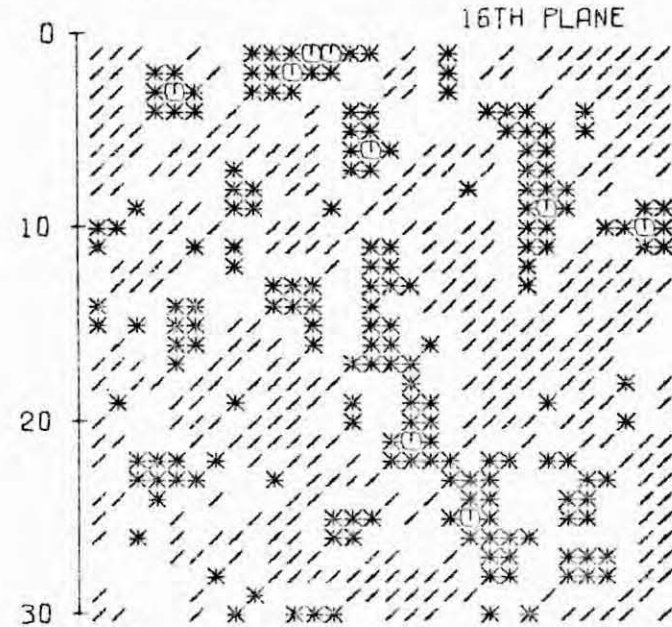


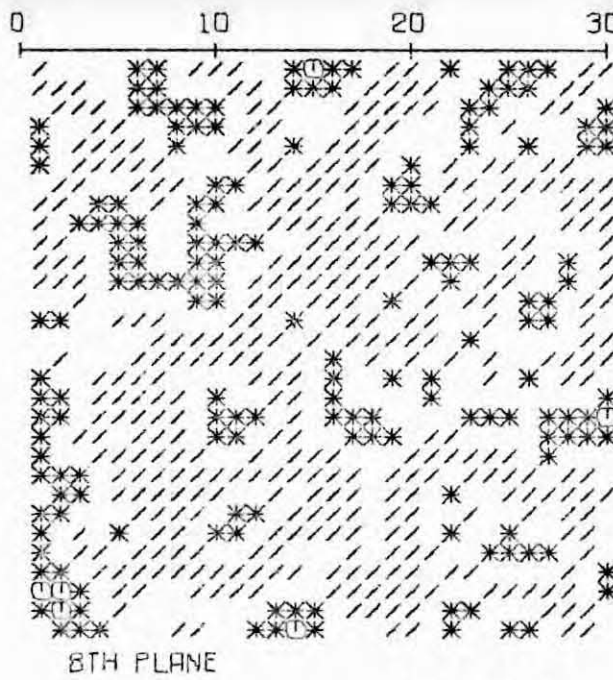
Fig. B3



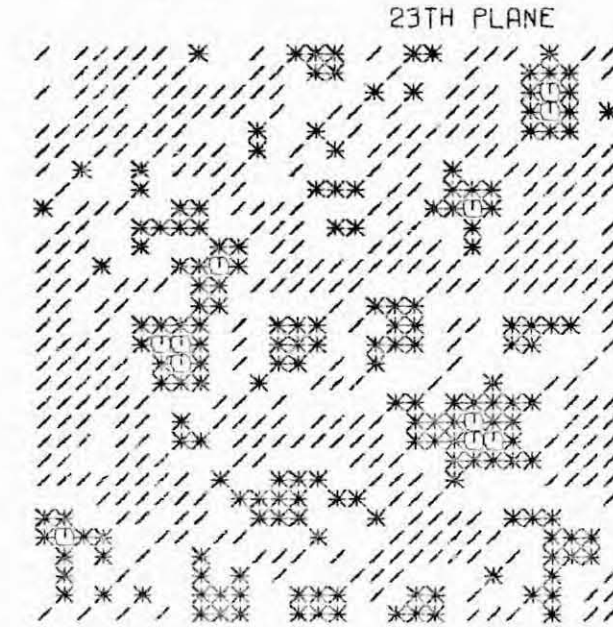
1ST PLANE



16TH PLANE



8TH PLANE



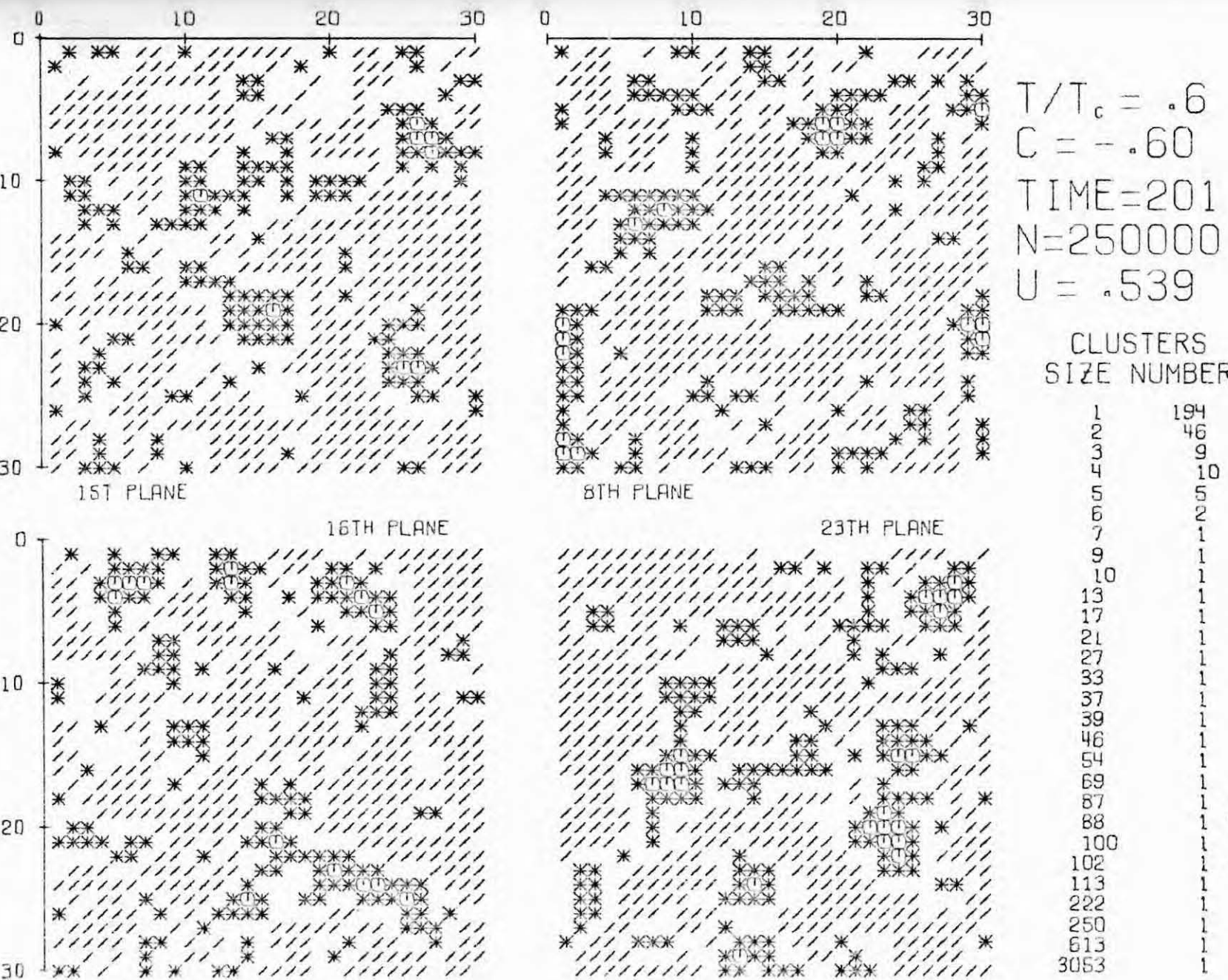
23TH PLANE

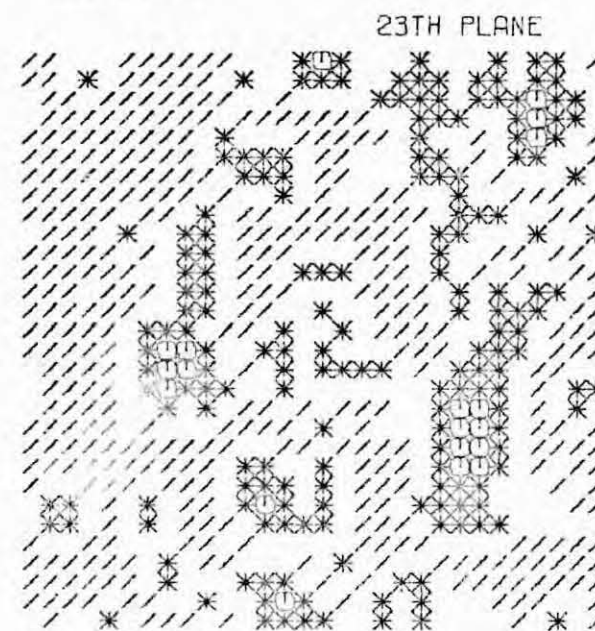
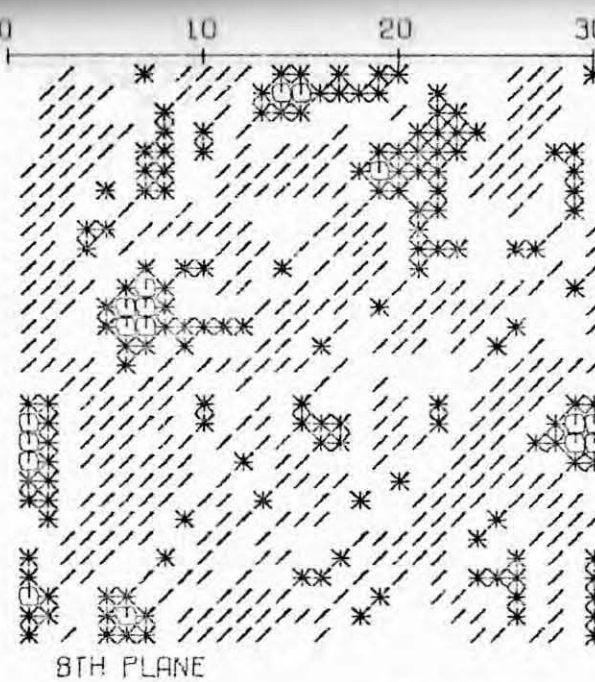
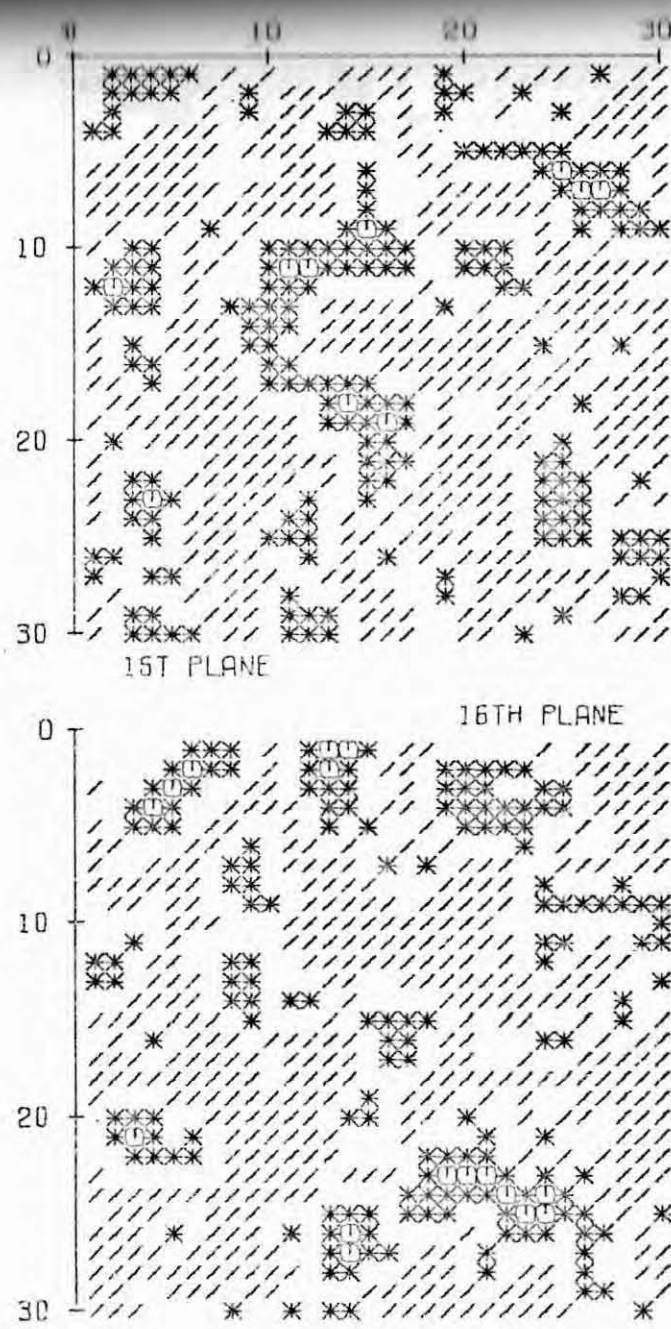
$T/T_c = .6$
 $C = -.60$
 TIME=108
 $N=150000$
 $U = .598$

CLUSTERS
SIZE NUMBER

1	260
2	36
3	18
4	5
5	7
6	3
7	1
8	1
9	1
10	1
11	1
12	1
13	2
14	1
15	1
16	1
17	1
18	1
19	1
20	1
21	1
22	1
23	1
24	2
25	1
26	1
27	1
28	1
29	1
30	1
31	1
32	1
33	1
34	1
35	1
36	1
37	1
38	1
39	1
40	1
41	1
42	1
43	1
44	1
45	1
46	1
47	1
48	1
49	1
50	1
51	1
52	1
53	1
54	1
55	1
56	1
57	1
58	1
59	1
60	1

Fig. B4



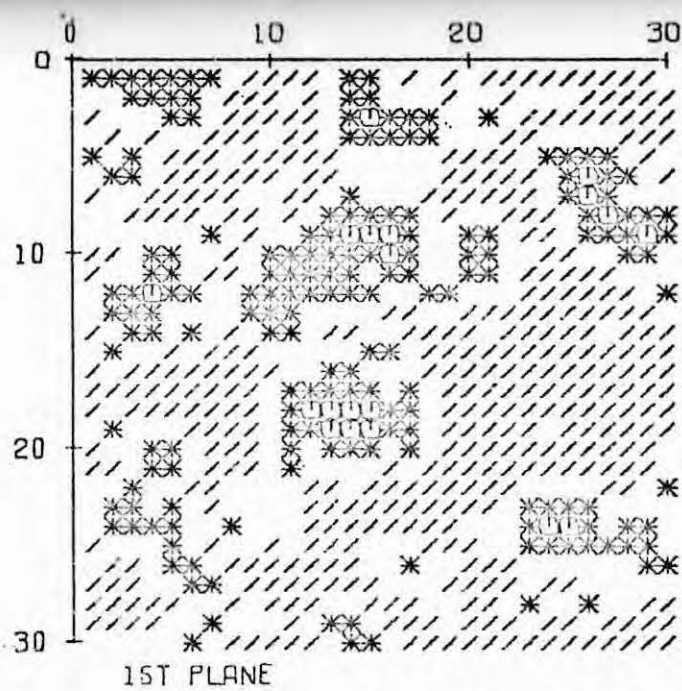


$T/T_c = .6$
 $C = -.60$
 TIME=250
 $N=300000$
 $U = .538$

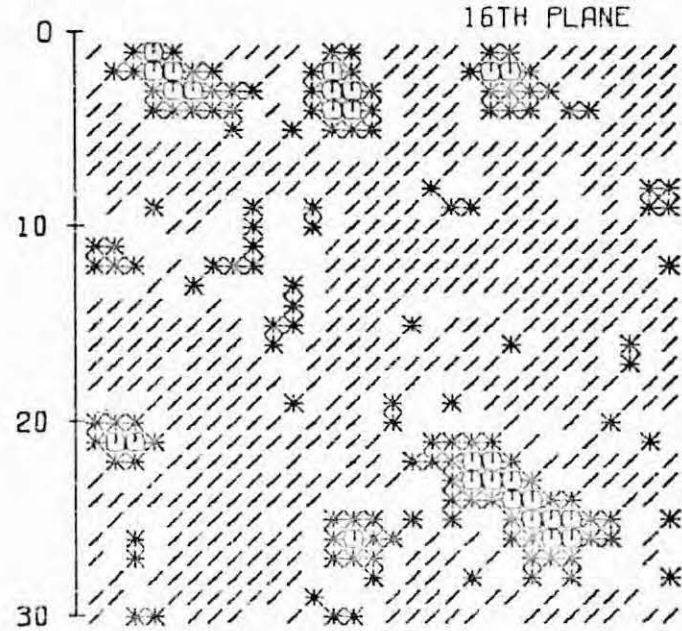
CLUSTERS
SIZE NUMBER

1	219
37	37
14	14
4	4
4	0
0	0
2	2
2	1
1	1
1	1
1	1
1	1
11	11
21	21
22	22
25	25
36	36
41	41
42	42
50	50
52	52
53	53
56	56
67	67
104	104
106	106
672	672
3618	3618

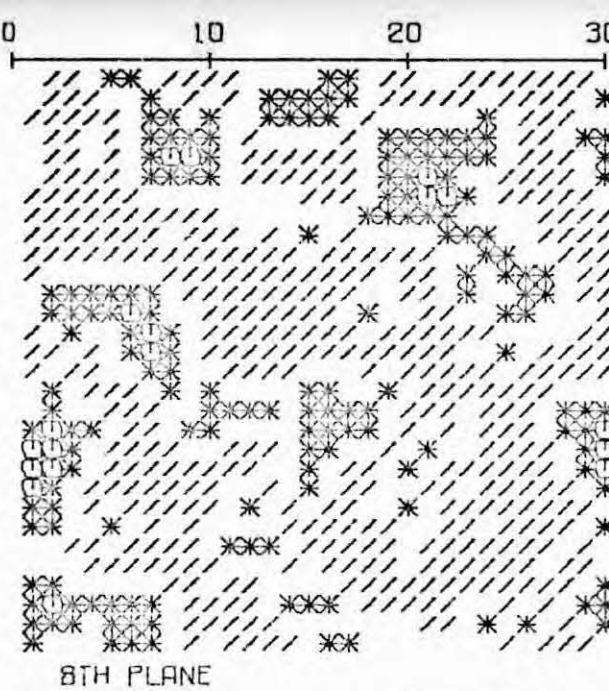
Fig. B6



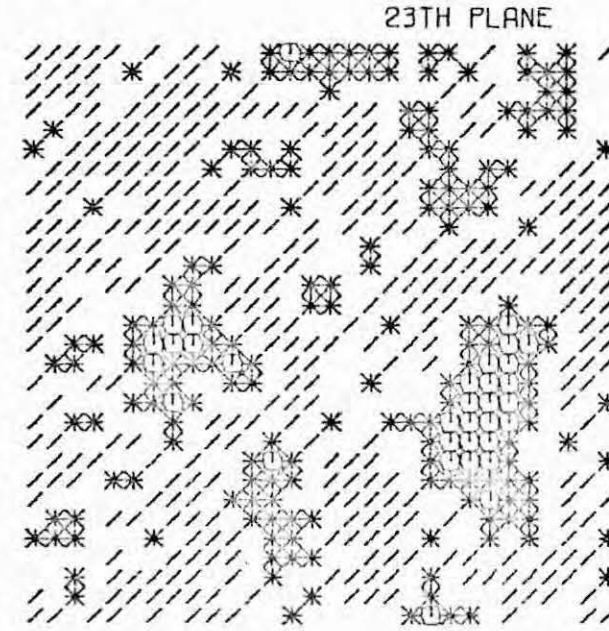
1ST PLANE



16TH PLANE



8TH PLANE



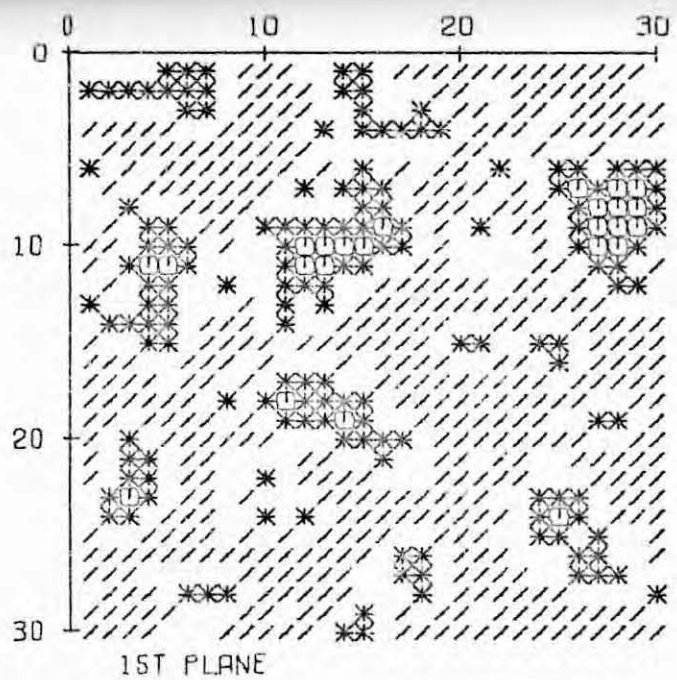
23TH PLANE

$T/T_c = .6$
 $C = -.60$
 TIME=352
 $N=400000$
 $U = .499$

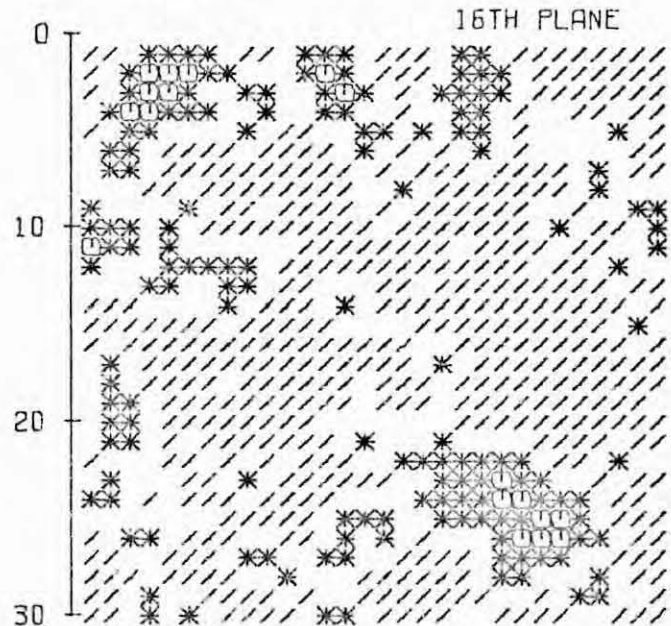
CLUSTERS
SIZE NUMBER

218	46
12	14
3	6
4	2
5	1
6	1
7	1
8	1
9	1
10	1
11	1
16	1
38	1
41	1
55	1
93	1
122	1
224	1
1457	1
2917	1

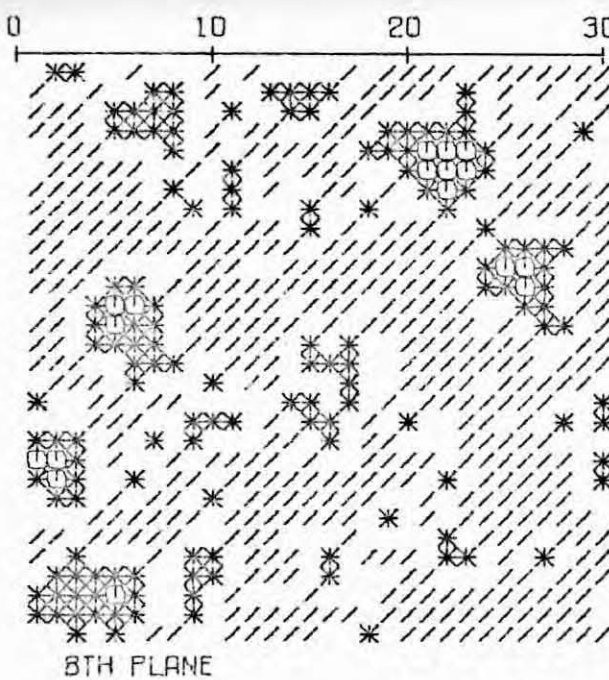
Fig. B7



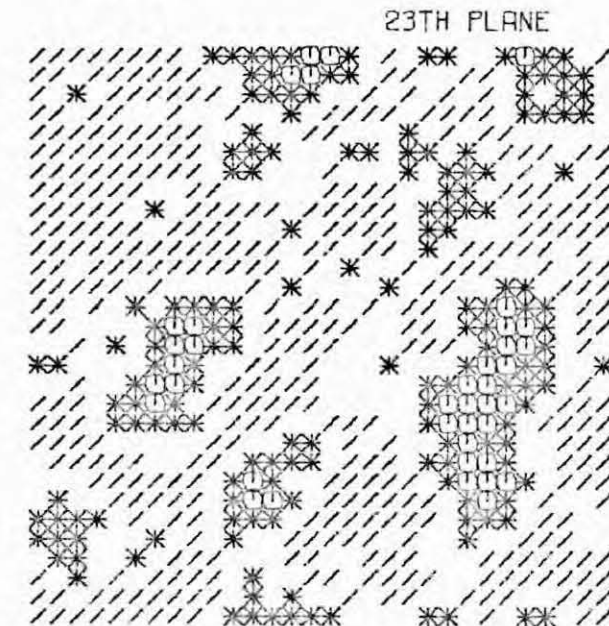
1ST PLANE



16TH PLANE



8TH PLANE



23TH PLANE

$T/T_c = .6$
 $C = -.60$
 TIME=461
 $N=500000$
 $U = .488$

CLUSTERS
SIZE NUMBER

1	235
2	47
3	23
4	22
5	1
6	2
7	1
11	1
12	1
36	1
45	1
57	1
71	1
74	1
101	1
128	1
138	1
167	1
191	1
218	1
240	1
317	1
353	1
368	1
547	1
1892	1

Fig. B8

$T/T_c = .6$
 $C = -.60$
 TIME=572
 $N=600000$
 $U = .474$

CLUSTERS
SIZE NUMBER

1	234
2	44
3	12
4	7
5	4
6	1
7	1
8	1
9	1
10	1
11	1
12	1
13	1
14	1
15	1
16	1
17	1
18	1
19	1
20	1
21	1
22	1
23	1
24	1
25	1
26	1
27	1
28	1
29	1
30	1
31	1
32	1
33	1
34	1
35	1
36	1
37	1
38	1
39	1
40	1
41	1
42	1
43	1
44	1
45	1
46	1
47	1
48	1
49	1
50	1
51	1
52	1
53	1
54	1
55	1
56	1
57	1
58	1
59	1
60	1
190	1
211	1
213	1
266	1
294	1
304	1
720	1
2714	1

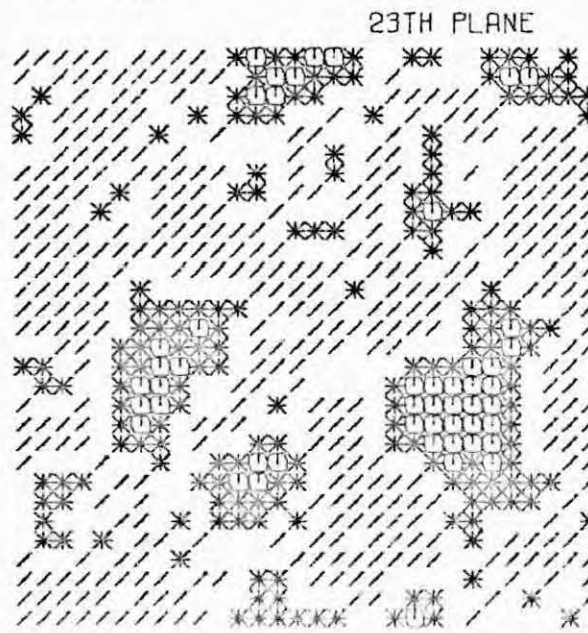
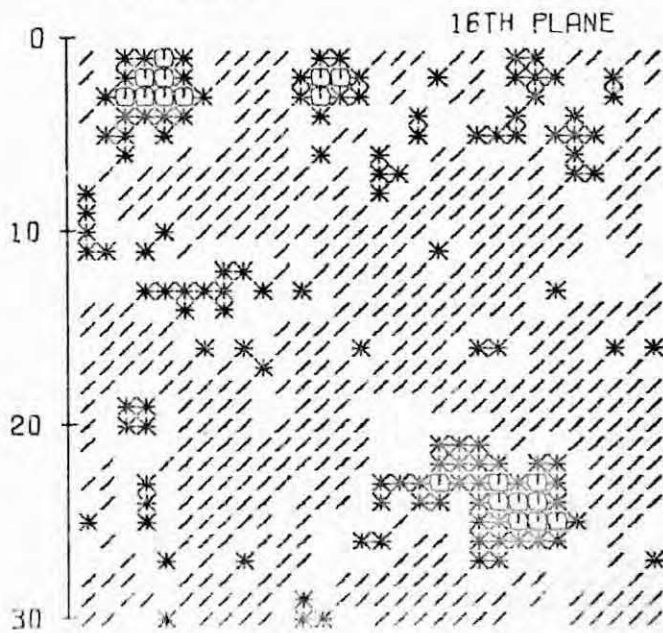
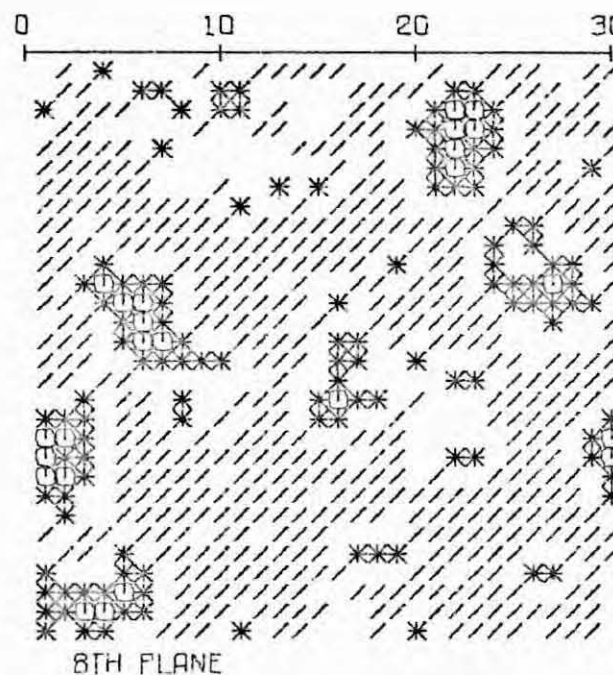
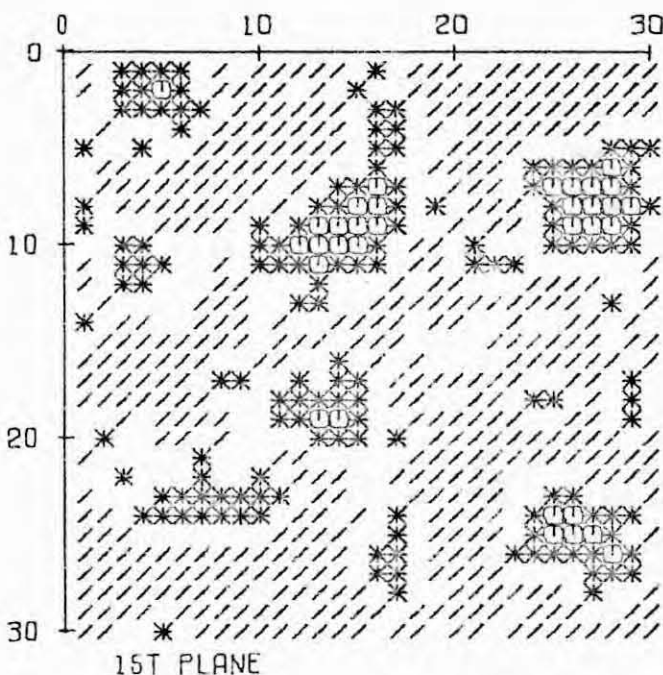
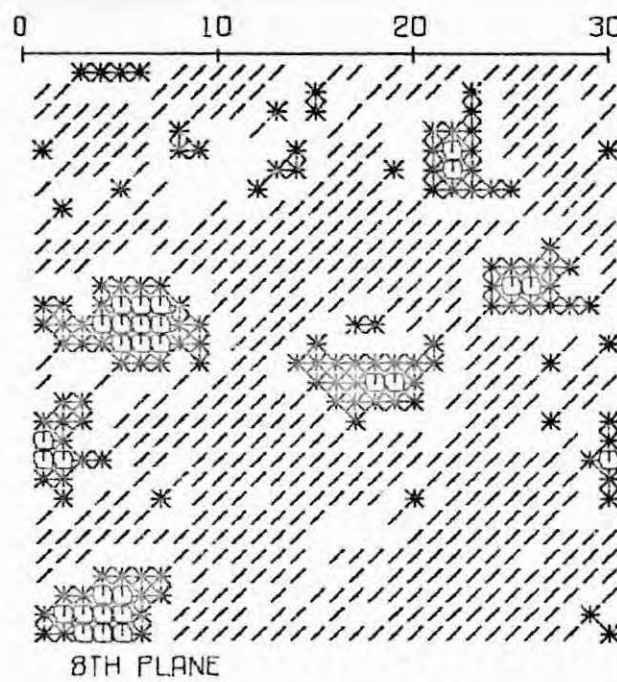
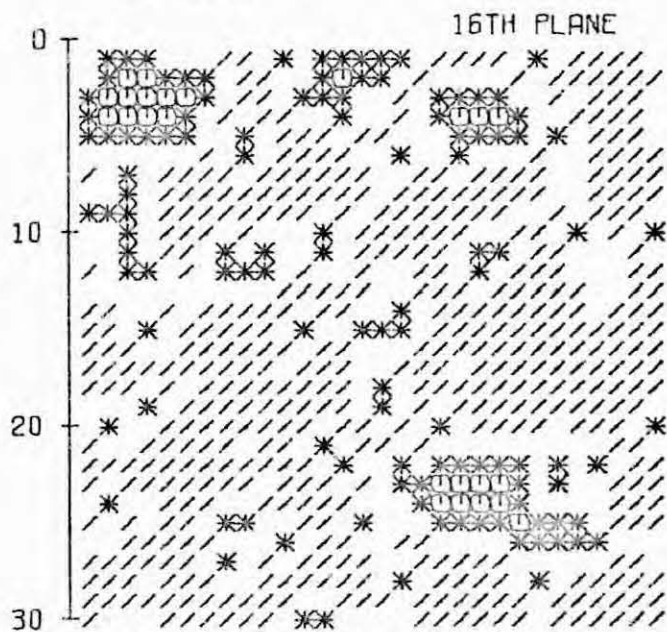
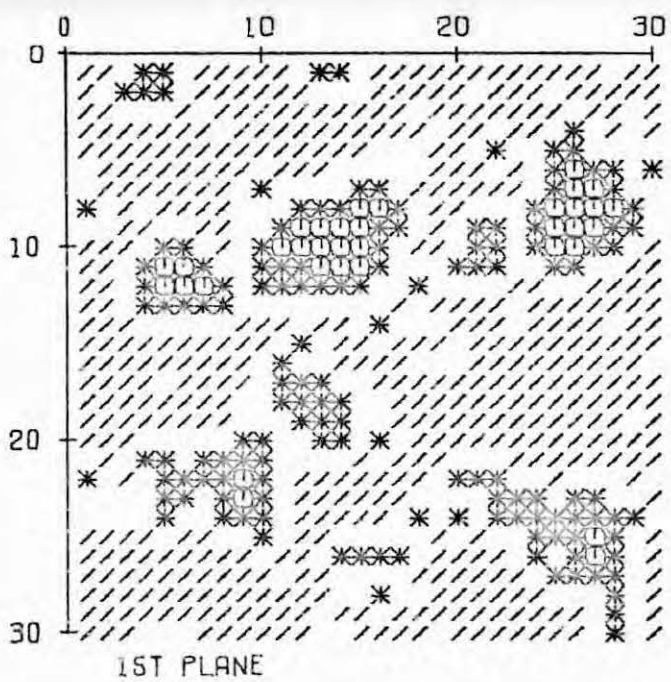


Fig. B9

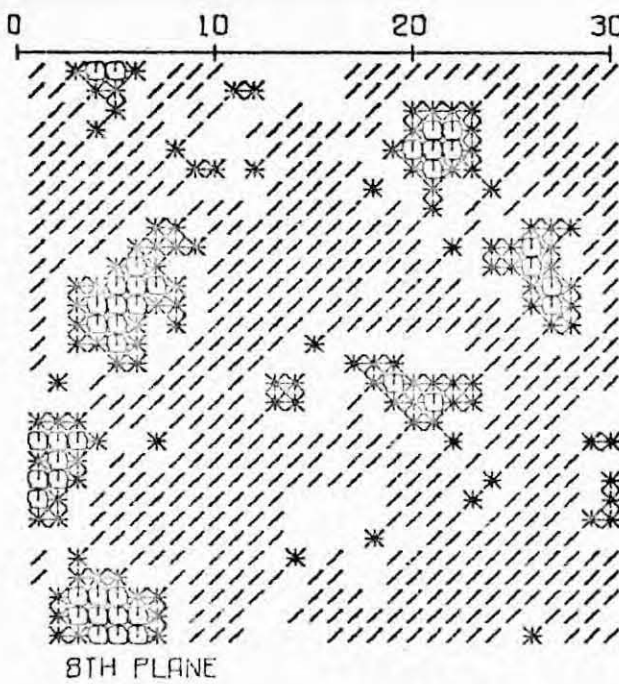
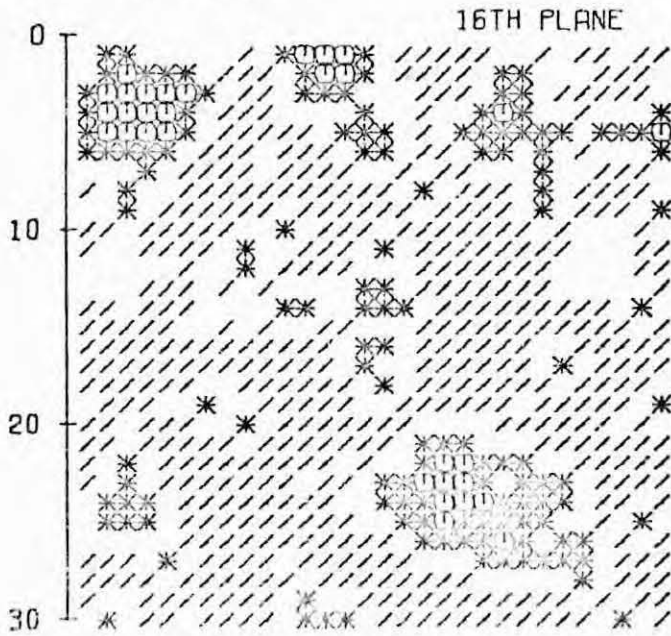
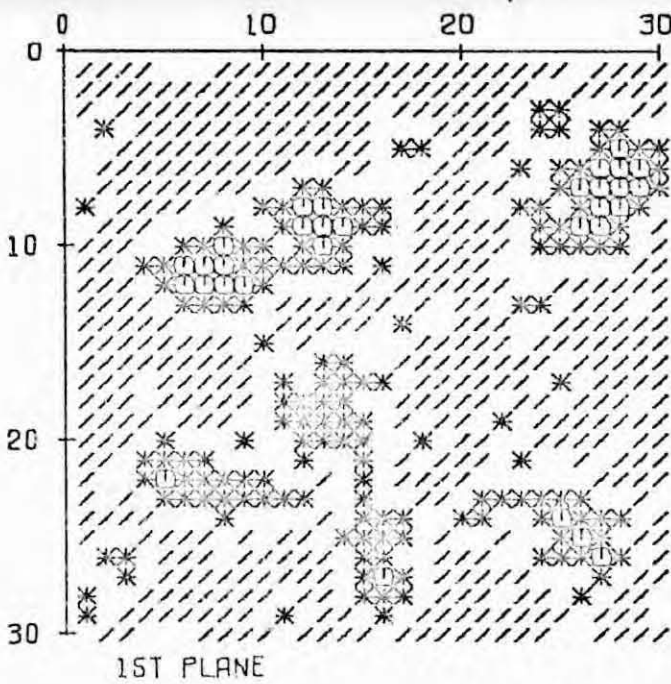


$T/T_c = .6$
 $C = -.60$
 TIME=810
 $N=800000$
 $U = .439$

CLUSTERS
SIZE NUMBER

1	244
2	50
3	65
4	2
5	1
8	1
10	1
53	1
69	1
73	1
77	1
125	1
321	1
323	1
362	1
461	1
828	1
2298	1

Fig. B10

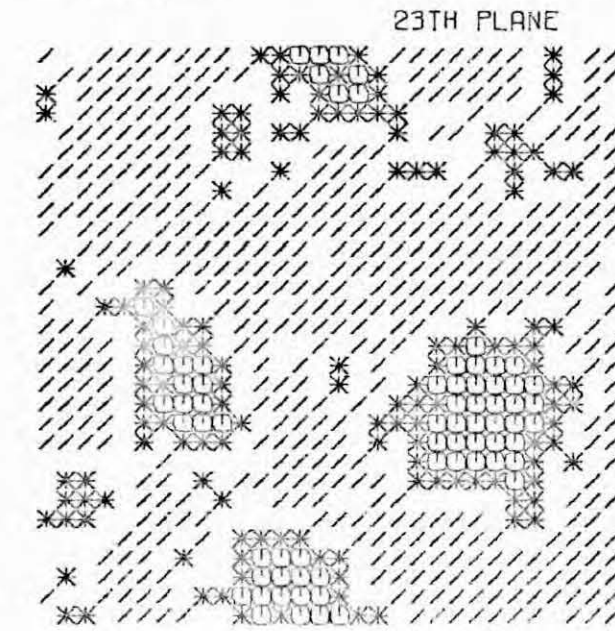
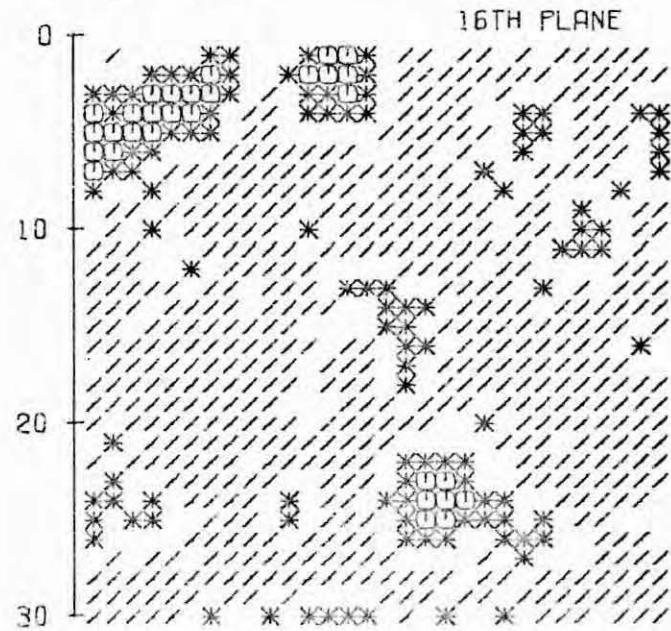
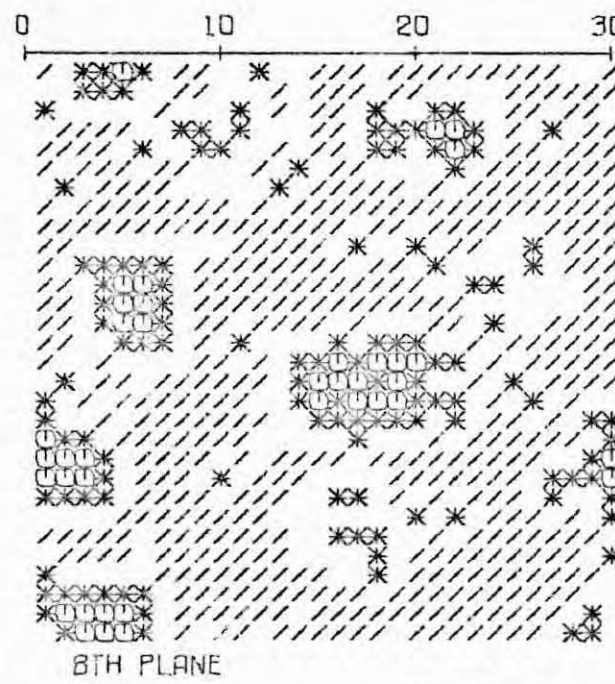
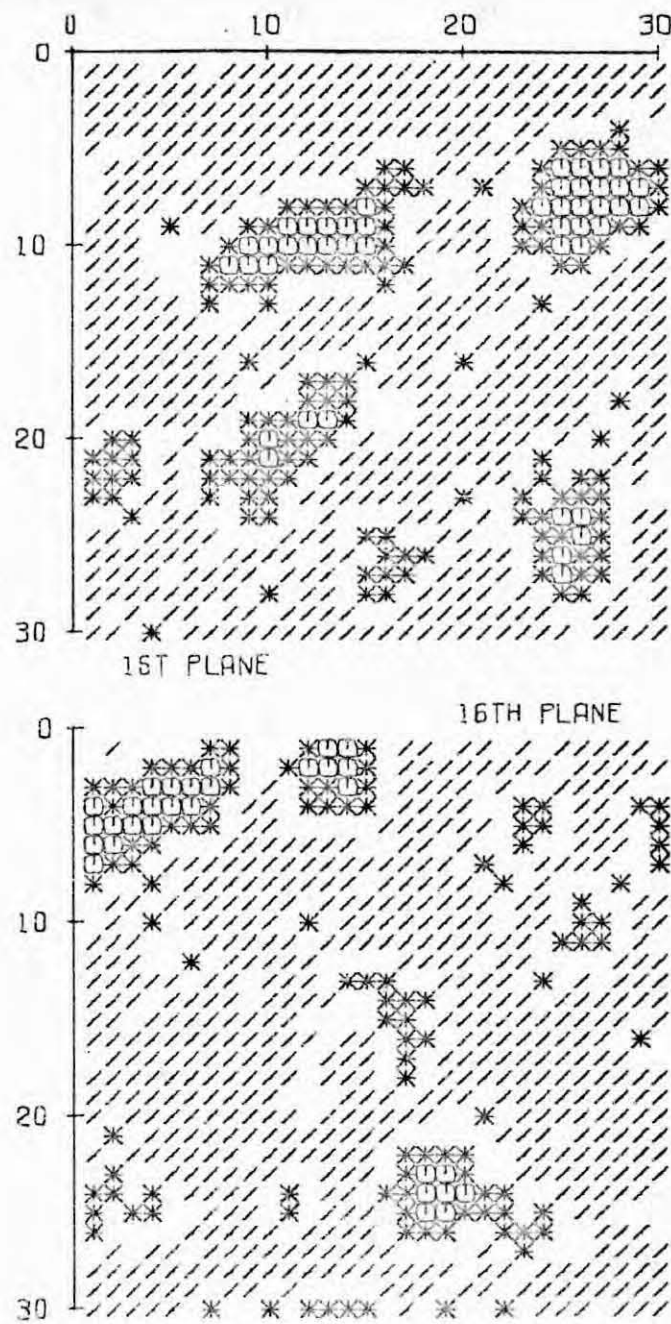


$T/T_c = .6$
 $C = -.60$
 TIME=1061
 $N=1000000$
 $U = .427$

CLUSTERS SIZE NUMBER

1	208
2	58
3	12
4	1
5	1
6	1
7	1
8	1
9	1
10	1
11	1
12	1
13	1
14	1
15	1
16	1
17	1
18	1
19	1
20	1
21	1
22	1
23	1
24	1
25	1
26	1
27	1
28	1
29	1
30	1

Fig. B11

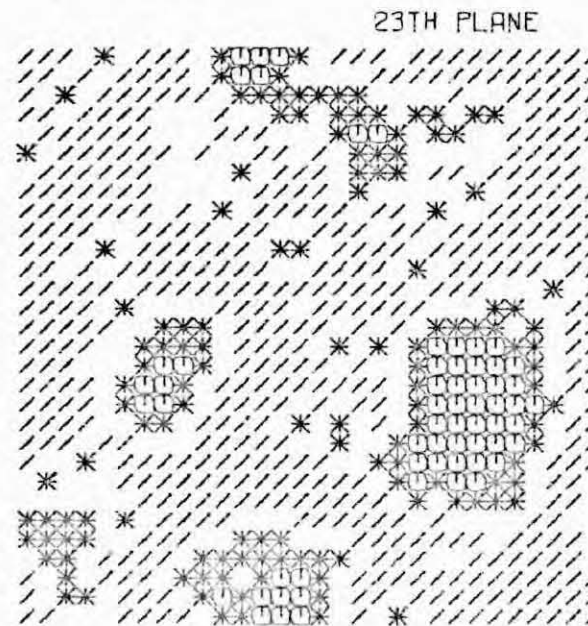
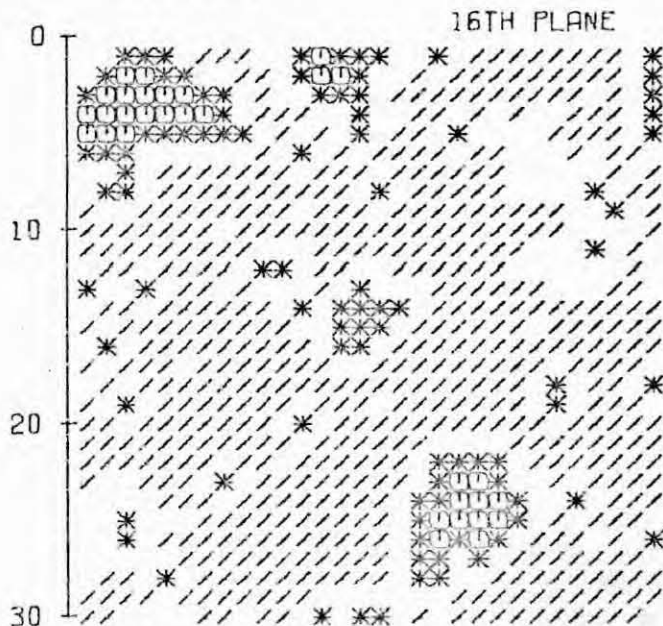
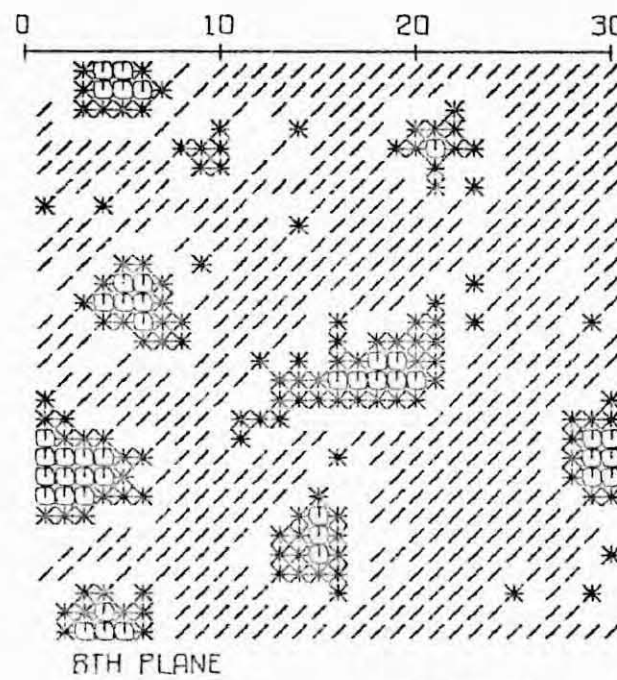
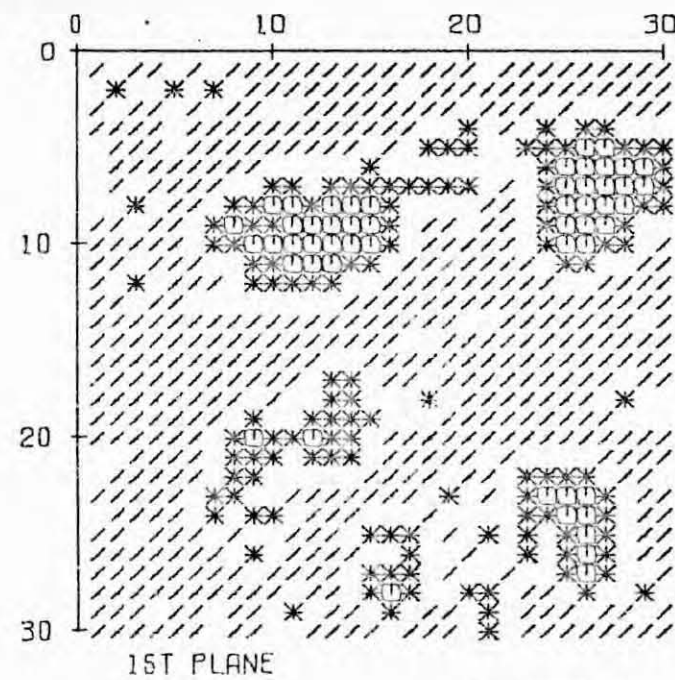


$T/T_c = .6$
 $C = -.60$
 TIME=1321
 $N=1200000$
 $U = .408$

CLUSTERS
SIZE NUMBER

226	46
11	4
25	1
93	1
109	1
125	1
221	1
326	1
665	1
728	1
2733	1

Fig. B12

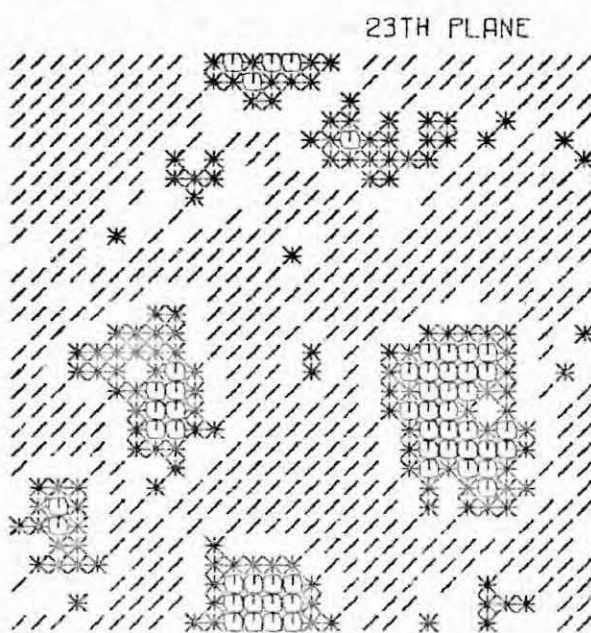
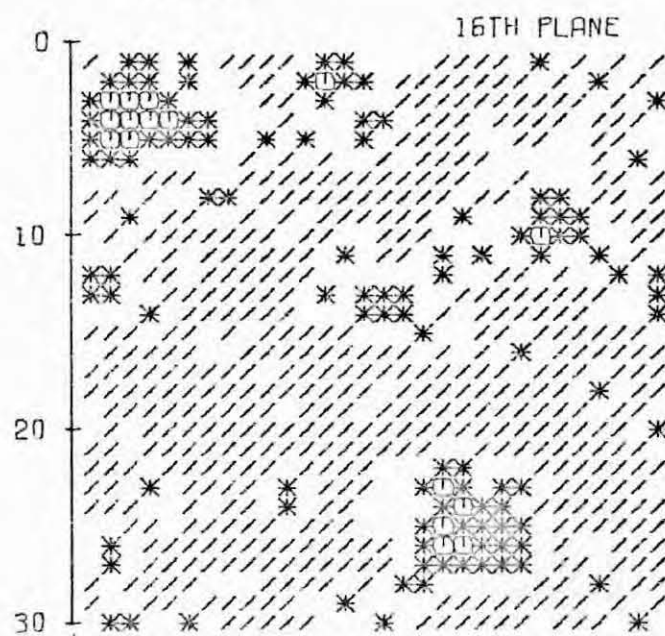
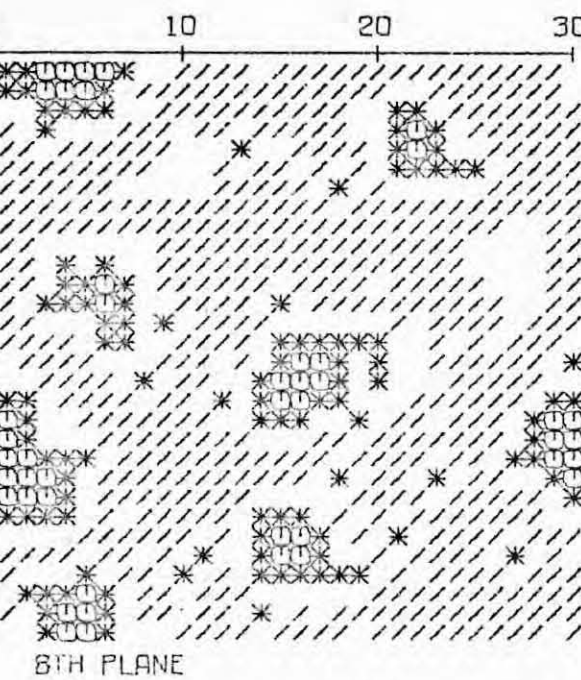
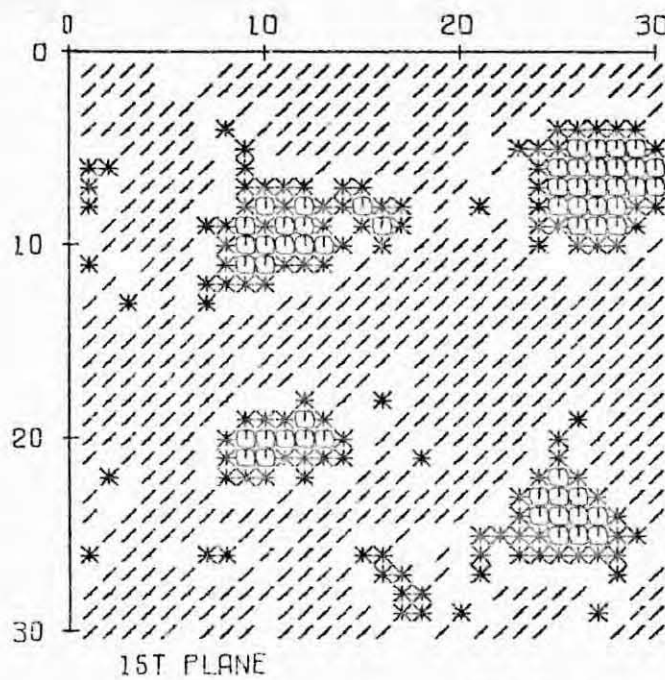


$T/T_c = .6$
 $C = -.60$
 TIME=1588
 $N=1400000$
 $U = .391$

CLUSTERS
SIZE NUMBER

1	210
2	320
3	10
4	96
5	427
6	746
7	871
8	2914

Fig. B13

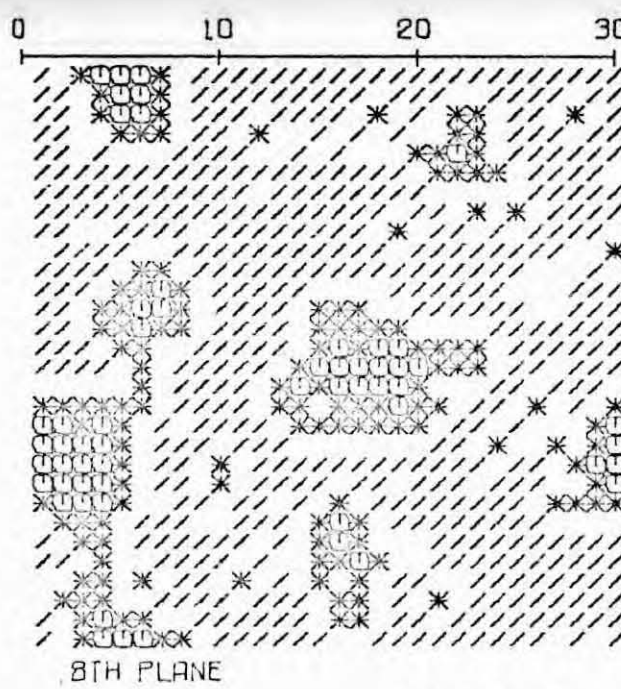
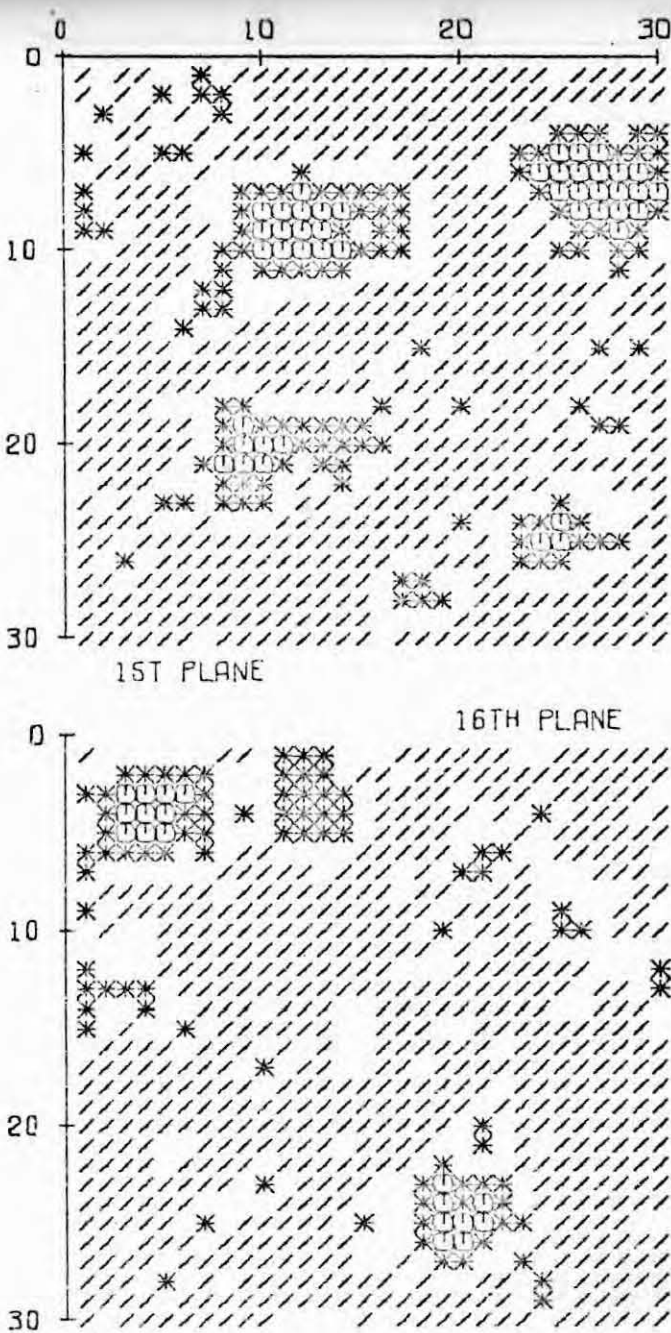


$T/T_c = .6$
 $C = -.60$
 TIME=1858
 $N=1600000$
 $U = .392$

CLUSTERS
SIZE NUMBER

1	258
2	33
3	18
4	5
5	1
6	2
7	1
8	1
9	1
10	29
11	86
12	99
13	117
14	196
15	363
16	376
17	406
18	678
19	2635

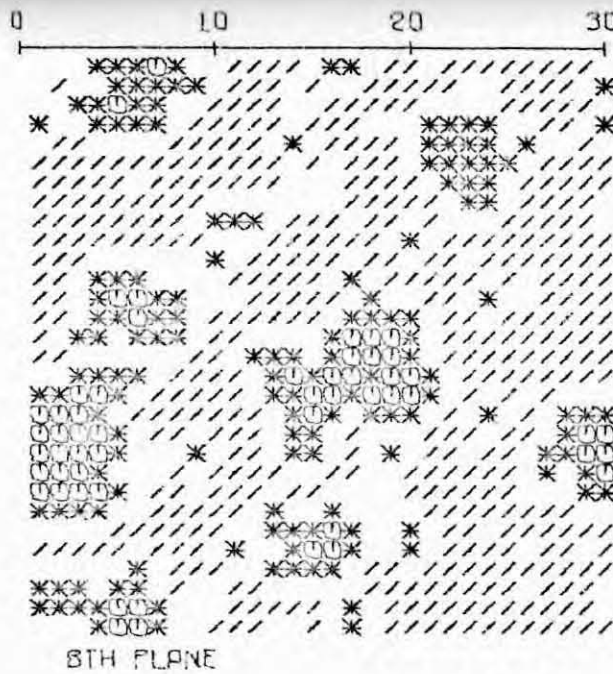
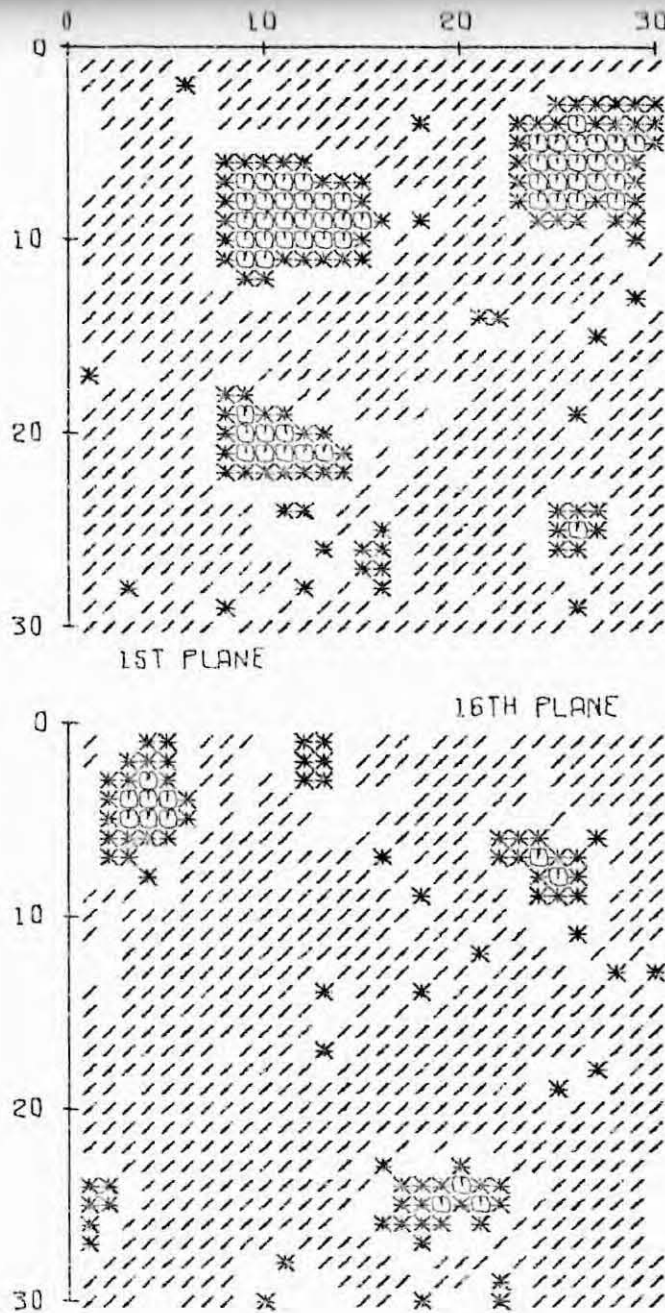
Fig. B14
250



$T/T_c = .59$
 $C = - .60$
 TIME=2130
 $N=1800000$
 $\cup = .384$
 CLUSTERS
 SIZE NUMBER

1	223
2	43
3	74
4	15
5	82
6	103
7	223
8	413
9	433
10	714
11	3023

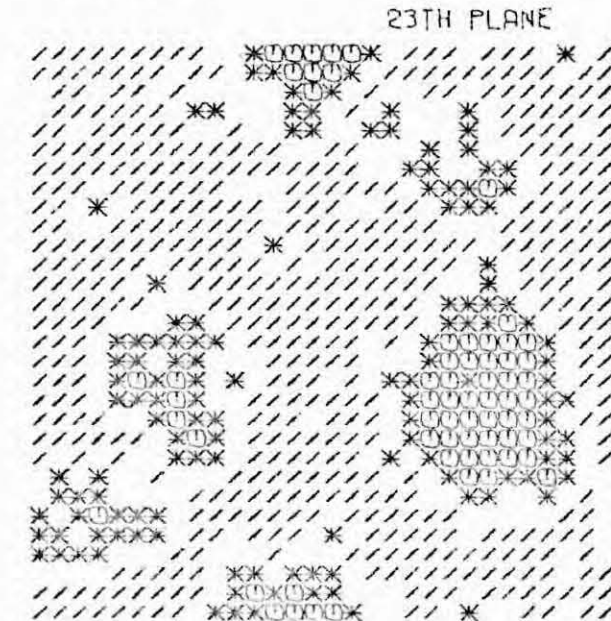
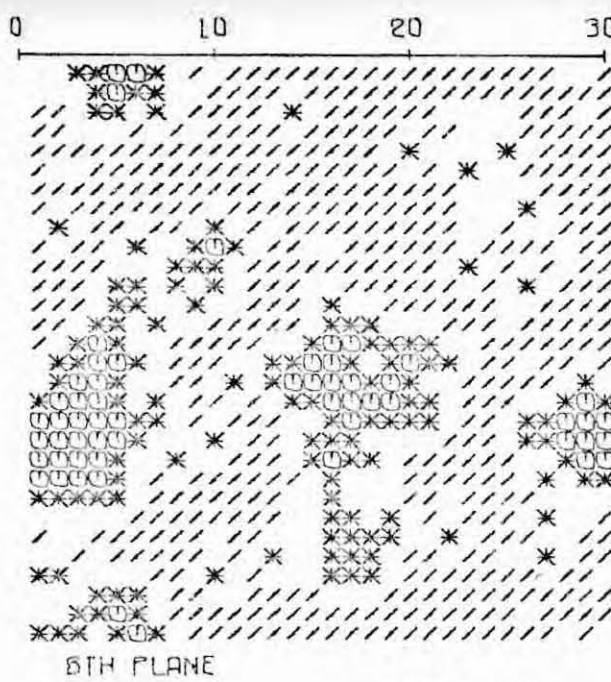
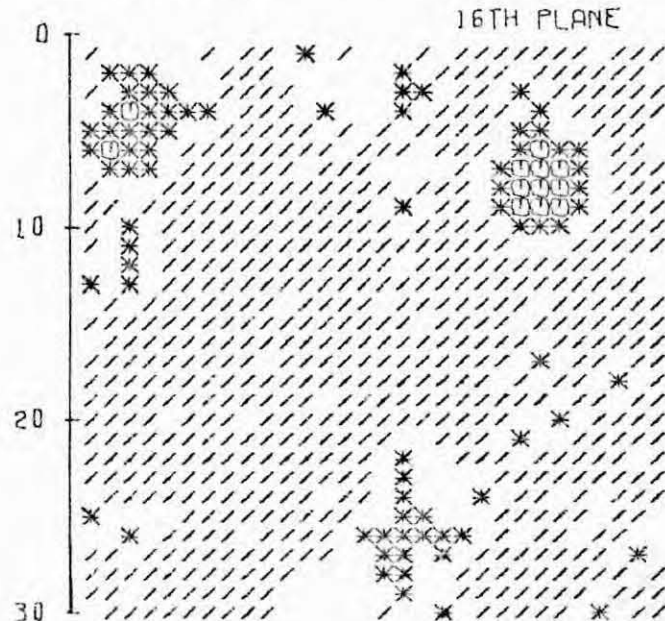
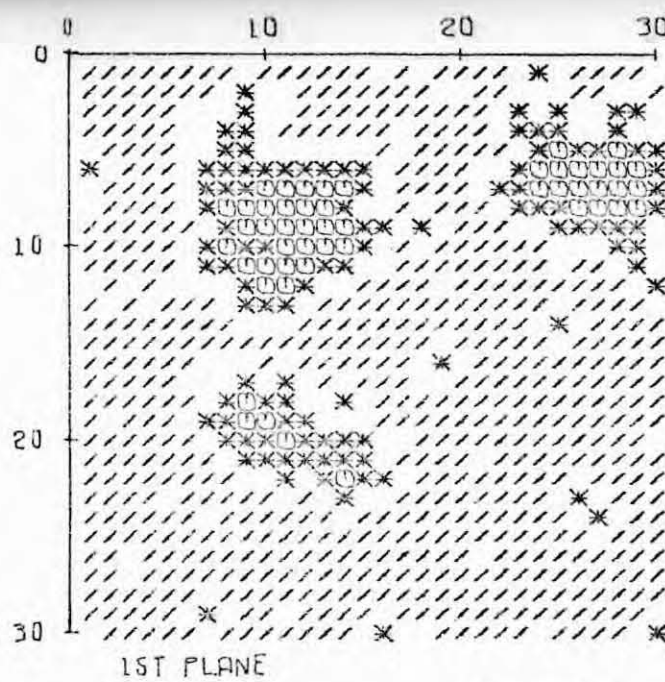
Fig. B15



$T/T_c = .59$
 $C = -.60$
 TIME=2546
 $N=2100000$
 $U = .374$

CLUSTERS
SIZE NUMBER

1	222
2	35
3	16
4	62
5	11
6	11
7	1
8	1
9	1
10	1
11	1
12	1
13	1
14	1
15	1
16	1
17	1
18	1
19	1
20	1
21	1
22	1
23	1
24	1
25	1
26	1
27	1
28	1
29	1
30	1
31	1
32	1
33	1
34	1
35	1
36	1
37	1
38	1
39	1
40	1
41	1
42	1
43	1
44	1
45	1
46	1
47	1
48	1
49	1
50	1
51	1
52	1
53	1
54	1
55	1
56	1
57	1
58	1
59	1
60	1
61	1
62	1
63	1
64	1
65	1
66	1
67	1
68	1
69	1
70	1
71	1
72	1
73	1
74	1
75	1
76	1
77	1
78	1
79	1
80	1
81	1
82	1
83	1
84	1
85	1
86	1
87	1
88	1
89	1
90	1
91	1
92	1
93	1
94	1
95	1
96	1
97	1
98	1
99	1
100	1
101	1
102	1
103	1
104	1
105	1
106	1
107	1
108	1
109	1
110	1
111	1
112	1
113	1
114	1
115	1
116	1
117	1
118	1
119	1
120	1
121	1
122	1
123	1
124	1
125	1
126	1
127	1
128	1
129	1
130	1
131	1
132	1
133	1
134	1
135	1
136	1
137	1
138	1
139	1
140	1
141	1
142	1
143	1
144	1
145	1
146	1
147	1
148	1
149	1
150	1
151	1
152	1
153	1
154	1
155	1
156	1
157	1
158	1
159	1
160	1
161	1
162	1
163	1
164	1
165	1
166	1
167	1
168	1
169	1
170	1
171	1
172	1
173	1
174	1
175	1
176	1
177	1
178	1
179	1
180	1
181	1
182	1
183	1
184	1
185	1
186	1
187	1
188	1
189	1
190	1
191	1
192	1
193	1
194	1
195	1
196	1
197	1
198	1
199	1
200	1
201	1
202	1
203	1
204	1
205	1
206	1
207	1
208	1
209	1
210	1
211	1
212	1
213	1
214	1
215	1
216	1
217	1
218	1
219	1
220	1
221	1
222	1
223	1
224	1
225	1
226	1
227	1
228	1
229	1
230	1
231	1
232	1
233	1
234	1
235	1
236	1
237	1
238	1
239	1
240	1
241	1
242	1
243	1
244	1
245	1
246	1
247	1
248	1
249	1
250	1
251	1
252	1
253	1
254	1
255	1
256	1
257	1
258	1
259	1
260	1
261	1
262	1
263	1
264	1
265	1
266	1
267	1
268	1
269	1
270	1
271	1
272	1
273	1
274	1
275	1
276	1
277	1
278	1
279	1
280	1
281	1
282	1
283	1
284	1
285	1
286	1
287	1
288	1
289	1
290	1
291	1
292	1
293	1
294	1
295	1
296	1
297	1
298	1
299	1
300	1
301	1
302	1
303	1
304	1
305	1
306	1
307	1
308	1
309	1
310	1
311	1
312	1
313	1
314	1
315	1
316	1
317	1
318	1
319	1
320	1
321	1
322	1
323	1
324	1
325	1
326	1
327	1
328	1
329	1
330	1
331	1
332	1
333	1
334	1
335	1
336	1
337	1
338	1
339	1
340	1
341	1
342	1
343	1
344	1
345	1
346	1
347	1
348	1
349	1
350	1
351	1
352	1
353	1
354	1
355	1
356	1
357	1
358	1
359	1
360	1
361	1
362	1
363	1
364	1
365	1
366	1
367	1
368	1
369	1
370	1
371	1
372	1
373	1
374	1
375	1
376	1
377	1
378	1
379	1
380	1
381	1
382	1
383	1
384	1
385	1
386	1
387	1
388	1
389	1
390	1
391	1
392	1
393	1
394	1
395	1
396	1
397	1
398	1
399	1
400	1
401	1
402	1
403	1
404	1
405	1
406	1
407	1
408	1
409	1
410	1
411	1
412	1
413	1
414	1
415	1
416	1
417	1
418	1
419	1
420	1
421	1
422	1
423	1
424	1
425	1
426	1
427	1
428	1
429	1
430	1
431	1
432	1
433	1
434	1
435	1
436	1
437	1
438	1
439	1
440	1
441	1
442	1
443	1
444	1
445	1
446	1
447	1
448	1
449	1
450	1
451	1
452	1
453	1
454	1
455	1
456	1
457	1
458	1
459	1
460	1
461	1
462	1
463	1
464	1
465	1
466	1
467	1
468	1
469	1
470	1
471	1
472	1
473	1
474	1
475	1
476	1
477	1
478	1
479	1
480	1
481	1
482	1
483	1
484	1
485	1
486	1
487	1
488	1
489	1
490	1
491	1
492	1
493	1
494	1
495	1
496	1
497	1
498	1
499	1
500	1

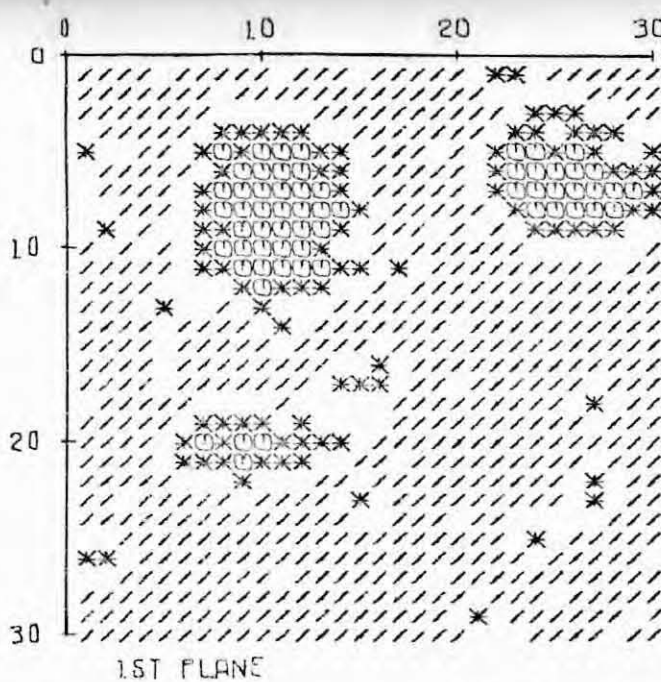


$T/T_c = .59$
 $C = -.60$
 TIME=2972
 $N=2400000$
 $U = .353$

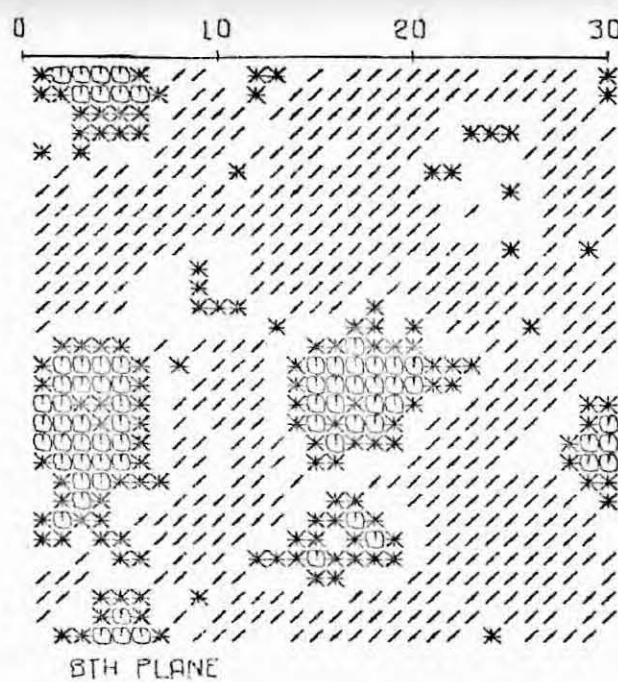
CLUSTERS
SIZE NUMBER

224	1
37	1
6	1
3	1
2	1
1	1
49	1
177	1
425	1
478	1
552	1
1540	1
1827	1

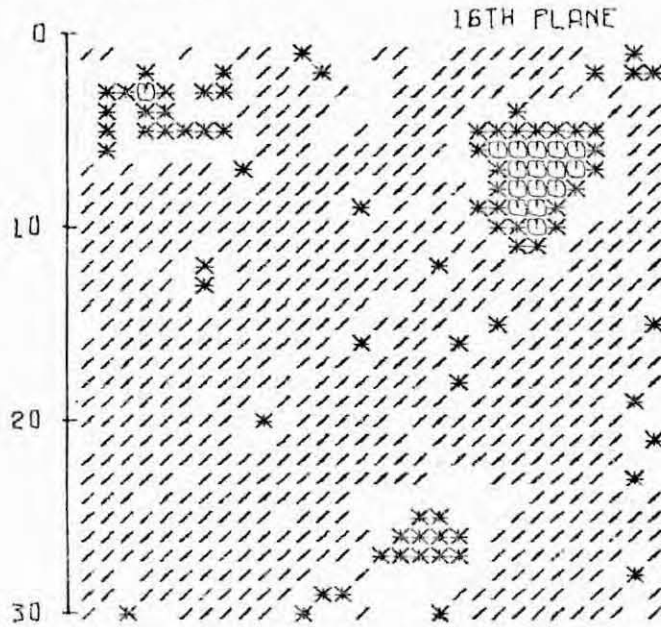
Fig. B17
253



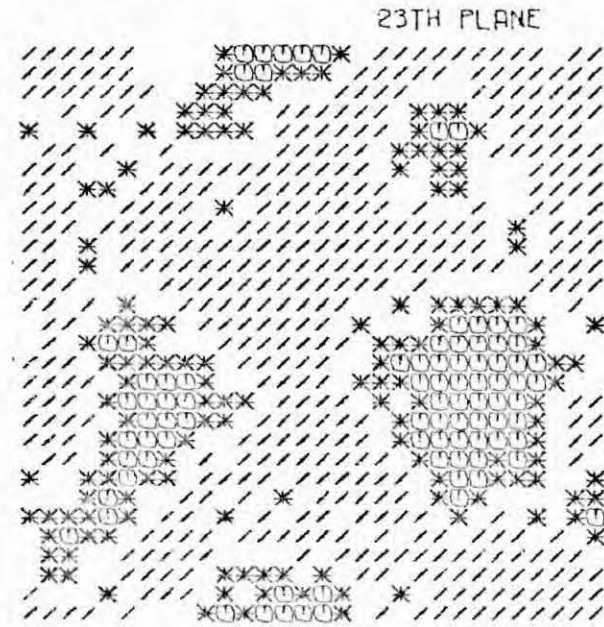
1ST PLANE



8TH PLANE



16TH PLANE



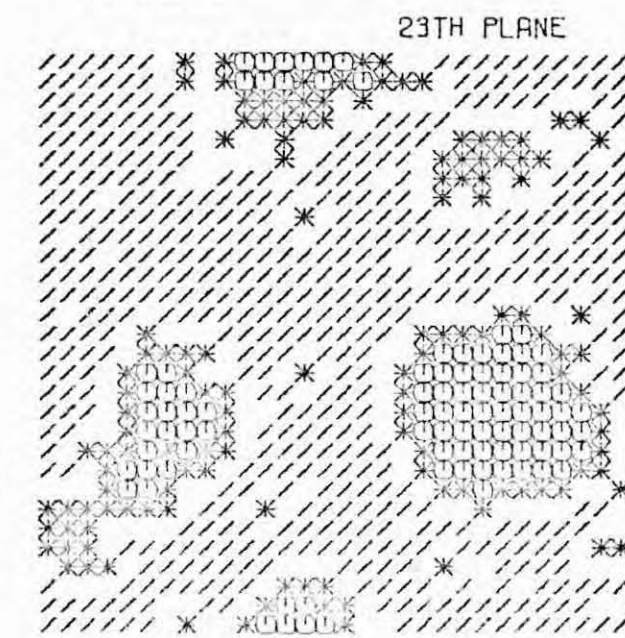
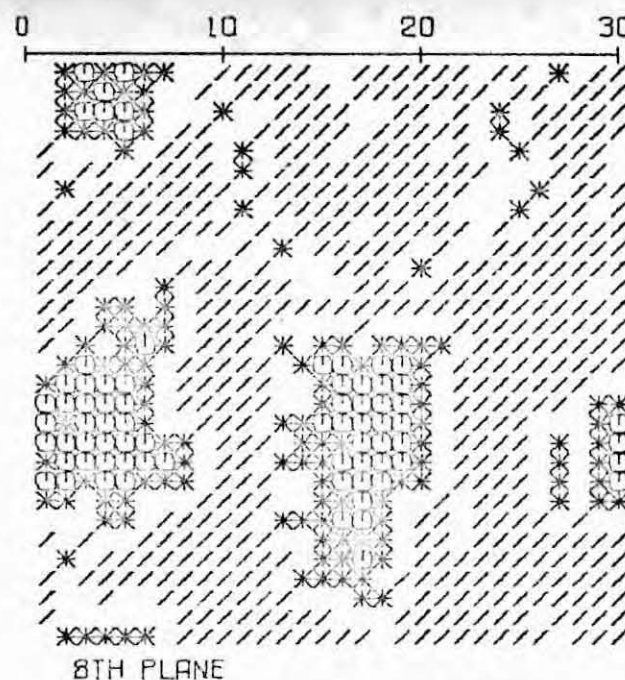
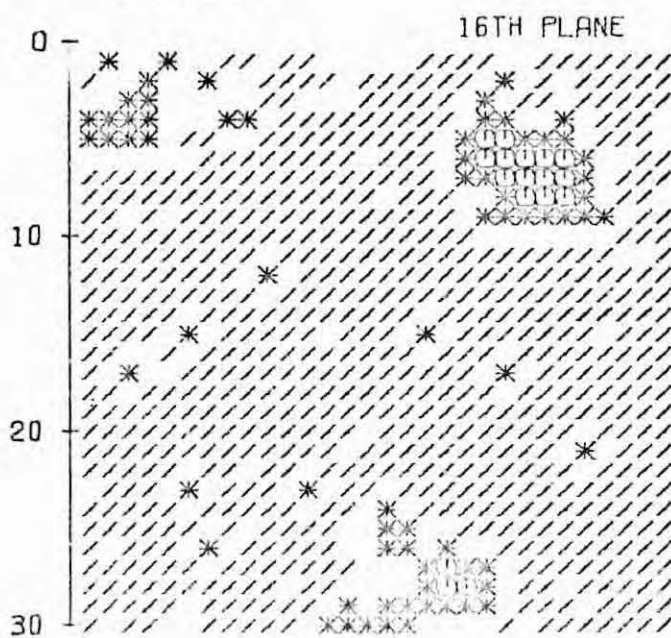
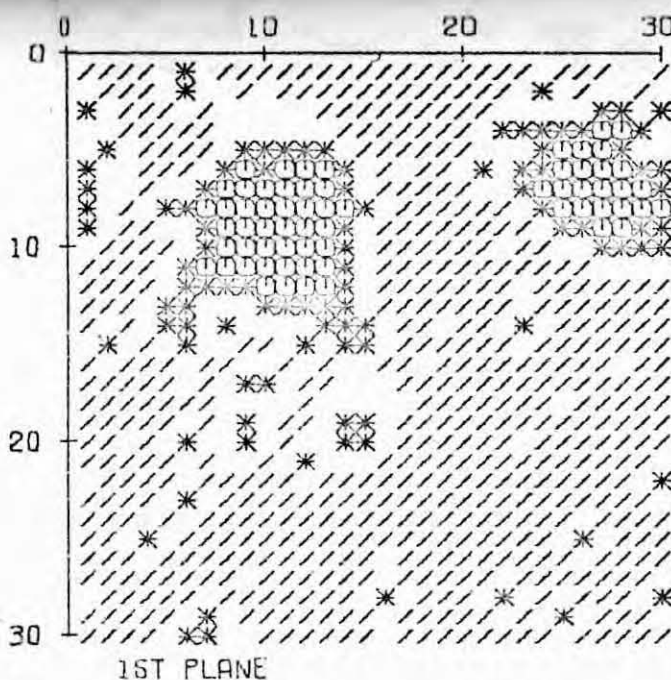
23TH PLANE

$T/T_c = .59$
 $C = -.60$
 TIME=3423
 $N=2700000$
 $U = .340$

CLUSTERS
SIZE NUMBER

235
39
1
0
2
502
955
1551
2017

Fig. B18

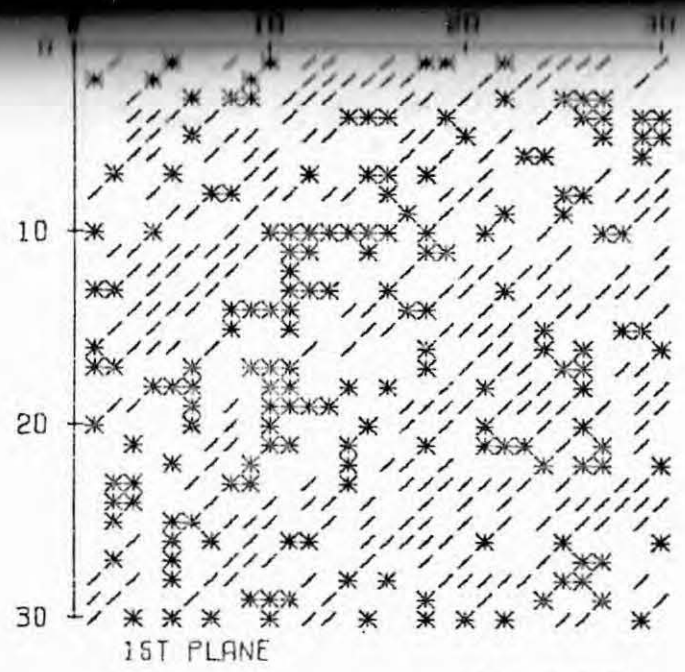


$T/T_c = .59$
 $C = -.60$
 TIME=3897
 $N=3000000$
 $U = .318$

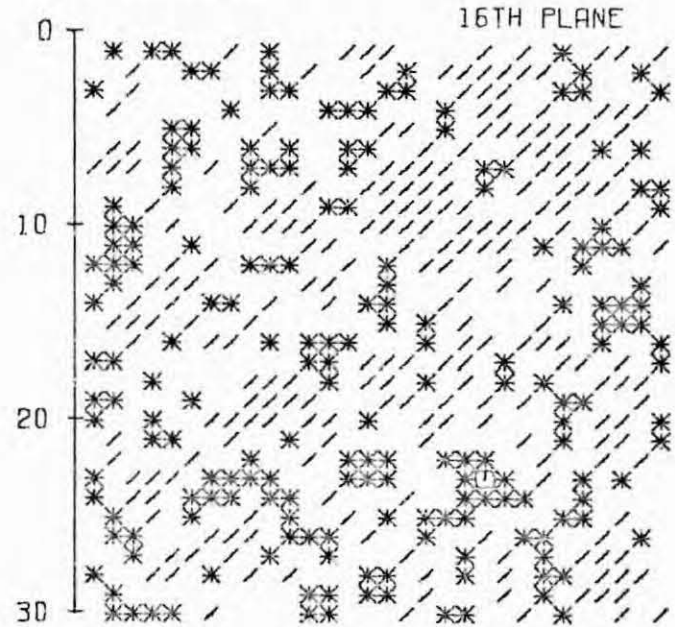
CLUSTERS SIZE NUMBER

	200	35	10	5	3	2	1
1	200	35	10	5	3	2	1
2	398	523	540	647	3021		
3							
4							
5							
6							
7							

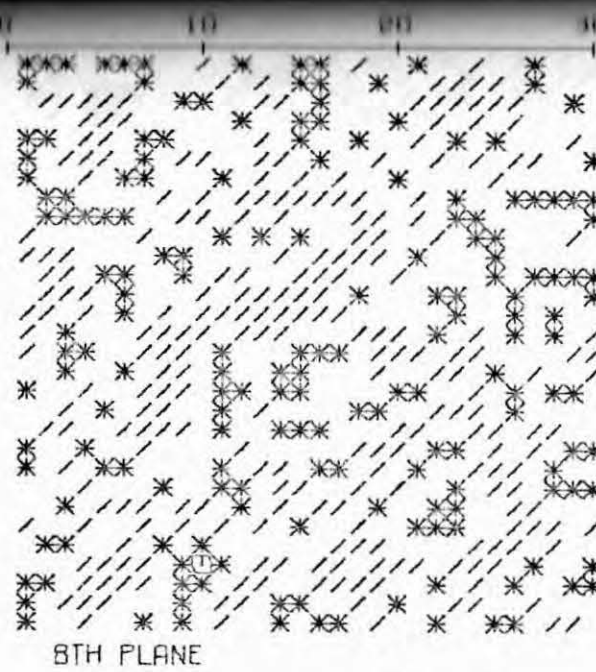
Fig. B19



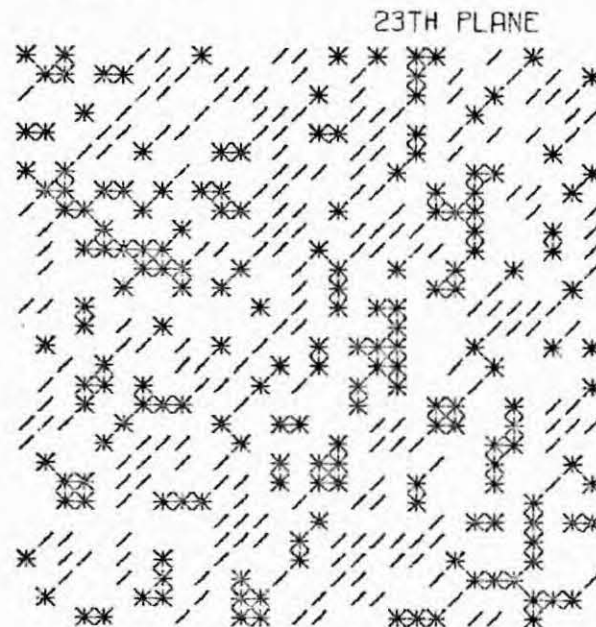
1ST PLANE



16TH PLANE



8TH PLANE



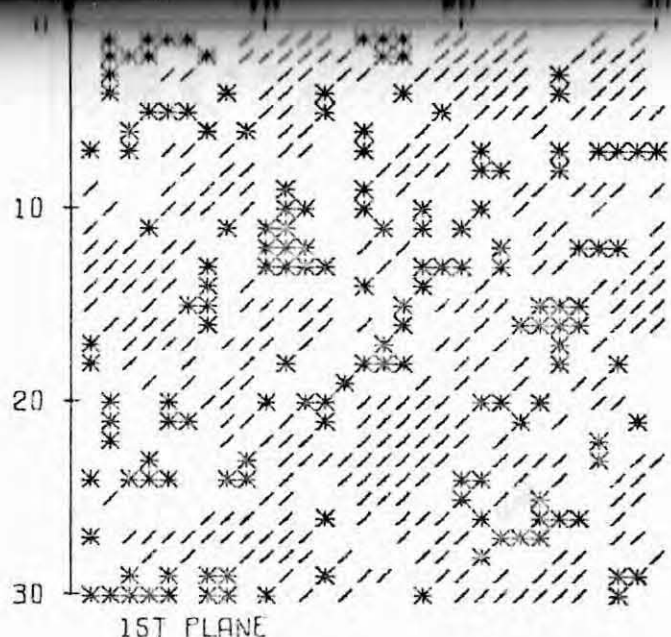
23TH PLANE

$T/T_c = .91$
 $C = -.60$
 TIME=9
 $N=25000$
 $U = .798$

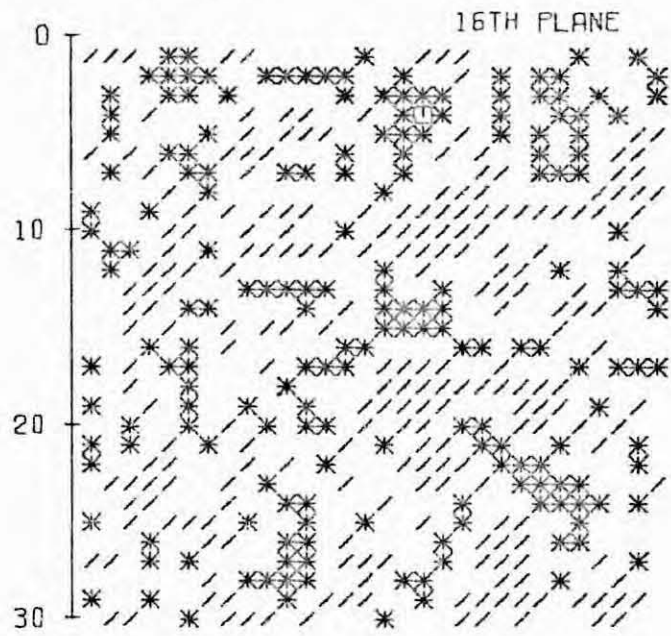
CLUSTERS
SIZE NUMBER

467
121
57
30
22
26
169
212
97
10
11
12
13
14
15
16
17
18
19
21
22
23
24
26
28
29
30
31
32
34
35
37
38
39
40
47
49
52
53
55
57
68
60
62
63
65
69
71
108
119
186
203

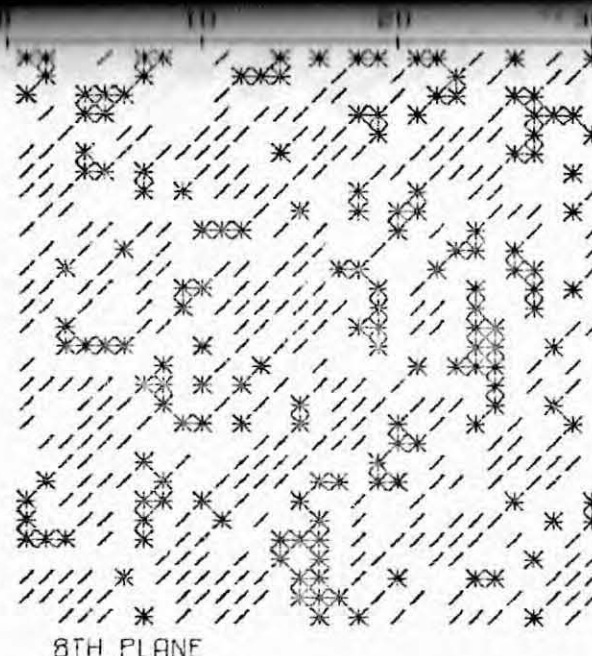
Fig. B20



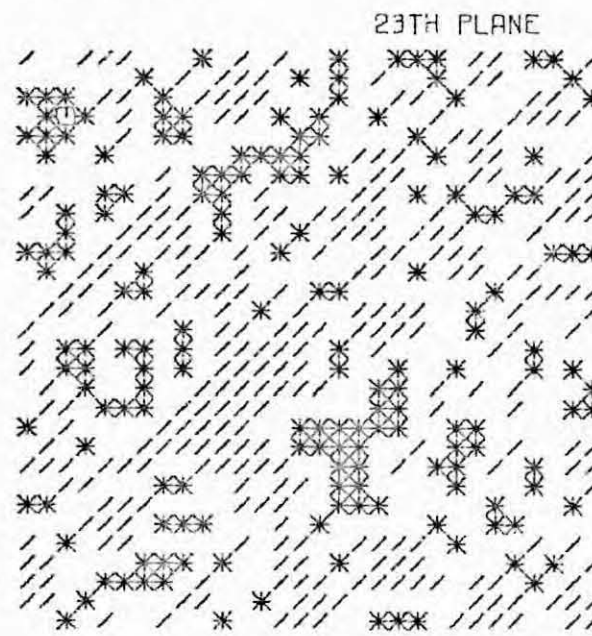
1ST PLANE



16TH PLANE



8TH PLANE



23TH PLANE

$T/T_c = .91$
 $C = - .60$
 TIME=62
 $N=150000$
 $U = .755$

CLUSTERS
SIZE NUMBER

1	440
2	126
3	48
4	22
5	6
6	11
7	10
8	9
9	10
10	11
11	12
12	13
13	14
14	15
15	16
16	17
17	19
18	20
19	21
20	22
21	24
22	25
23	26
24	27
25	29
26	31
27	35
28	36
29	40
30	44
31	46
32	51
33	58
34	62
35	83
36	199
37	215
38	275
39	289
40	341
41	421
42	572
43	635

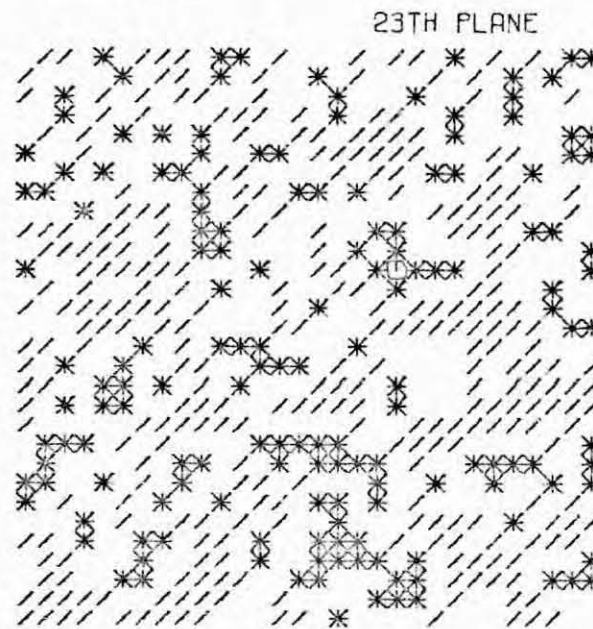
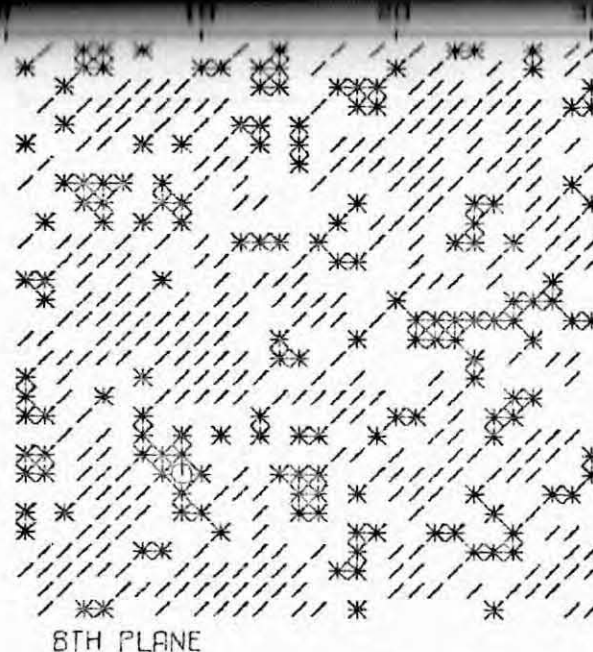
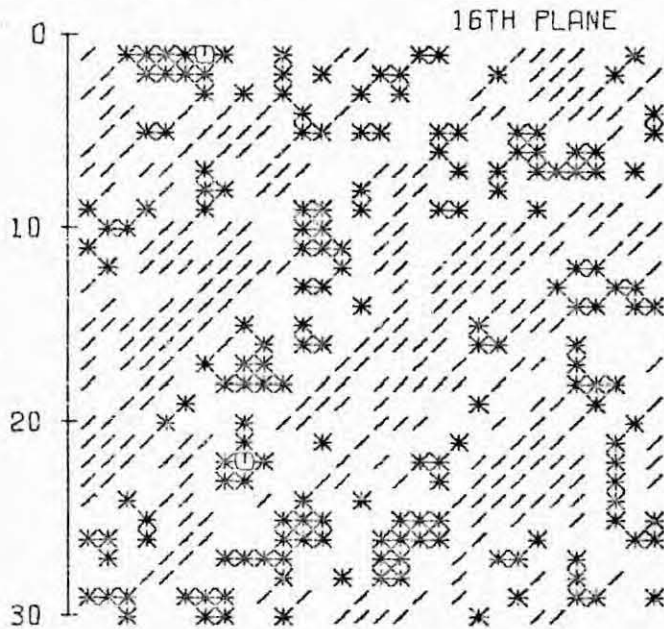
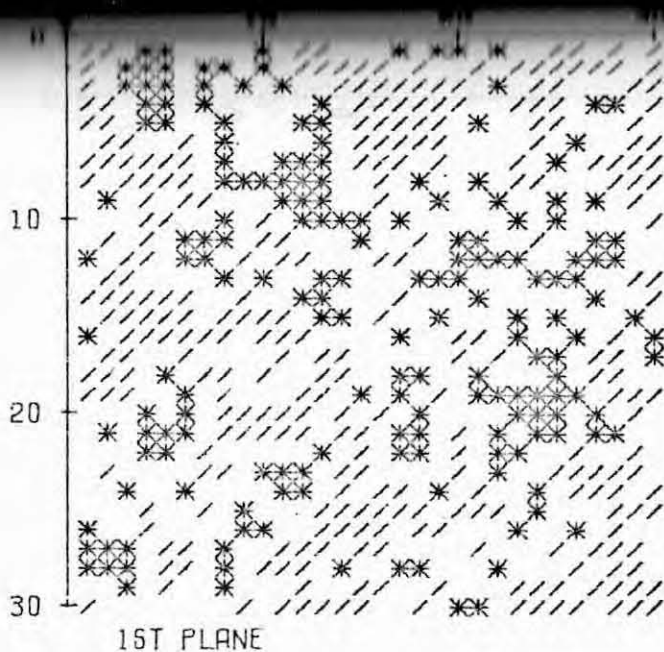
Fig. B21

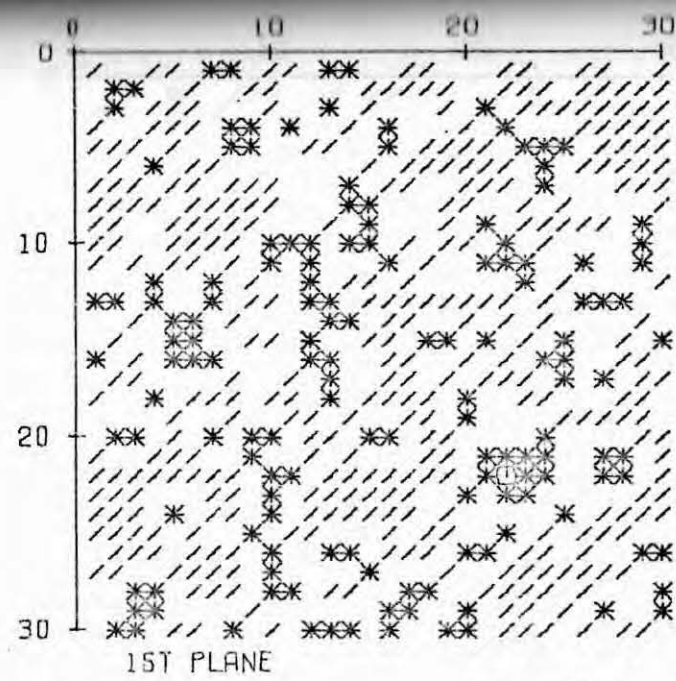
Fig. B22

$T/T_c = .91$
 $C = -.60$
 TIME=148
 $N=350000$
 $U = .747$

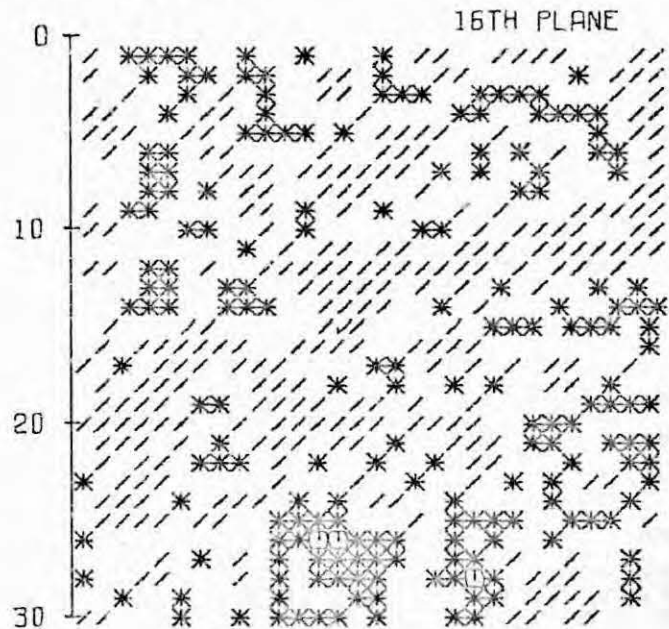
CLUSTERS
SIZE NUMBER

475
471
463
453
443
433
423
413
403
393
383
373
363
353
343
333
323
313
303
293
283
273
263
253
243
233
223
213
203
193
183
173
163
153
143
133
123
113
104
113
122
157
171
201
241
328
600
861

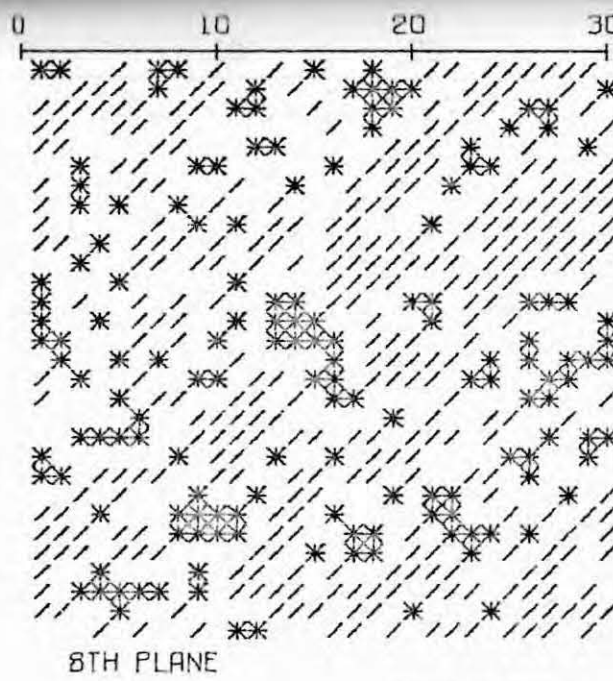




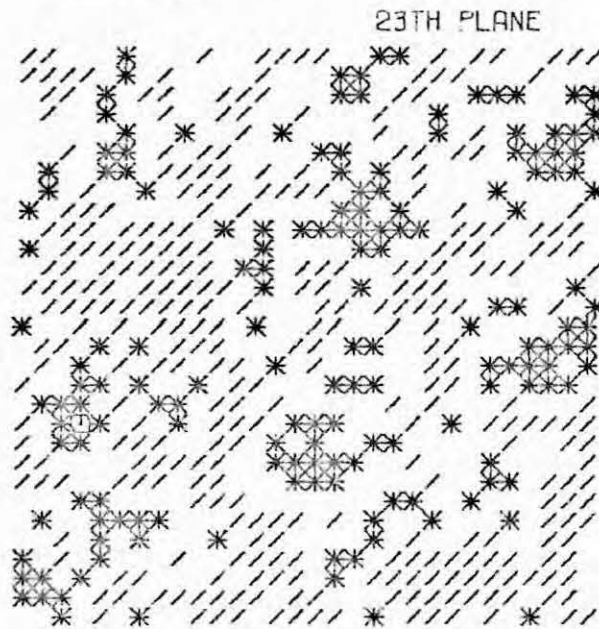
1ST PLANE



16TH PLANE



8TH PLANE



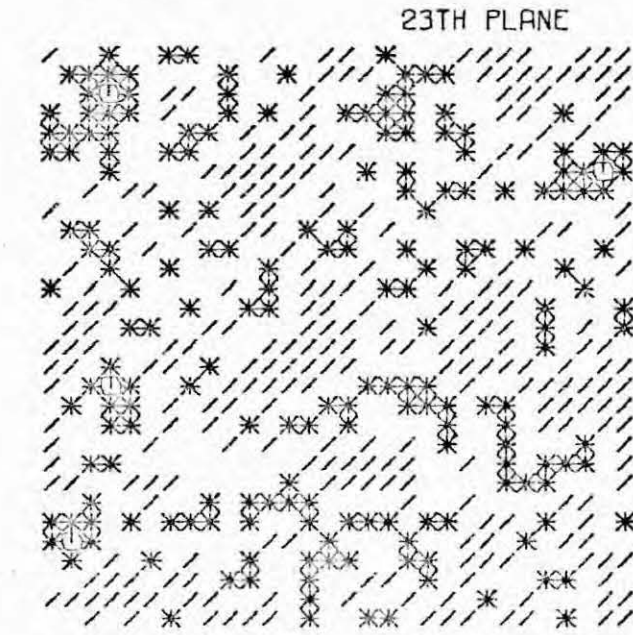
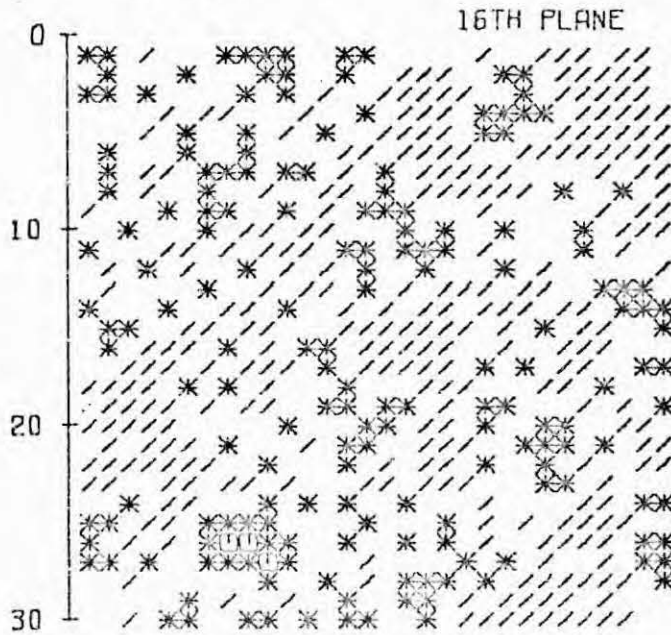
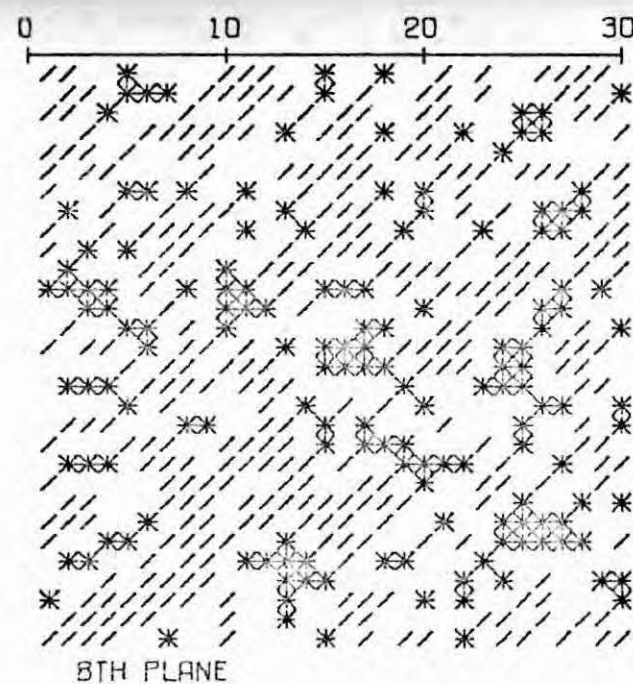
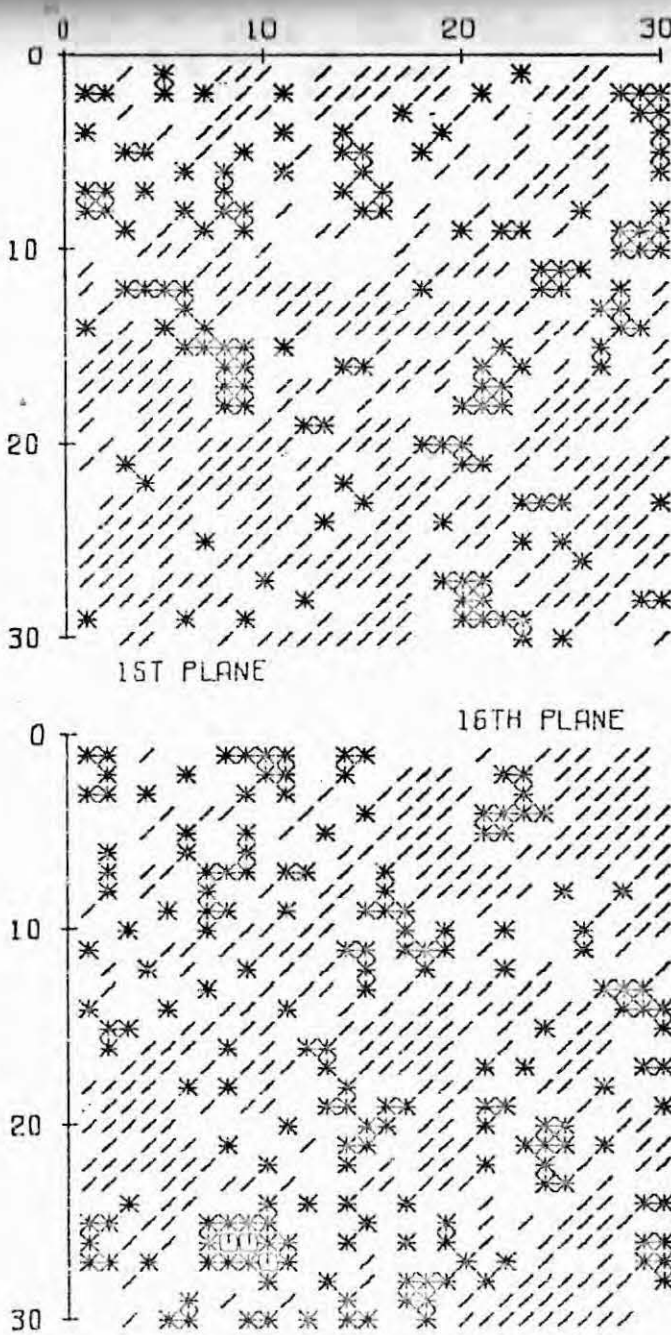
23TH PLANE

$T/T_c = .91$
 $C = -.60$
 TIME=237
 $N=550000$
 $U = .735$

CLUSTERS
SIZE NUMBER

458
112
57
34
16
10
8
7
84
1
2
3
5
6
7
9
10
11
12
13
14
17
19
20
21
23
24
29
30
34
31
38
50
52
56
64
73
99
100
215
233
240
274
315
359
520
728

Fig. B23
259



$T/T_c = .91$
 $C = -.60$
 TIME=348
 $N=800000$
 $U = .731$

CLUSTERS
SIZE NUMBER

1	459
2	107
3	56
4	26
5	18
6	7
7	137
8	66
9	13
10	10
11	12
12	13
13	14
14	15
15	16
16	17
17	19
18	20
19	21
20	22
21	26
22	29
23	32
24	36
25	39
26	49
27	51
28	56
29	61
30	68
31	76
32	101
33	167
34	203
35	243
36	2436

Fig. B24

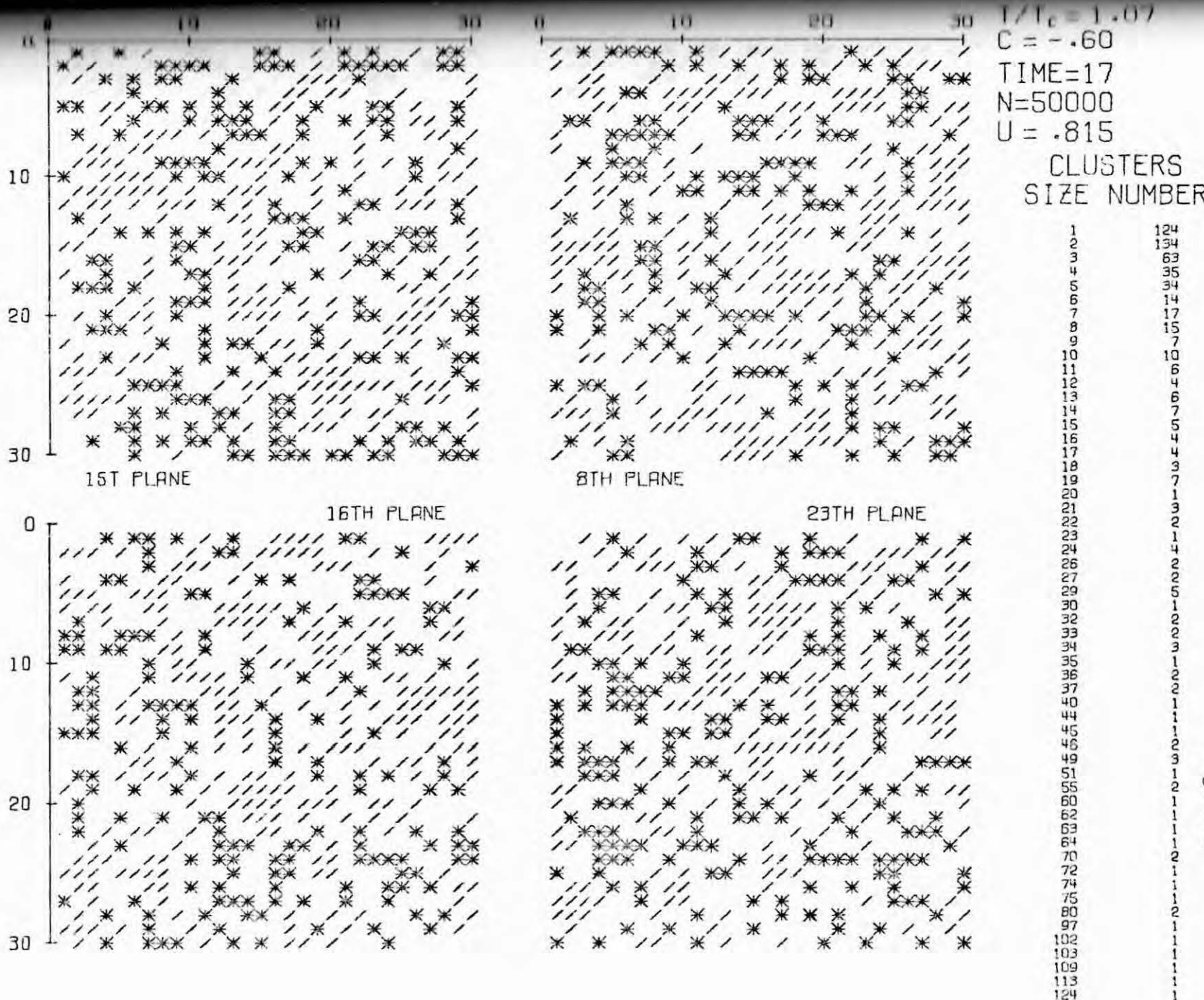
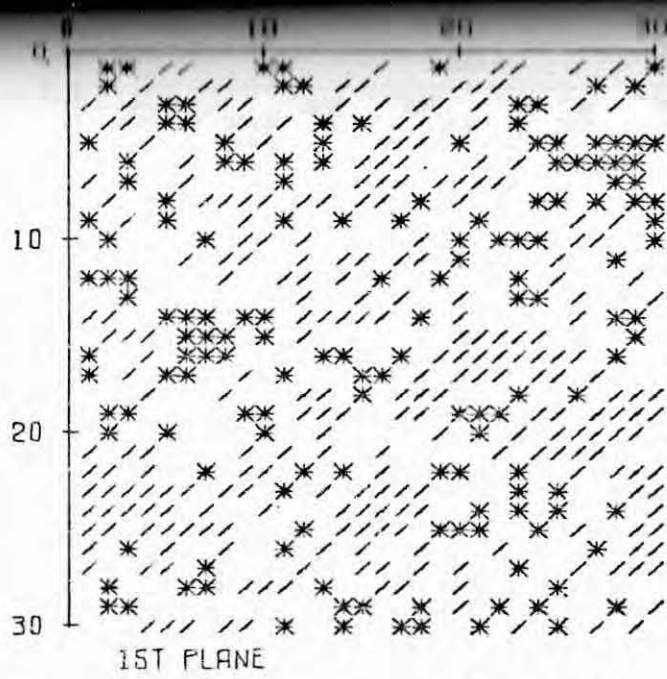
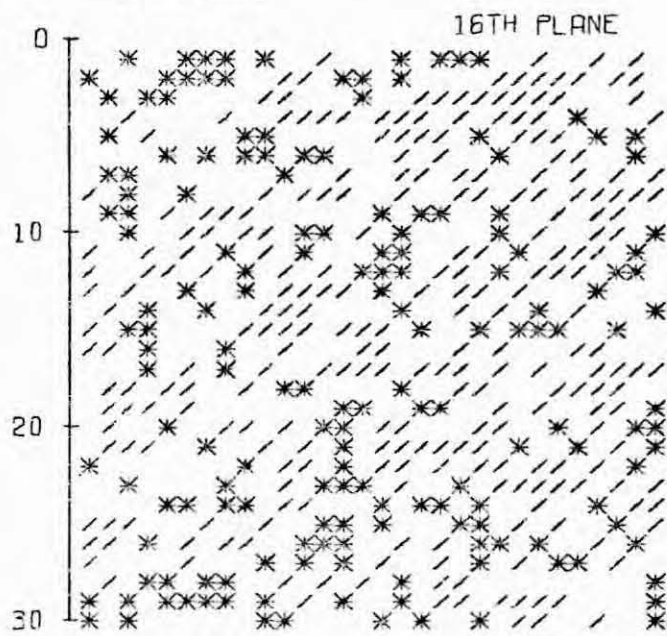


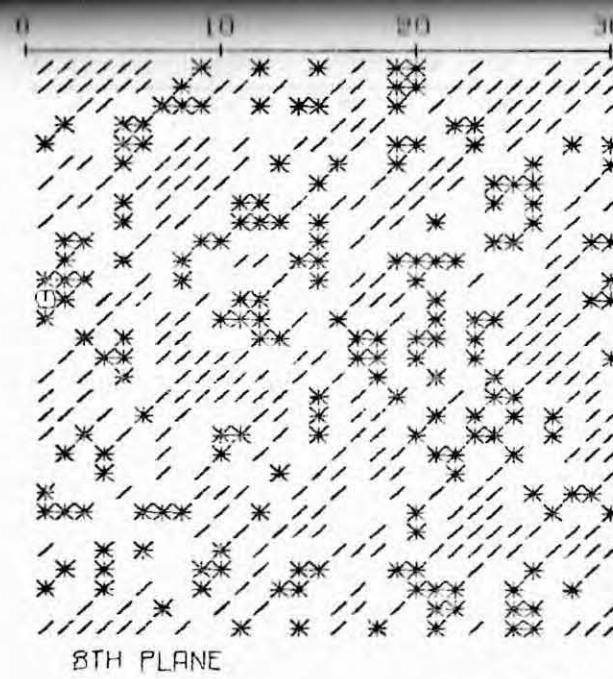
FIG. B25



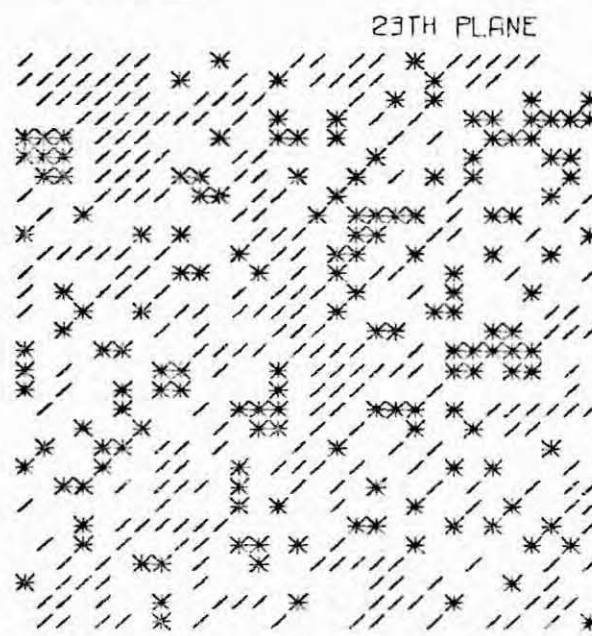
1ST PLANE



16TH PLANE



8TH PLANE

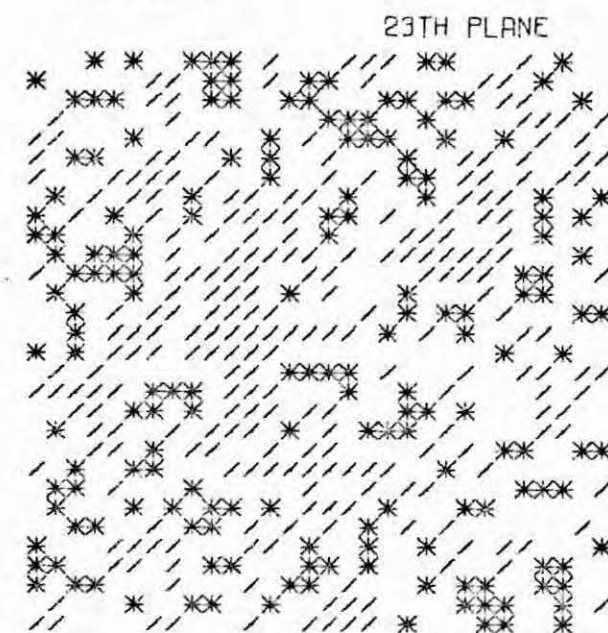
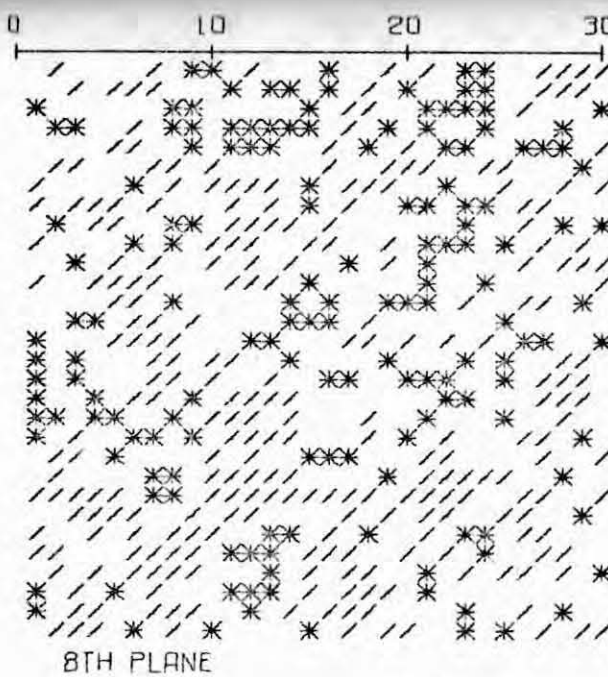
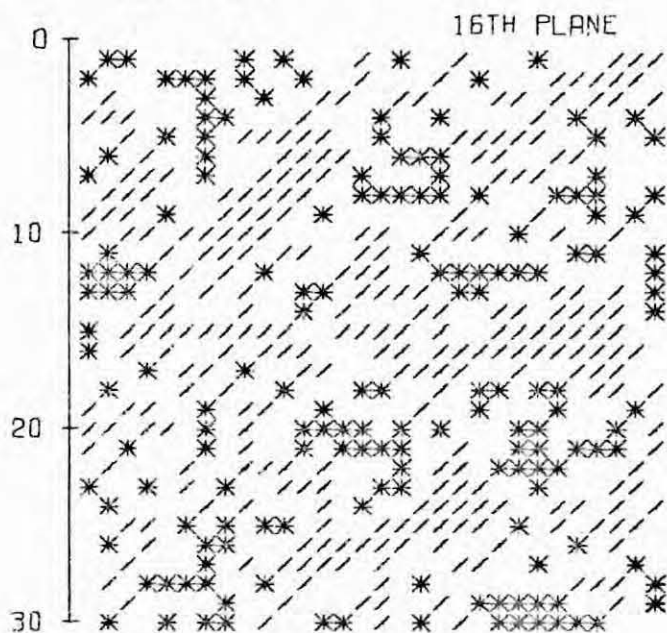
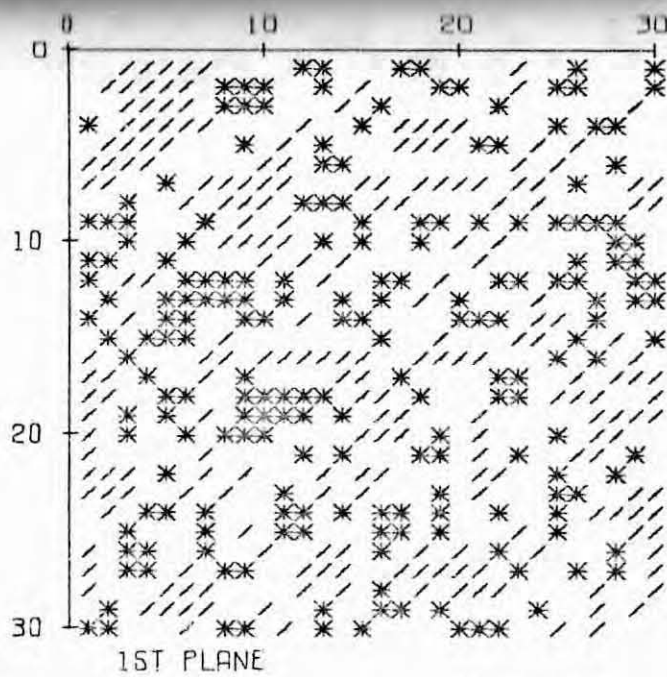


23TH PLANE

$T/T_c = 1.07$
 $C = -.60$
 TIME=89
 $N=250000$
 $U = .805$
CLUSTERS
SIZE NUMBER

1	366
2	120
3	73
4	40
5	27
6	20
7	11
8	11
9	10
10	6
11	6
12	6
13	6
14	6
15	5
16	5
17	4
18	4
19	3
20	3
21	3
22	3
23	2
24	2
25	2
26	2
27	1
28	1
29	1
30	1
31	1
32	1
33	1
34	1
35	1
36	1
37	1
38	1
39	1
40	1
41	1
42	1
43	1
44	1
45	1
46	1
47	1
48	1
49	1
50	1
51	1
52	1
53	1
54	1
55	1
56	1
57	1
58	1
59	1
60	1
61	1
62	1
63	1
64	1
65	1
66	1
67	1
68	1
69	1
70	1
71	1
72	1
73	1
74	1
75	1
76	1
77	1
78	1
79	1
80	1
81	1
82	1
83	1
84	1
85	1
86	1
87	1
88	1
89	1
90	1
91	1
92	1
93	1
94	1
95	1
96	1
97	1
98	1
99	1
100	1

262
Fig. B26

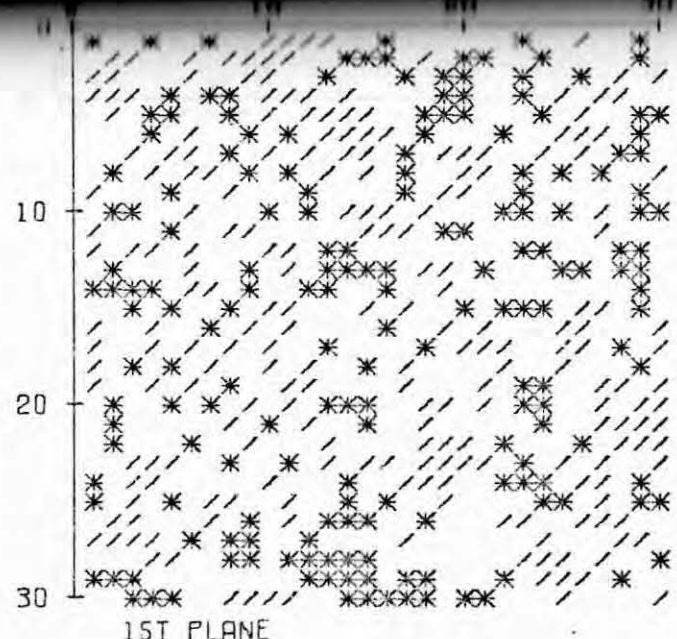


$T/T_c = 1.07$
 $C = -.60$
 TIME=252
 $N=700000$
 $U = .797$

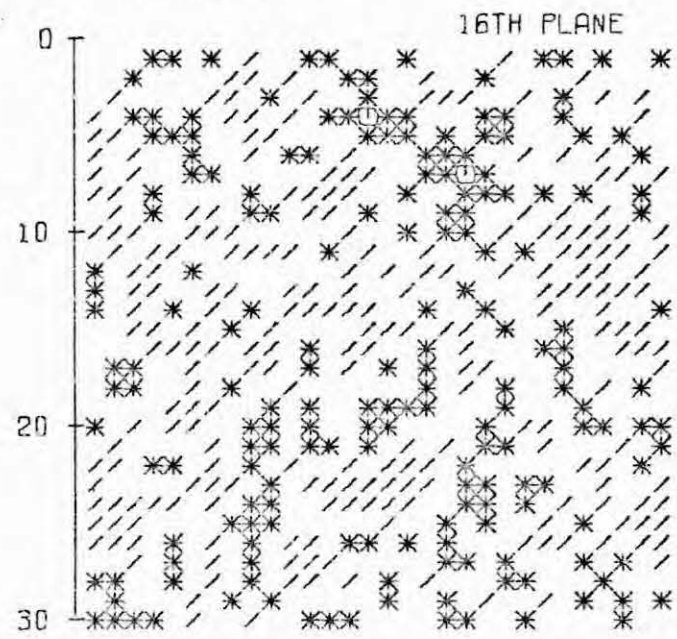
CLUSTERS
SIZE NUMBER

1
 2
 3
 4
 5
 6
 7
 8
 9
 10
 11
 12
 13
 14
 15
 16
 17
 18
 19
 20
 21
 22
 23
 24
 25
 26
 27
 28
 29
 30
 31
 32
 33
 34
 35
 36
 37
 38
 39
 40
 41
 42
 43
 44
 45
 46
 47
 48
 49
 50
 51
 52
 53
 54
 55
 56
 57
 58
 59
 60
 61
 62
 63
 64
 65
 66
 67
 68
 69
 70
 71
 72
 73
 74
 75
 76
 77
 78
 79
 80
 81
 82
 83
 84
 85
 86
 87
 88
 89
 90
 91
 92
 93
 94
 95
 96
 97
 98
 99
 100
 101
 102
 103
 104
 105
 106
 107
 108
 109
 110
 111
 112
 113
 114
 115
 116
 117
 118
 119
 120
 121
 122
 123
 124
 125
 126
 127
 128
 129
 130
 131
 132
 133
 134
 135
 136
 137
 138
 139
 140
 141
 142
 143
 144
 145
 146
 147
 148
 149
 150
 151
 152
 153
 154
 155
 156
 157
 158
 159
 160
 161
 162
 163
 164
 165
 166
 167
 168
 169
 170
 171
 172
 173
 174
 175
 176
 177
 178
 179
 180
 181
 182
 183
 184
 185
 186
 187
 188
 189
 190
 191
 192
 193
 194
 195
 196
 197
 198
 199
 200
 201
 202
 203
 204
 205
 206
 207
 208
 209
 210
 211
 212
 213
 214
 215
 216
 217
 218
 219
 220
 221
 222
 223
 224
 225
 226
 227
 228
 229
 230
 231
 232
 233
 234
 235
 236
 237
 238
 239
 240
 241
 242
 243
 244
 245
 246
 247
 248
 249
 250
 251
 252
 253
 254
 255
 256
 257
 258
 259
 260
 261
 262
 263
 264
 265
 266
 267
 268
 269
 270
 271
 272
 273
 274
 275
 276
 277
 278
 279
 280
 281
 282
 283
 284
 285
 286
 287
 288
 289
 290
 291
 292
 293
 294
 295
 296
 297
 298
 299
 300
 301
 302
 303
 304
 305
 306
 307
 308
 309
 310
 311
 312
 313
 314
 315
 316
 317
 318
 319
 320
 321
 322
 323
 324
 325
 326
 327
 328
 329
 330
 331
 332
 333
 334
 335
 336
 337
 338
 339
 340
 341
 342
 343
 344
 345
 346
 347
 348
 349
 350
 351
 352
 353
 354
 355
 356
 357
 358
 359
 360
 361
 362
 363
 364
 365
 366
 367
 368
 369
 370
 371
 372
 373
 374
 375
 376
 377
 378
 379
 380
 381
 382
 383
 384
 385
 386
 387
 388
 389
 390
 391
 392
 393
 394
 395
 396
 397
 398
 399
 400
 401
 402
 403
 404
 405
 406
 407
 408
 409
 410
 411
 412
 413
 414
 415
 416
 417
 418
 419
 420
 421
 422
 423
 424
 425
 426
 427
 428
 429
 430
 431
 432
 433
 434
 435
 436
 437
 438
 439
 440
 441
 442
 443
 444
 445
 446
 447
 448
 449
 450
 451
 452
 453
 454
 455
 456
 457
 458
 459
 460
 461
 462
 463
 464
 465
 466
 467
 468
 469
 470
 471
 472
 473
 474
 475
 476
 477
 478
 479
 480
 481
 482
 483
 484
 485
 486
 487
 488
 489
 490
 491
 492
 493
 494
 495
 496
 497
 498
 499
 500
 501
 502
 503
 504
 505
 506
 507
 508
 509
 510
 511
 512
 513
 514
 515
 516
 517
 518
 519
 520
 521
 522
 523
 524
 525
 526
 527
 528
 529
 530
 531
 532
 533
 534
 535
 536
 537
 538
 539
 540
 541
 542
 543
 544
 545
 546
 547
 548
 549
 550
 551
 552
 553
 554
 555
 556
 557
 558
 559
 560
 561
 562
 563
 564
 565
 566
 567
 568
 569
 570
 571
 572
 573
 574
 575
 576
 577
 578
 579
 580
 581
 582
 583
 584
 585
 586
 587
 588
 589
 590
 591
 592
 593
 594
 595
 596
 597
 598
 599
 600
 601
 602
 603
 604
 605
 606
 607
 608
 609
 610
 611
 612
 613
 614
 615
 616
 617
 618
 619
 620
 621
 622
 623
 624
 625
 626
 627
 628
 629
 630
 631
 632
 633
 634
 635
 636
 637
 638
 639
 640
 641
 642
 643
 644
 645
 646
 647
 648
 649
 650
 651
 652
 653
 654
 655
 656
 657
 658
 659
 660
 661
 662
 663
 664
 665
 666
 667
 668
 669
 670
 671
 672
 673
 674
 675
 676
 677
 678
 679
 680
 681
 682
 683
 684
 685
 686
 687
 688
 689
 690
 691
 692
 693
 694
 695
 696
 697
 698
 699
 700

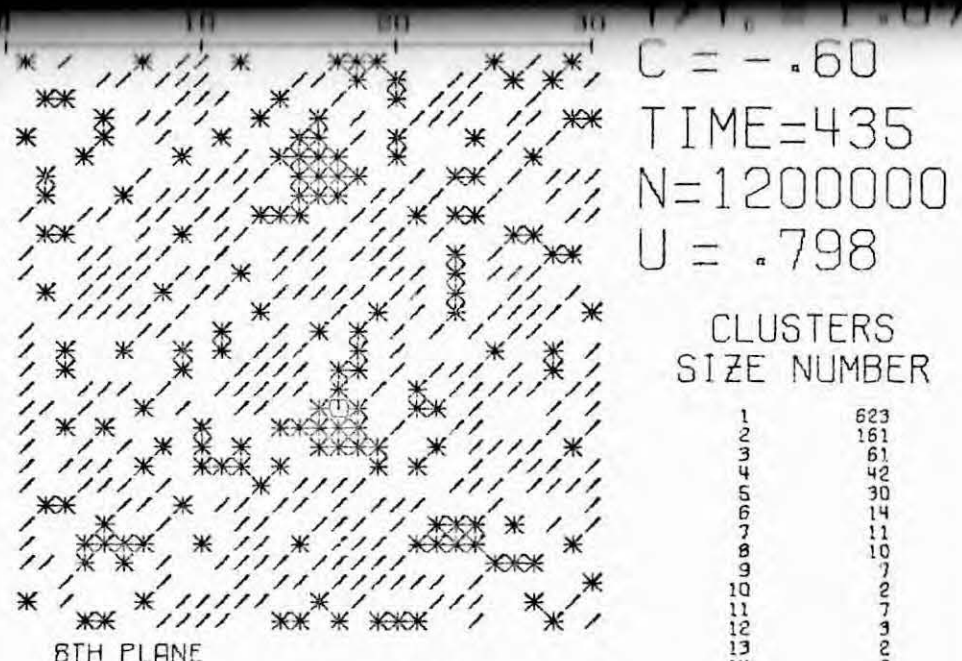
Fig. B27



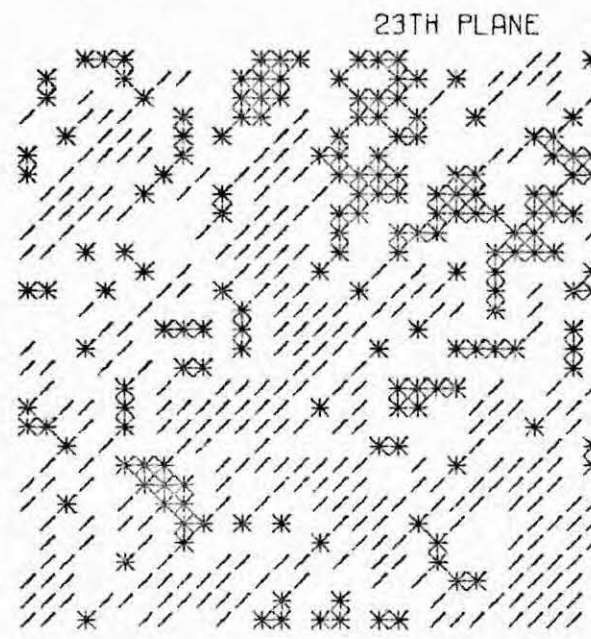
1ST PLANE



16TH PLANE



8TH PLANE



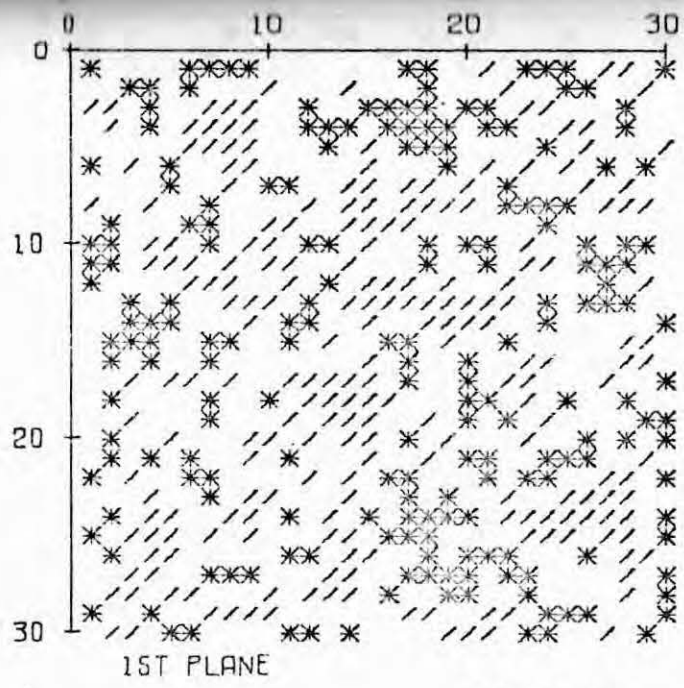
23TH PLANE

$C = - .60$
 $TIME = 435$
 $N = 1200000$
 $U = .798$

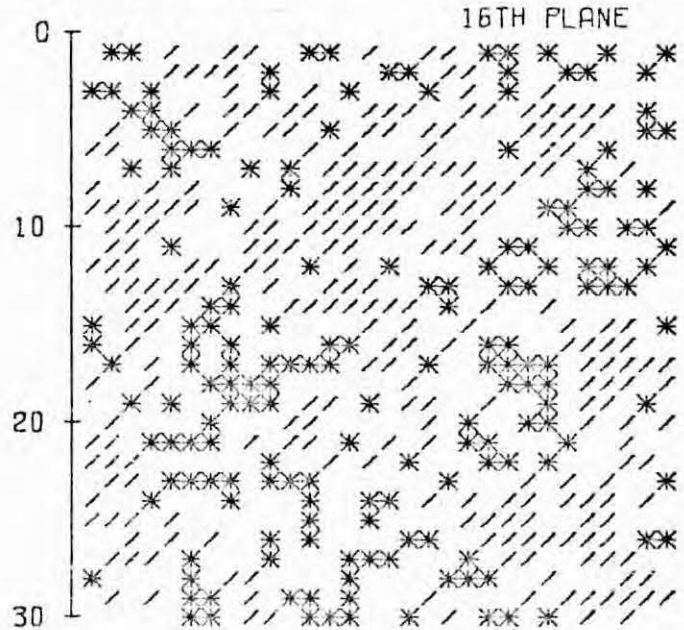
CLUSTERS
SIZE NUMBER

1	623
2	161
3	61
4	42
5	30
6	14
7	11
8	10
9	7
10	2
11	7
12	3
13	2
14	2
15	1
16	1
17	1
18	1
19	1
20	1
21	1
22	1
23	1
24	1
25	1
26	1
27	1
28	1
29	1
30	1
31	1
32	1
33	1
34	1
35	1
36	1
37	1
38	1
39	1
40	1
41	1
42	1
43	1
44	1
45	1
46	1
47	1
48	1
49	1
50	1
51	1
52	1
53	1
54	1
55	1
56	1
57	1
58	1
59	1
60	1
61	1
62	1
63	1
64	1
65	1
66	1
67	1
68	1
69	1
70	1
71	1
72	1
73	1
74	1
75	1
76	1
77	1
78	1
79	1
80	1
81	1
82	1
83	1
84	1
85	1
86	1
87	1
88	1
89	1
90	1
91	1
92	1
93	1
94	1
95	1
96	1
97	1
98	1
99	1
100	1
101	1
102	1
103	1
104	1
105	1
106	1
107	1
108	1
109	1
110	1
111	1
112	1
113	1
114	1
115	1
116	1
117	1
118	1
119	1
120	1
121	1
122	1
123	1
124	1
125	1
126	1
127	1
128	1
129	1
130	1
131	1
132	1
133	1
134	1
135	1
136	1
137	1
138	1
139	1
140	1
141	1
142	1
143	1
144	1
145	1
146	1
147	1
148	1
149	1
150	1
151	1
152	1
153	1
154	1
155	1
156	1
157	1
158	1
159	1
160	1
161	1
162	1
163	1
164	1
165	1
166	1
167	1
168	1
169	1
170	1
171	1
172	1
173	1
174	1
175	1
176	1
177	1
178	1
179	1
180	1
181	1
182	1
183	1
184	1
185	1
186	1
187	1
188	1
189	1
190	1
191	1
192	1
193	1
194	1
195	1
196	1
197	1
198	1
199	1
200	1
201	1
202	1
203	1
204	1
205	1
206	1
207	1
208	1
209	1
210	1
211	1
212	1
213	1
214	1
215	1
216	1
217	1
218	1
219	1
220	1
221	1
222	1
223	1
224	1
225	1
226	1
227	1
228	1
229	1
230	1
231	1
232	1
233	1
234	1
235	1
236	1
237	1
238	1
239	1
240	1
241	1
242	1
243	1
244	1
245	1
246	1
247	1
248	1
249	1
250	1
251	1
252	1
253	1
254	1
255	1
256	1
257	1
258	1
259	1
260	1
261	1
262	1
263	1
264	1
265	1
266	1
267	1
268	1
269	1
270	1
271	1
272	1
273	1
274	1
275	1
276	1
277	1
278	1
279	1
280	1
281	1
282	1
283	1
284	1
285	1
286	1
287	1
288	1
289	1
290	1
291	1
292	1
293	1
294	1
295	1
296	1
297	1
298	1
299	1
300	1

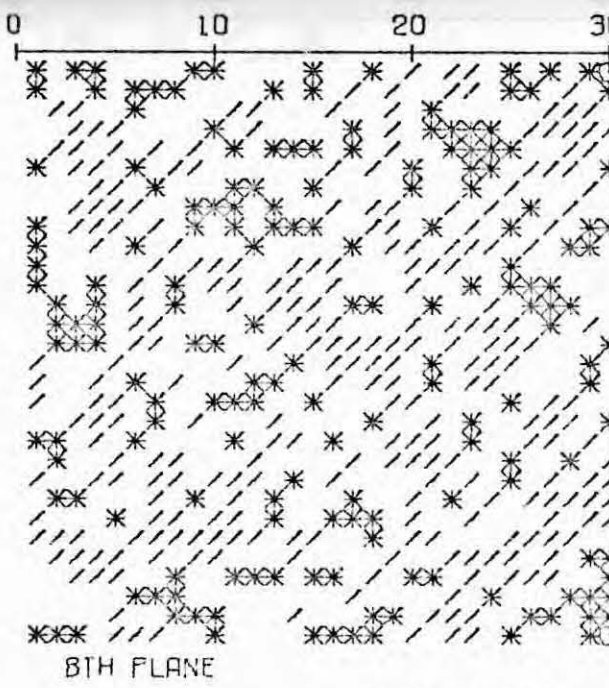
Fig. B28



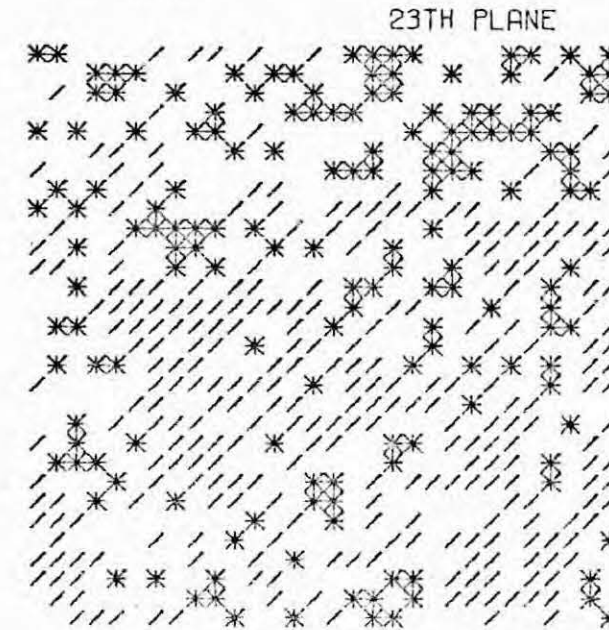
1ST PLANE



16TH PLANE



8TH PLANE



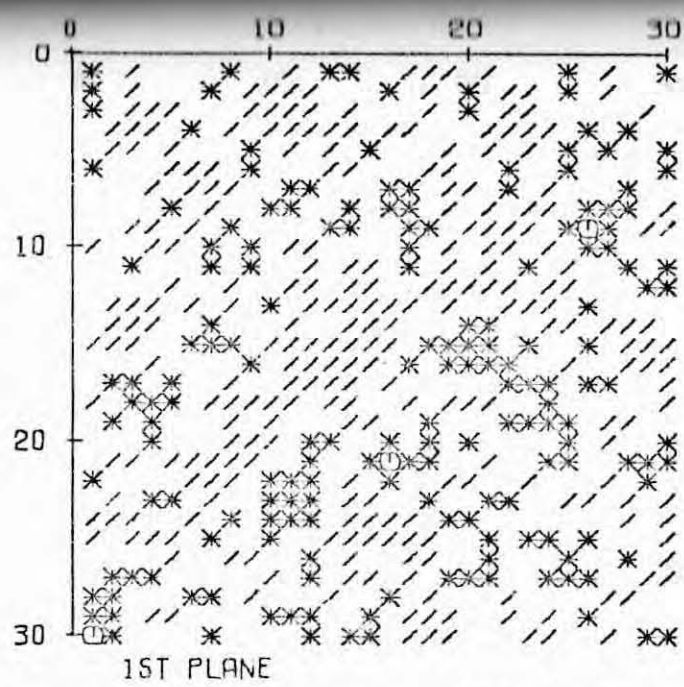
23TH PLANE

$T/T_c = 1.07$
 $C = -.60$
 TIME=581
 $N=1600000$
 $U = .796$

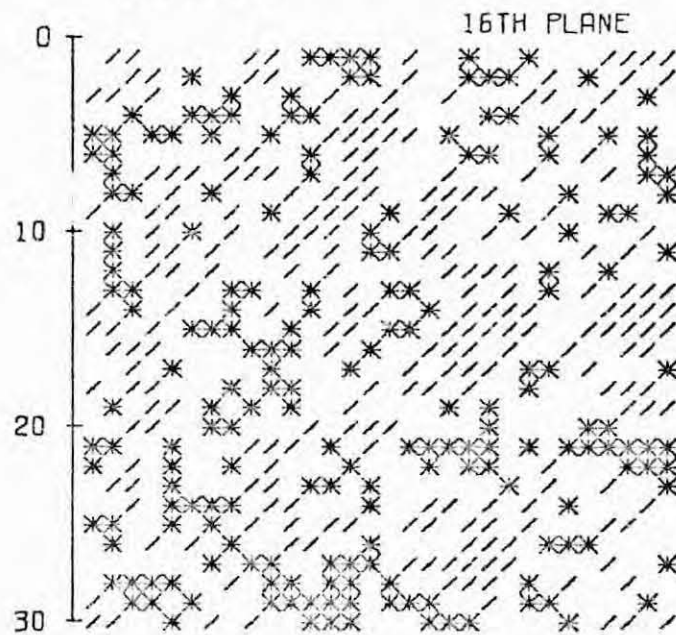
CLUSTERS
SIZE NUMBER

1	560
2	124
3	69
4	32
5	26
6	20
7	14
8	10
9	13
10	5
11	6
12	9
13	1
14	1
15	1
16	1
17	1
18	1
19	1
20	1
21	1
22	1
23	1
24	1
25	1
26	1
27	1
28	1
29	1
31	1
32	1
37	1
38	1
41	1
48	1
68	1
78	1
82	1
92	1
101	1
106	1
131	1
242	1
273	1
276	1
421	1
461	1

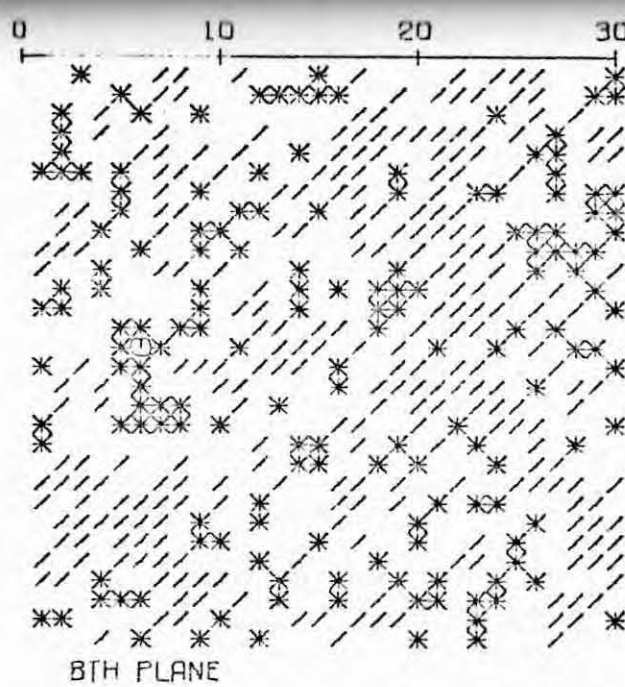
Fig. B29



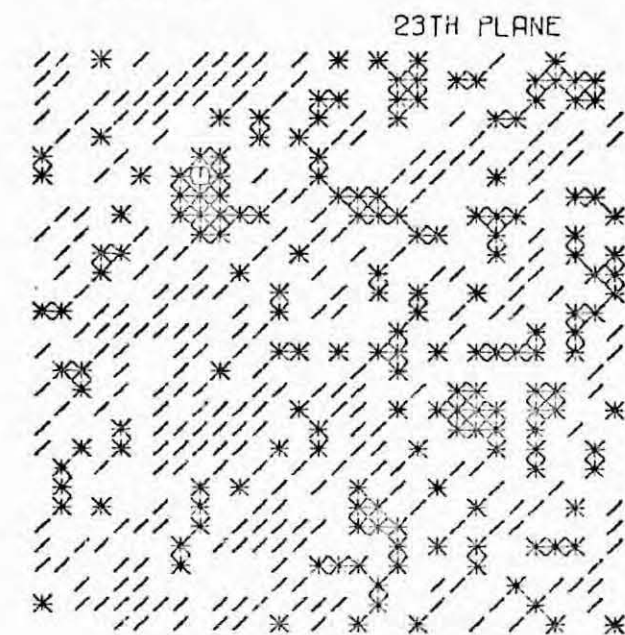
1ST PLANE



16TH PLANE



8TH PLANE



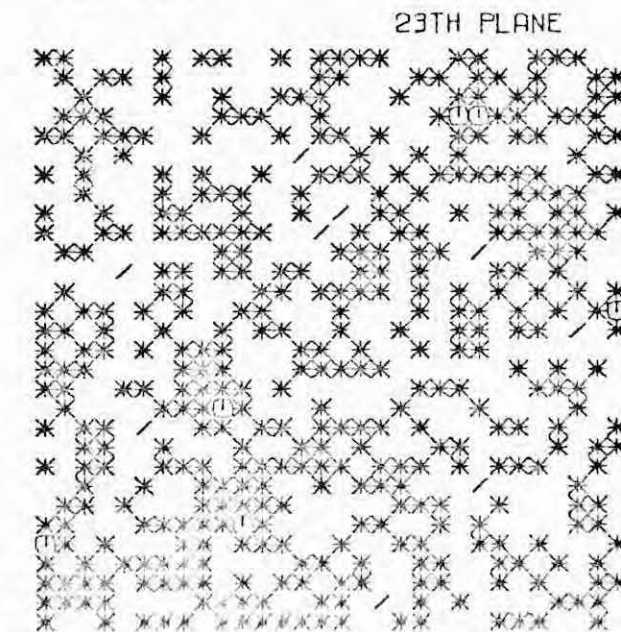
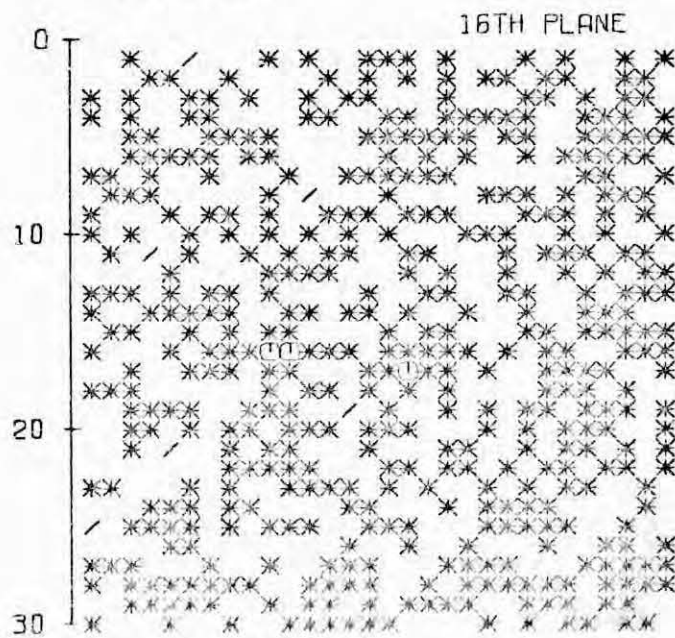
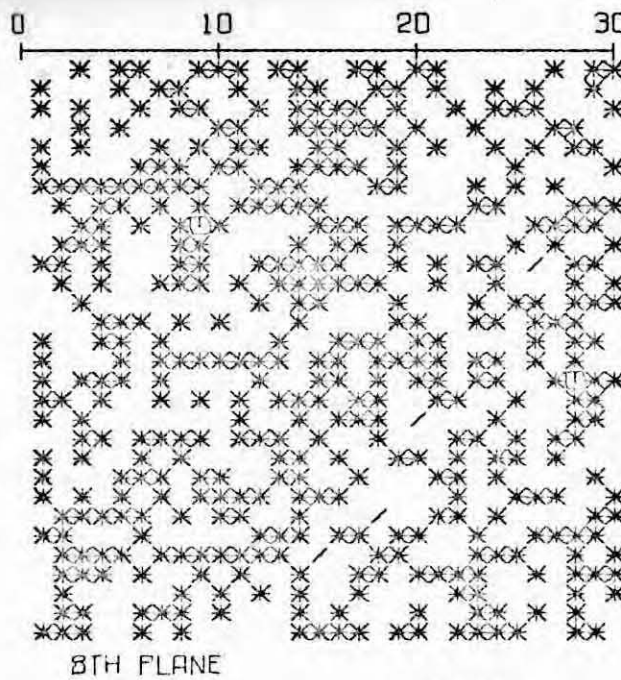
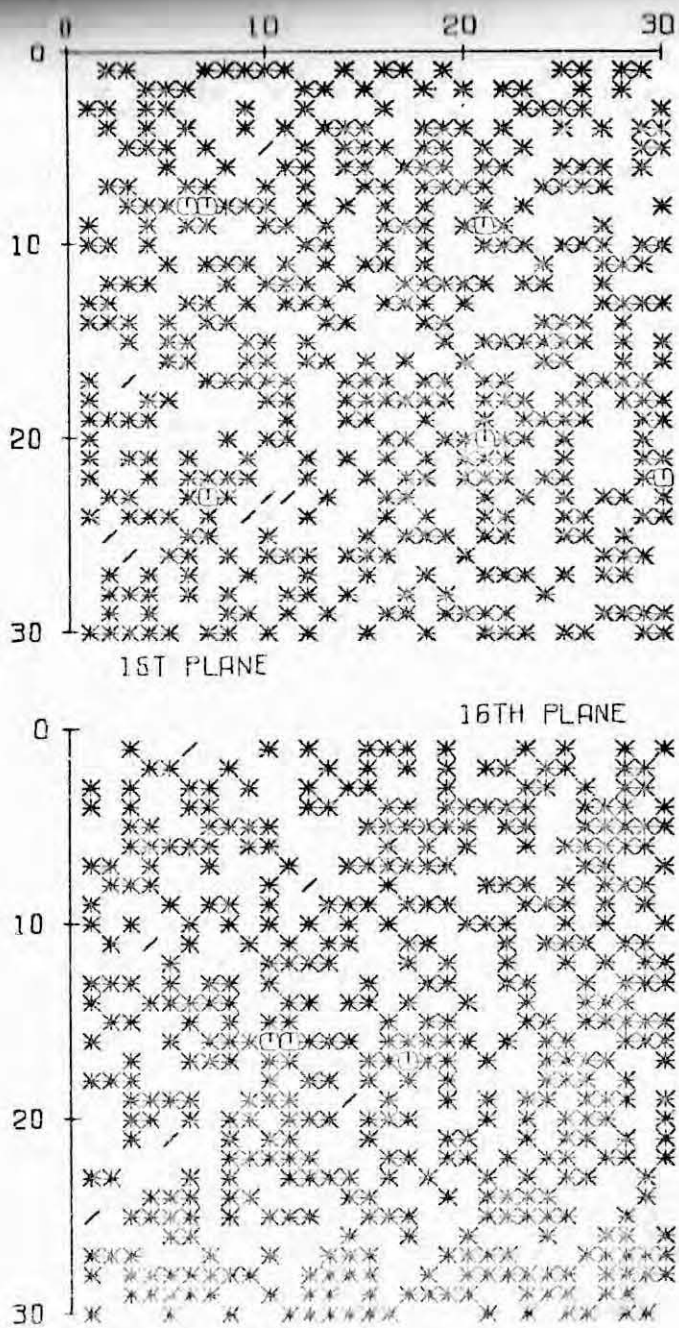
23TH PLANE

$T/T_c = 1.07$
 $C = -.60$
 TIME=727
 $N=2000000$
 $U = .796$

CLUSTERS SIZE NUMBER

570
131
73
40
26
19
12
13
57
35
14
11
13
14
15
16
17
19
20
21
22
23
24
25
27
29
29
32
33
35
36
37
38
43
47
56
60
61
62
69
82
87
93
102
107
152
281
285
448

Fig. B30

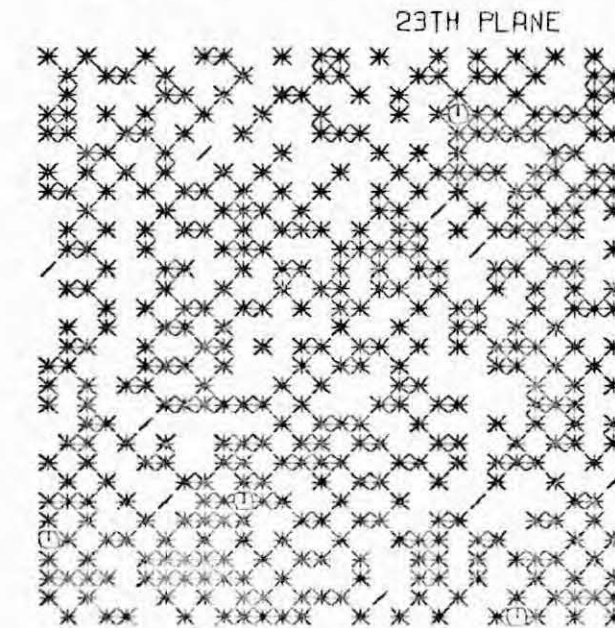
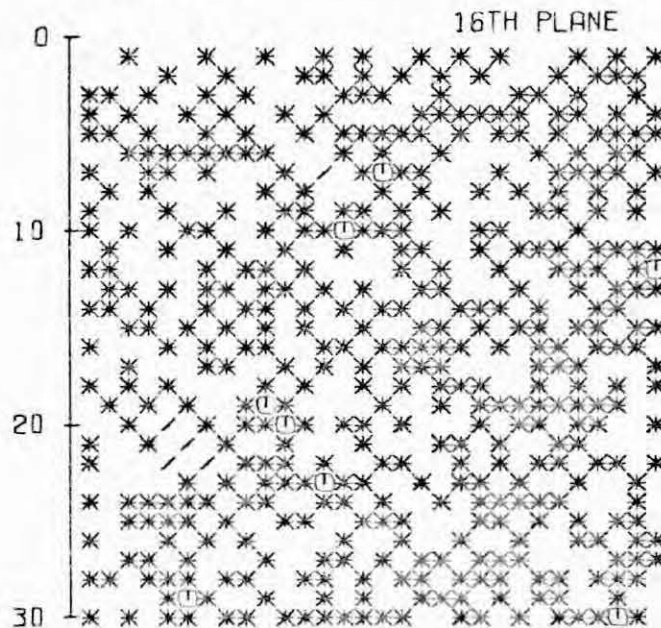
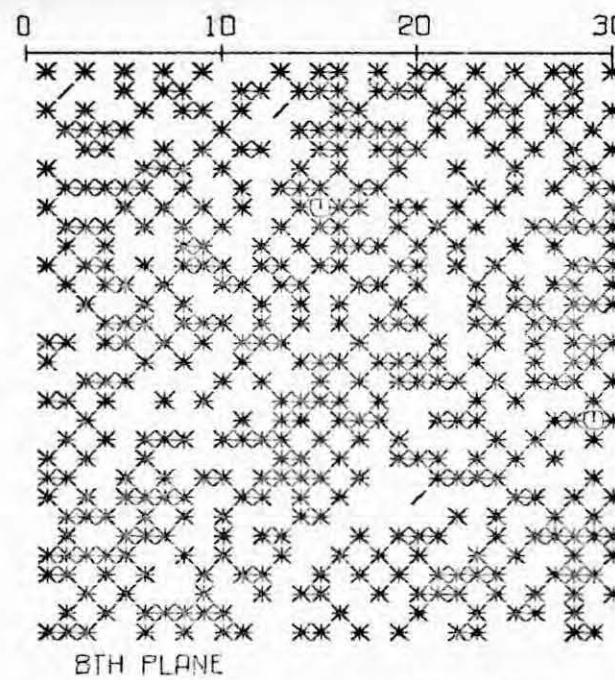
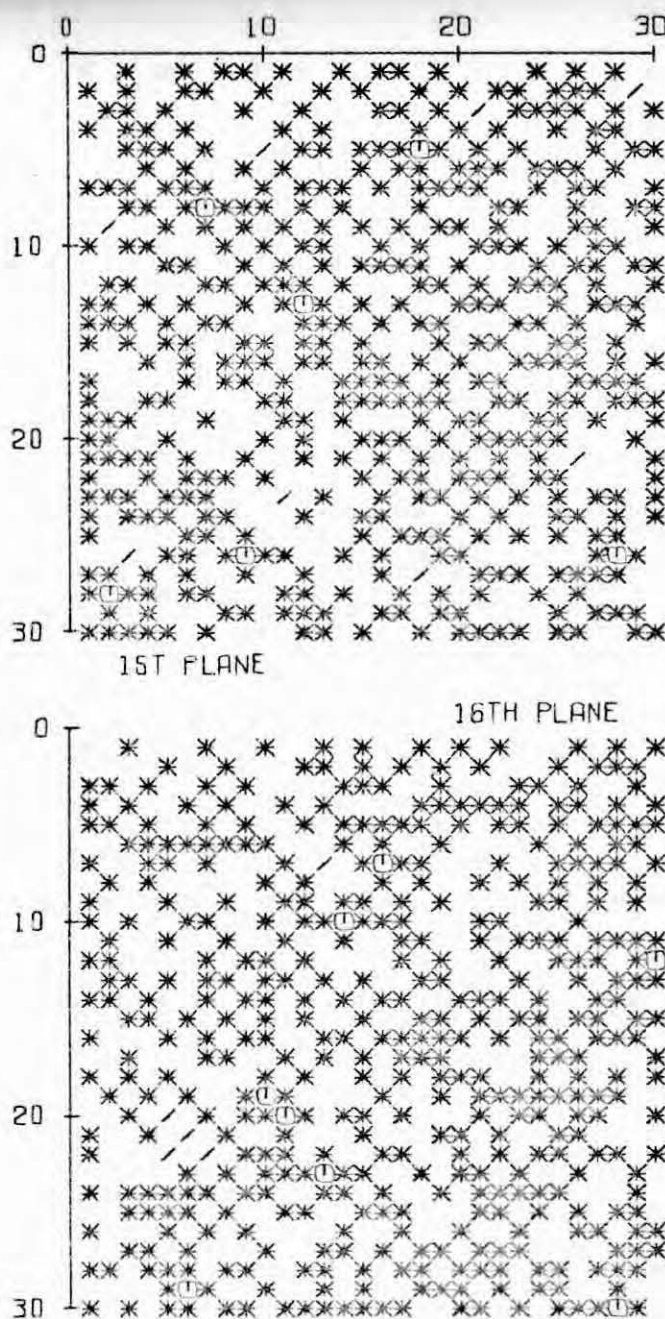


$T/T_c = .59$
 $C = .00$
 TIME=0
 $N=0$
 $U = 1.507$

CLUSTERS
SIZE NUMBER

241
186011111
13179

Fig. B31



$T/T_c = .59$
 $C = .00$
 TIME=1
 $N=5000$
 $U = 1.795$

CLUSTERS
SIZE NUMBER

1	2	3	4	5	6	7	8	9	10	11	12	13	14	15	16	17	18	19	20	21	22	23	24	25	26	27	28	29	30		
855	88	23	127	3	20	11	1	1	1	1	1	1	1	1	1	1	1	1	1	1	1	1	1	1	1	1	1	1	1	1	1

Fig. B32

$T/T_c = .59$
 $C = .00$
 TIME = 4
 $N = 15000$
 $U = 2.139$

CLUSTERS
SIZE NUMBER

1	2807
2	160
3	57
4	39
5	27
6	24
7	20
8	16
9	12
10	10
11	11
12	12
13	13
14	14
15	15
16	16
17	17
18	18
19	19
20	20
21	21
22	22
23	23
24	27
25	35
26	37
27	51
28	80
29	8684

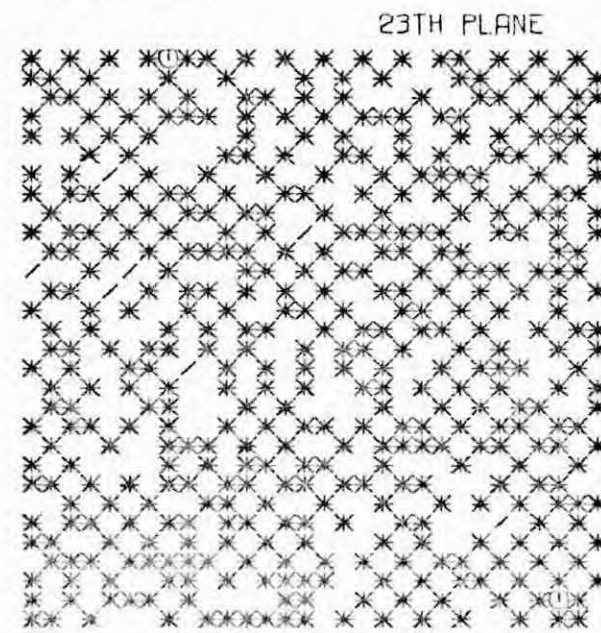
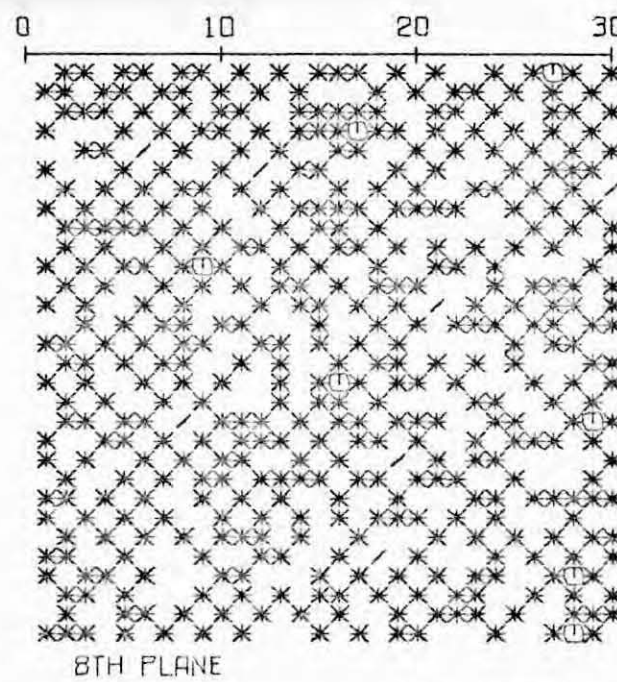
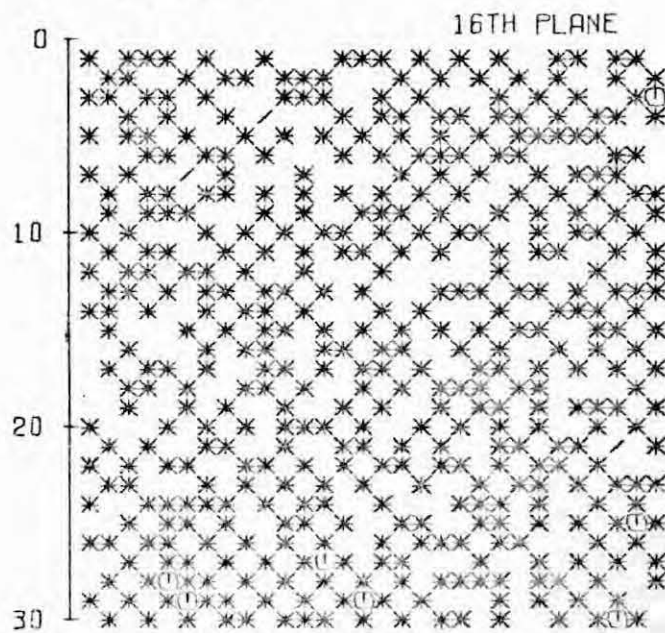
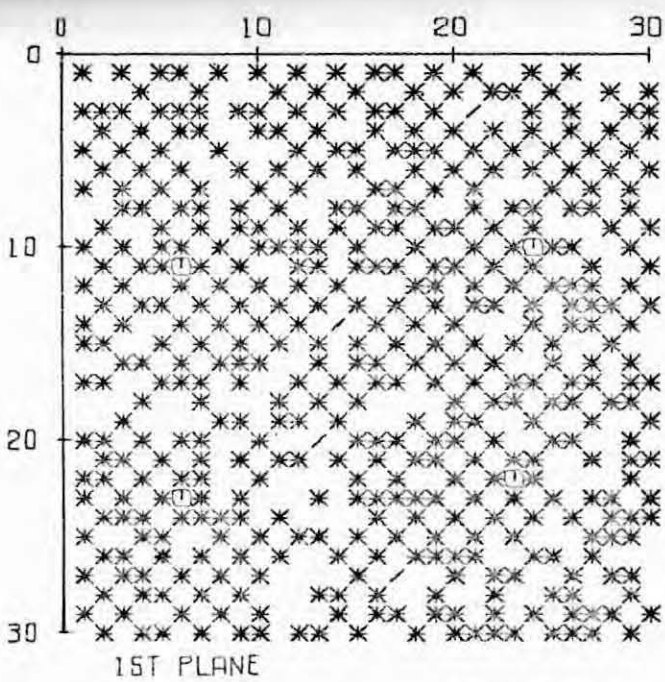
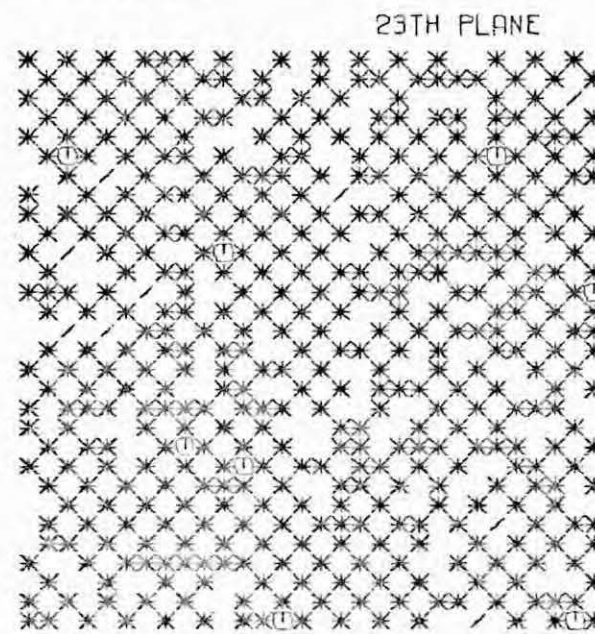
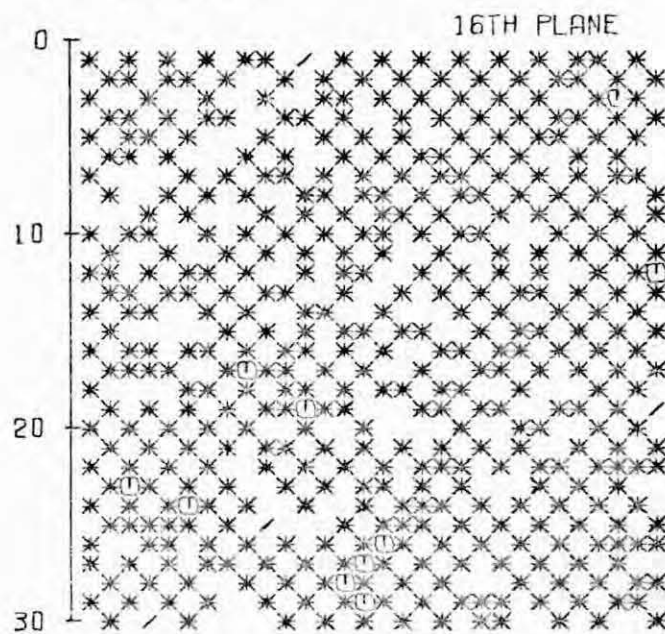
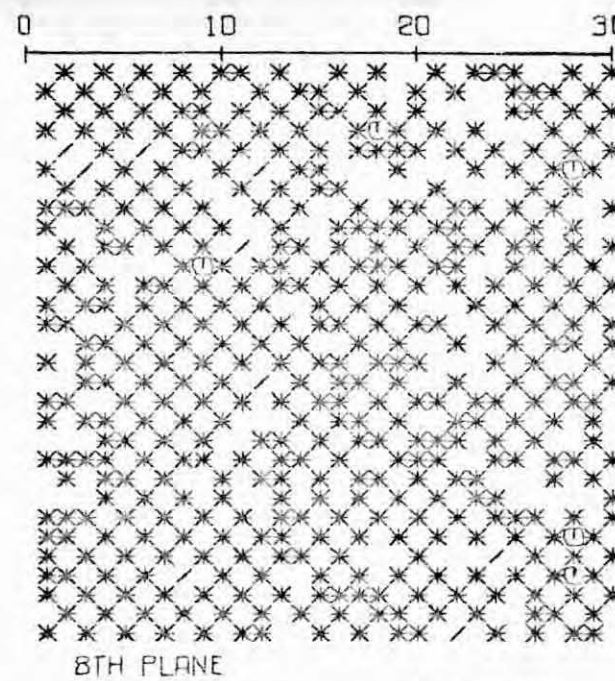
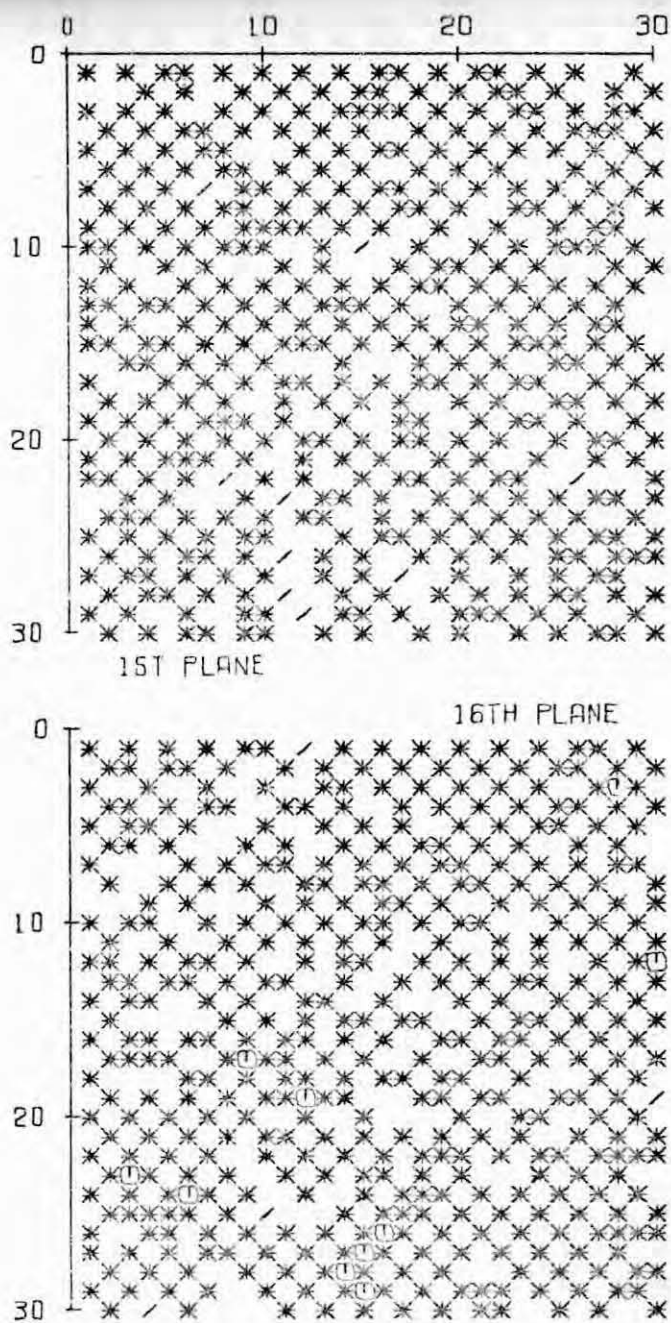


Fig. B33

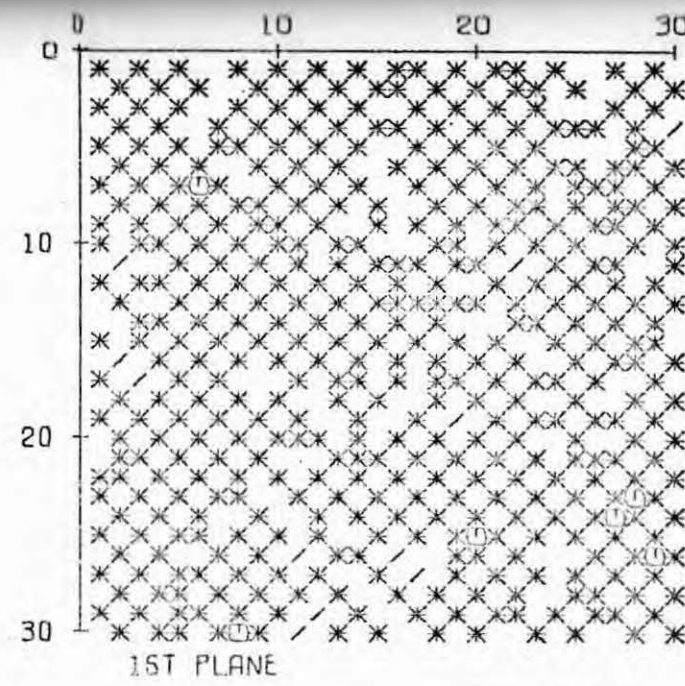


$T/T_c = .50$
 $C = .00$
 TIME=9
 $N=25000$
 $U = 2.334$

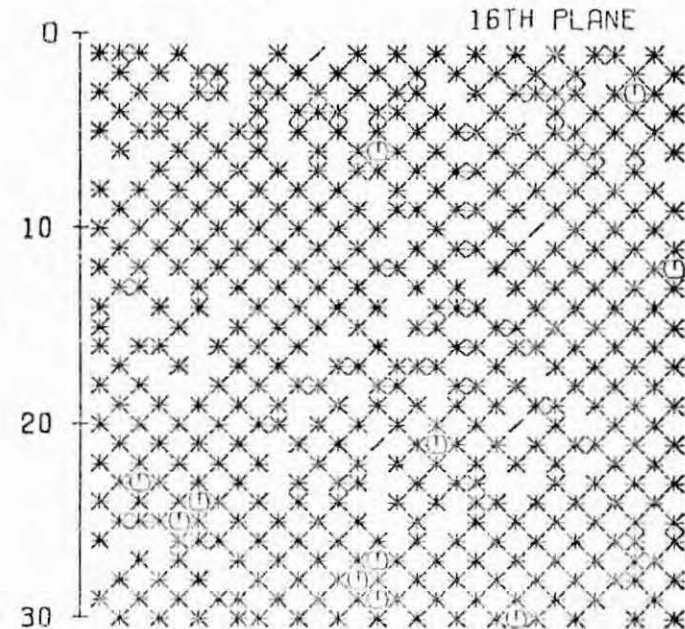
CLUSTERS
SIZE NUMBER

1	4750
2	142
3	71
4	35
5	20
6	32
7	46
8	17
9	10
10	7
11	12
12	8
13	6
14	1
15	16
16	2
17	19
18	20
19	21
20	22
21	25
22	26
23	27
24	30
25	31
26	32
27	35
28	36
29	37
30	44
31	47
32	51
33	56
34	59
35	60
36	62
37	64
38	81
39	134
40	149
41	150

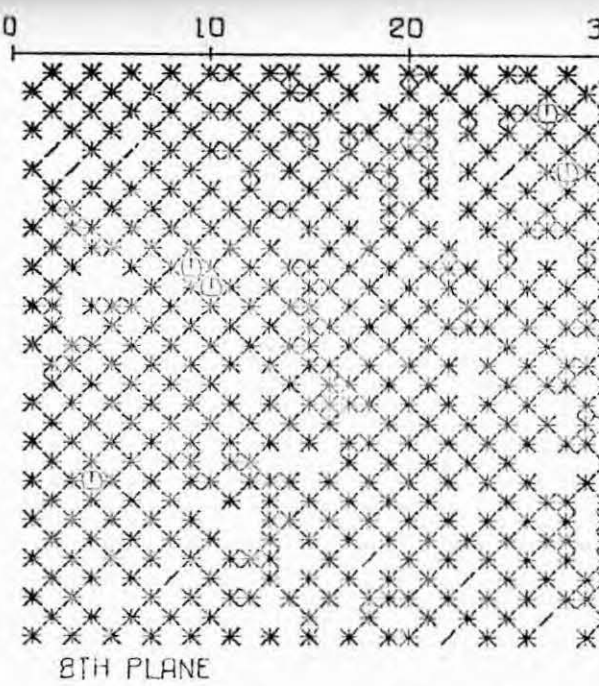
Fig. B34



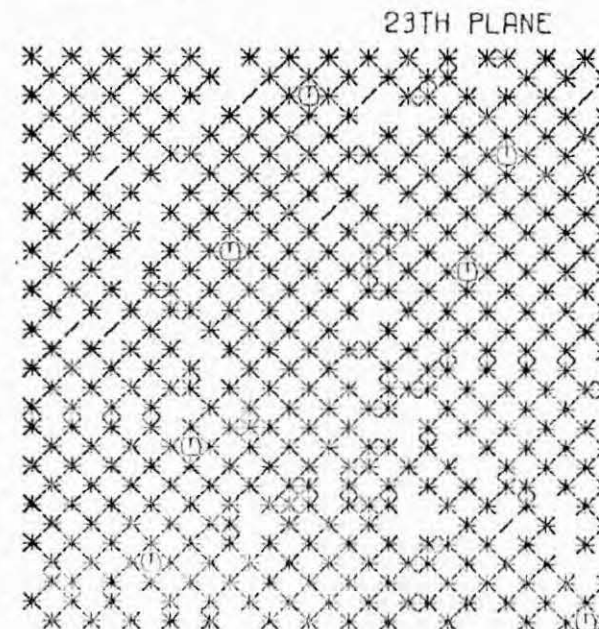
1ST PLANE



16TH PLANE



8TH PLANE



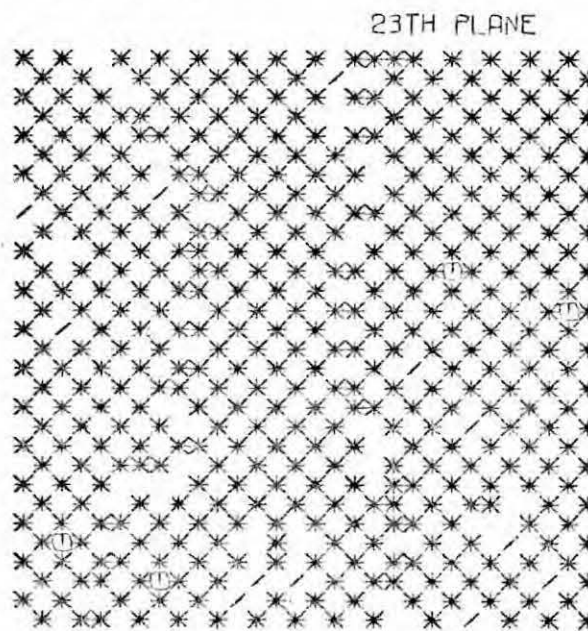
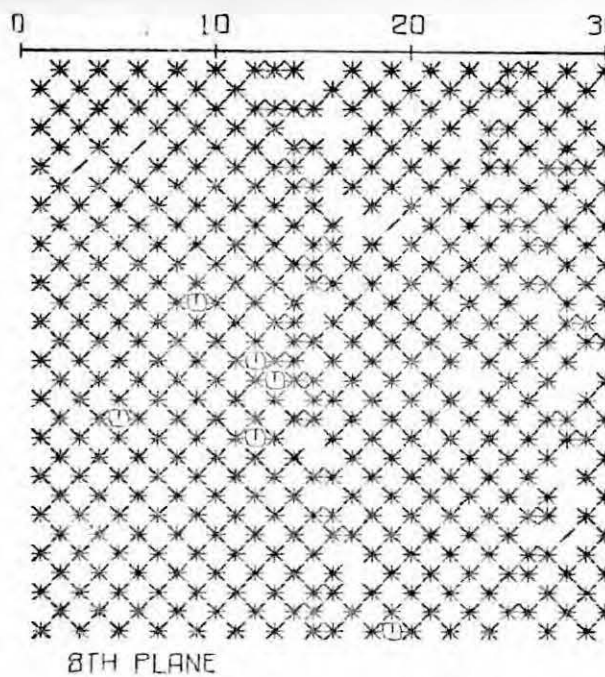
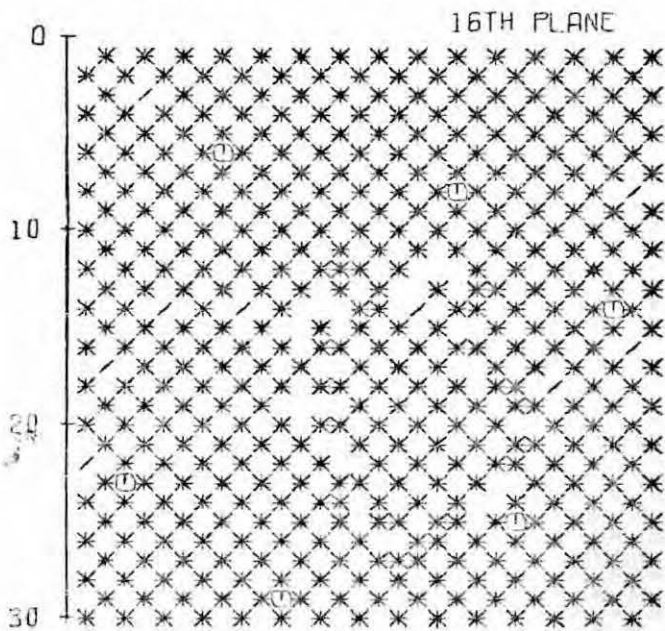
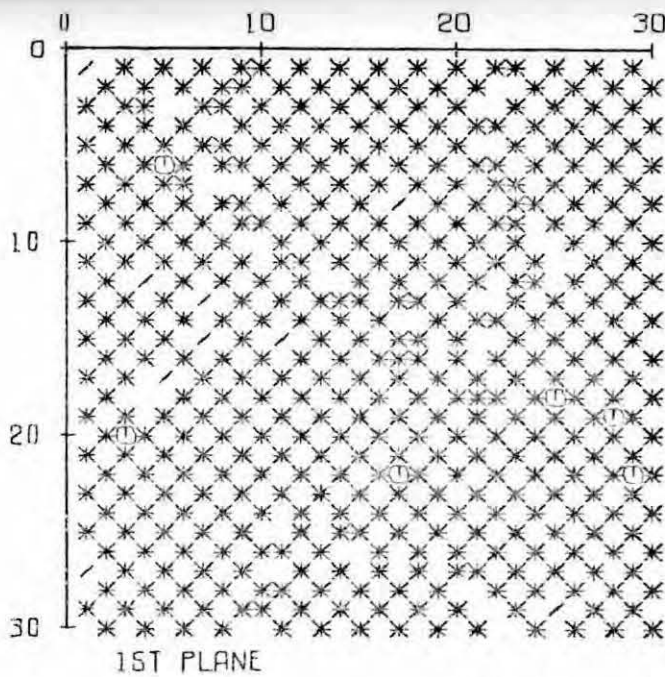
23TH PLANE

$T/T_c = .59$
 $C = .00$
 TIME=17.
 $N=35000$
 $U = 2.490$

CLUSTERS
SIZE NUMBER

1	6520
2	148
3	44
4	21
5	29
6	23
7	71
8	14
9	13
10	7
11	12
12	12
13	7
14	2
15	6
16	7
17	2
18	6
19	7
20	5
21	2
22	3
23	4
24	2
25	1
26	1
27	2
28	1
29	1
30	1
31	1
32	1
33	1
34	1
35	1
36	1
37	1
38	1
39	1
40	1
41	1
42	1
43	1
44	1
45	1
46	1
47	1
48	1
49	1
50	1
51	1
52	1
53	1
54	1
55	1
56	1
57	1
58	1
59	1
60	1
61	1
62	1
63	1
64	1
65	1
66	1
67	1
68	1
69	1
70	1
71	1
72	1
73	1
74	1
75	1
76	1
77	1
78	1
79	1
80	1
81	1
82	1
83	1
84	1
85	1
86	1
87	1
88	1
89	1
90	1
91	1
92	1
93	1
94	1
95	1
96	1
97	1
98	1
99	1
100	1

Fig. B35

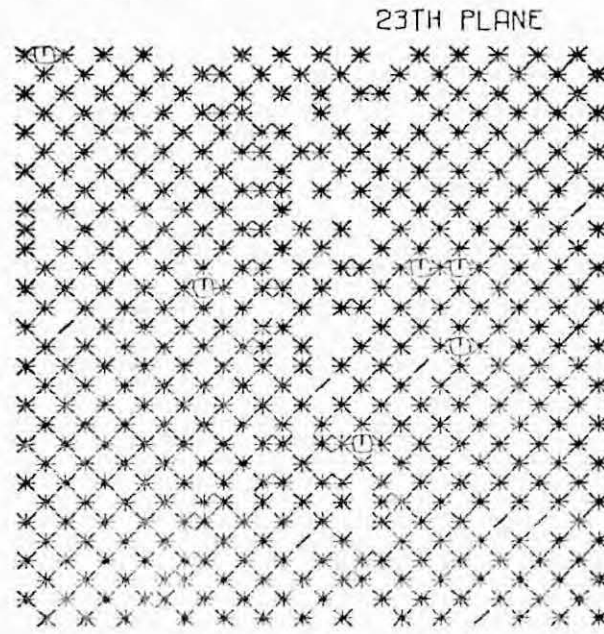
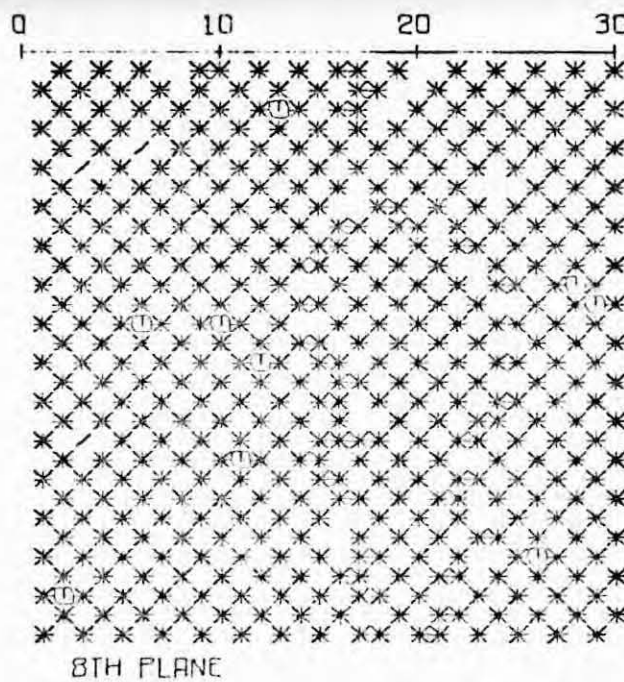
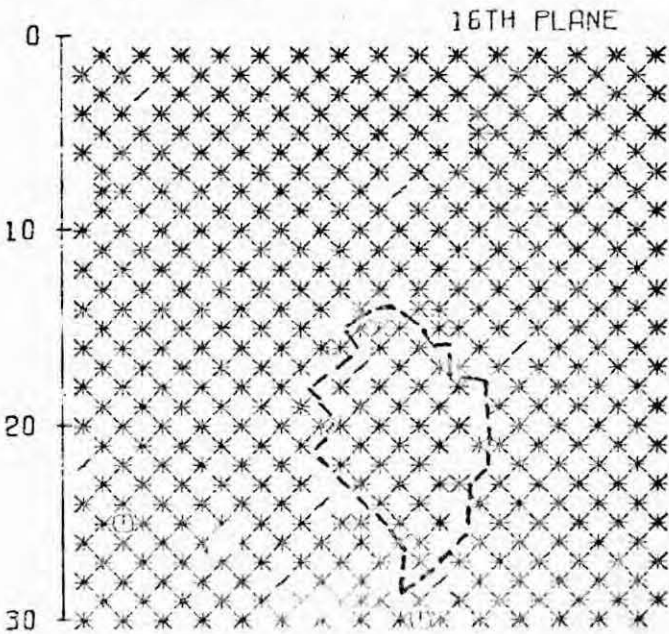
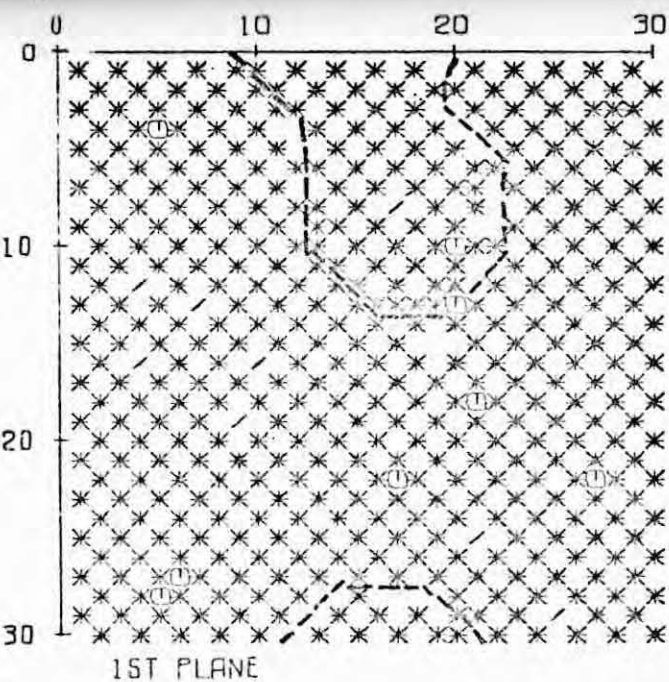


$T/T_c = .59$
 $C = .00$
 TIME = 77
 $N = 75000$
 $\langle J \rangle = 2.720$

CLUSTERS
SIZE NUMBER

1
2
3
4
5
6
7
8
9
10
11
12
13
14
15
16
17
18
19
20
21
22
23
24
25
26
27
28
29
31
32
33
35
36
38
39
41
42
47
49
50
52
53
60
61
62
63
75
83

Fig. B36

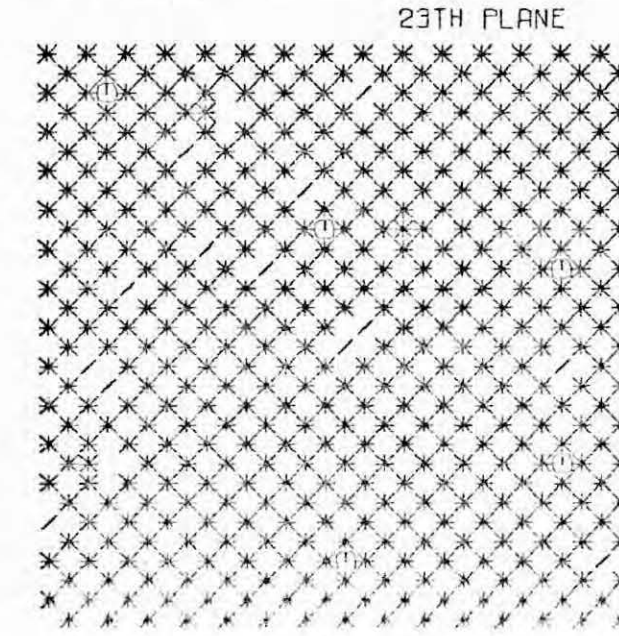
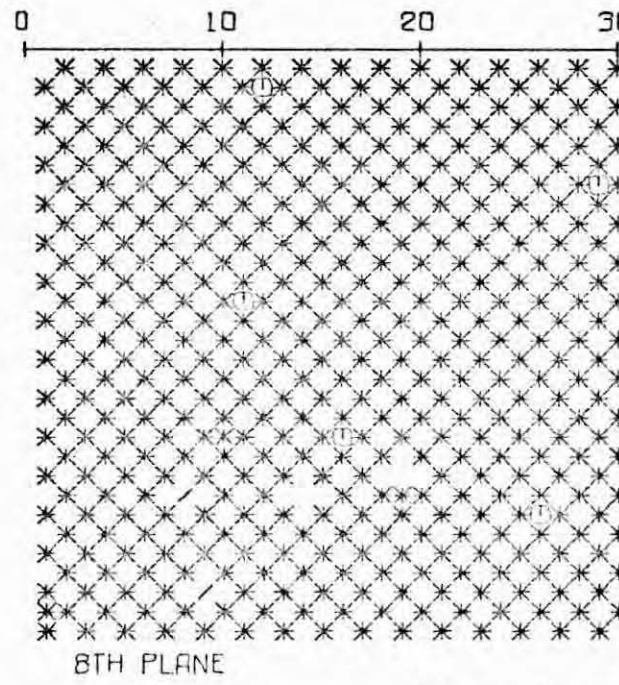
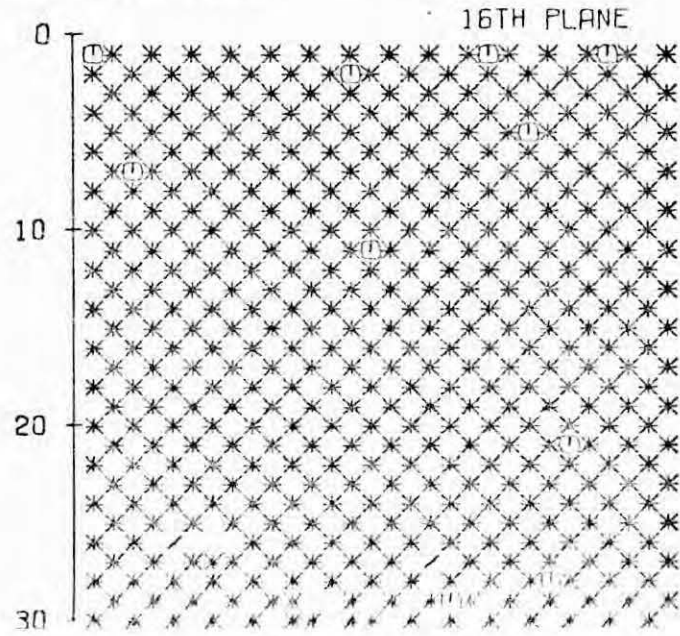
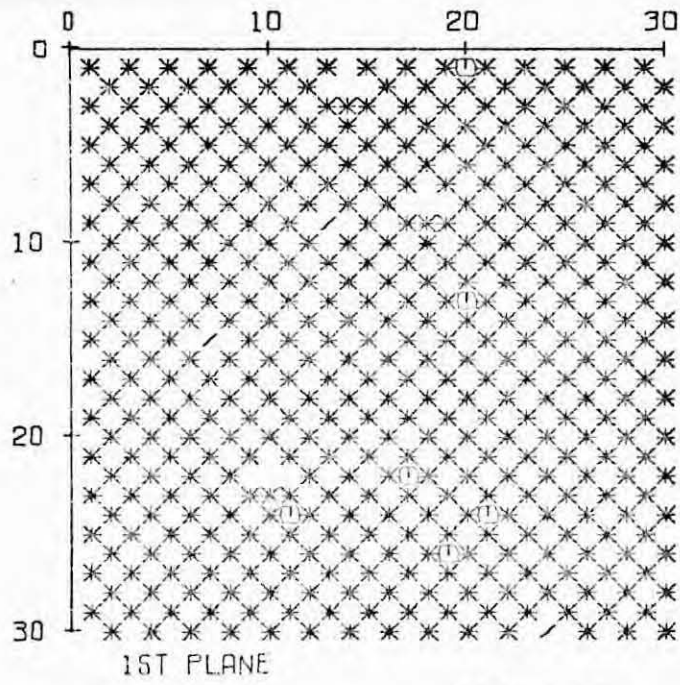


$T/T_c = .59$
 $C = .00$
 TIME=136
 $N=100000$
 $\langle I \rangle = 2.772$

CLUSTERS SIZE NUMBER

10179
57
19
13
10
32
126
460
124
658
177
23
19
13
10
11
12
13
14
15
16
17
18
19
21
22
23
27
26
27
29
30
33
43
62
69
71
95

Fig. B37

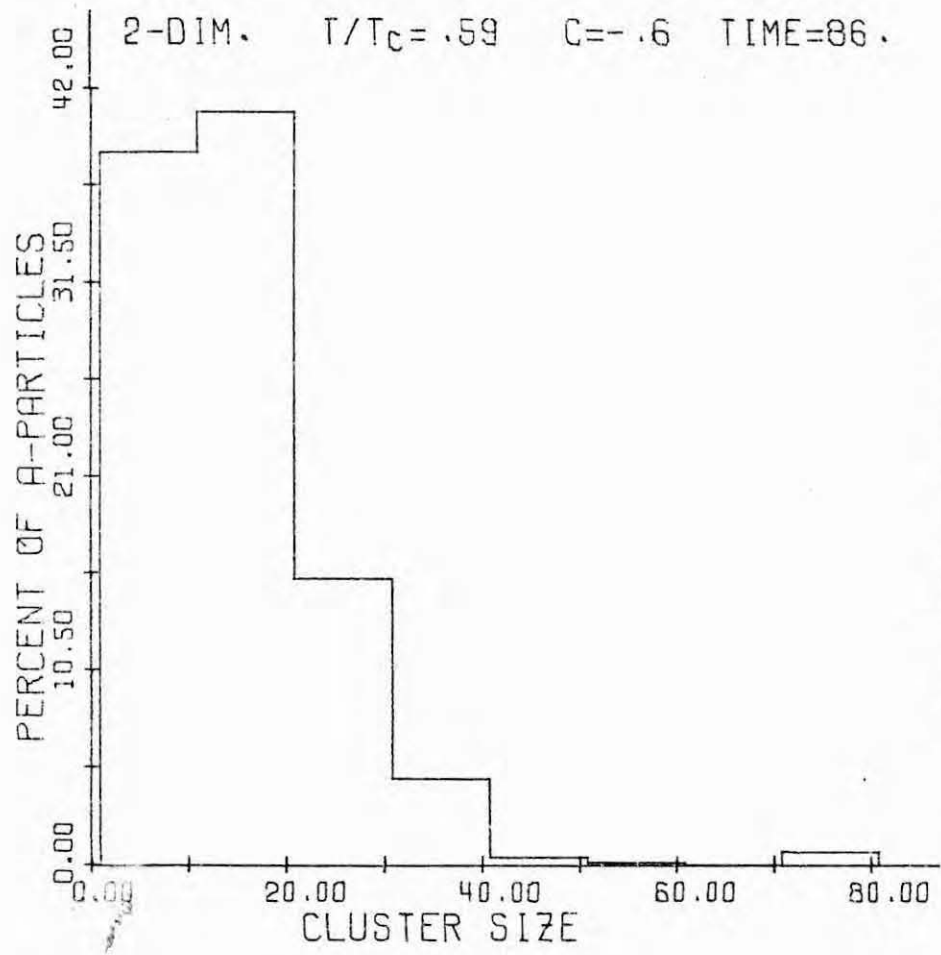


$T/T_c = .59$
 $C = .00$
 TIME=900
 $N=150000$
 $U = 2.917$

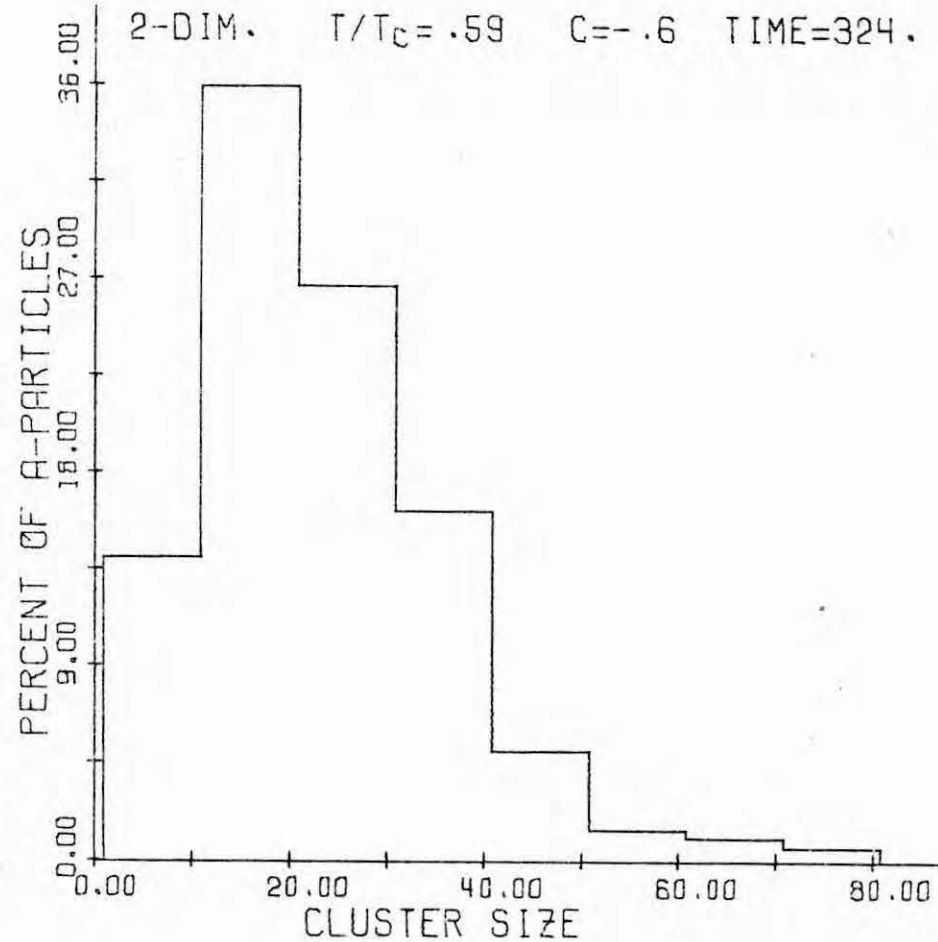
CLUSTERS
SIZE NUMBER

1	12212
5	80
6	30
7	113
9	1
10	11
11	12
12	13
13	14
14	15
15	16
16	2

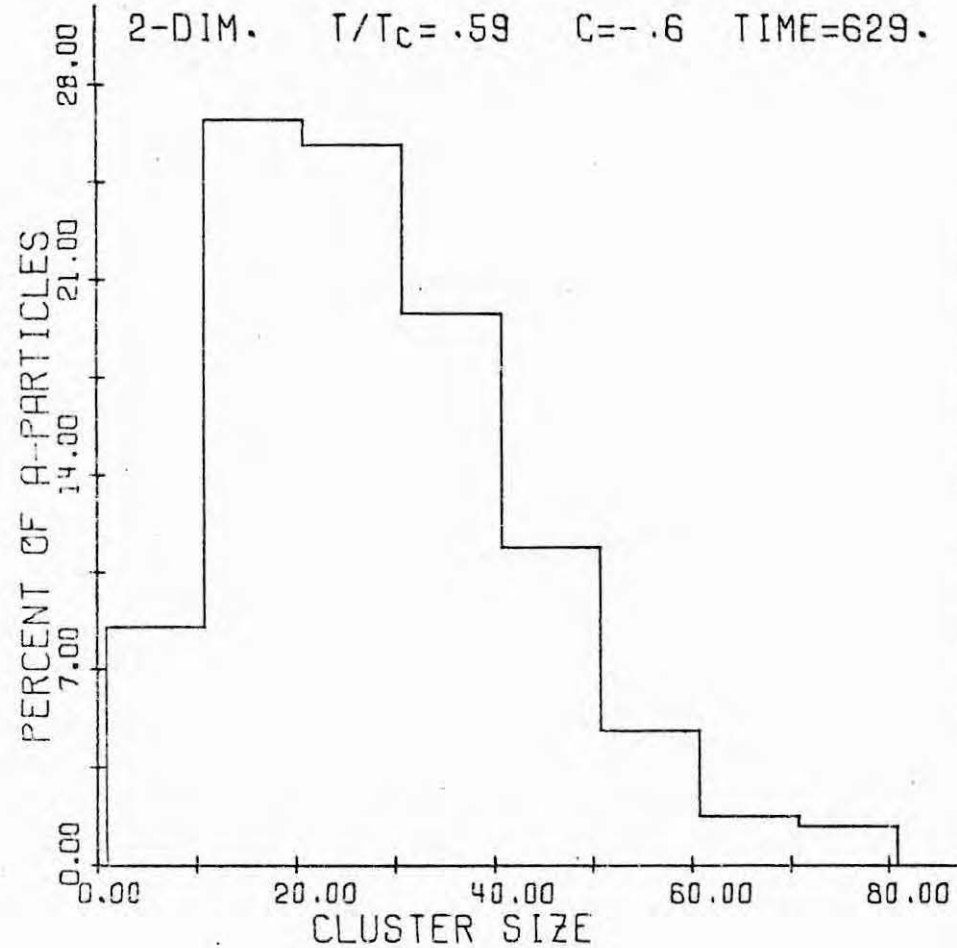
Fig. B38



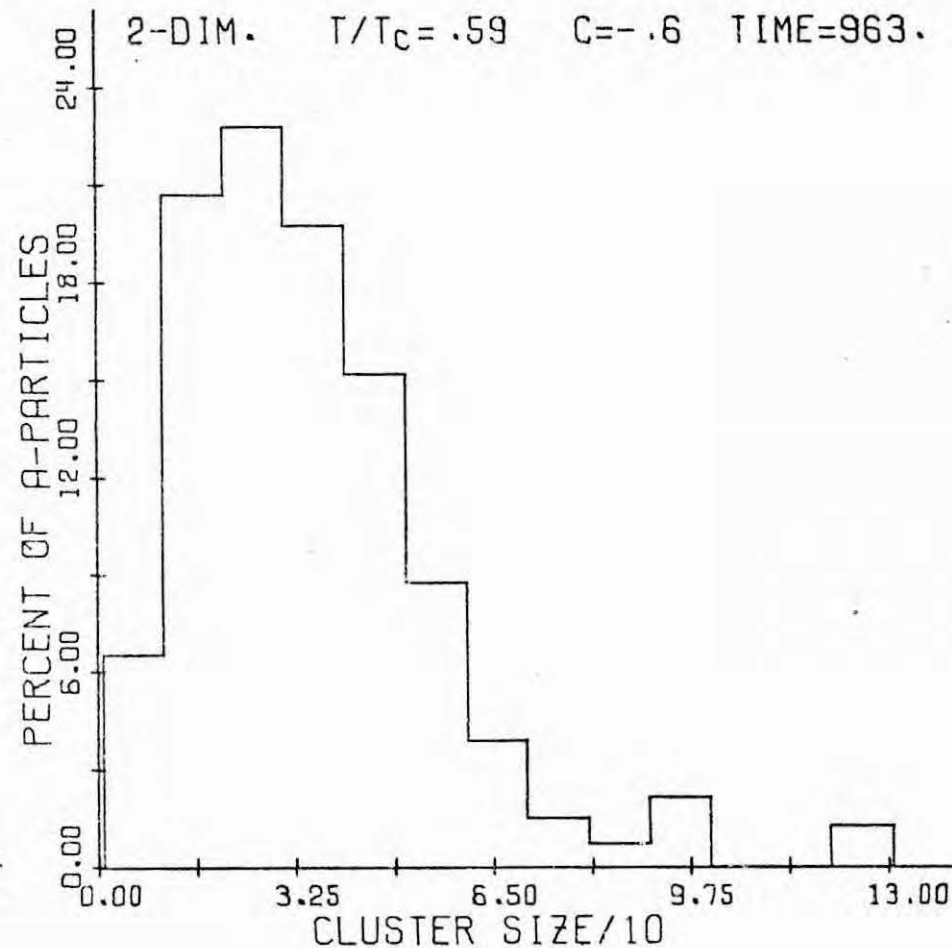
c.1



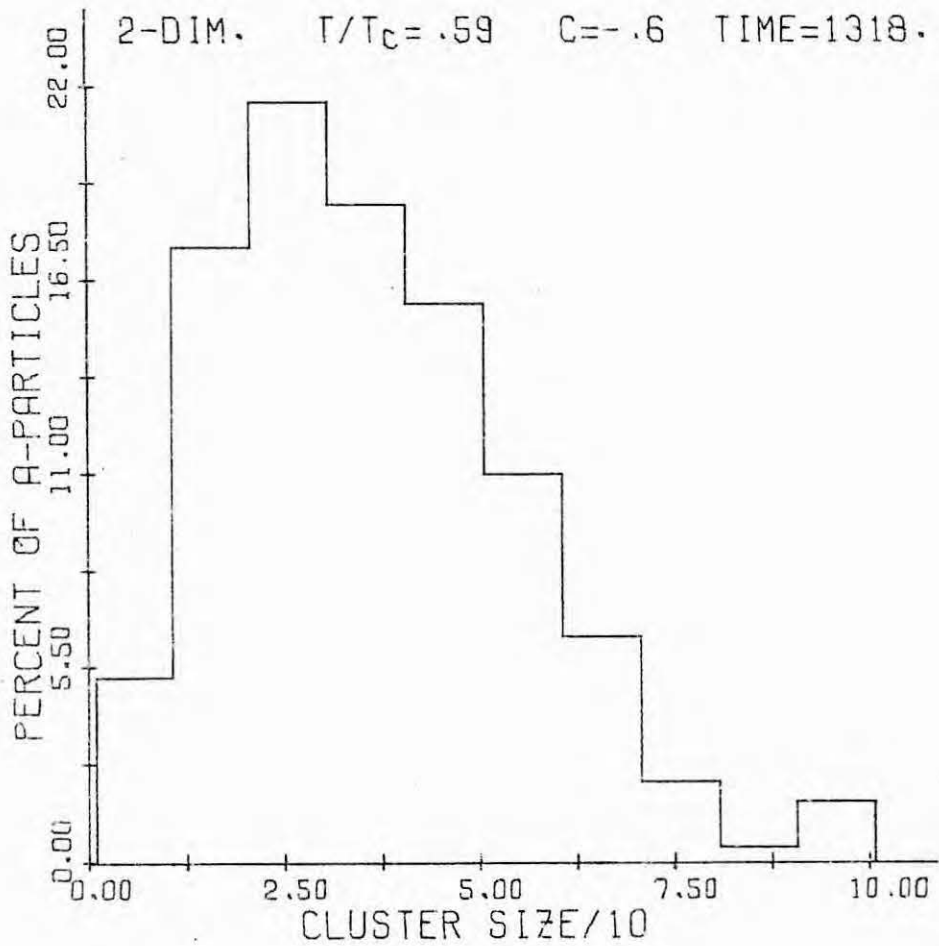
c.2



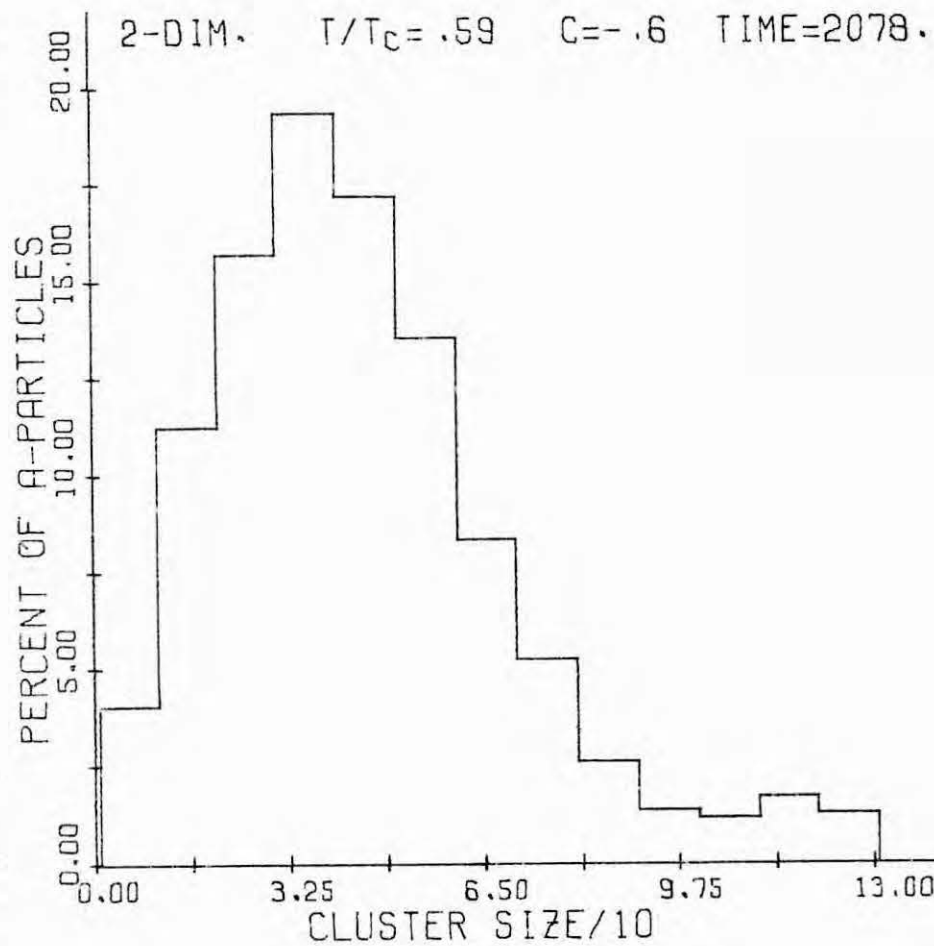
c.3



c.4

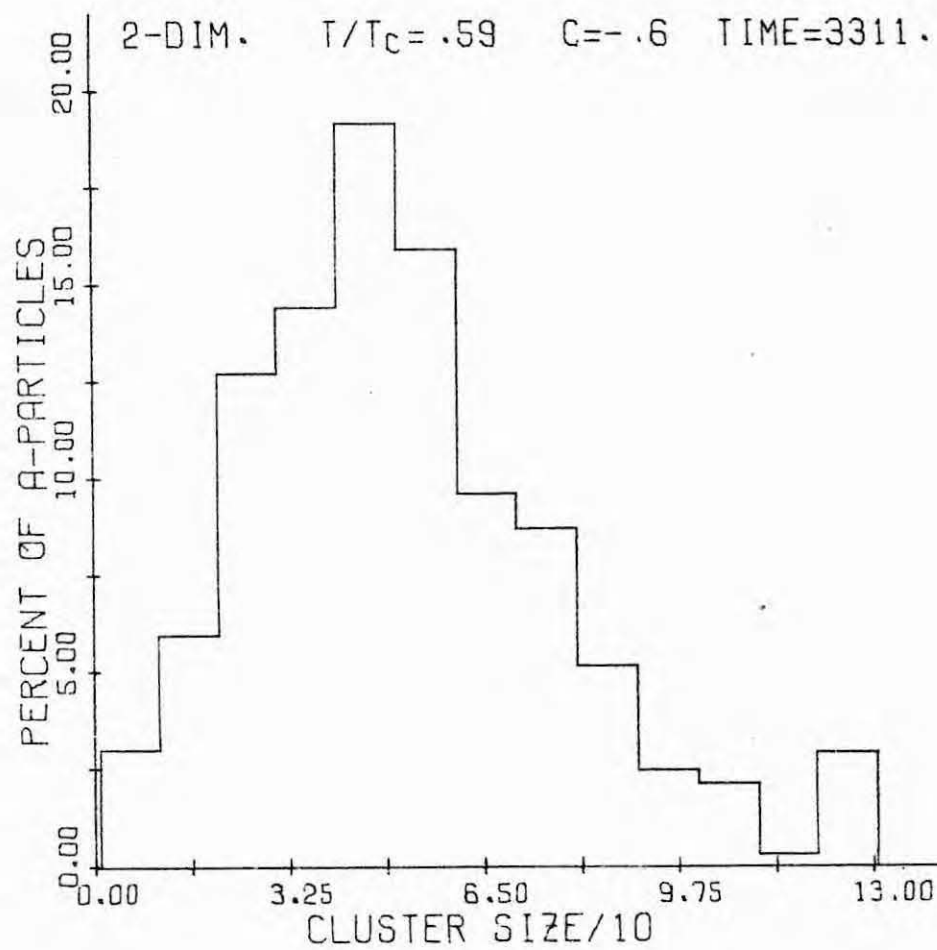
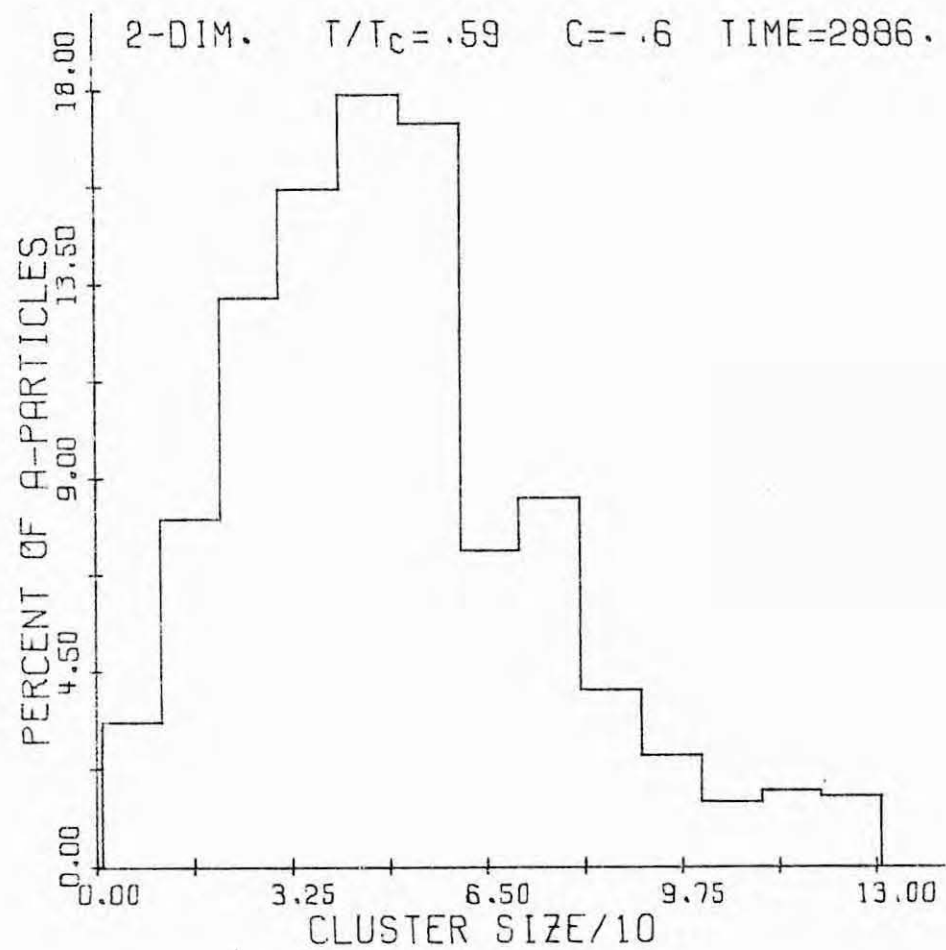


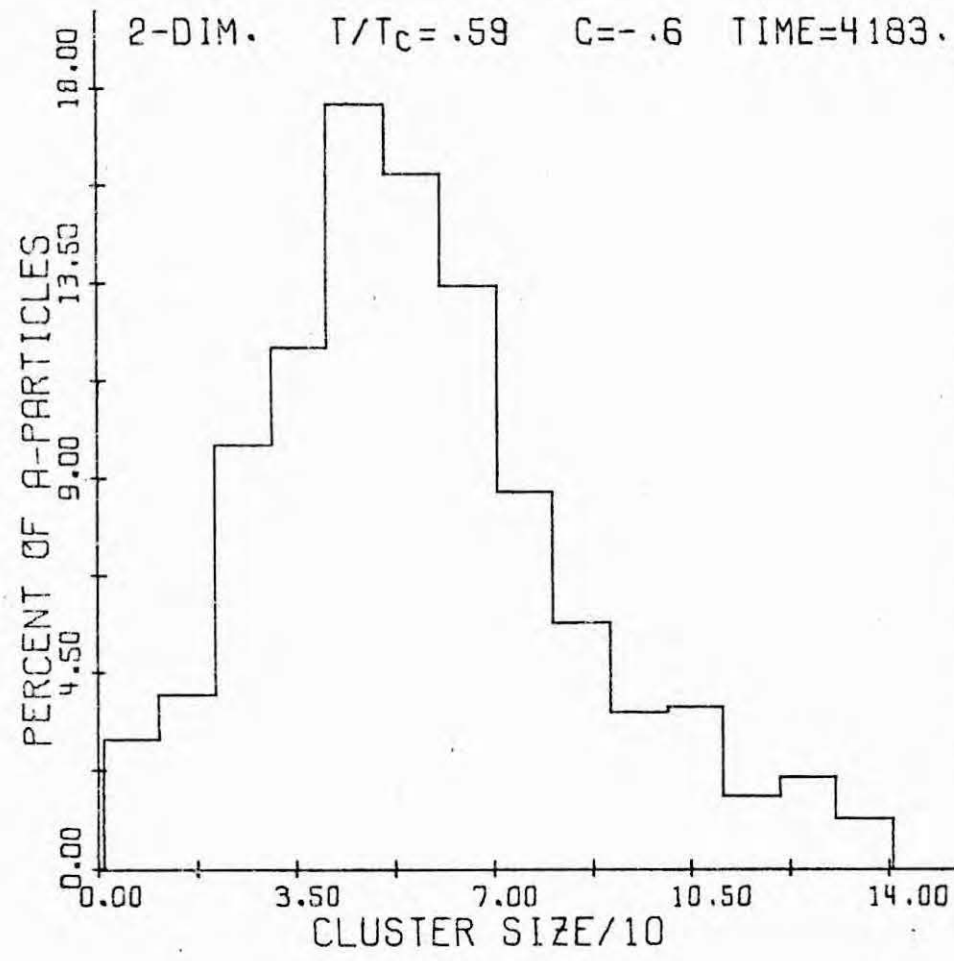
C.5



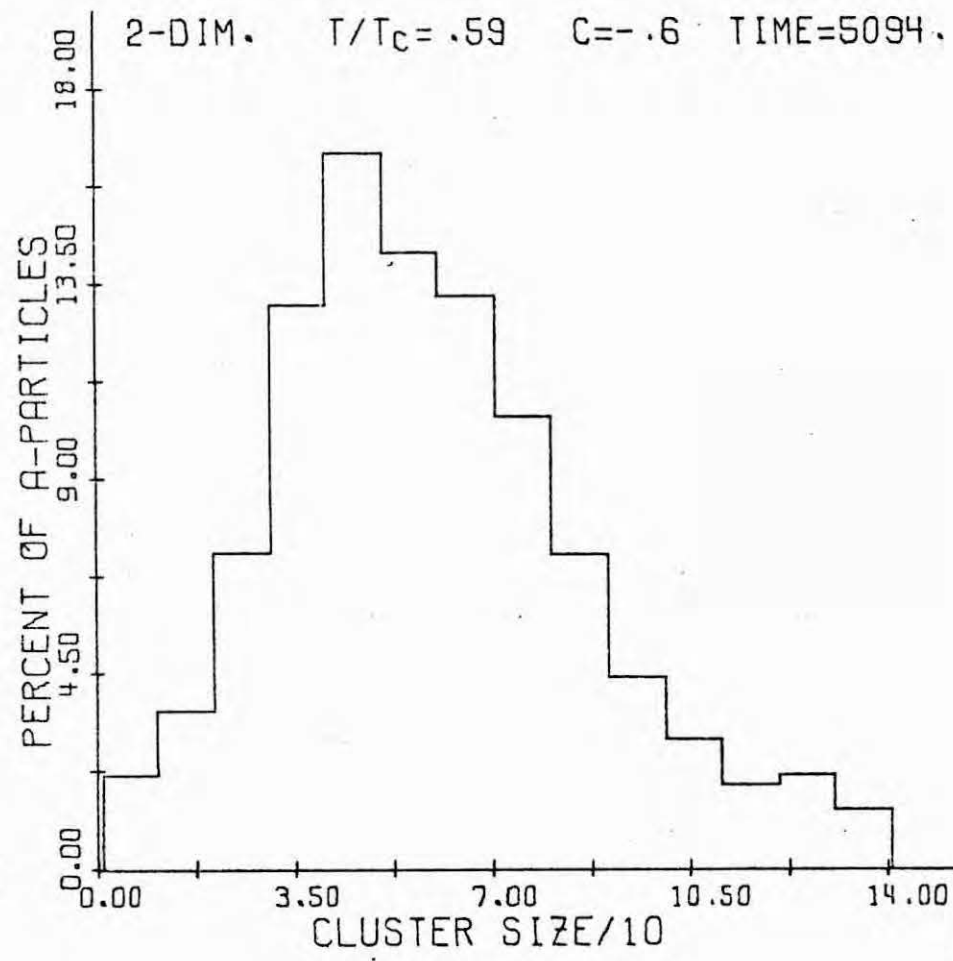
277

C.6

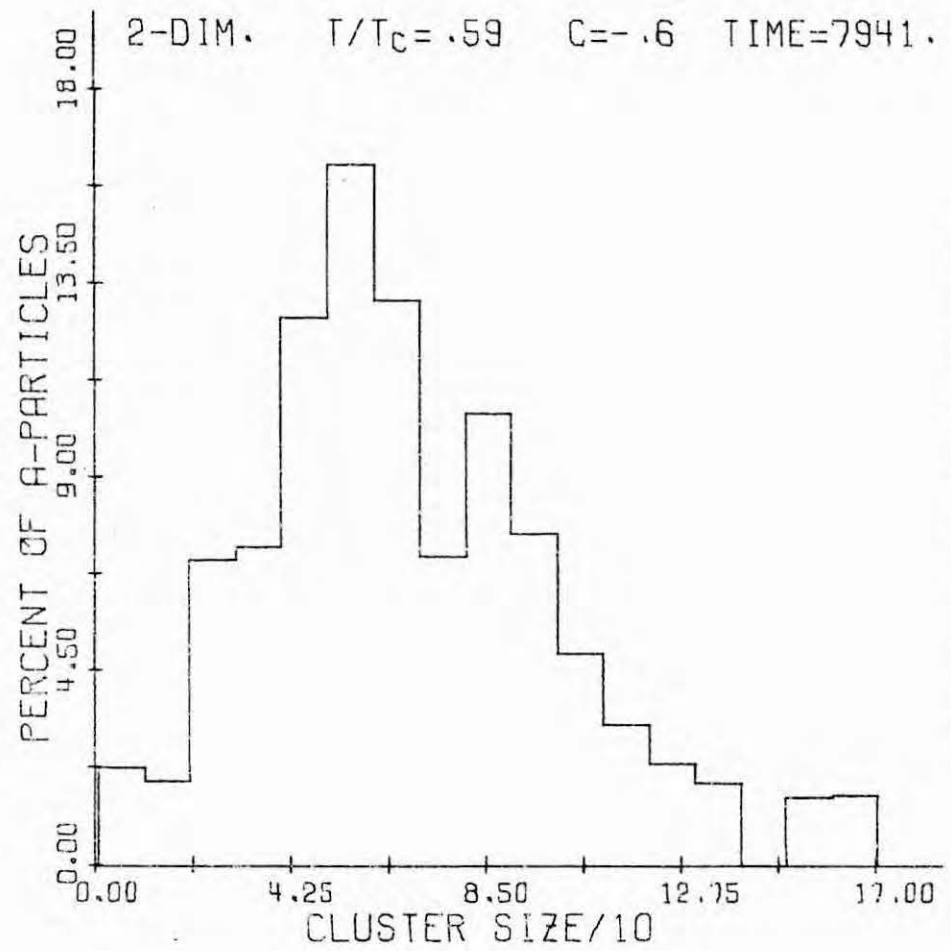




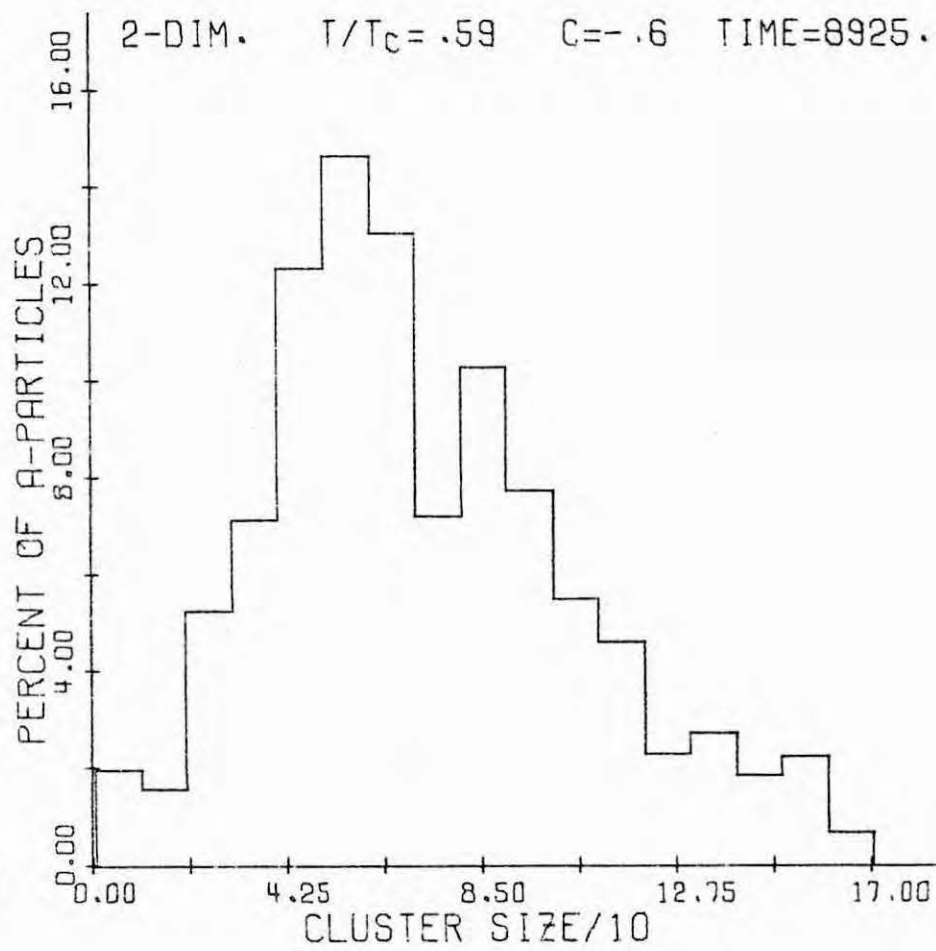
c.9



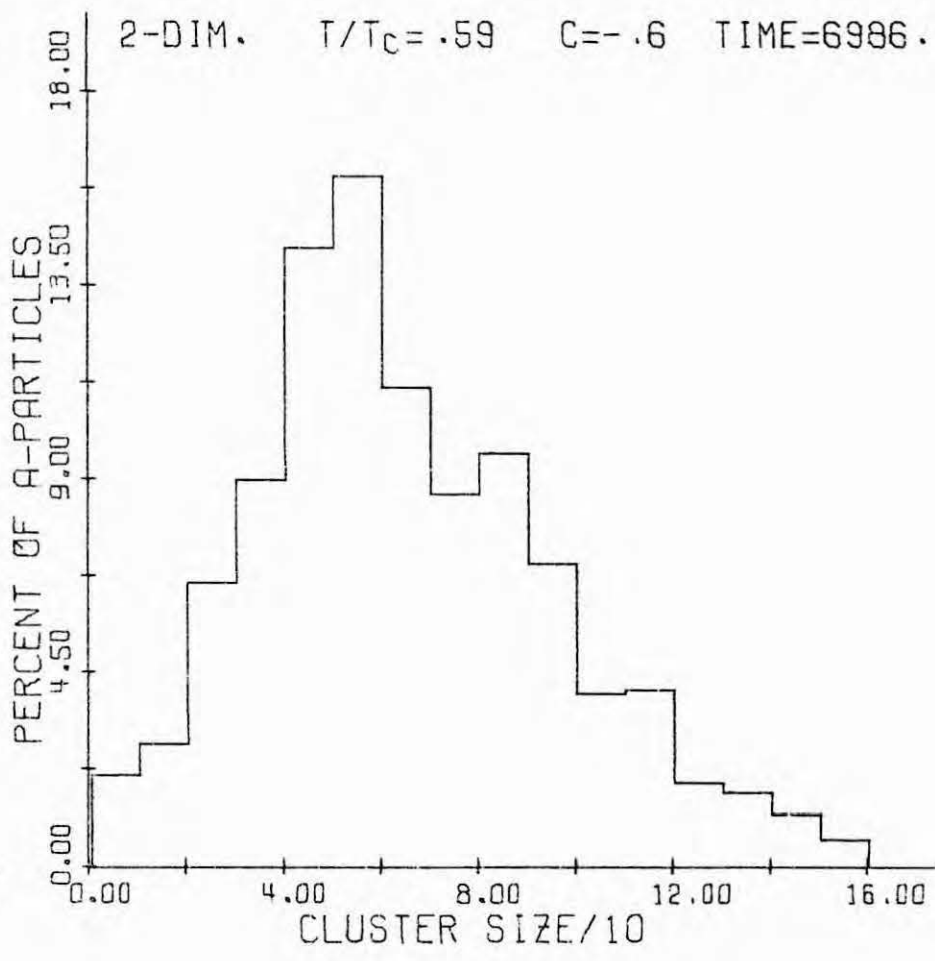
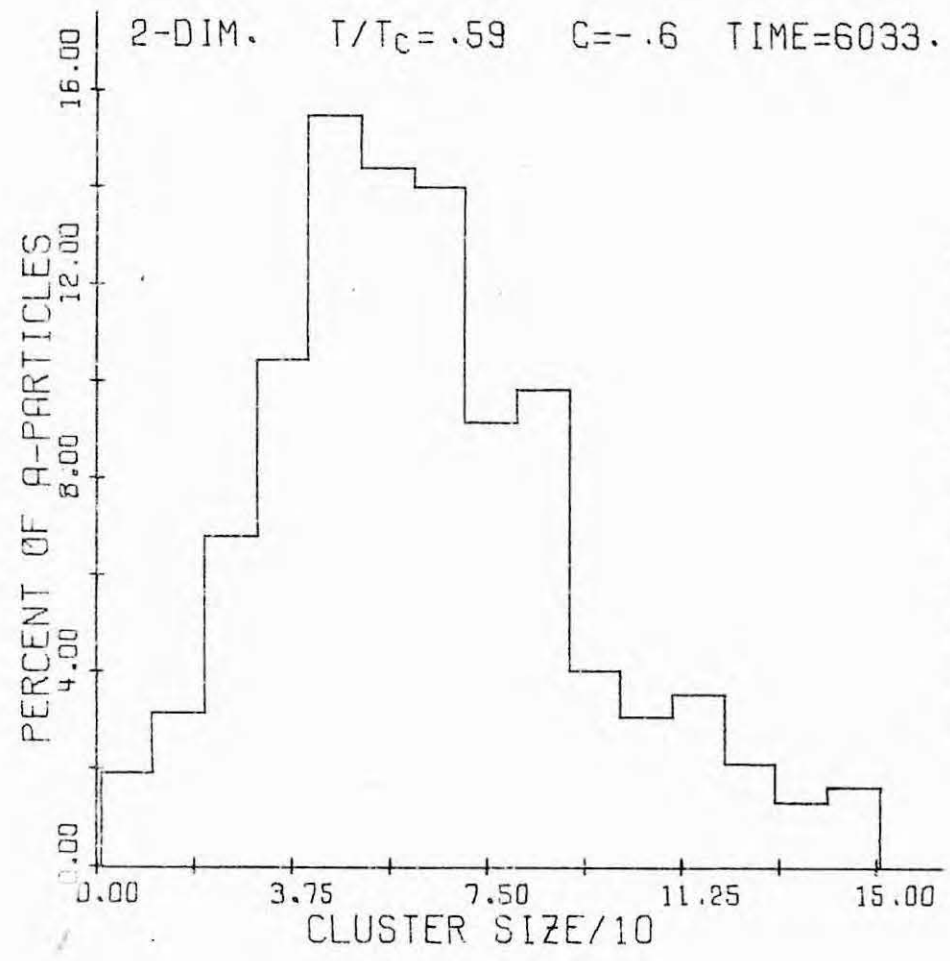
c.10

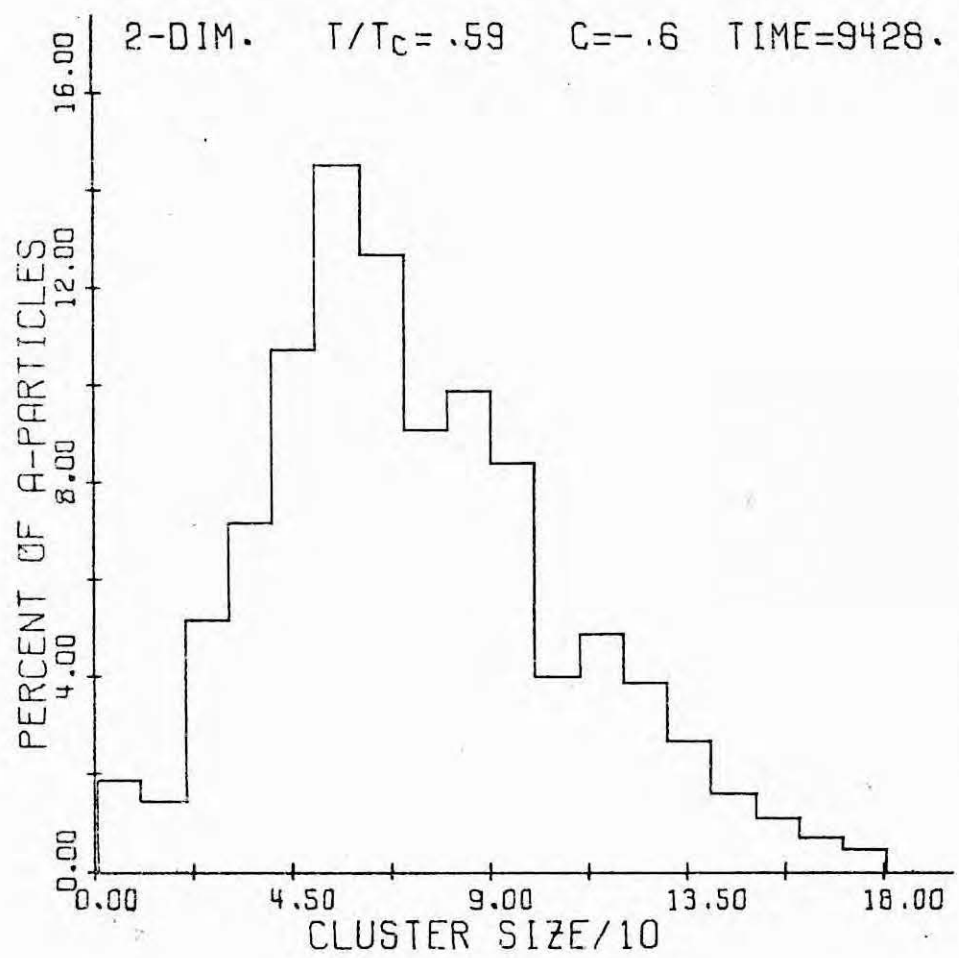


c.13

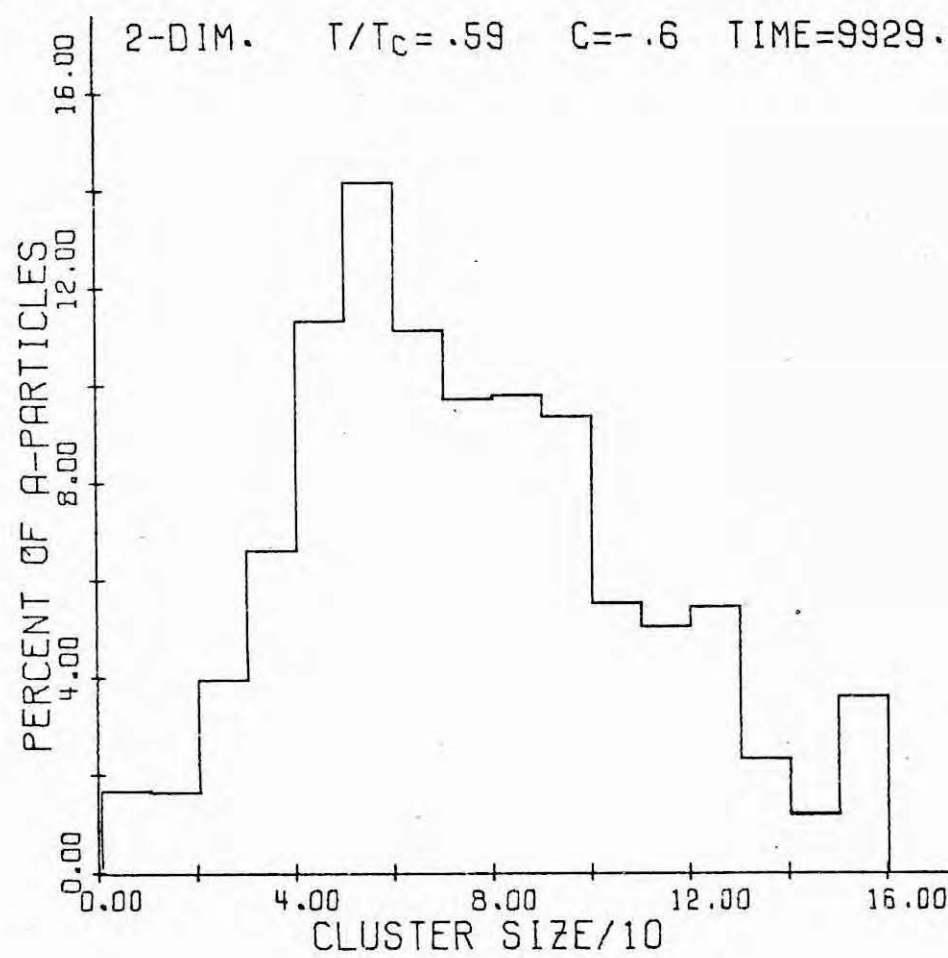


c.14

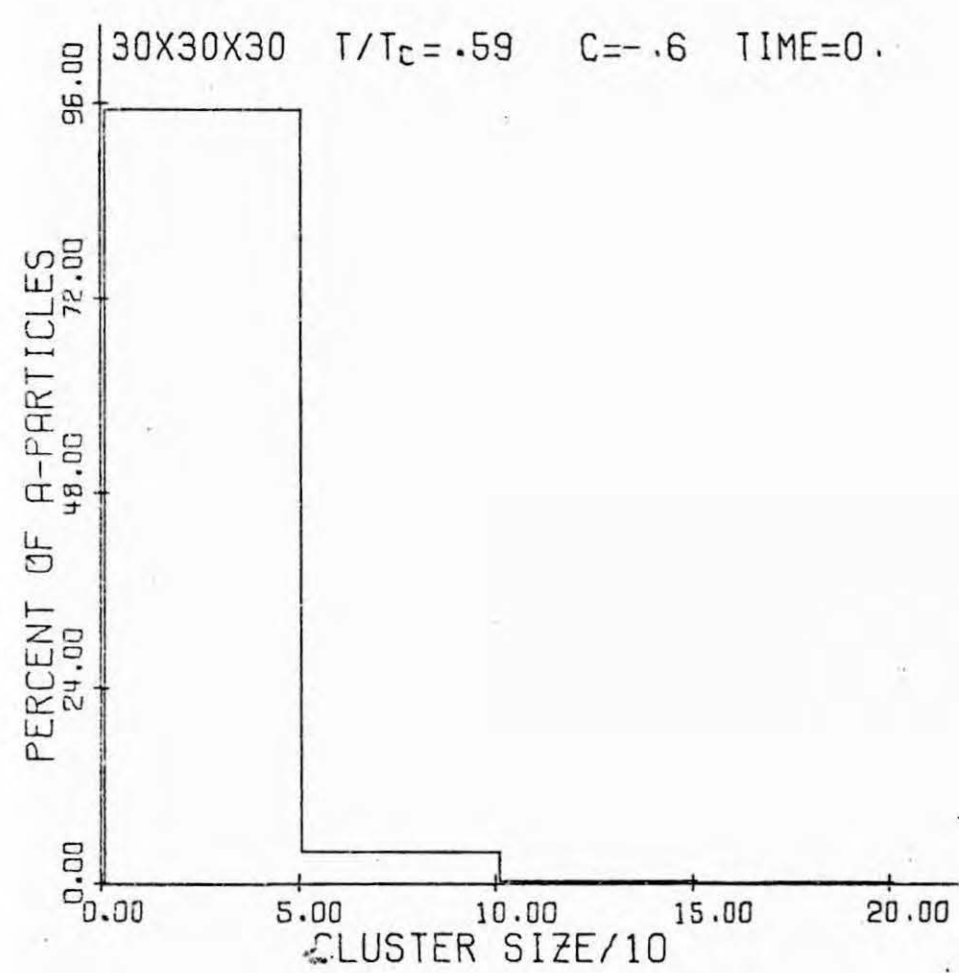




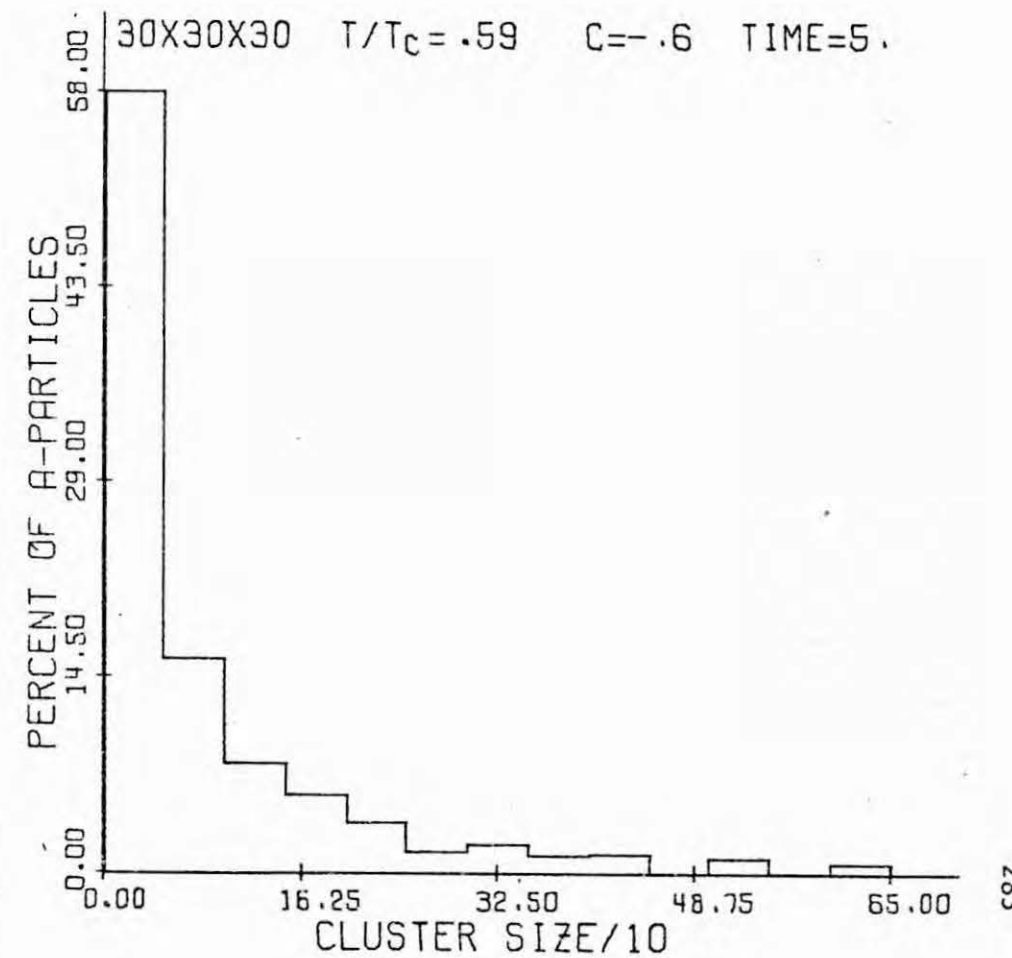
C.15



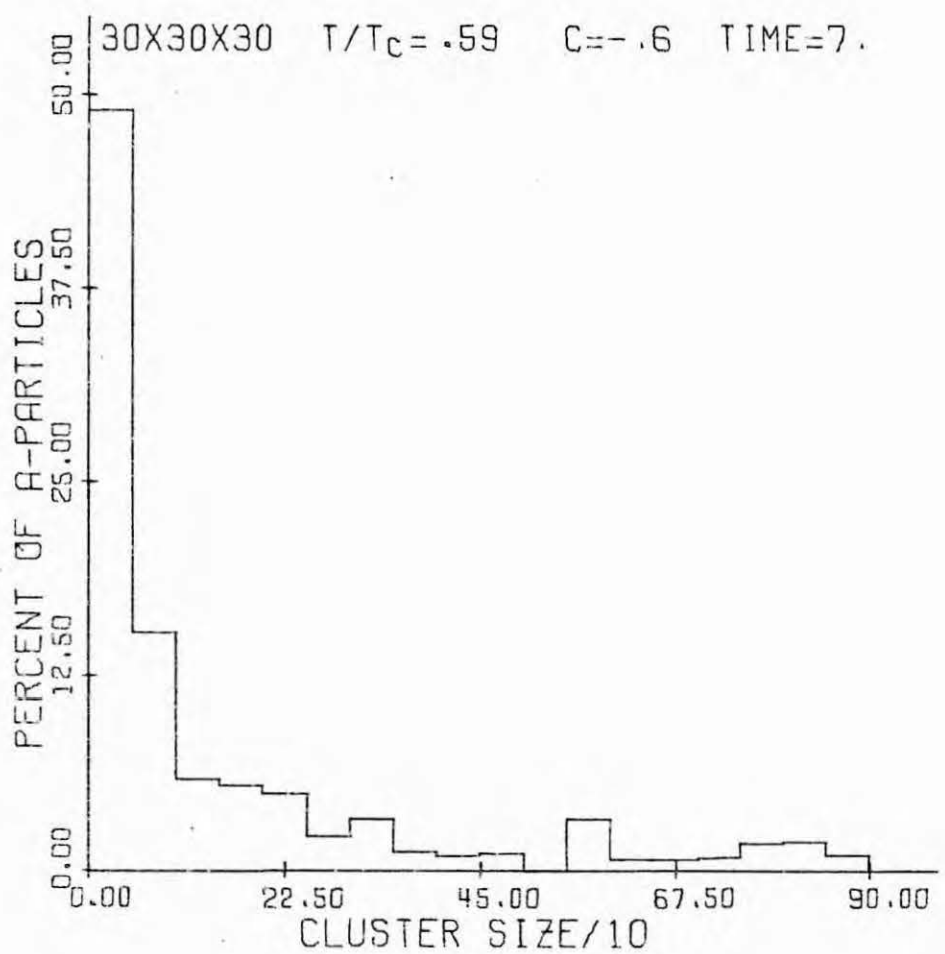
C.16



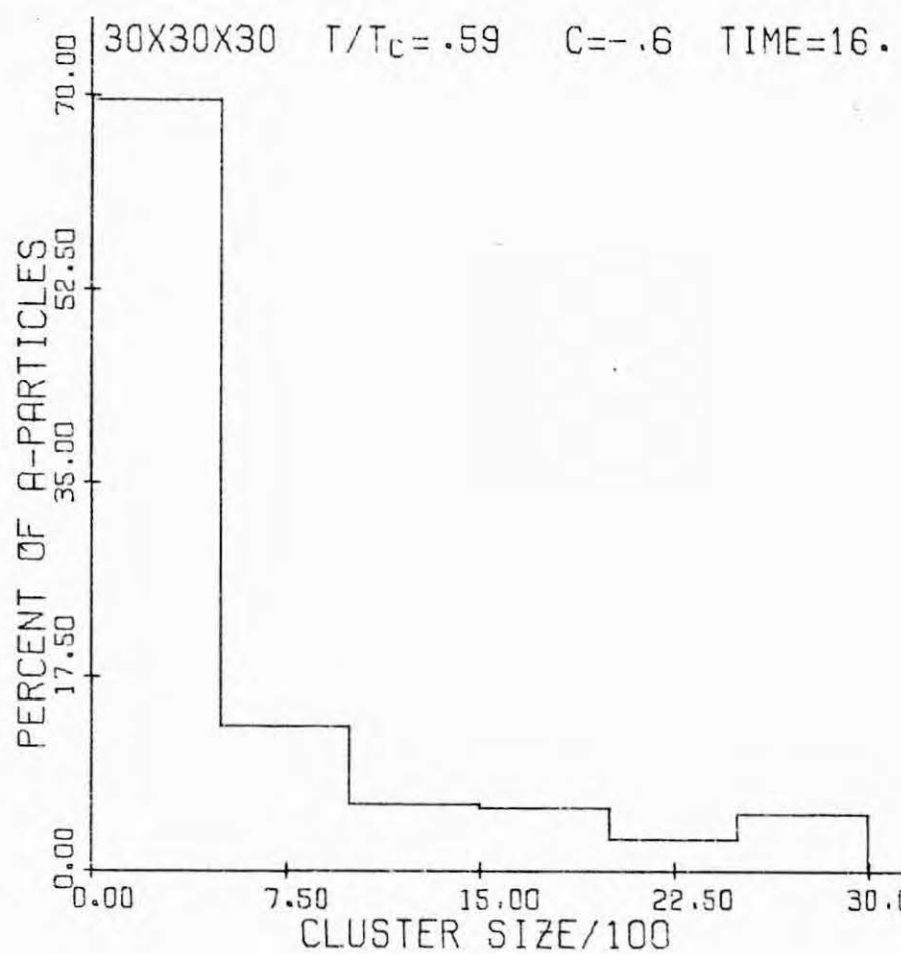
c.17



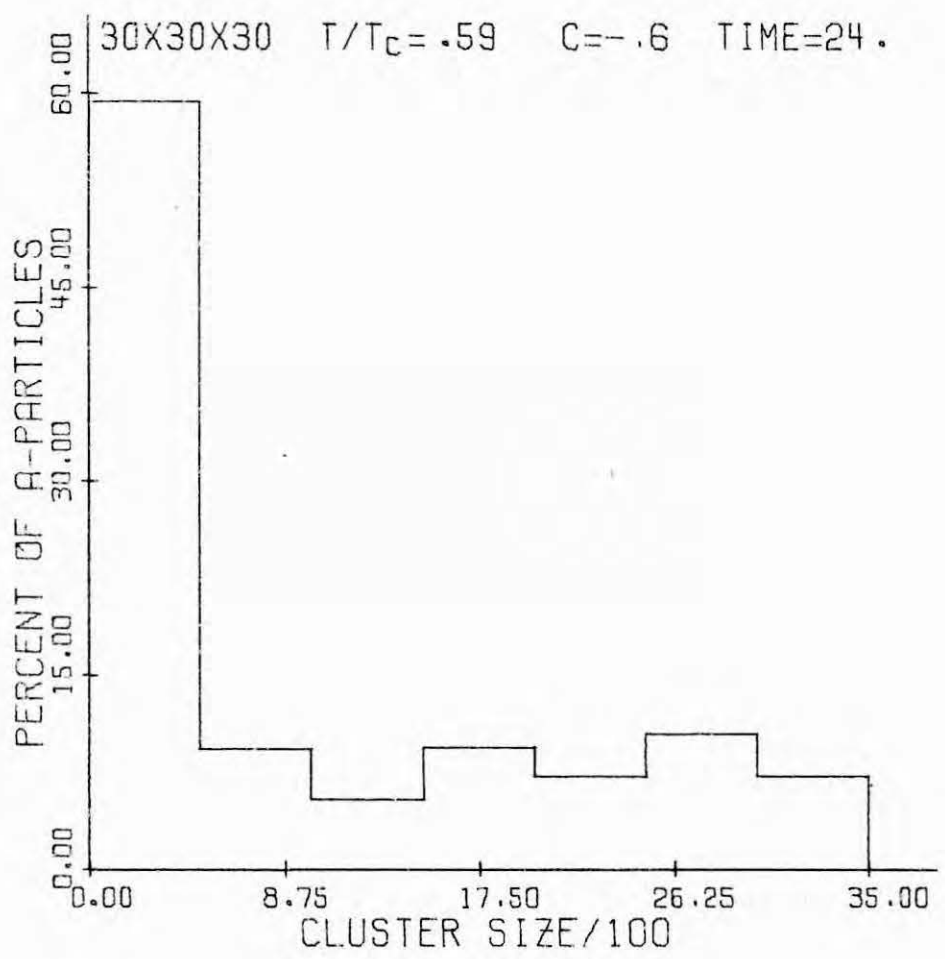
c.18



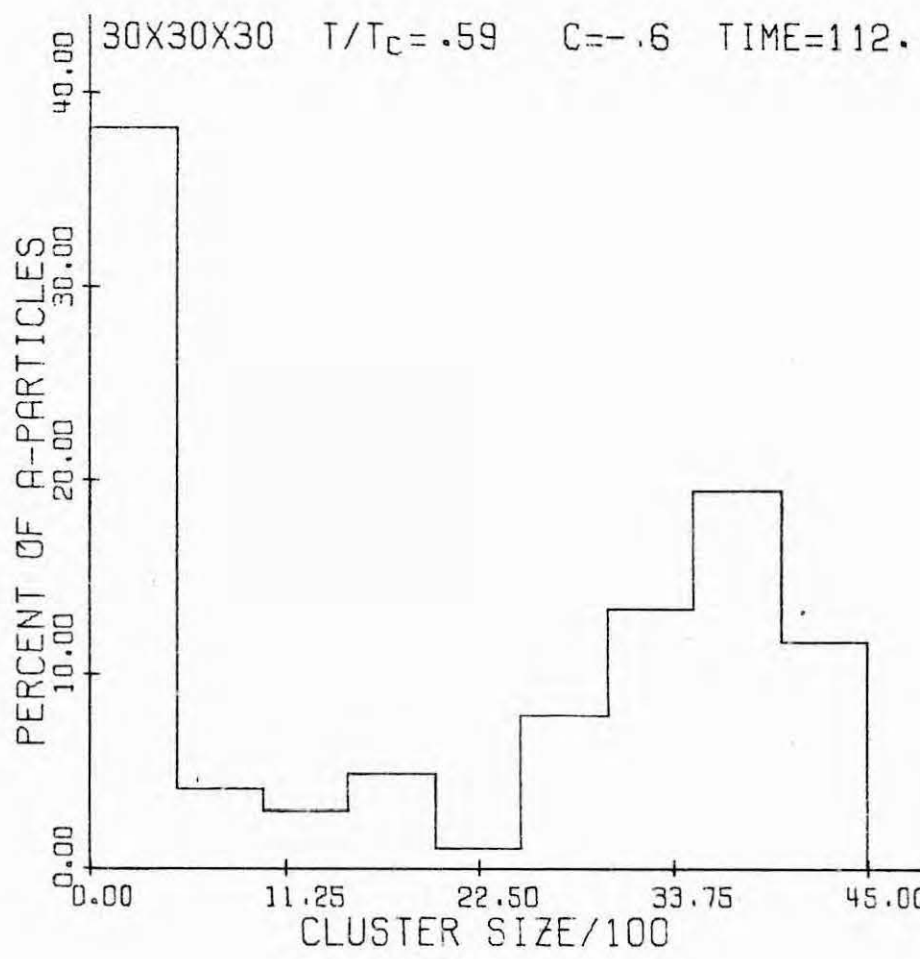
c.19



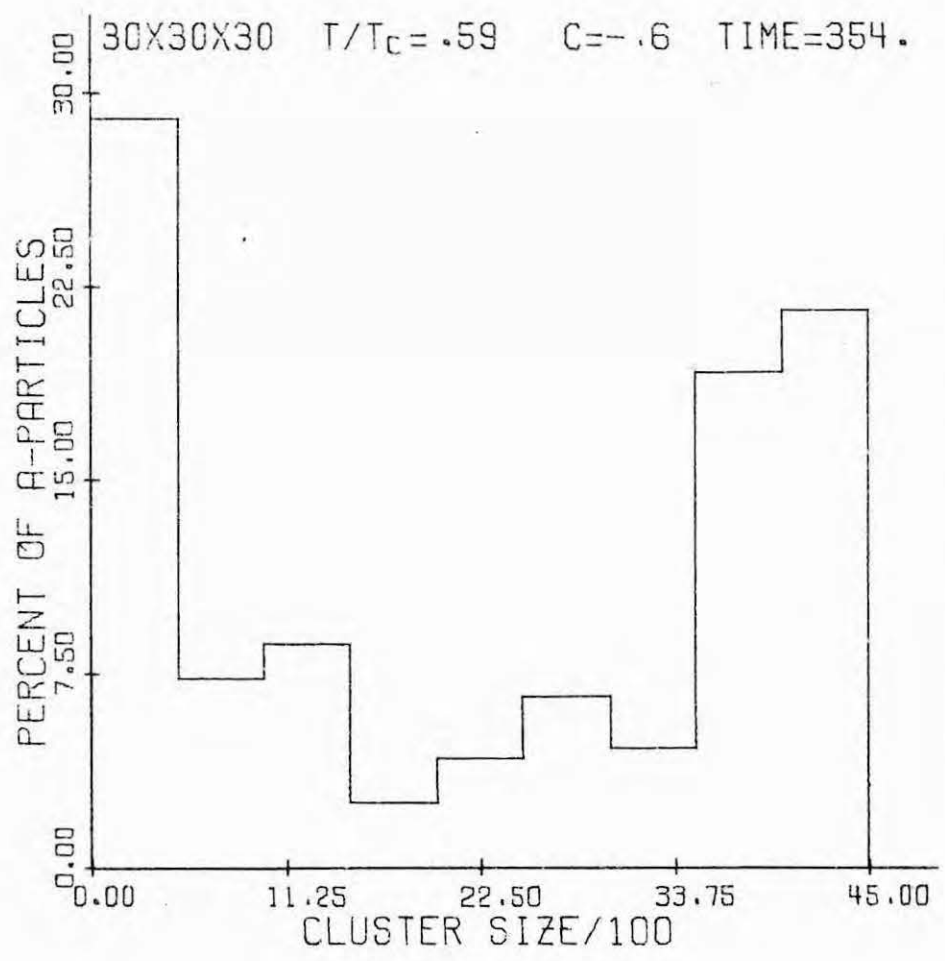
c.20



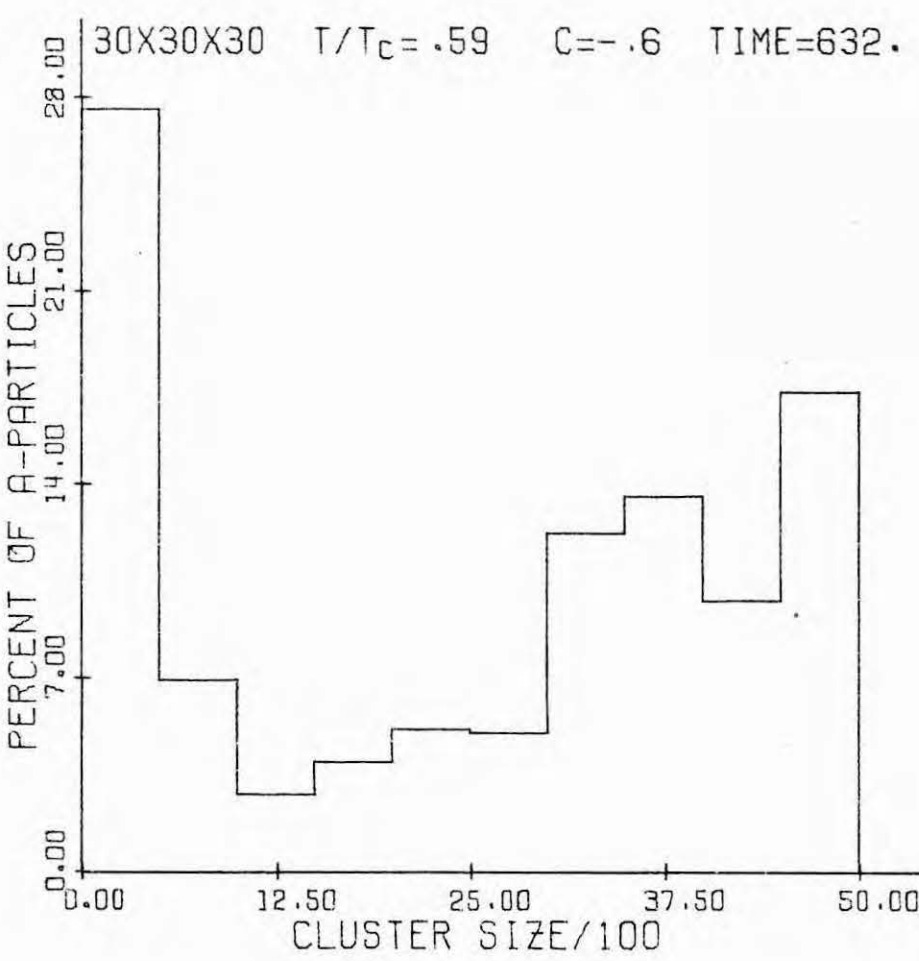
C.21



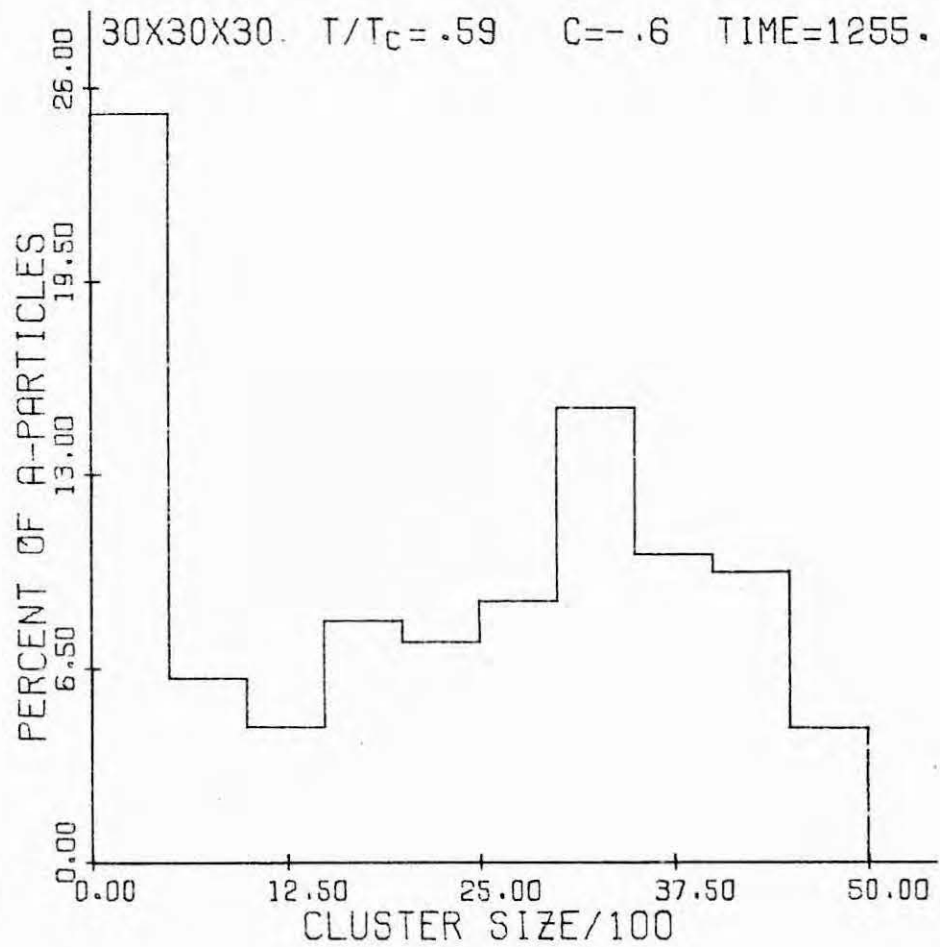
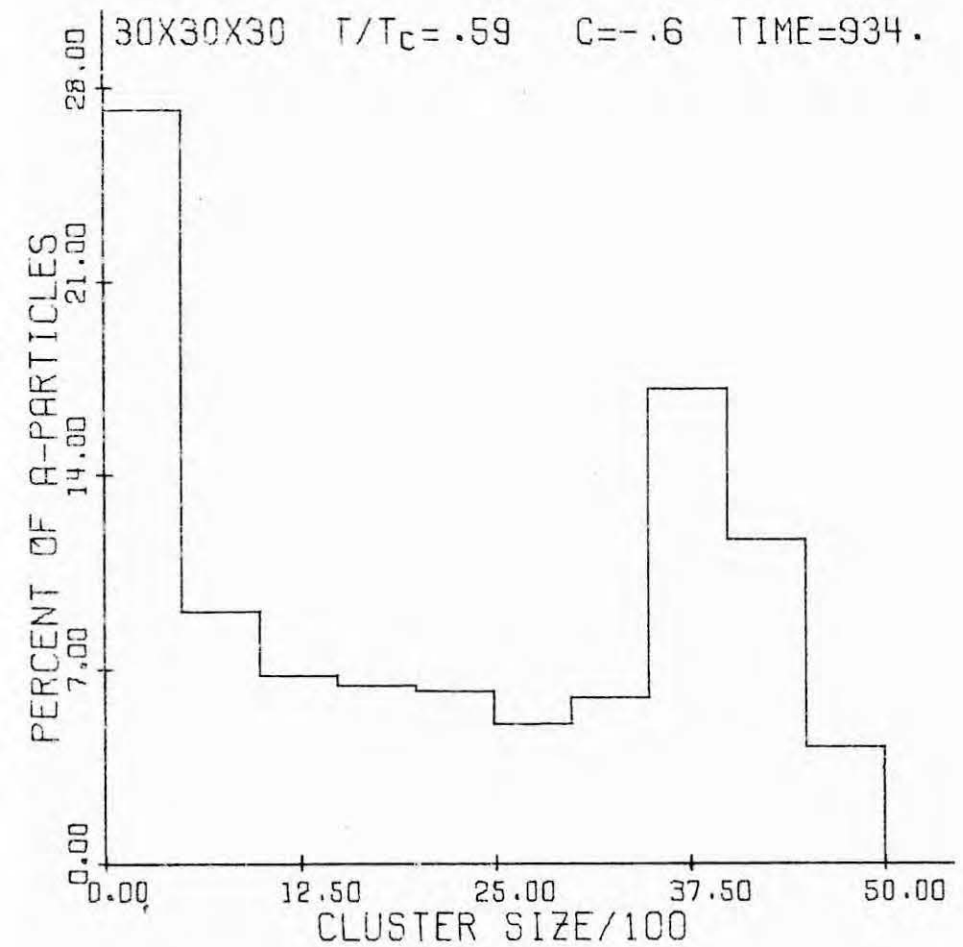
C.22

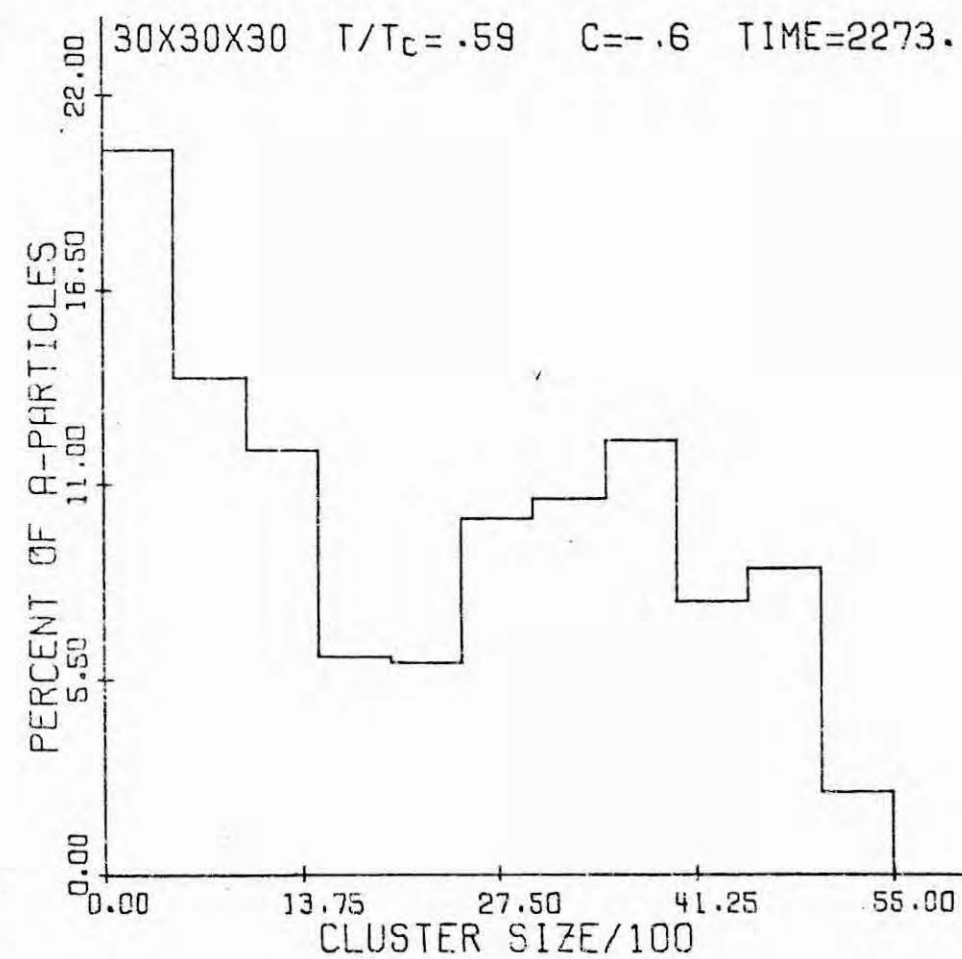
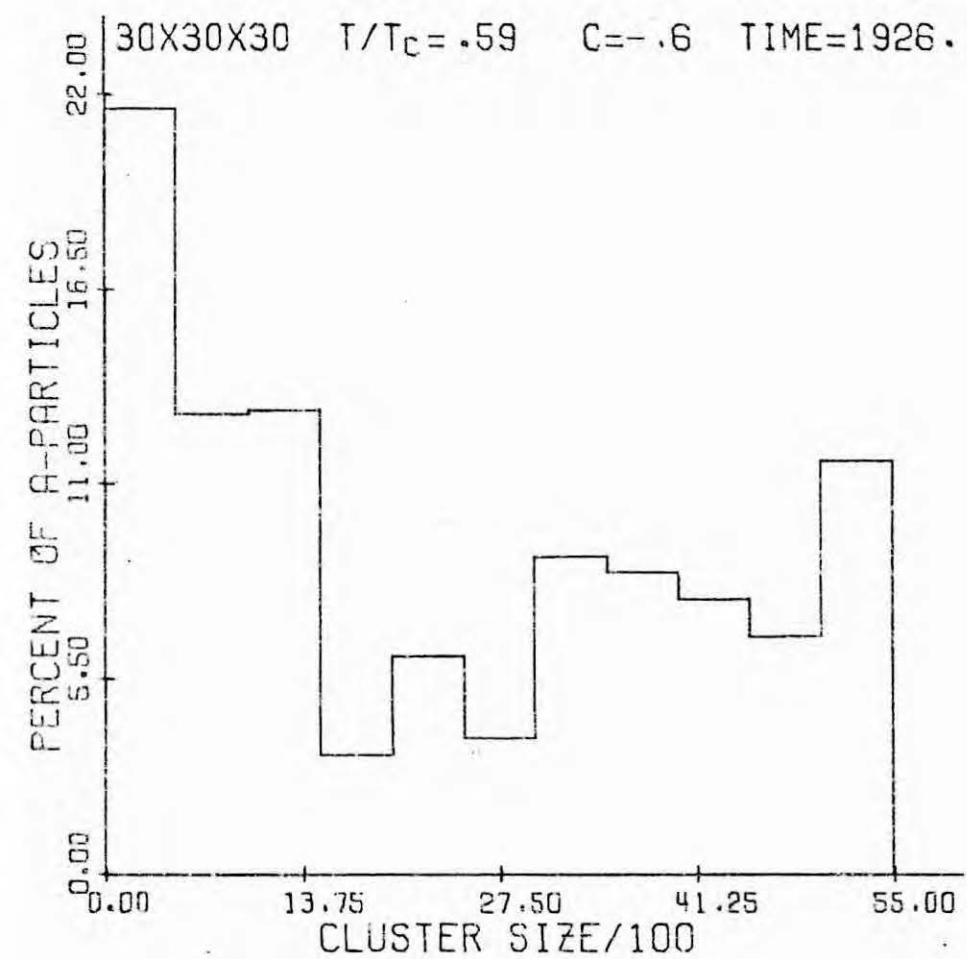


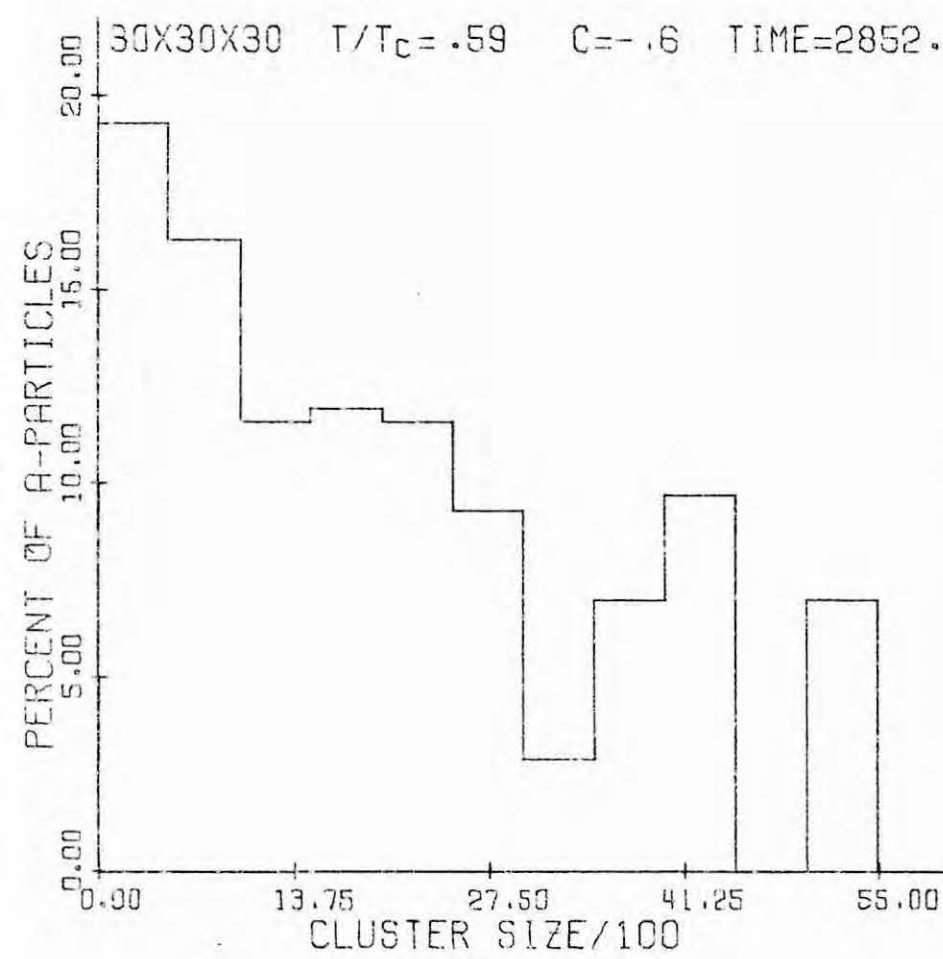
c.23



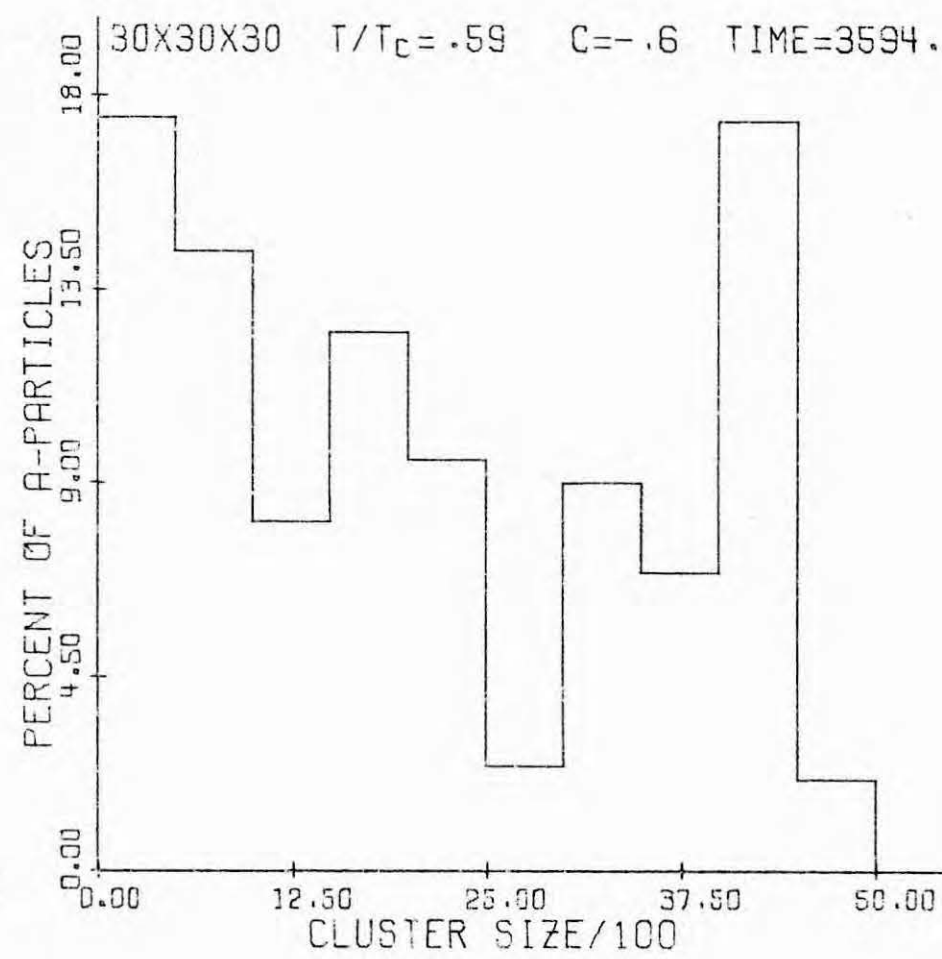
c.24



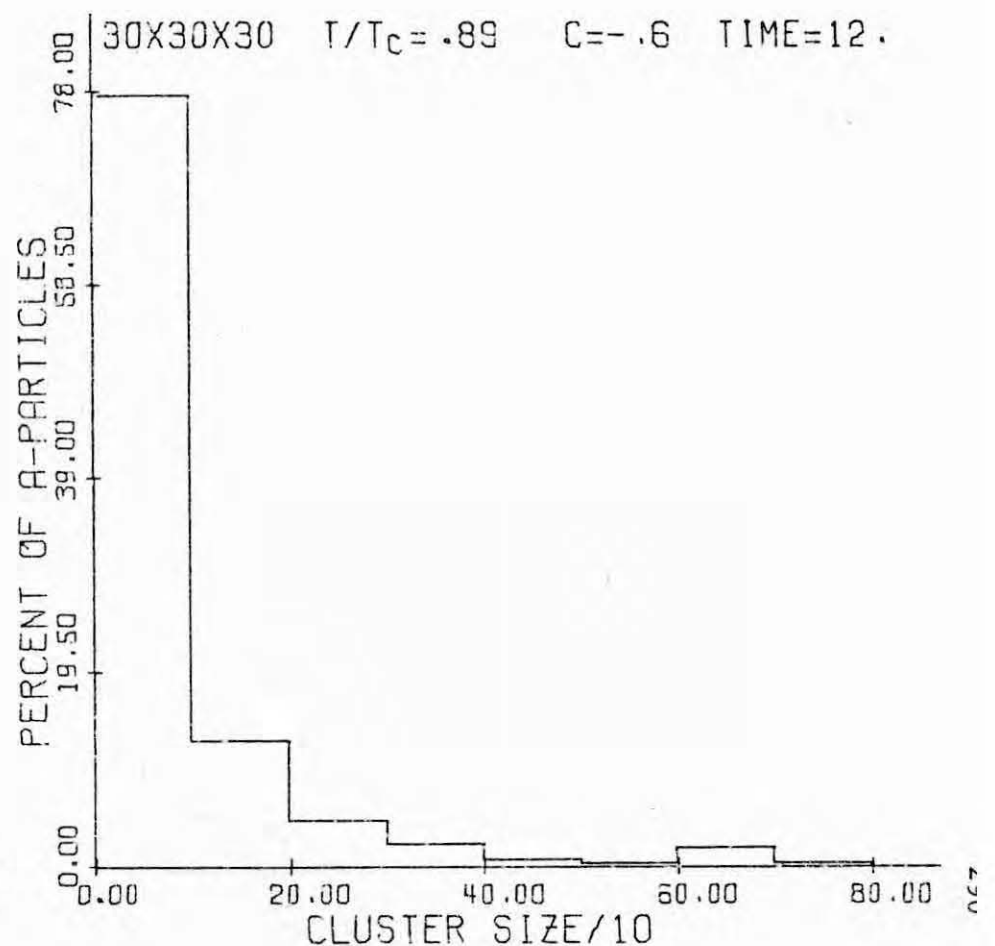
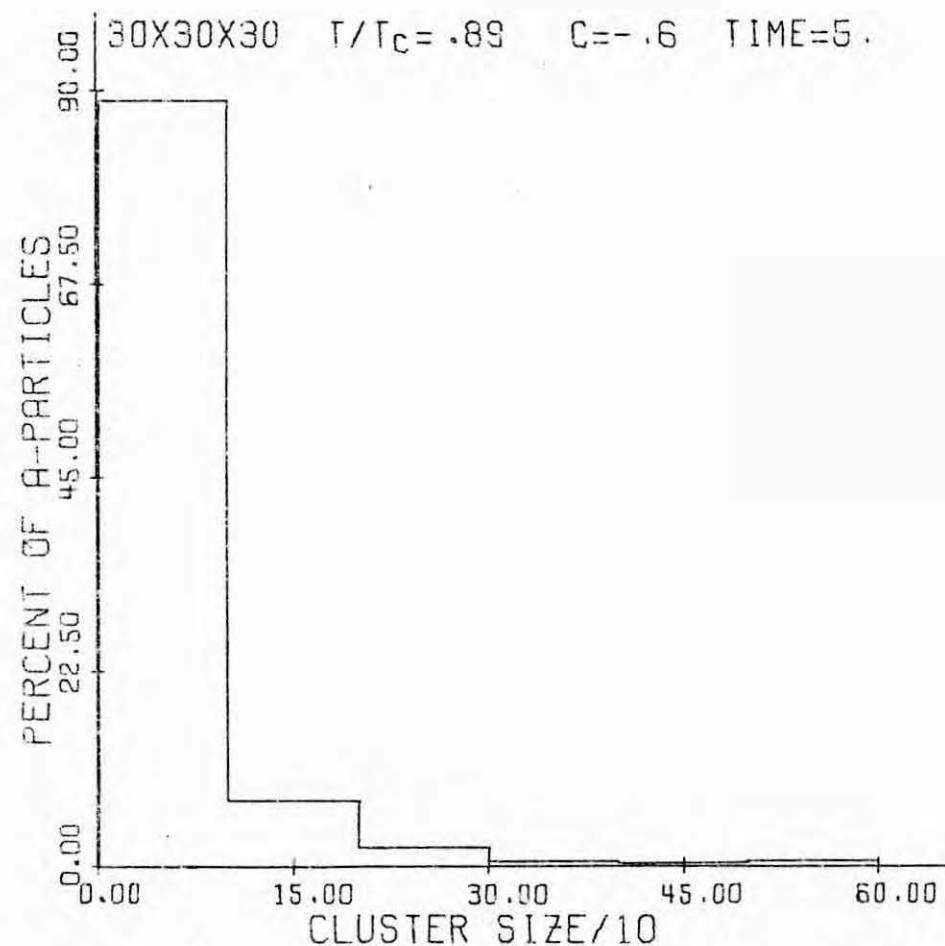


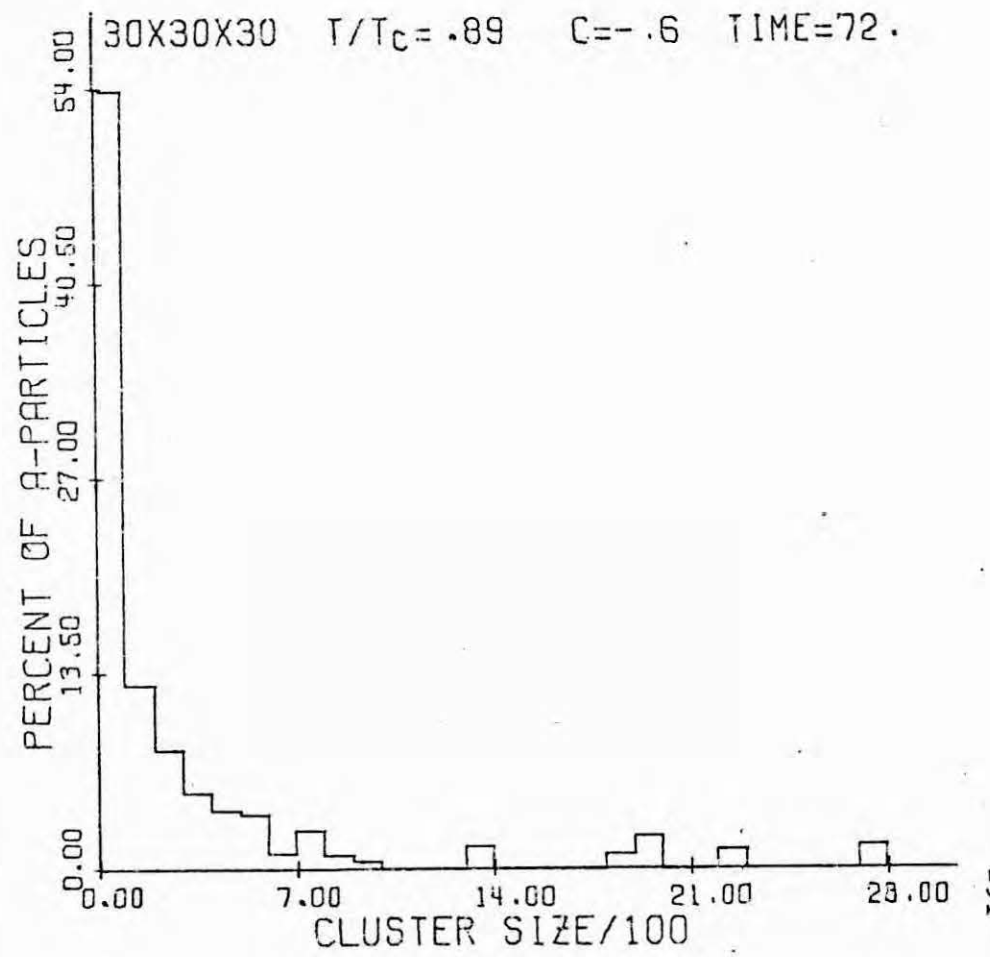
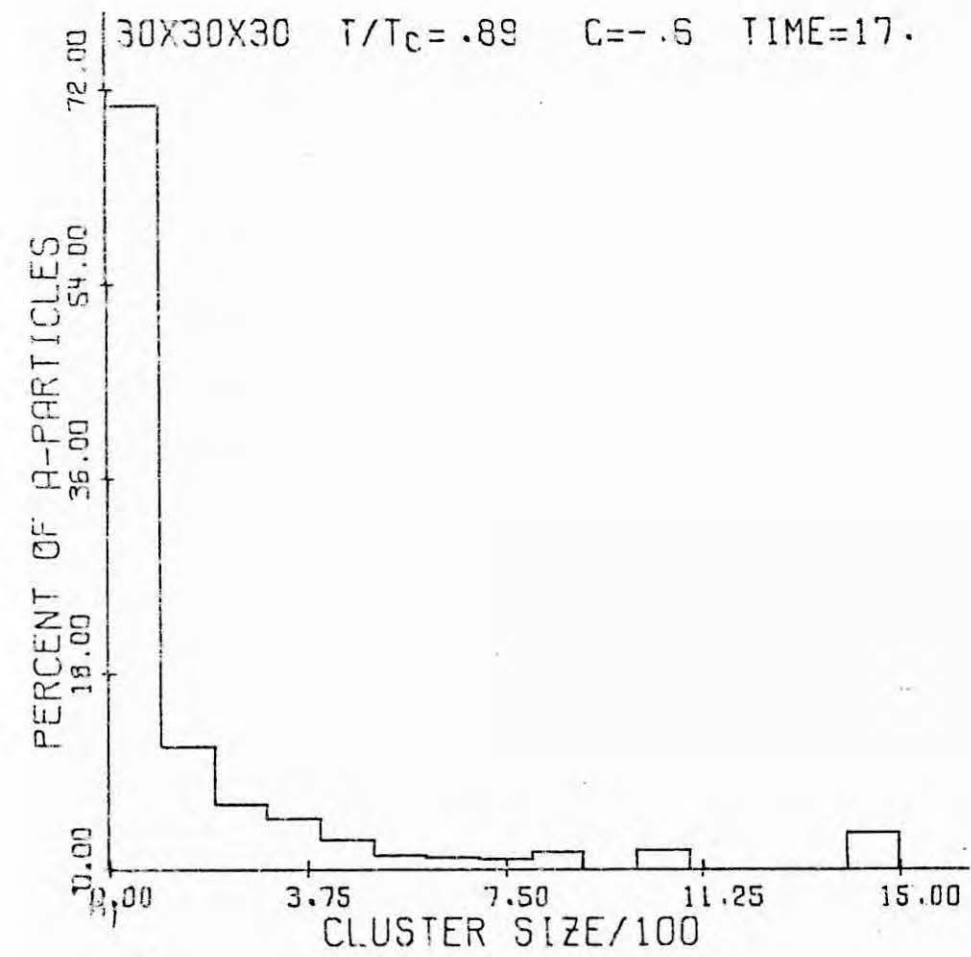


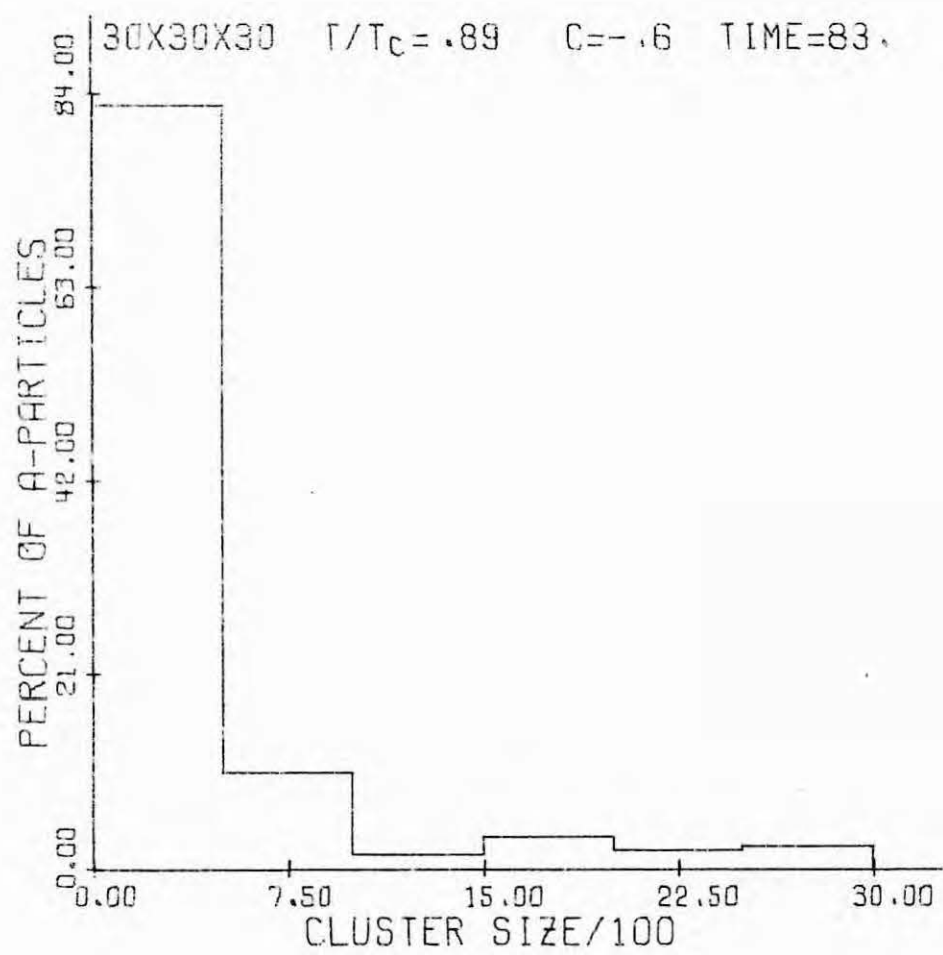
C.29



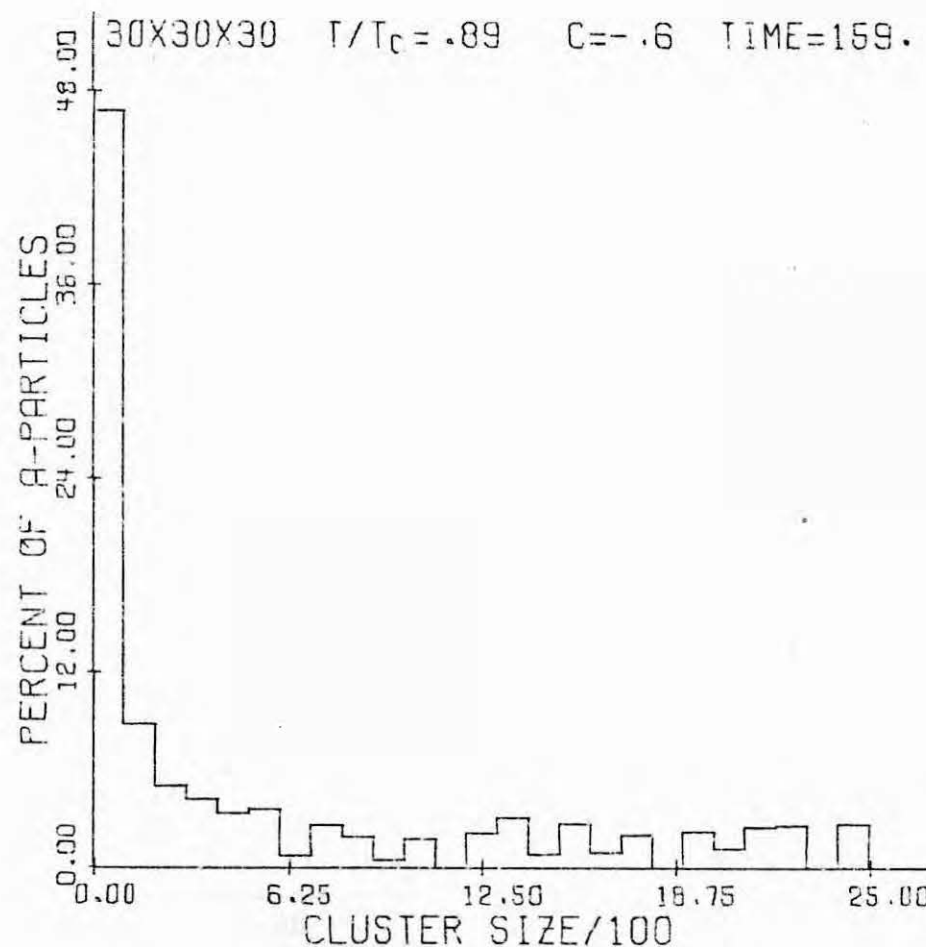
C.30



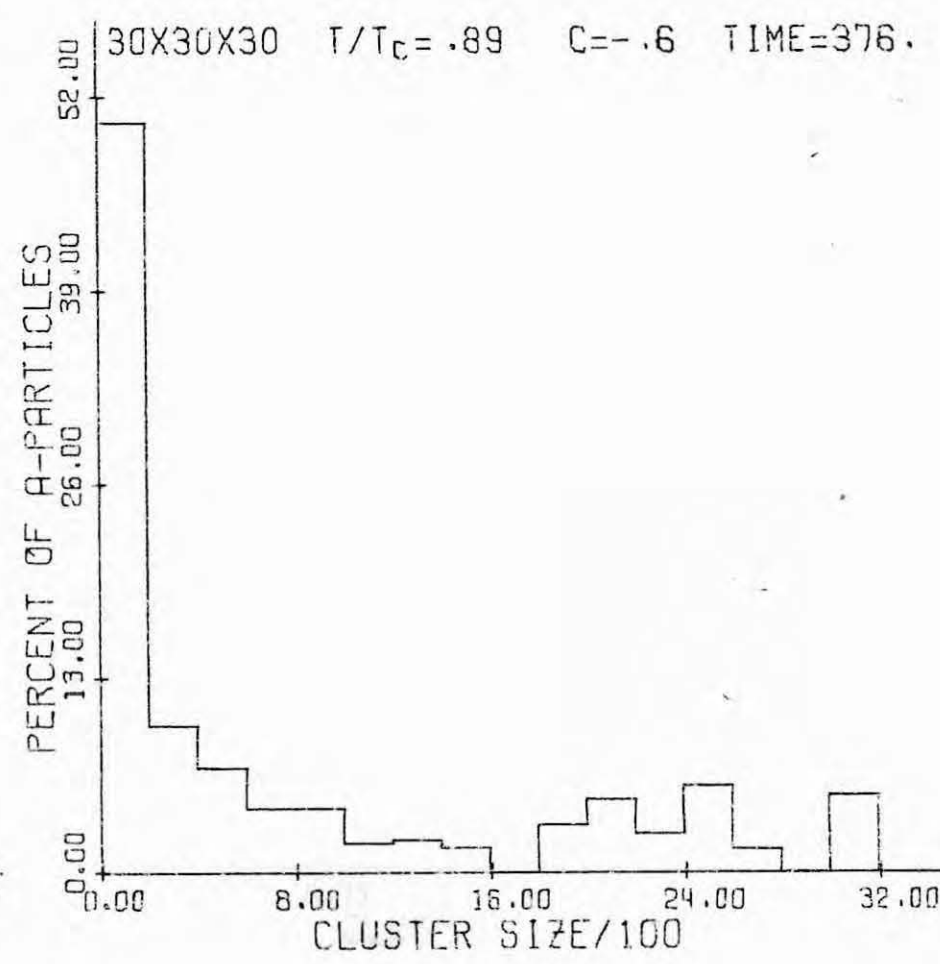
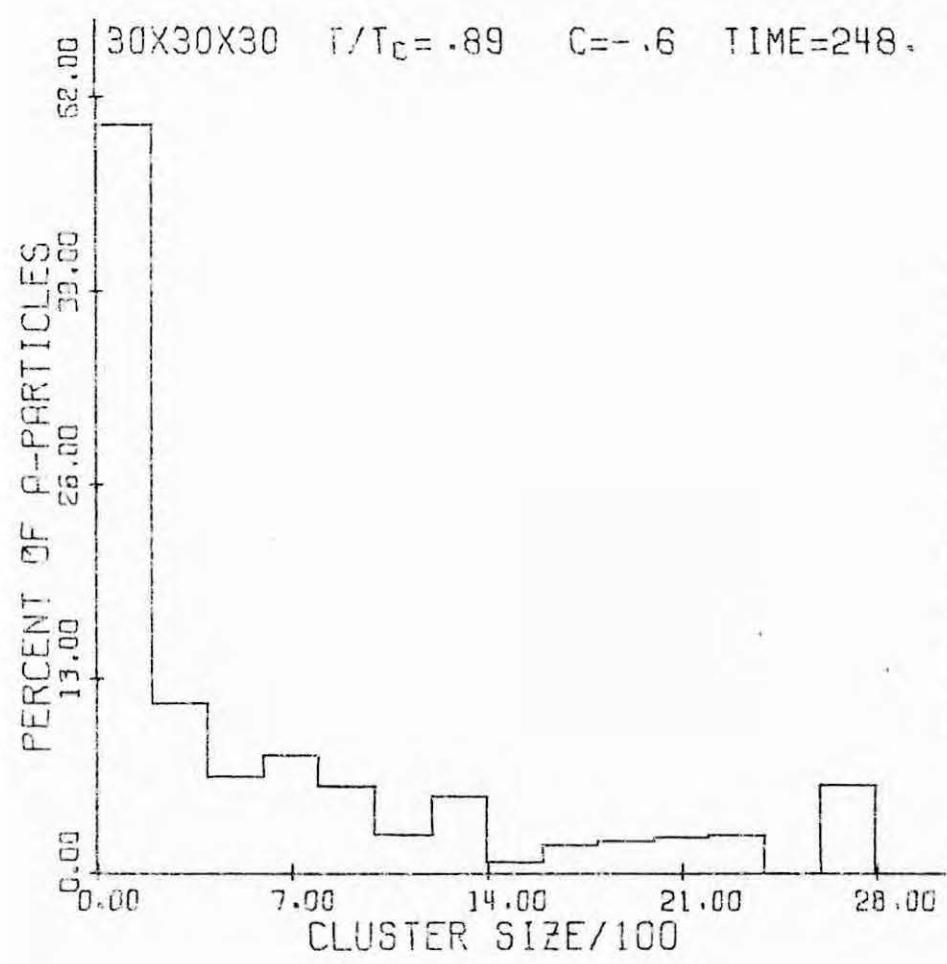


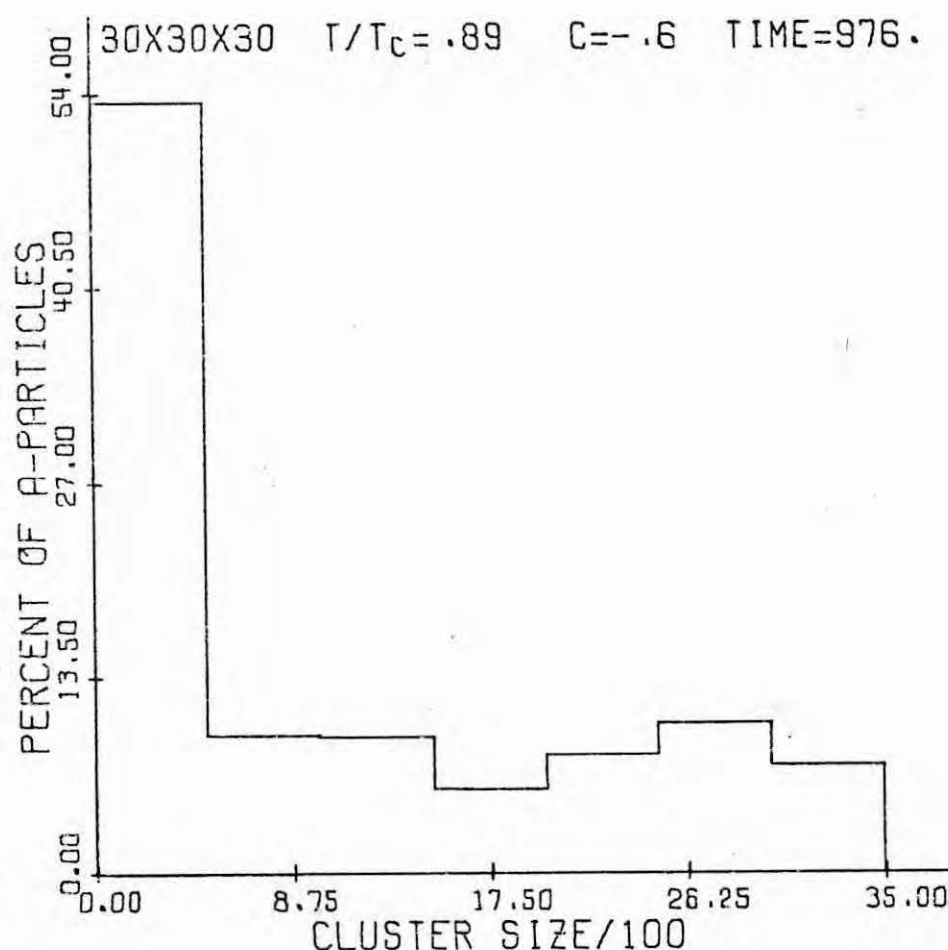
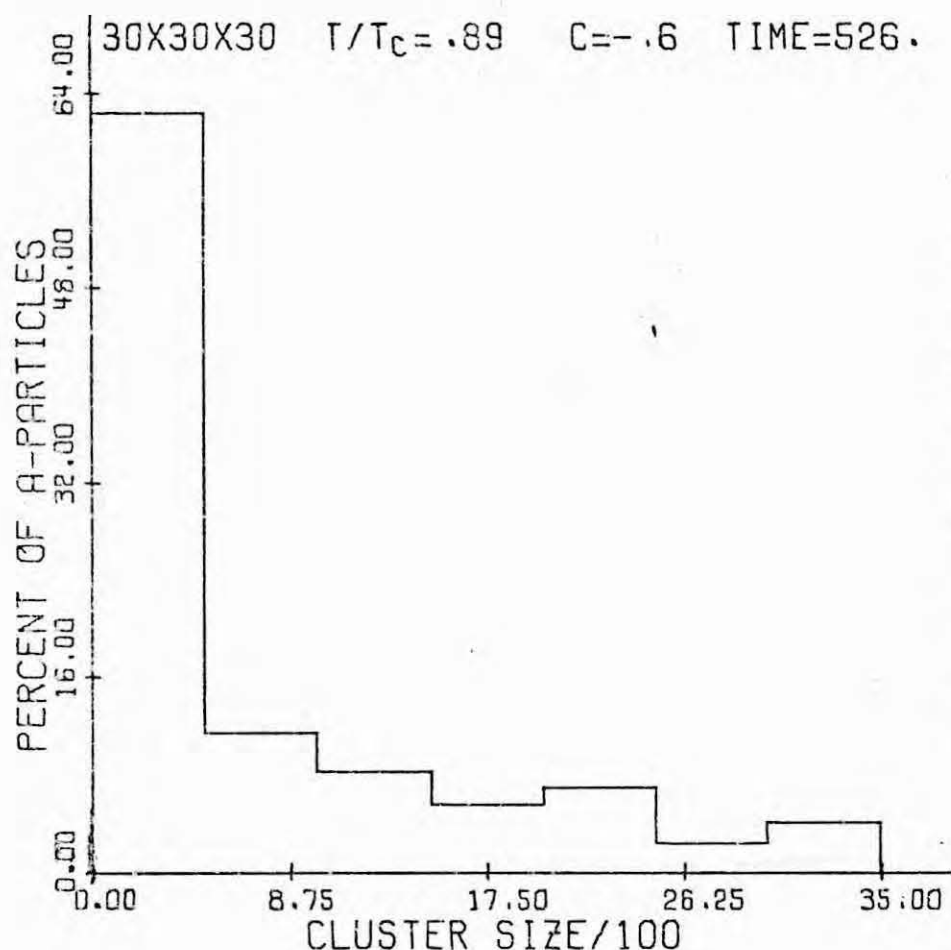


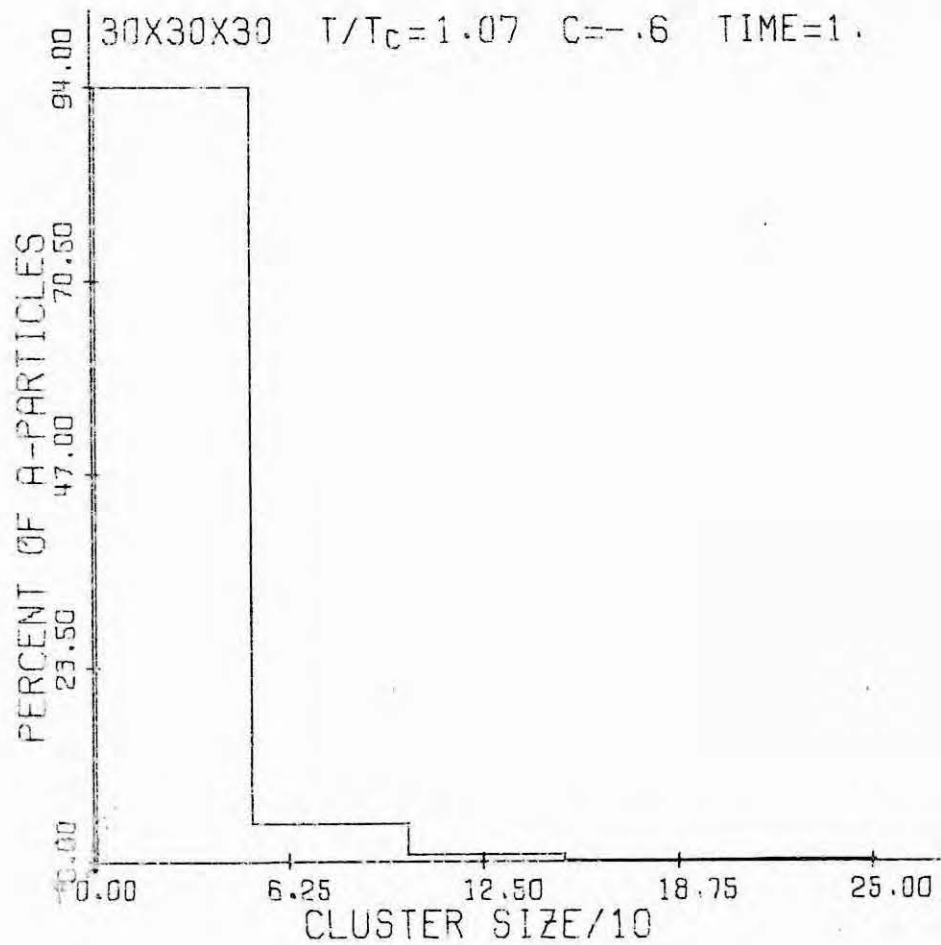
c.35



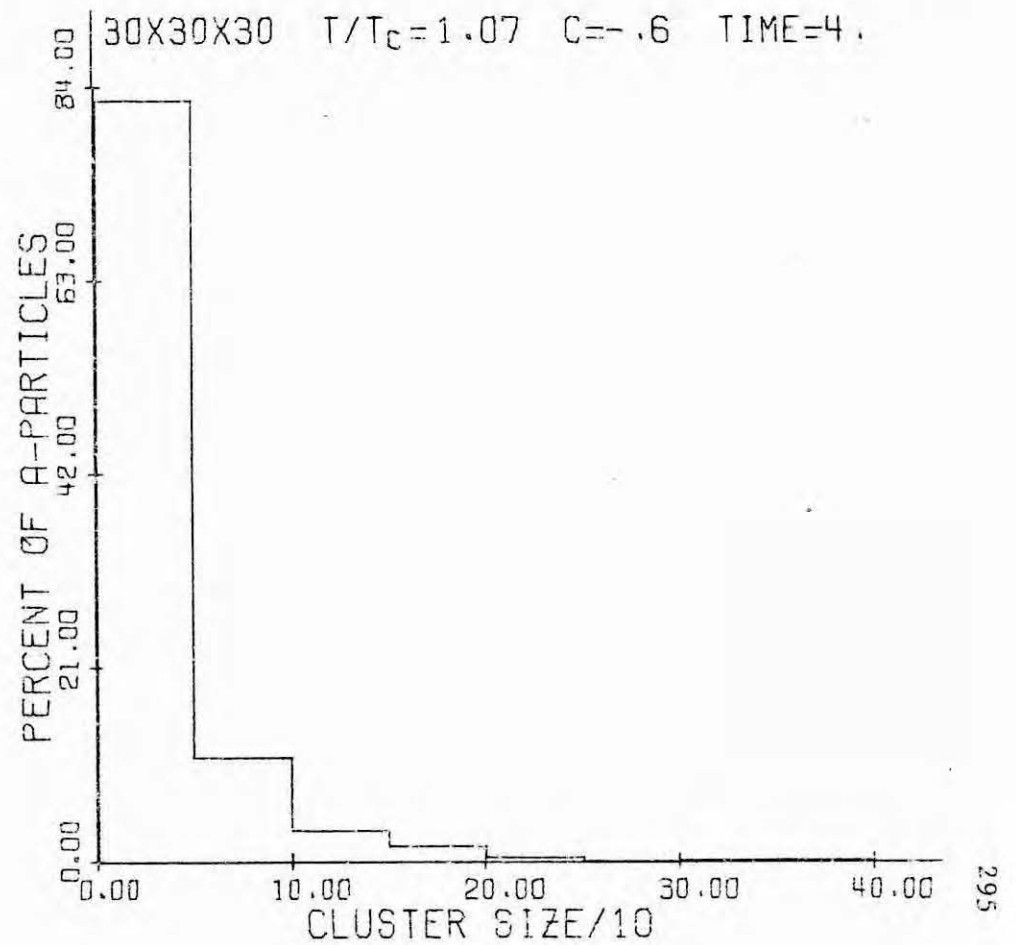
c.36



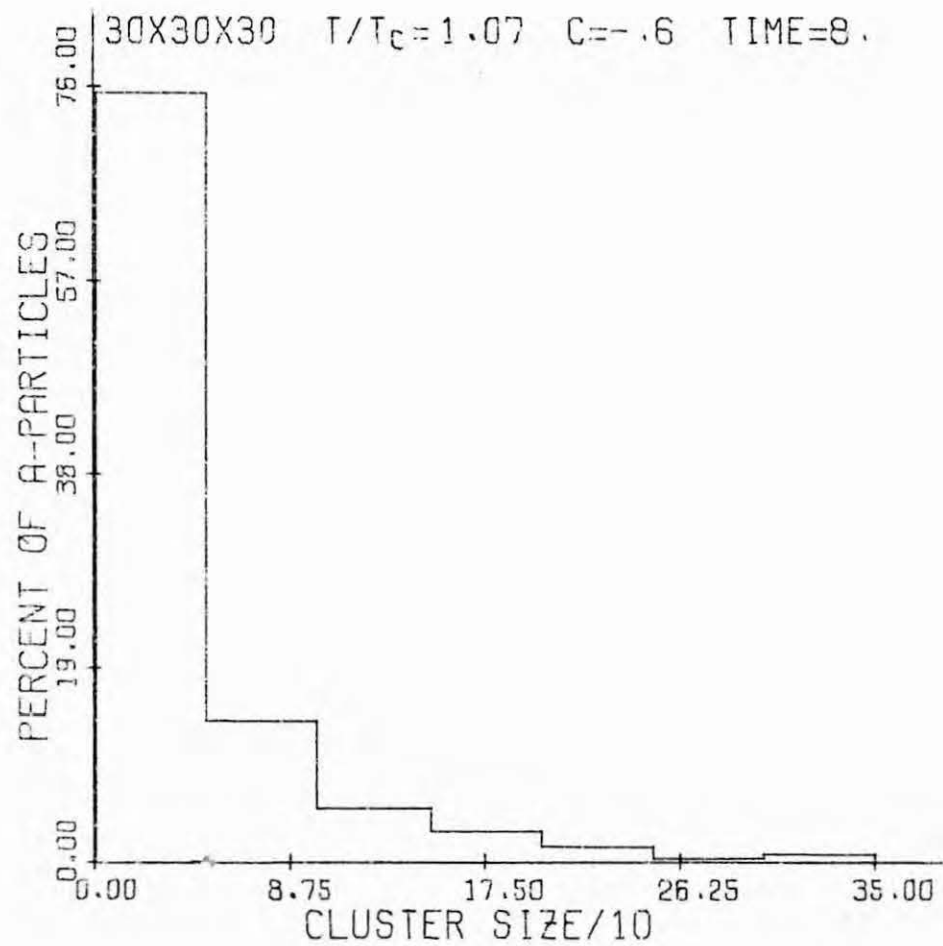




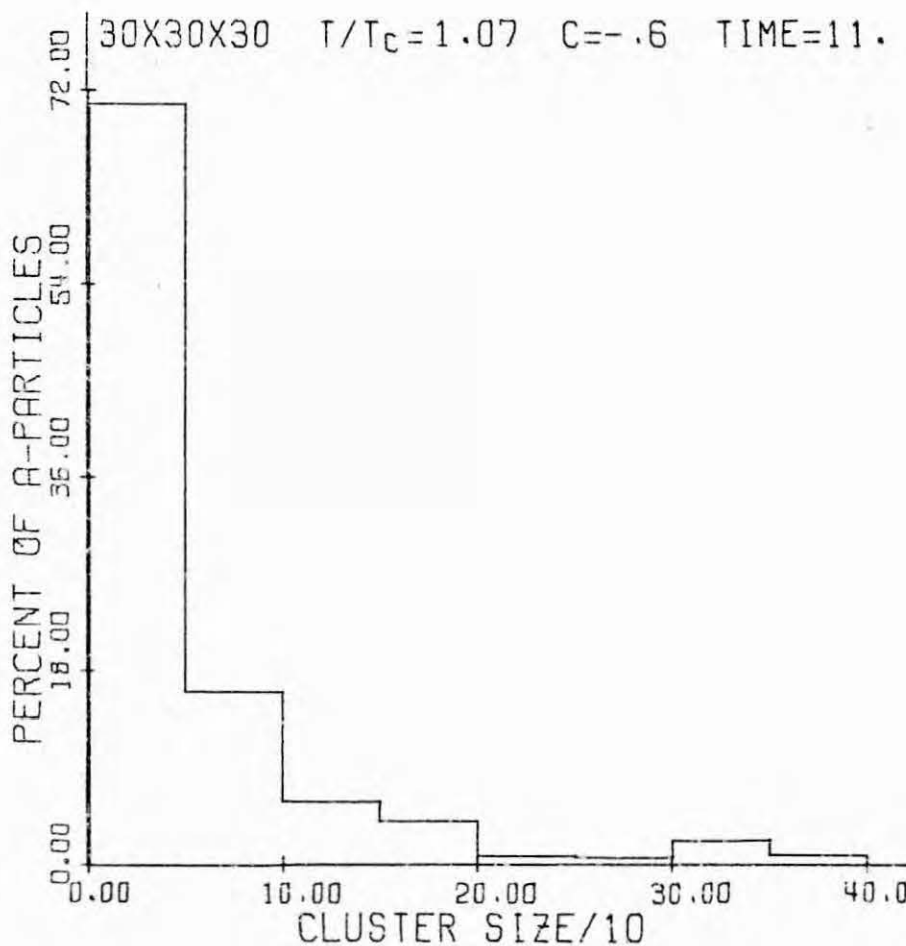
c.41



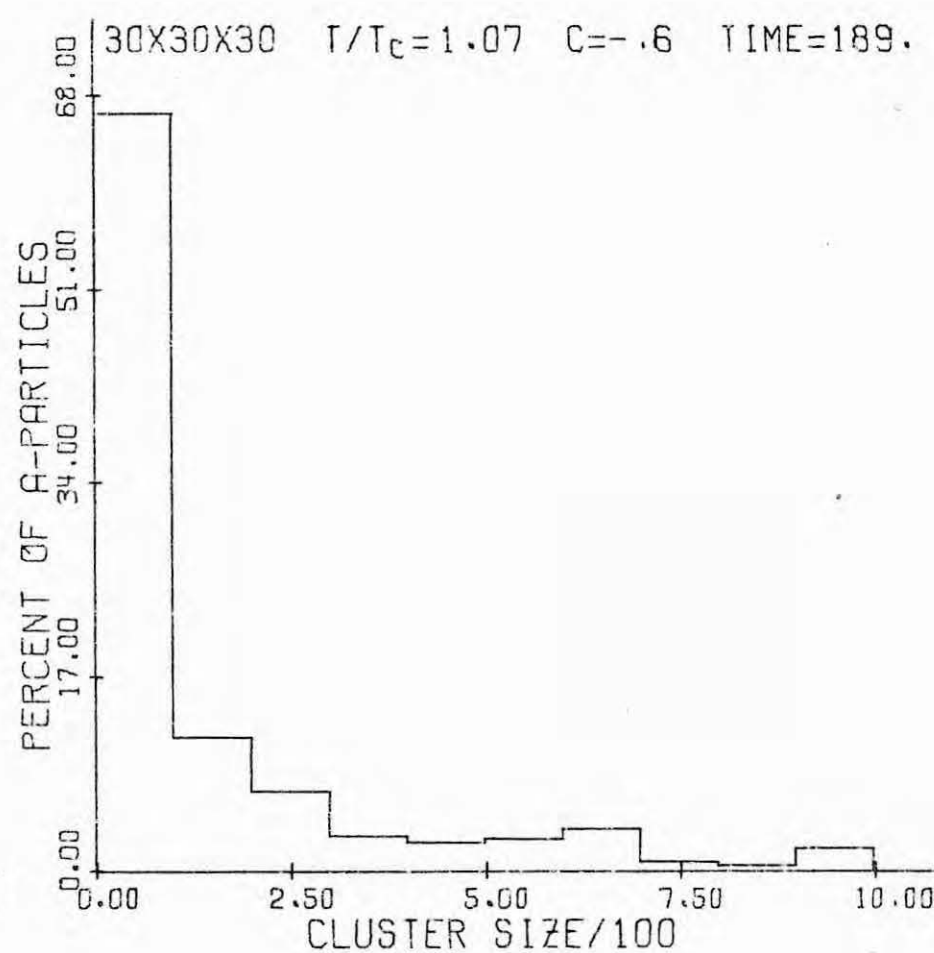
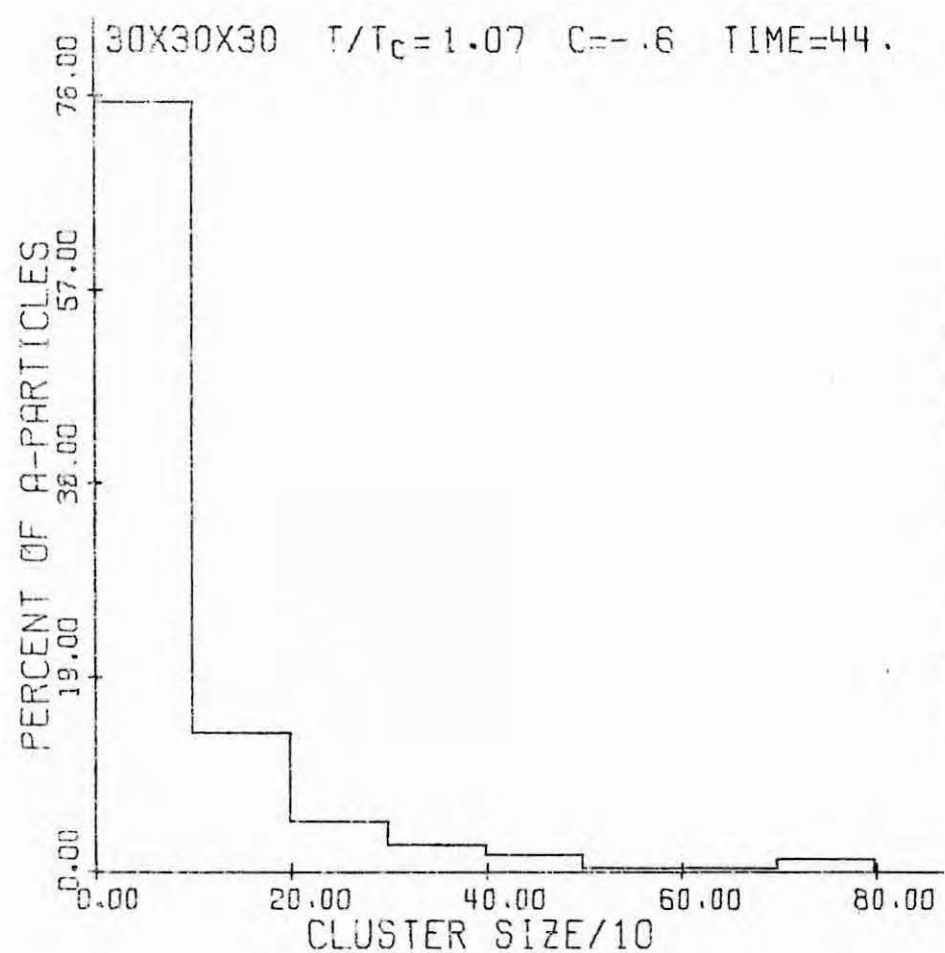
c.42

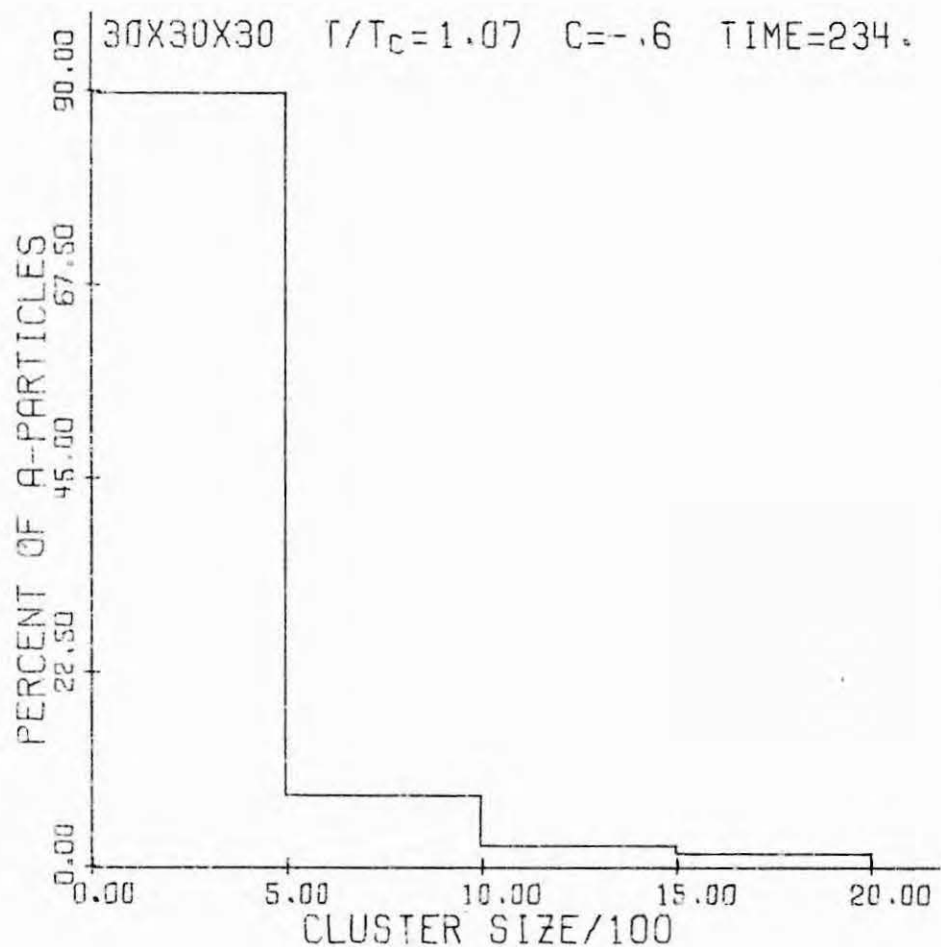


C.43

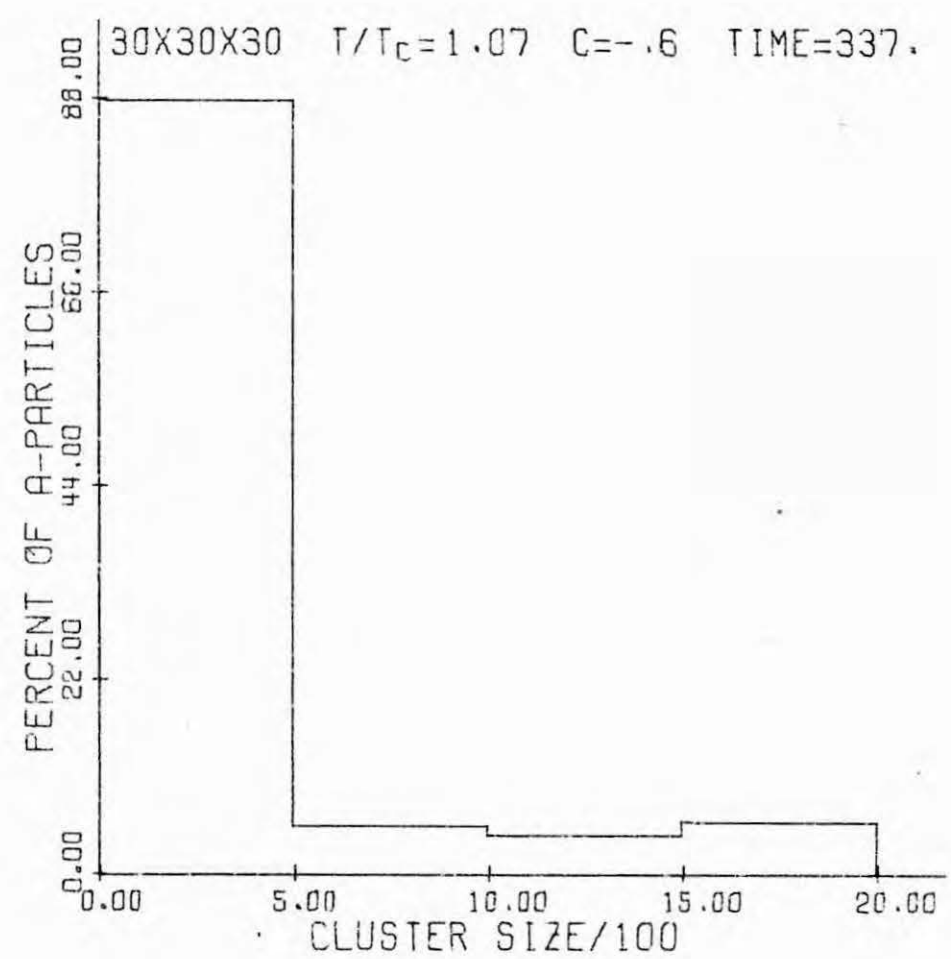


C.44

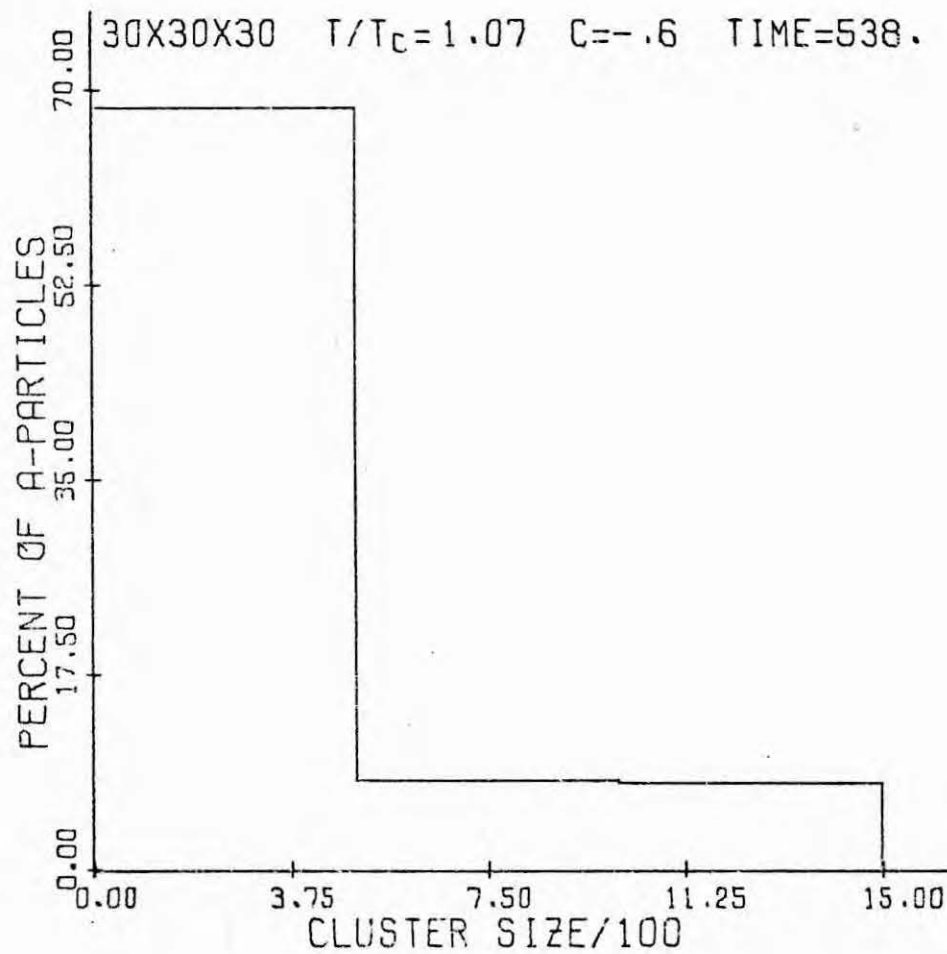
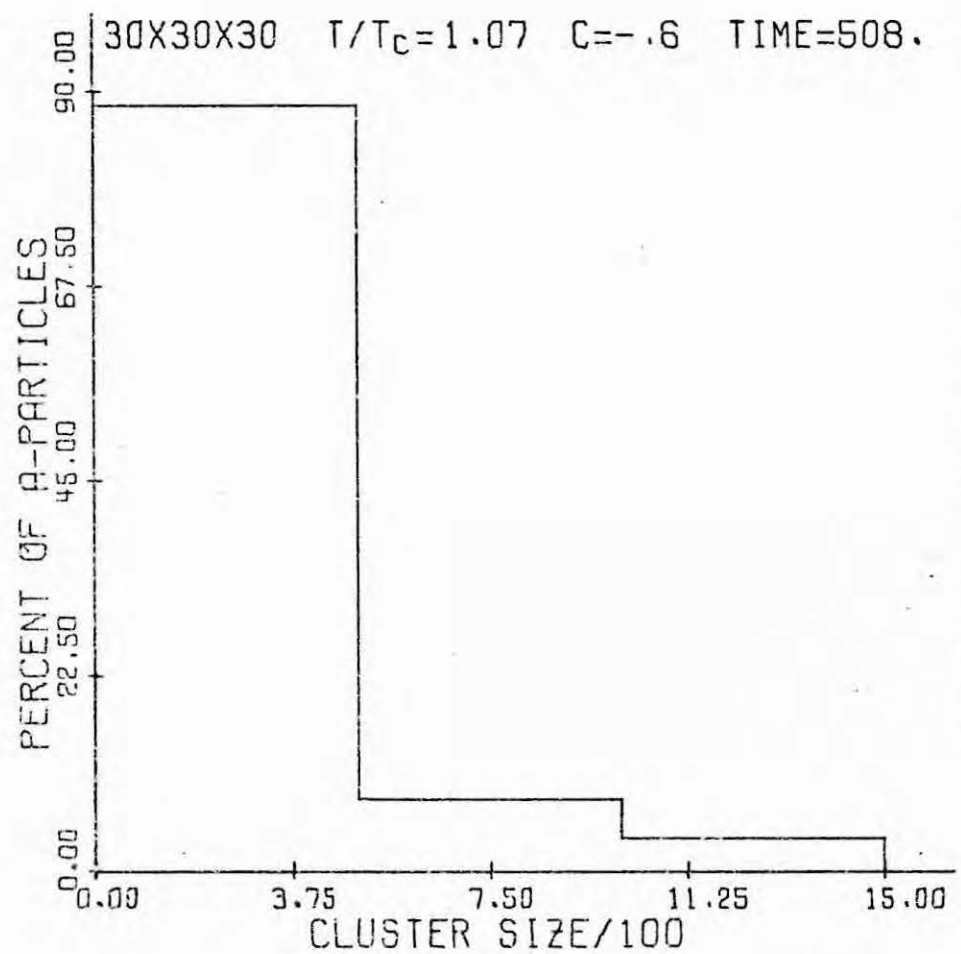


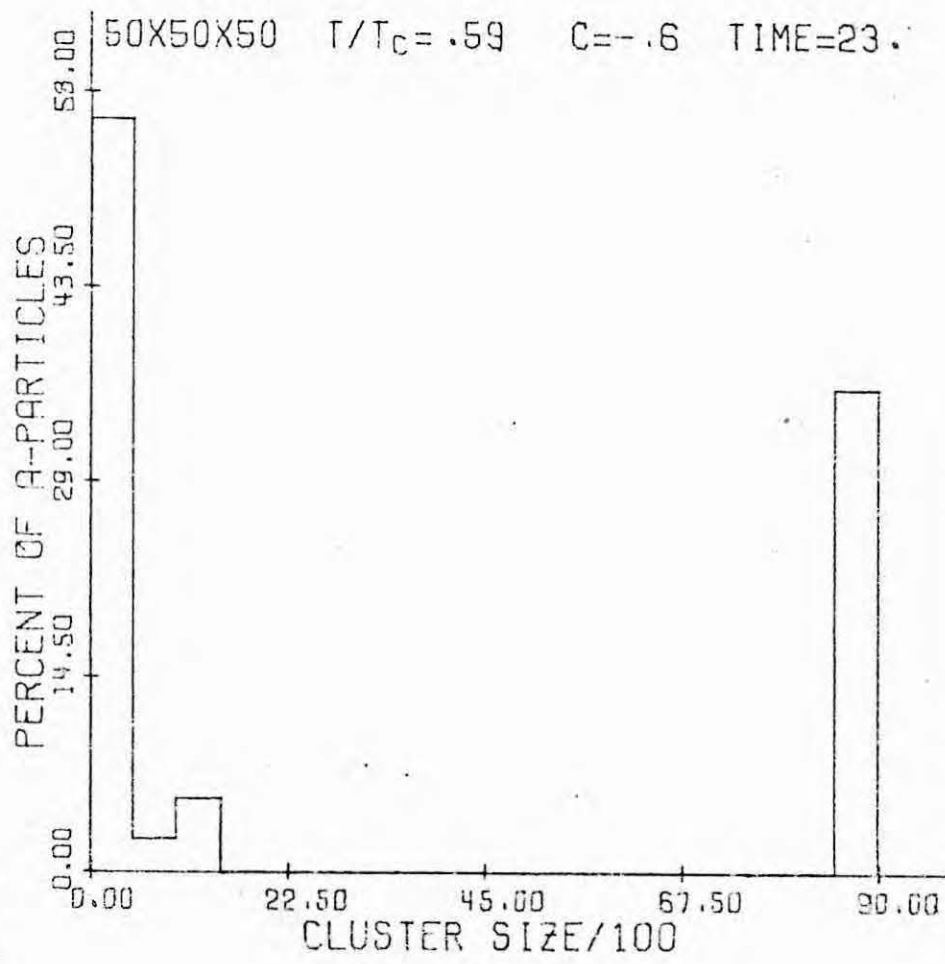
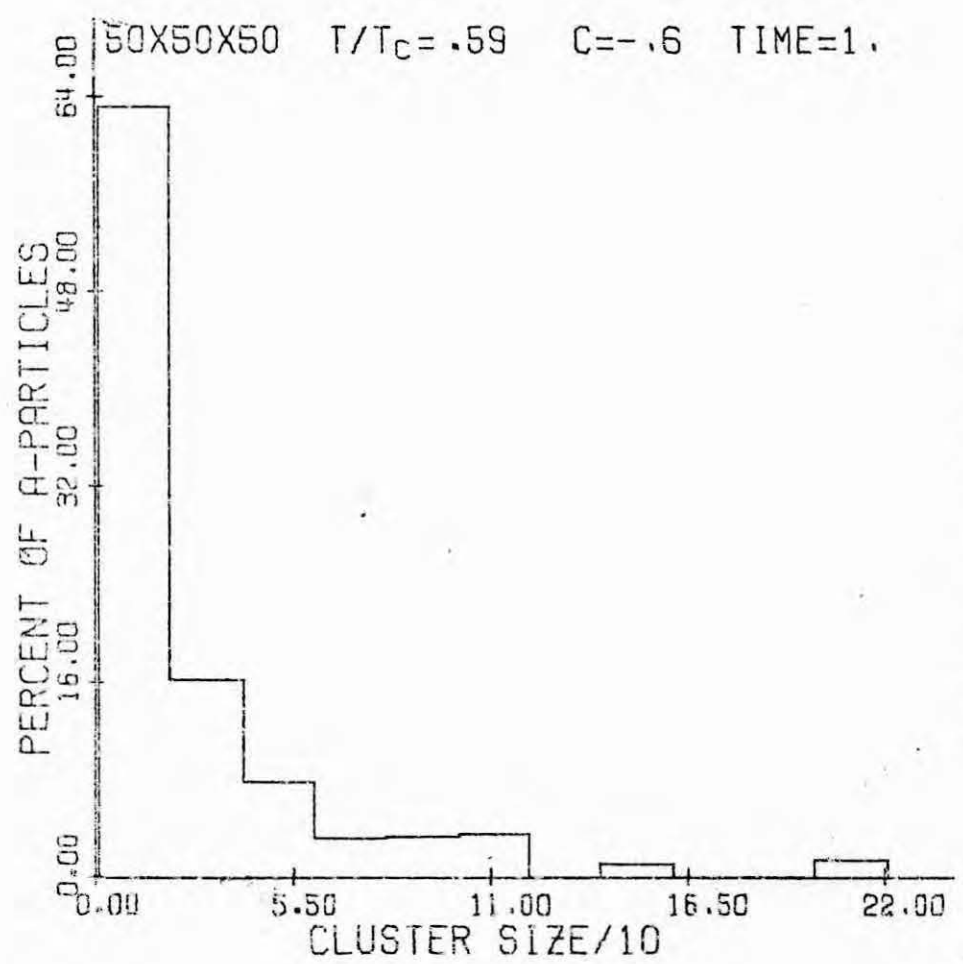


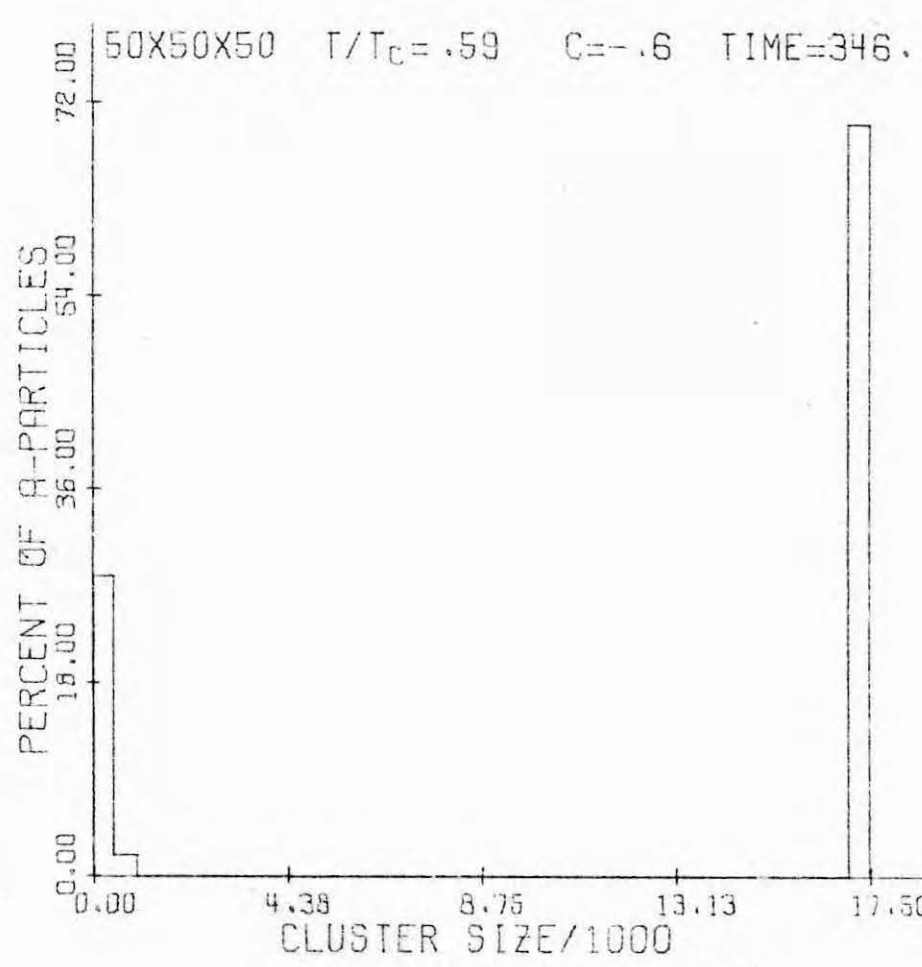
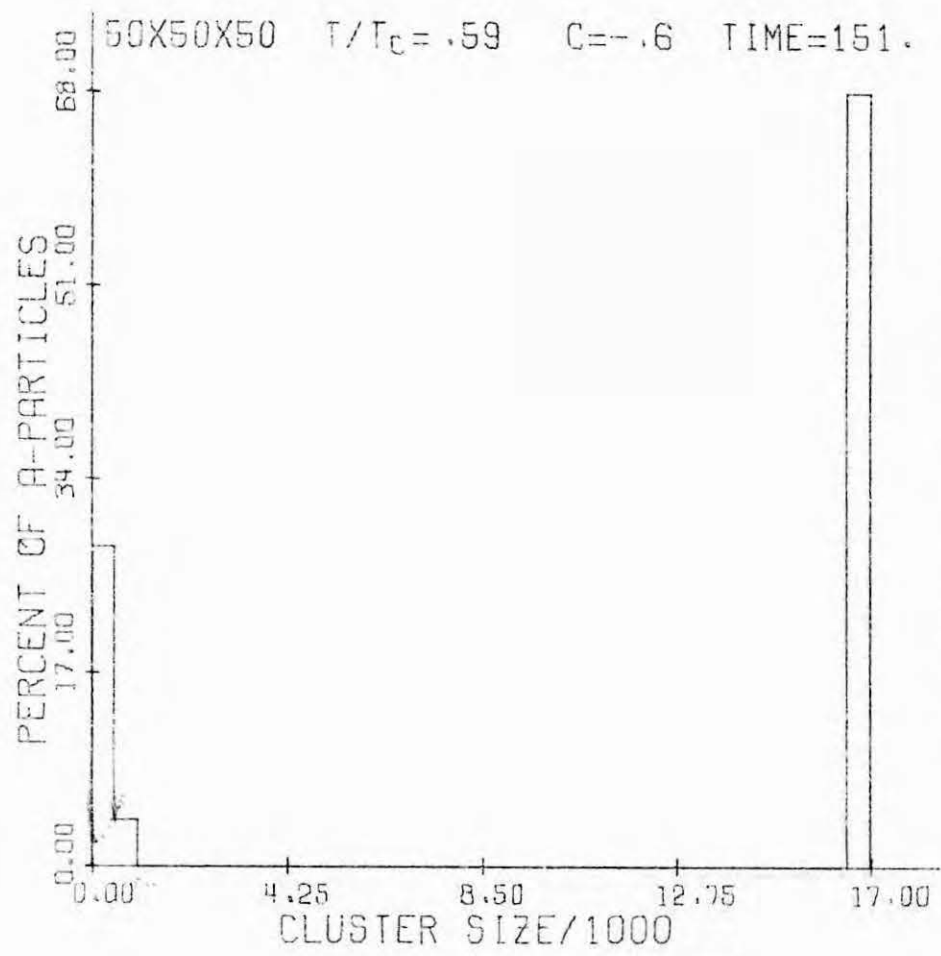
C.47

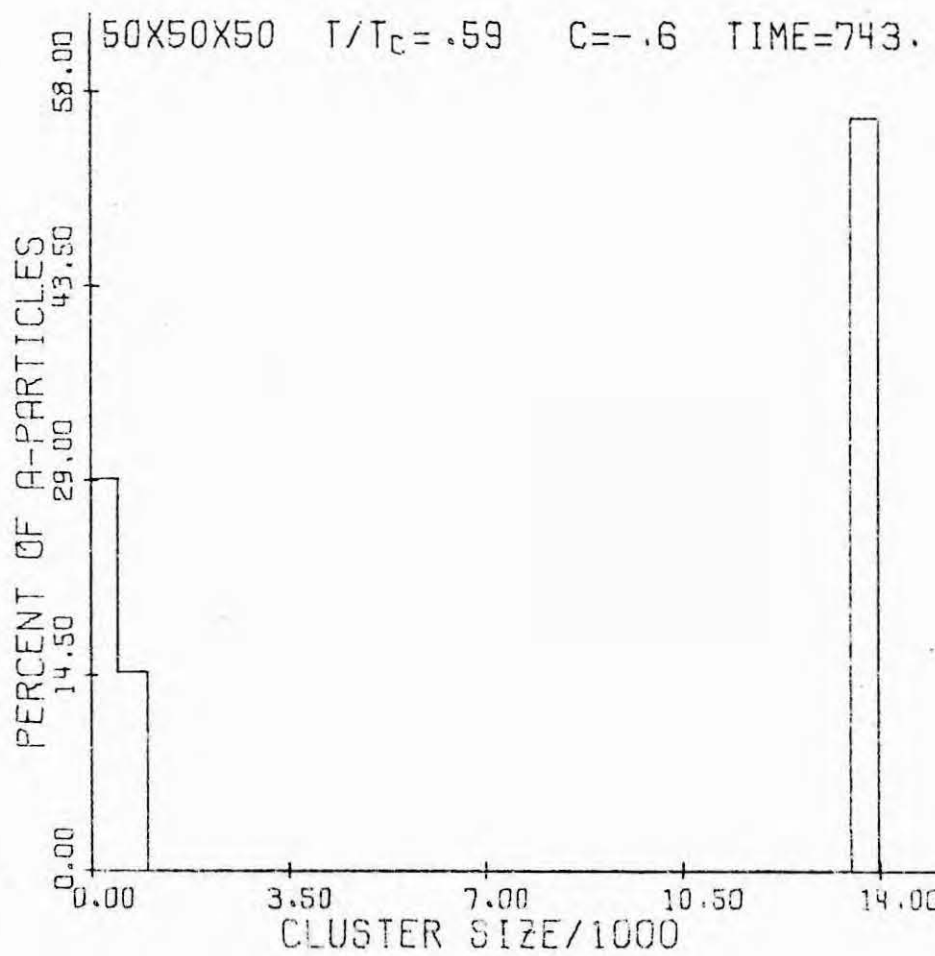
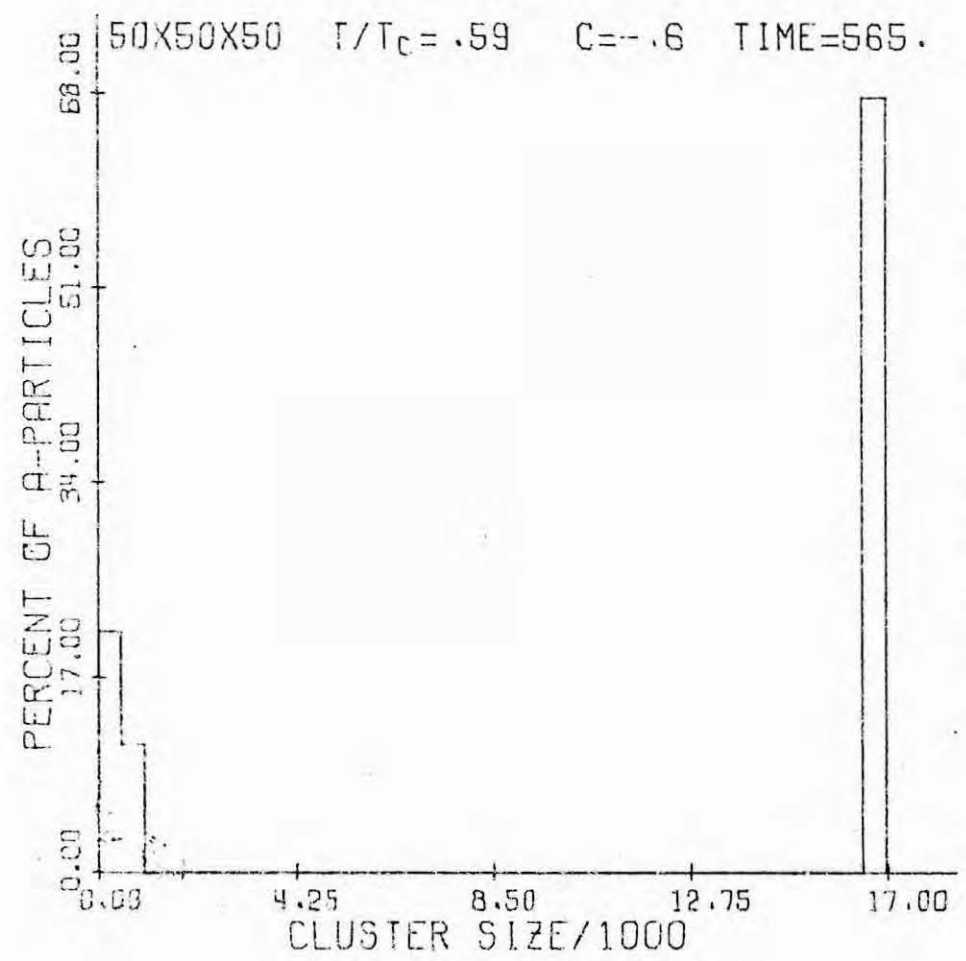


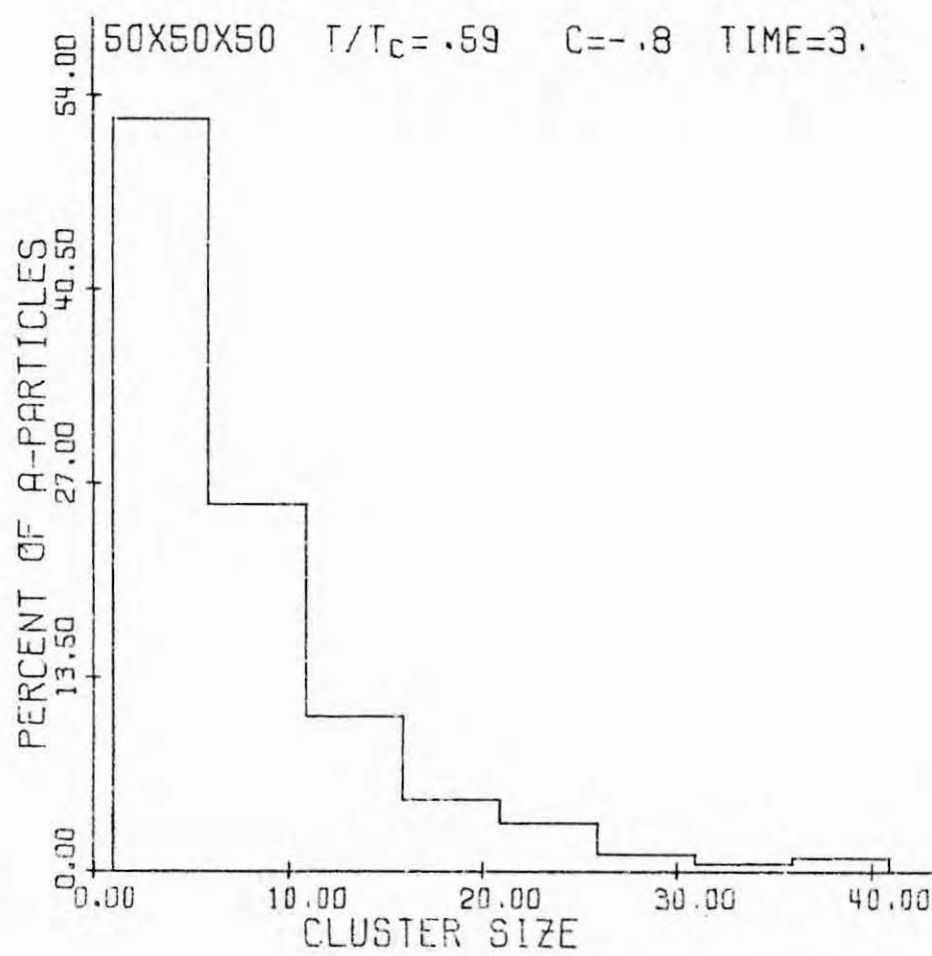
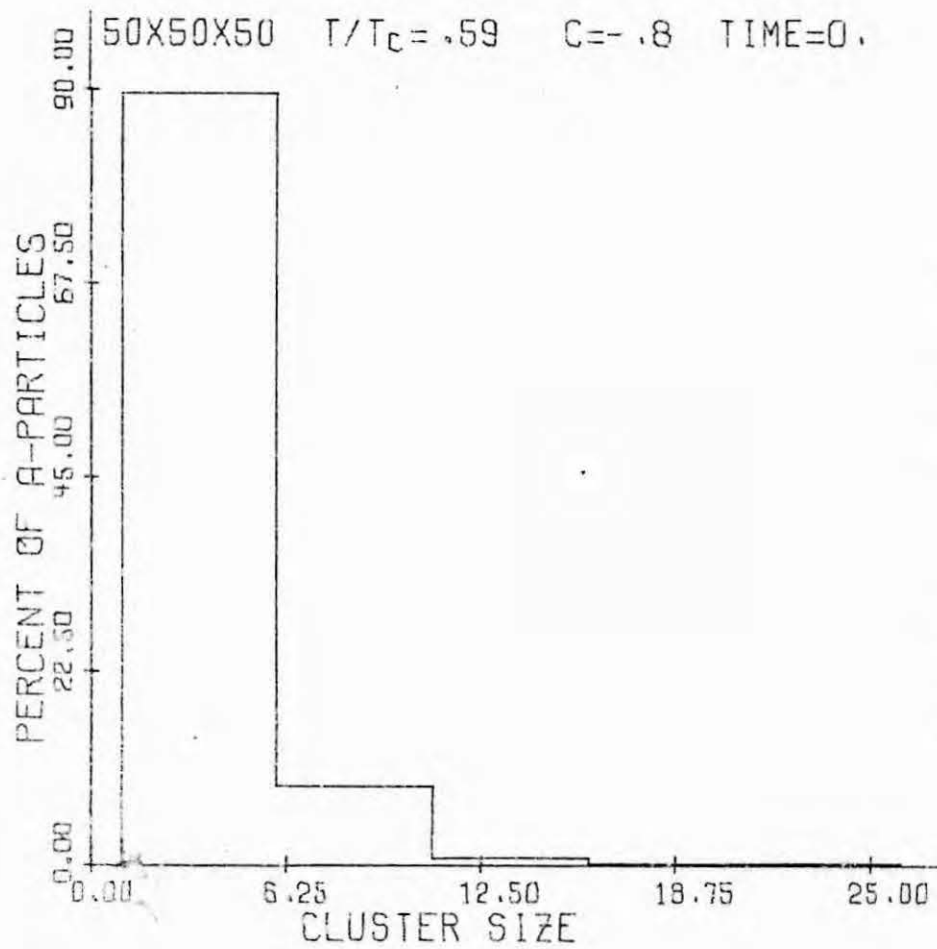
C.48

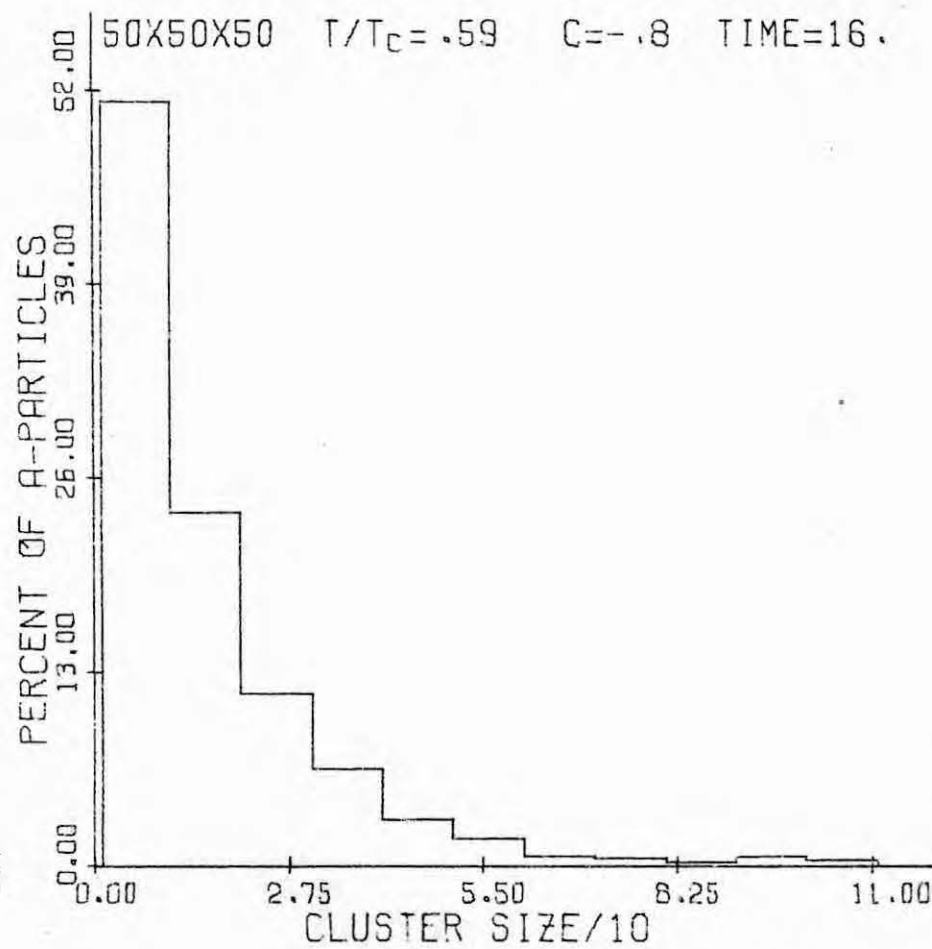
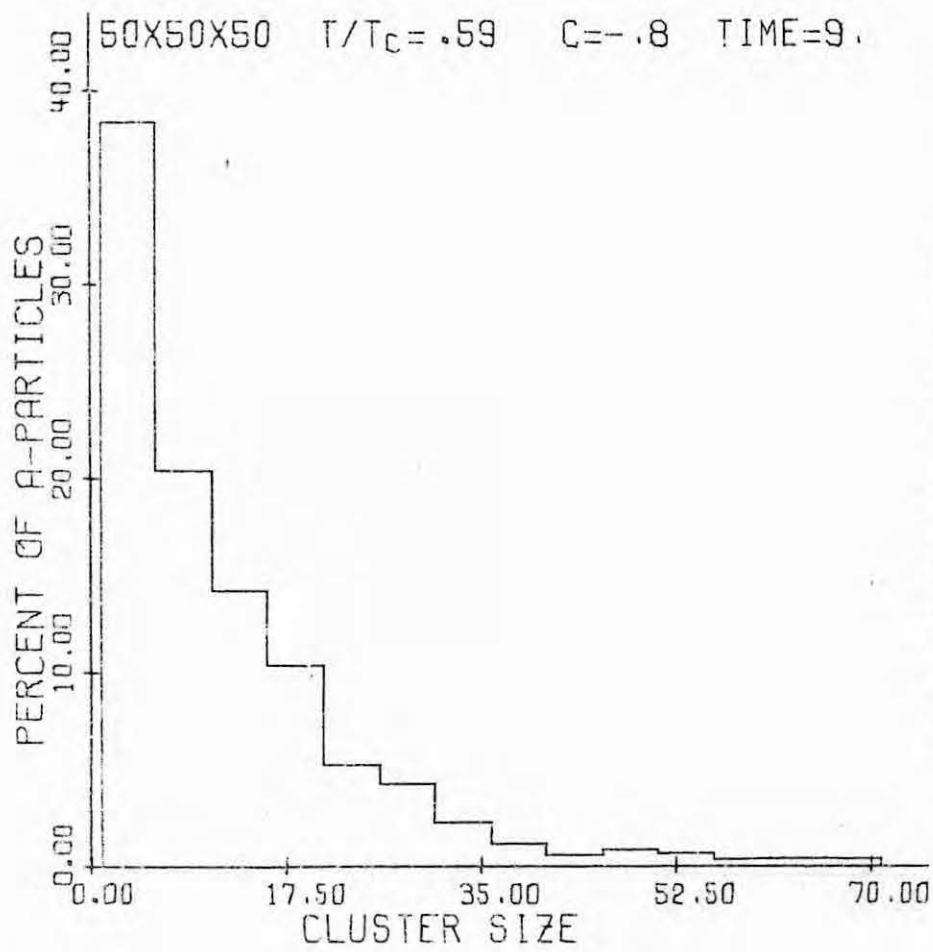


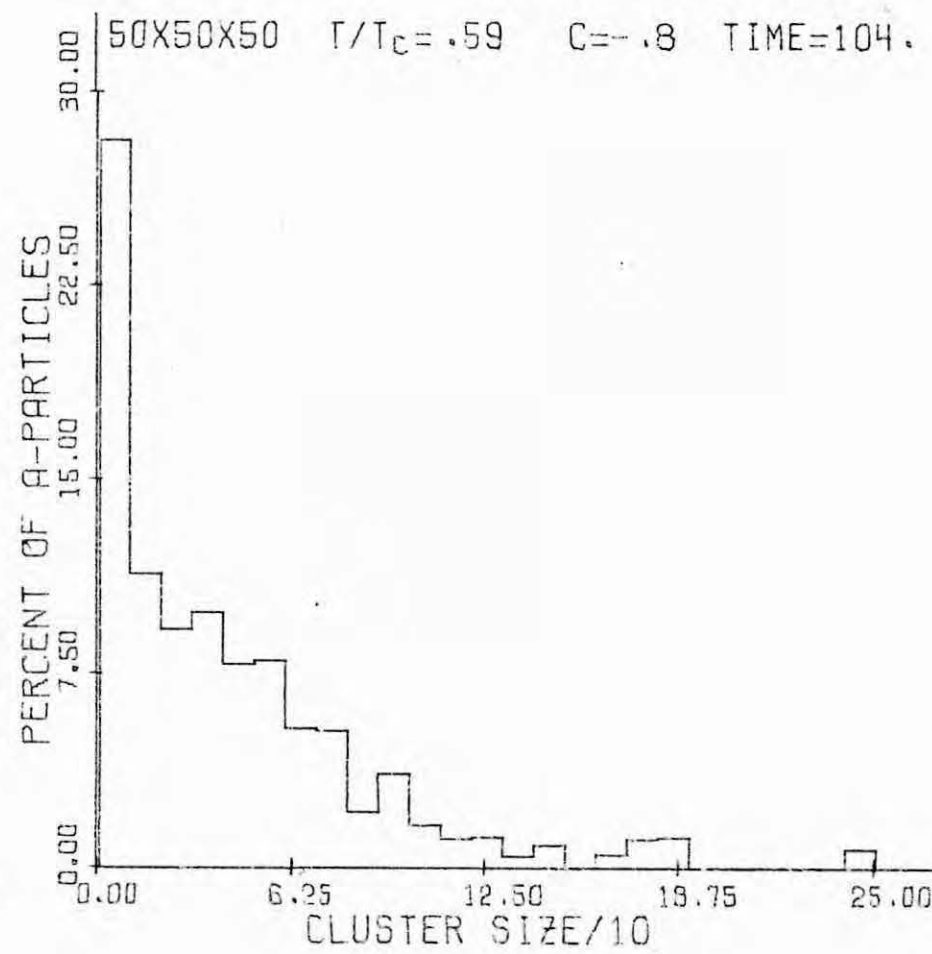
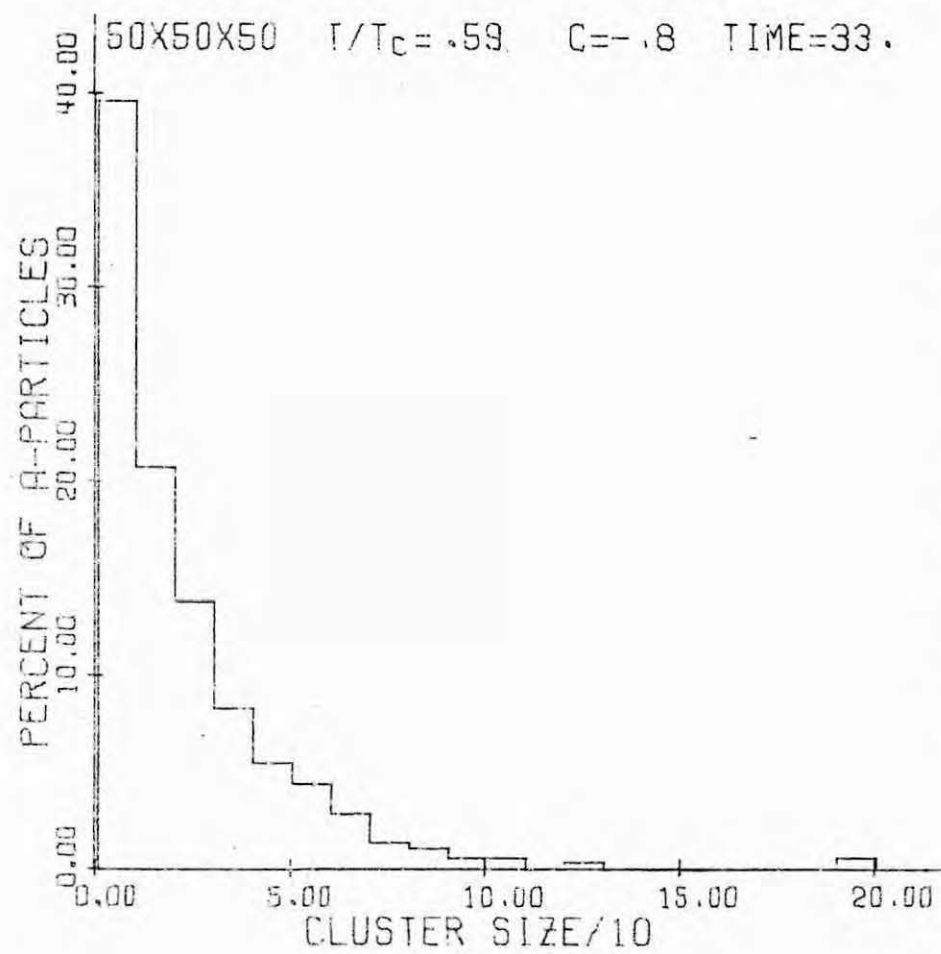


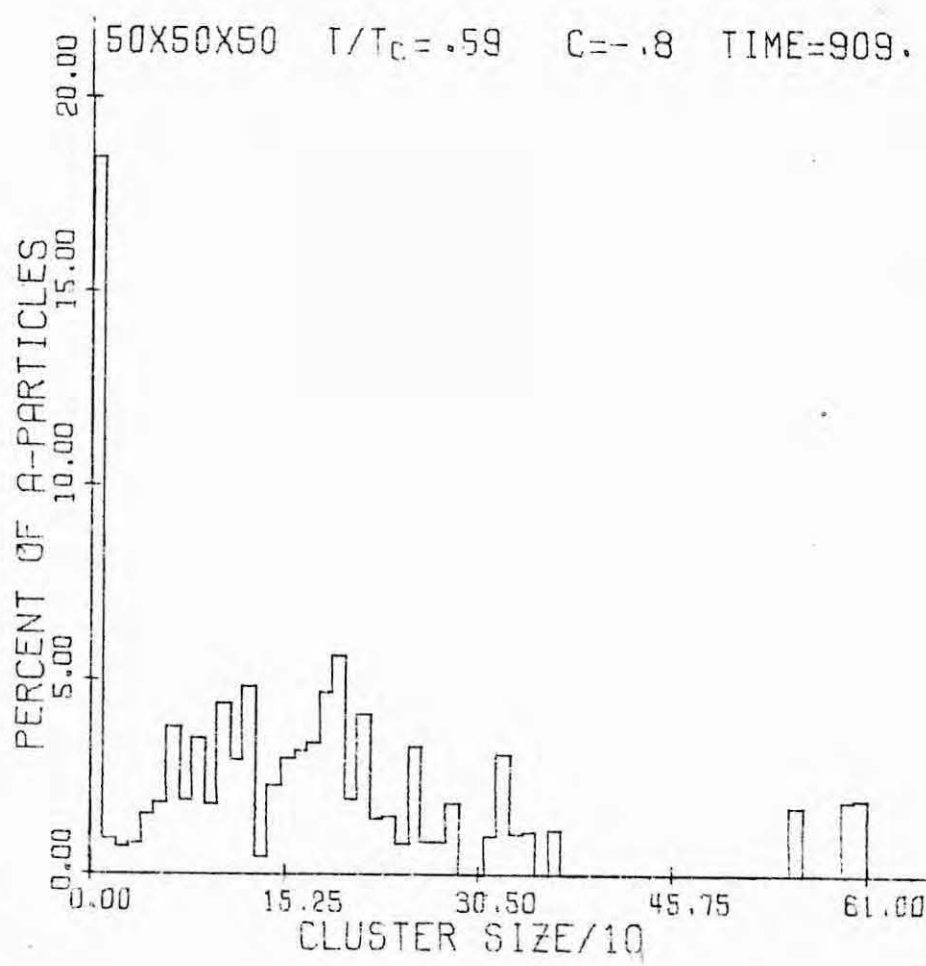
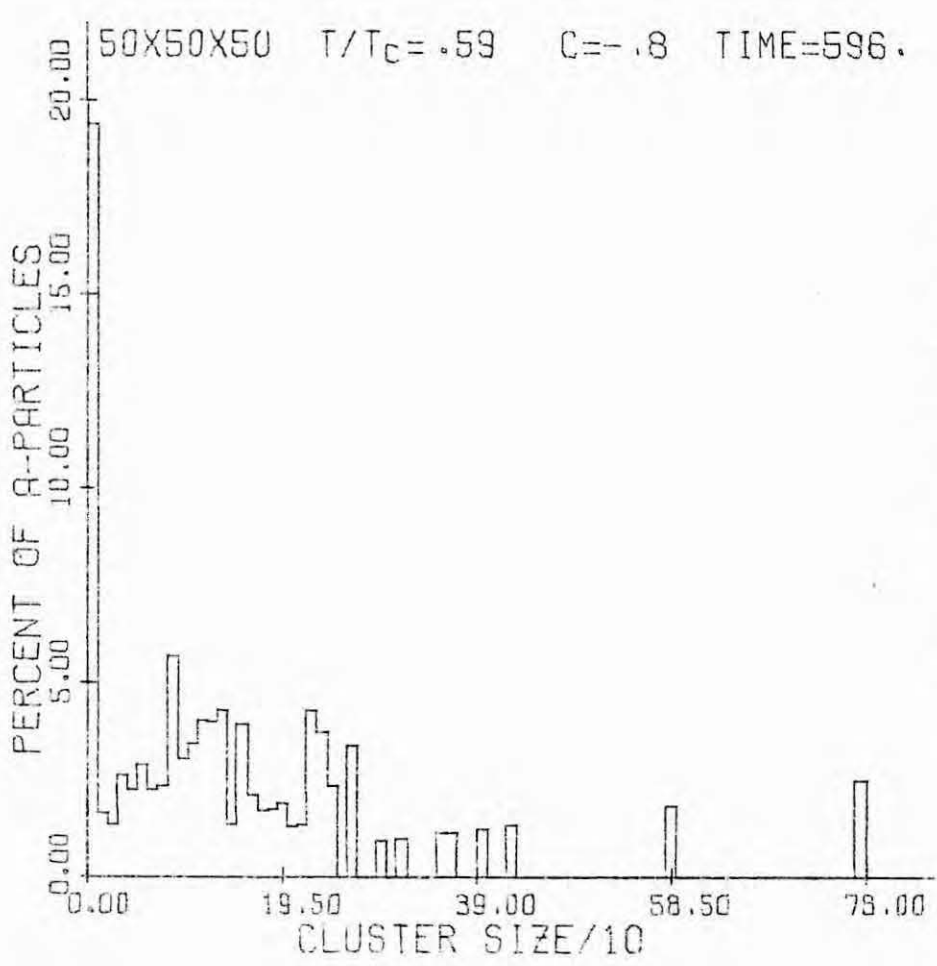


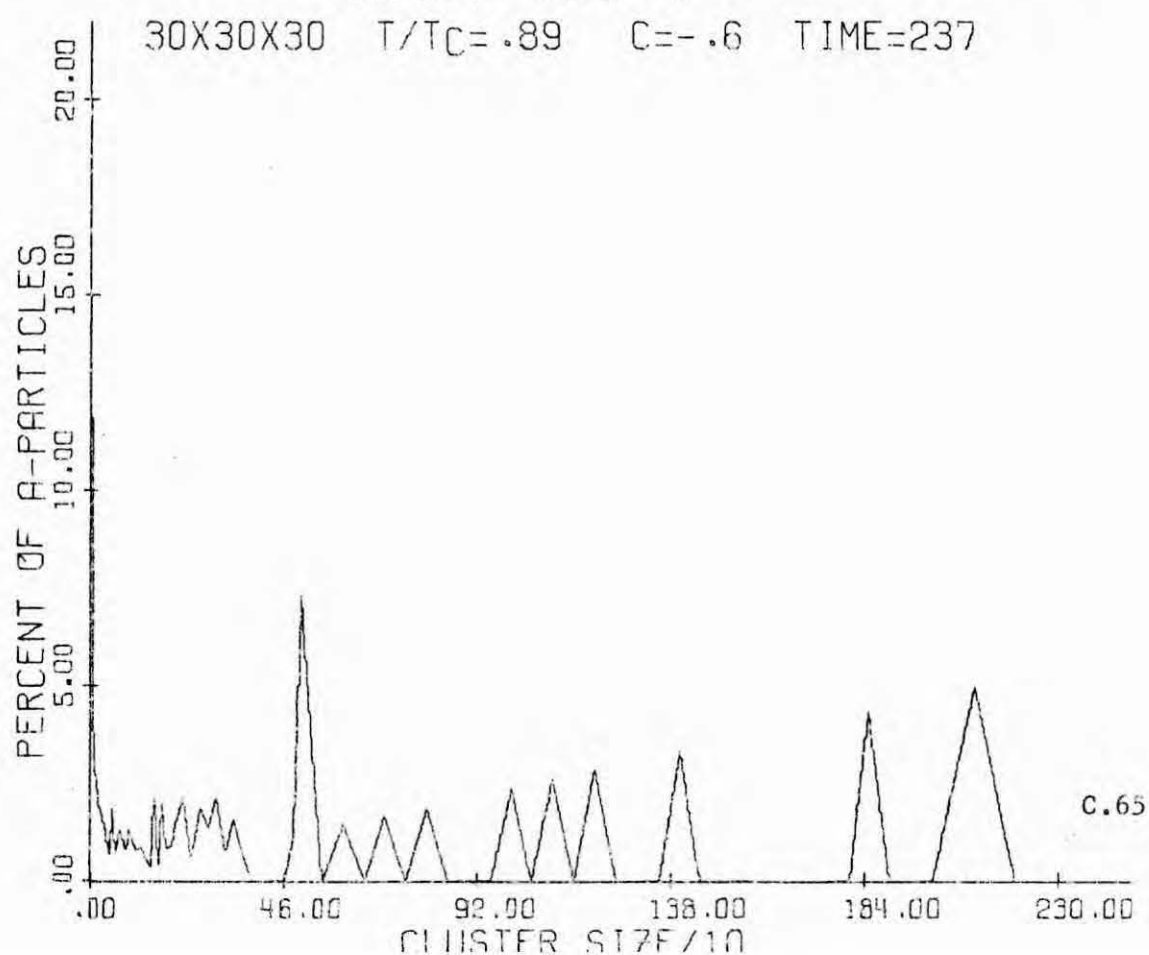
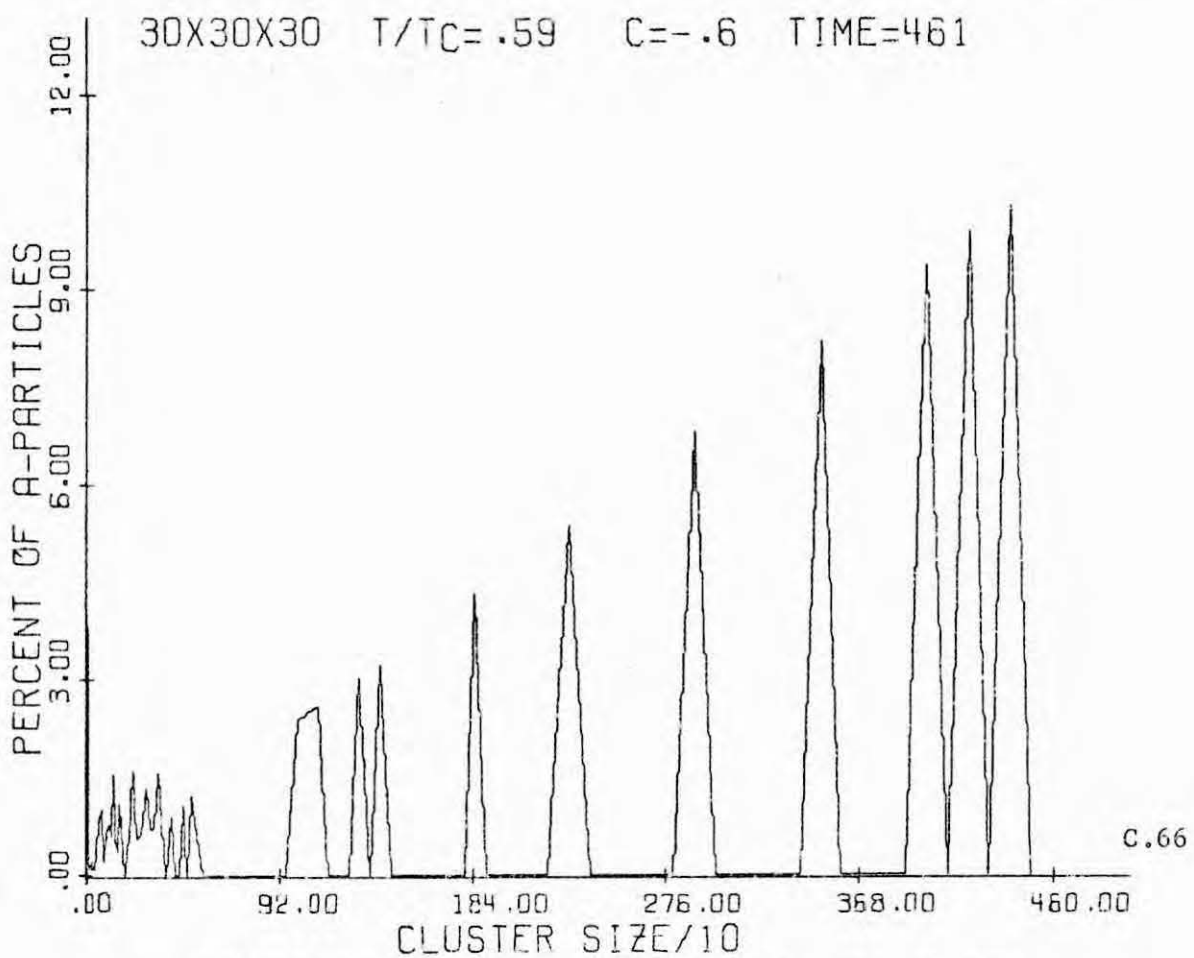


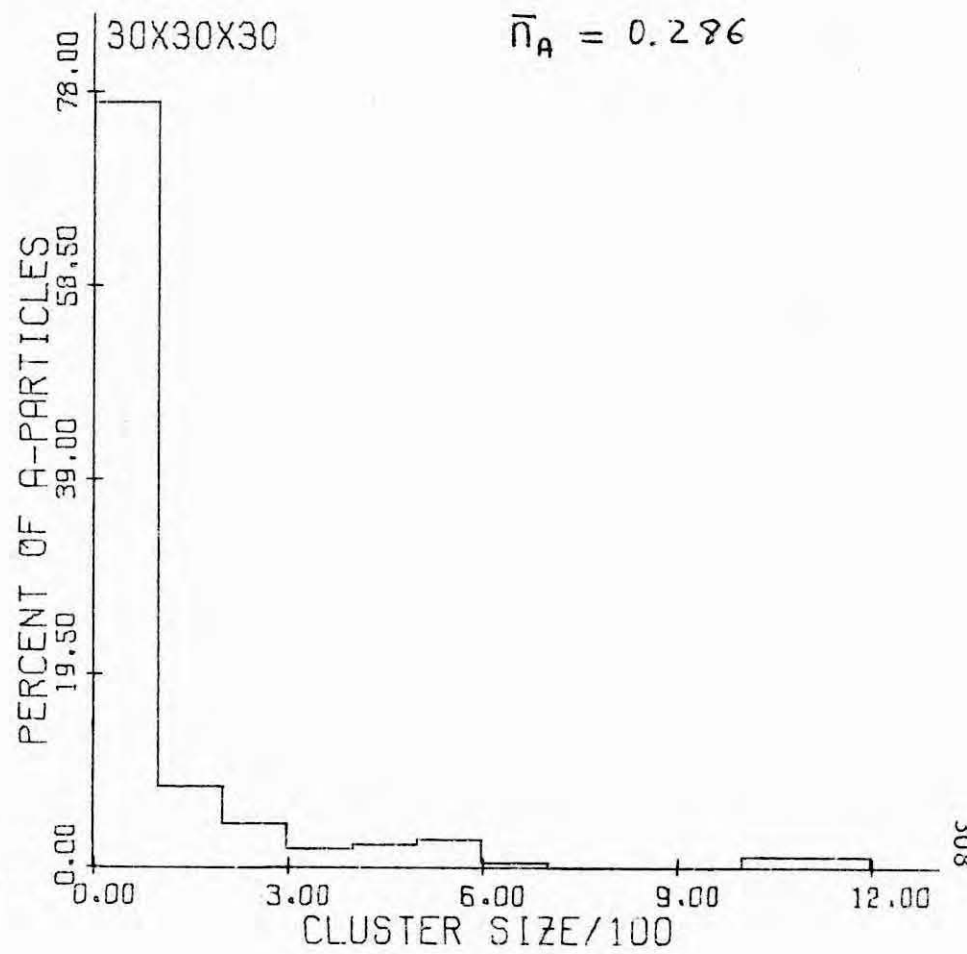
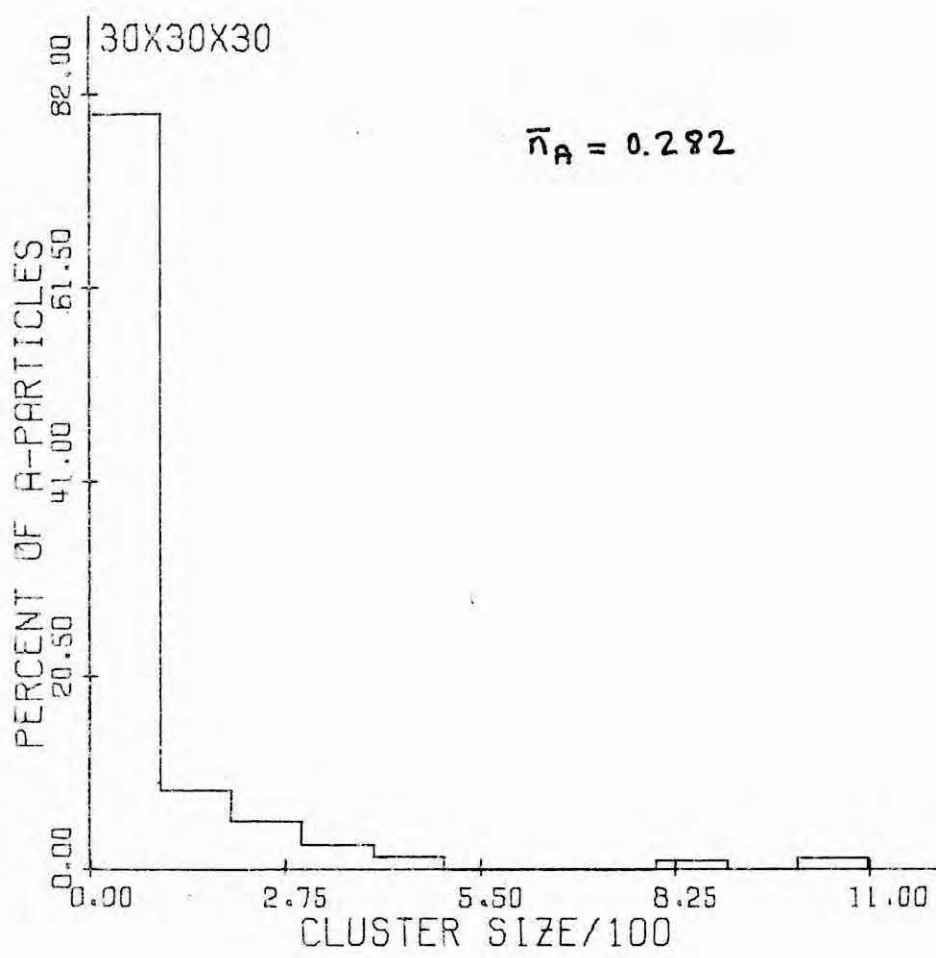


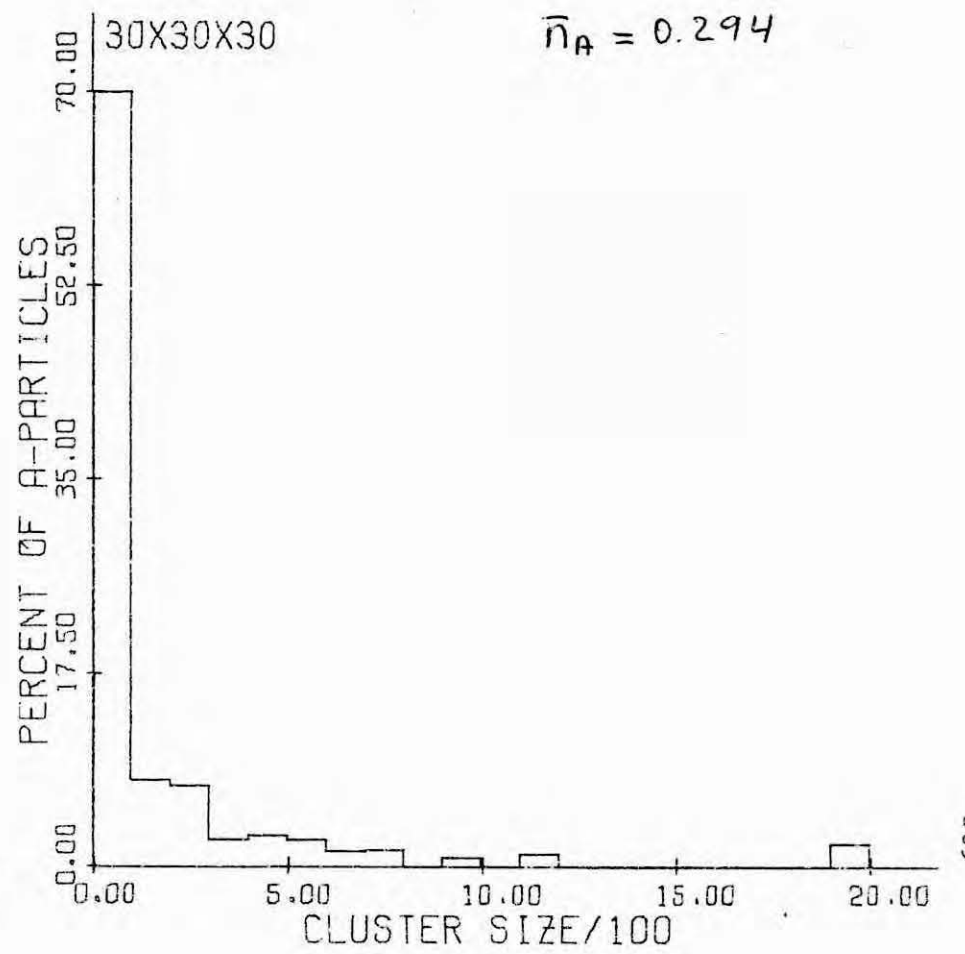
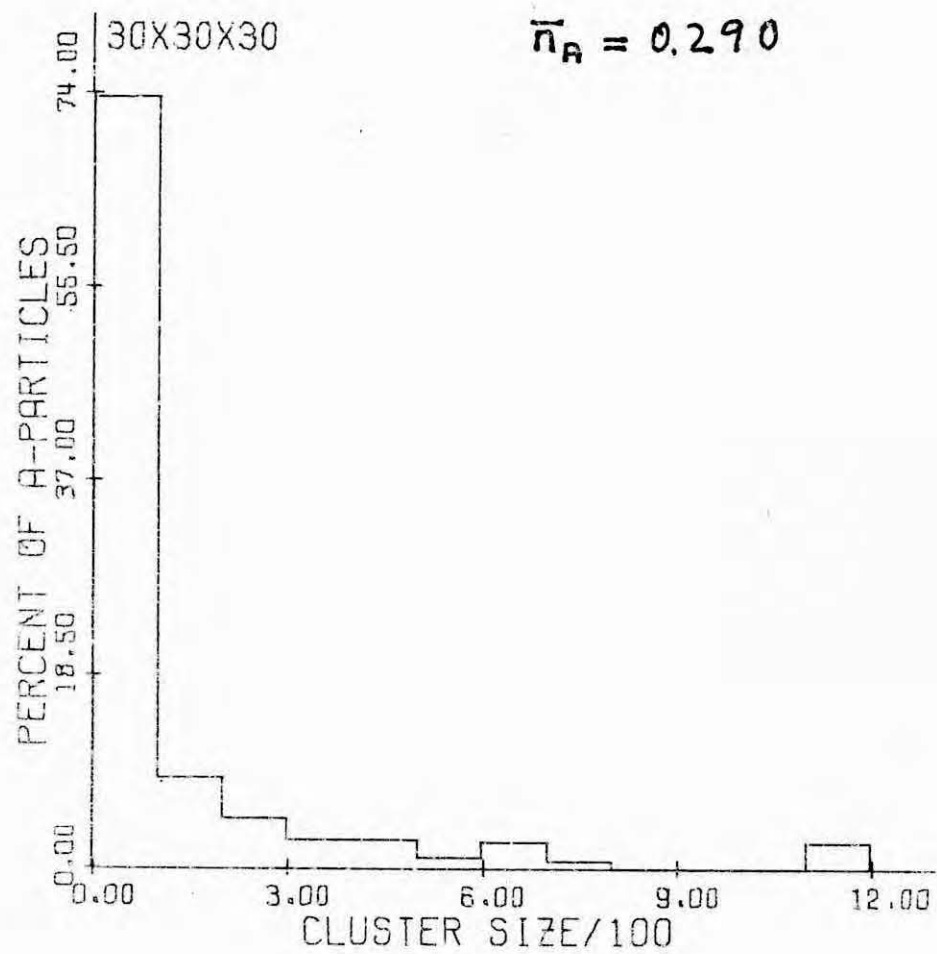


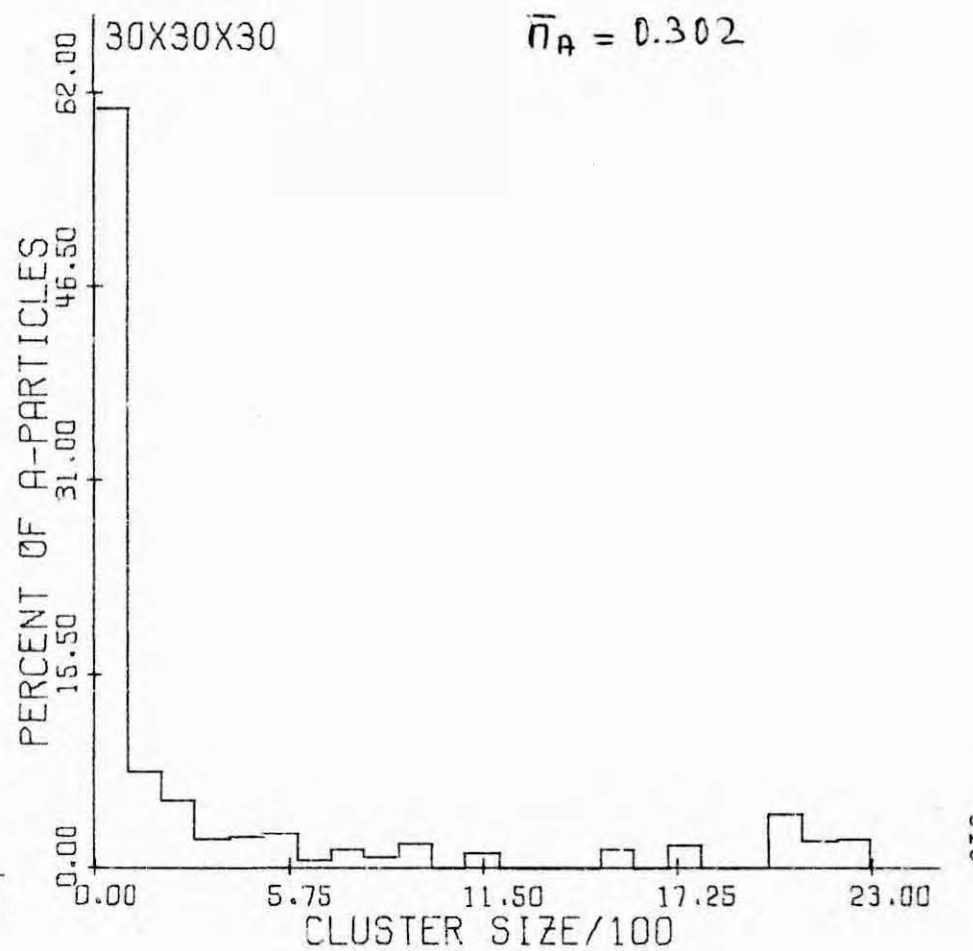
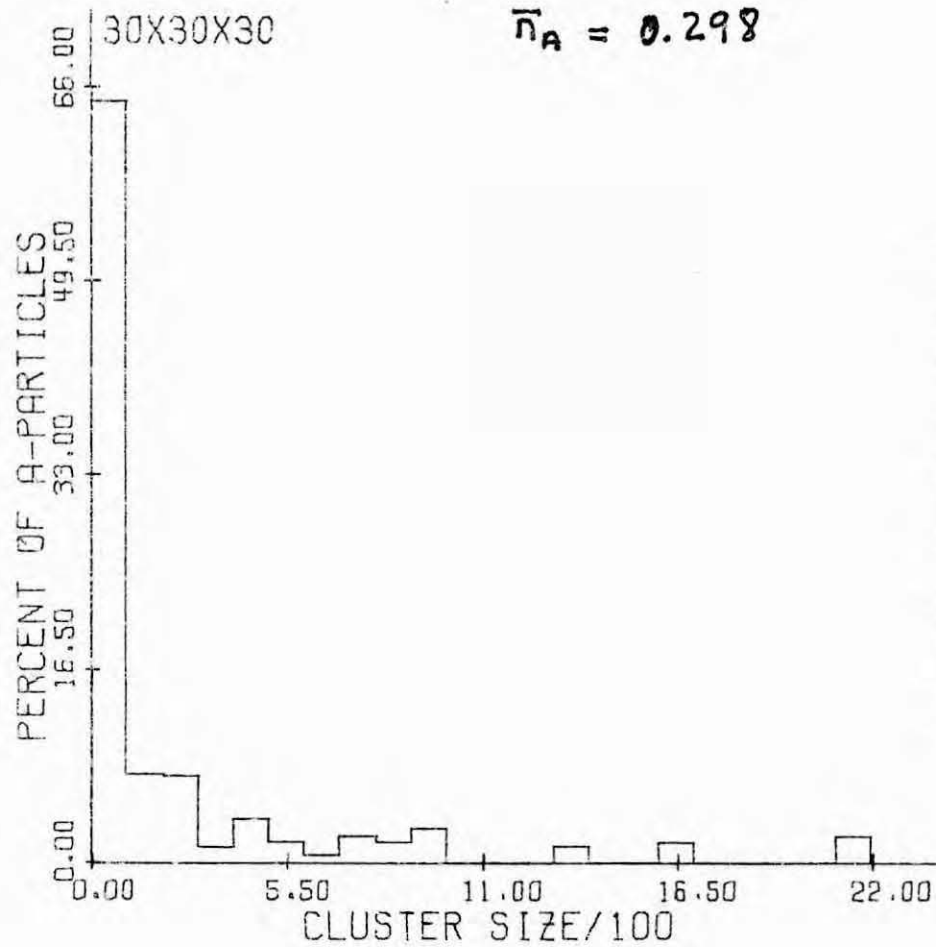


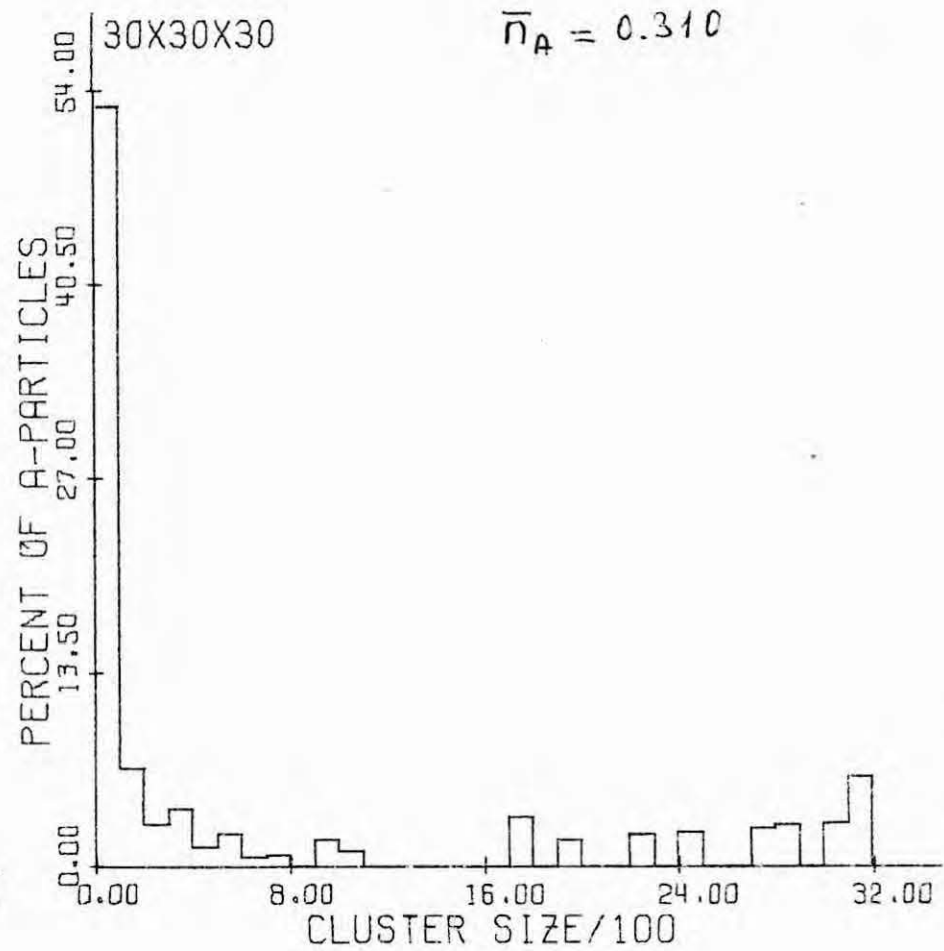
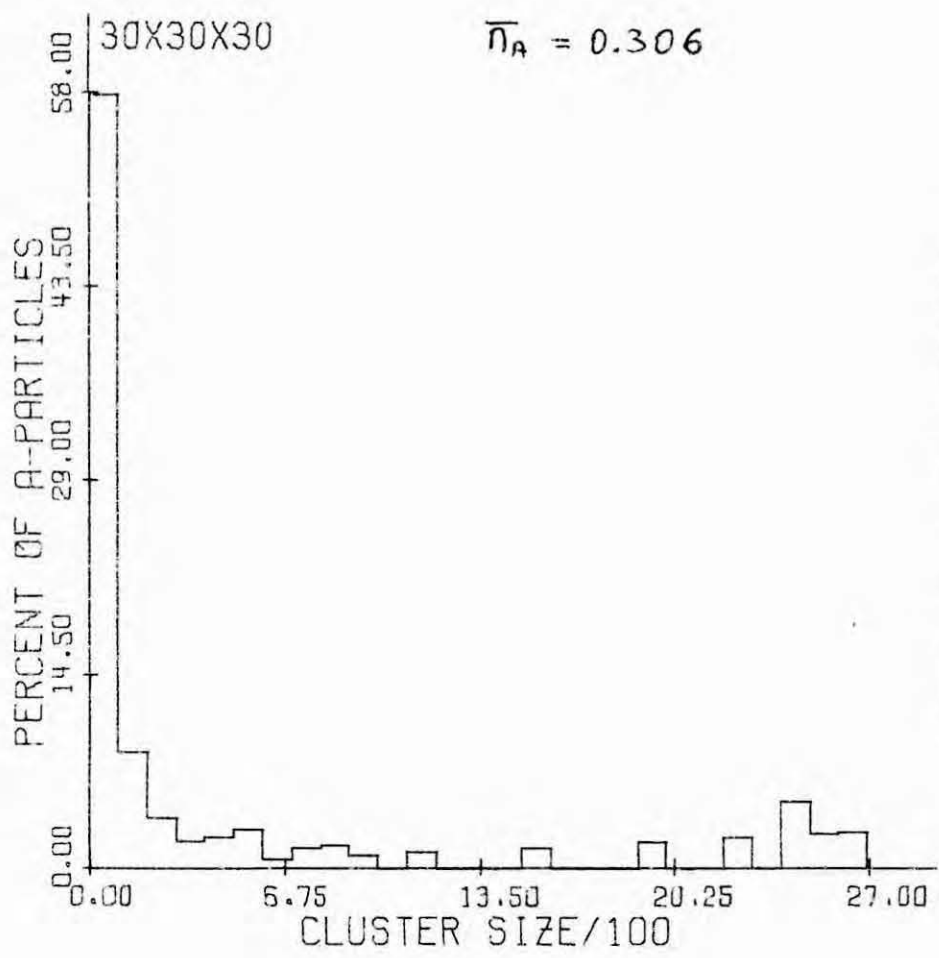


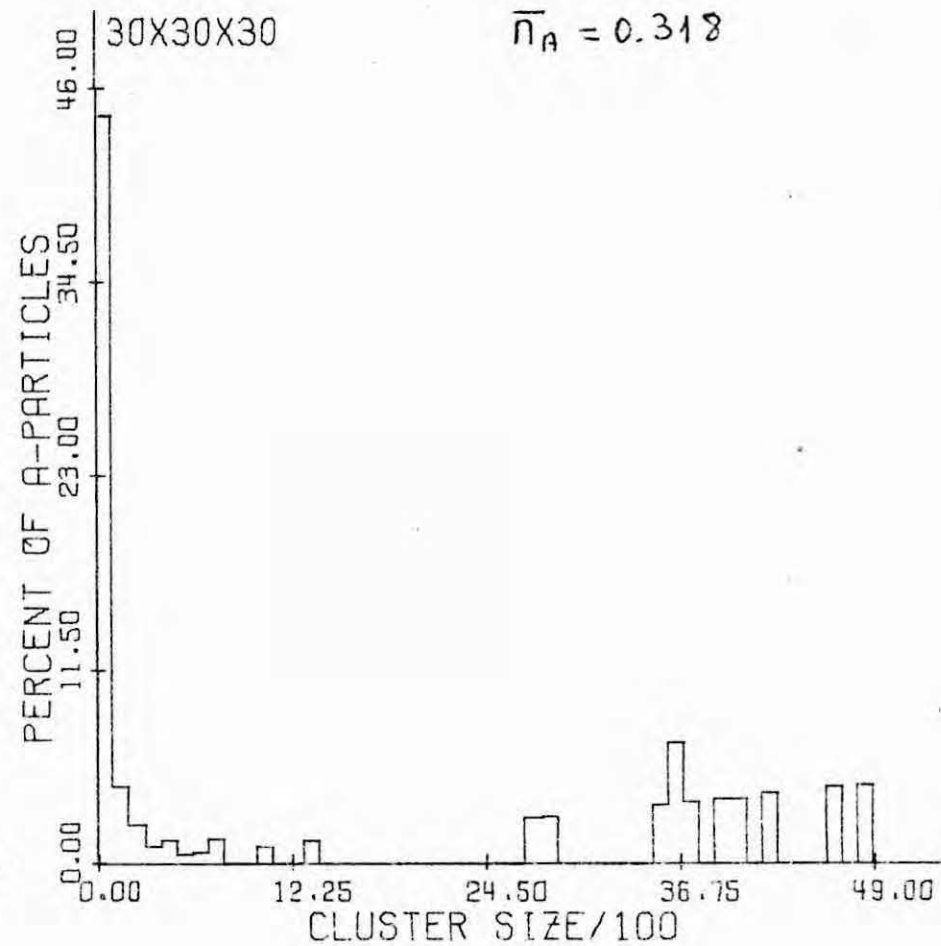
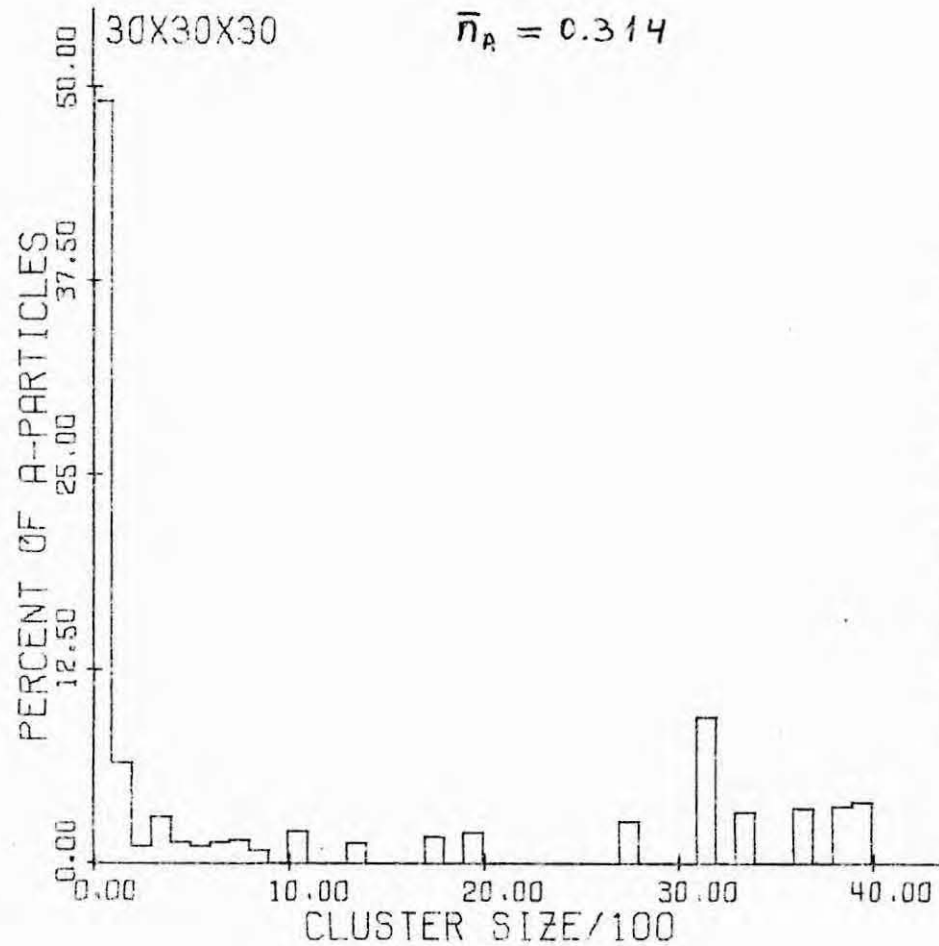


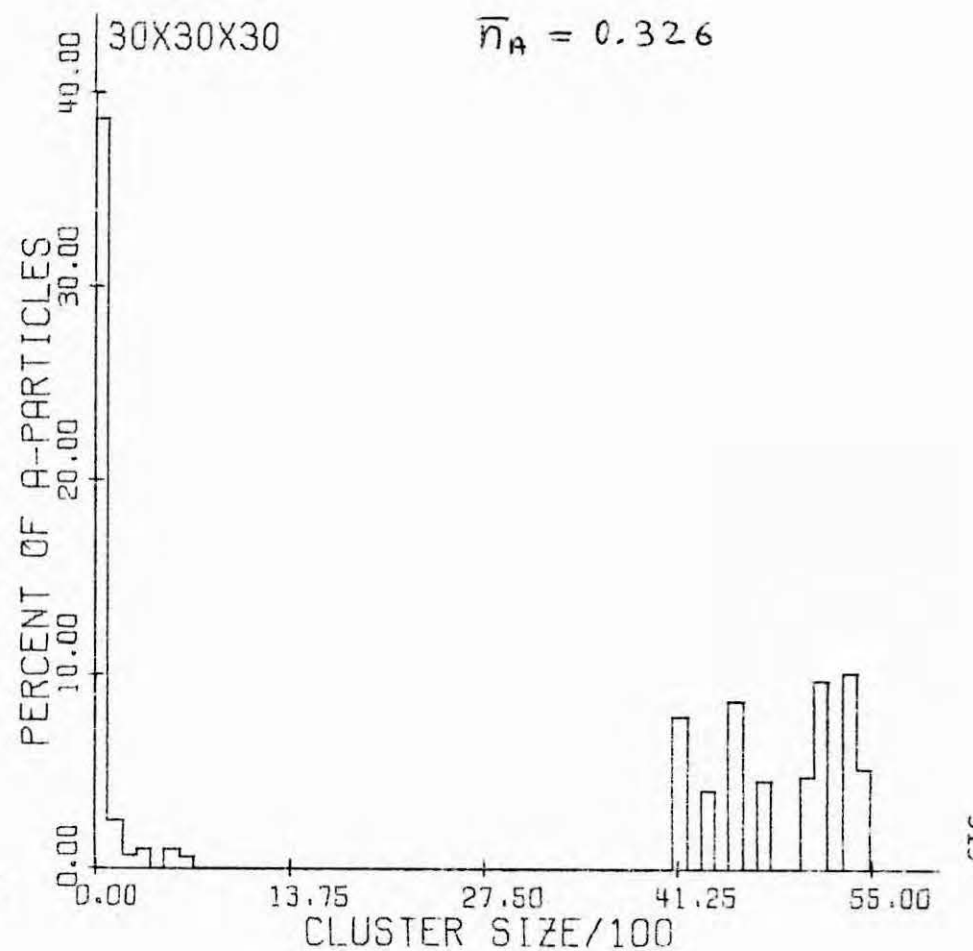
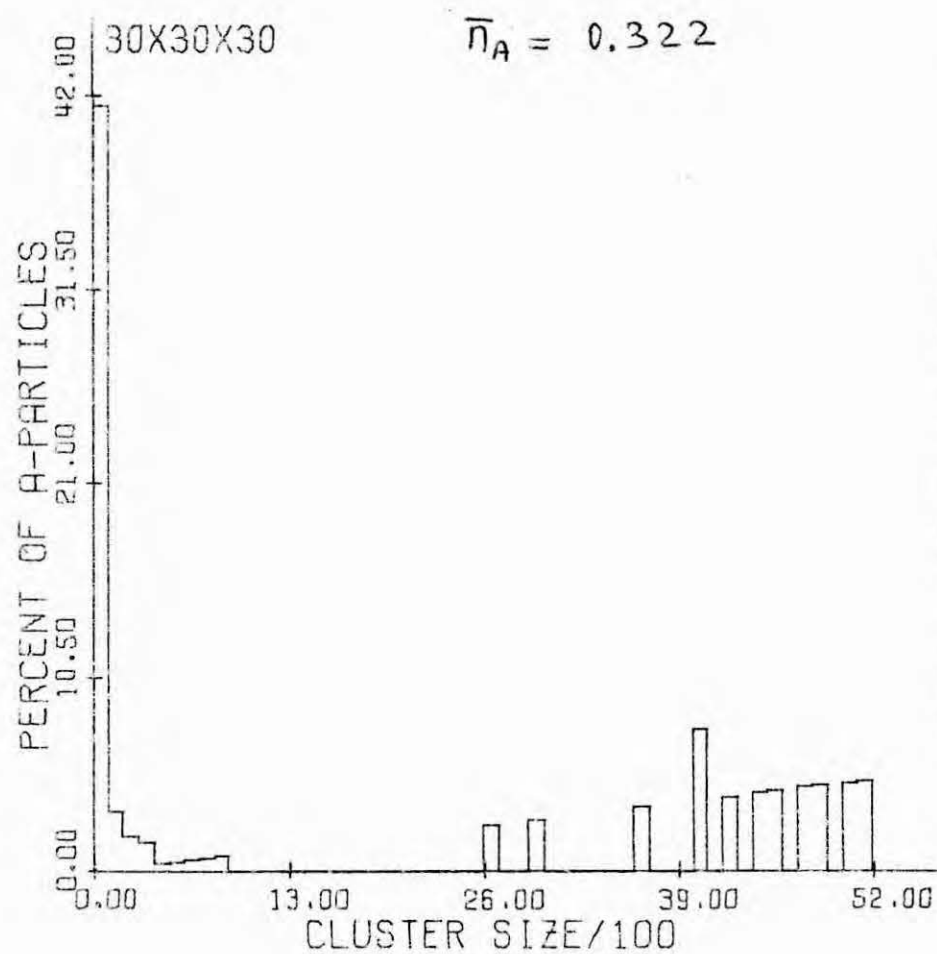


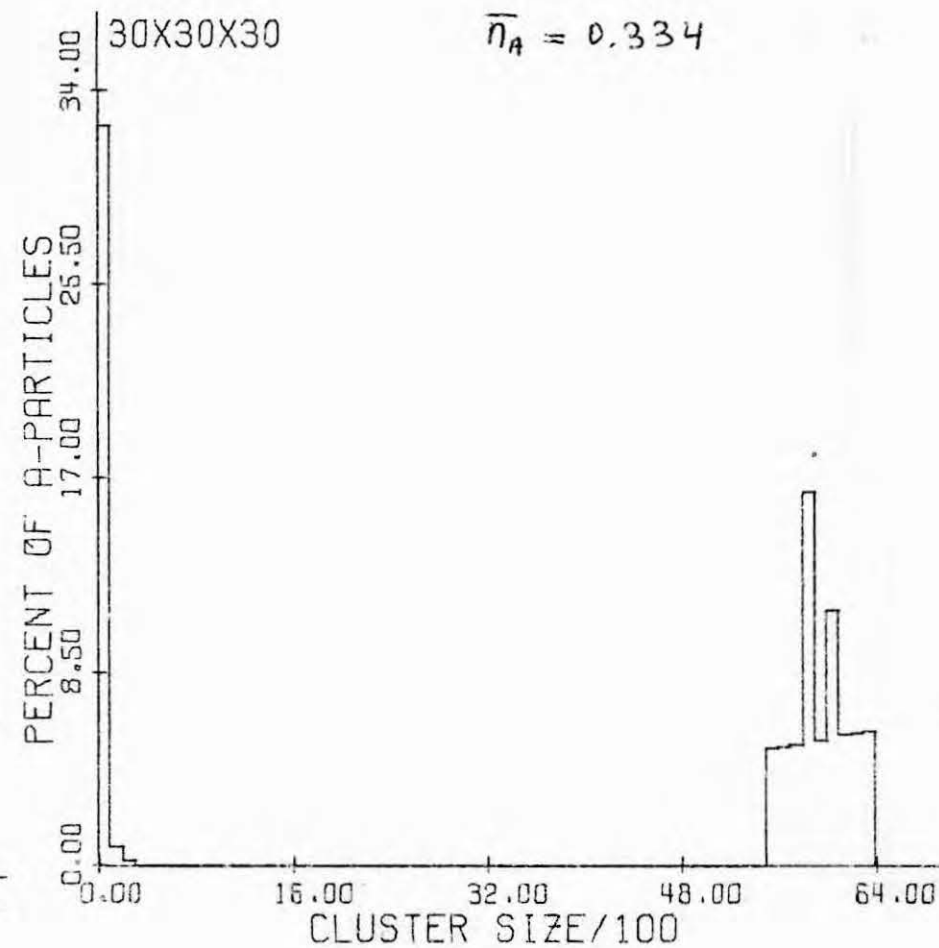
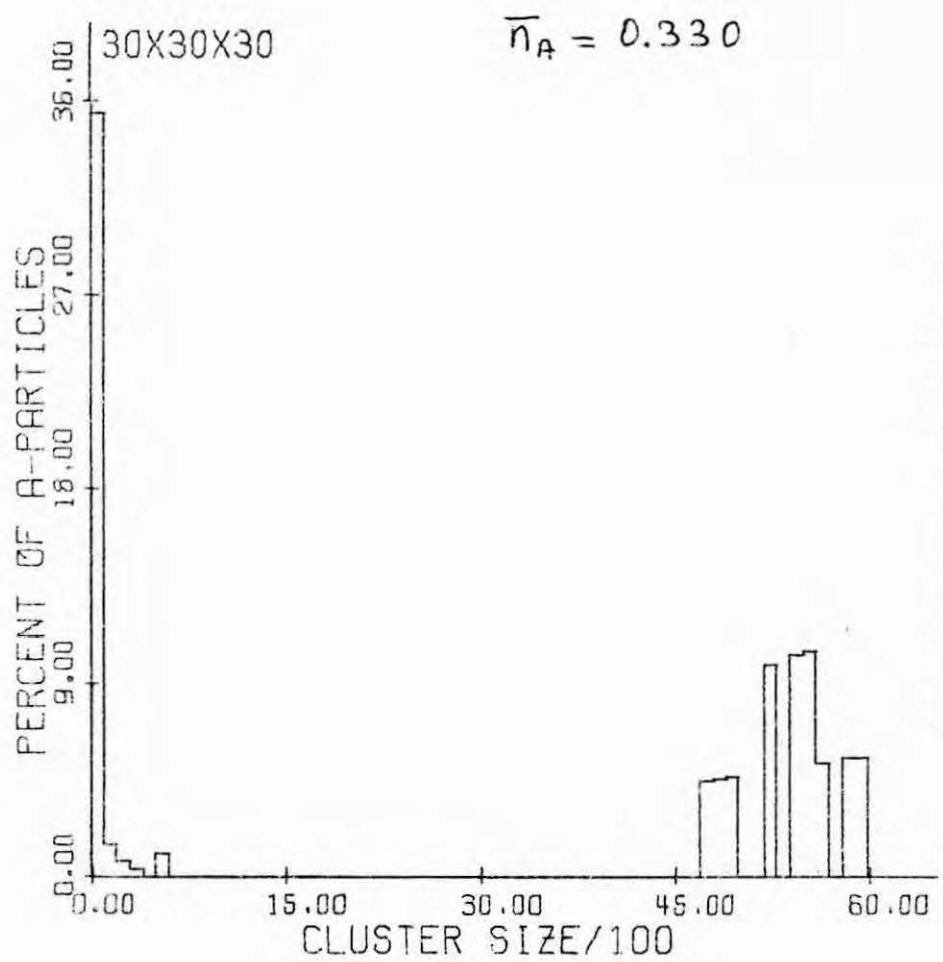


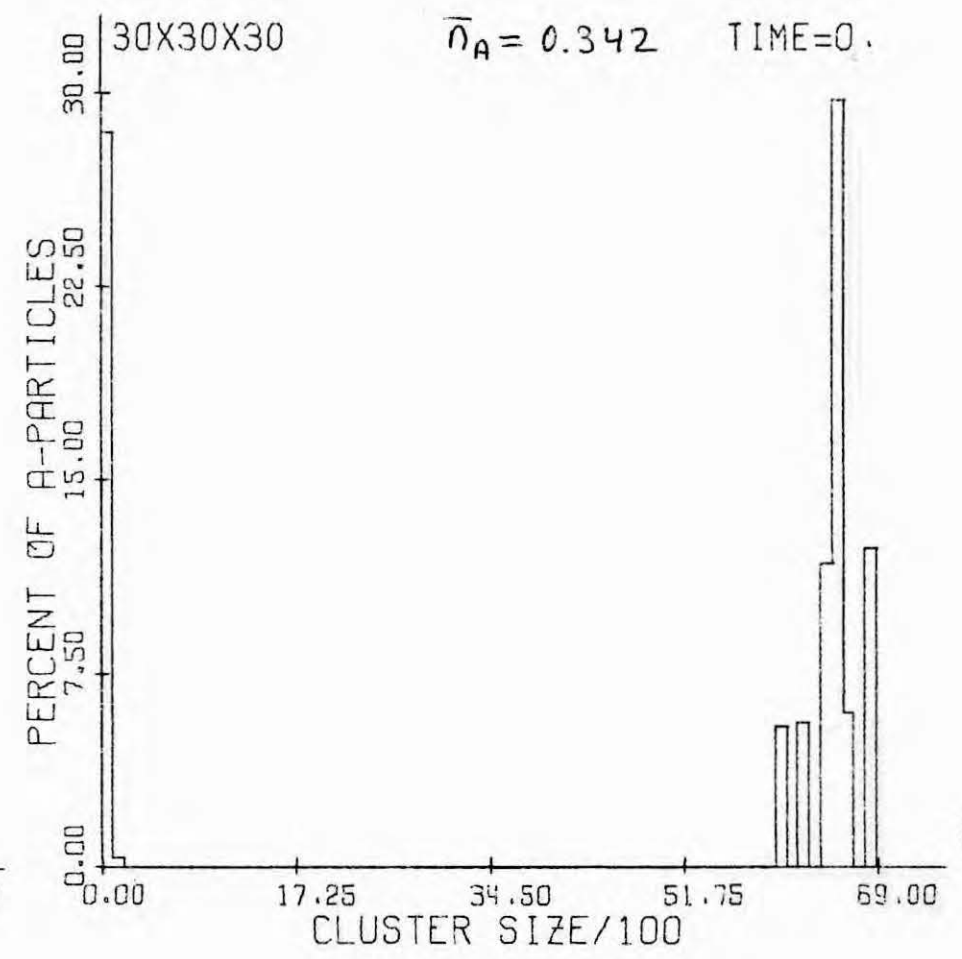
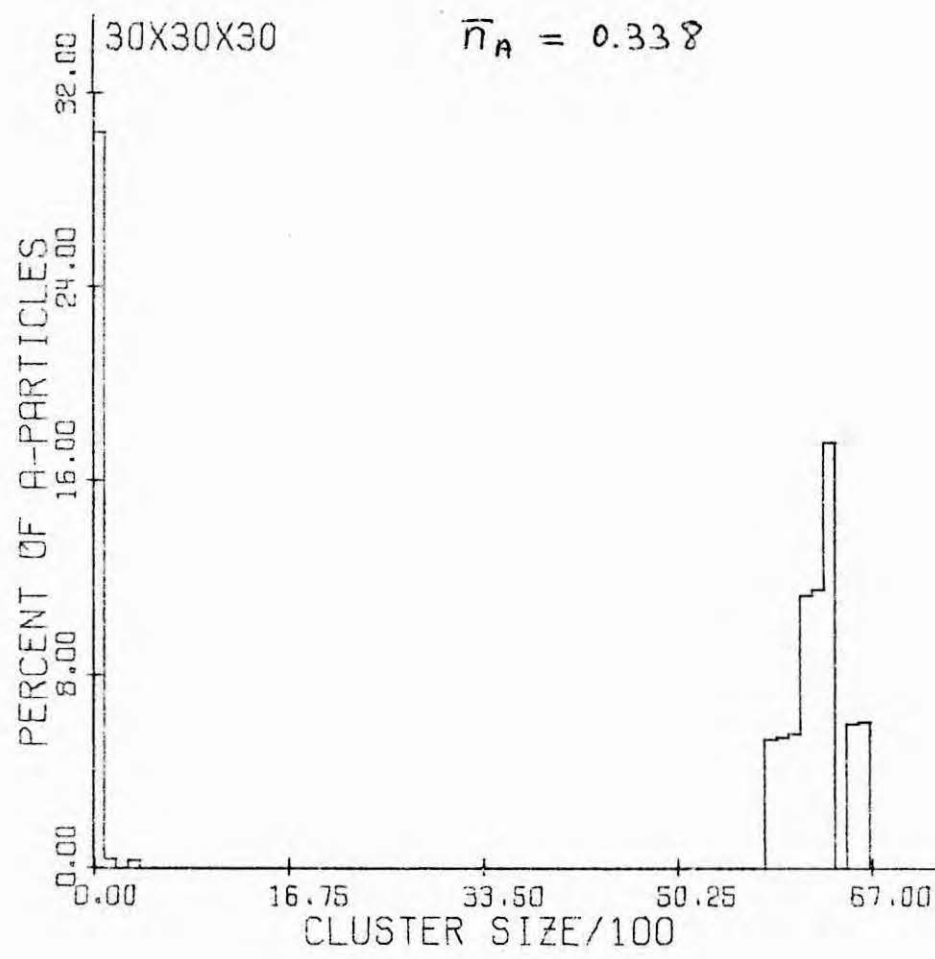


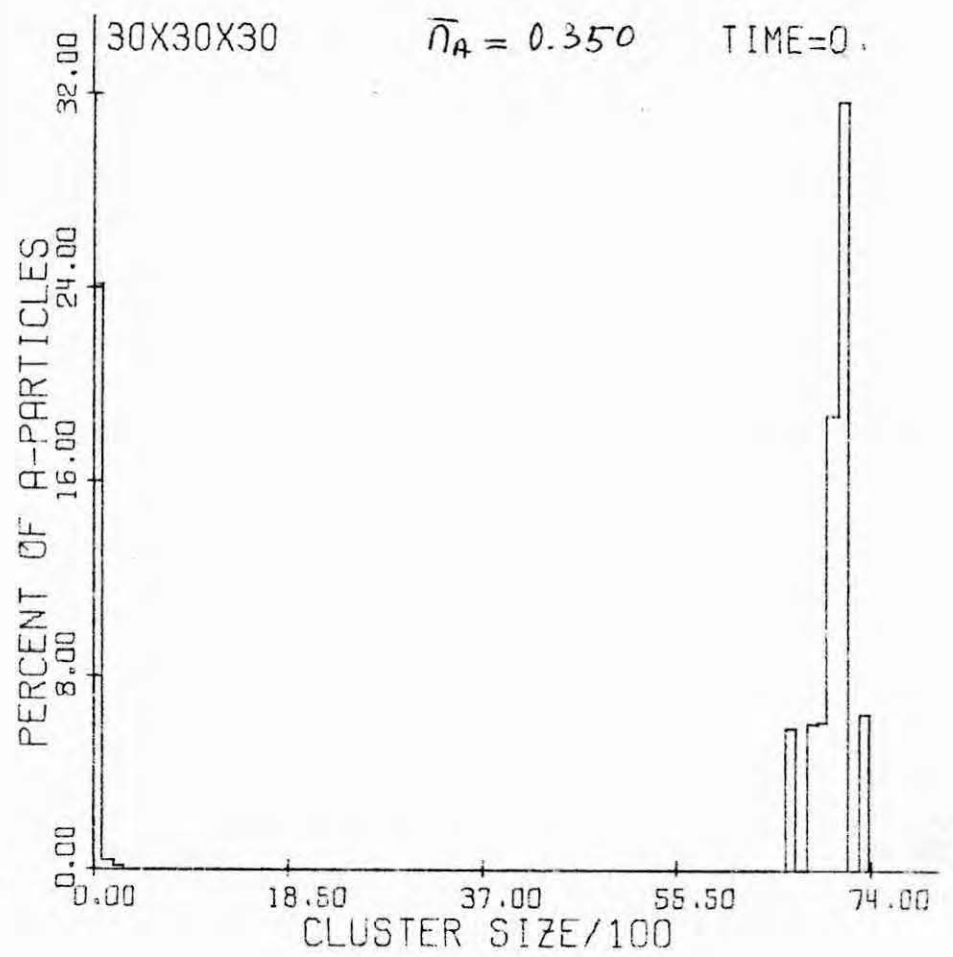
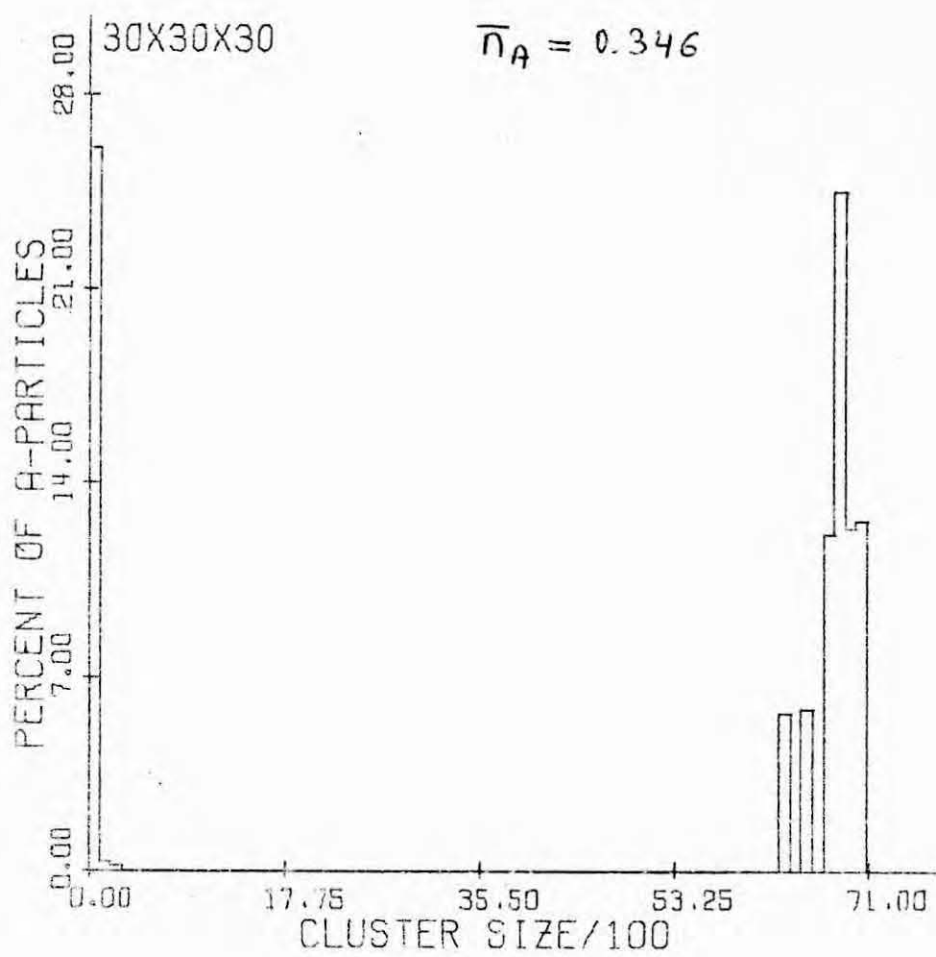


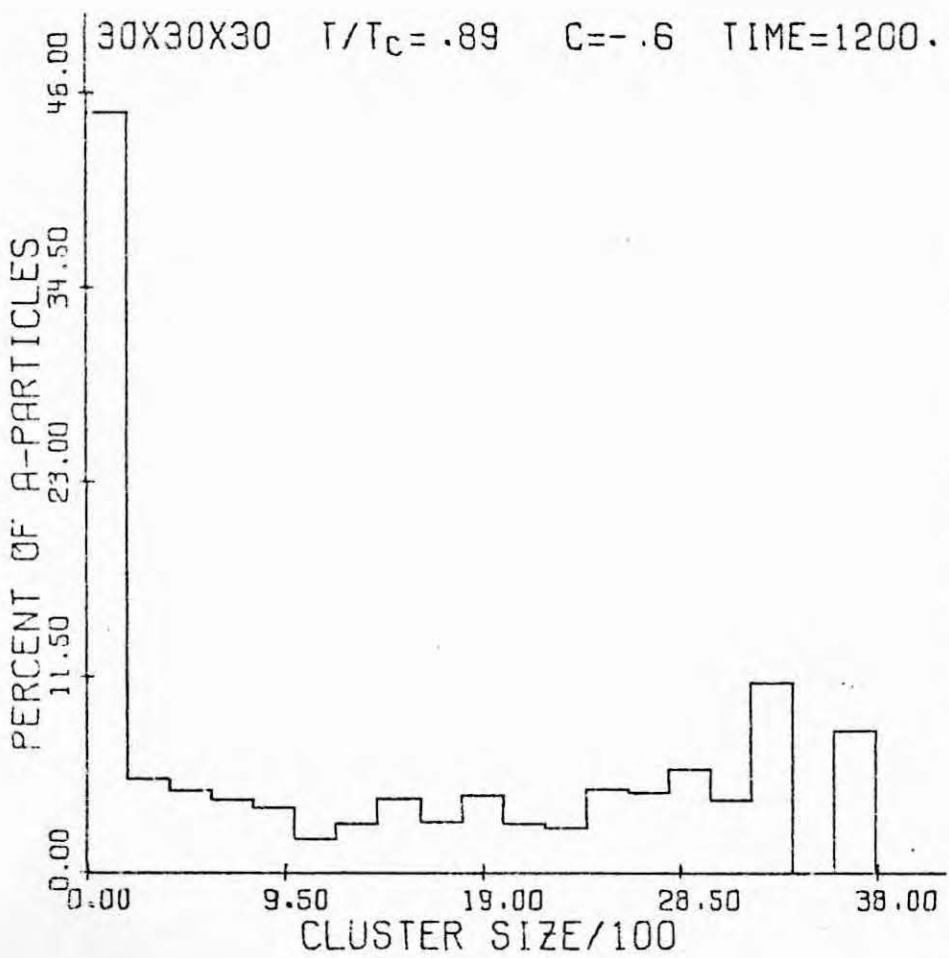




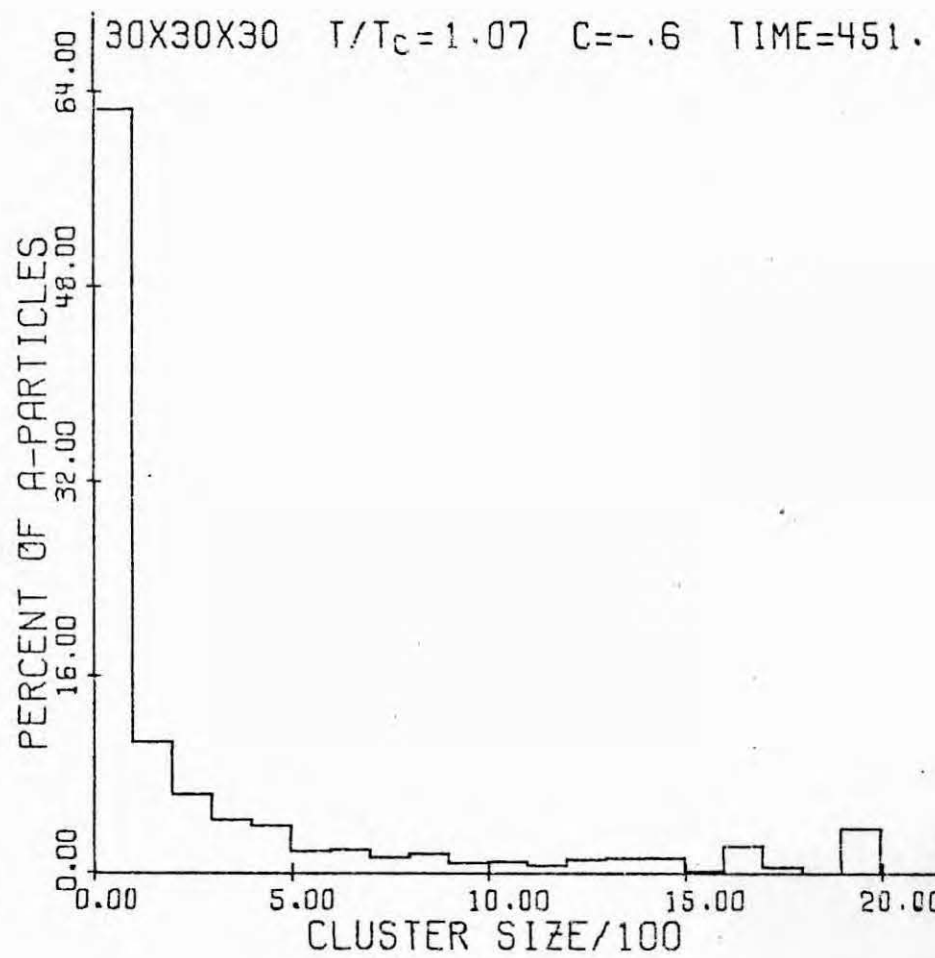








C.85



C.86